LEVEL II

ARL/STRUC-REPORT-363
ARL/MAT-REPORT-104

AR-000-724

DEPARTMENT OF DEFENCE

DEFENCE SCIENCE AND TECHNOLOGY ORGANISATION

AERONAUTICAL RESEARCH LABORATORIES

MELBOURNE, VICTORIA

STRUCTURES REPORT 363

MATERIALS REPORT 104

AIRCRAFT STRUCTURAL FATIGUE

Proceedings of a symposium held in Melbourne, 19–20 October, 1976

APPROVED FOR PUBLIC RELEASE

COPY No 13

APRIL 1977

LEVEL

AR-000-724

DEPARTMENT OF DEFENCE

DEFENCE SCIENCE AND TECHNOLOGY ORGANISATION

AERONAUTICAL RESEARCH LABORATORIES

STRUCTURES REPORT No. 363

MATERIALS REPORT No. 104

AIRCRAFT STRUCTURAL FATIGUE.

Proceedings of a symposium held in Melbourne, 19–20 October, 1976

SUMMARY

A Symposium on ARL work on Aircraft Structural Fatigue was held in October, 1976 in Melbourne. Nineteen technical papers were presented and these, together with questions and answers, comprise the bulk of the report. The papers cover:

Australian experience and research in Aircraft Structural Fatigue
fundamentals of fatigue and of fracture mechanics
data acquisition and interpretation
structural life prediction
current research and development in structural and materials fatigue

POSTAL ADDRESS: Chief Superintendent, Aeronautical Research Laboratories, Box 4331, P.O., Melbourne, Victoria, 3001, Australia.

[redacted]

VIBRATION TECHNIQUE

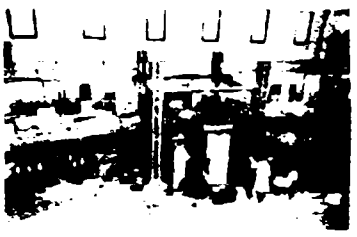

MEAN LOAD APPLIED BY HYDRAULIC JACKS AND SPRINGS

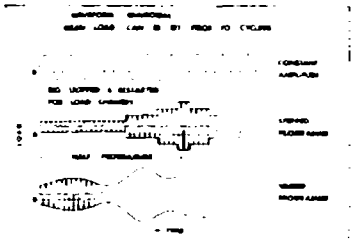

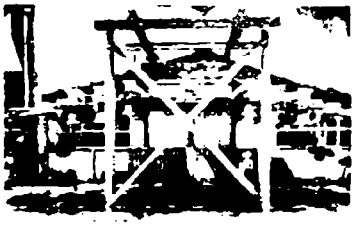

MEAN LOAD APPLIED BY DEAD WEIGHT AND SPRINGS

SIMPLE HYDRAULIC LOADING SYSTEM

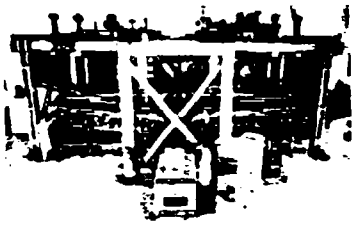

PRESSURE SWITCH SOLENOID VALVE BANG-BANG CONTROL

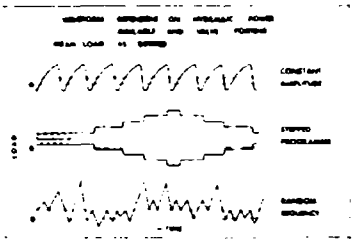

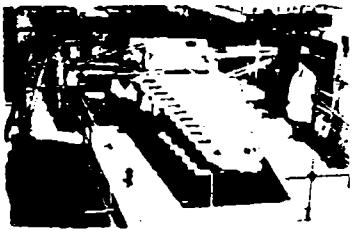

MECHANICAL VALVE BANG-BANG CONTROL

COMPUTER CONTROLLED SERVO HYDRAULIC -MULTI LOAD CHANNEL SYSTEM

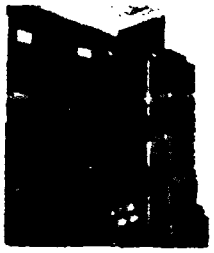

PDP 11 - COMPUTER

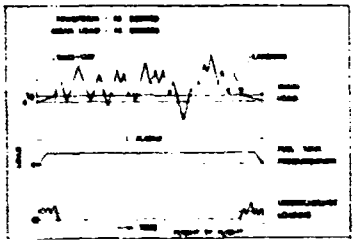

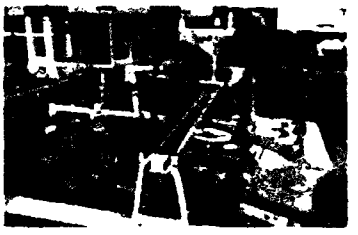

TEST RIG

A Symposium on ARL work on Aircraft Structural Fatigue was held on 19–20 October 1976 in Melbourne. It attracted an audience of 211 persons, comprised of a large contingent of Service personnel, academics, research workers, aircraft manufacturers and operators, air safety personnel, and many persons from the general engineering area of industry. Forty-four persons from interstate attended.

Nineteen technical papers were presented and these, together with the questions and answers, comprise the bulk of this report. As part of the Symposium a 28-board display was mounted illustrating examples of ARL research into Aircraft Structural Fatigue; the frontispiece shows a typical exhibit.

ORGANISING COMMITTEE

J. B. Dance (Convener)

F. P. Bullen

J. M. Finney (Secretary)

PREFACE

Australia has a very real interest in the problem of aircraft fatigue. The local civil airlines amass flying hours at a high rate, and military aircraft are frequently operated beyond the life guaranteed by the designers. It is a tribute to the air-worthiness authorities—the Air Transport Group of the Department of Transport, the RAAF and the RAN - and the operators, that Australia has an excellent safety record. Some of the credit for this record is also due, I believe, to the Aeronautical Research Laboratories, whose research work on fatigue has been conducted over a period of three decades. Indeed, ARL's international reputation probably owes more to its contribution to an understanding of fatigue than to any other single subject.

The total effort on fatigue work in Australia is shared by the operator, the regulating authorities, and the research workers. By international standards it is not large, but therein lies one of its significant advantages; the people know each other and hence very real co-operation is possible while the whole problem is maintained in proper perspective.

The symposium arose out of a suggestion by Mr. H. A. Wills--a former Superintendent of Structures Division - that the unique knowledge available at ARL for dealing with fatigue problems should be widely disseminated. The arrangements were in the care of a small ARL committee chaired by Mr. J. B. Dance, the then Superintendent of Structures Division. The fatigue work in that Division has been under his control for the last two decades; he retired a week after the symposium.

The opening of the symposium was to have been carried out by the Chief Defence Scientist, Dr. J. L. Farrands. Unfortunately, he was not able to be present, so his address was read: the text appears in full in the proceedings. Particular note was taken of his penultimate paragraph about codification of practice. The Laboratories are now paying close attention to the possibility of meeting his challenge.

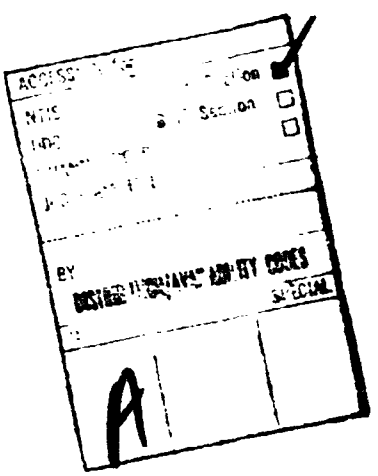

F. G. Bligh

(F. G. BLIGHT)
Chief Superintendent,
Aeronautical Research Laboratories

CONTENTS

OPENING ADDRESS BY DR. J. L. FARRANDS
CHIEF DEFENCE SCIENTIST

OPENING ADDRESS BY DR. J. L. FARRANDS CHIEF DEFENCE SCIENTIST

Mr. Blight, colleagues and visitors, I must apologise for not being able to be present to open this ARL Symposium on Aircraft Structural Fatigue. It is a subject which I find has a great deal of interest for me personally. It is furthermore a topic in which science can be immediately seen to have important social and economic implications.

Australia was one of the early leading countries in research on aircraft fatigue with participation by ARL, DCA and the RAAF. It owed its start, I believe, to the considerable insight of Mr. H. A. Wills when he was Superintendent of Structures.

The most important contribution in the early work was the repeated load tests on Mustang wings which was used as a basis for the data sheets on fatigue of aircraft structures put out by the Royal Aeronautical Society in UK.

After further civil work involving fatigue tests on Dove and Drover aircraft it was realised that military aircraft would also suffer fatigue failures, particularly in Australia because of the wish to obtain the longest possible life from this expensive equipment. Thus safe fatigue life investigations were commenced on Canberra, Hercules, Neptune, Winjeel and Vampire, the latter involving a full-scale fatigue test at ARL.

Full-scale tests were continued with Cessna and then Mirage which was completed over a year ago. This is probably the last overseas designed aircraft to be tested in Australia because there is now general recognition in other countries that a full-scale fatigue test is an essential part of the development of an aircraft.

In spite of the very good research work that has been done over the years there still remains a large number of unsolved problems. There are areas of contention in the interpretation of statistical methods. There needs to be a clearer understanding of the meaning of the advice that the scientists are giving.

In addition to these here-and-now problems there has to be attention to continual monitoring of new materials and new production processes. The lessons of the ultra high strength steel in the F111, and the subtleties and surprises of the corrosion problems should not be readily forgotten.

Fatigue and the associated problems of

(*a*) methods of calculating safe lives,

(*b*) fatigue properties of and crack propagation in aluminium alloys,

(*c*) methods of measuring flight loads in aircraft,

(*d*) statistical properties of fatigue fracture,

(*e*) non-destructive testing methods,

(*f*) the mechanism of damage in metals, and

(*g*) effect of environment on fatigue properties and safe life calculations

are all the subjects of continuing research.

The available resources clearly limit the effort which can be applied to these topics. It is a heavy responsibility of the research managers to ensure that the effort is properly distributed, reinforces success, and at the same time refrains from the merely interesting.

It has long been my belief that the knowledge within our community on this subject should be assembled. We have something to say to the world. I also believe that we should codify current practice, so that the basis for decision making should be explicit.

This symposium may be a good beginning for such a project. Certainly it will provide a summary of present knowledge and perceived problems.

What about codification of practice? Can the symposium help you to agree on this, and agree to do it.

If your symposium can go towards these two things it will have been worthwhile. I wish you well.

INTRODUCTORY PAPER

SAFETY AGAINST FATIGUE IN FLIGHT— A PERSPECTIVE OF AUSTRALIAN EXPERIENCE AND RESEARCH

by

F. H. HOOKE

SUMMARY

Metal fatigue in aircraft was not envisaged as a problem when the Aeronautical Research Laboratory was about to be established: it was seen to be significant after an aircraft accident in 1945, and this initiated a new and sustained thrust in the structures research programme.

At an early stage plans and procedures were formulated, and the Laboratory proceeded to carry out tests and acquire and interpret information, both on the endurance of structures and materials, and on the loading actions on the structure—information which was to be of great value to civil and military aviation in Australia and throughout the whole world. In 30 years the total of catastrophic fatigue failures was to rise to five, and, of these two resulted from the use of new high strength materials whose fatigue properties had not been properly explored in the laboratory before they were adopted.

These failures intensified and sharpened the research effort, leading to improvements in procedures and to better understanding of the way in which inspection can maintain structural integrity. The dissemination of Australian research results, and the overseas contact of Australian scientists, has produced a two-way flow of information which can be said to have significantly improved aircraft fatigue performance and fatigue evaluation.

1. INTRODUCTION

The problem of fatigue of metals, though by no means new in the field of engineering, was not regarded as particularly significant to aircraft during the second world war or immediately thereafter, when what was then the Structures and Materials Section of the CSIR Division of Aeronautics was in its infancy.

There had, it is true, been fatigue failures in the primary structure of some military aeroplanes overseas during the war, but these were regarded as having resulted from poor design, and therefore remediable by the use of adequate design and stress analysis procedures. Of the many problems on which the advice of the Division of Aeronautics was sought during the war, three only were concerned with fatigue; a failure of a Gipsy Major engine crankshaft, a failure of a Jowett Javelin motor crankshaft, and a question whether the welding of steel tubes of similar strength but of different composition caused a deterioration of the static and fatigue strengths.

In January 1945 there occurred an event which was to reshape the Laboratory's research programme: it was the crash of the Stinson airliner VH-UYY at Spring Plains in Victoria with the loss of ten lives. The weather conditions were fine and could in no way have contributed directly to the accident. An examination of the wreckage[1] showed that fatigue failure had occurred in a joint of the welded steel tube structure carrying tension loading between the port outer wing and the centre section, and that another fatigue crack had grown to a less advanced stage at another welded joint area.

It has only been recently learnt that, by 1945, Swiss aircraft designers had rejected the "birdsmouth" type of welded joint used in the Stinson, in favour of butt-welded joints, because of the relatively inferior fatigue performance of the former.

The significance of this accident to Australia was that it revealed that fatigue failure under normal fluctuating flight loads was not a remote possibility as had been previously thought, but was a serious risk: it drew attention to the disadvantages of welded steel structures from the fatigue viewpoint, and it catalysed the study of all factors entering into the problem of aircraft fatigue.

Following the Stinson accident a meeting was held between Division of Aeronautics and Department of Civil Aviation personnel at the Laboratory to plan to obtain the information required to elucidate the fatigue problem. The decisions, as recorded, were:

(*a*) DCA to contact overseas airworthiness authorities regarding steps being taken to determine a safe working life of aeroplane structures.

(*b*) DCA to install flight load measuring instruments in civil aircraft.

(*c*) The Division of Aeronautics to contact overseas research institutions to obtain any available data and proposals for future works in respect of—

  (i) magnitudes and frequencies of applied loads,

  (ii) methods of assessing the endurance life of various types of structure under these loads.

(*d*) The Division to consider performing flight tests to obtain specific data on loads and stresses in aircraft when flying in normal and adverse weather conditions.

(*e*) The Division to investigate endurance limits of typical structures and components.

Arising out of these recommendations approaches were made in person and by letter to overseas authorities, and surveys of information were made which revealed that nowhere was it considered possible to design for a specified life expectancy nor did methods of estimation of fatigue life expectancy exist in a form suitable for adoption by an airworthiness authority. Some limited information was obtained on the frequencies and magnitudes of applied flight loads; at Farnborough the effects of fluctuating loads on aircraft components were being explored in a general way[2] and the basic idea of establishing life expectancy from the relevant load and fatigue data had been put forward by Bland and Sandorff;[3] but a logical approach and concrete factual data which could be regarded as relevant to Australian flying conditions or Australian operated aircraft were completely lacking.

It is a tribute to the foresight of Mr. H. A. Wills, the first Head of the Structures and Materials Section, that he saw this as a potentially growing problem demanding for its solutions the development of specific procedures and the obtaining of specific data both on the fatigue behaviour of structures and on the loading actions occurring.

This work proceeded enthusiastically. Within a few months the hydraulically controlled wing test rig, being used at the time to investigate the static strength of Australian-built Mosquito wings[4] was mechanised and a Mosquito wing was fatigue tested[5] with some surprising results. As far as is known no wing testing rig capable of this performance then existed elsewhere in the world. In December 1946 the current state of knowledge was exposed in a Symposium on "The Failure of Metals by Fatigue", organised at Melbourne University. The papers covered a very wide field, and included several on aircraft fatigue by overseas specialists (little more definitive than the results of the overseas inquiries of the previous year), and contributions from the Division of Aeronautics by Johnstone and Hooton on "Methods of investigating the fatigue properties of materials" and "The measurement of dynamic strain" respectively. In retrospect the Symposium proved most valuable in bringing together expertise from the world over; it is nevertheless not too harsh a criticism to say that it revealed more areas of ignorance than of knowledge, since, for example, it became apparent that no means was available to design against fatigue the simplest of machine parts, viz., a shaft in fluctuating torsion with a fillet radius blending a smaller diameter to a larger one.

Meanwhile the research programme of the Structures and Materials Section began to get under way. After surveying the meagre literature, studies were made of the fatigue strength of machine parts,[6] methods for extrapolating fatigue data,[7] and for calculating the endurance strength of aircraft.[8] Because it had become clear that fatigue loading on civil aircraft came primarily from the fluctuating loads caused by atmospheric turbulence, particularly in adverse weather conditions, theoretical studies were made of the response of aircraft to gusts.[9,10] Flight load measurements were instituted on civil DC-3 aircraft[11] within Australia and on RAAF Lincoln[12] and Dakota transports within Australia and overseas, while laboratory investigations were made of the performance of measuring instruments.

By September 1947 the various aspects of the problem had been brought to a sufficiently definitive stage for Wills to present to the Institution of Engineers, Australia a detailed statement of the situation.[13] He showed that, because of a number of factors, including:

(*a*) the steady increase in working stresses,
(*b*) the increase in cruising speeds,
(*c*) the increase of dynamic effects with increasing aircraft size, and
(*d*) the introduction of new materials having higher static strength but unchanged fatigue properties,

the likelihood of fatigue failures of the primary structure was increasing and would continue to increase in the future.

In a sample calculation using hypothetical data, it was shown that gusts of a low order (below the load factor 0·5 or a gust velocity of about 6 f.p.s.) could well be ignored when considering fatigue damage; and maximum damage occurred with gusts having a vertical velocity of about 12 f.p.s. Using the by then familiar cumulative damage hypothesis, a life to failure of about 9000 hours was calculated. When it is remembered that the utilisation of civil aircraft in this country was particularly high, and not uncommonly aircraft used to accumulate between 3000 and 4000 flying hours per year on short stage operations, the significance to Australian operators of the fatigue problem was clear.

This analysis reiterated the immediate need for further data and further research on such topics as:

(*a*) fatigue behaviour of full scale aircraft structures under laboratory tests,
(*b*) fundamental fatigue properties of specimens of various aircraft materials under a wide range of maximum and minimum loads,
(*c*) fluctuating flight loads experienced on Australian air routes (desirably to be recorded with statistical recording instruments), and
(*d*) the dynamic behaviour of the structure under suddenly applied loads.

Investigations of fatigue behaviour of full scale structures proceeded with the testing of fourteen aluminium alloy wings of Boomerang fighter aircraft—the wings being of single spar type with compression skin stiffened internally with corrugated sheet. The wings (which were

made in Australia by Commonwealth Aircraft Corporation), were tested at a variety of fluctuating load amplitudes, and an S-N curve was established. When compared with the reputed behaviour of riveted joints in the same material at low alternating stresses there was reasonable agreement, but in tests at loads approximating 40% of ultimate design load the wing life was only one-twentieth of the reputed life of riveted joints, and a little inferior to the life of Typhoon tailplanes previously tested by Oaks and Townshend at the RAE, Farnborough.[14]

In May 1949, at the invitation of the Royal Aeronautical Society, Wills presented a paper on the same topic to the Second Anglo-American Aeronautical Conference held in New York.[15] Its message and its conclusions were the same as those of the earlier Institution of Engineers paper, while the sample calculation of fatigue life was updated using the actual full scale fatigue data from Boomerang wings, giving a safe lifetime of 14,900 hours. Two years later a safe lifetime of one-fifth of that figure was to be applied to an aircraft type in service.

2. THE NINETEEN FIFTIES

As far as the Structures Laboratory (now the Structures and Materials Division of the Aeronautical Research Laboratories, Department of Supply) was concerned, the 1950s were the era of "Mustang Wing Tests".

After World War 2, a large number of Australian- and US-built Mustang aircraft became surplus, and the wings were acquired, for the purpose of further investigating at full scale the fatigue properties of aluminium alloy structures as then constructed, as had been recommended following the Stinson accident.

Initially the endurance was to be investigated under constant amplitude loading and different specimens were tested with various mean and alternating loads.

By 1955 over 170 wings had been tested, deriving the A-M Diagram for Mustang Wings, and providing a data base, the use of which, with a cumulative damage hypothesis, would permit the calculation of endurance of these wings under any sequence of service loads, whether military fighter, trainer, civil transport or whatever.[16] In addition the tests revealed the sorts of structural details in Mustang wings where fatigue first became apparent: sharp cornered holes in evenly stressed panels, concentrations of stress where load carrying members converge, etc.: they also showed the way in which fatigue cracking developed, and that the predominant failure location varied with the load amplitude. The endurance of various failure locations corresponded with those of notched specimens of material with a K_T* of 3·6 and 4·2.[23] Tests were carried out on specimens preloaded to between 85% and 95% of mean ultimate failing load, and these revealed what was shown by Heywood[17] on specimens, lugs, wing booms and tailplanes, viz. that high preloads can considerably enhance the endurance.

The results of the constant amplitude tests became well known and used throughout the aeronautical design world, and were incorporated into Issue 2 of the Royal Aeronautical Society (now ESDU) Data Sheet on "Endurance strength of complete wings and tailplanes (aluminium alloy material)".[18] They were also combined by ARL with other overseas data to give the 24ST Structures A-M diagram, and this was used for some years in Australia for life estimation, using a large scatter factor, until the conviction had grown that a single test result from the structure in question was preferable to several hundred test results from other sorts of structures.

There had been a growing feeling within ARL and elsewhere that the cumulative damage hypotheses and procedures required verification, that fatigue airworthiness testing with one fluctuating load amplitude was inadequate, and that the testing should be spread over at least three load amplitudes. ARL therefore decided to represent the service load experience by a multi-load-level test with loads applied in random sequence. Langford of DCA[19] enunciated a proposed fatigue airworthiness requirement for aircraft wings, which specified programme loading at these amplitudes—a simplification of the procedure initiated 16 years earlier by Gassner,[20] but yet more complex than was then the current practice. Woodgate,[21] of Trans Australia Airlines, questioned the validity of procedures for calculating the damaging effects of the air-ground-air loading cycle, and pointed out that the proposed three-load-level programme had not been designed to represent these loads.

---

* Theoretical stress concentration factor.

ARL therefore proceeded to further tests of Mustang wings under four different varying load histories:

(*a*) A three-level programme of gust loads.

(*b*) A multi-load-level random gust load history derived from the same spectrum.

(*c*) The same multi-load-level random gust history with a periodic air-ground-air cycle.

(*d*) A multi-load-level random manoeuvre load history.

The results of these investigation were described in a series of reports by Johnstone, Payne, Ford, Patching, Kepert, Rice, *et al.*[16,23,24,25] From these it was concluded that, having the complete A-M diagram for the wings in question, the endurance to final failure could be well predicted for each of the three gust load histories using the linear cumulative damage hypothesis, provided that the largest positive load in the history was assumed paired with the largest negative load, the second largest with its complement, and so on (denoted Hypothesis H_1). This procedure had been current practice at ARL for the previous decade. Under the manoeuvre load history the prediction method was found to underestimate the endurance, but as this was conservative it continued to be adopted.

It was also concluded that a full scale fatigue test was necessary to adequately estimate fatigue life, so as to avoid errors intrinsic in estimation based on pre-existing data for "similar structures". Although Mustang wings were not "fail safe" in design nor strictly in practice, it was concluded that in potentially fail safe structures full scale testing was necessary to determine fatigue critical areas and the way fatigue failures develop. It was also concluded that a programme load test was the most feasible method of representing service loads, and that a simplified three-load-level test proposed by Langford gave close agreement with a random load sequence.

The constant amplitude data, when combined with overseas data from other structures showed a total variability (variance) of $s^2 = 0{\cdot}32^2$, and the variance between makes was $s^2 = 0{\cdot}25^2$ while that within makes was $s^2 = 0{\cdot}20^2$. This latter figure was about 3½ times the variance for Mustang wings alone ($s^2 = 0{\cdot}116^2$) and, appearing conservative, was used for a number of years as a variance to provide a scatter factor for a desired probability of failure, when variability data were not available for the structures in question.

While the Laboratories were testing wings which were not designed as fail-safe, the Australian airlines operated aircraft which the manufacturers claimed to embody such features, and the Department of Civil Aviation began to be concerned whether the claims of safety of such structures could be substantiated. The requirements for such substantiation are knowledge of all the critical points of the structure at which fatigue cracks may initiate, an assurance that cracks will not initiate simultaneously in parallel redundant members, an evaluation of the strength of redundant structure with a member cracked, an assurance that such a crack will be found by inspection if such inspections are timed regularly, and an assurance of the adequacy of the strength with one member cracked. The approach necessary to provide adequate assurance of safety was very fully discussed by R. R. Shaw in a paper to the *Aeronautical Journal*.[22]

Concurrently with the full scale fatigue test investigations, basic studies of the mechanism of fatigue of metals were being made by Wood and Head[26] and by Davies and Mann,[27] and on statistical properties of strength and endurance,[28] while a theoretical model for fatigue crack propagation in metals was devised and studied by Head.[29] Fatigue testing techniques were devised and improved for the testing of material specimens (again following the recommendations of Wills) as early surveys showed that test results could be meaningless without adequate control on metallurgical variables, manufacturing and testing procedures. Investigations covered the effects of surface finish,[30] various methods and degrees of heat treatment[31] and of protection coatings,[32] and various processes for forming fastener holes in sheet material, to name just a few.

In October 1951, complacency and a leisurely approach to fatigue was shaken by the crash of a Dove aircraft, VH-AQO, at Kalgoorlie as a result of primary structural failure. This aircraft had flown more than 9000 hours when the failure occurred, in an area having no obviously severe stress raiser, and no apparent source of unusually high nominal stress. Members of DCA accident investigation team were flown to the scene of the accident in another Dove, VH-AZY (also with about 9000 hours). When the fatigue failure in the crashed aircraft was identified, inspection of VH-AZY revealed cracks on the right- and left-hand sides of the wing carry-through structure, similarly located to the critical crack in VH-AQO. No aircraft elsewhere in the world had exceeded 3000 hours service at that time.

The accident raised several urgent questions:

"Why should a failure occur in an aircraft carry-through component whose strength complied with specification requirements, which had neither excessive nor avoidable stress raisers, poor design, faulty manufacture nor any other obvious reason for rejection?";

"Did the increase of all-up weight from 8000 to 8500 lb have any significant effect?"; and

"Could such an early failure have been predicted from a knowledge of the flight loads and the fatigue properties of the structure?".

In an endeavour to answer these questions an assessment of life was made at ARL. An immediate difficulty was the lack of data specifically applicable to the problem. The frequencies of gust loads were estimated, using data from V-g recorders functioning in DC-3 aircraft operating in Western Australia, supplemented by data on small gusts derived from the USA. No fatigue data of any sort were available for the material DTD363 of which the failed part was made, so data from the Boomerang and Mustang tests were used, after adjustment for the higher strength material using comparisons between riveted joint performances of high strength 75S alloy and lower strength 24ST alloy.

This life assessment revealed[33] that:

(*a*) An early failure would have been predicted (scatter range 3200 hours to 15,000 hours).

(*b*) The scatter in lives of identical structures (deduced from fixed amplitude laboratory tests) is greater than was generally realised. The service life figure must be chosen below the minimum calculated figure.

(*c*) The increase in permitted all-up weight from 8000 lb for the prototype to 8500 lb for production models would have had a negligible effect on life.

(*d*) If the part had been designed in 24ST to the same static design load factors, an increase in the life of from three to five times would have resulted, with a negligible weight penalty.

The analysis accented the need for additional research on properties of DTD363 alloy, if it was to continue to be used in aircraft construction, and for a rational service life test. A service life test for this wing was proposed, but not implemented. A type of fluctuating load test had been made by the manufacturer on a test wing, even though none was mandatory by the airworthiness authority. It was the Australian view that this test was too mild to be representative of the Australian operating conditions. It has subsequently appeared that the test specimen was a wing (and centre section) which had already been subjected to a static test to design ultimate load, and hindsight makes it clear that the test specimen's fatigue endurance would have been enhanced thereby, in a way which did not occur on aircraft for service.

This accident confirmed, if confirmations were necessary, the fears regarding the deterioration of safe operating lives of newer aircraft, and the Department of Civil Aviation decided to undertake a detailed fatigue analysis of every regular passenger transport aircraft type operating in Australia. An immediate action was to extend the flight load data collection programme to Dove, Bristol Freighter and Viscount aircraft and to prepare a generalised survey of materials fatigue data in preparation for the proposed analyses.

In November 1953 there occurred the crash of a Bristol Freighter aircraft of the RAAF, within sight of the Mallala aerodrome while undertaking "navigational training" duties, on the day prior to an air display there.

Analysis of the wreckage revealed that the structure, though not old in flying hours, had significant structural deterioration in the way of worked rivets, ill-fitting stressed-door bolts, and a small unrepaired fatigue crack, sufficient to reduce its strength significantly below design strength but not necessarily below limit strength, and it had failed in a high load and high speed manoeuvre.

The mid 1950s saw a growing interest in experiments on the accumulation of fatigue damage in irregular load sequences. Numerous ideas were current, including the inertia-loaded notched specimens to be carried in an aircraft, designed to fall off when the aircraft was about to become unsafe, or the specimen loaded by replay of a tape recording of the stress history recorded in flight. An ingenious testing technique of fatigue testing under random noise history was developed in 1955 by Head and Hooke.[34] A small notched specimen was loaded by amplified electronic random noise; an absolutely random process in which all of the statistical properties of the fluctuating wave form were completely specified by only three parameters, the mean

frequency, the r.m.s. value and the coefficient of damping. This technique has since been used and further developed in the UK, USA and Europe.

The year 1956 saw the International Conference on Fatigue of Metals, held in London and New York jointly by the Institution of Mechanical Engineers and the American Society of Mechanical Engineers. Australia was represented, in person, and by four papers, covering full scale testing, small specimen random noise testing, and effects of fretting in fatigue. At the same time a broad survey of the current state of the art of structural fatigue research, and of current problems in fatigue life estimation, was made.[38]

In 1957 there occurred in Brussels the Conference of the relatively young International Committee on Aeronautical Fatigue, with Australia participating as part of the British delegation. The possibility of Australia's membership was raised and subsequently effected, so that at the 1959 Conference in Amsterdam Australian membership was confirmed and papers on fatigue of wing structure by Payne[36] and on the safety of fail-safe wing structures by Ferrari, Milligan, Rice and Weston[37] were read.

3. THE SIXTIES

Early in 1960 the need for research in relation to civil aircraft problems became sufficiently acute, that the Department of Civil Aviation made arrangements with the Department of Supply to fund eleven additional research positions in the Structures and Materials Divisions, in order to apply greater effort upon basic and applied projects for DCA. The additional staff, some recruited from the UK, brought enhanced progress to a number of the studies of DCA interest, particularly in relation to the studies of operating loads on transport[35] and agricultural aircraft.[39]

Airworthiness investigations on the Dove aircraft had led to fatigue tests by the manufacturer of a pair of mainplanes which had been in service for about 16,000 hours in Western Australia. The manufacturer's test was carried out at constant amplitude, viz. at 1 $g \pm$ the load of a 12 fps. EAS. vertical gust, and it endured until a total equivalent lifetime of 57,350 hours. There was, however, considerable doubt in the Department of Civil Aviation and in the Aeronautical Research Laboratories concerning adequacy of single-load-level testing to represent a gust spectrum with ground to air cycles (when the only S-N data were results pooled from tests on other wings), and doubt also on the significance of the life of 57,350 equivalent hours of service and laboratory testing. It was therefore decided to carry out a laboratory test at ARL of a complete wing and carry-through structure under a five-load-level block programme sequence, in which one of the blocks was to represent the ground load effect. The wings had been modified in a highly loaded area near their root by the splicing-in of a length of steel spar boom in the lower part of the main spar, and the tests were intended to reveal the properties of the wing as a whole, the life of the modified boom and splice, and that of the tension boom of the carry-through structure. The tests continued for a period of nine years till the wings failed catastrophically at a life of 135,000 equivalent hours. To reach this lifetime the carry-through tension booms had to be replaced a number of times.

The tests showed firstly that the test endurance of wing carry-through tension booms of the original design (having a nominal stress of 12,000 p.s.i. per g) was very close to the mean service life of the boom causing the crash and of another found cracked in service. The dimensions of booms varied from 3% under to 11% above nominal area, and surprisingly, the test life of the smallest boom was the longest. A modified boom (having a nominal stress of 8200 p.s.i. per g) in the same material showed a fourfold increase in mean endurance, but a scatter range of 4½ to 1, thus confirming a conclusion concerning scatter.[33] Eventually these booms were made in steel.

The wings generally suffered some 60 cracks of varying severity in the skin and round cutouts: some were patched and some were untouched. An unanticipated catastrophic failure occurred at 70,000 hours in the spar some nine feet from the wing root, where the tension spar boom is spliced in manufacture, and the final collapse at 135,000 hours occurred at a fatigue crack just outboard of the splice of the modification steel insert into the wing.

The tests[40,41] were taken as confirming the validity of the laboratory representation of the Western Australian service spectrum, and also the merits of a multi-load-level programme as compared with a single-load-level programme test for getting realistic endurance data. They

showed also that a wing not designed as fail safe could suffer many nuisance and non-critical cracks, and that the repair of these will provide no safety against catastrophic collapse at some hidden area where cracking is out of reach of detection methods. The tests also conclusively demonstrated that for an aircraft of this type and in this material, a working stress of 12,000 p.s.i. per g was too high to permit a useful life.

Crack initiation and propagation in the carry-through structure was so variable in location and rate that, with inspection methods available then (and possibly now), it could not be treated as safe-by-inspection; both the wing carry-through structure and the wings themselves had to be treated as "safe life" and, with modifications designed by the manufacturers, reasonably economic safe lives were achieved.

During the next two years the subject of fatigue was to become a matter of major concern to the RAAF, first through the issuing in the UK of a safe life figure for Lincoln bombers, a figure which had already been exceeded by the Australian fleet of Lincolns, and secondly, by the adoption by the RAF and the RAAF of a new type of bombing manoeuvre for Canberras, called "Loft Bombing", which involved the aircraft in severe manoeuvre loads applied just before the bombs were released, 500 hours of which service was reputed to exhaust the available fatigue life of the aircraft.

The conclusion had long been held that life evaluations for specific aircraft could not be confidently based upon generalised loading action data. Accordingly, flight load investigations were set in hand, using unattended recording instruments, in Canberra, Sabre, Vampire, and Winjeel aircraft, while later, when Mirage aircraft were chosen as Australia's front-line aircraft, every aircraft of the fleet was fitted with a flight load recorder on delivery to the RAAF, as a precaution against the possible need for such data. Thus began a reverse defence technological spin-off; fifteen years of basic and applied research, triggered by a civil aviation need, suddenly found application in a defence area. Though these investigations carried the priorities accorded to the Services, nevertheless the needs of DCA were not entirely submerged, and similar studies were carried out on Douglas DC-6 and Viscount transport aircraft, and on Cessna, Beaver, Prospector and Cropmaster agricultural aircraft.

The grounding of the Lincoln fleet could not be countermanded. Studies by ARL of the Canberra problem of loft bombing,[42,43] revealed that, it being a long range aircraft, fuel was a large part of the disposable load, and the original flight fuel usage procedure was to use fuel from wing tanks first and fuselage tanks last. The proposal and adoption of a new procedure of using fuselage fuel first optimised the inertia relief from wing-carried fuel, and markedly reduced the manoeuvre stresses at fatigue critical regions. The fatigue damage analysis was developed into a simple formula so that the calculated consumption of available safe fatigue life could be updated regularly from operational and flight records. In consequence a fleet life-of-type of over 20 years was achieved with confidence throughout that the fatigue risk was negligibly low.

Attention was then directed, both in the UK and Australia, to fatigue of Vampire jet trainers. UK tests had revealed a most critical region in the lower part of the outer wing main spar at a point where, merely to provide attachment for a piece of wing skin, four screw holes were drilled into the spar boom. UK analyses prescribed a safe life of about 2000 hours, but the UK would not support the same life for Australian-built Vampires because of a difference in the diameter of these four screws, and evidence from a small specimen test series at the RAE, Farnborough, suggesting that screws as used in Australian aircraft were inferior in fatigue performance to those as used in the UK. A wing test programme was therefore commenced in Australia, using a loading spectrum identical with that used in the UK tests, to establish the life of the Australian-built wings. A suggestion had been made for "desensitising" the critical area by drilling out the screw holes and replacing them with cylindrical pinned Chobert rivets, and a number of wings were tested to evaluate this modification. The results of the tests[44] showed conclusively that the life of Australian-built wings was superior to that of UK-built wings, that the proposed modification was ineffectual, and that fatigue cracking in a number of other "nuisance" areas occurred. As the spar tension boom was the critical component, two tests were carried out on wings in which a cracked tension spar boom was extracted and a new boom riveted in its place. It was conclusively demonstrated that the life could be doubled by so doing. The Vampire wing has several stress-carrying doors covering openings through which wing fuel tanks are inserted. The tests also showed that fatigue life was enhanced by continuously maintaining a high standard

of tightness of the screws attaching these doors, but use could not be made of this result, as it was only learnt after service aircraft had operated for long periods with a lesser standard of tightness. Life evaluations for the Australian load spectrum based upon these tests, showed adequate life for the RAAF's purposes, and the expedient of replacing spar booms was not utilised.

During the early 1960s the RAAF also operated the Winjeel trainer, Sabre fighter, Hercules transport and Neptune maritime reconnaisance aircraft. None of these aircraft had been the subject of fatigue study in the design stage, though Sabre had subsequently been fatigue tested by the manufacturer to investigate whether it could be regarded as fail safe. Because of RAAF concern for the safety of all its aircraft, and because it was beyond the capacity of ARL to investigate them all at the same time, it was decided to engage the services of the aircraft industry initially in a training role under the supervision of ARL to investigate the life of each of these types. The plan would relieve ARL of engineering work load and would build up industry's expertise in the calculation phase and in the conduct of airworthiness tests leaving ARL freer to press ahead with more basic work and newer developments. The plan was put into effect with Commonwealth Aircraft Corporation co-operating most enthusiastically, and the scheme operated to mutual benefit. During this period was developed the idea of determining fatigue critical areas (sometimes known as "control points") from a survey of the regions of high nominal stress and an estimation of the local stress concentration factors. Study of the Winjeel aircraft, which had been designed by CAC, showed that in each of the fatigue critical areas except one, the structure was inspectable and had "fail-safe" properties, so that safety could be, and in fact was, achieved by inspection for cracks at regular intervals. The one non-fail-safe area was in a continuous chordwise bolt-angle joint, and an adequate safe life at this point was validated by a component test, under stress conditions very carefully established from comprehensive flight strain surveys.

Although it is true that military aircraft are employed for shorter lifetimes than civil aircraft, it may be taken as a tribute to the co-operation between the Laboratories and industry that there has never been a fatigue failure in service of any RAAF aircraft type validated in this way.

In September 1963 and again in July 1964, agricultural aviation was shocked by the crashes of two Beaver aircraft, all the more disturbing because safe life estimates had already been promulgated for this type,[46,47] and these had been based upon component fatigue tests by the manufacturer. At the request of DCA further more detailed flight tests were undertaken[48,49] to support a re-examination of the problem.[50] This work showed that although the pattern of operating agricultural aircraft was fairly standard, there was an extraordinarily large variability in the applied loads, as a result of variations in the severity of atmospheric turbulence conditions, and variations in the severity of manoeuvring loads imposed by different pilots: it also revealed that assembly alignment of the wing strut lug produced additional bending stresses not present in the component fatigue test, thus giving further support to the now universal practice of validating the safe life by a complete structural fatigue test. And when, soon after, a fatigue problem was suspected in Cessna aircraft, used in both military and civil roles, a full scale test was set in hand by ARL, using a test spectrum which was an agreed compromise between the military and civil conditions.

During this period concern grew in relation to the confidence which could be placed in fatigue life estimates. Confidence is the antithesis of variability, and an intensive study was made by Ford, Graff and Payne[51] and by Jost and Verinder[52] of statistical aspects of structural endurance, and by Patterson[53,54] of statistical aspects of applied loads. These studies were eventually to convince the authorities that assessment of fatigue risk is notional rather than precisely quantifiable: that estimates can only be estimates for the many based on tests on the few: that the absolute in safety does not exist; and that inspectability engenders more confidence than non-inspectability.

During this period also, materials fatigue testing was to investigate a number of relevant effects in aircraft alloy behaviour, including fretting,[55] vapour and grit blasting,[56] aged structure,[57] storage and cleaning and batch to batch variations. Particularly significant were tests on an aluminium alloy containing 0·3% silver, Australian invented and patented, with the aim of giving improved stress corrosion and fatigue properties. This alloy was later to be used in the Swedish SAAB Viggen fighter.

The materials fatigue laboratory being virtually the only competent fatigue testing laboratory in Australia also found time to perform fatigue tests for non-aeronautics customers, the Snowy Mountains Authority and others, on welded low alloy steel, on precipitation hardened stainless steel, on welded normalised Mn. Si steel, on high tensile notch tough steel, and so on.

The nature and characteristics of the turbulent atmosphere continued to be an unsolved problem, as it had been described by Wimperis in 1937 in recommending the establishment of aeronautical research in Australia: "There is necessary the acquirement of knowledge of such aspects of atmospheric structure as the size and intensity of vertical air currents, upward and downward. Vertical currents having estimated speeds of as much as 30 feet per second are not uncommon in Britain and America. Whether such conditions in Australia are more or less severe than this is unknown, and in view of the rapidity with which conditions alter in this country, it is possible that higher 'load factors' in construction may be found desirable." For fatigue analysis purposes the choice had been made to acquire load history data specific to any fleet of aircraft whose fatigue safety was in question. The data were used directly as an input to a life calculation or a laboratory test programme; they were, however, often expressed in terms of "effective gust velocity" by the use of a crude inverse transfer function. It was considered that, if the transfer function of an aircraft could be accurately known, then the characteristics of the atmosphere (the input) could be determined from a recorded response, and if the transfer functions of two aircraft were accurately known, the response of the second, when passing through a particular patch of turbulence could be calculated from the response data of the first.

Since the turbulent atmosphere is critical to the ultimate design strength of transport aircraft, and, with respect to all aircraft, to their controllability, especially when servo controls or active controls are used, and to their stability, as well as to their fatigue life in service, atmospheric turbulence deserved study in its own right.

Little real progress occurred until instrumentation was developed capable of recording a time history of the components of turbulent velocity along a line of flight, independently of the response behaviour of the aircraft carrying the measuring instrument (a gust probe). It was in 1963 that this significant step forward was made in the study of the atmospheric environment in Australia, through the implementation of a UK–Australian co-operative research programme to measure high altitude atmospheric turbulence over Australia. This programme was managed for Australia by Rider and for the UK by Anne Burns. The UK provided a Canberra measuring aircraft with gust probe, while Australia provided ground, meteorological and flight record analysis facilities. A significant number of mild to moderately severe turbulence events was encountered, located, explored and measured,[58,59] contributing very significantly to the rather meagre world knowledge, and providing data for analysis for a decade or more.

In 1966 ARL were invited to participate in the USAF programme "HICAT" which extended clear air turbulence measurements into the stratosphere wherein SST aircraft of the 1970s were expected to operate. A specially instrumented V-2 aircraft operated from Christchurch, NZ, during June 1966, and RAAF Base Laverton during July 1966. From data tapes for the Australian flights ARL made a detailed examination of stratospheric turbulence in the Australian region.[60] With Concorde flights into Australia now a reality, it is interesting to recall that the Hicat experiment recorded significantly higher frequency of CAT in Australia than any other region which was sampled.

By 1967 concern was being felt for the fatigue safety of the RAAF Mirage and it was apparent that gust loading, particularly on the fin, would have to be established for RAAF operations of this aircraft. Co-operative engineering by ARL, GAF and the Ordnance Factory, Maribyrnong led to the design and manufacture of a sophisticated gust probe capable of measuring the full vector gust velocity at speeds including supersonic flight.

During 1968–9, measurements of gust velocity and aircraft response were collected including three flights of severe low level turbulence in the vicinity of Richmond, New South Wales, on 11 September 1969. Analysis of the data [61,62,63,64] confirmed the existence of significant dynamic response to gusts of the Mirage IIIO.

These data were of particular value in deriving a test load spectrum when it later became necessary to undertake a fatigue test in Australia.

During 1967 Mann published a monograph on Fatigue of Materials for engineers[65] through Melbourne University Press.

The year 1967 was particularly significant for Australian fatigue research, for in that year the International Committee on Aeronautical Fatigue had chosen Australia as host country for its Conference and Symposium. A number of overseas papers was presented, some by their authors in person, and the meeting of overseas and Australian scientists proved stimulating to both. The Department of Supply sponsored the Symposium, to which the opening address was given by Mr. Wills, by then Chief Scientist of the Department of Defence. Proceedings of the Symposium were edited by Mann and Milligan.[66]

4. THE F-111 ERA AND LATER

Australia officially took delivery of the first of its order of 24 F-111 aircraft in Forth Worth on Wednesday 4 September 1968, but the delivery was halted when the news became public that eight days earlier the F-111 wing test article had failed almost at the commencement of its fatigue test programme. This event assumed greater public significance than any other fatigue failure in Australia's history. The RAAF immediately consulted the Aeronautical Research Laboratories for assistance in interpreting the significance of the failure, in interpreting the technical information as it became available from the USAF and the manufacturer, and in providing continued advice upon which the RAAF could make its decision that the remedies proposed or implemented by the manufacturer rendered the aircraft suitable for acceptance.

The swing wings of this aircraft were pivoted upon a centre section or "wing carry-through-box", shaped roughly like a large coffin with a bolted on lid with lugs at each end of the base and lid, and made of ultra-high-strength D6ac steel—the first-ever use of a monolithic ultra-high-strength steel structure of such size in aircraft. This first failure occurred in this box, in a region remote from welding, commencing at a taper-lock bolt hole. Metallurgical study showed the reamed surface to be different from others, and to incorporate a layer first described as "untempered martensite" and later described as "white etching constituent", and it was opined that it could have resulted from drilling the glass-hard steel, after heat-treatment, with a blunt drill. Subsequent experiments were never to demonstrate convincingly that the metallurgical structure could be duplicated by blunt drilling, nevertheless disassembly and reworking of all of the 270 bolt-holes in the 24 Australian aircraft and in all the USAF fleet was implemented. Substantiation of the specified life was never to depend upon one single test, and the next test specimen, denoted FW-1, although performing much better, did not achieve its test target life, nor did a third test specimen, denoted FW-2, from which it could only be concluded that the inadequacy was not merely metallurgical, but was an inadequacy in fatigue design capability, resulting from the dearth of prior experience in constructing, designing and operating with this material.

In order to analyse and find a solution to this problem the US Government set up an independent F-111 Scientific Advisory Board, under the chairmanship of Professor Holt Ashley, and comprising experts on all branches of fatigue from all over the USA and this Board continued to function until late 1971.

ARL's response to the RAAF's request for assistance was to make available scientists as thought necessary to visit Fort Worth where the aircraft were designed and being manufactured, to obtain at first hand information necessary in relation to determing F-111's fatigue performance in the Australian scene; to set up the ARL Scientific Advisory Panel, under the chairmanship of the Chief Superintendent, Dr. J. L. Farrands (now Chief Defence Scientist), to coordinate every facet of Australia's fatigue expertise and provide the best possible advice to the RAAF; and to second three ARL scientists to the Australian Scientific Advisory Team, led by Air Commodore D. R. Cuming, which, in June 1969 spent several months in the USA evaluating the aircraft with all of the data available, finally recommending to the Secretary, Department of Defence and the Chief of Air Staff, not to accept the aircraft until substantial redesign of the carry-through-box and further work on other parts were performed. In retrospect it is impossible to avoid the conviction that Australia's rejection of the aircraft convinced the USAF procurement agency that the aircraft as delivered by the manufacturer was not good enough for the USAF, and that no effort of scientific investigation or political persuasion should be spared to upgrade the aircraft to a level above USAF criticism and the more open criticism of Australian appraisal.

In this era there was a lack of knowledge of the fatigue performance of ultra-high-strength steels in aircraft primary structure, as there had been of the high strength aluminium alloy

DTD363 when the Dove accident had occurred eighteen years earlier. Most of what was known had been determined by the manufacturer in tests of large components which duplicated the rear lower edge of the wing carry-through-box. At Australia's request twelve additional of these large components were provided by the USAF to Australia to explore gaps in knowledge, particularly on the scatter of performance of this construction and on the performance under the projected Australian usage spectrum. Testing of these specimens required the design and construction by ARL of a 500,000 lb testing machine (which came to be known as the Humphries* rig), under high priority and in a very short time scale.

Australian tests revealed a new problem: very rapid fatigue crack propagation in some specimens. This was identified by scientists of ARL Materials Division to be due to corrosion effects of various fluids used during the manufacturing operations. When one of the matching halves of each suspectedly corrosion-affected specimen was returned to the manufacturer for analysis the ARL conclusions were eventually agreed.

Meanwhile, late in 1969 one aircraft crashed as a result of a pre-existing crack which had escaped production inspection - its location being in a wing pivot fitting of the same D6ac material. After much scientific thought on both sides of the Pacific, the solution eventually adopted to establish structural integrity, in the presence possibly of pre-existing cracks or of residual fluids with corrodent properties, was to proof load every aeroplane before delivery, or as soon as possible, for aircraft already delivered. The properties of steels are that their fracture toughness is lower at low temperature than at high temperature; and, as the aircraft operating envelope included flight at up to 55,000 ft, it was decided to adopt "cold proof testing" in a cold chamber at -40°C for all aircraft. The adoption of this procedure was vindicated by the fact that two from among the first 330 airframes failed on test. The test, in demonstrating some superabundance of strength for operation at ambient conditions, allowed for a limited amount of fatigue crack growth before strength would fall to the proof load value, and a routine of re-cold-proof-testing at recurring intervals was adopted to substantiate continued structural integrity.

During the two years of its existence before Australia accepted the aircraft the Scientific Advisory Panel examined every relevant aspect of the problem including scatter in fatigue of ultra-high-strength steels,[67,68] fatigue load monitoring in service,[69] surveys of fatigue information for ultra-high-strength steels [70] fracture mechanics and fatigue crack propagation,[71] comparisons between the US "Composite Mission Analysis" and RAAF proposed g spectra, and so on.

In the final outcome, the decision to accept was taken in December 1971, with 240 modifications to be incorporated before delivery, the major one being a teardown and replacement with new-design heavier wing carry-through-boxes.

During the F-111 investigation the research work of the Structures and Materials Divisions was surveyed, sharpened and redirected. The state of the art of fatigue life estimation was reviewed.[72] Structural reliability theory was further developed,[73,74,75,76] providing local estimates for permissible intervals between cold proof testing for Australia's F-111 fleet, and later, a basis for determining inspection intervals for Macchi centre sections,[77,78] now being operated on a "safe-by-inspection" basis. Fracture mechanics entered a new dimension, being related to fatigue crack propagation, expanding to address the phenomenon of fatigue crack retardation by high loads, using the technique of Wheeler's model.

By mid 1972 the fatigue spotlight turned to Mirage as the economic situation precluded their replacement, and several aircraft had reached their permissible safe life. The latter was based upon continuous load monitoring in flight, supported by shorter time flight strain tests, and on a simplified fatigue test carried out by the manufacturer some 15 years earlier. Because of the simplistic nature of that two-load-level programme test carried out upon the wing spar alone, a larger scatter factor had been applied than would have been applied to a more representative fatigue test result, and in the prospect of benefitting by a lower scatter factor, and in the sure knowledge that a more representative test would engender greater confidence, such a test was commissioned by the RAAF and undertaken by ARL with assistance from the industry. Flight load data were reviewed and the load sequence was made as representative as possible[80] and a computer controlled multi-jack test rig was built, to apply accurately controlled loads upon a single test wing.[82]

---

* Humphries was the General Dynamics engineer who conceived this test specimen.

The wing failed catastrophically and without warning after 35,000 simulated flights, at the same location as in the French test and at the same equivalent lifetime. The complete wing was not inferior in fatigue to the wing spar. The catastrophic failure, occurring in the wing spar, was shown by a technique of backward-looking fracture analysis[81] to have been present for more than half the lifetime. It was, however, preceded by a crack in the integral fuel-tank skin, commencing at about one quarter of the final life, though this crack did not significantly weaken the wing. Had the sequence been repeated in service leaking fuel would have given prior warning of fatigue. After collapse the wing spar was found to have eight other cracks in bolt holes, some as large as 5 mm long and 10 mm deep, and it may be concluded that, if no crack had initiated at the collapse location, collapse would have occurred at some other location soon thereafter. It was significant, however, that the wing did not crack in the lug at the root - the location calculated to be the most critical. The result gave confidence in the adoption of a lower scatter, and therefore an extended safe life. Close liaison is being maintained with Switzerland, where a complete airframe is to be fatigue tested, with a view to determining with greater confidence the safe life of other regions.

Within this period of intense activity upon the more specific problems of fatigue life assessment, much thought has also been given to the objectives, philosophies and procedures of fatigue testing.[72] The Commonwealth Advisory Aeronautical Research Council has requested members to compare their methods of deriving safe lives for airframes (and engines) with a view to standardisation of procedures, and as a follow up, the subject became a major topic for discussion at the Eighth Symposium of the International Committee on Aircraft Fatigue held in Lausanne, Switzerland, in 1975.[83] The last word on the subject has not yet been spoken, for the topic of Aircraft Life Estimation is the major topic for the Ninth Symposium of ICAF in Darmstadt in 1977. I do not doubt that Australia will have something to say.

REFERENCES

1. Osborne, C. J. — Examination of Failures in Stinson Model A Wing Structure. CSIR Div. of Aero. Rep. SM134, 1945.
2. Marmion, L., and Starkey, R. D. — Repeated Load Tests of Modified Typhoon Semi-span Tailplanes. RAE Tech. Note No. SME279, October 1944.
3. Bland, R. B., and Sandorff, P. E. — The Control of Life Expectancy in Aeroplane Structures. Aero. Engineering Review, Vol. 2, no. 3, p. 7, August 1943.
4. Johnstone, W. W. — Review of Current Methods for Strength Testing of Aircraft Wings. ACA Report 28, 1946.
5. Johnstone, W. W. — Repeated Load Tests on a Mosquito Wing. CSIR Div. of Aero. Rep. SM59, 1946.
6. Patterson, M. S., and Wills, H. A. — Strength of Machine Parts for Fluctuating Loads. CSIR Div. of Aero. Rep. SM82, 1947.
7. Wills, H. A. — A Method of Obtaining Fatigue Endurance Curves for any Load Range Ratio. CSIR Div. of Aero. Note S&M155, 1947.
8. Hooke, F. H., and Wills, H. A. — A Procedure for Calculation of the Endurance Strength of Aircraft Structures. CSIR Div. of Aero. Note SM152, 1947
9. Radok, J. R. M. — The Motion and Deformation of Aircraft in Atmospheric Disturbances. CSIR Div. of Aero. Rep. SM89, 1947; also Rep. SM101, 1947; Rep. SM105, 1947; Rep. SM133, 1949; and Rep. SM138, 1949.
10. Hooke, F. H. — The Influence of Aeroplane Characteristics on the Response to Gusts of Various Forms. CSIR Div. of Aero. Rep. SM144, 1949; also SM170, 1951; and Rep. ACA 54, 1954.
11. Hooke, F. H., and Ferstat, Q. — V-g Recorder Results from a DC-3 Aircraft Operating Between Perth and Darwin. CSIR Div. of Aero. Rep. SM135, 1949
12. Hooke, F. H. — Load Frequency Measurements on a Lincoln Aircraft. CSIR Div. of Aero. Note SM150, 1947.
13. Wills, H. A. — The Life of Aircraft Structures. Journal of I.E. Aust., Vol. 20, No. 10, October 1948.
14. Oakes, J. K., and Townshend, P. H. — Fluctuating Load Tests on Typhoon Tailplanes. RAE Report No. SME 3354, 1945.
15. Wills, H. A. — The Life of Aircraft Structures. Proc. Second International Aeronautical Conference, New York, 1949; Institute of the Aeronatucial Sciences Inc., p. 361.
16. Johnstone, W. W., and Payne, A. O. — Determination of Fatigue Characteristics of Mustang P51D Wings. ARL Rep. SM 207, January 1953.
17. Heywood, R. B. — The Effect of High Loads on Fatigue. IUTAM Colloquium on Fatigue, Stockholm, May 1955, ed. Waloddi Weibull and Folke K. G. Odqvist, Springer Verlag, p. 92.
18. Royal Aeronautical Society (now ESDU) — Endurance of Complete Wings and Tailplanes. Data Sheet on Fatigue E.02.01, Issue 2, June 1958.
19. Langford, P. S. — An Airworthiness Fatigue Requirement for Civil Aeroplane Wings. AARC 35, CAARC Rep. 290, September 1955.
20. Gassner, E. — Strength Investigations in Aircraft under Repeated Application of the Load. Luftwissen, Vol. 6, No. 2, February 1939; also RTP Trans. 1415 and NACA Tech. Memo 1087.

21. Woodgate, B. G. — Some Notes on a Proposed Airworthiness Requirement for Wing Structure Fatigue Life.
AARC 53 and CAARC Rep. CC323, October 1955.

22. Shaw, R. R. — The Level of Safety Achieved by Periodic Inspection for Fatigue Cracks.
J. Roy. Aero. Soc., Vol. 58, 720, 1954.

23. — Fatigue Characteristics of a Riveted 24ST Aluminium Wing.
Part I – "Testing techniques", J. L. Kepert and C. A. Patching, ARL Rep. SM246;
Part II – "Stress analysis", M. K. Rice, Rep. SM247;
Part III – "Experimental results", J. L. Kepert, C. A. Patching, J. G. Robertson, M. Rice;
Part IV – "Analysis of results", D. G. Ford and A. O. Payne, Rep. SM263;
Part V – "Discussion of results and conclusions", J. Kepert, C. A. Patching, D. G. Ford, W. W. Johnstone, A. O. Payne, M. Rice.
Rep. SM268, 1956–59.

24. Kepert, J. L. — Determination of Fatigue Prone Areas in Aircraft Wings Using a Progressive Repair Technique.
ARL Rep. 246, 1958.

25. Payne, A. O., and Squire, N. L. — The Failing Stress of Mustang Wings Weakened by Fatigue Cracks.
ARL Note 257, 1959.

26. Wood, W. A., and Head, A. K. — Some New Observations on the Mechanism of Fatigue of Metals.
ARL Rep. SM158, 1950.

27. Davies, R. B., and Mann, J. Y. — Structural Changes During Rotating Bending Cantilever Fatigue Tests on Annealed Copper.
ARL Rep. Met. 10, 1954.

28. Head, A. K. — Statistical Properties of Fatigue Data on 24ST Aluminium Alloy.
ARL Note SM180, 1950.

29. Head, A. K. — The Growth of Fatigue Cracks.
Phil. Mag., p. 925, 1953.

30. Mann, J. Y. — The Effect of Surface Finish on the Fatigue Resistance of 24ST Aluminium Alloy.
ARL Rep. SM147, 1950.

31. Mann, J. Y. — The Effects of Re-heat-treatment and Overheating on the Fatigue Properties of 24S Aluminium Alloy.
ARL Rep. SM185, 1957.

32. Finney, J. M. — The Effects of Pickling and Anodising on the Fatigue Properties of 2L40 and DTD683 Aluminium Alloys.
ARL Rep. SM255, 1957.

33. Hooke, F. H. — Preliminary Note on the Fatigue Life of an Aeroplane Constructed of High Strength Aluminium Alloy under Australian Operating Conditions.
ARL Tech. Memo SM27, 1952.

34. Head, A. K., and Hooke, F. H. — Random Noise Fatigue Testing.
International Conference on Fatigue of Metals, I. Mech. E. London, p. 301, 1956.

35. Hooke, F. H. — Operating Loads and Safe Life Evaluation of Aircraft.
J.I.E. Aust. 36, 1, 1964.

36. Payne, A. O. — The Determination of the Fatigue Resistance of Aircraft Wings by Full Scale Testing; Full Scale Fatigue Testing of Aircraft Structures. Proceedings of ICAF Symposium, Amsterdam 1959; Pergamon Press. p. 76, 1961.

37. Ferrari, R. M., Milligan, I. S., Rice, M. K., and Weston, M. R. — Some Considerations Relating to the Safety of Fail-Safe Wing Structure.
Ibid., Ref. 36, p. 413.

38. Hooke, F. H., and Langford, P. S. — Australian Work on Aircraft Fatigue and Life Evaluation. Aircraft Engineering, Vol. 28, No. 334, December 1956.

39. Foden, P. — Agricultural Aircraft: Typical Load Spectra and some Observations on Airworthiness. ICAF Conference, Melbourne, 1967.

40. Ellis, R. Graff, D. G., and Mitchell, B. J. — Dove Wing Fatigue Test. ARL Note SM408, 1974.

41. Ellis, R., and Graff, D. G. — Fatigue Testing of DH104 "Dove" Centre Section Tension Booms. ARL Note SM409, 1974.

42. Hooke, F. H., and Jost, G. S. — Formula for Assessment of Fatigue Life of Australian Canberra Aircraft. ARL Rep. SM285, 1961

43. Hoskin, B. C. — A Comparison of Two Investigations of Fatigue Life of Canberra Aircraft. ARL Rep. SM293, 1964.

44. Bruton, R. A., and Patching, C. A. — Fatigue Tests of Vampire Aircraft. Report in preparation.

45. Barnard, M. H., and Agar, E. — Safe Life Predictions for Vampire Wing Components. ARL Note SM389, 1964.

46. Jost, G. S., and Lacey, G. C. — Safe Life Estimates of the de Havilland Beaver Wing Structure. ARL SM TM98, 1960.

47. Bruce, G. P. — A Review of the Safe Life of the de Havilland Beaver Wing Strut Attachment. ARL SM. TM. 123, 1964.

48. Foden, P. — Flight Load Spectra for Beaver Aircraft on Agricultural Operations. ARL Note SM312, 1966.

49. Foden, P. — Agricultural Aircraft Typical Load Spectra and some Observations on Airworthiness. ARL Note SM317, 1968.

50. Foden, P. — Mean Life Estimates for Wing Strut of Beaver Aircraft in Asymmetrical Operation. ARL Note SM316, 1968.

51. Ford, D. G., Graff, D. G., and Payne, A. O. — Statistical Aspects of Fatigue Life Variation. ARL TM. SM105, 1961; Proceedings of ICAF Symposium, Paris 1961; Pergamon Press, p. 179, 1963

52. Jost, G. S., and Verinder, F. E. — A Survey of Fatigue Life Variability in Aluminium Alloy Aircraft Structures. ARL Rep. SM329, 1971.

53. Patterson, A. K. — Estimation of Response Parameters and Confidence Intervals in Flight Testing, with Application to Experiments on Beaver Aircraft. ARL Rep. SM309, 1965.

54. Patterson, A. K. — A Statistical Study of Flight Loads on a Cropmaster Agricultural Aircraft. ARL Rep. SM 320, 1966.

55. Mann, J. Y. — The influence of Fretting on the Fatigue Strength of Materials and Components. ARL Rep. SM296, 1964.

56. Douglas, R., and Simpson, R. — Fatigue Tests on Vapour Blasted and Grit Blasted 2L65 Alloy. ARL Note SM295, 1964.

57. Finney, J. M. — The Relationship Between Aged Structure and the Fatigue Behaviour of Aluminium Alloys. Part 1—ARL Rep. SM 324, 1969. Part 2—ARL Rep. SM325, 1969.

58.	Burns, Anne, and Rider, C. K.	Project Topcat: Power Spectral Measurements of Clear Air Turbulence Associated with Jet Streams. RAE TR 65210, September 1965.
59.	Rider, C. K.	Project Topcat: A Study of the Gust Velocity Power Spectra for Six Flights in Clear Air Turbulence. ARL Rep. SM317, August 1967.
60.	Rider, C. K., and Thomson, M. R.	Clear Air Turbulence in the Australian Stratosphere. ARL Note SM362, January 1971.
61.	Rider, C. K., Thomson, M. R., and Verinder, F. E.	Measurement of Extreme Mechanical Turbulence During Low Level Flights by Mirage A3-76. ARL Rep. SM333, May 1971.
62.	Rider, C. K., Sparrow, J. G., Thomson, M. R., and Verinder, F. E.	Variation in Wing Strains Measured During Three Low Level Flights by Mirage A3-76 in Severe Mechanical Turbulence. ARL Note SM401, December 1973.
63.	Rider, C. K., Sparrow, J. G., and Thomson, M. R.	Fin Strains in Mirage A3-76 During Flights in Severe Turbulence. ARL Note SM407, 1974.
64.	ARL	Annual Report, p. 16, 1967.
65.	Mann, J. Y.	Fatigue of Materials. MUP, 1967.
66.	Mann, J. Y., and Milligan, I. S.	Aircraft Fatigue: Design, Operation and Economic Aspects. Pergamon Press, 1972.
67.	Hoskin, B. C., and Ford, D. G.	Scatter Factor in Aircraft Fatigue Life Estimation. ARL Note 350, 1970.
68.	Scientific Advisory Panel	Interpretation of the Scatter Factor by ARL. ARL Note SM373, 1972.
69.	Patterson, A. K.	Fatigue Monitoring in the USA—A Report of Overseas Visit, January 1971. ARL Memo SM200, 1971.
70.	Simpson, R.	Fatigue of Ultra High Strength Steels – A Survey of the Literature. ARL Note 378, 1972.
71.	Hoskin, B. C.	Simple Theoretical Studies of Fatigue Crack Propagation Using a Fracture Mechanics Approach. ARL Note SM372, 1971.
72.	Hooke, F. H.	Fatigue Life of Safe-Life and Fail-Safe Structures—A State-of-the-Art Review. ARL Rep. SM334, 1971.
73.	Diamond, P., and Payne, A. O.	Reliability Analysis Applied to Structural Tests; Advanced Approaches to Fatigue Evaluation. ICAF, NASA SP309, p. 275, 1971.
74.	Hooke, F. H.	A Comparison of Reliability and Conventional Estimation of Safe Fatigue Life and Safe Inspection Intervals: Advanced Approaches to Fatigue Evaluation. ICAF, NASA SP309, p. 667, 1971.
75.	Payne, A. O.	A Reliability Approach to Fatigue of Structures. ASTM STP511, 1974.
76.	Hooke, F. H.	Probabilistic Design and Structural Fatigue. The Aeronautical Journal, p. 267, June 1975.
77.	Howard, P. J., and Woodbury, S. P.	Crack Propagation—Macchi Centre Section Lower Spar. ARL Rep. SM TM213, 1972.
78.	Diamond, P., and Grandage, J.	A Proposed Inspection Procedure for the Macchi Centre Section. ARL Note SM394, 1973.
79.	Mann, J. Y.	Fatigue Testing, Objectives, Philosophies and Procedures. ARL Rep. SM336, 1972.
80.	Howard, P. J.	Development of a Load Sequence for a Structural Fatigue Test. Symposium on Fatigue in Aircraft Structures, ARL, October 1976.

81. Goldsmith, N., and Anderson, B. E. — Unpublished note. ARL, 1975.
82. Howard, P. J., Patching, C. A., and Payne, A. O. — Life Estimation by Parametric Analysis. ICAF Symposium, Lausanne, Switzerland, 1975.
83. Hooke, F. H. — Search for Unified Methods of Fatigue Life Estimation. ICAF Symposium, Lausanne, Switzerland, 1975.

DISCUSSION

R. B. Douglas (Department of Transport)

I would like to comment on the historical aspects of Dr. Hooke's presentation. Firstly, in the RAAF Bristol Freighter accident, fatigue was on'y a relatively minor contributory factor, and the accident perhaps should not be classed as a fatigue accident.

Secondly, Dr. Hooke has made no direct mention, either in his written paper or in his presentation, of the most tragic and spectacular of all Australian fatigue accidents, Viscount aircraft VH-RMQ at Port Hedland in 1968. This accident had a significant effect on subsequent fatigue work, and on the attitude of the Australian operator and the (then) Department of Civil Aviation.

No mention has been made of the two Australian helicopter fatal fatigue accidents, nor of the two fatal accidents following propeller fatigue failures. Indeed, it is disappointing to note that the theme of this Symposium is limited mainly to structural fatigue of aeroplanes, heavily laced with Mirage and F-111; and that rotorcraft and accessories like power plants, propellers, and landing gears, have largely missed out.

Dr. F. H. Hooke

I think it appropriate to regard the RAAF Bristol Freighter accident as a fatigue accident, in view of the findings of the team which investigated it. The wing had failed in a primarily torsion mode, and the failure path proceeded right round the wing torsion box, starting from an unrepaired fatigue crack in the skin. The wing had other aspects of structural deterioration also. It will be appreciated that it is difficult to determine exactly the strength of such a cracked structure; nevertheless the investigators concluded that the strength had fallen to a value below ultimate design strength, but not below limit strength. In my opinion it would not have failed under the applied loads if the structure had been intact.

I agree with Mr. Douglas that mention should have been made of the Viscount aircraft VH-RMQ accident at Port Hedland in 1968. I do not know if it was more tragic or more spectacular than other fatigue catastrophes, but it proved to be most significant, in that it caused the then Department of Civil Aviation to ban further use of that type of aircraft in Australia—an action which I believe it had not taken before or since.

Limitations of space have prevented me from detailing failures of propellers, power plants, landing gears, etc., and although the Laboratories have been involved in accident investigations of helicopters, we have done no research on the subject, apart from what might be regarded as a mechanical engineering investigation on rotor gear boxes. I think Mr. Douglas is right, that there is probably a large amount of information on non-structural fatigue investigations, but these were beyond the scope of my paper.

FUNDAMENTALS

MECHANISMS OF FATIGUE AND FRACTURE

by

S. P. LYNCH

SUMMARY

This paper reviews mechanisms of fatigue and fracture with particular reference to the author's research at ARL. Overload fracture, liquid-metal embrittlement, stress-corrosion cracking, fatigue-crack initiation, fatigue-crack growth and corrosion-fatigue are discussed and related. Observations suggest that crack growth in many metallic materials generally occurs by plastic flow and that fracture characteristics are determined mainly by the distribution of slip around crack tips. This distribution governs ductile versus brittle behaviour and is influenced by microstructure, stress intensity, temperature and environment; the effects of environment are attributed mainly to chemisorption at crack tips and are discussed in some detail. Changes in microstructure induced by cyclic stress, and the association of such changes with initiation and growth of fatigue cracks, are also examined. Relationships between crack-growth rates and stress-intensity factors, and the application of mechanistic understanding are then briefly discussed.

1. INTRODUCTION

Design of components and predictions of crack-growth rates, even when based on linear-elastic fracture mechanics, have limited accuracy since the effects of

(*a*) plasticity,

(*b*) microstructure, and

(*c*) environment

on crack initiation and growth are not adequately taken into account. Useful predictions of crack-growth rates under complex conditions, however, should be possible by using fracture mechanics in conjunction with analyses of plastic strain around cracks on the basis of an understanding of mechanisms of fracture. The author's research at ARL has been mainly concerned with the mechanistic aspect, particularly with respect to fatigue and corrosion-fatigue, since these processes are involved in the majority of service failures.

Corrosion-fatigue obviously cannot be considered without understanding

(*a*) fatigue in inert environments, and

(*b*) stress-corrosion cracking (SCC).

Likewise, fatigue and SCC cannot be understood without considering critical (overload) and sub-critical crack growth under sustained stress in inert environments. A review of the mechanisms of all these processes, with particular reference to the author's own work is presented in this paper in the order indicated in Appendix I; particular attention is given to fracture surfaces since studies of fracture-surface topography (after fracture under controlled conditions) not only provide information regarding atomic mechanisms of fracture but also aid diagnosis of service failures. Some common fractographic characteristics, general fracture trends, and terms used in the present paper, are outlined in the Appendix. References 1–6 give comprehensive reviews of the various subjects.

2. OVERLOAD FRACTURE

2.1 General Considerations

In general terms, the reduction of elastic strain energy provides the driving force for crack growth. At the atomic level, fracture may occur by

(*a*) tensile separation of atoms at crack tips, or

(*b*) shear movement of atoms at crack tips.

Elastic strain energy may also be relaxed by plastic flow, producing blunting of (initially sharp) crack tips. These processes are discussed in more detail below; factors determining ductile versus brittle behaviour are then considered, followed by some examples from the author's studies on tensile fracture in Al-Zn-Mg alloys.

2.2 Crack Growth by Tensile Rupture of Interatomic Bonds

The work required to propagate cracks by tensile rupture of bonds (Fig. 1), with only elastic deformation around crack tips, is equal to the surface energy of the crack faces. (This energy balance leads to the well-known Griffith's criterion.) To allow for the plastic flow which may be associated with fracture by tensile rupture of bonds, a plastic-work term (corresponding to the extra energy required to move dislocations in the stress field of cracks) is added to the true surface energy.

Materials in which dislocation movement is extremely difficult, e.g. diamond at low temperatures, or materials with abnormally weak atomic bonding across some plane, e.g. mica, probably fracture by a bond-rupture process. Petch[7] and Beachem,[7a] however, suggest that true (absolute) brittleness is rarer than commonly supposed (a view shared by the present author and discussed further in connection with liquid-metal embrittlement and corrosion-fatigue), and that fracture in most materials occurs by plastic flow, i.e. shear movement of atoms.

2.3 Crack Growth by Shear Movement of Atoms

As summarised by Petch,[7] any injection of dislocations into, or emergence of dislocations (of opposite sign) from, the solid at the crack tip will extend the crack – although the details may be complex. Several workers[8,9] have proposed that crack growth may occur by alternate shear on slip planes intersecting crack tips (Fig. 2*a*) to produce "flat", cleavage-like fracture surfaces parallel to low-index crystallographic planes. For example, alternate shear on {111} slip planes in f.c.c. materials could produce {100} fracture surfaces; in b.c.c. materials, {100} fractures could occur by alternate shear on {112} or {110} planes and, in c.p.h. materials, alternate shear on pyramidal planes could produce fracture surfaces parallel to basal planes.

2.4 Blunting of Crack Tips

In many materials, crack-opening displacements (CODs) are accommodated by (plastic) blunting of crack tips as well as by crack growth. A dislocation/crack-tip interaction producing blunting is shown in Figure 2*b*. In specimens below general yield, extensive blunting requires large strains ahead of cracks; large strains in small volumes of material ahead of cracks generally require the operation of at least five independent slip systems (von Mises-Taylor criterion) and interpenetration of slip bands and cross-slip.[10]

The large plastic strains during blunting often result in separation of second-phase particle/matrix interfaces, or fracture of brittle particles ahead of cracks, so that voids (internal cracks) are produced. Further crack-opening causes further plastic flow in the crack-tip region with some crack advance and void growth; eventually, the ligament of material separating external cracks and voids necks down and voids link up with external cracks (Fig. 3). The term microvoid coalescence (MVC) is generally used for this mode of fracture and both fracture surfaces are covered by "dimples". MVC is a very common fracture mode and dimples have been observed after fracture by overload, SCC, and fatigue.

2.5 Ductile Versus Brittle Behaviour

It is commonly suggested that ductile versus brittle behaviour depends on the σ/τ ratio,[11] where σ is the tensile stress required to break atomic bonds at crack tips and τ is the shear stress required to move dislocations near crack tips (Fig. 3). Decreasing σ, or increasing τ, increases the tendency for (true) brittle fracture. This criterion, however, only differentiates the relative tendencies for fracture by tensile separation of atoms and fracture by shear movement of atoms. In many common materials, however, it is proposed that ductile *and* brittle crack growth occurs by plastic flow and that the balance between crack growth (by movement of dislocations on slip planes intersecting crack tips) and crack-tip blunting (general dislocation movement around cracks) provides a better explanation for ductile versus brittle behaviour. Thus, the greater predominance of slip on planes intersecting crack tips over general slip favours brittle behaviour (Fig. 4). Expressed in a different way, ductile-brittle behaviour depends on τ_s and ϵ_g, where τ_s is the stress required to produce rapid crack growth by extensive nucleation (and/or egress) of dislocations at crack tips and ϵ_g is the general strain in an element of material ahead of cracks at a stress of τ_s; ϵ_g will depend on the number of slip systems operating and the ease of slip on each system, and on the ease of cross-slip and interpenetration of dislocations in this element (Fig. 4).

According to a criterion based on ϵ_g, if the stress required for dislocation nucleation/egress at crack tips (τ_s) was decreased without affecting the stress required for general slip, then crack growth would occur at lower stresses and less general slip would be activated, i.e. ϵ_g would decrease and fractures would be associated with reduced ductility. (This situation is applicable to LME and is discussed in detail later.) Likewise, if τ_s was increased without changing the stress required for general dislocation activity, then ϵ_g would also increase. Generally, however, factors which restrict dislocation activity (e.g. precipitation hardening) will increase both τ_s and the stress required for general slip; moreover, slip flexibility is probably hindered to a greater extent than dislocation nucleation/egress at crack tips, so that hardening processes decrease ϵ_g. This is consistent with the observation that higher strength materials usually have lower fracture strains. The transition from ductile to brittle fracture in b.c.c. and c.p.h. materials, with decreasing temperature, could be explained along the above lines, since the number of slip systems operating and slip flexibility (and, hence, ϵ_g) decrease with decreasing temperature.

2.6 Tensile Fracture of Al-Zn-Mg

High purity Al-Zn-Mg alloys (on which the commercial 7000 series is based) have been extensively studied since they are the strongest of the aluminium alloys and their high strength-to-weight ratio makes them attractive for aircraft applications. These alloys have low fracture toughness, and poor fatigue and stress-corrosion characteristics and, hence, studies have aimed at understanding and improving these characteristics. Their high strengths are achieved by precipitation-hardening (solution treatment at ~450°C, then quench to 0–100°C and age at 100–180°C) and the resulting microstructures are characterized by fine dispersions of small precipitates ($MgZn_2$) in grain interiors, coarser dispersions of larger precipitates along grain boundaries, and precipitate-free zones (PFZs) adjacent to grain boundaries (Fig. 5 inset).

Tensile fractures of high-strength Al-Zn-Mg alloys (both high purity and commercial) are intercrystalline and the microstructure of grain-boundary regions predominantly controls the initiation and growth of cracks.[12] Since deformation of very thin soft layers is normally constrained by surrounding harder regions, yielding of precipitation-hardened grains usually occurs, then slip concentrates in PFZs. (PFZs behave differently during fatigue (discussed later).) The mechanism of tensile fracture involves preferential plastic deformation in "soft" PFZs, nucleation of voids by separation of grain-boundary particle/matrix interfaces, and growth to coalescence of voids resulting in dimpled fracture surfaces (Fig. 5). Fracture toughness is usually low because the blunting accompanying crack growth is limited by the narrow PFZs and large number of grain-boundary precipitates. Toughness, crack-blunting and the size and depth of voids observed after fracture all decrease with

(*a*) increasing area fraction of grain-boundary precipitates, and

(*b*) decreasing PFZ width, if the area fractions of precipitates are small,

as illustrated in Figure 6.

Fracture surfaces of specimens with very narrow PFZs and/or large densities of grain-boundary precipitates (very low fracture toughness) appear to be flat and dimples are not observed in many areas (Fig. 5). However, since extremely small dimples (near the limit of resolution of replicas) are observed in some areas, it seems quite probable that even smaller dimples (below the limit of resolution of replica techniques) are present on apparently flat surfaces. Alternatively, flat fractures would result if crack growth occurred by shear at crack tips with insufficient strain ahead of cracks to nucleate voids. (It is less likely that flat intercrystalline fractures are produced by "tensile separation of atoms" at crack tips, since it is known that grain boundaries can act as dislocation sources and there are "soft" PFZs adjacent to boundaries.)

The behaviour of narrow (~0·1 μm) PFZs in the Al-Zn-Mg during tensile and fatigue stressing (the latter is discussed later) was simulated on a larger scale by "model" specimens—the larger scale facilitating observation of the deformation and fracture processes. Model specimens consisted of a soft layer (e.g. of lead or tin), some hundreds of micrometers thick, sandwiched between (and bonded to) harder regions (e.g. of Pb-Sn-Sb alloy) (Fig. 7). Tensile fracture of model specimens (as with Al-Zn-Mg specimens) involved deformation concentrated in soft layers resulting in MVC. Fracture-surface dimples in model specimens were about 3–4 orders of magnitude larger and deeper than those produced after fracture of Al-Zn-Mg (Fig. 8). Fracture by MVC occurs in a wide variety of materials and circumstances, probably because the process is able to operate over such widely different microstructural scales.

3. SUB-CRITICAL CRACK GROWTH UNDER SUSTAINED STRESS

3.1 Inert Environments

Sub-critical crack growth under sustained stress in inert environments generally does not occur in engineering/aircraft materials at ambient temperatures. At higher temperatures (normally >0·5 melting point), thermally activated (creep) processes, such as diffusion, dislocation cross-slip, climb, grain-boundary sliding, may result in crack growth. In high purity Al-Zn-Mg alloys, however, slow crack growth (10^{-7} m/sec) associated with creep does occur at room temperature;[13] at higher temperatures (~160°C), crack-growth rates in dry air or paraffin oil are quite rapid (~10^{-5} m/sec) at high stress intensities and crack growth occurs by MVC probably as a result of thermally-activated dislocation glide.

3.2 Aggressive Environments (SCC, LME)

3.2.1 General Comments

Many mechanisms have been proposed for SCC,[2] but there is no general agreement that any of the proposed mechanisms is valid for any particular system. This situation has arisen largely because of the variety and complexity of reactions that can occur between material and environment. SCC theories fall into four main classes (Fig. 9) based on

(*a*) dissolution (e.g. of anodic precipitates),

(*b*) (oxide) film formation followed by fracture of the films,

(*c*) diffusion of embrittling species (such as hydrogen) ahead of cracks, and

(*d*) embrittlement due to chemisorption at crack tips.

(The theories have also been applied to corrosion-fatigue.)

All the above theories and combinations of them have been proposed to explain SCC in aluminium alloys. In recent work,[14,15] the author has attempted to resolve some of the controversies regarding mechanisms of SCC and corrosion-fatigue. Studies have been undertaken of sub-critical crack growth under sustained and cyclic loads in Al-Zn-Mg alloys in various environments, viz. liquid metals, aqueous solutions and water-vapour/air. Liquid-metal environments were studied since, in the cases selected, the environment-metal reaction could only involve chemisorption of liquid-metal atoms at crack tips. Thus, an indication of the relevance of chemisorption (compared to other processes) to SCC and corrosion-fatigue should be obtained. Liquid-metal embrittlement (LME) is also of practical importance in some circumstances, e.g. transport of cadmium from surface plating to tips of cracks in steel can enhance crack growth; this effect can occur below the melting point of cadmium due to surface diffusion.

3.2.2 Liquid-Metal Embrittlement

The very rapid crack growth and the negligible mutual solubilities of solid and liquid metals in many systems indicate that neither diffusion of liquid-metal atoms into solids nor dissolution of the solid metal is necessary for the growth of cracks. In the past, it has been assumed[3] that chemisorption of liquid-metal atoms lowers the tensile strength, σ, of atomic bonds at crack tips without significantly affecting the shear stress, τ, required to move dislocations, so that crack growth then occurs by repeated adsorption and breaking of bonds at low applied stress. Fracture surfaces produced by such a "bond-rupture" process would be flat and little deformation would be associated with fracture. It is implicit that, if some dislocations do move in the stress fields of such cracks, they generally do not intersect crack tips or cause blunting.

In recent studies[14,15] of LME, slip densities and distributions indicated that dislocations did intersect crack tips. Moreover, dimpled fracture surfaces, observed after LME, indicated that microvoids nucleated and grew ahead of cracks and, hence, that some blunting did occur at crack tips. Some examples are

(*a*) LME of Al-Zn-Mg alloys resulted in dimpled fracture surfaces; however, compared to overload fracture the dimples were smaller, shallower, and more elongated, and deformation in grains was not as extensive (Fig. 10).

(*b*) In the Sn/Pb-Sn-Sb "model" specimens (described earlier), where crack growth in air produced very large, deep dimples, fracture in liquid gallium resulted in very shallow dimples on intercrystalline facets (Fig. 11).

(*c*) Fracture of polycrystalline cadmium in liquid gallium occurred with near-zero reduction of area, while specimens tested (in tension) in air elongated considerably and necked down to a chisel edge (RA $\sim 100\%$) (Fig. 12). LME fractures showed cleavage-like and brittle intercrystalline facets (Figs. 13, 14) which were covered by shallow, elongated dimples (revealed by examination at high magnifications) (Fig. 15).

Thus, it is concluded that, although LME is associated with considerably less plastic deformation (and much less crack-tip blunting) than fracture in air, crack growth in liquid-metal environments occurs by plastic flow (shear movement of atoms) rather than by tensile separation of atoms at crack tips.

LME could be explained on the basis that chemisorption of liquid-metal atoms facilitates nucleation and movement of dislocations on slip planes intersecting crack tips. There is evidence[16] that, since atoms at surfaces (in vacuum) have fewer neighbours than atoms in the interior, the lattice-spacings in the first few atomic layers differ from those in the interior (Fig. 16). It has been suggested[17] that such "surface-lattice distortion" should hinder the nucleation

and egress of dislocations at surfaces. Since chemisorption of environmental species at surfaces should reduce this "surface-lattice distortion"[18] (Fig. 16), nucleation and egress of dislocations at surfaces (crack tips) could be facilitated by adsorption.

Adsorption-activated dislocation nucleation/movement on slip planes intersecting crack tips would produce sub-critical crack growth (by shear) and would also result in fractures with reduced ductility (less crack-tip blunting).* As discussed earlier, the balance between crack growth and crack-tip blunting should be determined by the relative proportions of slip on planes intersecting crack tips compared to "general" slip ahead of cracks. Chemisorption can promote the former (r_i decreased) but cannot affect the stress required for general dislocation movement ahead of cracks.† Thus, crack growth can occur at lower stresses and dislocations ahead of cracks are then not activated to the same extent (ϵ_p decreased) in liquid-metal environments.

3.2.3 Environmental Factors

The degree of embrittlement of solid metals by liquid metals varies widely and depends on the metals involved, their composition, the microstructure of the solid, and temperature. On the basis of the mechanism of LME outlined above, larger reductions in "surface-lattice distortion" by adsorbed species should produce greater embrittlement. Increased coverage of the surface by chemisorbed atoms‡ should also increase embrittlement since longer (surface) dislocation sources, which probably require lower activation stresses, may then be nucleated. Thus, embrittlement should be promoted by high affinities of adsorbates for metals, accompanied by high activation energies for any reaction - the latter determines the relative life of adsorbates on metal surfaces before chemical reactions (dissolution, compound formation) occur. This prediction is consistent with the general trends (from limited data) noted[3] for embrittlement couples; embrittlement is unlikely if the two metals involved readily form high-melting-point compounds or show significant mutual solubility, and large interaction energies betweeen solid and liquid are conducive to embrittlement.[19]

There is no apparent reason why chemisorption of species other than metal atoms should not cause some embrittlement, although metal-metal interactions are likely to be much stronger than metal/non-metal interactions. Evidence (discussed below) supports this contention and suggests that adsorption-activated dislocation movement is probably the most important factor in hydrogen embrittlement (HE), SCC and corrosion-fatigue.

3.2.4 Hydrogen-Embrittlement and Stress-Corrosion Cracking

The hydrogen (gas)–iron (solid) couple satisfies most criteria suggested as prerequisites for LME and hydrogen–metal bonding is essentially metallic. The mechanism proposed above for LME could therefore be applicable to HE, although HE is more complex than LME since hydrogen can readily diffuse into materials. This proposal is consistent with many characteristics of HE and, in particular, with observations of iron surfaces in the presence of hydrogen using field-ion microscopy; this work[20] suggests that nucleation of dislocations is catalysed by adsorption of hydrogen.

Analogies between SCC and LME[21] suggest that similar mechanisms are involved in both effects, e.g. cleavage-like fractures are observed for aluminium single crystals and polycrystalline cadmium (Figs. 13, 14)[14] in liquid metals, austenitic stainless steels in boiling $MgCl_2$, titanium alloys in methanol and others.[2] Thus, a mechanism of adsorption-induced alternate shear, producing cleavage-like fracture surfaces, could be applicable to many cases of SCC. Previous objections[2] to an "adsorption-induced-cleavage" mechanism of SCC were mainly based on the unlikely operation of a "bond-rupture" process during SCC. (It was assumed that cleavage occurred by "bond-rupture".)

The case for a common mechanism for LME and SCC, in Al-Zn-Mg for example, is supported by the following observations. Immersion of pre-cracked and loaded (to near K_c) DCB specimens (of a particular heat treatment) in aqueous KI solution resulted in an increment of

* An effect of adsorption on flow behaviour of uncracked specimens, with small surface-to-volume ratios, would not be expected and is not observed.

† The high density of conduction electrons in metals screens out effects of chemisorption within a few atomic distances of the surface; non-metals behave differently.

‡ Preferential chemisorption along grain-boundary/surface intersections would favour intercrystalline fracture.

very rapid sub-critical crack growth within 1 sec. of immersion. Such rapid rates (~ 10 mm/sec) of cracking in aqueous solutions (as in LME) strongly suggest that adsorption is responsible; other proposed mechanisms of SCC involving dissolution, diffusion of hydrogen ahead of cracks, oxide film formation/fracture, are unlikely to have time to occur. In addition, fracture-surface appearance of LME and SCC fractures and the extent of deformation accompanying crack growth are similar; for example, sub-critical crack growth of Al-Zn-Mg (for particular heat treatments) in liquid-metals, aqueous solutions and water vapour/air produces dimpled fracture surfaces (Figs. 10, 17, 18) with dimples becoming smaller and shallower with decreasing stress intensity. Dislocation nucleation/movement, activated by adsorbed water molecules, would explain these observations of SCC; other explanations are less probable. (In the case of SCC in water-vapour/air (20% RH), dissolution cannot be involved since there is no liquid electrolyte at crack tips at this humidity. Hydrogen gas has no significant effect on (fatigue) crack growth in aluminium alloys and "hydrogen-embrittlement" explanations for SCC in aluminium alloys do not seem likely. Results cited in favour of hydrogen-embrittlement of aluminium alloys can be explained in other ways. For example, reduced ductility of aluminium alloys due to pre-exposure to water-vapour/air during aging, suggested by some workers[22] to be associated with diffusion of hydrogen into specimens, is probably the result of intercrystalline pitting.[15])

In some instances, other mechanisms of SCC could occur in conjunction with, and contribute to, crack growth by adsorption-induced slip. In fact, dissolution processes probably predominate during initiation of SCC and during crack growth at low stress intensities, especially in "corrosive" environments. SCC by adsorption-activated plastic flow at crack tips is consistent with the general trend that alloys of higher fracture toughness are more resistant to SCC. Effects of microstructure and environment on sub-critical crack growth can generally be understood (qualitatively) in terms of the balance between crack-tip blunting and crack growth discussed for overload fracture (2.5). A more quantitative analysis would require a more detailed understanding of adsorption and its effects on τ_d.

4. FATIGUE—SUB-CRITICAL CRACK GROWTH UNDER CYCLIC STRESS

For convenience, the process of fatigue is generally sub-divided into various stages viz. crack initiation, stage I crack growth and stage II crack growth; the last can also be sub-divided according to stress-intensity regimes (Figs. 19*a*, *b*).

4.1 Initiation of Fatigue Cracks

The initiation of fatigue cracks in a wide variety of materials is associated with the intrusion/extrusion phenomena, whose main features are summarized in Figure 20.[23] Extrusions and intrusions generally occur along slip bands and grain boundaries (Figs. 21, 22) and are asociated with localized fatigue-induced, or pre-existing, soft layers ($\sim 0{\cdot}1$ μm thick). In Al-Zn-Mg alloys, intrusion/extrusion occurs at PFZs adjacent to grain boundaries (Fig. 23) and at transcrystalline slip bands in which re-solution of age-hardening precipitates has occured.* In single-phase materials, fatigue can produce local softening along slip bands by recrystallisation or possibly by formation of very fine sub-grain structures.

Numerous mechanisms proposed for intrusion/extrusion (reviewed in Reference 4) gave no consideration to the associated microstructural changes and were generally unsatisfactory. Improved understanding of fatigue crack initiation has been gained by comparing[23] the behaviour of model specimens (soft layers ~ 100 μm thick sandwiched between harder regions (Figs. 25, 7)) with those of soft PFZs and slip bands in Al-Zn-Mg. Deformation of model specimens in compression (and under cyclic compressive loads) results in extrusions of thin ribbons of soft material (Figs. 26, 27). Similarities between model extrusions and fatigue extrusions were

(i) the extrusions sometimes "curled over",

(ii) the extrusions were tapered,

* There has been some controversy whether precipitate-free slip bands in aluminium alloys are induced by fatigue or are formed prior to fatigue by the quenching and aging processes. However, it was shown[24] that fatigue initially produces narrow discrete bands of high dislocation density in "quench-bands" which usually contain only a slightly lower-than-normal density of precipitates. Re-solution of precipitates then occurs within these bands, probably by a dislocation-enhanced diffusion process; dislocations then re-arrange into a fine sub-grain structure within the precipitate-free bands.

(iii) the harder material adjacent to the extrusions deformed similarly,
(iv) extrusion markings (parallel to the extrusion direction) were found on the surfaces of both types of extrusions, and
(v) striations occurred on the surfaces of extrusions at right-angles to the extrusion marks (in model specimens, these were found only after *repeated* compressive loading).

Tensile tests on model specimens showed that soft zones were "sucked-in", thereby producing intrusions (Fig. 28). Thus, it was concluded that the model specimens successfully simulated the behaviour of very thin soft layers in "real specimens". Experimental observation of deformation occurring during intrusion/extrusion in model specimens demonstrated that intrusion/extrusion involved preferential plastic deformation within soft layers and relative displacement of hard and soft regions by shear close to their interfaces; this pattern of deformation is predicted by slip-line-field theory. Hence, it is reasonable to assume that similar deformation occurs in PFZs during fatigue-crack initiation (intrusion).

Some apparent discrepancies were found between the behaviour of model specimens (which was generally consistent with the predictions of macroplasticity theory) and the behaviour of PFZs in Al-Zn-Mg. In particular, intrusion/extrusion at pre-existing PFZs at grain boundaries occurred at much lower stresses than predicted, but not until after a considerable number of stress cycles; intrusions/extrusions then occurred only along short lengths of PFZs and extrusions were much longer than predicted. Experimental observations showed that intrusion/extrusion formation corresponded to the production of sub-grains within PFZs. It is concluded that, although deformation of very thin soft layers surrounded by harder material is normally highly constrained, the fine sub-grain structures formed in soft layers during fatigue permits their extensive deformation at relatively low stresses. The precise role of sub-grains in relaxing the constraint is not clear, although the presence of sub-grain boundaries at the interfaces of the hard and soft regions, where intense shear occurs, is probably significant.

Since intrusions are the precursors of stage I fatigue cracks, the process of crack initiation under cyclic stress can be summarized thus:

(i) cyclic stressing produces localised microstructural changes and the formation of thin soft layers sandwiched between harder regions (although soft layers may already be present in some materials),
(ii) fine sub-grain structures form in soft layers and enable intrusion (crack initiation) to occur during (local) tensile half-cycles,
(iii) formation of slip steps (or oxide films) on intrusion surfaces or other factors prevent reversal of interfacial shear associated with intrusion during unloading and/or reversal of stress.

4.2 Fatigue-Crack Growth

Stage I crack growth occurs by the progressive development and linking-up of intrusions along slip bands (Fig. 24 inset). Sub-grain formation often occurs initially along short lengths of slip bands/PFZs, resulting in intrusion "tunnels" or "holes"; subsequent sub-grain formation between tunnels enables their linking-up by intrusion. Similarities between intrusion/extrusion, stage I and stage II crack growth, viz.

(i) the association of each with soft slip bands, PFZs and sub-grain structures,
(ii) the similar crack morphologies, i.e. tunnels at surfaces or crack tips extending into slip bands/PFZs,
(iii) the similar striations on intrusion/extrusion surfaces and stage I and stage II fracture surfaces,

all suggest that stage II crack growth can also occur by an intrusion process, illustrated in Figure 29. The change from stage I to stage II crack growth probably occurs when the stress intensity (and amount of slip) at crack tips increases sufficiently to produce soft slip bands on several planes in the plastic zone ahead of cracks. Crack growth then occurs on those soft slip bands/PFZs for which the resolved normal stress is most favourable.

After a crack growth increment by intrusion, compressive deformation does not reverse the process but brings the opposite crack faces closer together and deforms the fracture surfaces immediately behind the crack tip (Fig. 30); the next tensile half-cycle re-opens the crack and produces another increment of crack growth. This loading–unloading sequence may produce striations with a roughly saw-tooth profile with peak matching peak on opposite fracture surfaces, as is often observed (Fig. 31).

At low stress intensities, striation spacings are often larger than expected from crack-growth rates measured by other methods, and average crack-growth rates may be less than atomic spacings; these observations suggest that crack growth does not occur along all the crack front on every stress cycle. Crack growth probably does not always occur because, on some cycles, there is no soft band/sub-grain structure ahead of cracks (cf. crack initiation). In the absence of soft bands ahead of cracks, crack-opening displacements could be accommodated by plastic blunting without significant crack growth (Fig. 32); the tensile strain ahead of cracks is then reversed during the compressive half-cycle. The cyclic deformation ahead of cracks, which is associated with their opening and closing, may produce soft layers and sub-grain structures, such that crack growth can proceed by intrusion.

In many instances, fatigue-crack growth may occur in the absence of soft layers ahead of cracks by the process of alternate shear (or alternate shear plus blunting) described earlier. Several workers[9,25,26] have proposed mechanisms of fatigue-crack growth based on this process. Factors such as microstructure, stress intensity, and environment, probably determine if crack growth occurs by alternate shear or by intrusion of soft layers. Intrusion is probably most common at low stress intensities (and, therefore, during initiation and stage I crack growth), in inert environments, and in ductile materials. At high stress intensities, CODs are often accommodated by crack growth (alternate shear), crack-tip blunting and formation of microvoids ahead of cracks; dimples and striations, or just dimples, are then observed. Fatigue-crack growth by alternate shear (in "aggressive" environments) is discussed further in 4.3.2. Regardless of the precise mechanism, fatigue occurs because CODs are accommodated by crack growth, while crack-closing displacements are accommodated by deformation of the fracture surface immediately behind the crack tip, i.e. the forward slip processes are not reversed when the stress is reversed.

4.3 Effect of Environment on Fatigue

4.3.1 Crack Initiation

Surface-pitting produced by corrosion can sometimes facilitate crack initiation. For example, prior corrosion of Al-Zn-Mg alloys, producing intercrystalline pitting (probably involving dissolution of anodic grain-boundary precipitates), reduces the number of cycles required for fatigue-crack initiation.[27] (Heat-treatment of pre-corroded specimens before fatigue-testing improves their fatigue life, probably because grain-boundary migration/grain growth occurs; corrosion pits are then not always located at grain boundary-PFZs and hence are not as effective.[27]) Crack initiation also occurs in fewer cycles when specimens are fatigued in aggressive environments (compared to inert environments); this probably results from the effects both of pitting and adsorption on the activation of surface sources of slip (described earlier).

In some cases, oxide films formed on surfaces by environmental reactions can increase resistance to fatigue-crack initiation by suppressing sub-surface plasticity and formation of slip bands.[28]

4.3.2 Crack Growth

In many materials, fatigue in aqueous environments generally results in quite large increases in crack-growth rates, compared to those in air, and in fracture surfaces characterised by "brittle" striations; "ductile" striations are generally produced in air. "Brittle" striations, often on {100} facets, are particularly favoured by low cyclic frequencies and applied anodic potentials,[29] and can be suppressed by cathodic potentials[29] and/or addition of inhibitors to aqueous solutions.[30] Both "ductile" and "brittle" striations are often observed on fracture surfaces (Figs. 33, 34), probably because of local variations in microstructure and/or potential along the crack front; brittle striations (Fig. 33) are probably associated with locally anodic regions, possibly arising at positions where the crack front intersects voids nucleated ahead of cracks.

Fatigue of pure aluminium single-crystals in liquid-metal environments[27] produced "brittle" striations, and increased rates of crack-growth, compared to "ductile" striations in air. Observations on the polished sides of specimens revealed the deformation associated with crack-opening (Fig. 35) and crack-closing (Fig. 36) displacements. (In these specimens, crack fronts were fairly straight and fracture surfaces appeared the same at the edges of specimens as at the centre; hence slip at the surface is probably reasonably representative of the deformation occurring in the centre of specimens.) These results indicated that crack growth occurred by alternate

shear *at* crack tips and that crack closure occurred by slip *behind* the crack tip. In these tests, crack-growth increments were about three times the crack-tip opening displacements. (After removing liquid metal from the crack, CODs in air were accommodated by blunting at the crack tip (Fig. 32).) The mechanism of crack growth and formation of "brittle" striations, based on these observations, is illustrated in Figure 37 and is similar to mechanisms proposed by Schijve[31] and Neumann.[26]

The change from "ductile" to "brittle" striations and the increased crack-growth rates produced by "aggressive" environments are consistent with the general criterion for ductile versus brittle behaviour described earlier, viz. that chemisorption of certain species facilitates dislocation nucleation/movement on slip planes intersecting crack tips and favours crack growth rather than crack-tip blunting. Such an effect may change the mechanism of fatigue-crack growth from "intrusion of soft layers" to "alternate shear"; if crack growth in inert environments occurs by alternate shear, then chemisorption may simply reduce the amount of blunting associated with crack growth by alternate shear.

Oxide films can influence fatigue-crack growth through their effect[28] on dislocation movement near surfaces at crack tips. Moreover, well-defined "ductile" striations, observed after fatigue in air, are not commonly observed after fatigue in vacuum,[32] probably because compressive deformation in vacuum produces slip over all the fracture surface formed during the tensile loading, due to the easier egress of dislocations in the absence of an oxide film (Fig. 30*b*).

In most common environments and at cyclic frequencies normally encountered, there is probably insufficient time for dissolution processes to contribute significantly to crack growth. In aluminium alloys, diffusion of hydrogen ahead of crack tips does not seem to be involved in corrosion-fatigue, since abrupt changes in electrochemical potentials result in sharp changes in crack-growth rates and fracture-surface appearance;[29] results generally suggest that adsorption characteristics are the most important feature of environments.

Inert environments usually result in slower crack-growth rates than in air. Thus, for Al-Zn-Mg, crack-growth rates in stage II (in fluctuating tension) are slower in inert liquids (dodecanol, silicone oil) than in air.[33] In stage I (in reversed torsion), however, crack-growth rates in inert liquids were much faster than in air. This difference in the influence of environment could arise because, in stage I, crack-opening and shearing displacements are restricted by fretting of opposing fracture surfaces, whereas fretting does not usually occur in stage II. Inert (and non-inert) liquids can lubricate rubbing fracture surfaces and also "pump" fretting product from cracks, thus enabling larger crack-opening and shearing displacements (and hence greater crack-growth rates) to occur. These effects illustrate the dangers involved in applying results to situations different from those under which the data was obtained.

5. APPLICATION OF MECHANISTIC UNDERSTANDING

The determination and prediction of the effects of different variables on fracture processes have obvious practical significance and are intimately related to the understanding of basic mechanisms and processes. Outlined below are some examples of the application of fundamental studies to

(i) alloy development,
(ii) materials selection and testing methods,
(iii) inspection techniques (NDI), and
(iv) life prediction.

Research on fatigue and fracture of aluminium alloys has shown that the presence of large (iron–silicon rich) second-phase particles facilitates nucleation of fatigue cracks and reduces fracture toughness;[34] production of "cleaner" materials thus results in improved properties. Understanding of the role of soft PFZs in crack initiation and growth suggests that further improvements in properties may result if PFZs are either eliminated (preventing very localised concentration of deformation) or increased in width (so that slip is more dispersed and more crack-tip blunting can occur). Improved mechanistic understanding also suggests that the better SCC resistance of overaged alloys is associated with decreased area fractions of grain-boundary precipitates—not with coarser matrix precipitates, as previously suggested by some workers.[2] Thus, further research aimed at improving SCC resistance should concentrate on modifying grain-boundary precipitates rather than matrix precipitates.

An understanding of the effects of environment on fracture suggests that environmentally-induced crack growth could be inhibited by alloying the solid metal with an element chosen to

react rapidly (e.g. to produce compounds) with the environment, so that effects of chemisorption are reduced (see 3.2.3). Results[35] with LME demonstrate this approach. Inhibition of sub-critical crack growth is also possible by modifying the environment (e.g. adding inhibitors, cathodic protection, changing operating temperature). Since it is considered that chemisorption is the most important aspect of environmental reactions, further research should be concentrated in this area (rather than, for example, on dissolution processes) to give further improvements in fracture resistance. In contrast, the ability of certain environments to facilitate fracture can be used to advantage, e.g. in metal-cutting processes.[35]

An appreciation of fracture mechanisms and knowledge of variables affecting fracture processes provides a better basis for selection of existing materials when designing components for particular applications and environments. Mechanistic understanding should also contribute to resolving whether or not short-term tests under laboratory conditions can be applied to long-term service conditions; improvements in, and standardisation of, test methods could also result. Fundamental principles of fracture also show how various crack-growth processes (e.g., fatigue, SCC, corrosion-fatigue) are interrelated. Hence, it should be possible to predict the resistance of materials to corrosion-fatigue from data on SCC and fatigue in inert environments, thus reducing the amount of empirical testing. Some work[36] along these lines has been attempted, but not with great success; however, this is not surprising since it was assumed that SCC and fatigue occurred independently of each other during corrosion-fatigue. Better results should be possible on the basis of mechanistic understanding.

Understanding should provide an input into inspection techniques (NDI). For example, the knowledge that fatigue "damage" prior to crack initiation is associated with localised micro-structural changes and formation of fine sub-grain structures may enable detection of such "damage"; it could also provide a basis for determining if repair of such "damage", (e.g. by heat treatment), is possible. A precursor of fatigue prior to cracking, has long been sought as a means of assessing residual life. The identification of the microstructural change during pre-cracking stages of fatigue is thus an important step.

Considerable research has been directed towards prediction of rates of fatigue-crack growth and determination of residual life of components. Semi-empirical equations relating the rate of crack growth to power functions of the stress-intensity factor, K, have been developed. However, such equations lack a mechanistic rationale, and, therefore, often fail to predict effects of material properties and environment. Considerations of the mechanisms of fatigue-crack growth indicate that crack-growth increments per cycle, da/dN, should be related to crack-tip-opening displacements (CTODs). For example, direct observations showed that crack-growth increments in aluminium single-crystals in a liquid metal were three times the CTODs (Fig. 35). In general, $da/dN \propto B \cdot \Delta\,\mathrm{CTOD}_{eff}$ where $\Delta\,\mathrm{CTOD}_{eff}$ is the range of CTOD over which plastic deformation (alternate shear process) occurs at crack tips, and B is a crack-tip-blunting factor. As discussed in earlier sections, B is related to the distribution of slip around crack tips and will be determined by microstructure, environment (frequency), and stress intensity. If crack growth involves the formation and intrusion of soft layers, then da/dN will be controlled by $\Delta\,\mathrm{CTOD}_{eff}$ and the rate of formation of, and dimensions of such soft layers.

Stress intensity, K, and da/dN, are related because K is related to the CTOD by the expression $\mathrm{CTOD} = 4K^2/\pi\sigma_y E$, where σ_y is the yield stress of the material and E is Young's modulus. The sigmoidal shape of the $\ln da/dN$ v. $\ln \Delta K$ curve (Fig. 19) probably arises because of different mechanisms of crack growth; at low K, growth is discontinuous and probably occurs by intrusion of soft layers, while crack growth at high K involves alternate shear and MVC processes.

It is concluded that, at present, mechanistic understanding is sufficiently advanced to provide qualitative explanations for most observed effects and is able to provide a basis for systematic experiments to determine empirical "constants" in predictive crack-growth equations. However, further work is required to improve basic understanding and, particularly, to apply such understanding.

REFERENCES

1.	Liebowitz, H. (ed.)	Fracture: An advanced Treatise, Vol. 1, Microscopic and Macroscopic Fundamentals. Academic Press, 1968.
2.	Scully, J. C. (ed.)	The Theory of Stress-Corrosion Cracking in Alloys. NATO, Brussels, 1971.
3.	Kamdar, M. H.	Embrittlement by Liquid Metals. Progress in Materials Science, 15, 289, 1973.
4.	Laird, C., and Duquette, D. J.	Mechanisms of Fatigue Crack Nucleation. In Reference 6, p. 88.
5.		Fatigue-Crack Propagation. ASTM STP415, Philadelphia, Pa., 1967.
6.	Devereux, O. F., McEvily, A. J., and Staehle, R. W. (eds)	Corrosion Fatigue: Chemistry, Mechanics and Microstructure. NACE, 1971.
7.	Petch, N. J.	Metallographic Aspects of Fracture. In Reference 1, p. 351.
7a.	Beachem, C. D.	Microscopic Analyses of Cleavage Mechanisms. 2nd Int. Conf. on Mechanical Behaviour of Materials, Boston, 1976 (to be published).
8.	Pelloux, R. M. N.	Crack Extension by Alternating Shear. Eng. Frac. Mech., 1, 697, 1970.
9.	Garrett, G. G., and Knott, J. F.,	Crystallographic Fatigue Crack Growth in Aluminium Alloys. Acta Met., 23, 841, 1975.
10.	Kelly, A.	Strong Solids. Clarendon Press, Oxford, 1973.
11.	Kelly, A., Tyson, W. R., and Cottrell, A. H.	Ductile and Brittle Crystals. Phil. Mag., 15, 567, 1967.
12.	Lynch, S. P.	Tensile Deformation and Fracture in High-Strength Al-Zn-Mg Alloys. Met. Sci. J., 7, 93, 1973; and ARL Metallurgy Note 86, December 1972.
13.	Speidel, M. D.	Current Understanding of Stress Corrosion Crack Growth in Aluminium Alloys. In Reference 2, p. 289.
14.	Lynch, S. P.	Concerning the Mechanism of Liquid-Metal Embrittlement—Crack Growth in Aluminium Single Crystals and Other Materials in Liquid-Metal Environments. ARL Report, No. 102, 1977.
15.	Lynch, S. P.	Mechanisms of Stress-Corrosion Cracking and Liquid-Metal Embrittlement, Particularly in High Strength Al-Zn-Mg Alloys. ARL Report, No. 101, 1977.
16.	Latanision, R. M.	Characterisation of Metal Surfaces. In Reference 6, p. 185.
17.	Fleischer, R. L.	Effects of Non-Uniformities on the Hardening of Crystals. Acta Met., 8, 598, 1960.
18.	Uhlig, H. H.	Metal Surface Phenomena. In Metal Interfaces, p. 312, ASM, 1952.
19.	Kelly, M. J., and Stoloff, N. S.	A Bond Energy Approach to Liquid-Metal Embrittlement. 6th Int. Conf. Metallic Corrosion, Sydney, 1975.

20. Clum, J. A. — The Role of Hydrogen in Dislocation Generation in Iron Alloys. Scripta Met., 9, 51, 1975.

21. Nichols, H., and Rostoker, W. — Analogies between Stress Corrosion Cracking and Embrittlement by Liquid Metals. Trans. ASM, 56, 494, 1963.

22. Speidel, M. O. — Hydrogen Embrittlement of Aluminium Alloys? In Hydrogen in Metals (eds. I. M. Bernstein and A. W. Thompson), p. 249, ASM, 1974.

23. Lynch, S. P. — A New Model for Initiation and Growth of Fatigue Cracks. Met. Sci. J. 9, 401, 1975; ARL Metallurgy Report 94, May 1974.

24. Lynch, S. P., and Ryder, D. A. — The Fatigue Behaviour of a Superpure and a Commercial Al-Zn-Mg Alloy. Aluminium, 49, 748, 1973.

25. Laird, C., and Smith, G. C. — Crack Propagation in High Stress Fatigue. Phil. Mag., 7, 847, 1962.

26. Neumann, P. — New Experiments Concerning the Slip Processes at Propagating Fatigue Cracks. Acta Met., 22, 1155, 1974.

27. Lynch, S. P. — Unpublished work.

28. Grosskreutz, J. C. — The Effect of Surface Films on Fatigue-Crack Initiation. In Reference 6, p. 201.

29. Stoltz, R. E., and Pelloux, R. M. — Mechanisms of Corrosion Fatigue Crack Propagation in Al-Zn-Mg Alloys. Met. Trans., 3, 2433, 1972.

30. Stoltz, R. E., and Pelloux, R. M. — Inhibition of Corrosion Fatigue in 70'5 Aluminium Alloys. Corrosion, 29, 13, 1973.

31. Schijve, J. — In Reference 5, p. 533.

32. Meyn, D. A. — The Nature of Fatigue Crack Propagation in Air and Vacuum for 2024 Aluminium. Trans. ASM, 61, 42, 1968.

33. Lynch, S. P., and Ryder, D. A. — The Fatigue Behaviour of Two Al-Zn-Mg Alloys. Scripta Met., 6, 181, 1971.

34. — Advances in the Physical Metallurgy of Aluminium Alloys. Met. Trans., 6A, 624, 1975.

35. Westwood, A. R. C. — Control and Application of Environment Sensitive Fracture Processes. In Effects of Chemical Environment on Fracture Processes (eds. C. J. Osborn and R. C. Gifkins), p. 1, 3rd Tewksbury Symposium on Fracture, 1974.

36. Gerberich, W. W., Birat, J. P., and Zackay, V. F. — In Reference 6, p. 396.

APPENDIX I

Order of Presentation of the Various Fracture Processes Considered in this Paper, their General Fracture-Surface Characteristics and Definitions of Some Fracture Terms as Used in the Present Paper.

(1) OVERLOAD[1] — BRITTLE (Shallow dimples, cleavage-like); DUCTILE (Macroscopic shear, deep dimples)

(2) LIQUID-METAL EMBRITTLEMENT[2] — Dimples

(3) STRESS-CORROSION CRACKING[3] — Cleavage-like; Brittle intercrystalline

(4) FATIGUE — INITIATION[4] (Extrusions, intrusions); CRACK GROWTH[5] (Ductile striations, dimples)

(5) CORROSION FATIGUE[6] (Brittle striations, cleavage-like, intercrystalline)

"Ductile"—Associated with "large" amounts of plasticity
"Brittle"—Associated with "small" amounts of plastic deformation
"Cleavage-like"—Brittle fractures with "flat" fracture surfaces parallel to low-index crystallographic planes, often with "river lines"—see below

} Mechanisms of fracture are not implied

"River lines", etc.—A feature of many fracture surfaces (overload, SCC, LME, fatigue) are arrays of steps usually running approximately in the (local) direction of crack growth; these steps generally arise because cracks in adjacent areas initiate (or re-initiate) and grow on slightly different levels (due to inhomogenieties) and are then linked by fracture of material between adjacent cracks. Steps are often confluent ("river" lines) since interaction of stress fields of adjacent cracks favours their coalescence. In other cases, cracks may radiate from certain areas and fracture surfaces may have a "fan-like" or "feathery" appearance. Certain patterns of steps do not necessarily indicate a particular mode of fracture.

"Dimples"—Depressions on both fracture surfaces produced by a microvoid-coalescence process.

"Striations"—Lines delineating positions of crack fronts, usually produced by fatigue; "brittle" striations have much flatter profiles than "ductile" striations, thus

"brittle" "ductile"

FIGURES

Large arrows on micrographs indicate directions of crack growth.
EM - electron micrographs of secondary carbon replicas.
SEM – scanning electron micrographs.

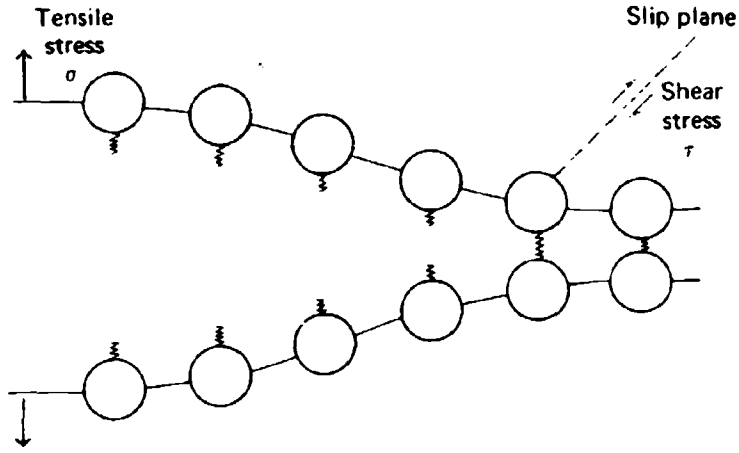

Fig. 1. Diagram schematically illustrating crack growth by tensile rupture of interatomic bonds at crack tips; shear along slip plane does not occur.

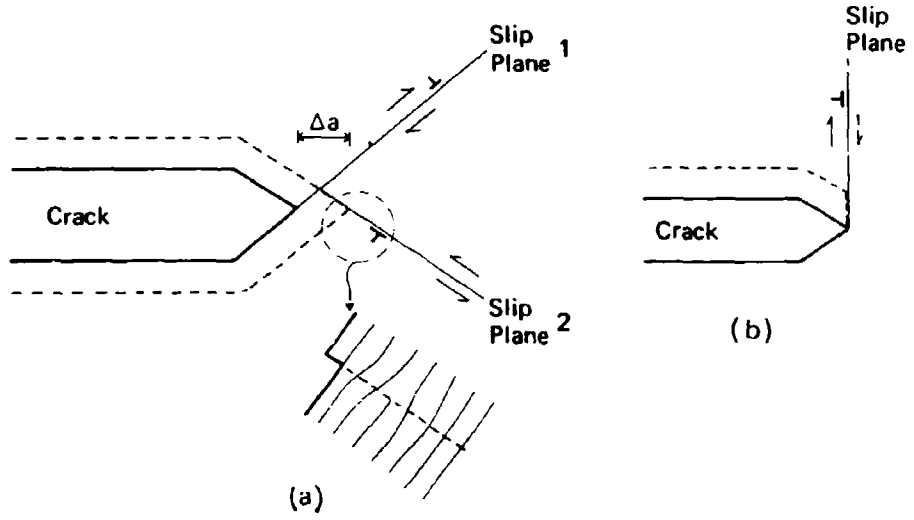

Fig. 2. Diagrams schematically illustrating (a) crack growth by shear movement of atoms at crack tips, i.e, crack-growth increment, Δa, produced by movement of dislocations on slip plane (1) then (2): (b) blunting at crack tips – extensive blunting also requires large strains ahead of cracks. Arrows indicate shear displacements on slip planes.

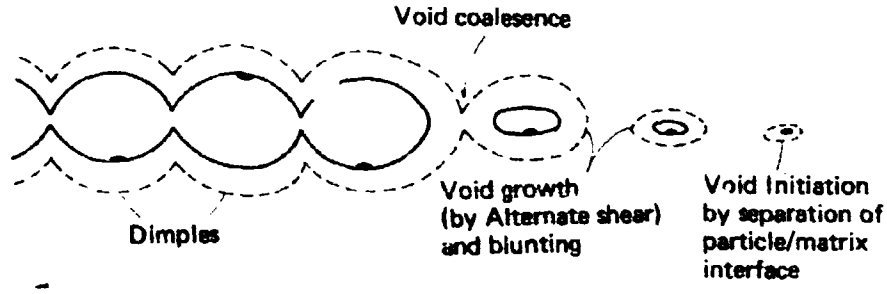

Fig. 3. Diagram schematically illustrating crack growth by micro-void coalescence; dotted lines indicate effect of increasing COD.

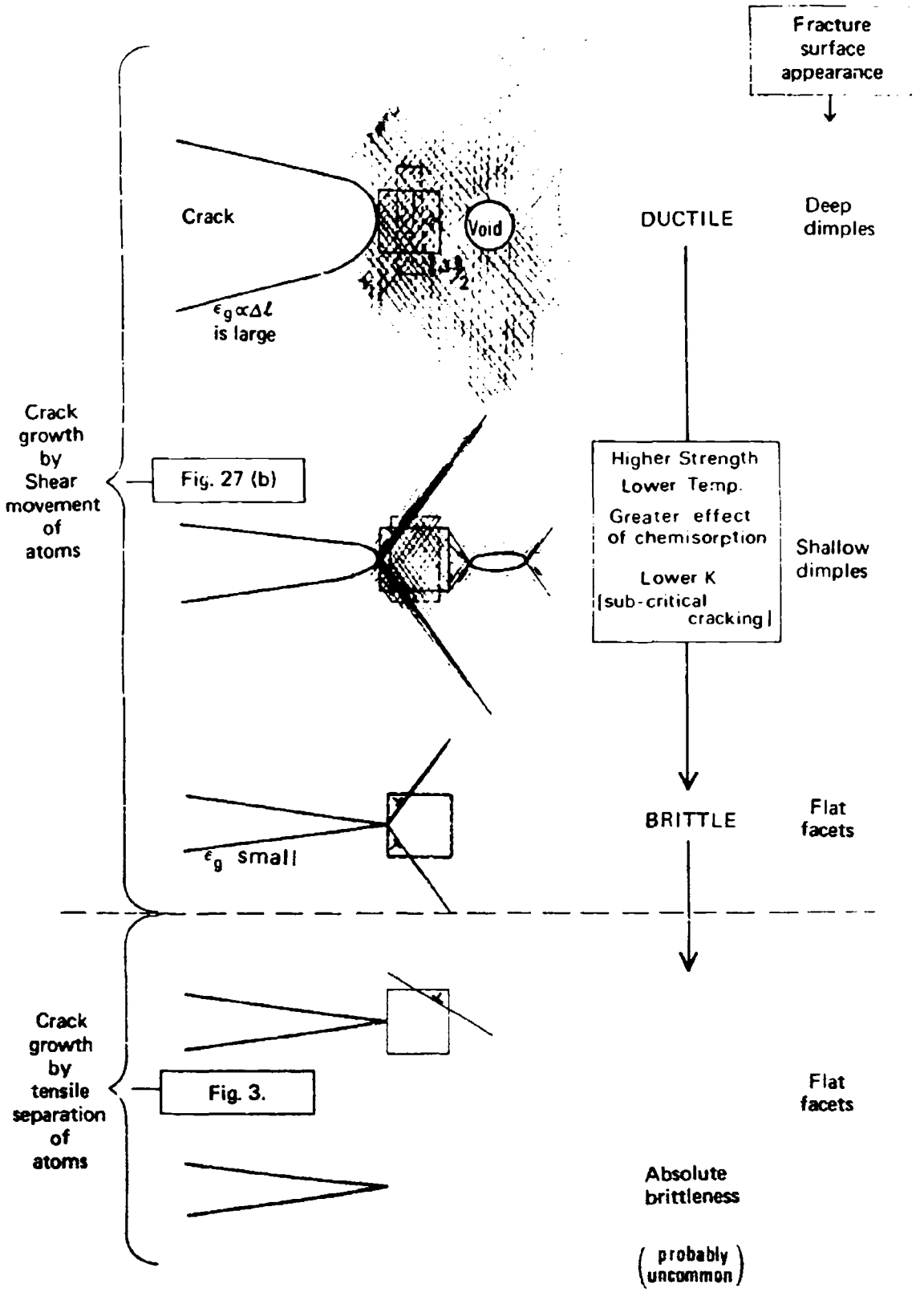

Fig. 4 Diagram illustrating transition from ductile to brittle behaviour with decreasing amounts of 'general' slip ahead of cracks.

Fig. 5. Fractograph (EM) after tensile fracture in a high-strength Al-Zn-Mg alloy showing dimples and flat areas on intercrystalline facets; inset (TEM) shows microstructure of grain-boundary regions in Al-Zn-Mg.

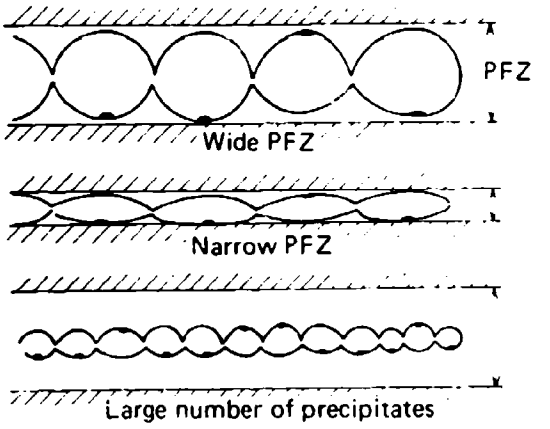

Fig. 6. Diagrams illustrating variation in dimple size (and amount of blunting at crack tips) with PFZ width and density of grain-boundary precipitates in Al-Zn-Mg.

Fig. 7. Optical micrograph of 'model' specimen consisting of a soft layer (of lead) sandwiched between and bonded to harder regions (of Pb-Sn-Sb alloy); cf. Fig. 5, inset.

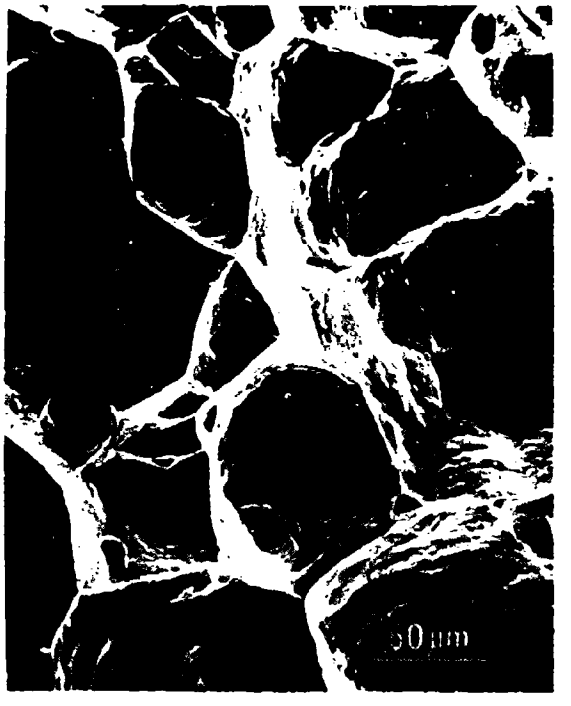

Fig. 8. Fractograph (SEM) after tensile fracture of model specimen (Fig. 7) showing large deep dimples.

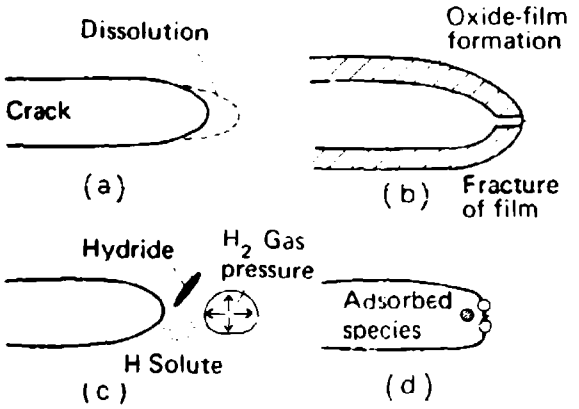

Fig. 9. Diagram illustrating proposed SCC mechanisms based on (a) dissolution (b) oxide-film formation then fracture of oxide film, (c) diffusion of hydrogen ahead of cracks, and (d) chemisorption at crack tips.

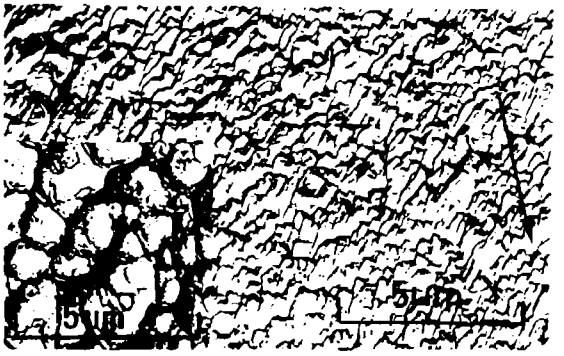

Fig. 10. Fractographs (EM) after fracture of Al-Zn-Mg in liquid metal and (inset) in air showing change in dimple appearance associated with change in environment.

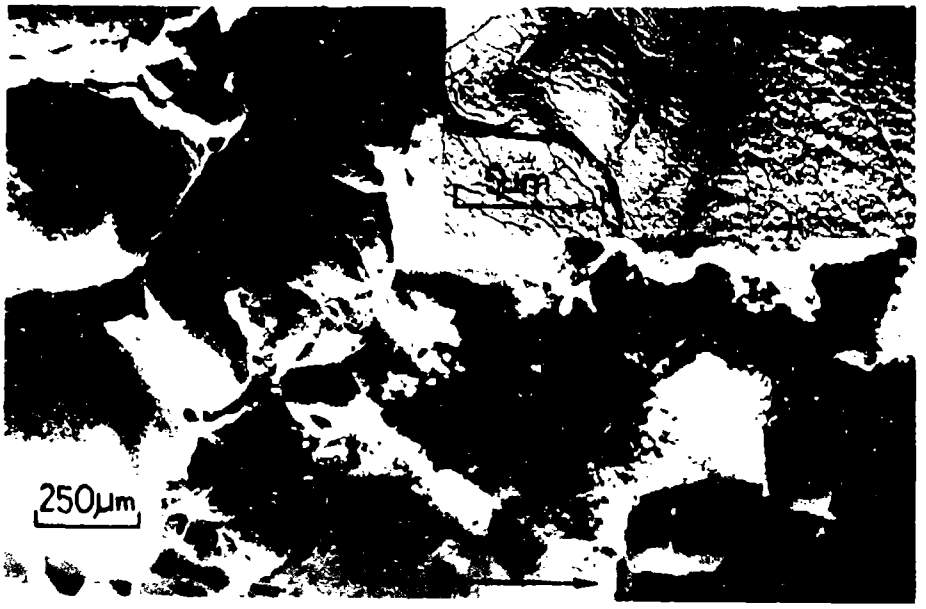

(a)

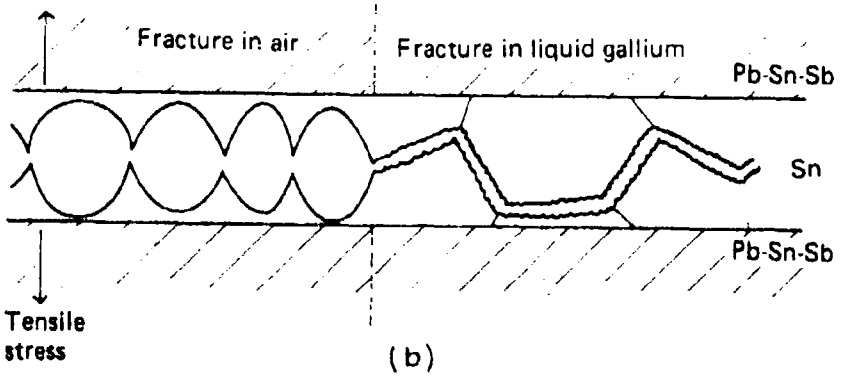

Fig. 11. (a) Fractograph (SEM) of Pb-Sn-Sb/Sn 'model' specimen partially cracked in air, producing large deep dimples, followed by brittle intercrystalline fracture in liquid gallium; (inset) fractograph (EM) of brittle intercrystalline areas showing very shallow dimples, (b) schematic diagram of fractured specimen.

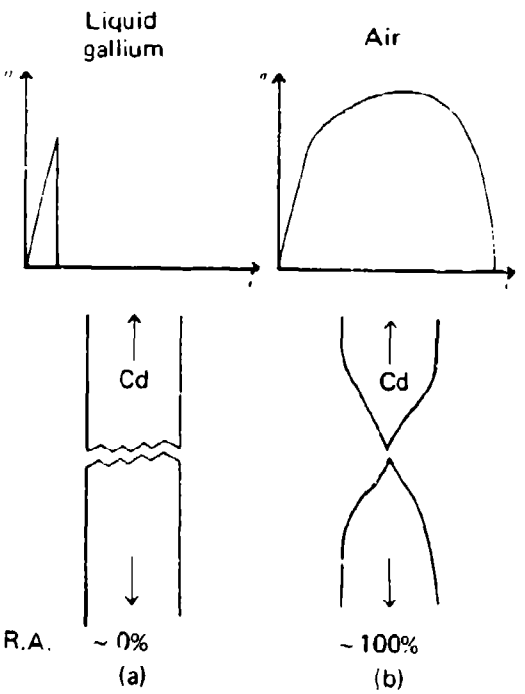

Fig. 12. Diagrams showing stress-strain curves and fracture appearance of tensile specimens of cadmium tested in (a) liquid gallium and (b) air.

Fig. 13. Fractograph (SEM) of cadmium after fracture in liquid gallium showing 'flat' cleavage-like and brittle-intercrystalline facets.

Fig. 14. Fractograph (optical) of cadmium after fracture in liquid gallium showing 'river lines' on a cleavage-like facet.

Fig. 15. Fractograph (EM) of cadmium after fracture in liquid gallium showing shallow dimples on a facet similar to those shown in figs. 13, 14.

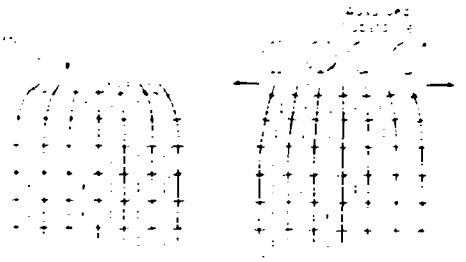

Fig. 16. Diagram schematically illustrating effect of chemisorption on 'surface-lattice distortion' (after Uhlig[18]).

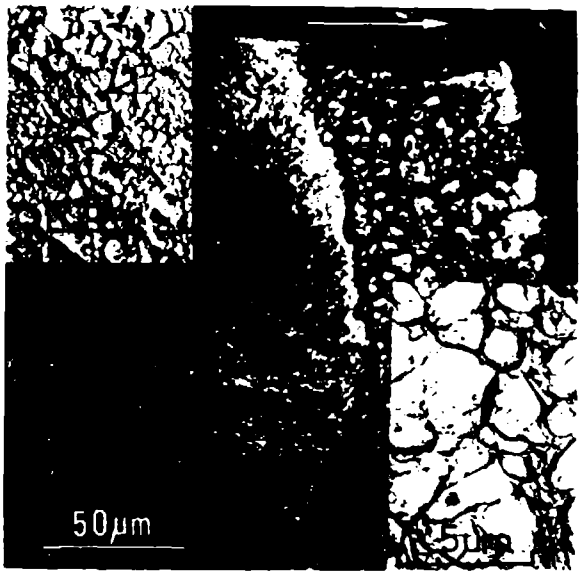

Fig. 17. Fractography (optical) after SCC/overload in Al-Zn-Mg showing transition and change in dimple size from SCC (High K — distilled water) to overload in air. Top insert (fractograph (EM)) shows dimples produced by SCC; bottom insert (fractograph (EM)) shows dimples produced by overload.

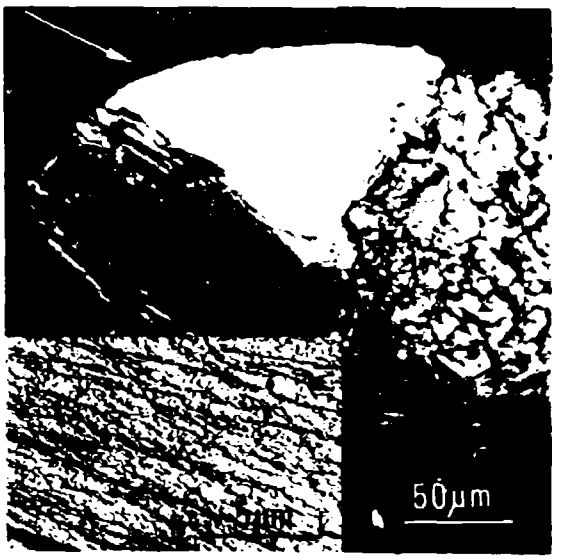

Fig. 18. Fractograph (optical) after SCC/overload in Al-Zn-Mg showing transition from SCC (low K — distilled water) to overload in air. Inset (fractograph (EM)) shows very shallow dimples produced by SCC.

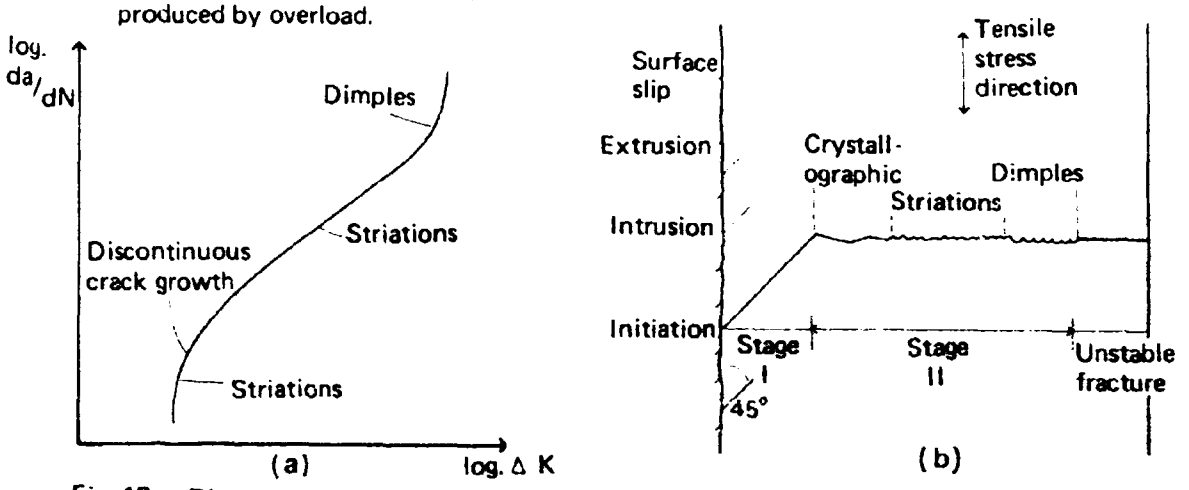

Fig. 19. Diagrams illustrating stages of fatigue; (a) shows typical crack-growth rate versus stress-intensity curve, (b) depicts typical features of fracture surface and its orientation.

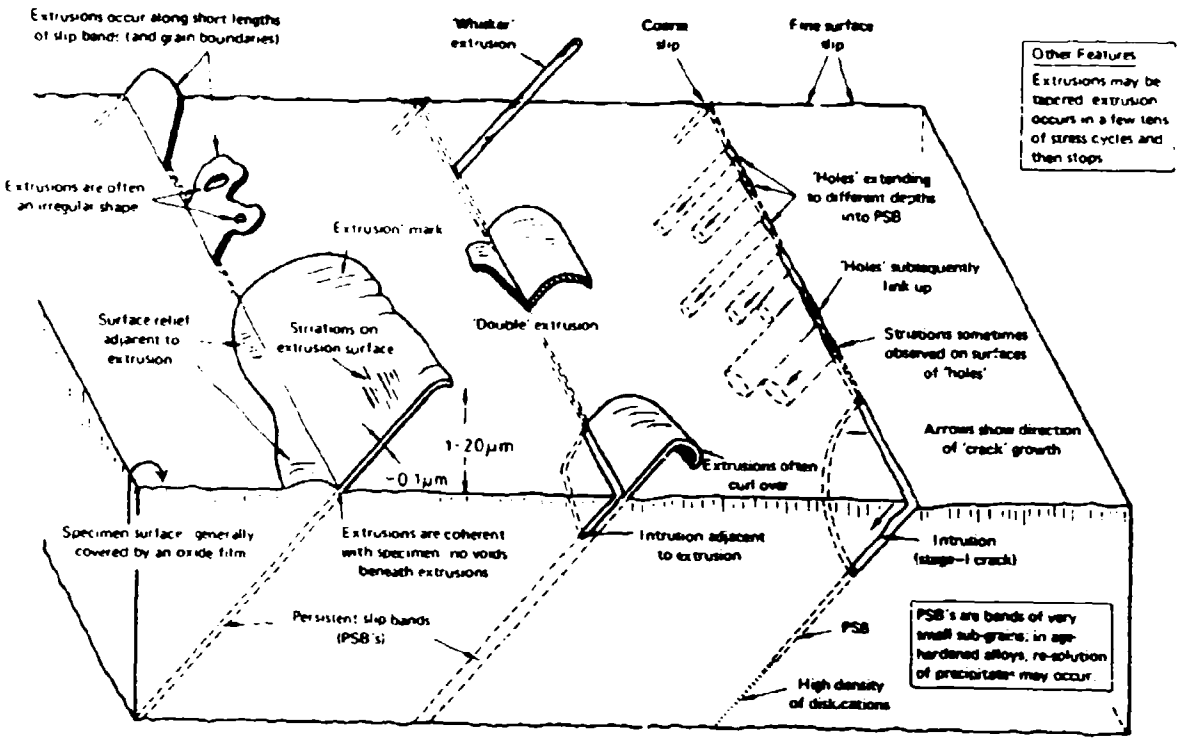

Fig. 20. Diagrammatic summary of important features of slip-band extrusion and intrusion. Specific details depend on material, stress, environment, etc.

Fig. 21. Optical micrograph of surface of Al-Zn-Mg after torsional fatigue (± 4¾° twist, 2 x 10^3 cycles) showing slip-band extrusions and intrusions.

Fig. 22. Optical micrograph of surface of D6AC steel (quenched and tempered) after torsional fatigue (± 4¾° twist, 8 x10^4 cycles) showing slip-band cracks (intrusions) across martensite plates.

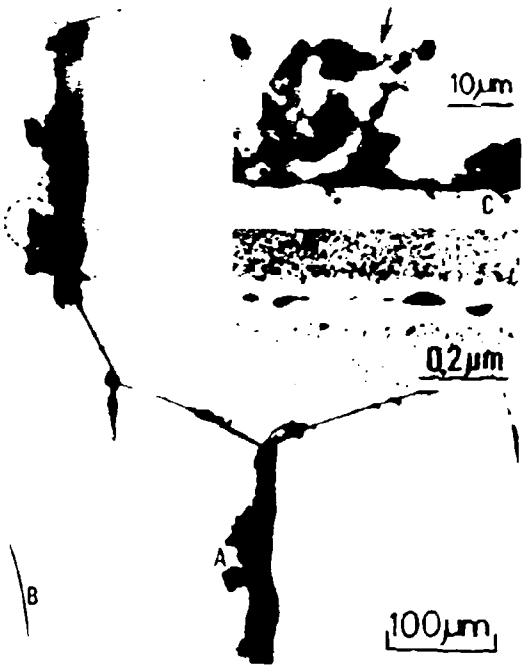

Fig. 23. Optical micrograph of surface of Al-Zn-Mg after torsional fatigue ($\pm 3^{\circ}$ twist, 5×10^3 cycles) showing extrusions (A) and intrusions (B) at grain boundaries. Extrusions project up to 12 μm above specimen surface. Insert (1) shows circled region at higher magnification; note double extrusions (C) and striations (arrowed). Lower insert(2) (electron micrograph) shows microstructure at grain boundaries.

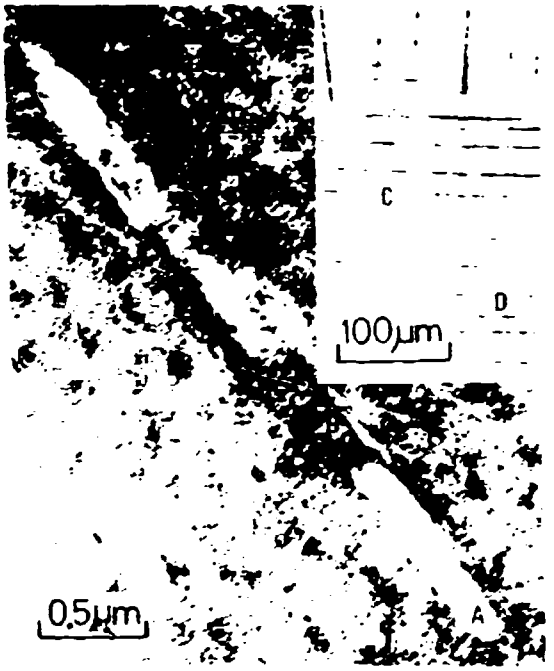

Fig. 24. Electron micrograph of PSB in Al-Zn-Mg after torsional fatigue ($\pm 4\frac{3}{4}^{\circ}$ twist, 2×10^3 cycles). Fatigue-induced re-solution of precipitates has occurred within PSB; note sub-grains (A) and high dislocation density (B) in PSB. Insert shows optical micrograph of PSB's (C) and holes (D) extending into PSB's.

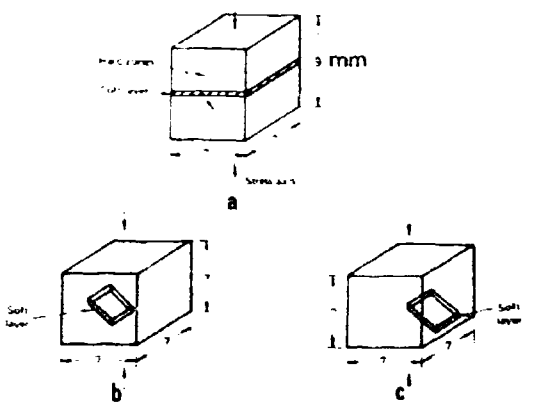

Fig. 25. Diagrams showing configurations of model specimens with respect to the applied stress.

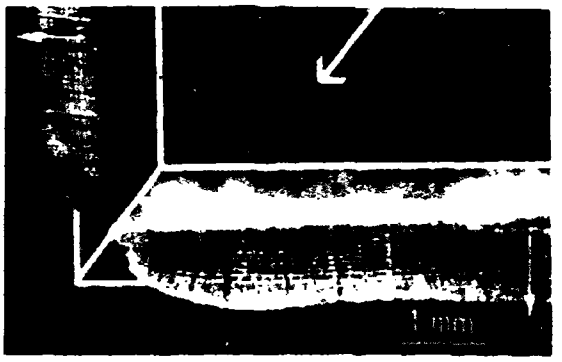

Fig. 26. Photomacrograph of 'model' specimen (Fig. 25(a)) after repeated compression (approximate specimen configuration and axis of compression is indicated) showing extrusion of soft layer. Note extrusion marks parallel to extrusion direction (small arrows) and striations at right angles to extrusion marks.

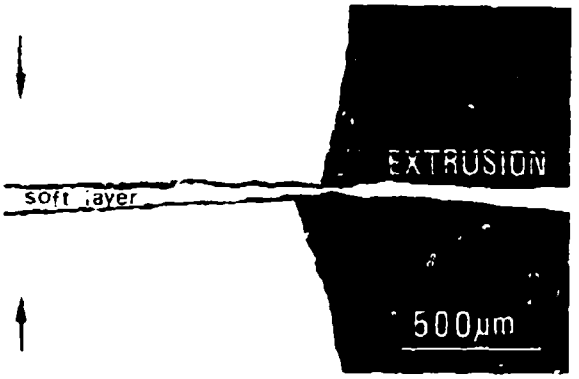

Fig. 27. Optical micrograph of taper-section through extrusion in brass/tin model specimen (Fig. 25(a)). Note deformation of hard material adjacent to extrusion. Horizontal taper magnification x ~ 6¾.

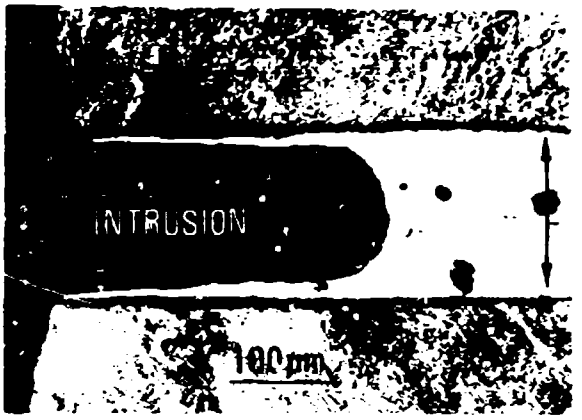

Fig. 28. Optical micrograph of longitudinal section of Pb/Pb-Sn-Sb model specimen after tensile deformation (stress axis indicated by arrows) showing intrusion of soft layer.

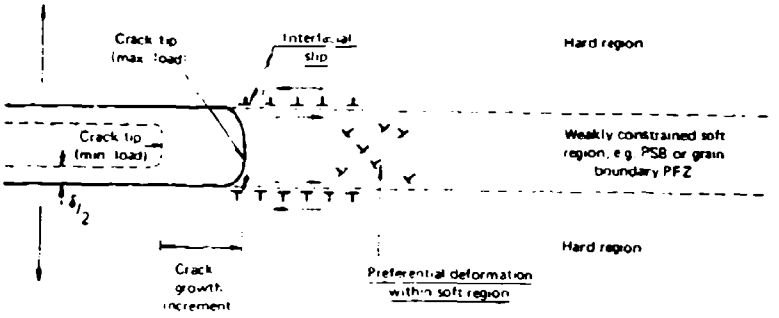

Fig. 29. Diagram illustrating mechanism of fatigue-crack growth by intrusion of weakly constrained soft layer.

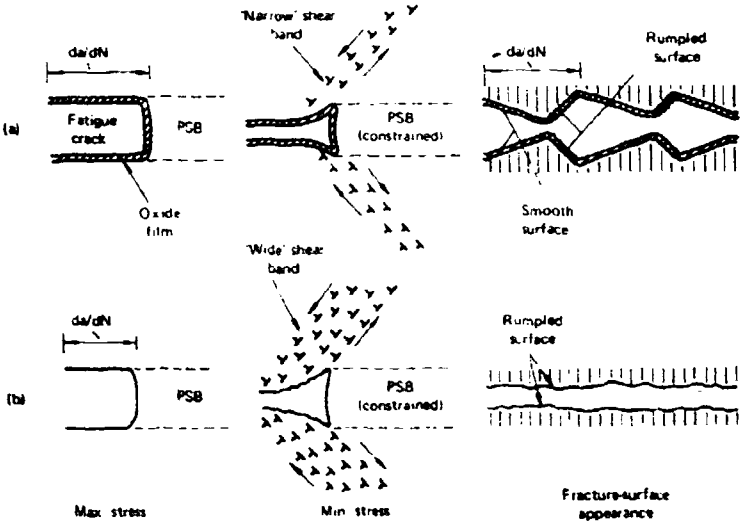

Fig. 30. Schematic diagrams showing deformation of fracture surface close to crack tip during unloading: (a) in air producing well-defined striations; (b) in vacuum.

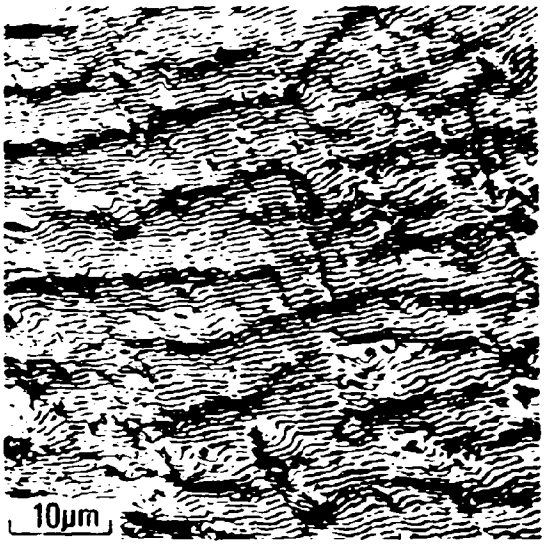

Fig. 31. Fractograph (optical) after fatigue of Al-Zn-Mg in air showing well – defined striations.

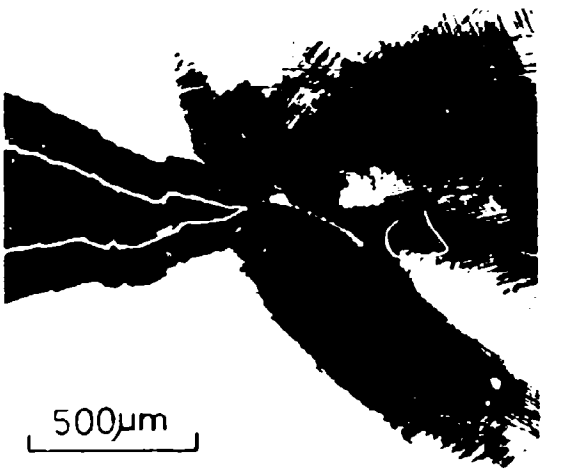

Fig. 32. Optical micrograph of crack in an aluminium single crystal specimen showing slip distribution associated with crack-tip blunting; the initially sharp crack t p blunts without significant crack growth when COD is increased in air.

Figs. 33, 34. Fractographs (EM) after fatigue of Al-Zn-Mg in NaCl solution showing ductile (D) and brittle (B) striations.

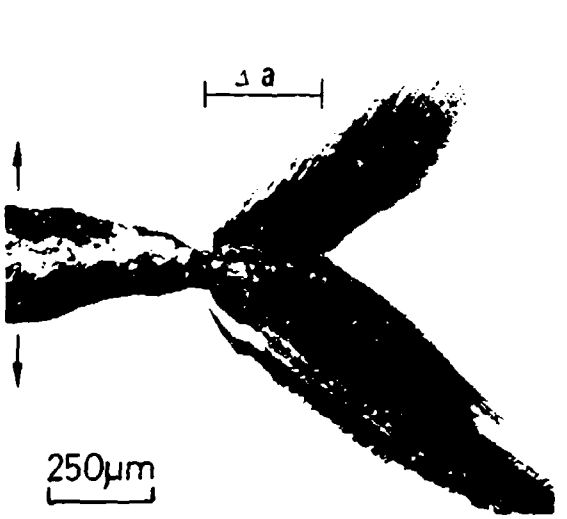

Fig. 35. Optical micrograph of aluminium single crystal (same specimen as Fig. 32) showing slip associated with crack growth increment, Δ a, when COD is increased in a liquid-metal environment, after polishing to remove surface slip due to previous crack growth.

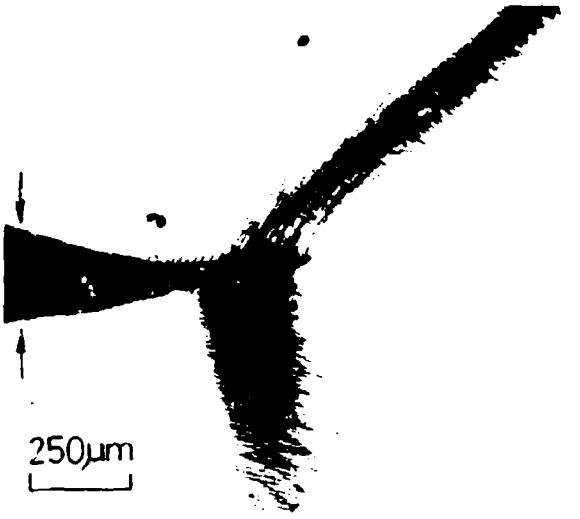

Fig. 36. Optical micrograph of aluminium single crystal (same specimen as Fig. 32) showing slip associated with crack-closing displacement (in liquid-metal environment).

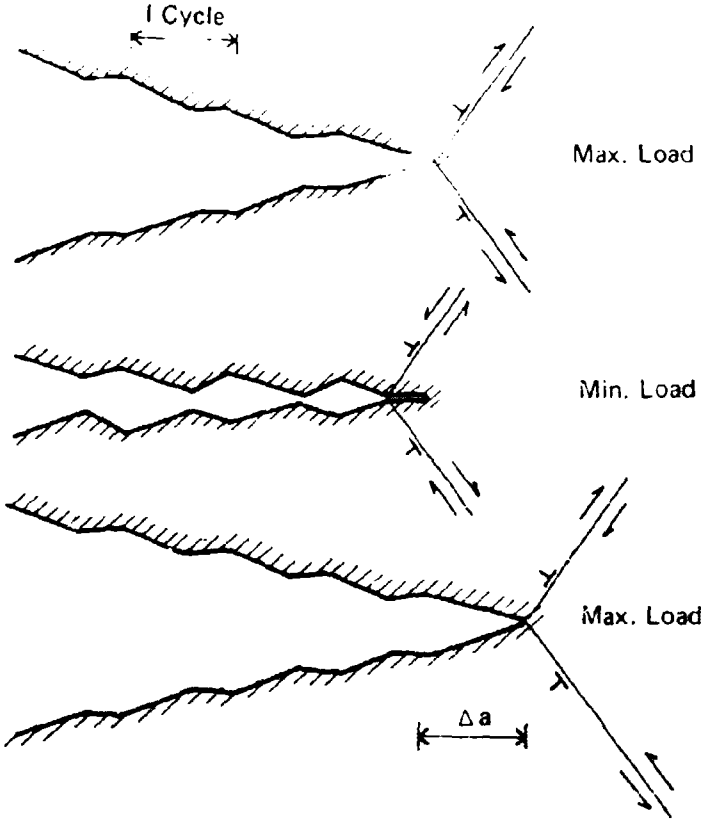

Fig. 37. Diagram illustrating mechanism of fatigue-crack growth (and brittle – striation formation) by alternate shear.

DISCUSSION

QUESTION—*J. D. Newton*
(SEC, Victoria)

I was interested in the comments you made on ductile and brittle striations. You attempted to differentiate between the two forms by using a model which explained their formation by two different sets of dislocation movements. Both the forms of striation therefore apparently require considerable dislocation movements to occur. It is difficult then to understand why one is designated brittle and the other ductile. In the illustration of the fracture surface replica, the ductile striations were indicated as those with the smaller spacing and the brittle with the larger spacing. If the range of stress intensity was increased then the spacing of the ductile striations would also increase. The key to the difference in the striations, if one actually exists, apparently lies in what you also mentioned, that the ductile striations occur when crack tip blunting takes place.

QUESTION—*Andrewartha*
(Tasmanian College of Advanced Education)

Both "brittle" and "ductile" striations result from ductile (slip) processes. There seems no advantage in thus subdividing striations.

QUESTION—*Keith R. L. Thompson*
(University of New South Wales)

Regarding the query raised by a previous questioner as to how one may distinguish between "ductile" and "brittle" striations, I would like to offer the following suggestions and would appreciate the speaker's comments on these suggestions.

I propose that the following criteria may be usefully applied to distinguish between the two types of striations as opposed to only comparing the relative striation spacing of contiguous striations; where the larger spacing is identified with brittle striation formation (Figures 33 and 34 in the paper).

(i) Does the fracture surface occupy, or lie close to, a low-index crystallographic plane?
(ii) Are cleavage steps or microscopic "river patterns" present which lie approximately parallel to the localised direction of crack propagation and perpendicular to any striations present?
(iii) Do these cleavage steps change their orientation upon crossing grain boundaries, increase in number and/or are new steps created when crossing tilt or twist boundaries in the material?

If the answers to the above questions are affirmative then I suggest that "brittle" striations may be positively identified. As the author is no doubt aware {100} fracture surfaces have been identified by Forsyth *et al.* Also the questioner has identified a {111} fracture surface in a type 2219 aluminium alloy which also fulfilled criteria (ii) and (iii) above.

In some recent fatigue crack growth studies conducted under laboratory air conditions on Type 315 and high nickel austenitic stainless steels and Incoloy 825, I have detected striations which lay approximately perpendicular to cleavage steps. The crystallographic orientation of the fracture planes in these materials has not yet been identified.

As the occurrence of "brittle" striations is usually considered to be indicative of an environmental accelerative influence on the crack growth process, I consider that it is important to establish criteria for their identification, particularly in the diagnosis of the cause of service failures.

Author's Reply

Taking questions and comments on ductile and brittle striations together: I agree with Dr. Thompson that it is useful to distinguish between ductile and brittle striations with regard to the diagnosis of service failures. The three criteria, suggested by Dr. Thompson, to identify brittle (cleavage) striations are certainly more characteristic of brittle striations than ductile striations but are not exclusive to brittle striations; for example, ductile striations (produced in inert environments) have also been observed in association with river lines and lying as facets parallel to low-index crystallographic planes. It is considered that an important difference between ductile and brittle striations is their profile—particularly the relative widths of the two "sides" of striations (see Figures 33, 34 and Appendix). This difference arises because, for a given ΔK, larger crack-growth increments occur during crack-opening in aggressive environments than in "inert" environments but the width of the "dark side" of the striation, produced by deformation of the fracture surface during crack closure, is not as affected by environment. Striation profiles are also determined by the material, ΔK and other factors as well as by environment and, hence, the fractographic determination of the role of environment in service failures should be based on comparison with fractures produced under controlled conditions.

The terms "ductile" and "brittle" (or "cleavage") are confusing to some extent in that the term "brittle" (and "cleavage") is sometimes used to describe an atomic mechanism of fracture by rupture of interatomic bonds. It is suggested that "brittle" and "cleavage" should be defined as in the Appendix.

QUESTION—*Dr. B. J. Wicks*
(ARL)

The application of your model to fatigue relies on the development of localised regions of intense strain within which softening occurs by the re-solution of precipitates. Yet you suggest that the model would be particularly valid at low stress intensities. At high stress intensities other mechanisms, such as alternate shear or plastic blunting, occur in the absence of a soft layer at the crack tip. It is not clear why microstructural instability should be limited to low stress intensities; in fact your model would seem more appropriate at high stress intensities where dislocation/particle interactions would ensure larger precipitate-free zones. Could you say something about the formation of the soft zones at high and low stress intensities.

One further question—Is there any reason to believe that material at a crack tip or along an intense slip band should be softer than the surrounding material, particularly for a cyclic hardening metal for which one would associate high cumulative plastic strains with an enhanced flow stress?

Author's Reply

At low stress intensities, crack growth increments per cycle da/dN are very small compared to plastic-zone sizes r_y, the material ahead of crack tips undergoes a considerable number of cycles of plastic strain and large accumulated strains arise. The ratio of da/dN to r_y is larger at higher stress intensities (crack growth usually occurs by microvoid-coalescence) and accumulated strains are less. Re-solution of precipitates and other microstructural changes leading to the formation of soft zones ahead of cracks are favoured by high dislocation densities associated with large accumulated strains. Thus, crack growth (and crack initiation) by intrusion of soft layers is more probable at lower stress intensities.

In age-hardening materials, precipitate-free zones at crack tips are obviously softer than surrounding regions; in work-hardened material, recrystallisation (work-softening) has been observed. In annealed materials where fatigue produces work-hardening, very small sub-grains are observed ahead of crack tips. The "mechanical properties" of such very fine sub-grain structures are not known and hence it is not clear whether crack growth occurs by intrusion or by other slip processes. More research is required to define the circumstances under which a particular mechanism of crack growth operates.

QUESTION—*P. Duane*
(GMH)

Is there any future for precipitation-hardening aluminium alloys, considering that these alloys are not dislocation free-and hence weak, soft, precipitation-free zones may form in the crystal?

QUESTION —*B. A. Parker*
(Monash University)

A comment on the first question—Intensive slip is a feature of the fatigue crack growth mechanism; intensive slip may be inhibited by the presence of larger second phase particles. Could this not give rise to an improvement in fatigue properties? Recent work at Monash has shown that the static tensile failure mechanism of an Al-Zn-Mg alloy may be changed from intercrystalline to transcrystalline by the incorporation of sub-micron particles.

Author's Reply

The presence of larger (0·1 to 1 μm) "dispersoid" particles does inhibit the formation of intense transcrystalline slip bands and the initiation and growth of transcrystalline cracks. Nevertheless, intense slip bands and re-solution of precipitates still sometimes occur in such microstructures. However, the main reason for the poor fatigue strength of aluminium alloys is the presence of pre-existing PFZs at grain boundaries. Thermomechanical processing (e.g. aging, deforming, aging) to produce more uniform precipitation gives some improvement. Improvement in properties (fatigue, fracture-toughness) has also been achieved by removing very large (10 μm) second-phase particles. These recent, modest, improvements and more careful design of components to minimise fatigue problems should ensure continued widespread use of aluminium alloys.

COMMENT—*B. Krishna Murthy*
(Monash University)

There is controversy whether the transgranular precipitate free zones observed in age-hardened Al alloys are due to the inhomogenities present before fatigue testing, or caused by the fatigue testing. Lynch[1] has shown that at least in Al-Zn-Mg alloys, the transgranular PFZs are due to both inhomogenities as well as the re-solution.

I would like to strike a note of agreement with this view, particularly in Al-4%Cu alloys. Support for this is obtained from an extensive search of the literature. It is illustrated schematically in Figures 38 and 39. The ill-defined PFZs of 0·5 μm width (Fig. 38) have transformed into clearly defined PFZs of width 1·5 μm after fatigue testing (Fig. 39). Thus the fatigue deformation may be initially concentrated in these ill-defined PFZs (containing less than the normal density of the precipitates). Intense deformation, in these narrow regions may then cause the precipitates to dissolve, leaving a clear PFZ, of increased width.

References

1. Lynch, S. P., and Ryder, D. A. The Fatigue Behaviour of Superpure and a Commercial Al-Zn-Mg Alloy, Aluminium, 49, 749, 1973.
2. Laird, C., and Thomas, G. Inter. J. Fract. Mech., 3, No. 2, 81, 1967.
3. Clark, J. B., and McEvily, A. J., Acta Met., 12, 1359, 1964.

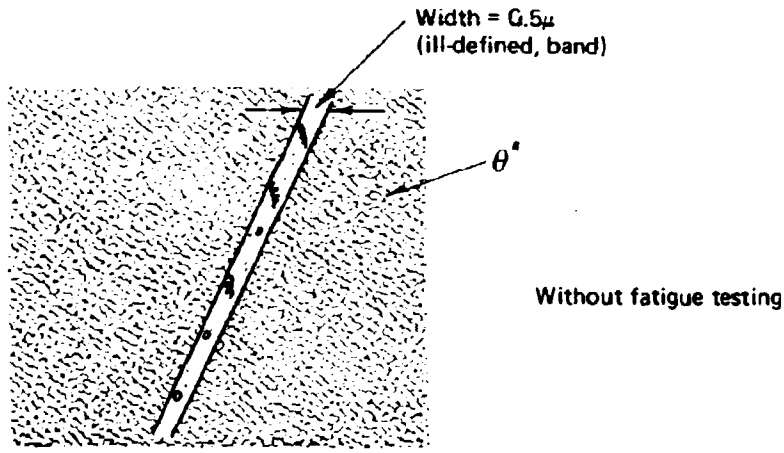

FIG. 38 ILL-DEFINED PFZ IN AGED (170°C/3 HRS) Al – 4% Cμ [REF. 2]

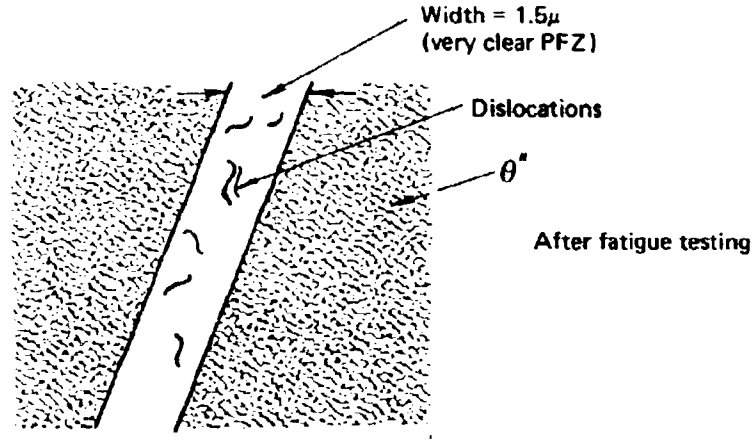

FIG. 39 CLEAR PFZ IN AGED (160°C/5 HRS) Al – 4% Cμ AFTER FATIGUE TESTING [REF. 3]

QUESTION—*L. M. Bland*
(ARL)

Would Dr. Lynch please say a little more about the possibility of the chemisorption mechanism of environmental influence being effective in the case of aluminium alloys (and steels) in an aqueous environment? May this mechanism, in such an environment, make a significant contribution to cracking propensity and, if so, may the adsorbed species be the water molecule or is it the hydrogen ion? (In the latter case it might be expected that the hydrogen would be absorbed some distance into the metal rather than remaining adsorbed at the crack surface.)

Author's Reply

The many close similarities between LME (only chemisorption possible), HE (chemisorption, diffusion possible) and SCC (chemisorption, diffusion, and other processes possible) suggest that chemisorption is the most important factor in environmentally induced cracking of aluminium alloys, steels and other materials. For example, fracture-surface appearance (which gives more information regarding mechanisms of fracture than any other factor) for steels in mercury, hydrogen, and water, and for aluminium alloys in liquid metals and water, are generally very similar and sometimes indistinguishable. (Details and full discussion are to be published in an ARL report on "SCC and LME in aluminium alloys" and in a paper on "Hydrogen embrittlement in steels" to be published in the proceedings of the "Hydrogen in Metals" conference, Paris, 1977.)

Aqueous environments facilitate crack growth in both steels and aluminium alloys while hydrogen influences crack growth in steels but not aluminium alloys. Thus, for aluminium alloys in aqueous environments, chemisorption of water molecules is probably involved in crack growth; for steels, chemisorption of water molecules or hydrogen atoms (produced by electrochemical reactions), or both, could be important. Further understanding will require more information on chemisorption and its effect on "surface-lattice distortion". It is considered that dissolved hydrogen (diffused from the surface) is probably not a significant factor in crack growth. However, the ease of diffusion of hydrogen from the surface could influence the extent of surface covered by chemisorbed atoms and, hence, could affect crack growth.

QUESTION—*M. T. Murray*
(CSIRO, Division of Tribophysics)

Why is microvoid coalescence a good model of fatigue in that the void is expanding in a reversible manner, or could be?

Author's Reply

Plastic deformation is not generally reversible on the atomic scale.

FRACTURE MECHANICS FUNDAMENTALS WITH REFERENCE TO AIRCRAFT STRUCTURAL APPLICATIONS

by

B. C. HOSKIN

SUMMARY

Fracture mechanics is being increasingly applied to problems associated with cracked, or potentially cracked, aircraft structures. Such applications include assessment of the residual strength of cracked components and also the prediction of fatigue crack growth. However, fracture mechanics is still very much a developing subject even as regards its fundamentals and, hence, in any application, it is important to bear in mind the limitations associated with some of its results. In the present paper a survey is made of basic fracture mechanics, with emphasis on those limitations likely to be of importance in aircraft structural applications.

NOTATION

a	Crack length (or half crack length)
r	Distance from crack tip
r_y	length of yield zone
x, y, z	Rectangular co-ordinates
B	Plate thickness
E	Young's modulus
G	Strain energy release rate
G_c	Strain energy release rate at fracture
J	Rice's integral
K	Stress intensity factor (subscripts I, II and III refer to "Modes")
K_c	Fracture toughness
K_{Ic}	Plane strain fracture toughness
N	Number of load cycles in fatigue
T_{ij}	Stress components ($i, j = x, y, z$)
U	Strain energy
δ	Measure of crack opening displacement
θ	Angular co-ordinate
σ	Applied tensile stress
σ_y	Tensile yield stress
τ	Applied shear stress
ν	Poisson's ratio

1. INTRODUCTION

Fracture mechanics, which can perhaps best be defined as the study of structures containing cracks or similar flaws, has found an ever-increasing application in the aeronautical field over the past decade or so.[1,2] This has come about because of the fairly widespread acceptance of the "damage-tolerant" and "fail-safe" philosophies in aircraft structural design.[3,4] These two concepts are not necessarily equivalent[5] but each has as its central feature the requirement that a structure must maintain an adequate degree of integrity despite having undergone some limited amount of damage.

An aircraft structure may be damaged for a variety of reasons. It may contain defects which have escaped detection during manufacture or it may have deteriorated in service due to fatigue or stress corrosion processes. It may have sustained accidental mechanical damage or, in the case of a military aircraft, battle damage. The commonest form in which such damage manifests itself is in the development of a crack, i.e. in the development of two free surfaces in the material separated by a very small but nevertheless distinct amount. This is virtually always the case for fatigue and stress corrosion damage; undetected manufacturing defects also are commonly of this form, partly because a crack is a type of defect that is not always easy to detect in a large built-up structure, even given the very refined non-destructive inspection (NDI) methods now available. Battle damage, of course, can involve the loss of major areas of a structure but, in the case of small arms fire, may consist of relatively small punctures from which cracks radiate.[5] If, from whatever cause, some crack-like defect be present in a structure, then it will generally grow by fatigue under the service loads into a genuine crack.

In the rational treatment of cracked aircraft structures two main problems arise. The first of these is concerned with the size of crack which can cause a catastrophic failure under a single load application; this is often termed the "residual strength problem". The second is concerned with the more or less gradual propagation of a crack from some initial size up to a critical size under the influence of a fatigue load spectrum.

As already indicated, fracture mechanics is specifically concerned with the behaviour of cracked structures so that its application here is certainly to be expected. The residual strength problem coincides with the classic fracture problem whilst fatigue crack propagation comprises part of what, in fracture mechanics, is usually called sub-critical crack growth. (The last named also embraces, for example, stress corrosion cracking.) However, although fracture mechanics has already established its usefulness in a variety of problems in the aero-space field,[7,8,9] it is important to realise that it is still very much a developing subject, even in its fundamentals, and to bear in mind the limitations associated with some of its results. In the present paper a survey is made of fracture mechanics from this point of view and with special reference to those results which have application to aircraft structures.

Fracture mechanics has a rapidly expanding literature. A fairly succinct account of the whole field has been given by Knott[10] and a very extensive one is given in the treatise edited by Liebowitz.[11] The symposia proceedings recorded in References 12–16 give detailed descriptions of recent developments in fracture mechanics, especially in the USA, and References 17 and 18 contain additional information on applications to aircraft structures.

2. NATURE OF CRACKS IN FRACTURE MECHANICS

In any analytical treatment certain idealisations are necessary regarding the geometry of a crack; those idealisations usually employed in fracture mechanics are now set down. First consider two-dimensional crack problems where the geometry is the same in all planes perpendicular to the thickness direction. A basic case here is that of a tension panel with a through-the-thickness crack (Fig. 1). It is assumed that:

(i) in the absence of any applied load the opposite faces of the crack, although distinct, are separated by an indefinitely small amount; and

(ii) the tip of the crack is sharp, as in a sharp edged notch, i.e. no radius of curvature is associated with the crack tip.

It is rather difficult to provide a satisfactory pictorial representation of such a crack (or slit), but the above conditions always apply even if they appear to be at variance with any of the illustrations.

The situation for three-dimensional crack problems is generally similar to that in two dimensions. Here the crack—or perhaps, more descriptively, the flaw—is taken as a disc-shaped void of infinitesimal thickness (Fig. 2). With the y-axis as shown (i.e., perpendicular to the crack plane and passing through it), then in any plane containing the y-axis the cross-section of the crack has the properties (i) and (ii) above.

The above idealisations would seem reasonable for fatigue cracks which are commonly of a "hairline" character. Further, any error associated with the idealisations should be of a conservative nature in the sense that it is difficult to conceive of a crack sharper than the idealised one.

Fracture theories have, however, been proposed in which these idealisations are not adopted. For example, in the two-dimensional case a crack has been considered as a long, narrow ellipse.[19] Here the radius of curvature at the crack tip is non-zero (though very small) and, generally, all results then become very sensitive to the value of this parameter. This approach has not obtained widespread acceptance.

3. ELASTIC SOLUTIONS FOR CRACKED STRUCTURES

3.1 General

Elasticity theory solutions for cracked structures have an important part to play in current fracture mechanics theory although taken by themselves they give only part of the story. In the first instance, these solutions may be thought of as applying exactly to ideally brittle materials, i.e. those which remain elastic up to the point of fracture. However, elastic solutions are also applied, under appropriate conditions, to problems of fracture in normally ductile materials such as the structural metals.

Following the pioneer work of Inglis[20]—of which a more accessible account of the method at least is given in Reference 21—exact analytical solutions for a limited number of two- and three-dimensional crack problems have been obtained using classical elasticity theory procedures.[22,23,24] These solutions usually relate to fairly simple geometries, such as an infinite plate with a straight crack or an infinite block with an elliptical (plan form) crack. For the present purposes the main feature of these solutions is the fact that, at some small distance r from the crack tip, certain of the stress components are found always to be proportional to $1/r^{\frac{1}{2}}$ and hence become infinite at the tip itself. In Appendix I a simple argument is given to show why such a result might, in fact, be anticipated.

Following Irwin[25] it has become the practice to describe any crack problem as belonging to one of three possible "Modes", according as to which of the stress components has the square root singularity. Consider the situation in the vicinity of the crack front in a three-dimensional problem and, in particular, consider the stresses on that plane in the material which represents an extension of the plane of the crack (Fig. 3). With the axes as shown (x-axis perpendicular to crack front, y-axis perpendicular to crack plane, z-axis tangential to crack front), then the stresses acting on the plane under consideration ($y = 0$) are (as always) a normal stress T_{yy} and two shear stresses T_{xy} and T_{yz}. If, of these three, the only one having the singularity is:

(i) T_{yy}, then the problem is of "Mode I, the opening or tensile mode type";

(ii) T_{xy}, then the problem is of "Mode II, the in-plane shearing mode type";

(iii) T_{yz}, then the problem is of "Mode III, the anti-plane or tearing mode type".

Prototypes for each case are shown in Figure 4 along with the associated deformations of the crack surfaces. (At the moment, however, there is no question of crack extension, i.e. these deformations are those occurring for cracks of constant length.) If more than one of T_{yy}, T_{xy} and T_{yz} has a singularity on the extension of the crack plane the problem is said to be of mixed-mode type.

3.2 The Stress Intensity Factor

Here the nature of the elastic stress distribution near the tip of a crack will be considered in more detail and it will be convenient to deal with the different modes separately. However, in all cases the results can be best described in terms of polar co-ordinates r, θ with origin at the crack tip (Fig. 5); it is assumed throughout that r is small compared with the crack length.

A study of the exact solutions referred to above shows that in all Mode I problems the stresses in the vicinity of the crack tip can be written in the form

$$\begin{aligned} T_{xx} &= \{K_I/(2\pi r)^{\frac{1}{2}}\} \cos\theta/2\,(1-\sin\theta/2 \sin 3\theta/2) + 0(1) \\ T_{yy} &= \{K_I/(2\pi r)^{\frac{1}{2}}\} \cos\theta/2\,(1+\sin\theta/2 \sin 3\theta/2) + 0(1) \\ T_{xy} &= \{K_I/(2\pi r)^{\frac{1}{2}}\} \cos\theta/2 \sin\theta/2 \cos 3\theta/2 + 0(1) \end{aligned} \tag{3.2.1}$$

where 0(1) denotes terms which are finite at $r = 0$. A general proof of the above result can be found in Reference 26.

The quantity K_I appearing in Equation (3.2.1) is termed the Mode I stress intensity factor (SIF) and, for reasons to be stated later, is a key parameter in current fracture mechanics theory. It can be seen that this single parameter completely categorises the stress state near the crack tip. Its explicit form varies from one crack problem to the next but it is always linearly proportional to the applied load (since the stresses in any elastic problem so vary) and contains a dependence on crack length and general structural geometry. For the case of a crack of length $2a$ in an infinite tension panel subjected to end stress, σ (e.g. Fig. 4*a*, where the crack length is small compared with the panel dimensions) it is found that

$$K_I = \sigma(\pi a)^{\frac{1}{2}} \tag{3.2.2}$$

The general definition of K_I is conveniently given by

$$K_I = \lim_{r \to 0} (2\pi r)^{\frac{1}{2}}\, T_{yy}\,(\theta = 0) \tag{3.2.3}$$

It follows that the stress intensity factor has the units of "stress . length$^{\frac{1}{2}}$". In the SI system the common unit is MN/m$^{3/2}$ or, equivalently, MPa.m$^{\frac{1}{2}}$; in the US system it is ksi.in$^{\frac{1}{2}}$ and in the Continental system kg/mm$^{3/2}$. (Conversion factors are 1 MPa.m$^{\frac{1}{2}}$ = 0·910 ksi.in$^{\frac{1}{2}}$ = 3·22 kg/mm$^{3/2}$.)

It might be observed that the inclusion of the 2π in Equations (3.2.1) and (3.2.3) is just a matter of convention to which most, but not all, authors subscribe; hence some care is necessary when consulting the literature on formulae for stress intensity factors. Also note that in Equation (3.2.1), $T_{xy} = 0$ on $\theta = 0$ as is required for a Mode I problem.

Similar results can be established for Mode II problems. As is shown in Reference 26, the crack tip stress field is now given by the following expressions:

$$\begin{aligned} T_{xx} &= -\{K_{II}/(2\pi r)^{\frac{1}{2}}\} \sin\theta/2\,(2+\cos\theta/2 \cos 3\theta/2) + 0(1) \\ T_{yy} &= \{K_{II}/(2\pi r)^{\frac{1}{2}}\} \sin\theta/2 \cos\theta/2 \cos 3\theta/2 + 0(1) \\ T_{xy} &= \{K_{II}/(2\pi r)^{\frac{1}{2}}\} \cos\theta/2\,(1-\sin\theta/2 \sin 3\theta/2) + 0(1) \end{aligned} \tag{3.2.4}$$

The quantity K_{II} is termed the Mode II stress intensity factor and is quite analogous to K_I. For the particular case of a crack of length $2a$ in an infinite panel subjected to a shear stress, τ, it is found that

$$K_{II} = \tau(\pi a)^{\frac{1}{2}} \tag{3.2.5}$$

The general definition of K_{II} is given by

$$K_{II} = \lim_{r \to 0} (2\pi r)^{\frac{1}{2}}\, T_{xy}\,(\theta = 0) \tag{3.2.6}$$

Note that in Equation (3.2.4) $T_{yy} = 0$ on $\theta = 0$ as required in a Mode II problem.

Finally, for a Mode III problem, the following results apply:[26]

$$\begin{aligned} T_{yz} &= \{K_{III}/(2\pi r)^{\frac{1}{2}}\} \cos\theta/2 + 0(1) \\ T_{zx} &= -\{K_{III}/(2\pi r)^{\frac{1}{2}}\} \sin\theta/2 + 0(1) \end{aligned} \tag{3.2.7}$$

where K_{III} is the Mode III stress intensity factor and is quite analogous to K_I and K_{II}. For an infinite block with a crack of length $2a$ (existing through the thickness of the block), which is subjected to a longitudinal shear stress q,

$$K_{III} = q(\pi a)^{\frac{1}{2}} \tag{3.2.8}$$

The definition of K_{III} is given by

$$K_{III} = \lim_{r \to 0} (2\pi r)^{\frac{1}{2}}\, T_{yz}(\theta = 0) \tag{3.2.9}$$

As it happens, Mode III problems are the most tractable from the mathematical viewpoint[27] but are probably of the least physical interest.

Expressions for the displacement components in the vicinity of the crack tip can be similarly established for all three modes; these turn out to be proportional to $r^{\frac{1}{2}}$ (see Appendix I) and the stress intensity factor is again the key parameter.[26]

A great deal of effort has been devoted to determining stress intensity factors for numerous crack problems using a variety of exact and approximate analytical techniques. General accounts

of these techniques, which are mainly restricted to two-dimensional problems, can be found in References 26 and 28. Special attention has sometimes been paid to collocation procedures.[29] Several compendia of the results obtained by all methods are now available.[30,31,32]

Recently, there has been a widespread development of finite element methods for determining stress intensity factors; see, for instance, References 33–41. Virtually all this work relates to two-dimensional problems. Different shaped elements have been used but a convenient procedure[41] seems to be to surround the crack tip by a regular polygon centred on the tip (Fig. 6). The stiffness matrix for such a "crack-tip element" can be calculated by using terms from the Williams[42] series expansion for the stress function in a cracked sheet. This approach enables the crack-tip element to be incorporated easily into a general purpose finite element programme.[43] Other finite element methods have been based on the so-called J-integral defined in Section 6.5[91] or on a special property of certain isoparametric elements.[92]

Thus it can be said that the determination of stress intensity factors for two-dimensional problems is well in hand. However, the situation is far less satisfactory for three-dimensional problems, and these are often encountered in practice. Important configurations here are the surface flaw (Fig. 7), which is discussed at length in References 44 and 45, and the cracked bolt hole (Fig. 8). The analytical difficulties are substantial for such problems and no convenient numerical method is yet available. Before passing on, attention is called to the fact that in three-dimensional problems, the stress intensity factor normally varies around the crack front.

3.3 Plane Stress and Plane Strain

When a thin elastic plate is loaded by forces in its own plane (the xy plane, say) it can be assumed that the only stresses arising are the in-plane ones T_{xx}, T_{yy} and T_{xy}; this situation is termed plane stress (more properly, generalised plane stress).[46] However, if a thick plate is similarly loaded but now constraints are applied so that there is no displacement in the thickness direction a condition of plane strain arises. In this last case it can be readily established from the basic elasticity equations that, as well as the in-plane stresses, there is a normal stress in the thickness direction given by[46]:

$$T_{zz} = \nu(T_{xx} + T_{yy}) \tag{3.3.1}$$

where ν is Poisson's ratio. It is important to distinguish these cases in fracture mechanics because as will be seen later, the out-of-plane stress has a very marked effect in inhibiting yielding, which in turn leads to significant reductions in the failure stress. However, provided the plan form geometry and the in-plane applied loading are the same in a plane stress and a plane strain crack problem the stress intensity factor is the same for each. There are (relatively small) differences in the displacements in each case.

When considering the crack tip stresses in a three-dimensional problem (at distances from the tip so small that the curvature in plan form of the crack front can be ignored) the problem can sometimes be usefully considered as approximately a plane strain one.[23,25]

4. ELASTIC-PLASTIC SOLUTIONS FOR CRACKED STRUCTURES

4.1 General

It has already been seen that a crack tip is an extremely severe stress concentrator, the elastic solution predicting infinite stresses right at the tip. For materials possessing some ductility, such as the metals used in aircraft structures, yielding must be anticipated around a crack tip, even for small values of the applied load. Thus it becomes necessary to carry out elastic-plastic analyses of cracked structures. These are very much more difficult than any purely elastic analysis. In fact, no generally accepted solution seems to have been yet obtained for the basic case of a small crack in a plane tension element (Fig. 1). One case for which a detailed elastic-plastic solution has been obtained is the Mode III problem of Figure 4c: this is sometimes also called the "anti-plane strain" or the "longitudinal shear" problem. Whilst of but limited interest for its own sake, the existence of this exact solution is very valuable for comparative purposes. It has been discussed at length by Rice.[26]

The study of the elastic–plastic behaviour of cracked structures is probably the major area of current basic fracture mechanics research. However, so far no conclusions of a comparable generality to those established for the elastic case can be drawn. In the following, a rather brief discussion is given of what seem to be the key results obtained to date.

4.2 Approximate Size of Plastic Zone at Crack Tip

The following procedure is commonly used for obtaining an "order-of-magnitude" estimate of the length, r_y, of the plastic zone measured along the line of prolongation of a crack. For brevity the discussion will be limited to Mode I problems but the same procedure can be applied to all modes.[47]

Consider a point P which is on the prolongation of the crack and which is on the boundary of the plastic zone (Fig. 9); such a point is common to both the elastic and plastic regions. The shear stress T_{xy} is zero at P so the stresses T_{xx} and T_{yy} are principal stresses. Now the distinction between plane stress and plane strain becomes important. As discussed in Section 3.3 above, the out-of-plane stress T_{zz} is different in the two cases. For plane stress,

$$T_{zz} = 0 \tag{4.2.1}$$

but for plane strain,

$$T_{zz} = \nu(T_{xx} + T_{yy}) \tag{4.2.2}$$

It is now assumed, firstly, that the stresses acting at P are as given by the purely elastic solution and, secondly, that the plastic zone is sufficiently small for the crack tip formulae to apply. (The first assumption is, at best, a rough approximation.) On setting $\theta = 0$ in Equation (3.2.1), it follows that, at P,

(i) for plane stress,

$$T_{xx} = T_{yy} = K_I/(2\pi r_y)^{\frac{1}{2}}, \; T_{zz} = 0 \tag{4.2.3}$$

(ii) for plane strain

$$T_{xx} = T_{yy} = K_I/(2\pi r_y)^{\frac{1}{2}}, \; T_{zz} = 2\nu K_I/(2\pi r_y)^{\frac{1}{2}} \tag{4.2.4}$$

Since P is also in the plastic zone, a yield condition must be satisfied there. According to Tresca's condition, yielding occurs whenever

$$\text{maximum of } \{|T_1 - T_2|, \; |T_2 - T_3|, \; |T_3 - T_1|\} = \sigma_y \tag{4.2.5}$$

where the T_i are principal stresses and σ_y denotes the tensile yield stress. As already remarked T_{xx}, T_{yy} and T_{zz} are principal stresses at P.

For plane stress substituting from Equation (4.2.3) into (4.2.5) immediately gives the result

$$r_y = (1/2\pi)\, K_I^2/\sigma_y^2 \tag{4.2.6}$$

whilst for plane strain use of Equation (4.2.4) with (4.2.5) gives

$$r_y = (1-2\nu)^2\, (1/2\pi)\, K_I^2/\sigma_y^2 \tag{4.2.7}$$

For a Poisson ratio value of 0·3 it would follow from the above that the length of the plastic zone in plane strain was only 0·16 times the length in plane stress, other things being equal. It seems to have become the practice in fracture mechanics to assume that, for plane strain,

$$r_y = (1/6\pi)\, K_I^2/\sigma_y^2 \tag{4.2.8}$$

Some discussion of this rather arbitrary assumption can be found on page 108 of Reference 47. However, as the whole analysis can only be viewed as extremely approximate the matter is hardly critical. (When the same procedure is applied to the Mode III case, where an exact answer is available, it gives a value for r_y which is precisely half the exact value.[47])

The above analysis can be readily extended to give the approximate shape of the whole plastic zone and not just its length.[47,48] One important feature of the above results is the indication that, for small scale yielding, the stress intensity factor remains a key parameter in the problem, here governing the size of the plastic zone. These indications are borne out by more complete analyses.[26]

4.3 Stress and Strain Fields in Plastic Zone

A reasonably clear picture of the stress and strain fields in the plastic zone around a crack tip is now starting to emerge. This has come partly from the exact solution to the anti-plane strain (Mode III) problem already referred to and partly from approximate analyses.[26] The main results are summarised in Figure 10.

For a purely elastic material, as already seen, the stress at a small distance r from the tip varies as $1/r^{\frac{1}{2}}$; since the strain is here directly proportional to the stress, it has the same variation. It follows that the product "stress × strain" which is of the nature of "work per unit volume" varies as $1/r$.

Consider now an elastic–perfectly plastic material. In such a material the stress can never exceed the yield stress. Hence the stress in the plastic zone is basically constant; for the purposes

of comparison this may be considered as a variation of the form $1/r$. On the other hand it now transpires that the associated strain varies as $1/r$. Thus the strain concentration has increased in severity compared with the elastic result. It will be noted, though, that the stress-strain product still varies as $1/r$.

Finally consider a work-hardening material, which in a sense is intermediate between the above two cases. Rice has indicated that here the stress and strain in the plastic zone vary as $1/r^p$ and $1/r^{1-p}$ respectively where p lies in the range $(0, 1/2)$ and can be related to the degree of work-hardening. Again the stress-strain product has a $1/r$ variation.

Reference 49 gives experimental results on the strain concentrations around crack tips which tend to confirm the above.

As already indicated in Section 4.2, the theoretical analyses also show that, as long as the size of the plastic zone is small compared with other lengths in the problem, and especially the crack length itself, the stress intensity factor retains its key role. However, for more extensive yielding it does not appear to be possible to establish a single parameter which characterises the state of affairs in the plastic zone.

4.4 The Dugdale Model

Because of the difficulties associated with the use of the classical theory of plasticity in crack problems, a simplified approach due to Dugdale[50] is sometimes adopted. Here an artifice is used to reduce the problem to an associated purely elastic problem. The model will be briefly described for the standard case of a crack of length $2a$ in a plane tension element subjected to an end stress, σ.

The key idea behind the model is shown in Figure 11. The actual crack is replaced by a fictitious one which is longer at each end by an amount r_y, the length of the yield zone. (This, of course, is initially unknown.) Over the lengths r_y, a stress equal to the tensile yield stress, σ_y, is applied. This problem is now treated as a purely elastic one. At the ends, P, of the fictitious crack, there will be a positive stress intensity factor caused by the applied stress, σ, and a negative stress intensity factor due to the crack surface stresses, σ_y. It is postulated that these two factors are of equal magnitude so that the net stress at P is finite. This condition serves to determine r_y and on carrying out the analysis in detail it is found that

$$r_y = a\{\sec(\pi\sigma/2\sigma_y) - 1\} \tag{4.4.1}$$

Dugdale compared this theoretical result with experimental data for mild steel and found a good agreement.

If the applied stress, σ, is small compared with the yield stress, σ_y, then on using the approximation

$$\sec x \simeq 1 + x^2/2 \tag{4.4.2}$$

it is found that Equation (4.4.1) reduces to

$$r_y \simeq a\pi^2\sigma^2/8\sigma_y^2 \tag{4.4.3}$$

In terms of the stress intensity factor K_I—see Equation (3.2.2)—this can be written as

$$r_y \simeq (\pi/8)\, K_I^2/\sigma_y^2 \tag{4.4.4}$$

This is the same sort of result that was obtained in Section 4.2, though the numerical coefficient is different. The Dugdale model is generally applied in plane stress situations so Equation (4.4.4) should be compared with Equation (4.2.6).

It might be noted that whereas classical plasticity theory predicts a diffuse plastic zone around a crack tip (much as in Fig. 9), the Dugdale model predicts a thin, narrow zone (Fig. 12). Actually, in the Dugdale model the plastic zone consists only of the area between the two surfaces of the fictitious crack in the region beyond the real crack tip. However, zones having roughly this shape have been observed in mild steel.[51]

As regards applications, the above theory has been mainly used in questions of fracture for low and medium strength steels. There seems to be little evidence on its applicability to aircraft materials such as high strength steels and aluminium alloys.

5. FRACTURE CRITERIA FOR IDEALLY BRITTLE MATERIALS

5.1 General

All the considerations to date have related to the stresses and deformations occurring in

cracked structures where the crack length was constant under application of load. Now attention is turned to the fundamental question of the conditions under which a crack will extend. For the moment only the classic fracture problem, where the crack undergoes a more or less unlimited extension under a single load application, is considered. It is convenient to commence by treating ideally brittle materials which, by definition, remain elastic up to the point of fracture. The situation for the structural metals will be considered later but, to anticipate, it can be said that results obtained here again find application.

One further restriction must be noted. Both here and in the next Section only Mode I (i.e., tensile) fracture is considered. The vast majority of fracture mechanics research has concentrated on this case which certainly seems to be the most important in practice. Some comments on other fracture modes are made in Section 7.

5.2 Griffith's Theory of Fracture

The original theory of fracture, and the one that from the theoretical viewpoint is still the most complete, is that due to Griffith.[52] Griffith was primarily concerned with the ultimate strength of a material containing microscopic cracks; present interest is in cracks of macroscopic size but this does not affect the physical argument.

Griffith set up an energy criterion for fracture involving, on the one hand, the elastic strain energy, U, in the structure (the "source" for promoting crack extension) and, on the other hand the work, W, that must be done in creating new crack surfaces (the "sink" for resisting crack extension). Griffith identified this last with the work that must be done against surface tension forces on the crack surface. For a two-dimensional crack problem Griffith's fracture criterion can be written in the general form

$$\mathrm{d}U/\mathrm{d}a = \mathrm{d}W/\mathrm{d}a \tag{5.2.1}$$

where a is a measure of the crack length.

Griffith then went on to evaluate explicitly the terms appearing in Equation (5.2.1) for the particular case of a plane tension panel under end stress σ and having a crack length $2a$. Actually, in his original paper he made an error in evaluating the left hand side of Equation (5.2.1) which he subsequently corrected with little comment and this has sometimes been the subject of some controversy. The easiest way of evaluating $\mathrm{d}U/\mathrm{d}a$ is to use the superposition result indicated in Figure 13. It can be shown[53] that the strain energy in the original problem, Figure 13*a*, is the sum of the strain energies for a panel with a crack under internal pressure, Figure 13*b*, and for an uncracked tension panel, Figure 13*c*. Since the strain energy in the last case is independent of crack length, it follows that $\mathrm{d}U/\mathrm{d}a$ has the same value in the first two cases, and, given the elastic solution, it is an elementary calculation to obtain it for the case of Figure 13*b*. At any rate, it is found that

(i) for plane stress,

$$\mathrm{d}U/\mathrm{d}a = 2\pi\sigma^2 aB/E \tag{5.2.2}$$

(ii) for plane strain,

$$\mathrm{d}U/\mathrm{d}a = 2(1-\nu^2)\pi\sigma^2 aB/E \tag{5.2.3}$$

where E denotes Young's modulus and B the panel thickness.

Turning now to the right-hand side of Equation (5.2.1) Griffith wrote

$$\mathrm{d}W/\mathrm{d}a = 4fB \tag{5.2.4}$$

where f is the surface tension and is considered as a material constant. (The factor 4 comes about because there are two crack tips and two new surfaces at each tip.) Thus, on applying the criterion (5.2.1), it follows that the critical stress to cause fracture is given by

(i) for plane stress,

$$\sigma = (2fE/\pi a)^{\frac{1}{2}} \tag{5.2.5}$$

(ii) for plane strain,

$$\sigma = (2fE/\pi a(1-\nu^2))^{\frac{1}{2}} \tag{5.2.6}$$

Griffith provided an experimental verification of his theory for glass, where he estimated f by linearly extrapolating measurements of surface tension made at high temperatures (700°C to 1100°C) (a procedure which would seem to be open to some criticism).

In current fracture mechanics notation, it is usual to introduce the symbol G (in honour of Griffith, and often written in script form to avoid confusion with the shear modulus) for the strain energy release rate associated with crack extension from a single tip; since, in the above problem, the crack extends symmetrically from each tip, there

$$2G = (1/B)\,dU/da \tag{5.2.7}$$

With this notation it follows that Griffith's fracture criterion can be written in the general form

$$G = G_c \tag{5.2.8}$$

where G_c is a material constant (in fact $G_c = 2f$).

5.3 Fracture Criterion in Terms of Stress Intensity Factor

Consider again the Griffith formula for the fracture stress and, for brevity, limit attention to the plane stress case. Equation (5.2.5) can equally well be written as

$$\sigma(\pi a)^{\frac{1}{2}} = (2fE)^{\frac{1}{2}} \tag{5.3.1}$$

The quantity on the left-hand side is simply the stress intensity factor, K, for the particular problem under consideration; see Equation (3.2.2). The term on the right-hand side is, with the present assumptions, a material constant. Thus the condition for fracture can just as well be written as

$$K = K_c \tag{5.3.2}$$

where K_c is a material constant. (Since only Mode I situations are being considered, the subscript I is here omitted.) Application of the Griffith criterion to other crack problems[53] again leads to results which can be written in the form (5.3.2) and Irwin[25] has established the general result. The key point in Irwin's proof is the demonstration that the strain energy release rate, G, is always related to the stress intensity factor, K, by

$$G = K^2/E \text{ for plane stress} \tag{5.3.3}$$

or,

$$G = K^2(1-\nu^2)/E \text{ for plane strain} \tag{5.3.4}$$

(Using Equation (5.2.7) it is immediately verified that Equations (5.2.2) and (5.2.3) represent particular cases of these relations.) That Equation (5.3.2) represents a general alternative formulation of the Griffith criterion follows by using the above relations in Equation (5.2.8). Also it might be noted that sometimes the strain energy release rate can be obtained directly, and then the above relations can be used to give the stress intensity factor.

5.4 Barenblatt's Theory of Fracture

Another approach to brittle fracture has been developed by Barenblatt.[54] Here, molecular cohesive forces are postulated as acting between the opposite faces of a crack near the tip providing the resistance to crack extension. It can be shown that this approach again leads to a fracture criterion of the form $K = K_c$. (Actually the formalism for this theory is very similar to that associated with the Dugdale model of Section 4.4 which it predated.)

6. FRACTURE CRITERIA FOR STRUCTURAL METALS

6.1 General

The establishment of a general criterion for the fracture of a structural metal is the central problem of fracture mechanics and it can be said at the outset that only partial solutions have been obtained so far. At first an attempt was made to apply Griffith's criterion unaltered but it was soon established from metal physics considerations,[55] that any "surface tension" on a crack in a metal was far too small to explain experimental results. Independently, Irwin and Orowan in the 1940s proposed that Griffith's criterion be modified by replacing the "surface tension" by "plastic work" as the mechanism now resisting crack extension.

An energy criterion of fracture of the form

$$G = G_c \tag{6.1.1}$$

is still written where G is the elastic strain energy release rate (just as for a brittle material). However, G_c is now the rate at which plastic work is done in crack extension.

In order to apply this criterion it is necessary to carry out an elastic-plastic analysis of the structure and to evaluate the changes in elastic strain energy and plastic work done as the crack extends. No generally accepted calculation seems to have yet been made: one reason for this lies in the difficulty of obtaining elastic-plastic solutions in the first place. Some approximate analyses have been performed,[56] but the results could not be used with confidence.

6.2 Elastic Fracture Mechanics

The difficulties associated with the application of the "modified Griffith criterion" just described led Irwin to investigate the simplifications that might ensue in cases where fracture occurred with only very limited plastic flow. In the first place it was proposed that now the elastic strain energy release rate could be computed from the purely elastic solution. Thus, the left-hand side of Equation (6.1.1) will be exactly the same as in the corresponding problem for a brittle material. As regards the plastic work term, no attempt was made to evaluate this explicitly. Instead it was assumed, and the justification for this is not especially apparent, that this would again be of the nature of a material constant.

Under these assumptions, the argument of Section 5.3 can again be used to express the fracture criterion (6.1.1) in the alternative form

$$K = K_c \tag{6.2.1}$$

where, again, K is the stress intensity factor and K_c is of the nature of a material constant, here termed the "fracture toughness". This result is, of course, formally the same as for a brittle material, but the following points of difference should be noted. For a brittle material, the Griffith theory provided an expression for K_c in terms of other, more basic, material constants as is implied in Equations (5.3.1) and (5.3.2). No corresponding relation has been obtained here. Also, for a brittle material K_c depended on the elastic constants and the "surface tension"; here, K_c is assumed to depend on the constants characterising the elastic and plastic behaviour of the material.

The criterion (6.2.1) is the one that has been almost universally used in predictions of the residual strength of cracked aircraft structures. The fracture toughness is regarded as the key material parameter and is normally determined by carrying out a fracture test on a standard cracked specimen for which the stress intensity factor is known. The critical value of the stress intensity factor is obtained by measuring the applied load and associated crack length at fracture: by virtue of (6.2.1) this is just the fracture toughness (which, of course, has the same units as the stress intensity factor). Once the fracture toughness is known Equation (6.2.1) can be used, in principle, to predict the weakening effect of any crack configuration for which the stress intensity factor is known. However, there are substantial difficulties in practice as discussed in the following.

6.3 Fracture Toughness

In Section 6.2 above, the fracture toughness was described as being "of the nature of a material constant". Unfortunately it is not a true material constant, tests on cracked plates showing that it varies markedly with plate thickness. The general sort of variation is as indicated in Figure 14. (For original test data see, for instance, References 4, 57 and 58.) The fracture toughness has a maximum value for small thicknesses and, as the thickness increases it decreases, finally becoming sensibly constant for some sufficiently large thickness. This constant value is termed the "plane strain fracture toughness" and is generally denoted by the symbol K_{Ic}. (This is a poor notation since the subscript "I" has already been associated with "Mode I" problems and the subscript "c" just denotes critical values; however, all the above discussion relates to "critical Mode I" situations irrespective of thickness effects.)

The reason for the variation of fracture toughness with thickness is believed to lie in the different way plastic zones develop in plates of different thickness. In thin plates it seems reasonable to expect plane stress conditions to apply. For thicker plates, even though no direct stress is applied in the thickness direction on the surface, it is considered that plane strain conditions will apply over some interior region due to constraints imposed by surrounding material on the material actually yielding. Now, it has been seen earlier that the length of the plastic zone ahead of a crack tip can be expected to be substantially larger for plane stress than for plane strain conditions. In general it is considered that the length of the plastic zone will vary through the thickness in the fashion indicated in Figure 15, i.e. outer plane stress zones surrounding an inner plane strain zone. When the length r_y of the plane strain zone is very small compared with the thickness of the plate it is considered that plane strain will prevail through most of the thickness. This variation in the nature of the plastic zone is also reflected in the different shapes of the fracture surfaces obtained in tests.[4,59]

At this stage it should be recalled that the whole theory of elastic fracture mechanics has been based on the stipulation that fracture occurs with only limited yielding. Although the theory

was originally developed using the type of argument given earlier now the theoretical justification seems to be made along slightly different lines. As remarked in Section 4.2, if only limited yielding occurs, it can be shown that the stress intensity factor remains the key parameter in determining the state of affairs around a crack tip. Therefore, under such circumstances, "it is considered reasonable" that a criterion such as (6.2.1) should apply.

However, just what constitutes an acceptably limited degree of plasticity is a matter of some contention. At least until recently there was a general view that fracture toughness tests were admissible only when carried out under essentially plane strain conditions. These conditions are generally formulated as[60]

$$B, a \geqslant 2{\cdot}5K_{Ic}{}^2/\sigma_y{}^2 \tag{6.3.1}$$

where B is the thickness of the specimen under test and a is the crack length. The implications of (6.3.1) can be seen as follows. The size of the plastic zone in a plane strain fracture may be approximately estimated by substituting K_{Ic} for K_I in Equation (4.2.8); this gives

$$r_y = (1/6\pi)\, K_{Ic}{}^2/\sigma_y{}^2 \tag{6.3.2}$$

Using (6.3.1) in this last gives

$$B, a \geqslant 15\pi r_y \simeq 47 r_y \tag{6.3.3}$$

Thus, when (6.3.1) holds, the plastic zone size at fracture should indeed be small compared with the other dimensions.

Details of the procedures to be employed in fracture toughness testing are given in the Standard[60] and some account of the more practical aspects can be found in References 61 and 62. Handbooks giving typical values of the fracture toughness of aircraft materials are available.[63,64] However, it should be pointed out that the fracture toughness of a material can be very sensitive to the exact nature of the heat treatment procedure employed in its manufacture. Cases have been reported[65] where apparently minor changes in heat treatment, which left the yield and ultimate strength and the elongation virtually unaltered, caused over 100% changes in fracture toughness; see also Reference 66. This shows the care that must be exercised in using handbook values of fracture toughness and also points up the difficulties in establishing a fracture theory that is based solely on classical continuum concepts.

The above paragraph has referred entirely to plane strain fracture toughness where the condition (6.3.1) has been implied. Regrettably this is a very restrictive condition in the sense that it is generally only satisfied for relatively thick plates, e.g. around 11 mm (0·4 in.) for 7075-T6 aluminium alloy and over 30 mm (1·3 in.) for 2014-T6 aluminium alloy. The required thickness is somewhat less for the ultra-high strength steels say, around 5 mm (0·2 in.). Much of an aircraft structure, however, comprises sheet material with a thickness of the order of 1·6 mm (0·064 in.) and, at the moment, there is no accepted method of fracture toughness testing for this situation (which is basically plane stress). One can, of course, always carry out a fracture test on a particular configuration and evaluate some nominal fracture toughness. The question, so far basically unanswered, is to what extent results so obtained can be applied to any other configuration. However, attention should be called to a very detailed "engineering solution" of fracture in aircraft-type built-up structures given by Broek.[4]

6.4 The Crack Opening Displacement (COD) Criterion

The main present alternative to elastic fracture mechanics is the so-called "crack opening displacement" (COD) approach.[67,68] Broadly, fracture is here considered to occur when the separation between the opposite faces of a crack as measured at some appropriate point attains a critical value. This criterion is often used in conjunction with the Dugdale model of a crack. It will be recalled that there the real crack was replaced by a longer fictitious one loaded at its ends. It follows that in the model there is a definite separation between points on the crack surface at a location corresponding to the tip of the real crack. Using the notation of Section 4.4 it can be established[56] that this separation, δ, is given by, for the case of a small crack in a tension panel,

$$\delta = (8\sigma_y a/\pi E)\, ln \sec(\pi\sigma/2\sigma_y) \tag{6.4.1}$$

The criterion for fracture is simply

$$\delta = \delta_c \tag{6.4.2}$$

where δ_c is of the nature of a material constant. When the applied stress, σ, is small compared with the yield stress, σ_y, it can be readily established that (6.4.1) reduces to

$$\delta = K^2/E\sigma_y \tag{6.4.3}$$

It follows that, in this case, the COD criterion is essentially the same as the elastic fracture mechanics one. However, at least in principle, the COD criterion can be applied in the presence of large scale yielding, Equations (6.4.1) and (6.4.2) then providing the required relation between applied stress and crack length at fracture for a tension panel. This approach is being widely developed for application to fracture problems in low and medium strength steels (where the Dugdale model appears to find its best application).

Some of the difficulties associated with the COD criterion have been outlined by Bluhm; see page 118 of reference 1. These centre around establishing a satisfactory test procedure for measuring a critical COD.

6.5 The J-Integral Criterion

The so-called J-integral is a mathematical formalism developed by Rice[69] which, when applied to problems of fracture occurring with little or no yielding, gives the same results as elastic fracture mechanics but which is also capable of being applied in the more general case.

For two-dimensional crack problems, the following line integral is defined

$$J = \int_C (W\mathrm{d}y - \vec{T} \cdot \partial\vec{u}/\partial x \, \mathrm{d}s) \tag{6.5.1}$$

where the co-ordinate system is as shown in Figure 16. Here C is a curve surrounding the crack tip which starts on the lower crack surface and ends on the upper one, s denotes the arc length along this curve, $\vec{T}$ denotes the stress vector and $\vec{u}$ the displacement vector. The quantity W is the strain–energy density so that the stress–strain law for the material is given by

$$\sigma_{ij} = \partial W/\partial \epsilon_{ij} \tag{6.5.2}$$

where σ_{ij} and ϵ_{ij} are corresponding stress and strain components. For a linearly elastic material W is a quadratic function of the strains and (6.5.2) is quite equivalent to Hooke's law. However, it is also possible to use (6.5.2) with other forms for W to give stress–strain laws appropriate to the deformation theory of plasticity. (These last are really only non-linear elastic laws and do not have a general validity but they can often be usefully employed for cases where the applied load is monotonically increasing.)

The physical significance of the J-integral is not especially evident from Equation (6.5.1) but it can be shown[26] that, for a linearly elastic material, J coincides with the strain energy release rate G. Since the Griffith criterion for a brittle material could be written as $G = G_c$ and, since for this case, $J = G$, it seems reasonable to investigate whether a criterion of the form

$$J = J_c \tag{6.5.3}$$

where J_c is of the nature of a material constant has a more general validity; in particular, whether it can serve without any restrictions about limited plasticity. This is currently being very actively studied, e.g. References 70–77, and results to date seem promising but the criterion could not yet be said to have been definitively established.

7. MIXED MODE FRACTURE

7.1 General

The discussion of fracture criteria in the preceding sections has been limited entirely to Mode I situations, i.e. to fracture under tensile loads where K_I is the only non-zero stress intensity factor. However, parts of an aircraft structure will commonly be subjected to shear stresses (along with tensile stresses) and thus there is interest in the behaviour of cracked elements under conditions where K_I and K_{II} are both non-zero. (Some attention has been paid in the literature to the situation where K_{III} is also non-zero[78] but this case will not be discussed here.)

7.2 Mode II Fracture

As indicated in Section 3.1, the basic case for Mode II fracture is a cracked plate under uniform shear (Fig. 4*b*) where K_{II} is the only non-zero stress intensity factor. The elastic solution indicates that points on the crack surfaces displace as shown in Figure 4*b*, a point on the top surface moving to the right and the corresponding point on the bottom surface moving to the left. It is frequently implied in the fracture mechanics literature that this type of deformation carries directly over into the fracture mode, the crack extending along its length with the top half

shearing off from the bottom half. However, there seems to be little experimental evidence of such a fracture mode in a metal plate. On the contrary, in some tests on aluminium alloy sheet, where the shear was applied by a "picture-frame" arrangement,[79] fracture occurred by the crack propagating at 45° to its original line (Fig. 17). No attempt was made to inhibit buckling in these tests, and this could have affected the results, but then in an actual aircraft buckling would also be virtually unrestrained. Experiments on cracked tubes under torsion, so that Mode II conditions approximately prevailed, have also been reported.[78] Once again the crack did not propagate along its own length.

It is, of course, possible to define a critical stress intensity factor K_{IIc} for the present case, irrespective of the direction of crack extension; however, if the crack does not propagate along its original line, this is only relevant to the first instant of extension since thereafter a different geometrical situation prevails.

7.3 Mixed Mode I-Mode II Fracture

Rather more attention has been paid to situations where both K_I and K_{II} are non-zero than to the pure Mode II case; this is partly because a simple type of test specimen is available here, namely, a tension panel with an oblique crack (Fig. 18). It can be seen from Figure 19 that the present problem can indeed be regarded as a combination of a Mode I and a Mode II problem. (The direct stresses parallel to the crack in Fig. 19*b* have no effect.) For a small crack of length $2a$ it can be easily established that the appropriate stress intensity factors are

$$K_I = \sigma \cos^2\alpha \, (\pi a)^{\frac{1}{2}} \tag{7.3.1}$$

and

$$K_{II} = \sigma \cos\alpha \sin\alpha \, (\pi a)^{\frac{1}{2}} \tag{7.3.2}$$

where σ denotes the applied stress and α is the angle shown. Several theoretical and experimental studies of this problem have been carried out.[4,76,80,81,82] The experiments have established that the crack extension is essentially perpendicular to the direction of applied tension (Fig. 20). On the theoretical side the aim has generally been to derive an "interaction formula" for fracture such as

$$c(K_I/K_{Ic})^m + d(K_{II}/K_{IIc})^n = 1 \tag{7.3.3}$$

Broek[4] has proposed taking $c = d = 1$ and $m = n = 2$ for aluminium alloy sheet (under plane stress conditions). Shah[76] found that $c = d = m = n = 1$ gave good agreement with results on thick plates of 4340 steel. At the moment, though, it does not appear possible to give any reasonably general criterion for mixed mode fracture.

8. FATIGUE CRACK PROPAGATION

8.1 General

There is currently a great deal of interest in establishing laws for fatigue crack propagation which are based on fracture mechanics concepts. The general functional form of these laws is

$$da/dN = f(\Delta K) \tag{8.1.1}$$

where da/dN denotes the rate of increase of crack length, a, with the number of load cycles, N, and ΔK denotes the stress intensity range over a load cycle (i.e., the difference between the stress intensity factors at the maximum and minimum loads for the cycle). Such laws are, at present, largely empirical although fracture mechanics theory is used to provide guidance on general forms. For reviews of the different laws proposed see, for example, References 4, 83, 84, 85 and 86. An introductory account of how such laws are used in considerations of the safe operating periods for cracked, or potentially cracked structures has been given in Reference 86, and an application to a specific aircraft is discussed in Reference 8. In the following a brief description is given of what seem to be the most widely used laws at present.

8.2 Laws for Constant Amplitude Cycling

The first law of the form (8.1.1) proposed and one that is still widely used today for constant amplitude cycling is that due to Paris. It is given by

$$da/dN = c(\Delta K)^n \tag{8.2.1}$$

where c and n are empirical constants. The exponent n is generally found to lie between 2 and 4

but higher values sometimes occur.[87] The parameter c, as well as varying with the material, may also be markedly affected by the test conditions (e.g. the environment).

The main alternative to Paris's law is one due to Forman. This can be written in the form[4]

$$da/dN = c(\Delta K)^n/(1-R)(K_c - K_{max}) \qquad (8.2.2)$$

where c and n are (in general) different empirical constants. Here R is the stress ratio which is the ratio of the minimum to the maximum stress in a load cycle, K_{max} is the stress intensity factor when the cyclic stress is at its maximum value and K_c is, as before, the fracture toughness. It can be seen that as the crack approaches its critical size for fracture, the law predicts an indefinitely large propagation rate.

Both the above laws have been shown to fit certain data quite well but the general applicability of either of them remains a matter of some contention.[4] Of course the whole question of fatigue is complicated by the relatively large scatter of experimental results commonly encountered.

8.3 Laws for Spectrum Loading

Both the previous laws can, in principle, be applied to the variable amplitude, or spectrum, loading normally experienced by an aircraft in service. However, neither takes account of what seems to be an important experimental fact, namely, that an occasional high (tension) load can markedly reduce the subsequent crack propagation rate.[4] Crack propagation laws which incorporate this effect have been constructed,[88,89] and shown to give agreement with limited amounts of experimental data. However, their generality remains uncertain. Reference should also be made to laws incorporating the so-called fatigue crack closure effects[90] which utilise fracture mechanics concepts.

9. CONCLUSIONS

In the present paper, a survey has been made of the current status of fracture mechanics from the point of view of aircraft structural applications. It is not simple to draw clear-cut conclusions since the subject is still very much a developing one. However, the following assessment is made:

(i) The stress intensity factor is a very useful parameter for characterising both the residual strength of, and the rate of crack propagation in, a structure. It can certainly be used in a qualitative fashion. For example, if by the design of some modification it can be established that the stress intensity factor is substantially reduced, then significant improvements can be expected in both static and fatigue strength.

(ii) The plane strain fracture toughness is likewise a very useful parameter for ranking a material as regards its resistance to fracture. However, it is a parameter which sometimes is very sensitive to the precise nature of the heat treatment process and care should be taken when using "handbook" values. There is a need for a satisfactory extension of the concept to the "sheet thickness" range.

(iii) The extent to which elastic fracture mechanics can be used for quantitative predictions of the residual strength of cracked components is a rather more difficult question. It can generally be used in the approximate calculations needed to assess the requisite sensitivity of NDI methods in a given situation. As regards structural applications the theory seems to have found its best applications for solid sections made in high-strength materials such as the ultra-high strength steels, the 7000 series aluminium–zinc–magnesium alloys and titanium alloys. The main difficulty likely to arise here is that of determining an appropriate stress intensity factor for a complex geometry.

(iv) The question of an appropriate law for fatigue crack propagation, especially under spectrum loadings remains very much an open one. Probably the best that can presently be said is that if a given law has been found to give good agreement with test results on a particular structure for a particular load spectrum, it is reasonable to employ the same law for assessing the crack propagation characteristics of the same structure under other related spectra. Generally, it would seem that comparative, rather than absolute, calculations should be made.

(v) In summary, when it is required to apply fracture mechanics to a structural problem in a predictive situation it would seem prudent, at present, to support the theoretical results with a reasonably representative test programme.

REFERENCES

1. Liebowitz, H. (ed.) — Fracture Mechanics of Aircraft Structures. AGARD-AG-176, NATO Advisory Group for Aerospace Research and Development, 1974.
2. Anon. — Application of Fracture Prevention Principles to Aircraft. US National Materials Advisory Board Report NMAB-302, 1973.
3. Anon. — Damage Tolerance in Aircraft Structures. ASTM STP 486, American Society for Testing and Materials, 1971.
4. Broek, D. — Fail-Safe Design Procedures. AGARD-AG-176, pp. 121–225 (see Reference 1 above).
5. Wood, H. A. — Application of Fracture Mechanics to Aircraft Structural Safety. Engineering Fracture Mechanics, vol. 7, pp. 557–64, 1975.
6. Jensen, J. E. — The Ballistic Damage Characteristics and Damage Tolerance of Wing Structural Elements. ASTM STP 486, pp. 215–29 (see Reference 3 above).
7. Tiffany, C. F. — Fracture Control of Metallic Pressure Vessels. NASA SP-8040, 1970.
8. Buntin, W. D. — Concept and Conduct of Proof Test of F-111 Production Aircraft. Aeronautical Journal, vol. 76, pp. 587–98, 1972.
9. Wood, H. A. — The Use of Fracture Mechanics Principles in the Design and Analysis of Damage Tolerant Aircraft Structures. Fatigue Life Prediction for Aircraft Structures and Materials, pp. 4-1 to 4-13; AGARD-LS-62, NATO Advisory Group for Aerospace Research and Development, 1973.
10. Knott, J. F. — Fundamentals of Fracture Mechanics. Butterworths, London, 1973.
11. Liebowitz, H. (ed.) — Fracture: An Advanced Treatise (vols. I–VII). Academic Press, New York, 1968–69.
12. Anon. — Stress Analysis and Growth of Cracks. ASTM STP 513, American Society for Testing and Materials, 1972.
13. Anon. — Fracture Toughness. ASTM STP 514, American Society for Testing and Materials, 1972.
14. Anon. — Progress in Flaw Growth and Fracture Toughness Testing. ASTM STP 536, American Society for Testing and Materials, 1973.
15. Anon. — Fracture Toughness and Slow Stable Cracking. ASTM STP 559, American Society for Testing and Materials, 1974.
16. Anon. — Fracture Analysis. ASTM STP 560, American Society for Testing and Materials, 1974.
17. Wood, H. A., Bader, R. M., Trapp, W. J., Hoener, R. F., and Donat, R. C. (eds) — Proceedings of the Air Force Conference on Fatigue and Fracture of Aircraft Structures and Materials. AFFDL TR 70-144, US Air Force Flight Dynamics Laboratory, 1970.
18. Wilhem, D. P. — Fracture Mechanics Guidelines for Aircraft Structural Applications. AFFDL TR 69-111, US Air Force Flight Dynamics Laboratory, 1969.
19. Kuhn, P. — Residual Strength in the Presence of Fatigue Cracks. AGARD Advisory Report 11, NATO Advisory Group for Aerospace Research and Development, 1967.
20. Inglis, C. E. — Stresses in a Plate Due to the Presence of Cracks and Sharp Corners. Transactions of Institute of Naval Architects, London, vol. 55, pp. 219–30, 1913.

21. Timoshenko, S. — Theory of Elasticity (1st ed., p. 175). McGraw-Hill, New York, 1934.
22. Sneddon, I. N., and Lowengrub, M. — Crack Problems in the Classical Theory of Elasticity. Wiley, New York, 1969.
23. Sih, G. C., and Liebowitz, H. — Mathematical Theories of Brittle Fracture. Fracture: An Advanced Treatise—Vol. II, Mathematical Fundamentals, pp. 67–190 (see Reference 11 above).
24. Sih, G. C. (ed.) — Mechanics of Fracture. Vol 1--Methods of Analysis and Solutions of Crack Problems. Noordhoff, Leyden, 1973.
25. Irwin, G. R. — Fracture. Encyclopedia of Physics, vol. 6, pp. 551–90. Springer, Berlin, 1958.
26. Rice, J. R. — Mathematical Analysis in the Mechanics of Fracture. Fracture: An Advanced Treatise, vol. II, Mathematical Fundamentals, pp. 191–311 (see Reference 11 above).
27. Hoskin, B. C. — Use in Fracture Mechanics of Coker and Filon's Approximate Elastic Solutions for Finite Width Structures. ARL Note SM 318, Aeronautical Research Laboratories, Australia, 1967
28. Cartwright, D. J., and Rooke, D. P. — Methods of Determining Stress Intensity Factors. RAE TR 73031, Royal Aircraft Establishment, UK, 1973.
29. Newman, J. C. — An Improved Method of Collocation for the Stress Analysis of Cracked Plates with Various Shaped Boundaries. NASA TN D-6376, 1971.
30. Sih, G. C. — Handbook of Stress Intensity Factors. Institute of Fracture and Solid Mechanics, Lehigh University, 1973.
31. Tada, H. — The Stress Analysis of Cracks Handbook. Del Research Corporation, Hellertown, Pa., 1973.
32. Rooke, D. P., and Cartwright, D. J. — A Compendium of Stress Intensity Factors. Her Majesty's Stationery Office, London, 1976.
33. Chan, S. K., Tuba, I. S., and Wilson, W. K. — On the Finite Element Method in Linear Fracture Mechanics. Engineering Fracture Mechanics, vol. 2, pp. 1–17, 1970.
34. Byskov, E. — The Calculation of Stress Intensity Factors Using the Finite Element Method with Cracked Elements. International Journal of Fracture Mechanics, vol. 6, pp. 159–67, 1970.
35. Walsh, P. F. — The Computation of Stress Intensity Factors by a Special Finite Element Technique. International Journal of Solids and Structures, vol. 7, pp. 1333–42, 1971.
36. Blackburn, W. S. — Calculation of Stress Intensity Factors at Crack Tips using Special Finite Elements. The Mathematics of Finite Elements and Applications (ed. J. R. Whiteman), pp. 327–336, Academic Press, London, 1973.
37. Robinson, J. — Integrated Theory of Finite Element Methods. Wiley, New York, 1973.
38. Papaioannou, S. G., Hilton, P. D., and Lucas, R. A. — A Finite Element Method for Calculating Stress Intensity Factors and its Application to Composites. Engineering Fracture Mechanics, vol. 6, pp. 807–823, 1974.
39. Hilton, P. D., and Sih, G. C. — Application of the Finite Element Method to the Calculations of Stress Intensity Factors. Mechanics of Fracture, vol. 1 (ed. G. C. Sih), pp. 426–83 (see Reference 24 above).
40. Wilson, W. K. — Finite Element Methods for Elastic Bodies Containing Cracks. Mechanics of Fracture, vol 1 (ed. G. C. Sih), pp. 484–515 (see Reference 24 above).
41. Jones, R., and Callinan, R. J. — A Finite Element Method for Calculating Stress Intensity Factors in Cracked Sheets.

ARL Report Struc. 360, Aeronautical Research Laboratories, Australia, 1976.

42. Williams, M. L. — On the Stress Distribution at the Base of a Stationery Crack. Journal of Applied Mechanics, vol. 24, pp. 109–14, 1957.

43. Callinan, R. J. — Programs for Calculating Stress Intensity Factors in Structures having Cracked Sheet Elements. ARL Tech Memo Struc. 244, Aeronautical Research Laboratories, Australia, 1976.

44. Swedlow, J. L. (ed.) — The Surface Crack: Physical Problems and Computational Solutions. American Society of Mechanical Engineers, 1972.

45. Keays, R. H. — A Review of Stress Intensity Factors for Surface and Internal Cracks. ARL Report SM 343, Aeronautical Research Laboratories, Australia, 1973.

46. Sokolnikoff, I. S. — Mathematical Theory of Elasticity (2nd ed., pp. 249-57). McGraw-Hill, New York, 1956.

47. McLintock, F. A., and Irwin, G. R. — Plasticity Aspects of Fracture Mechanics. ASTM STP 381, Fracture Toughness Testing and its Applications, pp. 84–113, American Society for Testing and Materials, 1965.

48. Rooke, D. P. — Elastic Yield Zones Around a Crack Tip. RAE TN CPM 29, Royal Aircraft Establishment, UK, 1963.

49. Bateman, D. A., Bradshaw, F. J., and Rooke, D. P. — Some Observations on Surface Deformation Round Cracks in Stressed Sheet. RAE TN CPM 63, Royal Aircraft Establishment, UK, 1964.

50. Dugdale, D. S. — Yielding of Steel Sheets Containing Slits. Journal of Mechanics and Physics of Solids, vol. 8, pp. 100–104, 1960.

51. Rosenfield, A. R., Dai, P. K., and Hahn, G. T. — Crack Extension and Propagation under Plane Stress. Proceedings of First International Conference on Fracture, vol. 1, pp. 223–58, Sendai, Japan, 1965.

52. Griffith, A. A. — The Phenomenon of Rupture and Flow in Solids. Philosophical Transactions of Royal Society of London, ser A, vol. 221, pp. 163–98, 1920.

53. Hoskin, B. C. — Applications of Elasticity Theory in Fracture Studies of Cracked Sheet. ARL Report SM 294, Aeronautical Research Laboratories, Australia, 1963.

54. Barenblatt, G. I. — The Mathematical Theory of Equilibrium Cracks in Brittle Fracture. Advances in Applied Mechanics, vol. 7, pp. 55–129, 1962.

55. Greenwood, G. W. — Concepts of Fracture Toughness. Fracture Toughness, ISI Publication 121, pp. 1–12, The Iron and Steel Institute, London, 1968.

56. Goodier, J. N., and Field, F. A. — Plastic Energy Dissipation in Crack Propagation. Fracture of Solids (ed. D. C. Drucker and J. J. Gilman), pp. 103–18, Interscience, New York, 1963.

57. Brothers, A. S., and Yukawa, S. — Fracture Test Methods and their Application. Application of Fracture Toughness Parameters to Structural Metals (ed. H. D. Greenberg), Metallurgical Society Conferences, vol. 31, pp. 35–68, Gordon and Breach, New York, 1966.

58. Srawley, J. E. — Plane Strain Fracture Toughness. Fracture: An Advanced Treatise, vol. IV, pp. 45–68, Engineering Fracture Design (see Reference 11 above).

59. Brown, W. F., and Srawley, J. E. — Plane Strain Crack Toughness Testing of High Strength Metallic Materials. ASTM STP 410, American Society for Testing and Materials, 1966.

60. Anon. — Standard Method of Test for Plane Strain Fracture Toughness of Metallic Materials.

ASTM Standard E 399–72. American Society for Testing and Materials, 1972.

61. Anderson, B. E., Ellis, R., and Ryan, N. E. — The ARL Fracture Toughness Testing Facility. ARL Note SM 405, Aeronautical Research Laboratories, Australia, 1974.
62. Ellis, R., and Anderson, B. E. — The Fracture Toughness of Large Structural Fatigue Specimens of D6ac Steel. ARL Note SM 410, Aeronautical Research Laboratories, Australia, 1974.
63. Anon. — Damage Tolerant Design Handbook. MCIC-HB-01, US Metals and Ceramics Information Center, Battelle Institute, 1972.
64. Lewis, G. I., Gardiner, R. W., and Peel, C. J. — Plane Strain Fracture Toughness Data for British Airframe Alloys. RAE TR 72224, Royal Aircraft Establishment, UK, 1973.
65. Feddersen, C. E., Moon, D. P., and Hyler, W. S. — Crack Propagation in D6AC Steel (An Evaluation of Fracture Mechanics Data for the F-111 Aircraft). MCIC Report 72-04, US Metals and Ceramics Information Center, Battelle Institute, 1972.
66. Ryan, N. E. — Relationship between Microstructure and Fracture Toughness in D6AC Steel. ARL Note Met. 103, Aeronautical Research Laboratories, Australia, 1974.
67. Burdekin, F. M., and Stone, D. E. W. — The Crack Opening Displacement Approach to Fracture Mechanics in Yielding Materials. Journal of Strain Analysis, vol. 1, pp. 145–53, 1966.
68. Dobson, M. O. (ed.) — Practical Fracture Mechanics for Structural Steel. UK Atomic Energy Authority, 1969.
69. Rice, J. R. — A Path Independent Integral and the Approximate Analysis of Strain Concentration by Notches and Cracks. Journal of Applied Mechanics, vol. 35, pp. 379–86, 1968.
70. Begley, J. A. and Landes, J. D. — The J-Integral as a Fracture Criterion. ASTM STP 514, pp. 1–20 (see Reference 13 above).
71. Bucci, R. J., Paris, P. C., Landes, J. D., and Rice, J. R. — J-Integral Estimation Procedures. ASTM STP 514, pp. 40–69.
72. Landes, J. D., and Begley, J. A. — The Effect of Specimen Geometry on J_{Ic}. ASTM STP 514, pp. 24–39.
73. Rice, J. R., Paris, P. C., and Merkle, J. G. — Some Further Results of J-Integral Analysis and Estimates. ASTM STP 536, pp. 231–45 (see Reference 14 above).
74. Merkle, J. G. — Analytical Applications of the J-Integral. ASTM STP 536, pp. 264–80.
75. Begley, J. A., Landes, J. D., and Wilson, W. K. — An Estimation Model for Application of the J-Integral. ASTM STP 560, pp. 155–169 (see Reference 16 above).
76. Landes, J. D., and Begley, J. A. — Test Results from J-Integral Studies. ASTM STP 560, pp. 170–86.
77. Underwood, J. H. — J_{Ic} Results from Two Steels. NEL Report 600, National Engineering Laboratory, UK, 1975.
78. Shah, R. C. — Fracture under Combined Modes in 4340 Steel. ASTM STP 560, pp. 29–52 (see Reference 16 above).
79. Ellis, R. — Residual Strength of Cracked Panels under Shear. ARL Note SM 393, Aeronautical Research Laboratories, Australia, 1973.
80. Erdogan, F., and Sih, G. C. — On the Crack Extension in Plates under Plane Loading and Transverse Shear.

Journal of Basic Engineering, Transactions of ASME ser. D. vol. 85, pp. 519–27, 1963.

81. Panasyuk, V. V., Berezhnitsky, L. T., and Kovchik, S. — Propagation of an Arbitrarily Oriented Rectilinear Crack During Extension of a Plate. NASA TT-402, 1965.

82. Hoskin, B. C., Graff, D. G., and Foden, P. J. — Fracture of Tension Panels with Oblique Cracks. ARL Report SM 305, Aeronautical Research Laboratories, Australia, 1965.

83. Pelloux, R. M. — Review of Theories and Laws of Fatigue Crack Propagation. AFFDL TR 70-144, pp. 409–16 (see Reference 17 above).

84. Bluhm, J. I. — Crack-Propagation Laws. AGARD-AG-176, pp. 95–109 (see Reference 1 above).

85. Bradshaw, F. J., and Rooke, D. P. — The Application of Fracture Mechanics to Material Selection and Structure Design in Aircraft. RAE TR 69122, Royal Aircraft Establishment, UK, 1969.

86. Hoskin, B. C. — Simple Theoretical Studies of Fatigue Crack Propagation Using a Fracture Mechanics Approach. ARL Note SM 372, Aeronautical Research Laboratories, Australia, 1971.

87. Ellis, R. — Fracture Mechanics Studies of Fatigue Crack Propagation in 2024 Aluminium Alloy Panels Containing Transverse Slits. ARL Note SM 379, Aeronautical Research Laboratories, Australia, 1972.

88. Wheeler, O. E. — Spectrum Loading and Crack Growth. Journal of Basic Engineering, Transactions of ASME, ser. D, vol. 94, pp. 181–86, 1972.

89. Keays, R. H. — Numerical Evaluation of Wheeler's Model of Fatigue Crack Propagation for Programmed Load Spectra. ARL Note SM 376, Aeronautical Research Laboratories. Australia, 1972.

90. Elber, W. — The Significance of Fatigue Crack Closure. ASTM STP 486, pp. 230–42 (see Reference 3 above).

91. Sharples, J. K. — Determination of Stress Intensity Factors for a Plate with Single Edge Crack using Finite Element Methods. NEL Report 615, National Engineering Laboratory, UK, 1976.

92. Henshell, R. D., and Shaw, K. G. — Crack Tip Finite Elements are Unnecessary. International Journal for Numerical Methods in Engineering, vol. 9, pp. 495–507, 1975.

APPENDIX
Occurrence of Square Root Function in Elastic Crack Problems

Here a simple argument is presented to indicate why the occurrence of the square root function might be anticipated in the elastic solutions to crack problems. Consider first the mathematical properties of the square root function defined in an unbounded plane region which has a slit extending from the origin to infinity along one of the co-ordinate axes (Fig. A1). This slit has exactly the same properties as those ascribed to an idealised crack in Section 2. It is convenient to work in terms of the complex variable

$$z = x + iy \tag{A1}$$

where x, y are the rectangular co-ordinates in the plane. Introducing polar co-ordinates (r, θ), as in Figure A2, it follows that

$$z = r \exp i\theta \tag{A2}$$

Consider now two points A and B on opposite faces of the slit. Just as in the elastic problem a crack represents a barrier as regards the transference of any tensile load (thinking of a Mode I problem), so is the slit here regarded as a mathematical barrier. The only valid mathematical paths linking A and B are those in which a circuit is made around the origin 0; it is not permissible to jump directly across the slit from A to B since this involves passing, albeit momentarily, out of the defined region. One permissible path is via the circle shown. Thus, it seems reasonable to characterise A by the value $\theta = 0$ and B by the value $\theta = 2\pi$. Note, however, that since

$$\exp i 0 \quad \exp i 2\pi = 1 \tag{A3}$$

it still follows that

$$z_A = z_B \tag{A4}$$

i.e., the actual co-ordinates of A and B are the same.

But consider the square root function. From Equation (A2)

$$\sqrt{z} = \sqrt{r} \exp i\theta/2 \tag{A5}$$

Evaluating this at A and B it follows that, despite Equation (A4),

$$\sqrt{z_A} - \sqrt{z_B} = 2\sqrt{r} \tag{A6}$$

Further insight is provided by some elementary geometrical considerations. Every point in the region of Figure A2 is characterised by a certain value of z. If, for each such point, the value of the square root function as defined by Equation (A5) is plotted the resultant region is as shown in Figure A3, i.e. the square root function conformally maps the infinite region with a slit (Fig. A2) on to the upper half plane (Fig. A3). Note especially that the re-entrant angle of 2π formed by the two faces of the slit at the origin has been "straightened out".

Now consider the physical situation for an elastic material with a crack. In the first place it can be shown that there exists a close connection between the solution of an elastic problem for a region of given shape and the function which conformally maps this region on to the upper half plane. The two are by no means necessarily identical but there is a connection: the reason for this lies buried rather deep in the theory of partial differential equations and will not be pursued here. Secondly, consider again the pair of points A and B of Figure A2 now treated as points of the material which are almost contiguous in the absence of any load. If a tensile load, whose line of action is parallel to the y axis is applied, then the vertical displacements v_A and v_B, say, of A and B will be oppositely directed as the crack opens up under load, i.e. there will be a result of the form

$$v_A - v_B = \delta \tag{A7}$$

where δ denotes the separation. The displacement of a point in an elastic body is always some function of the co-ordinates of that point in the undeformed condition; in the present case, then, it is necessary to find a functional form for the displacement which assumes different values depending on whether the point under consideration is on the top or bottom surface of the crack (always bearing in mind that the position co-ordinates of such a pair of points are virtually the same). By comparing Equations (A6) and (A7) it can be seen that the square root function satisfies this requirement. If the displacement is proportional to $\sqrt{r}$ then the stresses will be proportional to $1/\sqrt{r}$ since in an elastic material the stress is proportional to the strain, which last is a derivative of the displacement.

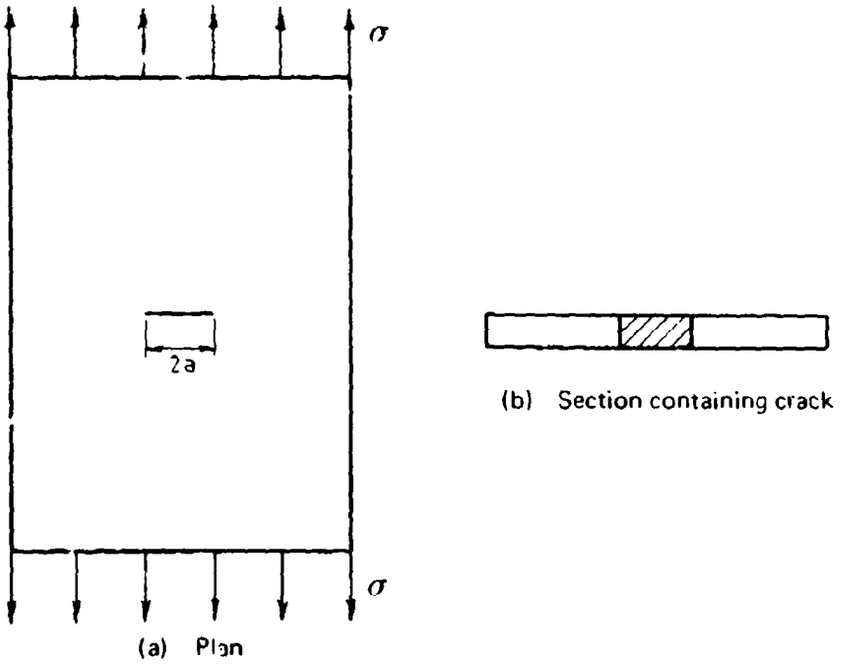

FIG. 1. TENSION PANEL WITH THROUGH-THE-THICKNESS CRACK; TWO-DIMENSIONAL PROBLEM.

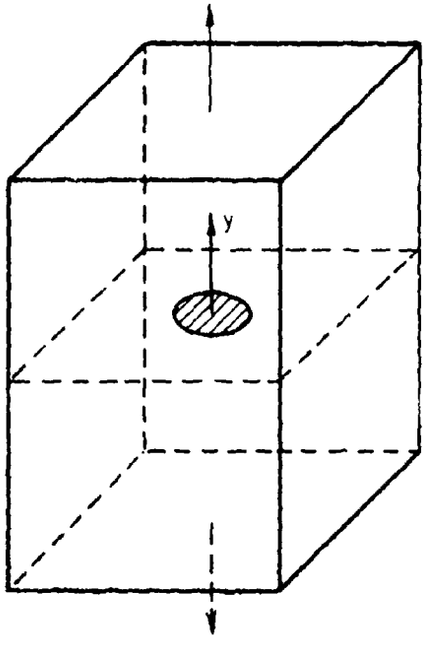

FIG. 2. THREE DIMENSIONAL CRACK PROBLEM

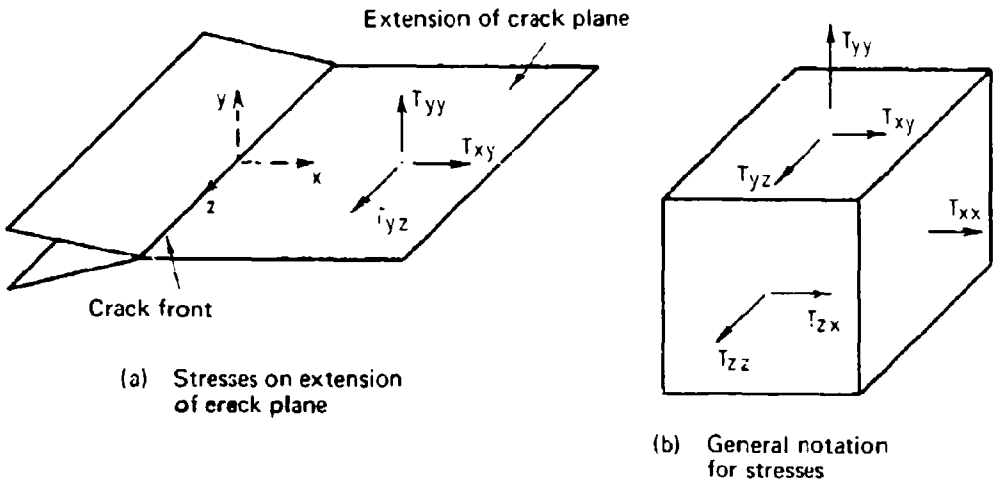

(a) Stresses on extension of crack plane

(b) General notation for stresses

FIG 3. CRACK TIP STRESSES

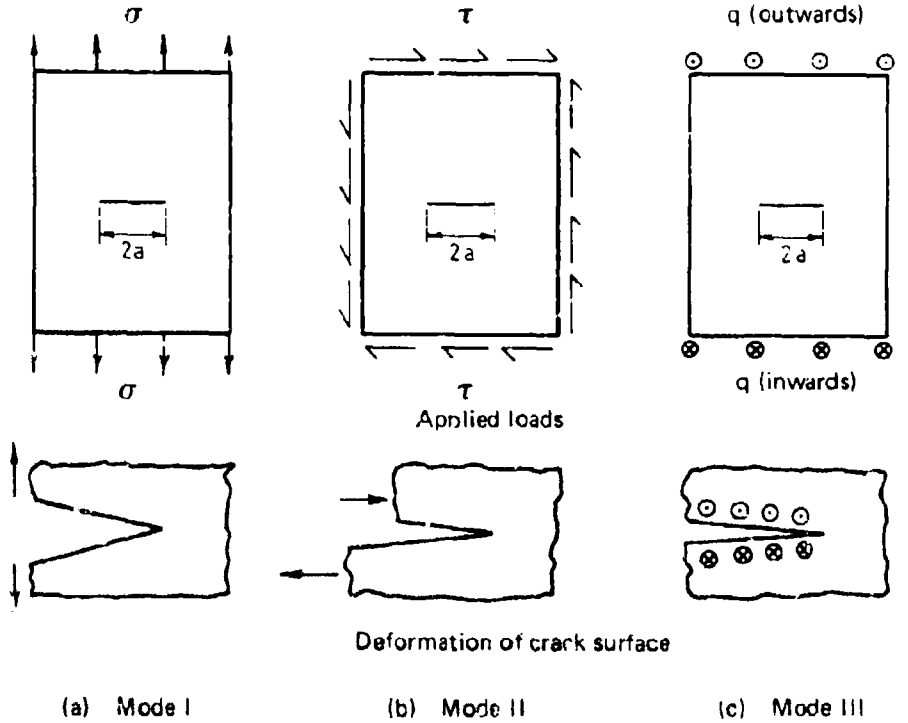

(a) Mode I (b) Mode II (c) Mode III

FIG. 4. THE THREE MODES IN FRACTURE MECHANICS

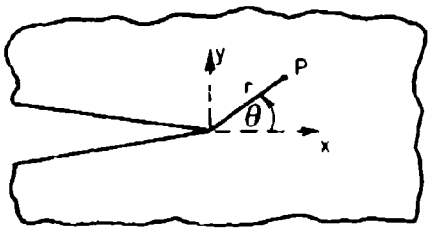

FIG. 5. POLAR CO-ORDINATES AT CRACK TIP

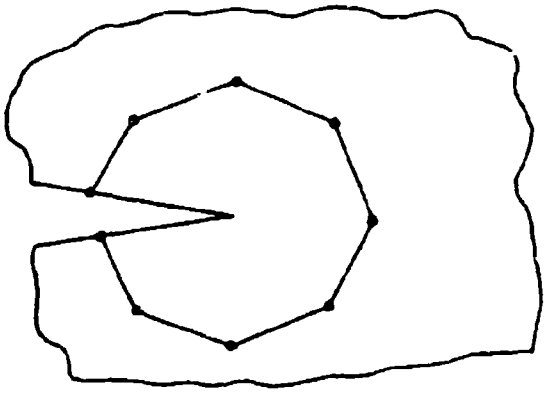

FIG. 6. CRACK TIP ELEMENT FOR FINITE ELEMENT ANALYSIS

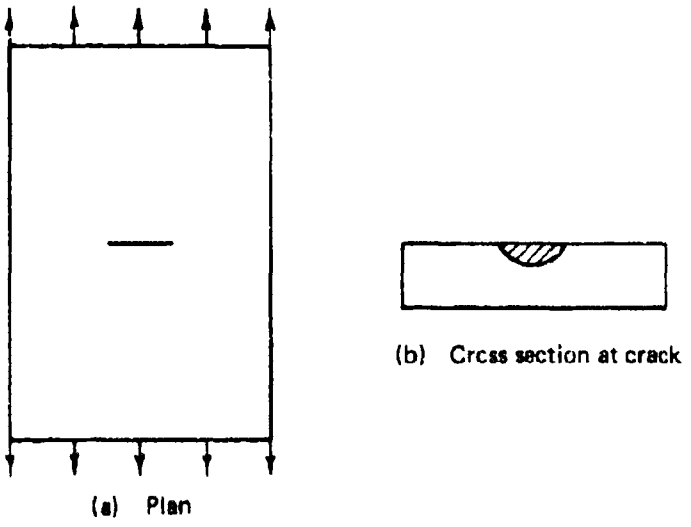

FIG. 7. THE SURFACE FLAW

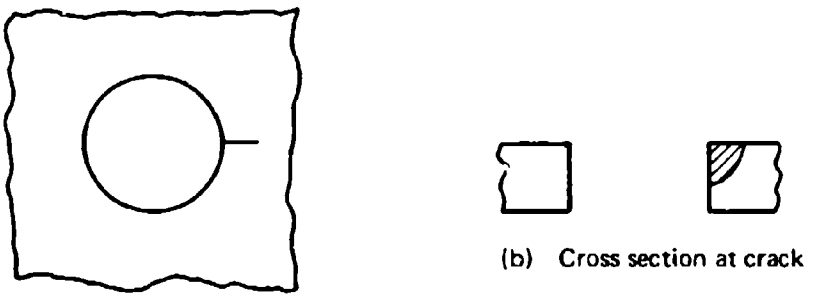

FIG. 8. CRACKED BOLT HOLE

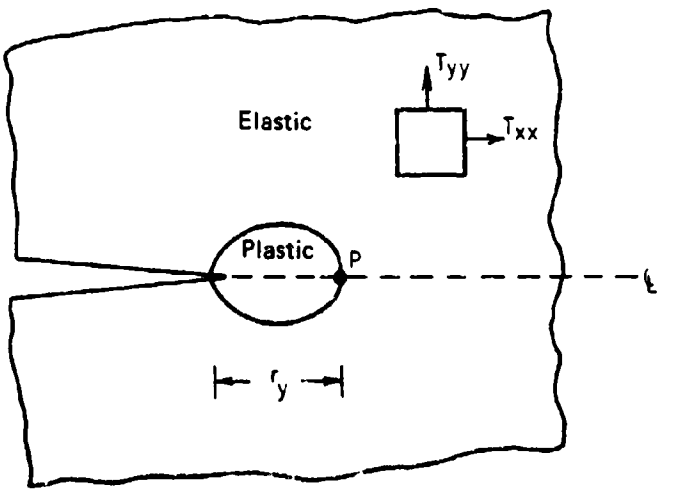

FIG. 9. PLASTIC ZONE AT CRACK TIP

Material	Stress-strain curve	Stress near crack tip varies as	Strain near crack tip varies as	Stress-strain product varies as
Elastic	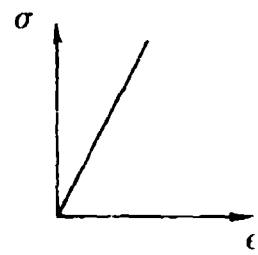	$\frac{1}{r^{1/2}}$	$\frac{1}{r^{1/2}}$	$\frac{1}{r}$
Elastic perfectly plastic	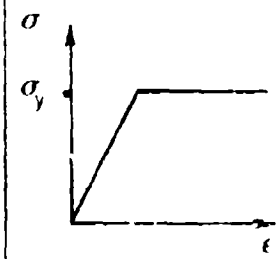	$\frac{1}{r^0}$	$\frac{1}{r}$	$\frac{1}{r}$
Work hardening	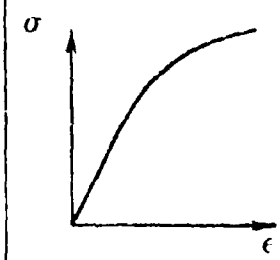	$\frac{1}{r^p}$ $(0<p<\frac{1}{2})$	$\frac{1}{r^{1-p}}$	$\frac{1}{r}$

FIG. 10. STRESS AND STRAIN VARIATION AT SMALL DISTANCE 'r' FROM CRACK TIP FOR DIFFERENT MATERIAL BEHAVIOUR

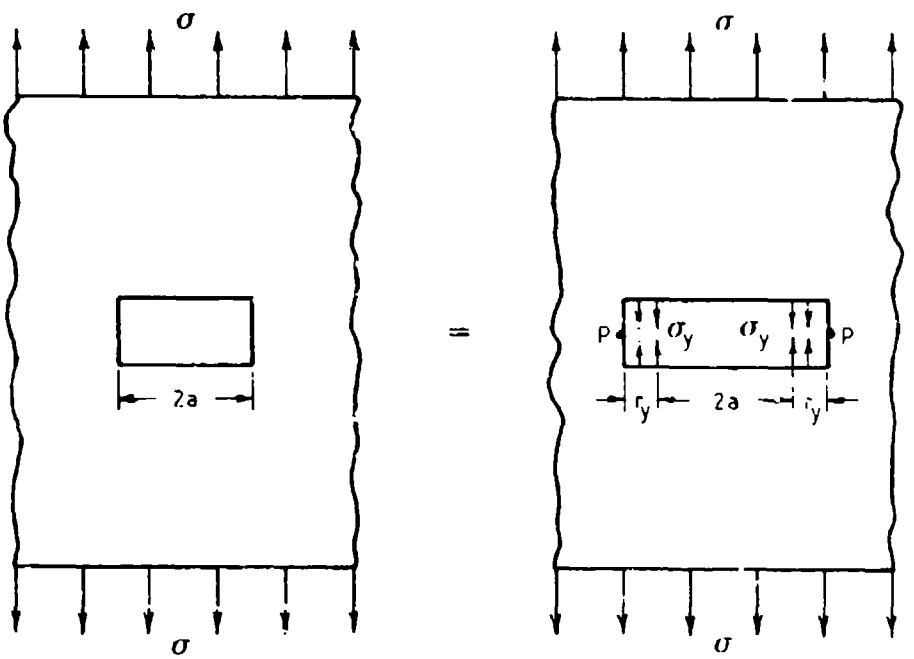

FIG. 11. THE DUGDALE MODEL OF CRACK TIP PLASTICITY

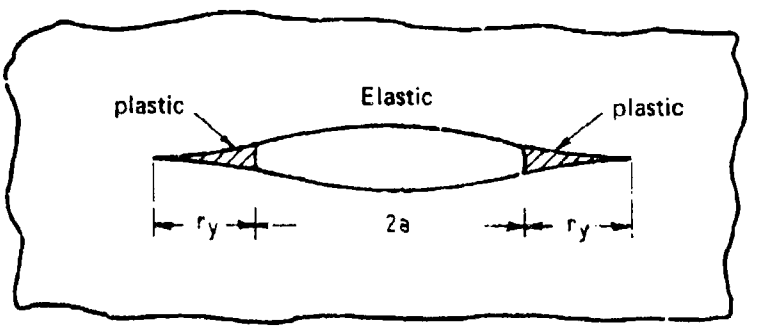

FIG. 12. SHAPE OF PLASTIC ZONE IN DUGDALE MODEL

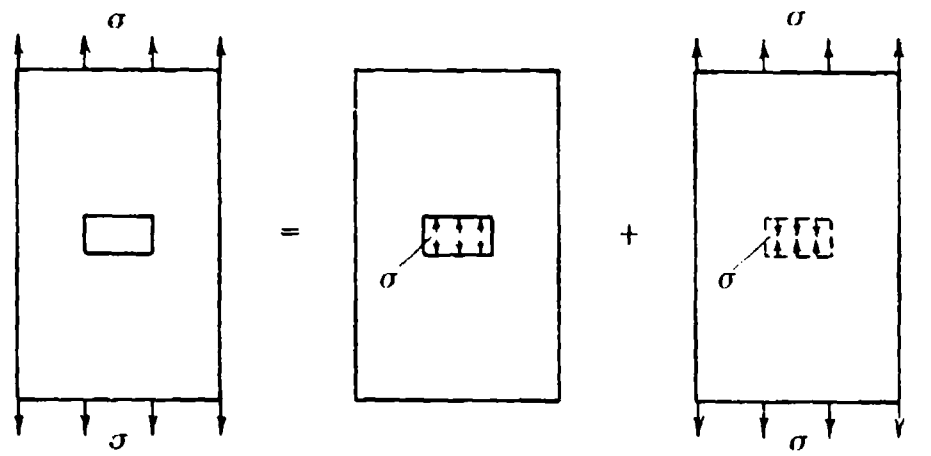

FIG. 13. SUPERPOSITION CASES FOR GRIFFITH PROBLEM

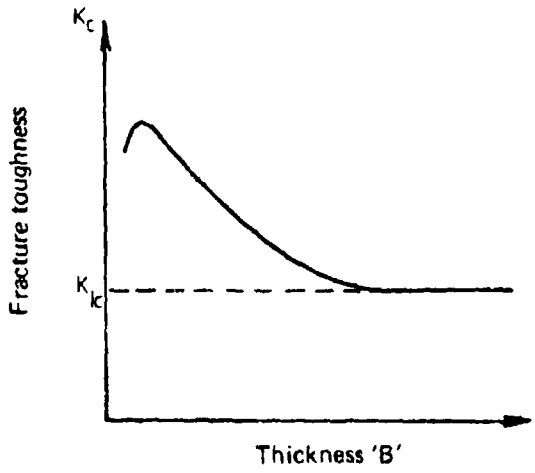

FIG. 14. VARIATION OF FRACTURE TOUGHNESS WITH PLATE THICKNESS

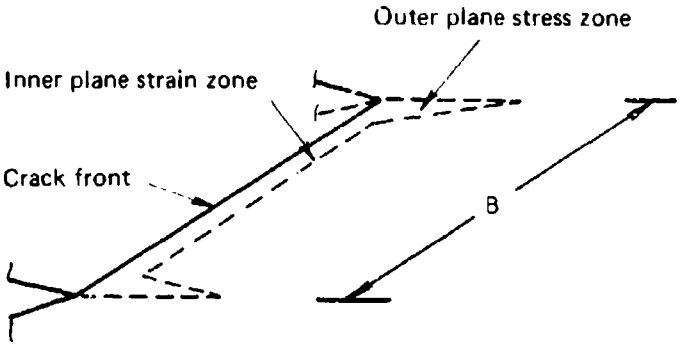

FIG. 15. VARIATION IN SIZE OF PLASTIC ZONE AHEAD OF CRACK TIP THROUGH THICKNESS OF PLATE

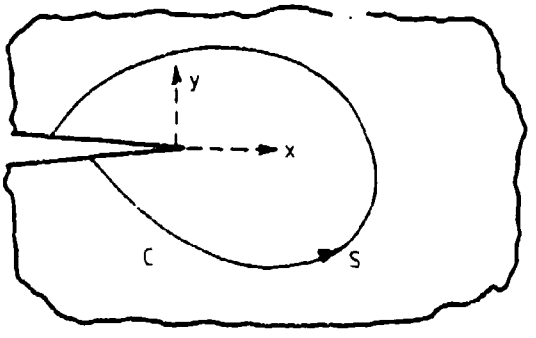

FIG. 16. AN INTEGRATION PATH 'C' FOR J-INTEGRAL

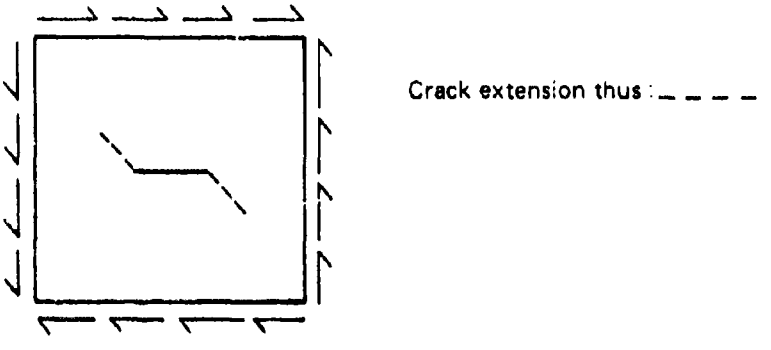

FIG. 17. OBSERVED CRACK EXTENSION UNDER SHEAR LOADS (MODE II PROBLEM)

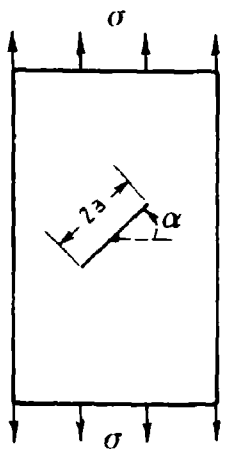

FIG. 18. TENSION PANEL WITH OBLIQUE CRACK

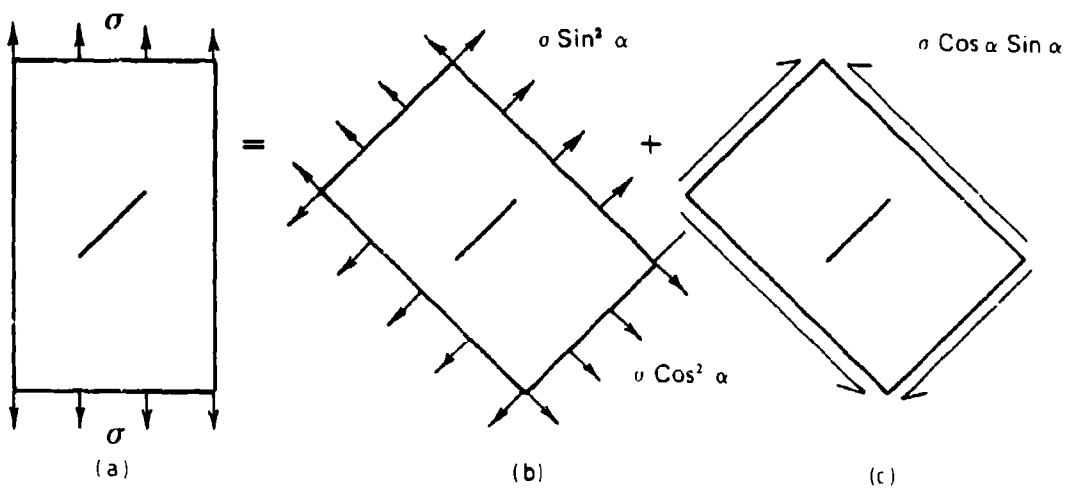

FIG. 19 TENSION PANEL WITH OBLIQUE CRACK AS SUPER POSITION OF MODE I AND MODE II PROBLEMS

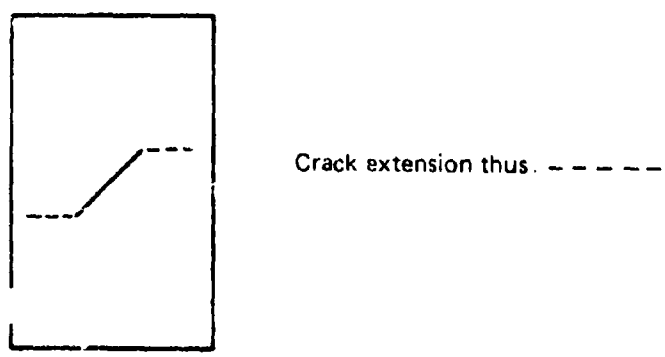

FIG. 20. CRACK EXTENSION IN TENSION PANEL WITH OBLIQUE CRACK

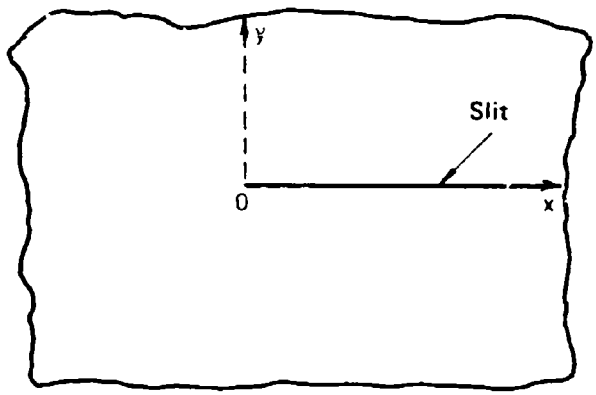

FIG. A1 INFINITE REGION WITH SLIT

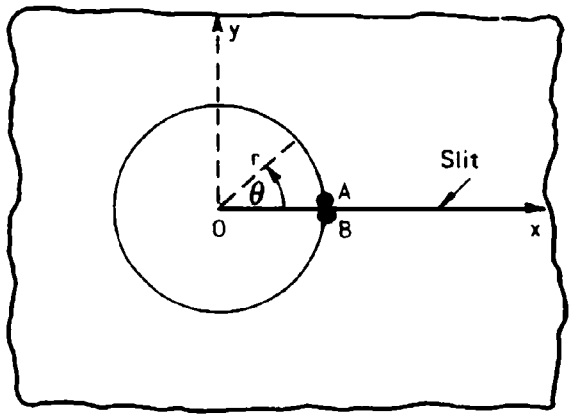

FIG. A2. CO-ORDINATE SYSTEMS FOR REGION WITH SLIT

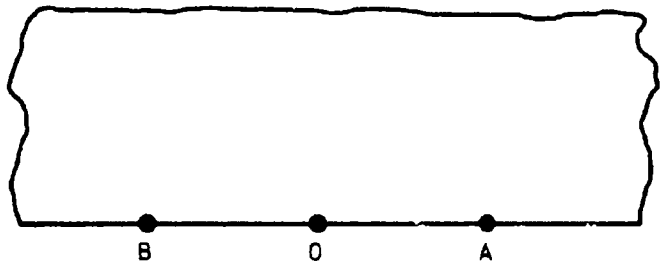

FIG. A3. CONFORMAL MAPPING OF REGION OF FIG. A2 BY SQUARE ROOT FUNCTION

DISCUSSION

QUESTION—*Dr. A. K. Head (CSIRO, Division of Tribophysics)*

The application of elastic fracture mechanics to static real fracture is often "justified" by saying that the plastic zone is small.

In applying FM to fatigue it is seen that this justification could be taken in two ways; that the size of the plastic zone is small or that the plastic deformation in the zone is small. The former is probably true enough in fatigue but the latter is not (when the total plastic deformation over the number of cycles is considered). Is there any indication as to the relative importance of size of zone smallness or total plastic deformation smallness for the validity of fracture mechanics?

AUTHOR'S REPLY

Whilst some analyses of fatigue crack growth which start from a postulated dislocation model have led to the typical fracture mechanics law of Equation (8.2.1) - see, for instance, B. A. Bilby and P. T. Heald, Crack Growth in Notch Fatigue, Proc. Roy. Soc. (A), vol. 305, pp. 429–39, 1968—the basis for all such laws is generally considered to be essentially empirical. However, it might be expected that the stress intensity factor would be a key parameter in any crack problem, either static or fatigue, where the geometric size of the plastic zone was small compared with the crack length because, in that case, a study of elastic-plastic solutions shows that, in the vicinity of the crack tip, all the apparent physical parameters of the problem (load, crack size, general geometry) appear combined in the stress intensity factor. (This, however, is not the case for large-scale yielding.)

QUESTION—*J. C. Ritter (MRL)*

I wish to add to Mr. Hoskin's observation that the commonly accepted formulae for estimating the plastic zone size, particularly in plane strain, are arbitrary and give approximate answers. These estimates apply only to the ideal case of homogeneous deformation at the crack tip. Real structural materials show varying degrees of non-uniform deformation determined by the presence of different phase particles in the microstructure. The resulting crack-tip deformation may be fairly uniform, as with quenched and tempered steels, or it may be broken up into bands of intense shear as with some age hardening aluminium alloys. The estimated plastic zone size then has little meaning; for example, K_{Ic} test specimen dimensions based on this estimate become spurious.

AUTHOR'S REPLY

My remarks on the approximate character of the formulae (4.2.6), (4.2.7) and (4.2.8) for estimating the size of the plastic zone were in the context of the classical continuum theory of plasticity. This last, of course, does not concern itself with microstructure phenomena and I could not comment on the added uncertainties associated with the type of effect raised by the questioner.

QUESTION—*Mike Murray (CSIRO, Division of Tribophysics)*

Mr Hoskin in his talk rightly, I think, implied that it was not possible to determine fracture toughness for a material without first fracturing it. I have been interested in this fact, and wonder whether one should be able to predict fracture toughness for a homogeneous, isotropic, elastic-plastic solid. Although no real solid would be expected to approximate closely to this description, the description itself represents an ideal limit from which we may gain some insight.

If we suppose our ideal solid to be

(*a*) capable of fracturing in the first place,

(*b*) capable of setting up a plastic zone around the crack tip, and

(*c*) that sufficient energy is dissipated during a stable propagation, so that we can ignore surface energy,

then it is difficult to conceive of any dimensional parameters other than E (Young's modulus for an opening mode crack) and σ_y (yield or appropriate flow stress) which could have a bearing on this problem. For the simplest dimensional analysis we require in addition a length, l, so that we might write

$$[G_{Ic}] \simeq \frac{[E]^2}{[\sigma_y]}[L]$$

We take $[\sigma_y]^{-1}$ because usually toughness increases as σ_y decreases. We find that if we write

$$[G_{Ic}] \simeq A\frac{E^2}{\sigma_y}b \qquad (A \text{ is a dimensionless constant})$$

and obtain σ_y from hardness ($\simeq 7\%$ strain), set $A \simeq 1$, and set L equal to about one atomic distance (abandoning the continuum solid), the equation *very roughly* gives the observed answer.

Use of the normal linear elastic fracture mechanics equation for plane strain plastic zone size

$$\sigma_y \quad \frac{1}{6\pi}\cdot\frac{E\,G_{Ic}}{(1-\nu^2)\,\sigma_y^2}$$

leads to a plastic zone size

$$r_y \simeq \frac{E^3}{\sigma_y^3}b$$

This equation then represents the automatic long range constraint that the ideal body places on the crack tip plastic zone size.

I must emphasise that this reasoning is highly speculative and may turn out to be valueless.

Dr. Ritter in his previous question has alluded to the idea of a short range effect which can overcome the long range one if particles of a second phase are present in a body. He suggests that the plastic zone concept might become inapplicable, and indeed for some cases he may be right. However, I have investigated one system (a WC–Co aggregate) which I regard as an extreme case of the short range effect, and find that it can be adequately described using a modified form of the normal LEFM approach. The limitation on plastic zone size in this case is simply the interfacial separations of the particles.

AUTHOR'S REPLY

Presumably if one could carry out a satisfactory elastic-plastic analysis of a cracked structure, and if one could then apply the Irwin–Orowan energy balance concept one would get a formula for the critical stress in which some quantity analogous to the fracture toughness appeared as a combination of the material constants of classical continuum analysis, such as Young's modulus and the yield stress. This was the type of analysis carried out by Goodier and Field (Reference 56 of the paper); see also P. L. Key, The Effect of Local Yielding on the Strain Energy Release Rate, Trans. of ASME, Journal of Basic Engineering, vol. 91, pp. 852–54, December 1969. However, as indicated in the paper, the results of such analyses—which generally involve substantial approximations—are not always easily interpreted. (Of course, whilst general energy considerations would suggest the reasonableness of the Irwin-Orowan concept as a necessary condition for fracture, it may not be a sufficient one and results derived from it may not be correct.) The point raised in Section 6.3 of the paper about changes in heat treatment which leave the standard elastic and plastic material constants unaltered but which may cause large changes in fracture toughness also is relevant here; if this turns out to be the general situation it is difficult to see how the fracture toughness would ever be reliably predicted by a classical continuum analysis.

The dimensional analysis presented by Dr. Murray is interesting but I do not have a clear understanding of the significance of the length parameter which it is necessary to introduce. I am not sufficiently familiar with the metal physics aspects of fracture to know whether fracture toughness can be adequately correlated with some linear dimension characterising the microstructure.

DATA ACQUISITION AND INTERPRETATION

FLIGHT LOAD RESEARCH AT A.R.L.

by

A. K. PATTERSON and C. K. RIDER

SUMMARY

Flight load research at ARL since 1947 has followed two distinct lines. One has been related to the need to establish valid flight load statistics for fatigue life estimation. The other has been the measurement of stress distribution using specially instrumented research-flight aircraft. Progress in the two activities has not been uniform, with significant advances being closely related to technological developments.

1. INTRODUCTION

ARL Report SM87—A Programme of Flight Load Research—was published[1] in February 1947 by the CSIR Division of Aeronautics. It set out the purpose and methods for routine monitoring of flight loads, but also argued the case for special research test flights to "study the correlation between accelerometer readings at the c.g. with peak stresses at the critical sections of the wings, particularly under dynamic loading conditions".

Nearly thirty years later, the same dichotomy of flight load research applies, albeit with a change in emphasis from civil to military aircraft. In consequence, it should be instructive to trace the development of flight load research at ARL and seek to identify factors which have led to significant progress

2. ROUTINE MONITORING OF FLIGHT LOADS

The aim of routine monitoring is to obtain valid statistical load data. Normally this implies the need for long-term sampling. To obtain good data it is essential that the instrumentation is reliable and data collection and extraction is simple and unambiguous. The NACA designed V-g Recorder which traces out an envelope of speed and load on a smoked-glass slide by the action of a stylus was used extensively by ARL from 1947 until 1952.[2] The instrument is a simple mechanical device, it was fairly easy to install and it appears to have been very reliable. Donely of NASA, in a paper to the Fifth ICAF Symposium in 1967, reported on a programme which collected more than 20,000 hours of data with V.g. recorders, an impressive performance since the data extraction is a tedious manual operation.

By its nature, the V-g recorder provides useful data only on the largest positive and negative loads occurring during the period for which each slide remains in the recorder. Frequent changes of recording slides cause serious logistic problems for a programme of routine monitoring. Infrequent changes lead to ambiguity in data interpretation, and reduction in the range of the load spectrum defined by the programme.

For these reasons, in 1952, ARL switched[4] to the RAE designed Counting Accelerometer. This instrument contained a large number of mechanical counters for recording the number of exceedances of positive and negative thresholds of acceleration, together with airspeed and altimeter indicators. An automatic camera, operated by a timing and relay system took photographs at ten-minute intervals. It is not surprising that, with such complexity, reliability was poor. Data returns[5] of less than 50% of the recording period were normal. The solution was to simplify the system by removing the automatic camera, and to read the counters when the aircraft was on the ground. Naturally this also removed the need for the airspeed and altitude indicators. Subsequently, ARL obtained nearly 18,000 hours of satisfactory recording[6] over a three year period of operations by two DC-6 aircraft owned by ANA.

Further simplification led to the RAE Fatigue Meter with a standard set of six acceleration threshold counters. With this instrument, a sample of 70,000 hours of flight load data[7] was obtained from ten Viscount aircraft owned by TAA. These large samples provided solid statistical data for flight load spectra applicable to aircraft operations similar to that for Viscount aircraft. However, because speed and height had been deleted from the data, it was no longer possible to determine either the altitude or location at which flight loads had been recorded, and it was not practical to use the flight load spectra for new aircraft operating either at much higher or much lower altitudes than the DC-6 or Viscount. Nor can the data be re-assessed to provide altitude-classified power spectra for the definition of gust loads in Australia. This has created a problem for assessing new aircraft designed against[8] the current MIL-SPEC.

More than 20 years after their first use in Australia, fatigue meters are monitoring the safe lives of Mirage III o and F-111c aircraft of the RAAF. For the F-111C, the variable geometry requires a need for more than one set of counters, thereby removing the simplicity and lack of ambiguity which previously characterised the instrument. For the Mirage, the wide range of

speeds at which loads could be applied to the structure created a need to fit V-g-h recorders[9] to five squadron aircraft in 1973. The V-g-h recorders were designed at ARL[10] to sample acceleration (g) twenty times each second, and speed (V) and height (h) once each second. Data were recorded in the form of frequency shift keying, using a ternary coding system, on a Philips EL 3002 cassette unit.

These recorders proved to be more reliable than the fatigue meters installed in the same aircraft. However the data extraction for the 650 hours of continuous recording proved to be a most time-consuming operation. Nevertheless, a valuable statistical sample of flight loads for a fighter aircraft was obtained and a useful check made on the load cycle counting accuracy of the fatigue meter. This confirmed[11] an earlier ARL investigation[12] which had revealed an uncertainty in the counting thresholds of fatigue meters. The V-g-h recorders also provided a picture of the frequency at which linking manoeuvres were performed. These are manoeuvres in which significant cycles of load occur about high mean levels of load and consequently are not recorded by the fatigue meter.

It is our opinion that the complications in load monitoring on the Mirage IIIo and F-111C aircraft are indicative that the fatigue meter's useful life may be limited. Currently we are working with BAC (Australia) Pty. Ltd. to develop a "range pair counter" for monitoring fatigue at 12 locations in an aircraft structure.[13] Strain cycles in the form of range pairs between every pairing of 15 different strain levels are counted and stored in the magnetic core memory of the unit. Read-out of the fatigue history may be obtained, as required, by using a digital magnetic tape cassette recorder.

The instrument, now called AFDAS (Aircraft Fatigue Data Analysis System) is based on two principles: firstly, that the most direct measure of stress which is available should be the one used; and secondly, that only data relevant to the fatigue calculation should be recorded. The first principle is met by using electrical resistance strain gauges, and the second by recording data as range pairs. It is considered that this approach by-passes the accuracy and computational problems inherent in obtaining stress from mathematical models which require measurements of aircraft state and motion. The data processing task is also greatly simplified in comparison with continuous recording systems which of necessity require the reading and rejection of data not required for fatigue analysis. The AFDAS equipment has the further advantage of potentially high reliability due to its completely solid state electronics.

Following extensive bench testing of the prototype, the AFDAS principle was confirmed by cross-reference to a continuous recorder simultaneously carried on four flights by a Mirage test aircraft. Reliability evaluation is currently in progress.

3. RESEARCH TEST FLIGHTS

A review of the last thirty years of test flight instrumentation reveals that progress has occurred in jumps rather than at a uniform rate. Techniques used in 1954 for measuring flight strains in a Dove,[14] in 1962 on a Vampire Trainer[15] and in 1966 on a Prospector agricultural aircraft[16] are quite similar to each other and indeed to the methods outlined in 1947 by ARL Report SM87. However significant advances in both the scope of instrumentation and the techniques for recording occurred between 1968–73 with the introduction of first analogue,[17] and then digital[18] magnetic tape recording of flight load data. The stimulus for these rapid advances was provided by the need to measure both temperature and strains throughout the structure of the RAAF Mirage IIIo aircraft.

The accuracy and detail in the load data which was obtained with the new tape recording system enabled us to establish with certainty such factors as the non-linearity of wing-spar strain/g under manoeuvre loads, and dynamic amplification of strain/g under gust loading. Table 1, extracted from SM Note 401[19] illustrates the weight of data which the tape recording system enabled us to apply to our flight load analysis.

A typical configuration of the digital Data Acquisition System (Fig. 1) allows 50 channels of data to be sampled 60 times per second for one hour. Submultiplexing has also been used to sample variables such as airspeed, altitude, fuel weight at a slower rate. Each sample is converted to a 12 bit digital word in "offset binary" code and these words are written as 2 bytes of 6 parallel bits on the tape, the seventh track being used for a parity check character. Data is blocked into records in a fully computer compatible format, using long records of 15,000 bytes so that inter-

record gaps take only 5% of tape length. During gap periods, incoming data is stored in a special "first-in, first-out" buffer memory so that a continuous time history is recorded. Use of a computer-compatible format eliminates the need for a special ground-replay station. Accuracy of recording approaches 0·1% and 10^7 data points are recorded on a typical research flight.

This system has been the subject of continuing development, and now includes remote multiplexing, analogue to digital conversion modules, and extended digital input facilities. To facilitate preliminary in-field evaluation of flight data, a quick-look system centred on a mini-computer has been developed.

In retrospect, the development of the present system can be closely related to the rapid expansion in the use of digital computer installations during the 1960s. In fact, since a PDP-10 computer was installed at ARL in 1968, the analysis of tape-recorded flight data has taken a major share of the core-time capacity of the installation.

It is interesting to compare the complexity of instrumentation for flight tests of the Vampire MK35 Trainer Aircraft[15] (1962) where "all [instrumentation] wiring in the aircraft was installed by the RAAF, in accordance with a simple wiring diagram supplied by ARL" with the flight test requirements for the Mirage fatigue investigation[20] (1970) where 182 drawings are listed for the wiring modifications to the test aircraft A3-76.

The new system has also changed drastically the staffing requirments for analysing the test data. In the days of photographic trace recording the most time-consuming function was the reading of traces,[21] and the Laboratories maintained a number of technical assistant positions for that purpose. The requirement now is for electronic designers, programmers and data analysts who can devise systems for ensuring the validity of the large samples of data. Such people must make decisions upon which depends the accuracy of large scale tests. Consequently they require the training and background which leads to professional qualifications.

4. FLIGHT LOAD RESEARCH DEVELOPMENTS DURING THE NEXT DECADE

We have seen that the techniques in use for flight load monitoring have not varied greatly since 1955 because the necessity for reliability in long term monitoring programmes required a simple electro-mechanical device such as the fatigue meter. The high reliability of modern solid state circuitry now permits the development of equipment with considerable data processing capacity for monitoring stress at a number of critical locations in an aircraft structure. At the same time the modern computer provides means of handling a greatly increased quantity of recorded data. In our opinion, the complexity and cost of the next generation of aircraft will provide the stimulus required to perfect new systems for flight load monitoring.

The situation for research test flying is quite different, with significant developments in recording techniques occurring in the last ten years. The data acquisition system now in use requires only minor modifications to be representative of the best of current technology. Its capacity is also compatible with modern data processing equipment.

The most likely changes in the next ten years will be the replacement of magnetic tape as the storage medium by magnetic bubble memories or charge coupled device memories. The present trend from analogue signal conditioning to digital processing will no doubt gather momentum, with increased use of digital filtering and data compression techniques.

It is interesting to note that the quality of the basic load monitoring transducer, the accelerometer, has improved steadily during the last fifteen years as a result of a quite different stimulus—the development of inertial guidance for space research. The development in strain gauge technology is also interesting. Ten years ago, semi-conductor strain gauges appeared to offer a promising alternative to the traditional resistance gauges. However, problems of temperature sensitivity and unreliability became apparent while simultaneous development of solid state amplifiers reduced the need for high gauge output. Additionally, the adoption of modern manufacturing techniques has improved both the reliability and performance of resistance gauges to a very high standard. The foil strain gauges (Baldwin Lima Hamilton FAB-12-12513) used[22] on Mirage A3-76 are clearly superior to the wire gauges (AB-11) used for Vampire flight tests in 1962. Consequently it appears unlikely that major changes in the flight load transducers will occur in the next ten years.

5. CONCLUSION

This review of techniques for flight load research at ARL has indicated that progress in flight load monitoring and research test flight instrumentation has been sequential, rather than parallel. The time scale of significant developments has been in intervals of around 15 years, similar to that for new aircraft type development, but significant influences have been exerted by developments in electronics, particularly those related to digital computers. It is likely that the trend towards miniaturisation of special purpose computers will result in the selection and compression of flight load data before recording, particularly for routine flight load monitoring. The increasing cost of aircraft replacement will provide the justification for this more sophisticated and expensive flight load monitoring equipment.

REFERENCES

1. Hooke, F. H., and Wills, H. A. — A Programme of Flight Load Research. CSIR Division of Aeronautics Report SM87, February 1947.
2. Hooke, F. H., and Baum, Q. — Gust Research with V-g Recorders on Australian Routes. ARL SM Rpt. 241, April 1956.
3. Donely, P., Jewel, J. W., Jnr., and Hunter, P. A. — An Assessment of Repeated Loads on General Aviation and Transport Aircraft. 5th ICAF Symposium, May 1967.
4. Baum, Q., and Hooke, F. H. — Counting Accelerometer Results from a Bristol Freighter Aircraft Operating in South-Eastern Australia. ARL S & M Note 207, August 1953.
5. Bacon, N. E. — Interim Note on Counting Accelerometer Results Obtained from Viscount Aircraft. ARL S & M Note 227, May 1956.
6. Higgs, M. G. J. — Analysis of Flight Loads on DC-6 Aircraft Obtained with Counting Accelerometers in Australia. ARL S & M Note 269, March 1961.
7. Bruce, G. P., and Hooke, F. H. — Flight Loads on Viscount Aircraft in Australia. ARL S & M Report 284, November 1961.
8. Austin, W. H., Jnr. — Development of Improved Gust Load Criteria for United States Air Force Aircraft. WPAFB, ASD Tech. Report SEG-TR-67-28, September 1967.
9. Anderson, B. E., Rider, C. K., Sparrow, J. G., and Thomson, M. R. — Preliminary Results from V-g-h Recorders in Five Mirage Aircraft. ARL Struc. Note 417 (Restricted), August 1975.
10. Patterson, A. K., and Adams, M. T. — Two Low Cost Aircraft Data Acquisition Systems. Institute of Instrumentation and Control Australia. 1975 Symposium.
11. Anderson, B. E., Howard, P. J., and Sparrow, J. G. — Setting and Firing Levels of Two Mirage Fatigue Meters. ARL Struc. Note 418 (Restricted), September 1975.
12. Nilsson, S. I. — An Examination of the Precision and Constancy of Fatigue Meters. ARL/SM Note 315, December 1966.
13. Ford, D. G., and Patterson, A. K. — A Range Pair Counter for Monitoring Fatigue. ARL/SM Tech. Memo 195, January 1971.
14. Brown, R. P., Forrester, C. L., and Hooke, F. H. — Strain Measurements in Flight on a Dove Aircraft. ARL/SM Tech. Memo 39, November 1954.
15. Barnard, J. M. H., and Gee, S. W. — Flight Tests of Vampire MK35 Trainer Aircraft. ARL/Sm Note 275, August 1962.
16. Visick, J. — Loading Actions on an Agricultural "Prospector" Aircraft. ARL/SM Note 309, August 1966.
17. Patterson, A. K., Sherman, D. J., and Thomson, M. R. — Mirage Stage 2 Fatigue Investigation Part 1—The Data Recording and Storage System. ARL/SM Note 380, September 1972.
18. Anderson, B. E. — Assessment of Some Aspects of the Aermacchi MB326H Fin Fatigue Tests. ARL/Struc. Note 421, 1976.
19. Rider, C. K., Sparrow, J. G., — Variation in Wing Strains Measured During Three Low Level Flights by Mirage A3-76 in Severe Mechanical Turbulence.

Thomson, M. R., and Verinder, F. E. — ARL SM Note 401, December 1973.

20. Moody, E. S., and Denchy, D. R. — Mirage Stage 1 Fatigue Investigation Part III—Instrumentation of Aircraft. ARL SM Note 348, January 1970.

21. Trayford, R. S. — Flight Load Spectra and Strain Prediction Equations for Ceres Aircraft. ARL Flight Note 41, March 1967.

22. Gee, S. W. — Mirage Stage 1 Fatigue Investigation Part 2—Gauging Mirage III-o Aircraft for Flight Testing. ARL SM Note 343, July 1969.

TABLE 1
Mirage A3-76: Flight 2 135

Ratios of RMS values of vertical acceleration (Z) and wing stresses for 100 second sample periods of severe turbulence flight data
(Sample rate 60 sec)

Sample no.	Flight direction	Tas (kts)	Fuel (gals)	RMS values		Ratios of RMS values			
				sZ (g)	s38T (ksi)	$\frac{s38T}{sZ}$ (ksi/g)	$\frac{s1C}{s38T}$	$\frac{s2T}{s38T}$	$\frac{s18T}{s1C}$
				Fuel Status 1					
1	W	391	773	·191	1·26	6·60	·569	·621	1·08
2	SW	436	734	·207	1·42	6·86	·565	·601	1·02
3	SW	397	706	·232	1·56	6·72	·563	·604	1·04
4	SW	410	675	·309	2·05	6·63	·571	·618	1·06
5	SW	411	655	·258	1·71	6·63	·566	·608	1·08
6	SW	416	636	·295	2·01	6·81	·570	·613	1·04
				Fuel Status 2					
7	SW	426	597	·317	2·10	6·621	·571	·617	1·03
8	SW	415	578	·289	1·87	6·46	·563	·608	1·06
9	NE	436	527	·271	1·58	5·83	·561	·604	1·38
10	NE	452	508	·345	2·05	5·94	·571	·622	1·26
11	NE	437	488	·375	2·16	5·75	·572	·621	1·27
12	NE	444	468	·307	1·81	5·90	·567	·608	1·29
13	NE	432	449	·340	1·91	5·62	·567	·621	1·34
14	NE	417	430	·254	1·47	5·79	·561	·603	1·27
15	SW	380	415	·242	1·50	6·18	·563	·609	1·04
16	SW	390	395	·326	2·01	6·17	·568	·612	1·06
17	SW	395	375	·278	1·74	6·25	·561	·607	1·08
18	SW	405	357	·285	1·77	6·21	·560	·606	1·08
				Fuel Status 3					
19	NE	425	293	·336	1·92	5·70	·567	·610	1·26
20	NE	424	273	·375	2·07	5·53	·566	·612	1·31
21	NE	432	254	·255	1·43	5·61	·560	·601	1·26
22	NE	395	200	·220	1·21	5·51	·556	·601	1·23

Extract from SM Note 401 (Reference 19).
Note: 38T, 1C, 2T are strain gauge positions on starboard wing; 18T is on port wing.

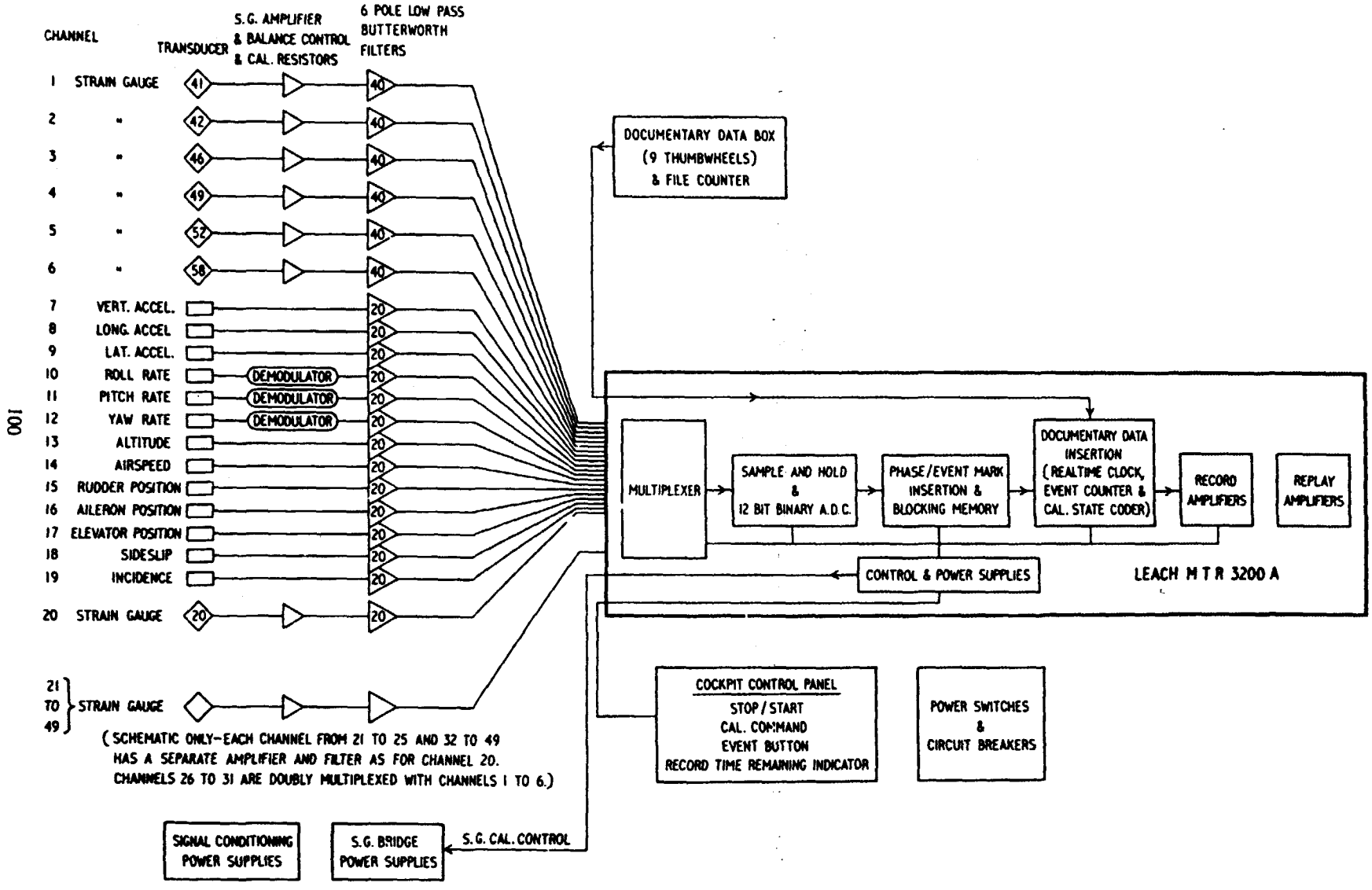

FIG. 1 LEACH DATA ACQUISITION SYSTEM

DISCUSSION

QUESTION—*H. A. Wills (Retired)*

About 1946, as part of ARL's general attack on the investigation of flight loads, Radok worked out some theory for the dynamic response of an aircraft, regarded as a resilient body, to atmospheric disturbances. This he later followed up with flight measurements on an instrumented Lincoln aircraft flown in turbulent conditions generated in winds over Mt. Elephant and Cape Woolamai--and obtained a measure of agreement with the theory.

It seems to me that a knowledge of the dynamic response of aircraft to impulsive loads would be valuable information for comparing the effects of different mission load spectra on a given aeroplane.

Has anyone done any recent work on this aspect?

Author's Reply

The research to which Mr. Wills refers was aimed at developing an analytical theory for predicting flexural and torsional deformations under gust loading, and some measure of agreement was obtained with experimental results.[1] However, by 1953, it was clear that statistical methods developed for the analysis of random time series were particularly suitable for the prediction of aircraft response to atmospheric turbulence.[2] The P.S.D. or power spectral density method establishes an invariant transfer function $T^2(f)$ between a specific aircraft response and a random gust input of constant "scale-length" and intensity. The transfer function may be calculated or experimentally determined. Once established, it is used to predict response exceedance statistics for different missions or anticipated aircraft usage.[3]

Since 1960 gust research at ARL has concentrated on the experimental determination of the power spectra of atmospheric turbulence at different flight altitudes and of the response of military aircraft to that turbulence. In 1963 we co-operated with the RAE to determine the scale-length of high altitude clear air turbulence which is commonly associated with upper level jet-streams.[4] In 1969 we measured the P.S.D. parameters of severe low level turbulence near Katoomba, New South Wales, and the response of a specially instrumented Mirage IIIo aircraft of the RAAF.[5] These results were used by Sherman to estimate the gust loading of a typical squadron aircraft.[6] More recently, measurements of gust input and response have been made for the Macchi MB326H trainer aircraft of the RAAF, and ground resonance tests have been carried out to provide accurate structural data for the development of a mathematical model of response.[7]

References

1. Radok, J. R. M., and Stiles, L. F.	The Motion and Deformation of Aircraft in Uniform and Non-uniform Atmospheric disturbances. CSIR Aero. Research Report ACA-41, 1948.
2. Press, H., and Mazelsky, B.	A Study of the Application of Power-Spectral Methods of Generalised Harmonic Analysis to Gust Loads on Airplanes. NACA Tech. Note 2853, 1953.
3. Hoblit, J., *et al.*	Development of a Power-Spectral Gust Design Procedure for Civil Aircraft. FAA Tech. Rept. ADS-53, 1966
4. Rider, C. K.	Project Topcat: A Study of the Gust Velocity Power Spectra for Six Flights in Clear Air Turbulence. ARL/SM Report 317, 1967.
5. Rider, C. K., Thomson, M. R., and Verinder, F. E.	Measurement of Extreme Mechanical Turbulence During Low Level Flights by Mirage A3-76. ARL/SM Report 333, 1971.
6. Sherman, D. J.	The Cumulative Exceedance Distribution for Accelerations Due to Turbulence Encountered by a Mirage. ARL/SM Tech. Memo 228, 1975.
7. Quinn, B., and Bailey, C. M.	Resonance Tests on a Macchi Aircraft. ARL/SM Tech. Memo 241, 1976.

GUST MEASUREMENTS AND THE N_0 PROBLEM

by

DOUGLAS JOHN SHERMAN

SUMMARY

The N_0 problem is the problem of interpreting level crossing counts of a process with a large number of small fluctuations superimposed on a lesser number of large fluctuations. It is shown that if fluctuations smaller than some specified amount are removed from a time history, the number of level crossings is reduced. An empirical formula is given for the amount of the reduction in a time series of atmospheric turbulence velocities.

NOTATION

Symbol	*Definition*	*Equation*
A	$A = \sigma_x/\sigma_w$	1.9
$\mathcal{AR}$	Aspect ratio	
a	Reference time	1.2
a	Parameter	3.2
b_1, b_2	Parameters	1.11
$C(\omega)$	Theodorsen function	2.4
C_{ij}	Range pair exceedance matrix component	
c	Wing chord	
D	Amplitude discriminant	
$F(\omega)$	Averaging factor to allow for spanwise variations in gust strength	2.8
F_{ij}	Matrix of range pair flags	
$\mathcal{F}\{\cdot\}$	Fourier transform	
f	Frequency (Hz)	
f_c	Cut-off frequency	2.1, 2.2
$H_x(f)$	Transfer function	1.3
$H_n^{(2)}(\omega)$	Hankel function of second kind	2.5
k	Wave number	2.9
L	Integral scale of turbulence	1.1
$L(p, q)$	Level crossing function	3.4
M_i	ith moment of $P_x(f)$	2.1, 2.2
$N(x)$	Frequency of up-crossing of level x	1.5
N_0	Frequency of up-crossing of level $\bar{x}$	1.6
$N_D(x)$	Frequency of up-crossing of level x when discriminant D has been applied to time series	
N_{00}	Value of N_0 with zero discriminant	3.1
P	Power spectrum P_x, P_w = Power spectrum of x, w, etc.	
P_1, P_2	Parameters	1.11
$p(\sigma_w)$	Probability density of σ_w	
$S(\omega)$	Sears function	2.3
t	Time	
t_i	Fraction of time spent in the ith altitude band	1.13
U	Relative velocity between observer and turbulent patch of air	
$w(t)$	Gust velocity	
$x(t)$	Aircraft response. In particular $x(t)$ is usually taken to be the vertical acceleration at the aircraft centre of gravity	
$x_D(t)$	The process obtained by smoothing $x(t)$ with an amplitude discriminant D	
$\bar{x}$	Mean value of x	
β_i	Coefficients	3.2, 3.7
δ	Amplitude discriminant	
σ	Standard deviation σ_x, σ_w = standard deviation of x, w	
ω	Non-dimensional frequency	2.6

INTRODUCTION

In turbulence, very small fluctuations in gust velocity occur very frequently and are responsible for a large number of level crossings in a stress time-history of an aircraft structure. This gives rise to the problem of defining the value of N_0, the mean frequency of upcrossings of the mean signal level. For a process with a von Karman power spectrum (e.g. idealised atmospheric turbulence) the N_0 value is theoretically infinite, and for practical atmospheric turbulence the N_0 value is exceedingly large and controlled largely by the dissipation of turbulence at wave lengths of the order of millimetres.

For aircraft response, the smoothing out effect when upgusts and downgusts occur simultaneously across the aircraft span must be taken into account. Even so, a large number of small load cycles are included in the response. It will be shown that if such small cycles are eliminated from a stress time-history, the parameter N_0 is reduced. Further the conventional formula for the gust-load exceedance curve must be modified.

The conventional method of counting or predicting numbers of load exceedances is inadequate because the inclusion or exclusion of small amplitude high frequency fluctuations can make great differences to numbers of exceedances. What is needed is a probability distribution of cycle amplitudes associated with the peaks occurring between each pair of levels at which upcrossings are counted or predicted.

1. THE METHOD OF CALCULATING GUST LOADS

In this section we will introduce the notation and the main assumptions involved in the power spectral density method of gust load analysis. The reader who is already acquainted with these may proceed directly to Section 2.

Atmospheric turbulence causes a large number of loads of minor severity on an aircraft, and a considerably smaller number of loads of greater severity. The expected number of loads of any severity can be estimated by either the "discrete-gust" method, or the so-called "power spectrum" method. Both methods have in common the fact that they can be divided into two parts. One part is the calculation of the aircraft response, which is only dependent on aircraft parameters (and, in the case of the power spectrum method, on the integral length scale of the turbulence). The other part is the calculation of the probability of occurrence of turbulence of different severities. This is a function of the part of the atmosphere through which the aircraft flies, but is independent of aircraft type.

Historically, the "discrete gust" method was developed first, and it is still satisfactory and very convenient for a non-flexible aircraft. It is the basis of the method adopted by the Engineering Sciences Data Unit (ESDU, May 1972)[1] but will not be further considered here. The "power spectrum" method is of greater generality, in that it can handle the case of a flexible aircraft. It is, however, of greater complexity because it requires the evaluation of two aircraft dependent parameters, and the evaluation of one of these—the parameter N_0—is, in some circumstances, an uncertain procedure. In the next section we will examine a significant problem involved in evaluating N_0.

The derivation of the power spectrum method is given by Press and Steiner (1958)[2] and the method has been adopted by the USAF (March, 1971).[3] Some recent determinations of the parameters defining the probability of occurrence of turbulence have been summarised by Garrison (1971).[4] Within a given patch of turbulence, the vertical velocity component, $w(t)$, is assumed to have a von Karman power spectrum,

$$P_w(f) = \sigma_w^2 \frac{2L}{U} \frac{1 + \frac{8}{3}(af)^2}{\{1 + (af)^2\}^{11/6}} \tag{1.1}$$

and this asymptotes to an $f^{-5/3}$ power law at high frequencies ($af \gg 1$). In this equation, U is the velocity of an observer relative to the turbulent patch of air, and f is an observed frequency.

L is the integral scale of turbulence, σ_w^2 is the variance of the velocity component, $w(t)$, and the reference time, a, is given by

$$a = 1{\cdot}339 \cdot 2\pi \cdot L/U \tag{1.2}$$

The reference time, a, is of the order of 10 seconds in many applications. (For example, an anemometer situated 10 m above the ground, with $L = 10$ m, and a speed of 8·4 m s, or an aircraft flying where $L = 200$ m at a velocity $U = 168$ m s.) A graph of $P_w(f)$ is given in Figure 1.

If the process, $w(t)$, is assumed to be a Gaussian process within the patch of turbulence under consideration, then so too is any linear function of $w(t)$. For example, the vertical acceleration of the aircraft, or the stress at some point on the aircraft, is commonly assumed to be a linear function of $w(t)$. Consider such a parameter, which will, for generality, be denoted $x(t)$. The aircraft is assumed to behave as a linear system with a transfer function $H_x(f)$, where

$$H_x(f) = \mathcal{F}\{x(t)\}/\mathcal{F}\{w(t)\} \tag{1.3}$$

with $\mathcal{F}\{\cdots\}$ being an operator to denote a Fourier transform. We have

$$P_x(f) = |H_x(f)|^2 P_w(f) \tag{1.4}$$

and because of the assumed Gaussian nature of the time series involved, Rice's[5] formula applies for the average frequency of upcrossings, $N(x)$, of the level x,

$$N(x) = N_0 \exp\{-(x-\bar{x})^2/2\sigma_x^2\} \tag{1.5}$$

where

$$N_0 = N(\bar{x}) = \left(\frac{\int_0^\infty f^2 P_x(f)\,df}{\int_0^\infty P_x(f)\,df}\right)^{1/2} \tag{1.6}$$

and

$$\sigma_x = \left\{\int_0^\infty P_x(f)\,df\right\}^{1/2} \tag{1.7}$$

is the standard deviation of the process $x(t)$. Equation 1.5 may be re-written in the form

$$N(x) = N_0 p(x)\,p(\bar{x}) \tag{1.5a}$$

where $p(x)$ is the probability distribution of the underlying time series $x(t)$. This latter equation holds more generally than for Gaussian processes. In fact it holds whenever the process $x(t)$ and its time derivative $dx(t)/dt$ are statistically independent. However, the argument has been restricted to the Gaussian case because it greatly simplifies considerations presented later (in Section 3).

It is convenient to re-write equation 1.5 in the form

$$N(x) = N_0 \exp\left\{-\tfrac{1}{2}\frac{(x-\bar{x})^2}{\sigma_w^2 A^2}\right\} \tag{1.8}$$

where

$$A = \sigma_x/\sigma_w \tag{1.9}$$

When an aircraft flies through patches of turbulence of different severity, the mean frequency of upcrossings, $N(x)$, of the composite case is a weighted average of equation 1.8, with the weighting factors being the probability density, $p(\sigma_w)$, of the occurrence of σ_w.

$$N(x) = N_0 \int_0^\infty p(\sigma_w) \exp\left\{-\tfrac{1}{2}\frac{(x-\bar{x})^2}{\sigma_w^2 A^2}\right\} d\sigma_w \tag{1.10}$$

It is known (see e.g. Press and Steiner (1958)[2]) that the probability distribution of vertical acceleration obtained from counting accelerometers and VGH meters can for an aircraft operating at fixed speed and altitude, usually be fitted fairly well by the empirical formula

$$N(x) = N_0\{P_1 \exp(-x/Ab_1) + P_2 \exp(-x/Ab_2)\} \tag{1.11}$$

where, in this case, x is the deviation of the acceleration from the 1 g steady flight value, and so $\bar{x} = 0$. By use of the known definite integral

$$\int_0^\infty \exp\left(-p^2x^2 - \frac{q^2}{x^2}\right) dx = \frac{\sqrt{\pi}}{2p} \exp(-2pq)$$

it may be shown that $p(\sigma_w)$ can be expressed as the sum of two folded normal distributions

$$p(\sigma_w) = \sqrt{2}\left\{\frac{P_1}{\sqrt{\pi}b_1}\exp\left(-\frac{\sigma_w^2}{2b_1^2}\right) + \frac{P_2}{b_2}\exp\left(-\frac{\sigma_w^2}{2b_2^2}\right)\right\} \quad (1.12)$$

if equation 1.10 is to reduce to 1.11 upon substitution of the expression for $p(\sigma_w)$. This expression will be used later, but for the present it is not necessary to use the precise form of the distribution of $p(\sigma_w)$: it is sufficient to merely argue that if $p(\sigma_w)$ is such that equation 1.10 reduces to the equation 1.11 in the special case when x is the deviation from the mean of the vertical acceleration of the aircraft, then it follows that 1.10 will also reduce to the equation 1.11 (with an appropriate choice of the parameters A and N_0) in the general case when x is the deviation from the mean of any other parameter which depends linearly on $w(t)$. In the special case $x = w$, $A = 1$, and the expression in braces in equation 1.11 is just the probability of encountering turbulence of any given severity. The parameters P_1, P_2, b_1, b_2 will be functions of altitude, climatic region, terrain, etc., but in practice it is usual to take averages over different geographic regions, depending on the relative amount of time that the average aircraft spends in each region. In this case the four parameters are functions only of altitude. The values given by Garrison are reproduced in Table 1 of this report. For a full evaluation of the average frequency of load on an aircraft, it is necessary to know the average fraction of time which an aircraft spends in each altitude band. Denoting the altitude bands by subscripts $i = 1, 2, 3, \ldots$ with corresponding fractions of time t_i in each band, so that

$$\Sigma t_i = 1.0 \quad (1.13)$$

we have, on taking a weighted mean of equation 1.11,

$$N(x) = \sum t_i N_0 \left\{P_1 \exp\frac{-(x-\bar{x})}{A b_1} + P_2 \exp\frac{-(x-\bar{x})}{A b_2}\right\} \quad (1.14)$$

2. THE N_0 PROBLEM

The parameters A and N_0 depend on the integrals

$$M_0 = \int_0^{f_c} P_x(f)\,df \quad (2.1)$$

$$M_2 = \int_0^{f_c} f^2 P_x(f)\,df \quad (2.2)$$

and these will only be convergent if the respective integrands are of order $f^{-1+\epsilon}$ with $\epsilon > 0$. The second of these integrals does not fulfill this condition in the case of atmospheric turbulence gust velocities when $x = w$ and $P_x(f)$, being given by the von Karman equation, asymptotes as $f^{-5/3}$. Thus a process with a von Karman spectrum has an infinite value of N_0. This is because such a process has a large number of very small amplitude (ripple) cycles which give rise to large numbers of level crossings, although they contribute very little to the variance of the signal.

Figure 1 shows how N_0 for a von Karman process increases without bound as the cut-off frequency, f_c, is raised. This example is an extreme case of the N_0 problem, which is how to deal with a process having many small cycles superimposed on a lesser number of large cycles.

In aeronautical applications, interest is directed not at the gust velocity $w(t)$ itself, but at the aircraft response, $x(t)$, which is obtained from $w(t)$ by a filtering process which attenuates the higher frequencies. In what follows, $x(t)$ will be taken to be the vertical acceleration of the aircraft centre of gravity. This case is traditionally considered to be the most important because many stresses are highly correlated with the aircraft acceleration.

To obtain the characteristics of the response requires a knowledge of the transfer function of an aircraft. In some applications it may be possible to measure the transfer function, in others it is necessary to compute the function from a model of the aircraft behaviour. Such models range from simple one degree of freedom models to very complex models allowing for several different structural oscillation modes as well as all the rigid body degrees of freedom. However, a multiplicity of models leads to spurious variations which makes it hard to compare results from different flight trials which have been computed in different ways. Houbolt (1970, 1971, 1975),[6,7,8] has written a "Design manual for vertical gusts based on power spectral techniques", in which he recommends the use of a consistent method of evaluating A and N_0, based on a simple one degree of freedom model (vertical translation only) flying in a one-dimensional gust field. The transfer function for such a model is the product of two factors, one of which takes account of aircraft parameters, and asymptotes to a non-zero constant at high frequency, and the other is

the Sears function which takes account of the unsteady aerodynamic response to a gust load on the wing. The Sears function[9] is given by

$$S(\omega) = \{J_0(\omega) - iJ_1(\omega)\}\, C(\omega) + iJ_1(\omega) \tag{2.3}$$

where

$$C(\omega) = \frac{H_1^{(2)}(\omega)}{H_1^{(2)}(\omega) + iH_0^{(2)}(\omega)} \tag{2.4}$$

$$H_n^{(2)}(\omega) = J_n(\omega) - i\, Y_n(\omega) \tag{2.5}$$

J_n and Y_n are Bessel functions of order n and ω is the conventional non-dimensional frequency based on the wing semi-chord, $c/2$,

$$\omega = 2\pi f(c/2)/U \tag{2.6}$$

The high frequency behaviour of the integrand of equation 2.2 depends on $|S(\omega)|^2$ which according to the Leipmann approximation[10] is given by

$$|S(\omega)|^2 = 1/(1+2\pi\omega) \tag{2.7}$$

$f^2 P_x(f)$ therefore behaves as $f^{-2/3}$, so that for this model N_0 is still theoretically infinite. Houbolt has proposed that this problem be overcome by choosing the cut-off frequency, f_c, to be the lowest cut-off frequency at which M_0 (equation 2.1) has practically attained its ultimate limit. He proposes to ignore any contributions to M_2 by higher frequencies.

There is, however, a more realistic way of overcoming the problem through noting that high frequency contributions to the isotropic turbulence gust structure cannot be adequately represented by a one-dimensional gust structure model. In this context, the term "high frequency" means that the wavelength of the gust is not large compared with the wing span. For a given, high wave-number contribution, the gust at one chordwise section will be upward whilst the gust at a distant chordwise section will be downward, and the resultant cancellation will wash out the high frequency effects. To formulate a simple quantitative model, consider a sinusoidal gust which is symmetrical about the longitudinal axis of the aircraft, so that the local lift per unit span varies as cos ky where y is the transverse co-ordinate. The average lift per unit span is the lift per unit span at the centre section multiplied by

$$F(\omega) = \frac{1}{\text{span}} \int_{-\text{span}/2}^{\text{span}/2} \cos \mathrm{k}y \, \mathrm{d}y \tag{2.8}$$

If the wave number, k, corresponds to the frequency, f, seen by the aircraft travelling at speed U, so that

$$k = 2\pi f/U \tag{2.9}$$

then the expression 2.8 becomes

$$F(\omega) = \sin(\omega \mathcal{A}R)/(\omega \mathcal{A}R) \tag{2.10}$$

Hence at high frequencies, the integrand of 2.2 behaves as

$$f^2 P_w(f)\, |S(\omega)|^2 \,.\, |F(\omega)|^2 = O(f^{-8/3}) \tag{2.11}$$

which gives a convergent integral. Figure 2 shows some examples of how the derived values of A and N_0 converge with increasing cut-off frequency. The ordinates of Figures 2*a* and 2*b* are proportional to A and N_0 respectively. The convergence of N_0 is almost complete by a cut-off non-dimensional frequency of $\omega = 4/\mathcal{A}R$. The corresponding cut-off value of af is obtained from

$$af = 1{\cdot}339\,(2L/c)\,\omega \tag{2.12}$$

The values of A and N_0 for a one degree of freedom model flying in a two dimensional gust field are functions of both the aspect ratio, $\mathcal{A}R$, and of $2L/c$. Figures 3 and 4 show convenient charts for obtaining the solution to such a model. These charts are similar to those given by Houbolt (1970, 1971, 1975) but differ in that the two dimensional structure of the gusts (which introduces a dependence on aspect ratio, whilst it allows a realistic evaluation of N_0) is taken into account. Further details of the derivation of Figures 3 and 4 are given by Sherman (1976).[11]

3. THE AMPLITUDE DISCRIMINANT METHOD OF COUNTING*

When data from flight trials are being analysed the input has already been subjected to some form of filtering. However, it is often desired to perform further smoothing on the signal, for

* Section 3 has been amended subsequent to the presentation at the conference.

example, to eliminate high frequency noise from the signal, or because small amplitude cycles are not considered significant.

With digital data, one way to do this is to use low pass digital filtering, but for purposes such as level crossing counting it is more efficient computationally to use an "amplitude discriminant" technique. The basic idea of the amplitude discriminant is to ignore any fluctuations in the time series where the difference in value between a peak and an adjacent trough is less than a prescribed value called the discriminant. The effect of such amplitude discriminant counting has been examined for a number of processes including actual turbulent measurements, but we first make two observations concerning the general shape which level crossing curves are expected to have when an amplitude discriminant is applied.

If the time series considered is Gaussian, then the level crossings (with zero discriminant) are fitted by Rice's level crossing equation (1.5). Further, Rice has shown that if the level, x, is sufficiently far from the mean, the number of extrema lying beyond x is approximately equal to the number of upcrossings of the level x, or in other words relatively few wrong-sided extrema lie far from the mean of a Gaussian process. Therefore the process of smoothing with an amplitude discriminant will make relatively little difference to the number of level crossings of levels which are far from the mean, although it will markedly reduce the number of crossings of levels near the mean.

The effect of applying amplitude discriminant counting to three different processes was studied. The processes chosen were:

(*a*) An ARMA model with a $-5/3$ slope of the power spectrum

$$x(t) = 0{\cdot}6x(t-1) - 0{\cdot}06x(t-2) + 0{\cdot}02x(t-3) + \epsilon(t) + 0{\cdot}15\epsilon(t-1) + 0{\cdot}02\epsilon(t-2) \qquad (3.1)$$

where the $\epsilon(t)$ are independent normally distributed random numbers with zero mean and unit variance.

(*b*) A sample of available atmospheric wind data from a ground based anemometer with a low noise (digital) measuring and recording system (see Section 2 of the Appendix)

(*c*) A simulated sequence of aircraft c.g. vertical acceleration measurements obtained by applying a one degree of freedom model of a rigid aircraft response[11] to the wind data in (*b*) above. The aircraft parameters chosen were:

$\mu = 20$
$AR = 7$
$\hat{c} = 5$ m
$U = 100$ m/s

For each of these processes Figure 5 shows a segment of the time history and Figure 6 shows a set of upcrossing curves for counts made with different amplitude discriminants. Figure 7 shows how, for two separate records of longitudinal wind velocity, N_0 decreases with increasing amplitude discriminant. The close agreement between the curves for the two different sets of data suggests that the relationship is fairly well established. The experimental points in Figure 7 may be fitted by the equation

$$N_0 = N_{00} \exp\{\beta_1(D/\sigma) + \beta_2(D/\sigma)^2 + \beta_3(D/\sigma)^3\} \qquad (3.2)$$

with the coefficients shown in the following table:

	β_1	β_2	β_3
Longitudinal wind speed	−0·24	−0·127	+0·00736
c.g. acceleration (or U_{de})	−0·11	−0·078	−0·00592

The various curves in Figure 6 appear to be fairly well fitted by the formula

$$N = N_0 \sqrt{\frac{1+a}{e^{x^2}+a}} \qquad (3.3)$$

Because of the condition that all the curves must asymptote to

$$N = N_{00}\, e^{-\frac{1}{2}x^2} \qquad (3.4)$$

at large x the parameter a is determined as

$$a = (N_{00}/N_0)^2 - 1 \tag{3.5}$$

so that 3.3 becomes

$$N/N_{00} = 1/\sqrt{e^{x^2} + a} \tag{3.6}$$

and this family of curves is shown in Figure 8. The variation of the parameter a with amplitude discriminant for the three processes studied is shown in Figure 9, together with the best fit parabola for each set of data. The equation for the parabola is

$$a+1 = (N_{00}/N_0)^2 = \exp\{\beta_1(D/\sigma) + \beta_2(D/\sigma)^2\} \tag{3.7}$$

with the coefficients shown in the following table:

	β_1	β_2
(*a*) ARMA process	0·316	0·224
(*b*) Longitudinal wind	0·595	0·164
(*c*) c.g. acceleration	0·127	0·229

Yamane *et al.* (1975)[14] have carried out amplitude discriminant counting on two filtered Gaussian noise processes, one with a low pass filter and one with a band pass filter. Equation 3.6 appears to fit both sets of data although no attempt was made to find the variation of a with the amplitude discriminant.

The data of Figure 6 have been normalised so as to remove the effect of varying intensity of turbulence. An estimation is therefore needed of the expected number of exceedance counts which would be obtained if counts were made in many patches of turbulence of different intensity but with a fixed value of the discriminant. Arguing by analogy with the development of equation 1.10,

$$N_D(x) = \int_0^\infty \frac{N_{00}\, p(\sigma_w)\, \mathrm{d}\sigma_w}{\sqrt{\exp\left[\dfrac{(x-\bar{x})^2}{\sigma_w^2 A^2}\right] + a}} \tag{3.8}$$

where $N_D(x)$ is the frequency of level crossings of level x, with discriminant D, and $p(\sigma_w)$ is given by equation 1.12. Thus

$$N_D(x) = N_{00}\left\{P_1 L\left(\frac{D}{b_1 A}, \frac{x-\bar{x}}{b_1 A}\right) + P_2 L\left(\frac{D}{b_2 A}, \frac{x-\bar{x}}{b_2 A}\right)\right\} \tag{3.9}$$

where, with the substitution $z = \sigma_w/b$

$$L(p, q) = \sqrt{\frac{2}{\pi}} \int_0^\infty \frac{\exp(-z^2/2)\, \mathrm{d}z}{\sqrt{\exp\left(\dfrac{q}{z}\right)^2 + \exp\left[\beta_1\left(\dfrac{p}{z}\right) + \beta_2\left(\dfrac{p}{z}\right)^2\right] - 1}} \tag{3.10}$$

The equation 3.10 differs from the usual equation $L(0, q) = \exp(-q)$ by the introduction of the polynomial in p/z. The function $L(p, q)$ is graphed in Figure 10, and it may be seen that as the discriminant, p, increases, the function becomes increasingly flat topped because the bulk of the records have small standard deviations, and so have a greater proportion of their level crossings removed by the application of a fixed discriminant rather than one with a fixed proportion of σ. Because the curves all asymptote to lines parallel to $\exp(-q)$, it is convenient to show the deviations from $\exp(-q)$ in the form $L(p, q)/L(0, q)$. These graphs are shown in Figure 11.

4. DISCUSSION

In the conventional "Power Spectrum" method of gust load analysis, the value of N_0 which is obtained will vary depending on the procedure used in removing small load cycles from the record. When using the amplitude discriminant method for normalised gust velocities in low level atmospheric turbulence, the level crossings are given by equations 3.3 and 3.5. However, when un-normalised data have a constant discriminant applied, the simple level crossing formula given by equation 1.11 and carried through into equation 1.14 is not applicable unless the filtering or amplitude discriminant is similar to that applied to the data from which equation

1.11 was evolved. For the general case equation 1.14 should be replaced by an equation based on the level crossing curves given by equation 3.9, for which the variation of the level crossing function with discriminant level is shown in Figure 10.

Logically, the procedure for choosing a discriminant level would depend on the relative fatigue damage done by load cycles of different amplitude, and this in turn depends on the particular S-N curve which is used.

One very big problem remains with the power spectral method, and that is the load to pair with each of the level crossings actually counted. This problem is solved if the complete variation of the number of level crossings with the size of the amplitude discriminant is known out to amplitude discriminants equal to the largest load cycle occurring in the record. Until recently, the only way to solve this problem in fatigue monitoring programs was to record a complete turning point load history of individual aircraft. This involved a considerable data storing and processing problem. A much better solution would appear to be the ARL range pair counter currently undergoing prototype testing at these laboratories. In the meantime, and for prediction work the continued use of the power spectral method of gust load prediction requires that a standard degree of filtering and amplitude discrimination be established, and that a standard variation of level crossing counts with amplitude discriminant be used in damage sums. Obtaining this standard variation will necessitate obtaining (as a research task) the variation of N_0 with amplitude discriminant for several records with different degrees of pre-filtering.

REFERENCES

1. ESDU — Average Gust Frequencies—Subsonic Transport Aircraft. Item No. 69023 with amendments A and B, May 1972.
2. Press, H., and Steiner, R. — An Approach to the Problem of Estimating Severe and Repeated Gust Loads for Missile Operations. NACA T.N. 4332, September 1958.
3. USAF — Military Specification—Airplane Strength and Rigidity—Flight Loads. MIL-A-008861A (USAF), March 1971.
4. Garrison, J. N. — An Assessemnt of Atmospheric Turbulence Data for Aeronautical Applications. Royal Aeronautical Society, London, Conference on Atmospheric Turbulence, 18–21 May 1971.
5. Rice, S. O. — Mathematical Analysis of Random Noise. Bell System Technical Journal: Vol. 23, No. 3, pp. 282–332, July 1944; Vol. 24, No. 1, pp. 46–156, January 1945.
6. Houbolt, J. C. — Design Manual for Vertical Gusts Based on Power Spectral Techniques. Wright-Patterson AFB Technical Report AFFDL-TR-70-106, December 1970.
7. Houbolt, J. C. — Frequency Response Functions and Human Pilot Modelling. AGARD Report No. 580, March 1971.
8. Houbolt, J. C. — Recommended Procedures for Processing Acceleration Data Obtained by Aircraft During Atmospheric Turbulence Encounter. AGARD Report No. 631, July 1975.
9. Sears, W. R. — Some Aspects of Non-Stationary Airfoil Theory and its Practical Application. Journal of the Aeronautical Sciences, Vol. 8, No. 3, pp. 104–108, January 1941.
10. Fung, Y. C. — Statistical Aspects of Dynamic Loads. Journal of the Aeronautical Sciences, Vol. 20, pp. 317–330, May 1953.
11. Sherman, D. J. — The Effect of Spanwise Gust Variations on the Transfer Function of an Aircraft Model with One Degree of Freedom. ARL Structures Note 431, 1976.
12. Patterson, A. K., Sherman, D. J., Thomson, M. R., and Woodall, G. — Low Level Wind Study—Bald Hills Instrumentation System. ARL Structures Note 414, May 1975.
13. Ford, D. G., and Patterson, A. K. — A Range-Pair Counter for Monitoring Fatigue. ARL Tech. Memo/Structures 195, January 1971.
14. Yamane, K., Takeuchi, K., Ono, K., and Asada, H. — Comparative Study of Counting Methods by Digital Simulation (in Japanese). National Aerospace Laboratory, TR-408, February 1975.

APPENDIX 1

Amplitude discriminant counting, fatigue meter counting and range pair exceedances

A practical method of counting level crossings with an amplitude discriminant involves having both a "counter" and a "previous minimum value" for the level crossings of each level considered. Then there are three phases in the counting program.

Phase 1 –Search consecutively through the time series until a value is encountered which is below the level for which counts are being made. Then:

Phase 2– Whilst the signal is below the level search for the lowest value and store this in the "previous minimum value". When the time series assumes a value greater than the level considered, proceed to phase 3.

Phase 3 –Whilst the signal is above the level considered search to find a value which is greater than the "previous minimum value" by at least D, the amplitude discriminant. If such a value is found, increment the counter by 1, reset the previous minimum value to be greater than the level considered, and revert to phase 1. If, however, the signal drops below the level before such a count has been registered, revert to phase 2.

For realisation on a simple machine this procedure may be modified, though the modified procedure will produce somewhat different results. The modified procedure involves having a "counter" and a "flag" corresponding to each level, x_i, at which counts are to be recorded. When the signal upcrosses a lower level, $x_i - D$, the flag is "set". When the signal upcrosses the level x_i the count is recorded and the flag is "fired" or returned to the "not set" state. No further counts will be recorded at that level until the time series falls again below the lower level. This procedure will be called counting with a "modified discriminant", and is essentially the counting procedure adopted by the fatigue meter. (In fact the fatigue meter differs from this description only in that it counts on a later part of the cycle. It sets the flag on upcrossing the level x_i, and increments the counter and fires the flag on downcrossing the level $x_i - D$.) This procedure is called a "downwards applied" discriminant (cf. the difference between forward differences and central differences in interpolation theory) because the oscillations which upcross both the lower level and the upper level are called upcrossings of the upper level, of the process with a modified discriminant applied. However, such a nomenclature leads to an asymmetry in the result. Consider, for example, a time series with a uni-modal distribution. For convenience we may assume the mode is also the mean value. If the level x_i is well above the mean then the level $x_i - D$ is closer to the mean, and is therefore crossed more frequently than x_i, whereas if x_i is below the mean the converse is the case. Thus for a symmetrically distributed time series and two levels x_i and x_j which are symmetrically placed about the mean there will be more upcrossings (with a downwards applied modified discriminant) of level x_i (above the mean) than of x_j (below the mean). It is therefore preferable to use a centrally applied discriminant whereby an oscillation which upcrosses both $x_i - D/2$ and $x_i + D/2$ is termed an upcrossing of the level x_i.

If we wish to study the effect of different size (modified) discriminants, we are led on naturally from the fatigue meter method of counting to the range pair exceedance method of counting. A discrete set of regularly spaced levels, x_1, x_2, x_3, etc., is chosen for counting, such that

$$x_i - x_j = (i-j)\,\delta$$

For each level, x_i, there is a whole set of flags F_{ij}, and a whole set of counters C_{ij}. Every time there is an upcrossing of level x_i the complete set of flags F_{ij} for $j = 1, 2, \ldots i$, is "set". Then when the signal falls back below the level x_j the flag F_{ij} is "fired" (i.e. returned to the "not set" state) and the counter C_{ij} is incremented by 1. Thus the set of counters C_{ii} on the leading diagonal contains the set of level crossings (with zero discriminant) of the levels x_i; the sub leading diagonal, $C_{i\,i-1}$, contains the level crossings of x_i with modified, downwards applied discriminant δ; the next diagonal, $C_{i\,i-2}$, contains the level crossings of x_i with discriminant 2δ, and so on. As with fatigue meter counting it is sometimes convenient to use a centrally applied discriminant instead of a downwards applied discriminant. (This is particularly so when counting the time

series obtained from a strain gauge with an unknown mean level, as the conventional presentation of fatigue meter counts is as exceedances of the level more remote from the mean or 1 g state.) In the sense of centrally applied modified discriminants the counter C_{ij} is the number of upcrossings of the level $\frac{1}{2}(x_i + x_j)$ with a discriminant $D = x_i - x_j \quad (i > j)$.

Relation between counting with an amplitude discriminant and counting with a modified amplitude discriminant

Consider the process $x_D(t)$ which arises after the process $x(t)$ has been smoothed with an amplitude discriminant D. The number of upcrossings $N_D(x_t)$ of a level x_t is greater than the number of upcrossings of the process with a modified discriminant applied (see Fig. 12). In the case of a downwards applied modified discriminant, the number of upcrossings of level x_t is (see Fig. 12*a*)

$$N_D(x) = \{\text{Number of minima of } x_D(t) \text{ between } x_t \text{ and } x_t - D\}$$

In the case of a centrally applied modified discriminant, the number of upcrossings of level x_t is (see Fig. 12*b*)

$$N_D(x) = \left\{\begin{array}{c}\text{Number of minima}\\ \text{of } x_D(t) \text{ between}\\ x_t,\ x_t - D/2\end{array}\right\} - \left\{\begin{array}{c}\text{Number of maxima}\\ \text{of } x_D(t) \text{ between}\\ x_t,\ x_t + D/2\end{array}\right\}$$

In the case of a Gaussian process with a large amplitude discriminant, D, applied, the majority of the oscillations in the trace go between (approximately) $-D/2$ and $+D/2$. Thus when counting with an amplitude discriminant at any level between these points, the number of upcrossings is almost constant. Figure 6 shows this flat-top effect. On the other hand when counting with a centrally applied modified amplitude discriminant, a nominal upcrossing of the level x implies actual upcrossings of both $x - D/2$ and $x + D/2$. If x is greater than zero the number of such pairs of events is governed by the number of upcrossings of $x + D/2$ (and vice versa if x is less than zero). Even a small increase in x above the zero (mean) level causes a significant decrease in the actual number of upcrossings of the level $x + D/2$ and so the graph at the number of upcrossings has a shape which is pointed at $x = 0$. This may be seen in Figure 13 (which is based on the same data as Fig. 6*b*).

APPENDIX 2

The anemometer data used in the range pair counting example

Figures 6*b* and 7 are based on anemometer data from nine miniature cup anemometer and direction vane pairs which were mounted on 10 m masts at Bald Hills, Queensland. The anemometers used digital (light chopper) transducers, and the wind run was recorded each second on a magnetic tape. (The Bald Hills experiment is described fully by Patterson *et al.* (1975).[12]) The record numbers C026 and C027 each refer to a two day file of data commencing on the afternoons of 26 and 28 January 1975 respectively. From these files were extracted records of longitudinal velocity component with durations of 512 seconds. Each record was divided into four segments, and records were only accepted for analysis if they met the following conditions (which were designed to ensure stationarity and the exclusion of non-turbulent or low wind speed records):

(*a*) The standard deviation of each segment was greater than 0·45 m/s, and also greater than 0·1 times the mean value of the segment.

(*b*) The kurtosis of each segment was less than 6.

(*c*) The mean value of each segment did not differ from the mean value of the entire record by more than $2\sigma_0$, where $\sigma_0 = \sigma_R/\sqrt{n}$, σ_R is the standard deviation of the entire record and the duration of the segment is $n = 128$ samples.

(*d*) The kurtosis of each segment did not differ from the kurtosis of the entire record by more than $2\sigma_K$, where $\sigma_K = \sqrt{24/n}$ is the standard deviation of the kurtosis of a Gaussian variable with sample size $n = 128$ points.

The resultant records accepted were as follows:

	*CO*26	*CO*27
No. of records	99	119
Total wind run	272·6 km	335·0 km
Mean wind speed	5·4 m/s	5·5 m/s

and the spectrum of the observed longitudinal component of wind velocity is shown in Figure 14. The various records accepted were normalized by subtracting their mean value and dividing each by its standard deviation. They were then counted with a range pair exceedance program and an amplitude discriminant counting program, and the results presented in Figures 6 and 7. The data have a somewhat skewed distribution because of the nature of the dynamic response of the anemometers. When a velocity change occurs the anemometer response depends on the run of wind which has travelled past. When the wind speed decreases momentarily from a moderate value to zero, the cups continue to rotate because of inertia, and this leads to a disproportionately low number of zero (or near-zero) values, and a disproportionately higher number of somewhat higher values. For higher wind speeds the necessary wind run goes past much faster, and the response becomes more nearly instantaneous. (The distance constant for the anemometers used was around 1 metre.) Thus at high speeds the anemometer record is essentially unaffected by the response of the anemometer.

TABLE 1 -
Turbulence Model Parameters
Quoted from Garrison (1971)[4]

Mission segment	Altitude (ft)	Gust component direction	P_1		b_1		P_2		b_2		L (ft)	
			Military	Civil	Military	Civil	Military	Civil	Military	Civil	Military	Civil
Low altitude contour	0–1000	Vertical	1·0	*	2·7	*	10^{-5}	*	10·65	*	500	*
Low altitude contour	0–1000	Lateral	1·0	*	3·1	*	10^{-5}	*	14·06	*	500	*
Climb, cruise, descent	0–1000	Vertical and lateral	1·0		2·51	3·903	·005		5·04	7·76	500	2500
Climb, cruise, descent	1000–2500	Vertical and lateral	·42		3·02	3·64	·0033		5·94	7·56	1750	2500
Climb, cruise, descent	2500–5000	Vertical and lateral	·30		3·42		·0020		8·17		2500	
Climb, cruise, descent	5000–10,000	Vertical and lateral	·15		3·59		·00095		9·22		2500	
Climb, cruise, descent	10,000–20,000	Vertical and lateral	·062		3·27		·00028		10·52		2500	
Climb, cruise, descent	20,000–30,000	Vertical and lateral	·025		3·15		·00011		11·88		2500	
Climb, cruise, descent	30,000–40,000	Vertical and lateral	·011		2·93		·000095		9·84		2500	
Climb, cruise, descent	40,000–50,000	Vertical and lateral	·0046		3·28		·000115		8·81		2500	
Climb, cruise, descent	50,000–60,000	Vertical and lateral	·002		3·82		·000078		7·04		2500	
Climb, cruise, descent	60,000–70,000	Vertical and lateral	·00088		2·93		·000057		4·33		2500	

* Low altitude contour is not applicable to commercial civil aircraft.

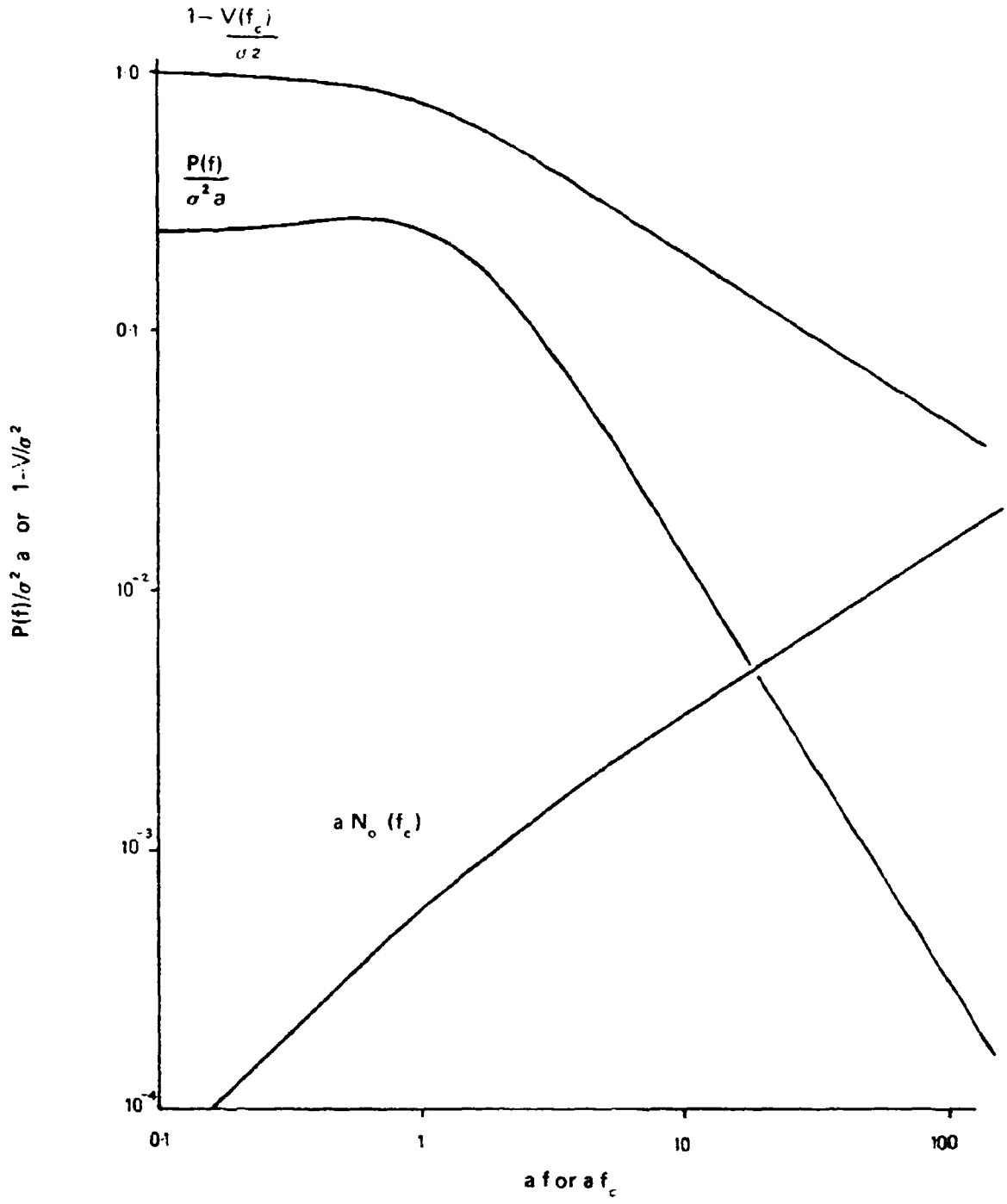

FIG. 1. VON KARMAN SPECTRUM AND VARIATION OF N_o WITH CUT-OFF FREQUENCY

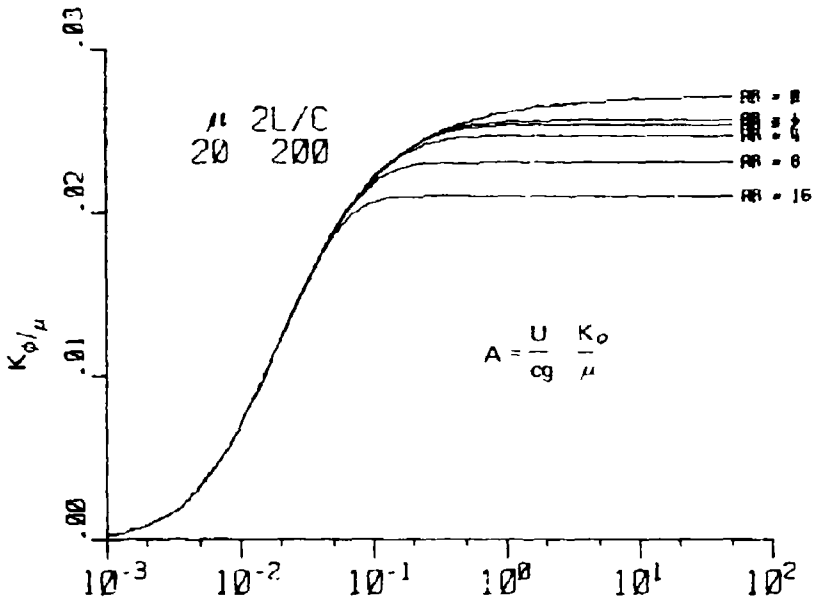

Fig. 2a Cut-off non dimensional frequency, ω_c

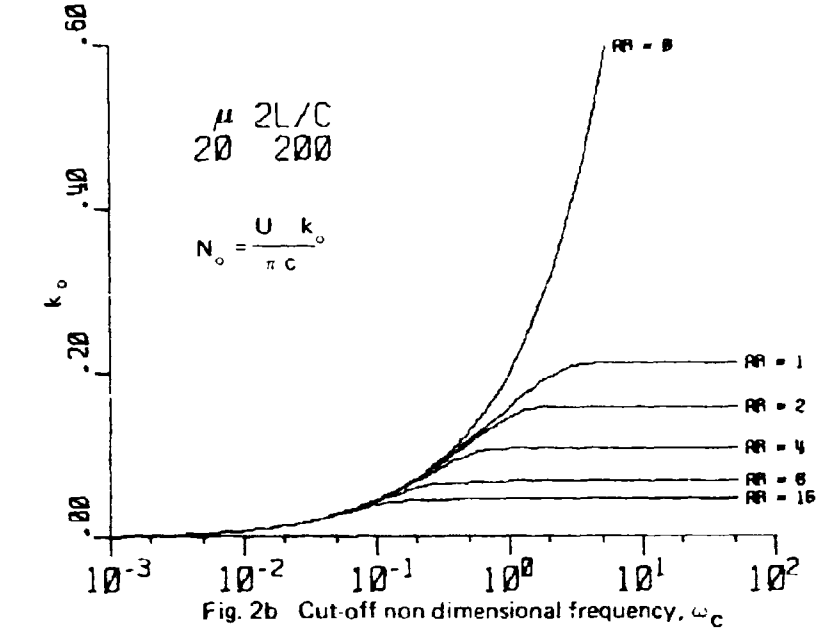

Fig. 2b Cut-off non dimensional frequency, ω_c

Fig. 2 THE CONVERGENCE OF A AND N_0 TOWARDS A LIMIT AS THE CUT-OFF FREQUENCY IS INCREASED

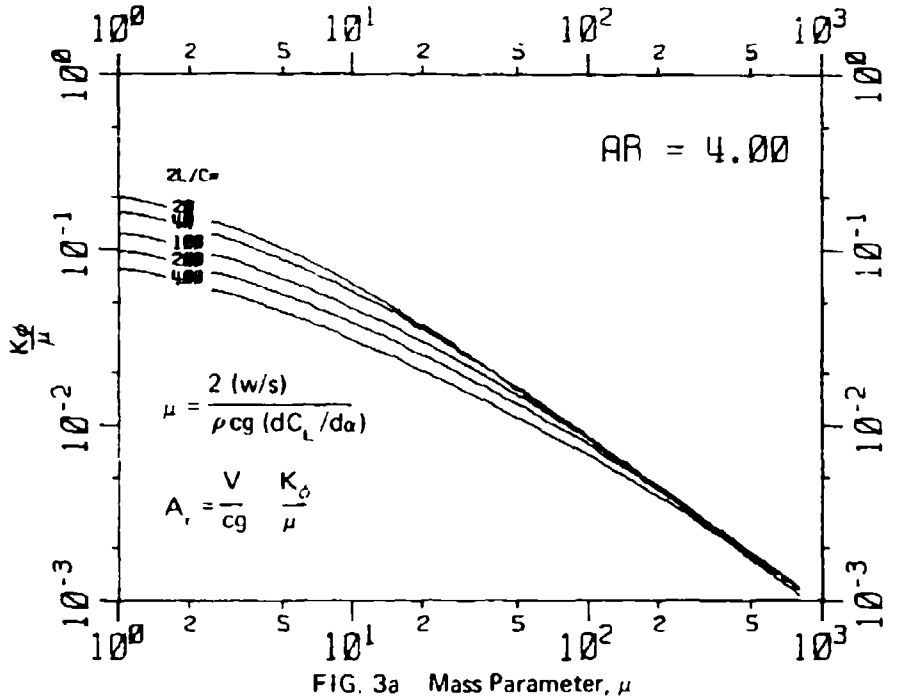

FIG. 3a Mass Parameter, μ

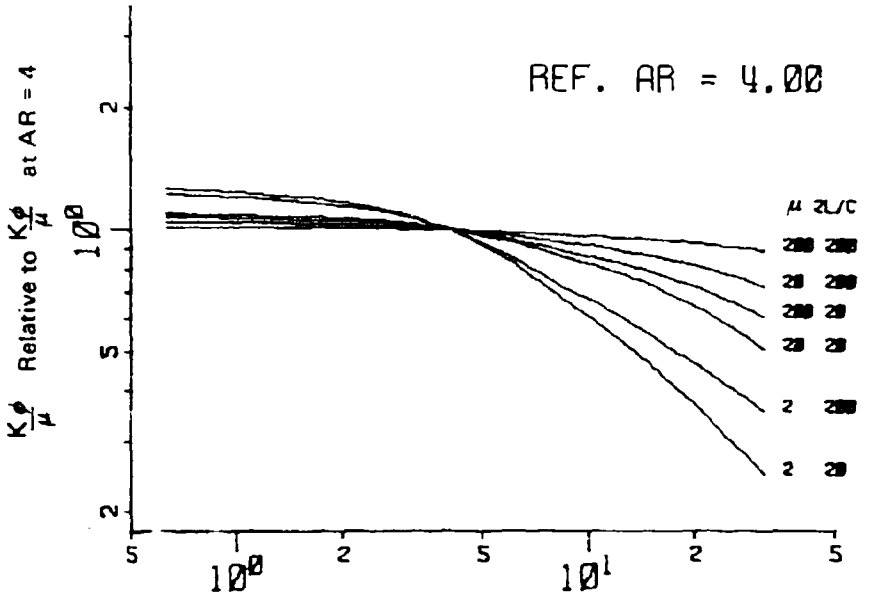

Fig. 3b Aspect ratio, AR

FIG. 3 THE A PARAMETER FOR THE C.G. VERTICAL ACCELERATION OF A ONE DEGREE OF FREEDOM AIRCRAFT MODEL IN THREE–DIMENSIONAL HOMOGENEOUS TURBULENCE

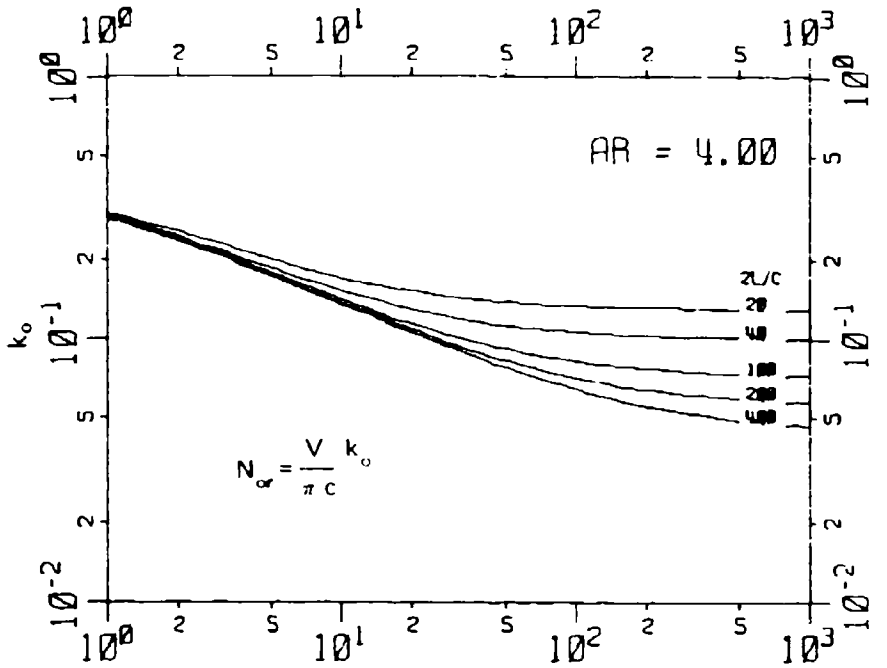

Fig. 4a Mass parameter μ

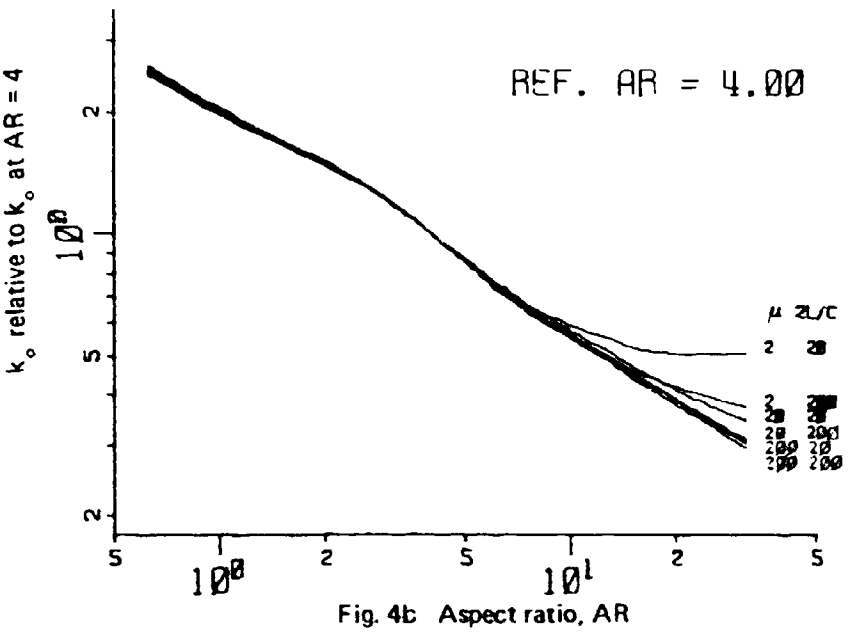

Fig. 4b Aspect ratio, AR

FIG 4. THE N_o PARAMETER FOR THE C.G. VERTICAL ACCELERATION OF A ONE DEGREE OF FREEDOM AIRCRAFT MODEL IN THREE-DIMENSIONAL HOMOGENEOUS TURBULENCE

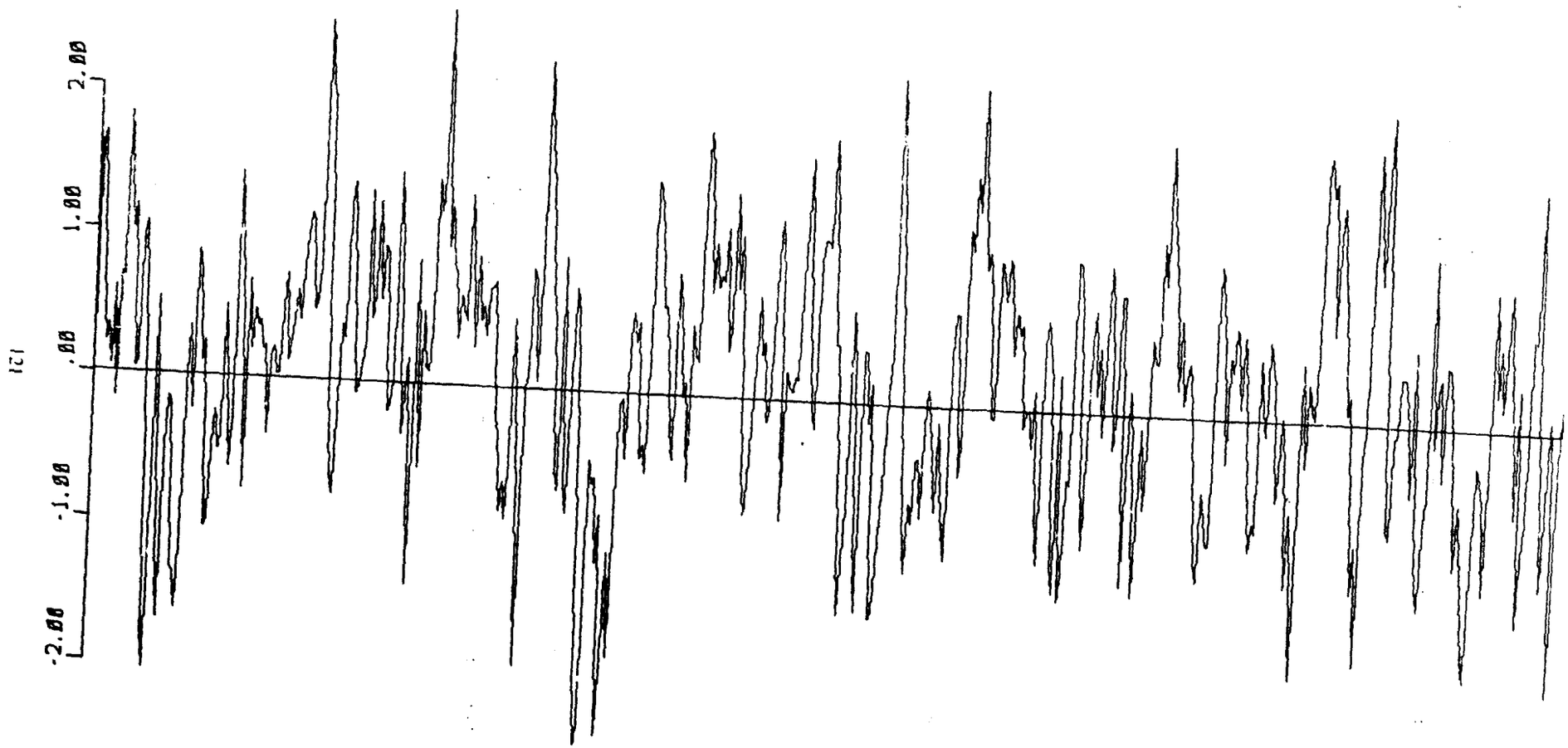

FIG. 5a. TIME SERIES GRAPH FOR ARMA MODEL

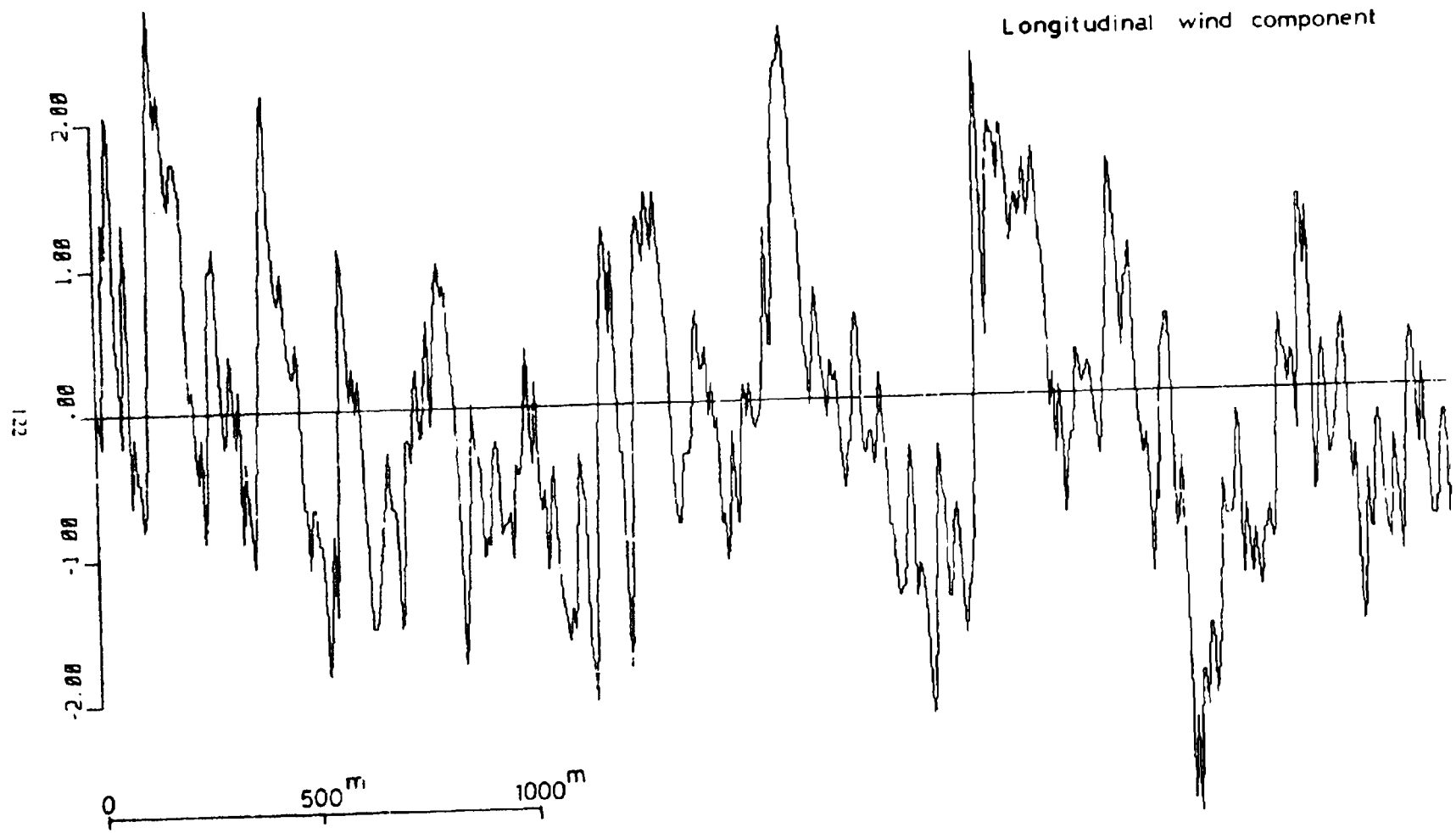

FIG. 5b. TIME SERIES GRAPH FOR LONGITUDINAL WIND
WIND VELOCITY COMPONENT

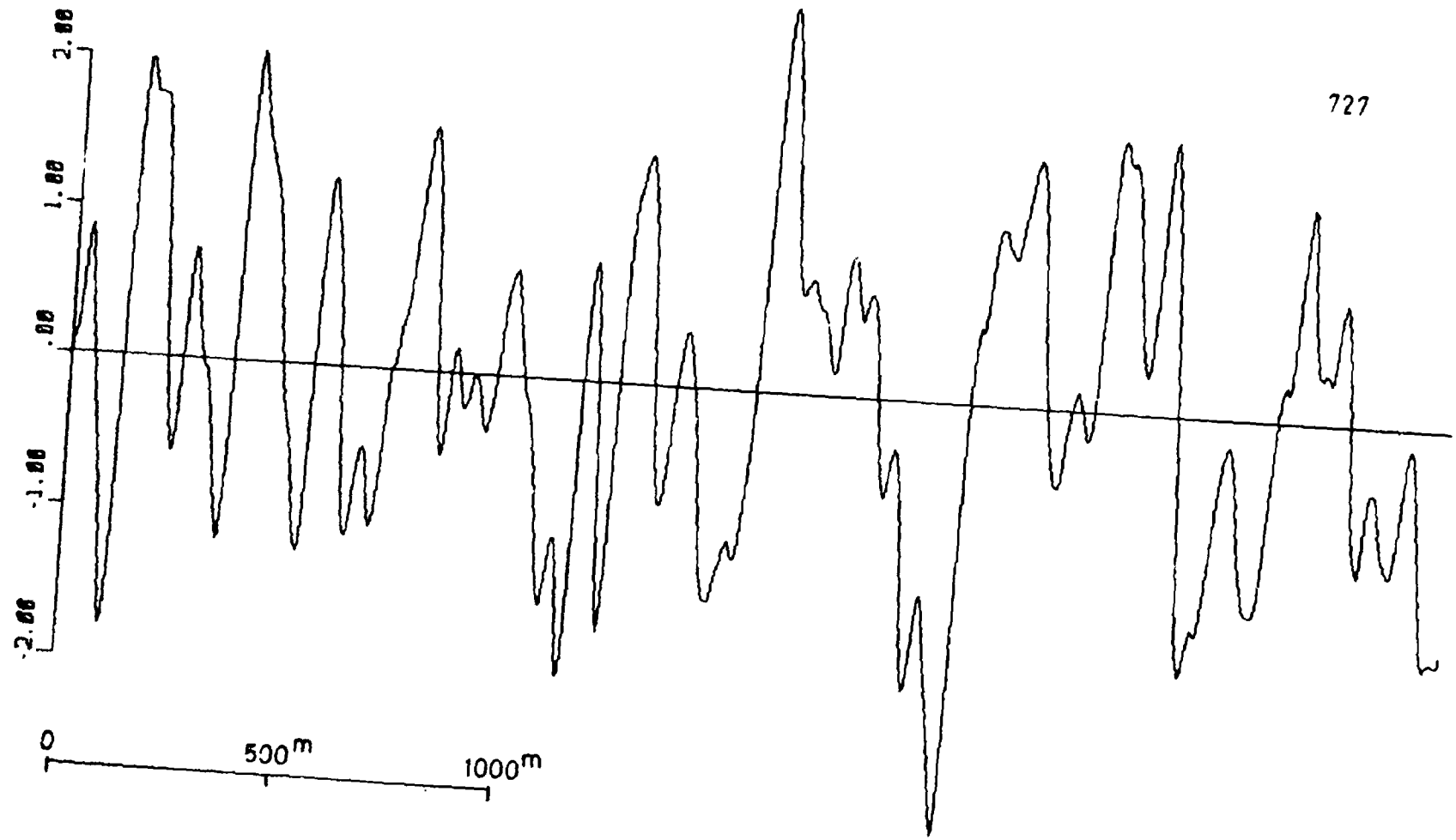

FIG. 5c. TIME SERIES GRAPH FOR U_{de} OR AIRCRAFT VERTICAL C.G. ACCELERATION

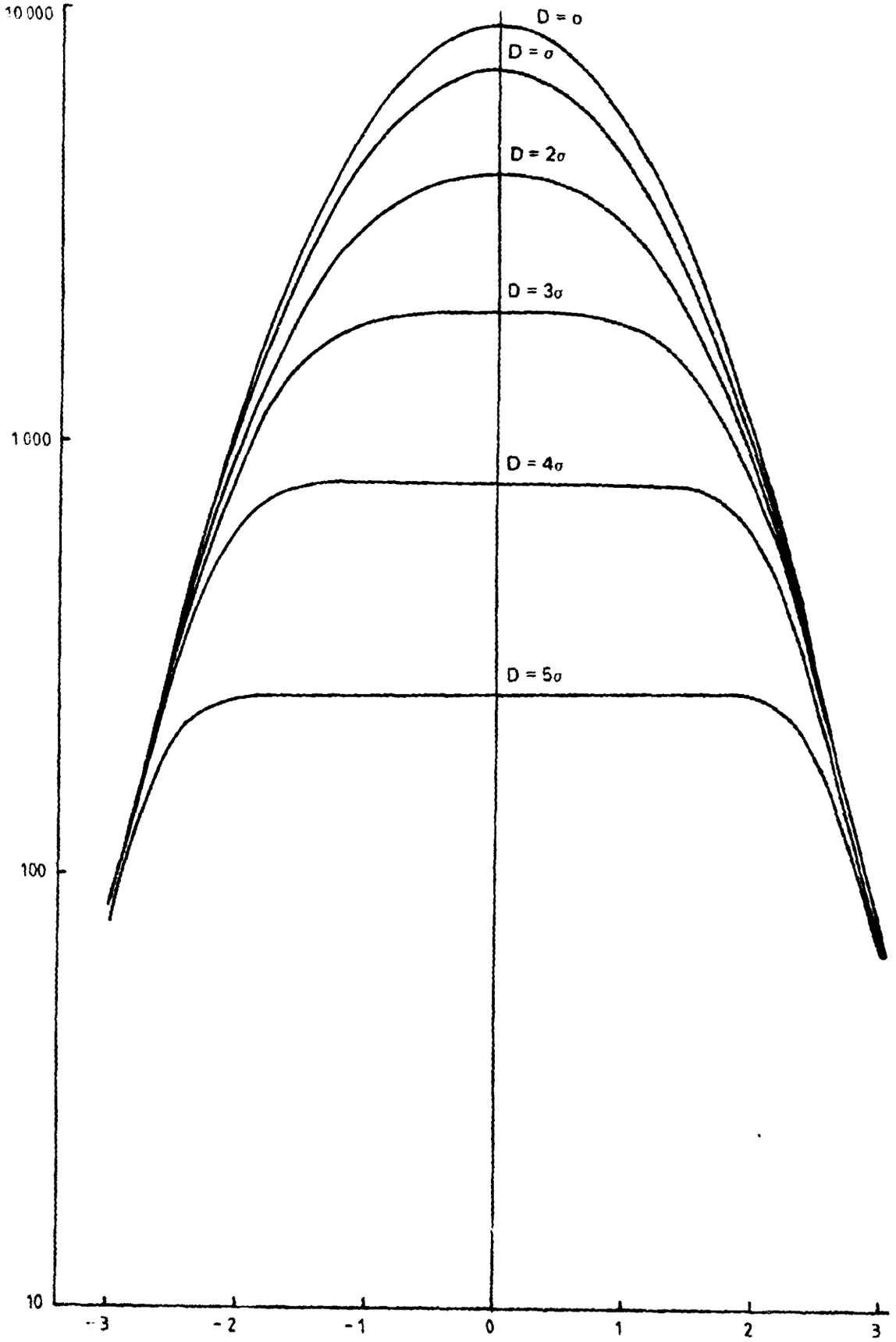

FIG. 6a. UP CROSSINGS WITH VARIOUS DISCRIMINANTS FOR ARMA MODEL

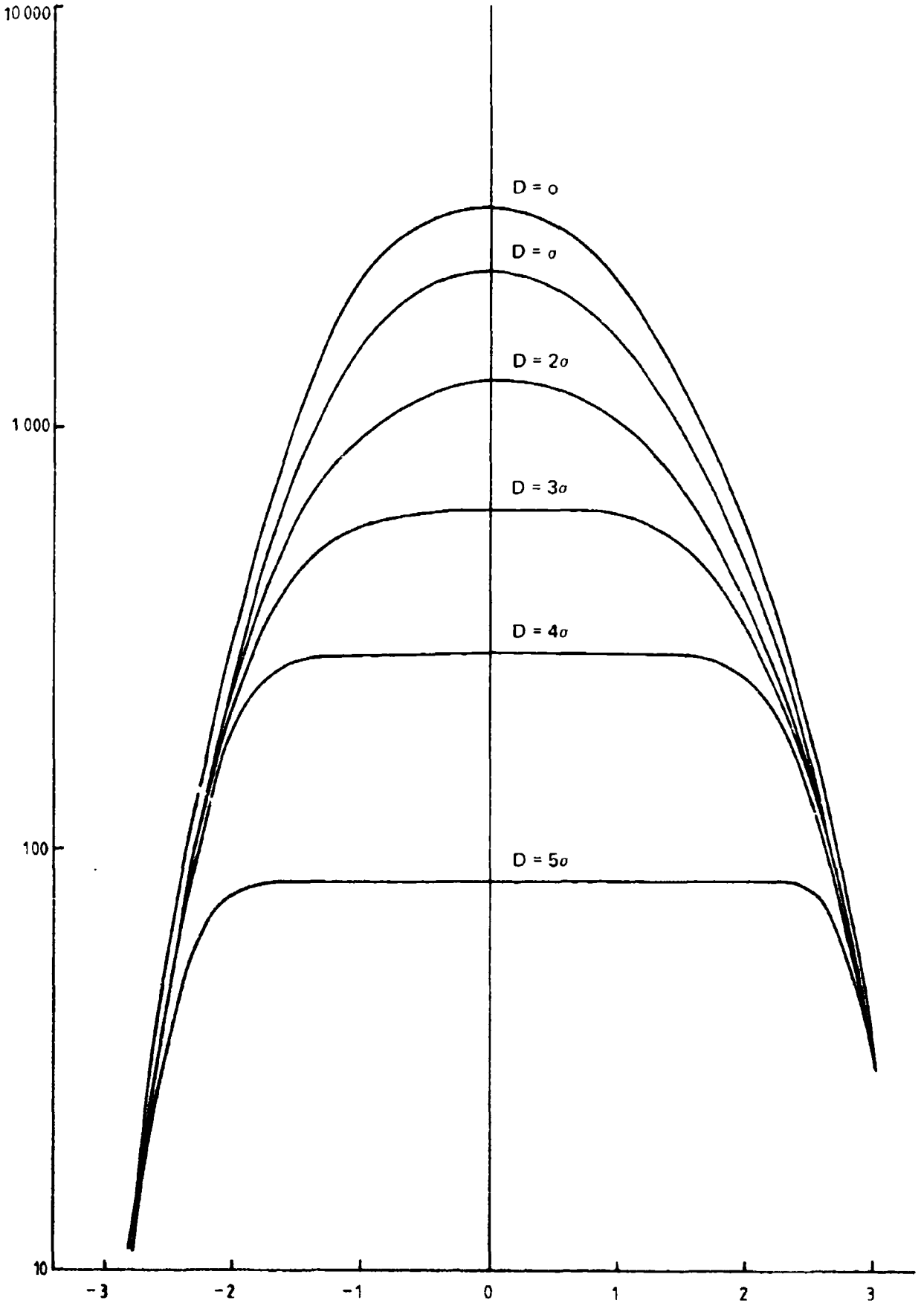

FIG. 6b. UP CROSSINGS WITH VARIOUS DISCRIMINANTS FOR LONGITUDINAL WIND VELOCITY COMPONENT

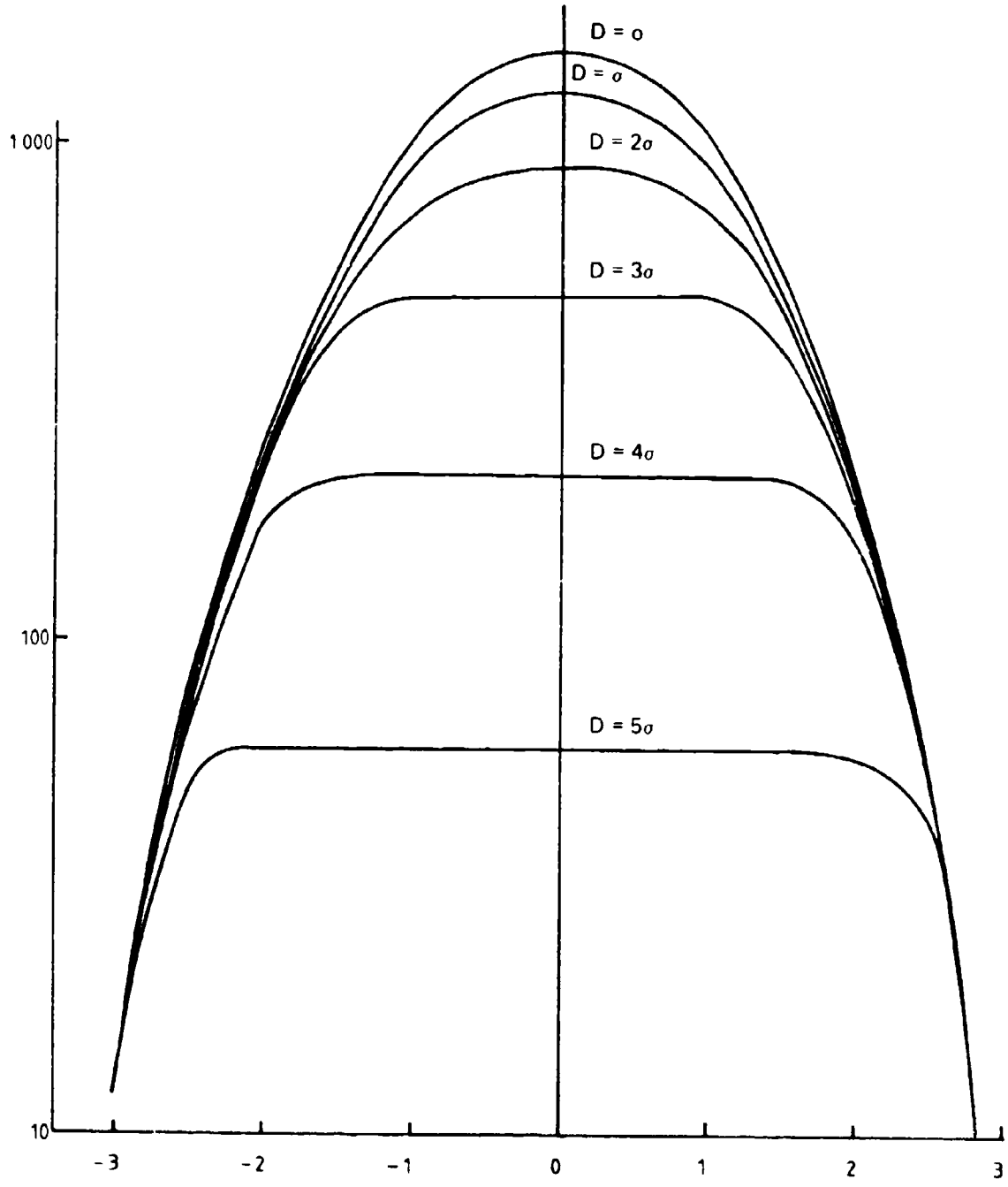

FIG. 6c. UP CROSSINGS WITH VARIOUS DISCRIMINANTS FOR U_{d_e} OR AIRCRAFT C.G. VERTICAL ACCELERATION

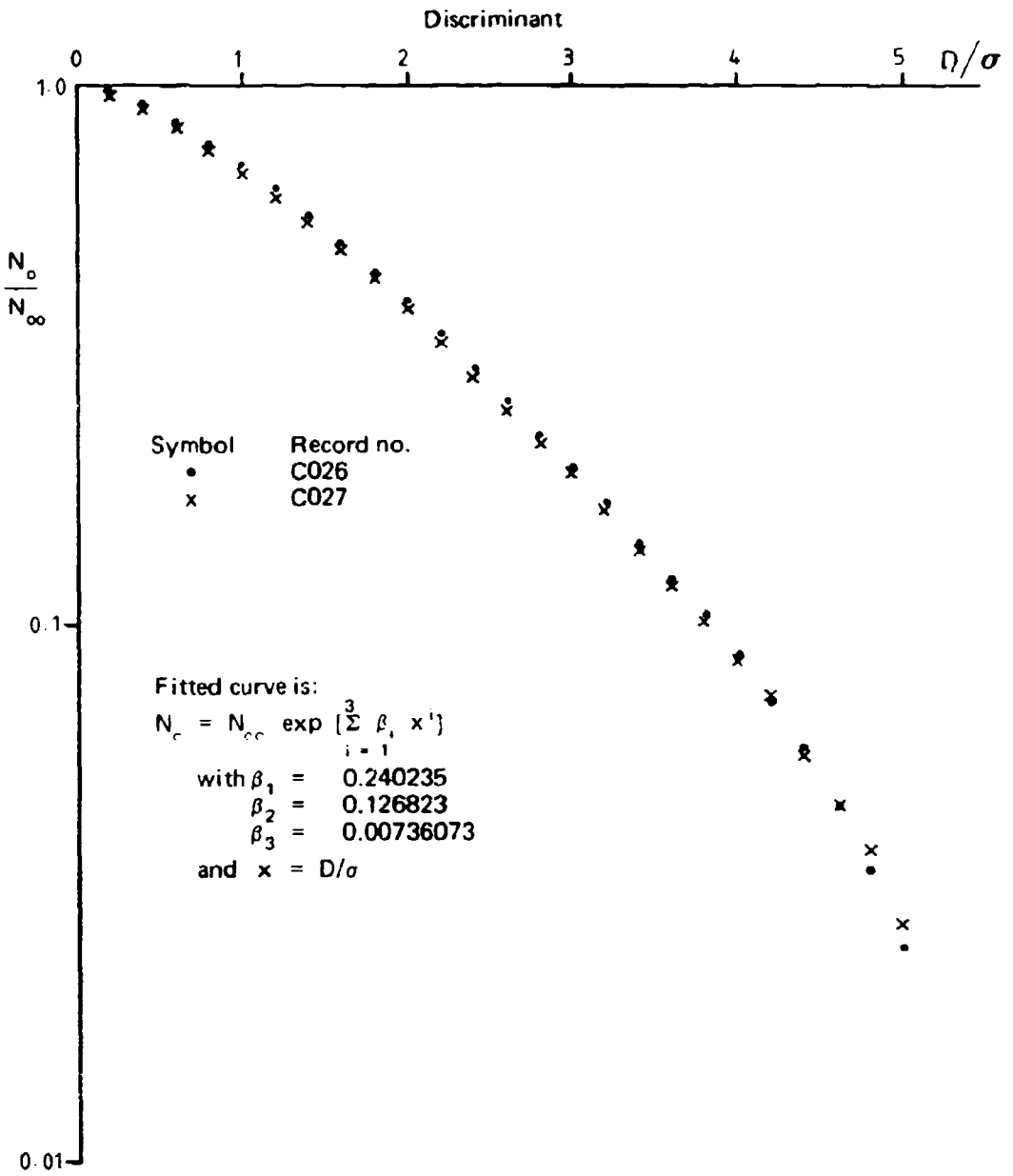

FIG. 7 VARIATION OF N_c WITH DISCRIMINANT, FOR LONGITUDINAL VELOCITY COMPONENT.

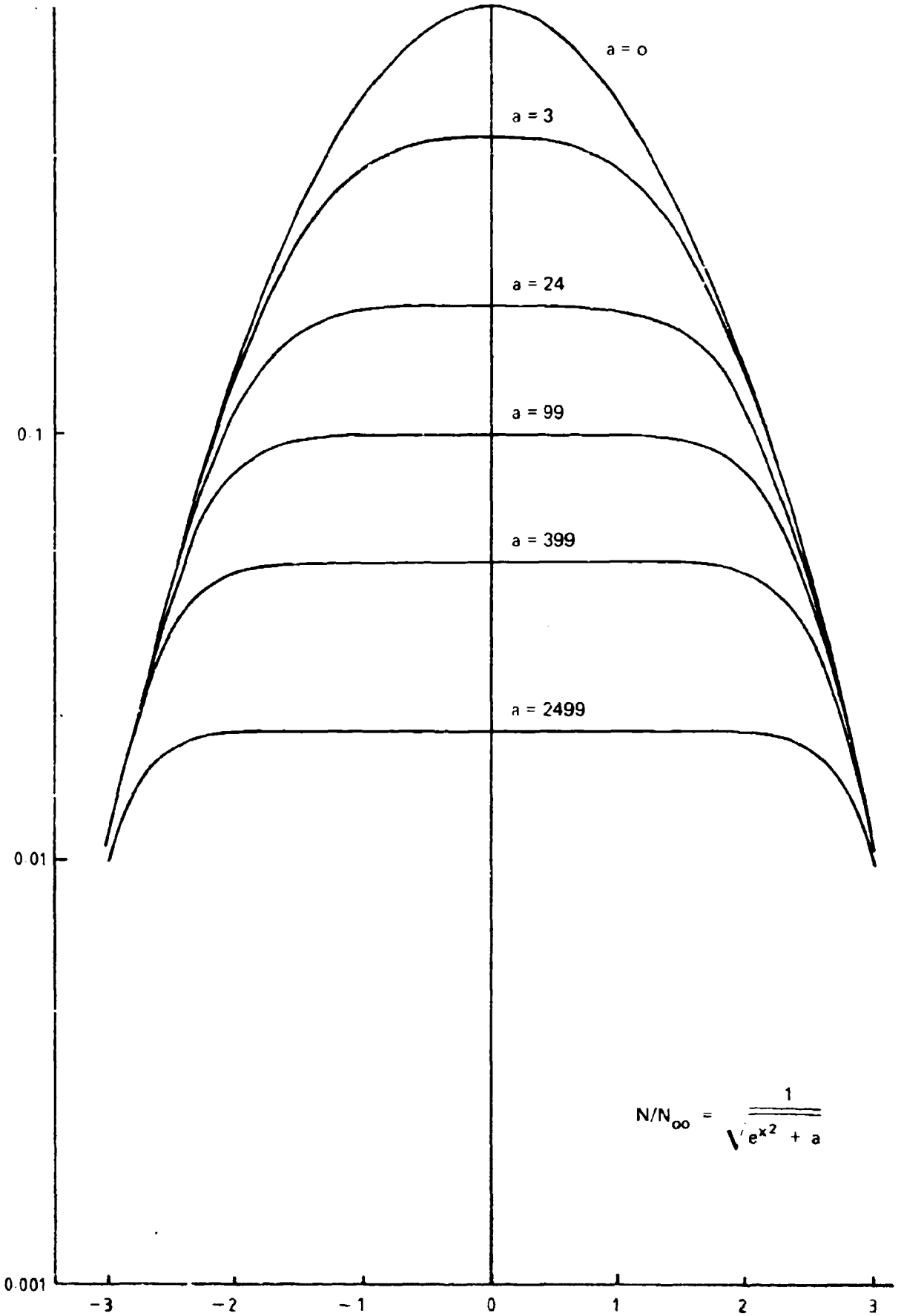

FIG. 8. THE EQUATION FITTED TO LEVEL CROSSING CURVES WITH VARIOUS AMPLITUDE DISCRIMINANTS

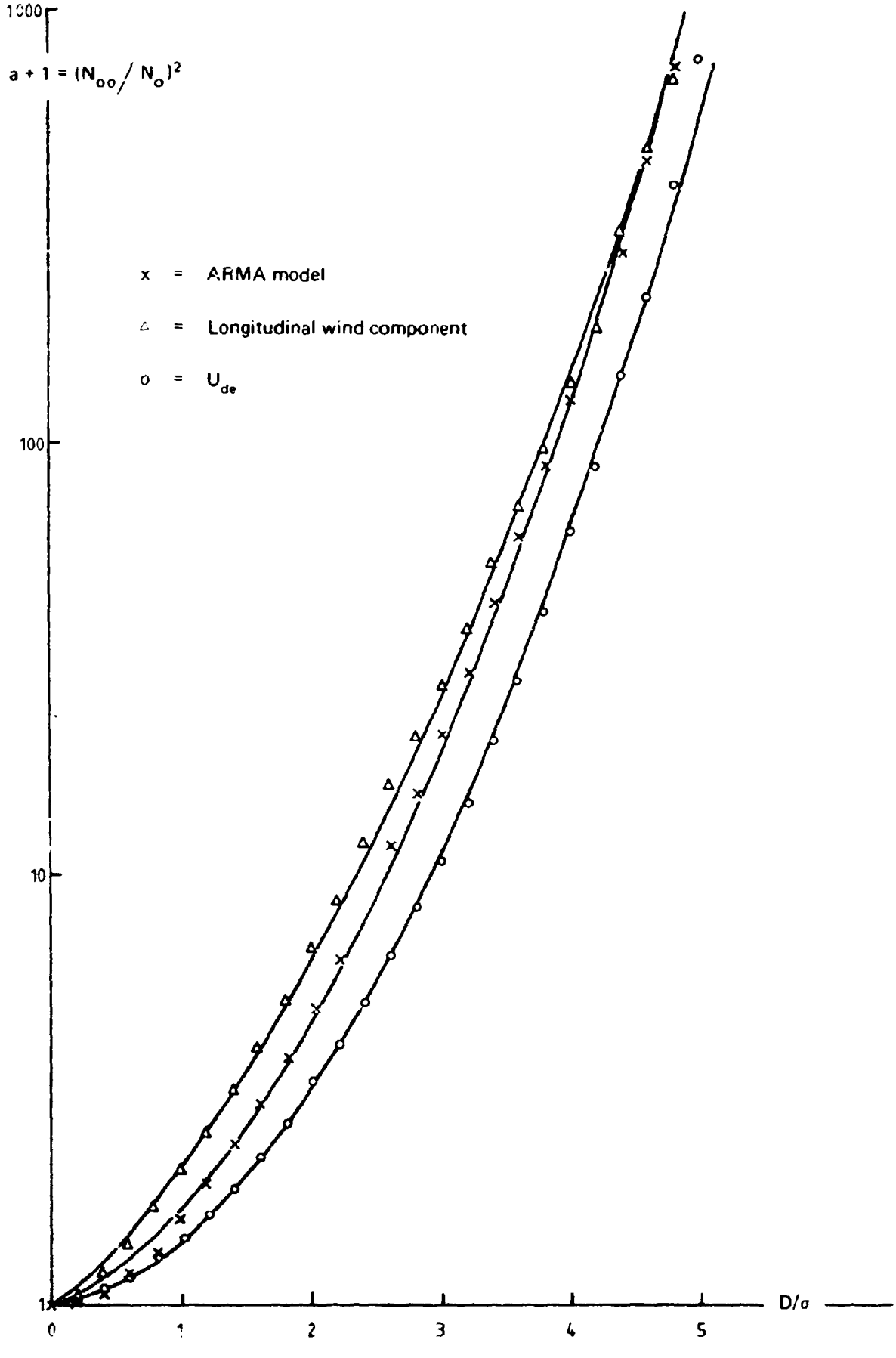

FIG. 9. VARIATION OF "a" WITH AMPLITUDE DISCRIMINANT

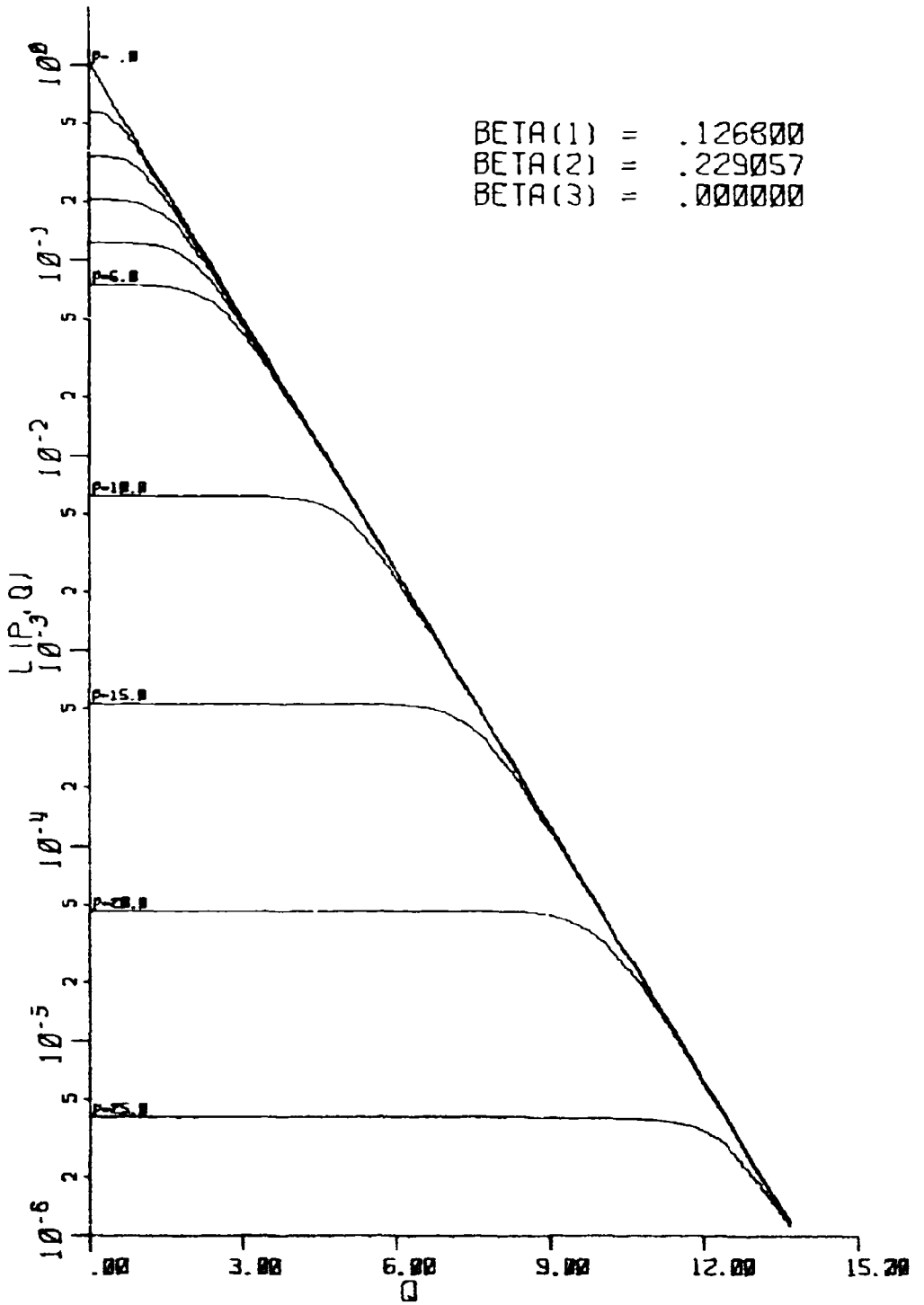

FIG. 10. LEVEL CROSSINGS FUNCTION L(p,q)

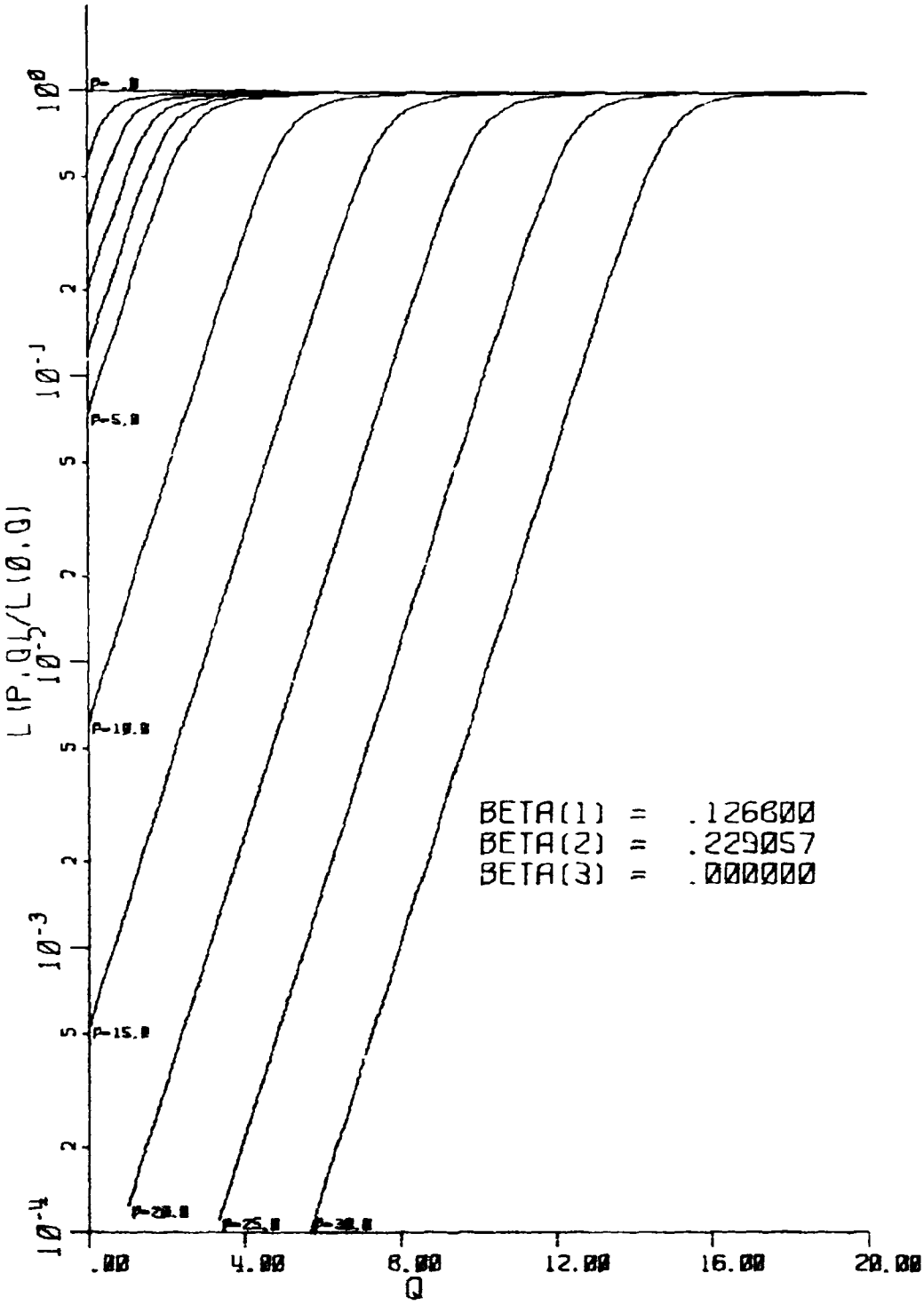

FIG. 11. LEVEL CROSSINGS FUNCTION L(p,q) AS FRACTION OF L(o,q) WHERE L(o,q) = EXP(−q)

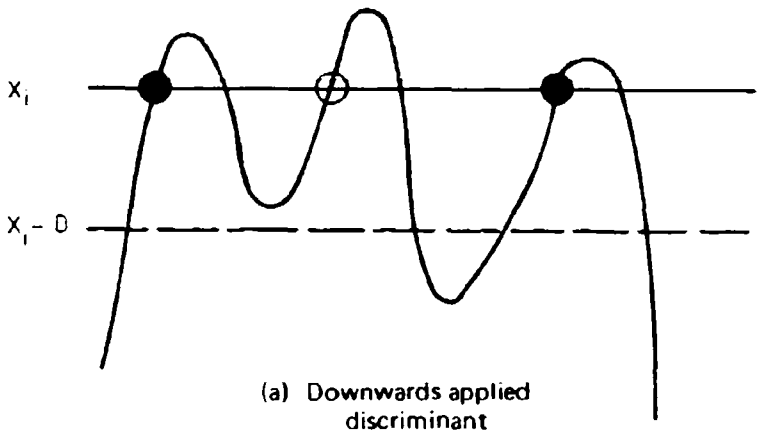

(a) Downwards applied discriminant

● = Upcrossing counted by both methods

o = Upcrossing not counted by modified discriminant method

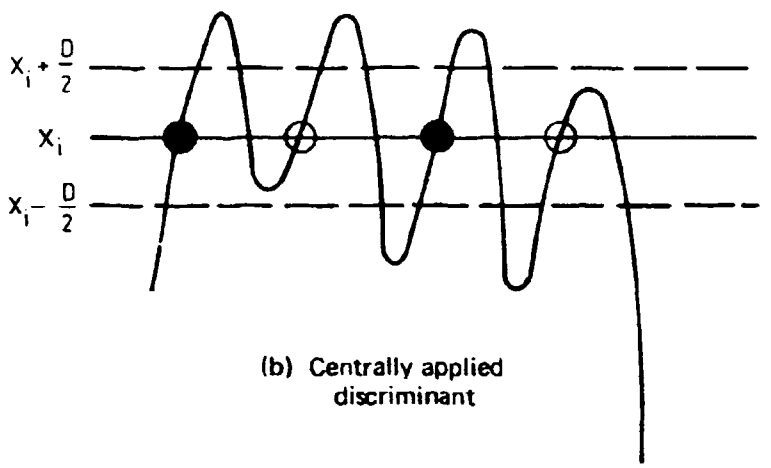

(b) Centrally applied discriminant

FIG. 12. RELATION BETWEEN LEVEL CROSSING COUNTING WITH AN AMPLITUDE DISCRIMINANT AND WITH A MODIFIED AMPLITUDE DISCRIMINANT.

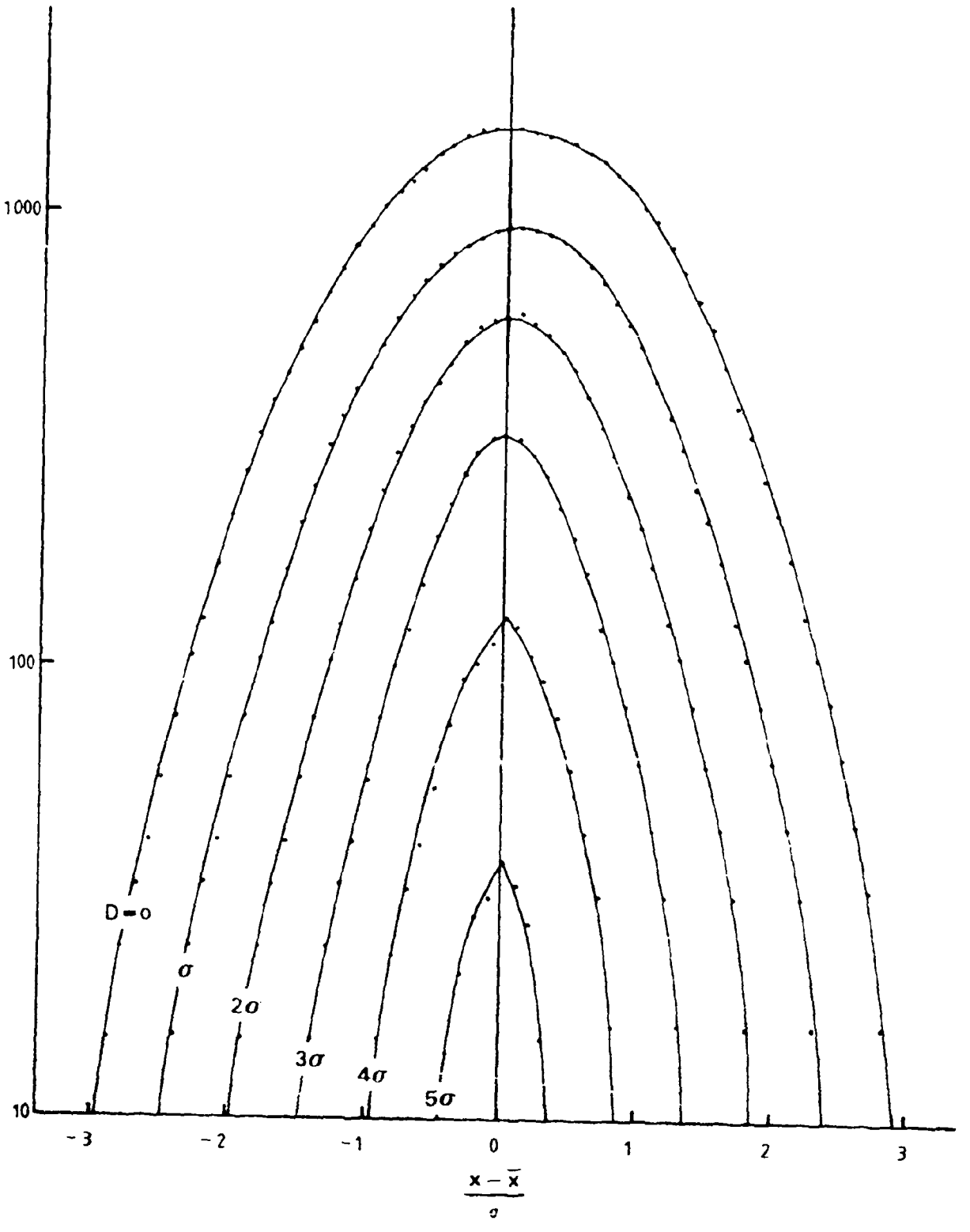

FIG. 13. LEVEL CROSSINGS OF U_{d_e} WITH VARIOUS MODIFIED DISCRIMINANTS

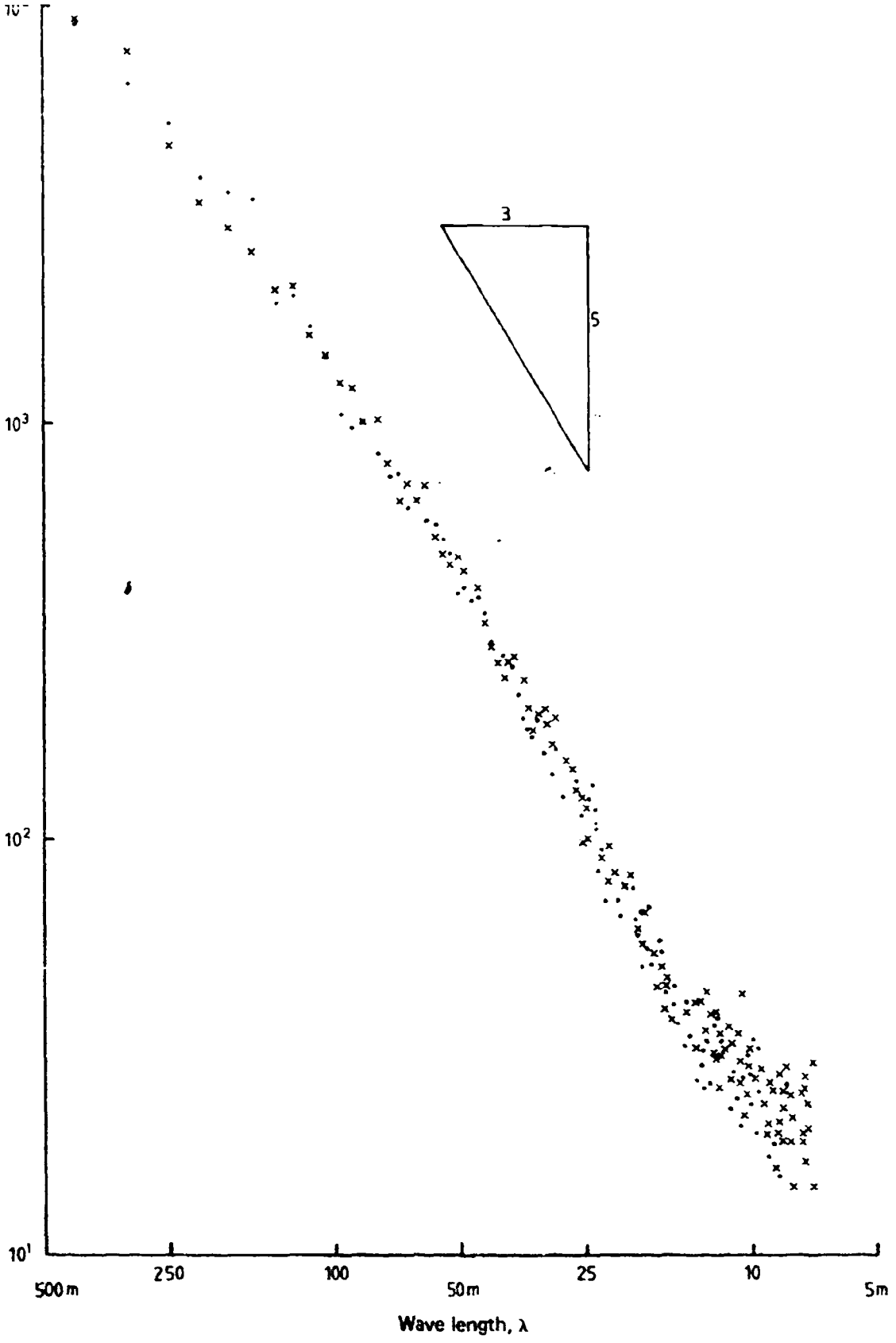

FIG. 14. SPECTRUM OF TURBULENT VELOCITY SIGNAL

DISCUSSION

QUESTION—*Sqn. Ldr B. Bryce, RAAF (Air Eng. Sc., Defair)*

In your talk you made the statement that a fatigue meter does not distinguish between a large amplitude crossing of a trip level, and a small amplitude crossing of the same level (ignoring cocking and firing for the moment). In practice, however, when a number of trip levels are used, and data resulting from hundreds of flight hours are plotted, the number of crossings of any "notional" trip level can be estimated by interpolation from the number of crossings of the actual trip levels. Would you agree with this?

Author's Reply

A set of fatigue meter counters appears to distinguish small cycles from large cycles in that two (or more) fatigue meter levels are crossed by a large cycle whereas only one level is crossed by a small cycle. However, the following two situations would not be distinguished by a conventional set of fatigue meter counters:

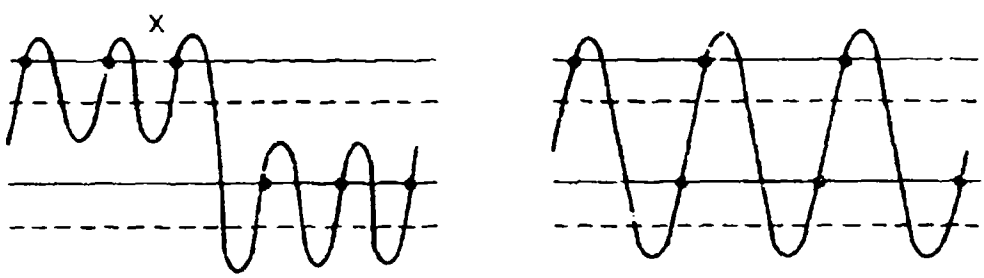

With a common firing level (e.g. 1 *g*) for all counters they would be distinguished, but at the cost of not counting the potentially damaging cycles at X.

DEVELOPMENT OF A LOAD SEQUENCE FOR A STRUCTURAL FATIGUE TEST

by

P. J. HOWARD

SUMMARY

A method for generating a load sequence for a structural fatigue test is described, and is illustrated by reference to the Mirage wing fatigue test.

Flight sequence and load spectra for this test were defined by fatigue meter data, and within-flight manoeuvre load sequences were derived from recorded time histories.

SYMBOLS AND ABBREVIATIONS

N_z	Normal load factor, the ratio of the current weight of an aircraft to its static weight
V	Aircraft velocity, kts
H	Aircraft altitude, ft
$\dot{\theta}$	Aircraft roll rate, deg sec
T	Type of flying
S	Stores carried
F	Fuel carried
Mission	A combination of T, S, and F
g	Acceleration due to gravity

1. INTRODUCTION

Given that a realistic load sequence is a desirable goal for a structural fatigue test, how can this be achieved and how much approximation is inevitable?

These questions are examined by a narrative study of a case history, the Mirage wing fatigue test, which represents the author's sole foray into the field.

2. THE AIRCRAFT

The Mirage IIIO is a delta wing interceptor (Fig. 1) which has been adapted for ground attack. Both roles involve rapid and severe manoeuvre loading accompanied by marked changes in altitude, H, and airspeed, V (Figs 2*a* and 2*b*). Indeed, they are the most spectacular and damaging of the ten or so types of flying (T) into which RAAF Mirage operations can be conveniently divided. The life history can be described by a succession of such flight types, of variable severity, separated by landings.

Every Mirage carries a counting accelerometer (fatigue meter) which stores on electromechanical counters the accumulated number of times that the aircraft acceleration normal to the wing surface passes any of eight preset levels. Counters cock as the acceleration represented is exceeded, but fire (register the count) only as the aircraft returns to within $\pm 0{\cdot}25\,g$ of the $1\,g$ level flight condition. These meters fail to record:

(1) load excursions which do not fire the counters (linking manoeuvres—shown A on Fig. 2*a*);
(2) load peaks between $-0{\cdot}5$ and $2{\cdot}5\,g$;
(3) the order of events;
(4) the magnitude of the turning points; and
(5) the state of all other aircraft parameters.

The last defect is important for Mirage because the load distribution over the wing depends strongly on current values of H, V, fuel (F), stores (S), and roll rate ($\dot{\theta}$) as well as the load factor (N_z).

The large store of fatigue meter data, about 200,000 flights, is of little help in establishing a load sequence. It adequately defines the N_z exceedance spectra for various missions (combinations of T, F and S), from counter readings, and mission sequence, from auxiliary records.

Other sources are needed to fill in the missing data. From a store of continuous time histories of aircraft parameters and structural strain responses, obtained during trials in 1969, RAAF fleet operators selected a set of flights which were typical of proposed Mirage operations and could therefore be used for defining load sequences.

This set of flights did not cover all possible missions which the Mirage is capable of performing: loads for these extra missions had to be estimated. Assistance in computing was provided by CAC,[1] who constructed a mathematical model of the load distribution for the aircraft. This model used current values of N_z, V, H, S, F and $\dot{\theta}$, and calculated loads distributed at the wing nodes. Where flights had to be synthesised, using only the measured N_z to define the load sequence, V and H had to be estimated from the type of flying, S and F from the initial state and the elapsed time, and $\dot{\theta}$ from N_z.

3. CONSTRAINTS

Besides the constraints imposed by limitations in data sources, additional constraints arose from the short timescale, limited resources and from a number of decisions.

The decisions of consequence to the creation of the load sequence were:

(1) flight-by flight loading would be applied;
(2) Manoeuvre, gust, air-ground and fuel pressurisation loadings would be represented, others would not;

(3) the loading system would allow for changes in distribution by using 14 independent computer controlled servo-hydraulic jacks connected by whiffle-trees to the wing;
(4) the jack loads would be stored as information on a standard 2,400 ft computer tape;
(5) to meet the desired time scale, the average number of loads per flight had to be limited to 100;
(6) only one control tape would be made. Decisions 3, 4 and 5 set the number of flights on this tape at 500;
(7) the overall load spectrum would be based on the averaged fatigue meter data for 1971 and 1972 and the flight sequence would conform to 1972 data, these being regarded by the RAAF as the best indicators of future usage.

4. TRUNCATION

In operations, the only constraint on the flight loads experienced by an aircraft is that the highest load should leave the structure intact. The limits of 500 flights per tape and 100 loads per flight fixed the maximum load to be automatically applied to the test at $7{\cdot}8\,g$ and the lowest load level at $1{\cdot}38\,g$ (Fig. 3). The intervening spectrum was defined by fatigue meter data for $N_z \geqslant 2{\cdot}5$, and by calculated gust data below this load. Because of rig design negative loads were truncated at $-1{\cdot}0\,g$ instead of $-1{\cdot}8\,g$ as required for one event in 500 hours. On our best prediction the truncations corresponded to Schijve's suggestion[2] that the highest loads should be that experienced 10 times in the service life, and to the fatigue limit of Heywood's curve B[3], the fatigue data used to predict the life at the root of the wing main spar.

Low loads were removed from the 16 sets of flight data to be used in defining the within-flight load sequences. This was achieved by extracting turning points in N_z separated by at least $0{\cdot}72\,g$, together with concurrent values of V, H, $\dot{\theta}$, F and strains at three spanwise main spar stations. This process compacted the data, pruned linking manoeuvres (perhaps over severely because of the high mean stresses sometimes involved) and eliminated all information on rate-of-change of N_z. Gust and ground loads and sequences were generated synthetically and were truncated on creation. The methods used for generating these loads are discussed later.

The highest naturally-occurring manoeuvre load in the sequence-generating flights was $7{\cdot}2\,g$, so that the upper truncation load had to be artificially introduced.

5. SEQUENCE OF FLIGHTS

It was assumed that the flight sequence in squadron usage was non-random, and that if the essence of order could be distilled it would be worth preserving.

The frequencies of different missions flown in 1972 were determined from fatigue meter data. A mission with a frequency less than 1 in 1000 (rounding to less than 1 flight in 500) was grouped with a similar mission of greater frequency. In case of doubt, the wing root bending moment, calculated for the initial fuel and stores from the CAC model, was used as a guide to mission similarity. Forty-four different missions remained and were given coded identification.

The 1972 sequence of flying, when re-labelled, showed strong pairwise ordering, in particular there was a pronounced tendency for adjacent flights to be identical missions. These attributes were quantified by producing, for each mission, two event frequency tables. The first showed the frequency with which the subject mission was followed by a different mission (transition probability). The second showed the frequency of occurrence of various run-lengths (number of times the mission was flown before different missions occurred). The ordering observed (runs of 10 identical missions were common and one case of 39 was seen) could be explained by bunching of training sorties, and a desire to minimise changes to aircraft configuration.

As analysed, the data related to 18,877 flights, and had to be compressed to 500 flights for the test. This was accomplished by multiplying all values in the frequency tables by 500/18,877. Fractional values in the transition probability matrix were eliminated by rounding. The run-length required a slightly more complicated treatment. Flights representing fractional frequencies of long runs were accumulated until an integral number of shorter runs could be formed.

Thus a frequency of 0·5 for a run of 12 and of 0·55 for a run of 11 (12 flights in all) became one run of 11 with one flight carried to shorter run-lengths. Small adjustments were made to these data to make the total of flights equal 500, and the total runs in both histograms the same (241).

The use of these tables is illustrated in Figure 4. The flight sequence for the test was derived by randomly selecting a mission (B), getting a run-length (2), deleting one from the run-length selected (2 − 1 = 1), selecting an allowed following flight from the transition probability table (A), deleting one from the box selected (4 1 3), and repeating the process until the data were used. In the illustration the first three flights are B, B, A.

The resultant test sequence necessarily conformed to the statistics built into its construction. Conceivably longer range order existed in the original data, but it was considered unrealistic to go beyond adjacent flights.

6. WITHIN-FLIGHT LOAD SEQUENCE

Manoeuvre Load Spectra

Fatigue meter data were processed to give N_z spectra for each of the 44 missions, scaled in the proportions used on the control tape. As this was being done, it was discovered that one type of flying code (80) had been used for high and low altitude versions of a mission in the approximate ratio of 3 high to 2 low. These versions had to be considered separately because altitude conditioned both the pressure distribution and the spectrum shape (high N_z is not easily achieved at high altitude). Eleven new missions were required; the N_z spectra for the split missions were generated by assigning all $N_z \geqslant 4{\cdot}5$ to low level and splitting the rest in proportion to the number of flights.

As this step was completed, the original, in retrospect over ambitious, plan to generate load distributions over the wing by putting current values of N_z, V, H, F and $\dot{\theta}$ into the CAC model collapsed. It was considered impossible within the available time to construct a computer model which would accept the distributed loads at 81 wing nodes, given by the CAC model, and compute 10 jack loads. To enable this to be done by hand, the 55 missions were reduced to 9 groups by combining missions having approximately similar flight profiles and loading histories. The N_z spectra for these 9 groups, Table 1, served as target spectra for the control tape.

Manoeuvre Load Sequence

Each of the 500 flights on the control tape was matched to one of the 16 load sequences obtained from the test flights by classifying the latter to current RAAF practice. A fatigue-meter like count on the control tape at this stage showed a disagreement between service and achieved spectra.

It was assumed that the load sequence would be substantially unchanged between different examples of a mission, but that the levels reached by individual turning points would be variable. A host of quasi-flights was generated by scaling every turning point on all sequences by the relation

$$N_Q = K(N_z - 1) + 1$$

where K had values in the range 0·8 to 1·4. This set was further extended by slightly changing a few turning point values so that they just crossed a counting level or the 1 g datum. Judicious and tedious selection from this set of data resulted in the nine target spectra being matched at the fatigue-meter counting levels, and the overall spectrum being matched at intervals of 0·5 g in the range $2{\cdot}5\,g \leqslant N_z \leqslant 6{\cdot}5\,g$. Arrangements were made to apply a load of 8·5 g manually every 5000 flights, but this was done irregularly, and for a load case which produced main spar strains less severe than those occurring with the 7·8 g load regularly applied.

Gust Spectrum

The fatigue meter cannot be used as a source of gust loads on Mirage since these are generally less than 2·5 g. Published data were used to generate a gust velocity spectrum which was transformed to a N_z spectrum by a measured transfer function for Mirage, and a load distribution was calculated based on a measured spar strain/N_z for gust. It was assumed that gusts were experienced mainly in low level roles, that they would occur independently of manoeuvre loads, that the random order of turning points was constrained so that troughs were the negatives of the preceding peaks, that the mean load was 1 g and that the manoeuvre loads already used were free of gust loads.

A gust N_z sequence, conforming to the spectrum and suitable for 500 hours, was generated

by random selection of loads quantised to 0·02 g in the range 1·5–3·0 g. This was cut into 169 equal segments each of which was fed into a low level flight ten typical flights are shown in Figure 5.

Landing and Pressurization Loads

Landing loads, important to the undercarriage and attachments, have only a minor influence on the stress history of the main spar. A simplified load sequence consisting of a rotation, a landing impact with springback, and a couple of bounces was inserted between each flight. These loads were applied through an undercarriage. At the same time the fuel tank was depressurised (on landing) and repressurised (on take-off) to the levels normally used.

The entire sequence of loads was transformed to a corresponding sequence of jack load instructions by a process beyond the scope of this paper.

7. DISCUSSION

Having put in a considerable effort, it would be nice to confidently assert that the ultimate in realism had been achieved, and that it was all absolutely necessary.

The process described can only be applied late in the life of an aircraft, or when a new design is expected to perform precisely as its predecessor. The load sequence derived can apply to, at most, one aircraft of the fleet, and probably is identical to none. It is realistic only in the sense that if an RAAF pilot conformed exactly to the N_z, V and H pattern used, he would not consider the flight to be atypical.

Gust loads accounted for 60% of the loads, and hence half the test time, and were generated synthetically from data of dubious relevance to Mirage operation. Substantiation of the reality of this component of the test is difficult.

The overall spectrum (level crossing exceedances) of manoeuvre loads agrees excellently with the measured spectrum. However, this forced agreement was based on an assumed firing level of the fatigue meter of 1·0 g, whereas subsequent work has shown that it is nearer 1·25 g. The applied spectrum was therefore about 10% too severe. The assumption, implied by the wholesale magnification of turning points values, that the sample of sixteen flights contains a proper ratio between fatigue meter and linking manoeuvres (i.e. that it is correct on a range-pair-mean counting basis) has yet to be tested.

The wing failed at a stress concentration slightly outboard of the control point used to determine the test load spectrum. The SN data judged appropriate for the actual failure site placed greater emphasis on the importance of low loads than did the data used to set up the test, so that the lower truncation level is suspect. Finally the load sequence used contained no readily identifiable blocks, and the problem of relating crack size to test duration by post-failure fracture analysis proved immense. It was eventually solved, but at a great cost in effort and by the exercise of considerable ingenuity.

So much for pessimistic comments, which surely apply in equal or greater measure to most similar tests.

More optimistically, the load sequence used represents all of the events seen by Mirage, and provides sufficient variety to allow recent advances in range-pair counting and sequence accountable damage techniques to be assessed. Perhaps when these assessments are completed the effect of sequence changes, e.g. application of high loads early in the life of the aircraft, will be calculable. All we will need then is a reliable load monitoring device which stores sequence as well as magnitude for each turning point.

8. CONCLUSION

A flight-by-flight sequence for a Mirage wing fatigue test was generated using.

(1) fatigue meter data to give flight order and manoeuvre load spectra;

(2) estimates of loads arising from atmospheric turbulence; and

(3) flight trial data to provide within-flight load sequences.

When combined with ground loading and pressurisation loads, the load sequences are believed to represent squadron usage as accurately as the available data permitted.

REFERENCE

1. Nankivell, J., and Beckett, R. — Mirage Wing Fatigue Test: Theoretical Wing Load Distributions. Commonwealth Aircraft Corporation Report No. AA276, January 1973.
2. Schijve, J. — The Endurance Under Programme Fatigue Testing. Full Scale Testing of Aircraft Structures. Proceedings of the Symposium held in Amsterdam 5–11 June 1959; International Series of Mimeographs in Aeronautics and Astronautics Division IX: Symposia Vol. 5, Pergamon Press, 1961.
3. Heywood, R. B. — Correlated Fatigue Data for Aircraft Structural Joints. Aeronautical Research Council Current Papers. C.P. No. 227, H.M.S.O., June 1955.

TABLE 1
Correspondence between desired and achieved spectra for various missions in wing fatigue test per 500 flights

Mission code	Source	F.M. level							
		−2·5	−1·5	−0·5	2·5	3·5	4·5	6·0	8·0
1	F.M.	—	—	2·8	2818·6	1444·2	661·6	42·0	0
	Tape	—	—	—	2822	1426	659	45	0
2	F.M.			1·1	400·8	168·2	67·0	3·1	
	Tape			—	400	169	67	4	0
3	F.M.			2·1	296·4	95·2	25·5	1·1	
	Tape			—	297	95	27	1	0
4	F.M.			3·6	484·7	133·1			
	Tape			—	485	133			0
5	F.M.			4·1	520·6	205·9	100·9	9·6	
	Tape			—	521	206	101	9	0
6	F.M.			3·5	493·1	244·6	122·8	22·9	
	Tape			—	489	249	124	23	0
7	F.M.			2·6	1333·8	588·5	214·7	13·4	
	Tape			—	1330	589	208	12	0
8	F.M.			9·8	421·3	156·7	50·7	5·4	
	Tape			28	420	162	56	6	0
9	F.M.			0·3	124·7	76·1	53·4	6·1	
	Tape			—	126	76	53	6	0
Total	F.M.	0·25	2	33·9	6888·9	3104·2	1295·9	105·8	0·5
	Tape	—	—	28	6890	3105	1295	106	0

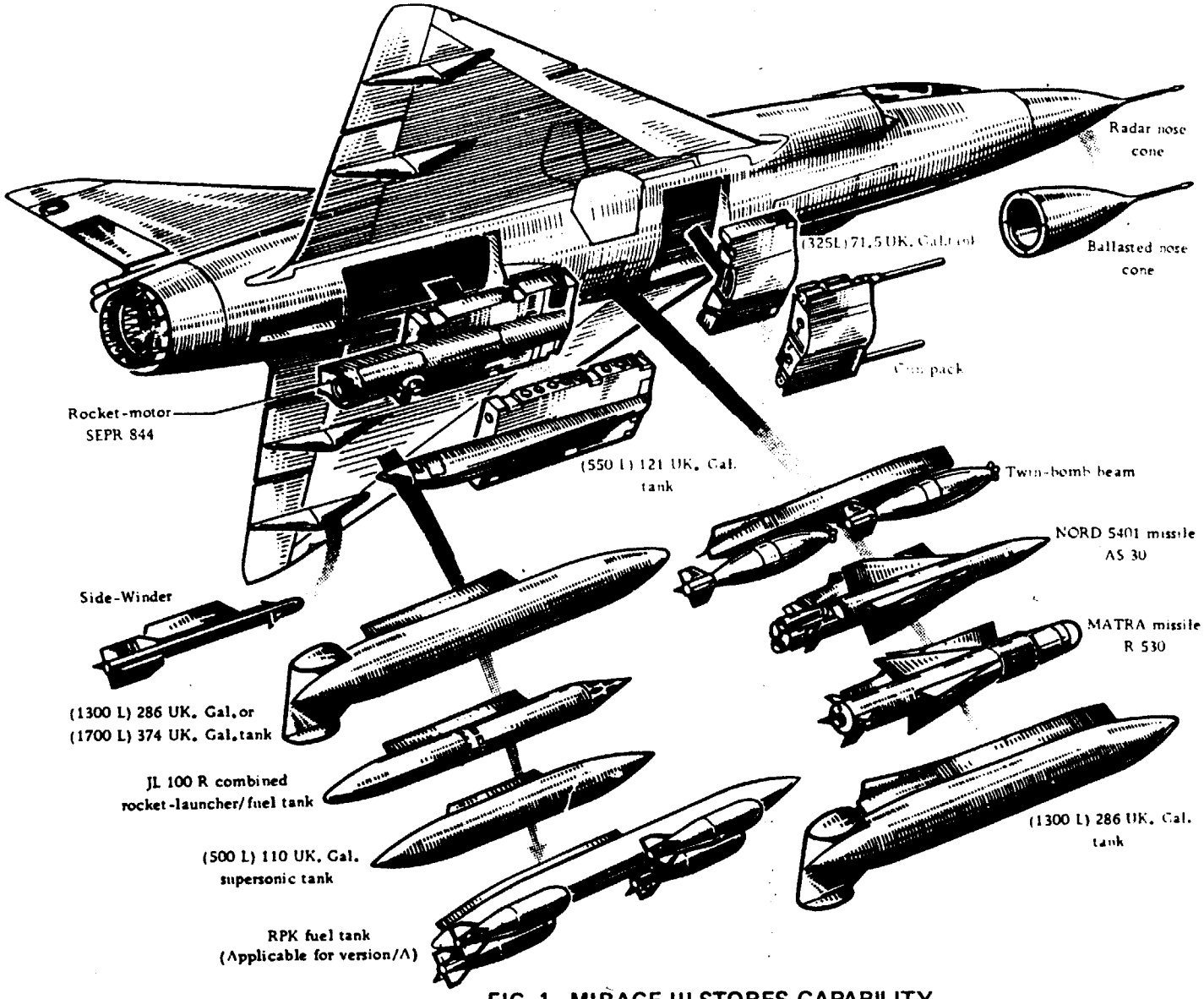

FIG. 1. MIRAGE III STORES CAPABILITY

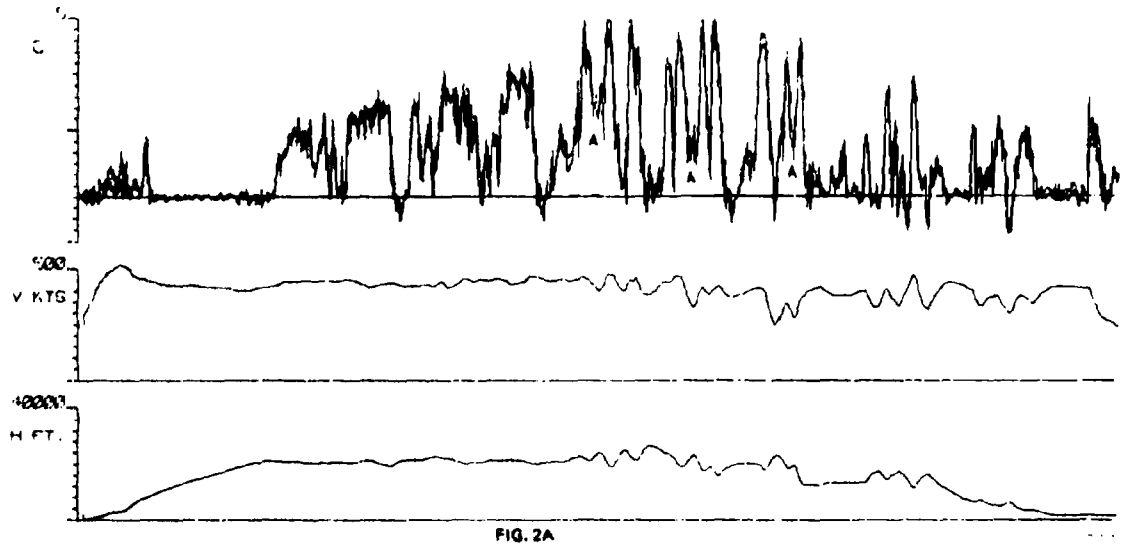

FIG. 2A

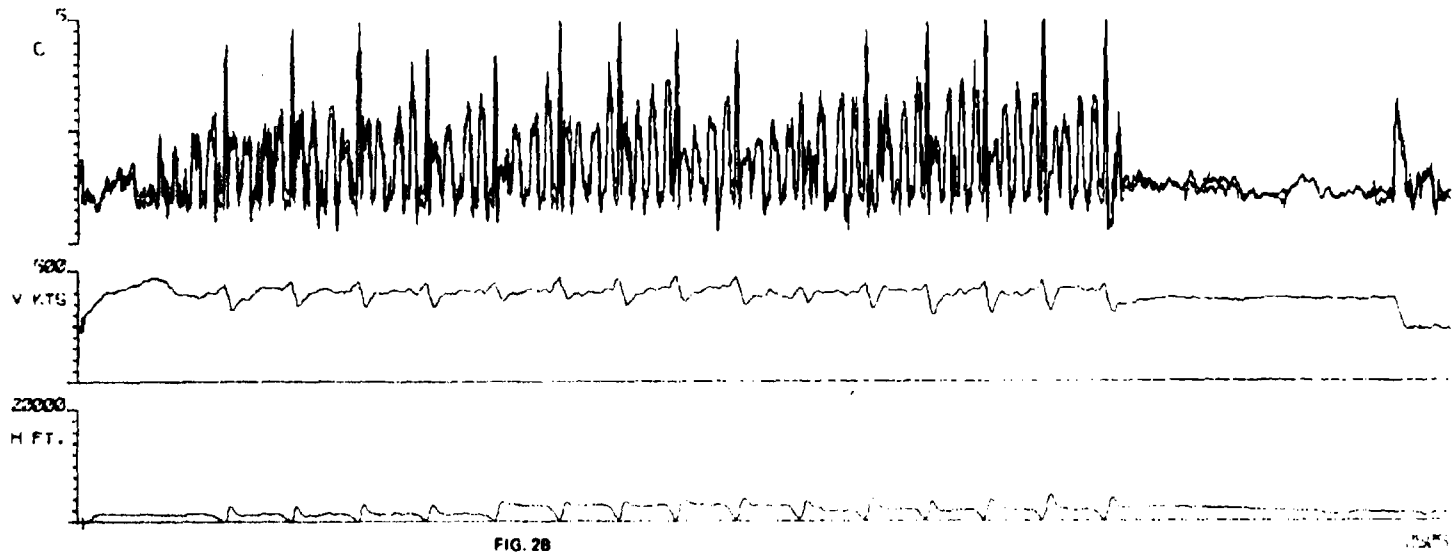

FIG. 2B

Figs. 2A, 2B LOAD, SPEED, ALTITUDE HISTORIES FOR TYPICAL MIRAGE SORTIES

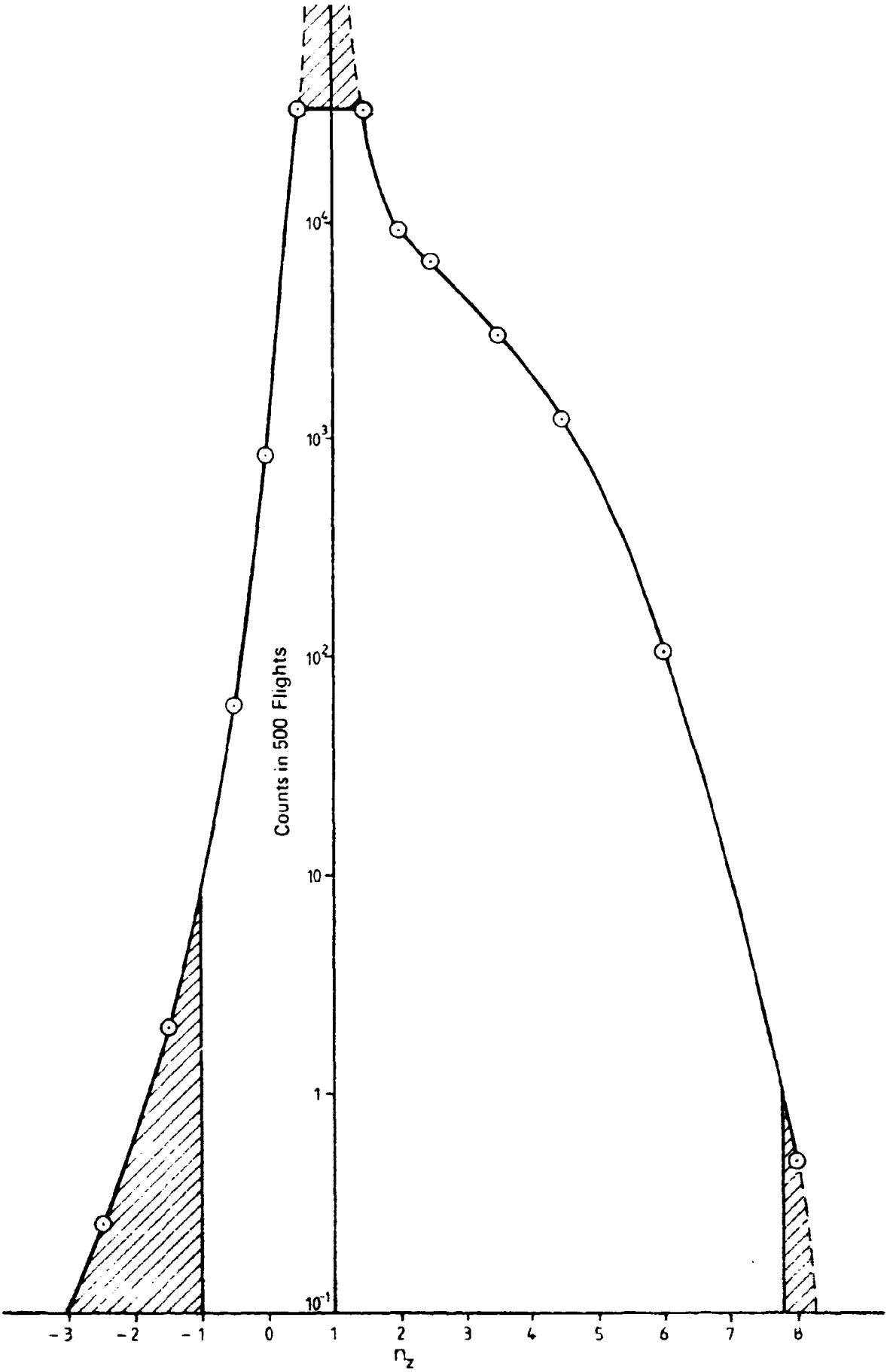

FIG. 3 LOAD SPECTRUM AND TRUNCATION

A	B	C	D	E	T	1	2	3	4	5
—		2	1	1	A	~~1~~	2			
~~3~~	—			3	B	3	~~1~~	1	1	
		—	1	1	C	1	1			
	7		—		D	2	2	1	1	1
			5	—	E	2	2	1		

B,B,A,—,—,—

FIG. 4. ILLUSTRATIVE DOUBLE MATRIX FOR GENERATIONS OF FLIGHT SEQUENCE

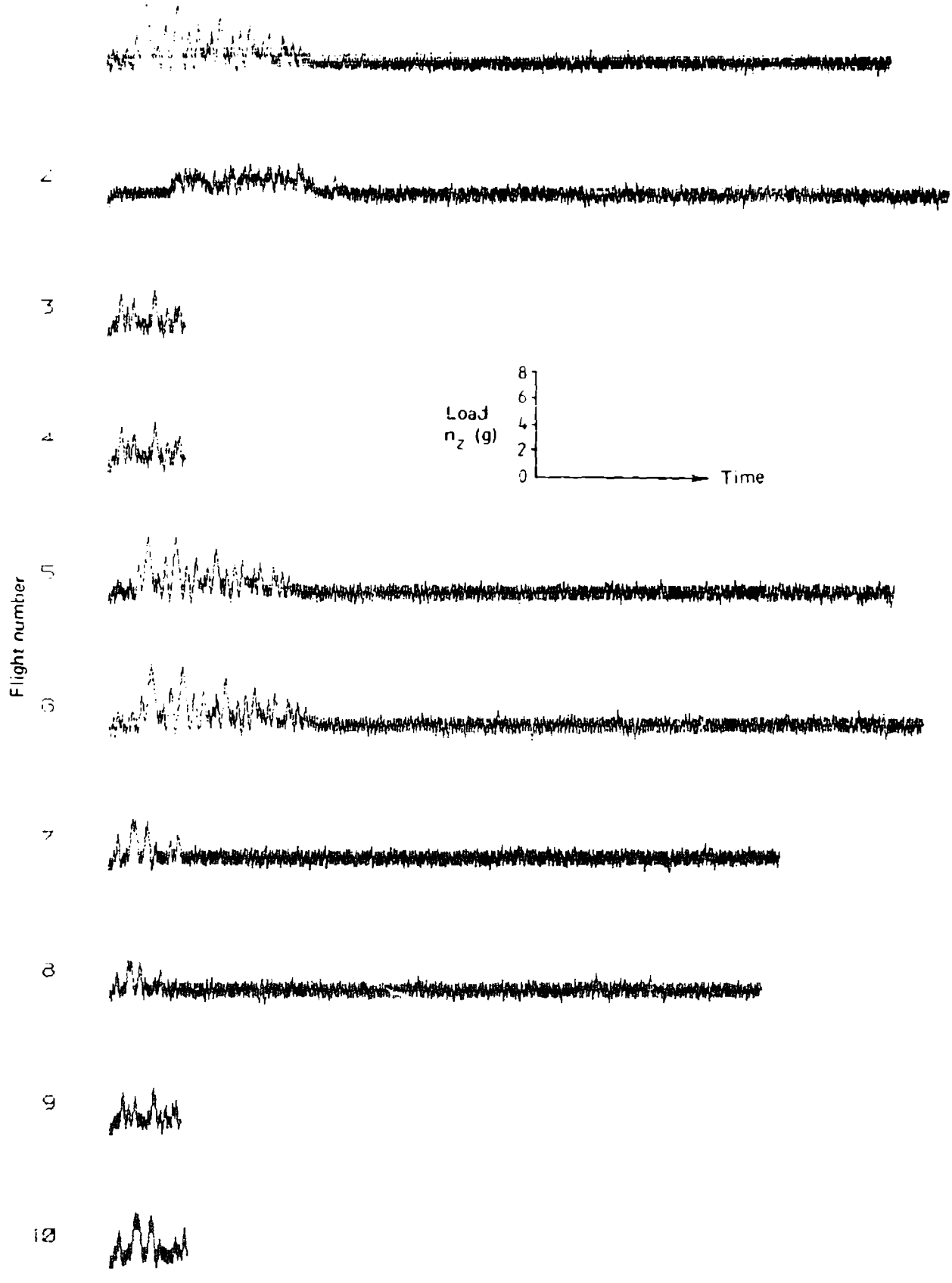

FIG. 5 TYPICAL LOAD SEQUENCES

FATIGUE S/N DATA IN RELATION TO VARIABILITY IN PREDICTED LIFE

by

J. M. FINNEY and J. Y. MANN

SUMMARY

Within the context of fatigue life prediction using S/N data, an investigation has been made of the variability which may arise from either fitting a mean curve to a given set of points or from sources affecting the data points themselves.

Given two sets of S/N data points, a number of people, including some experienced and some inexperienced in fitting S/N curves, were invited each to fit his own curves. From these, mean lives to failure were predicted for several multi-load-level spectra. For the experienced group the range of values of predicted life, from the largest to the smallest, and averaged over the several spectra, was 3:1 for one set of data points and 2·4:1 for the other set. The ranges of values for the inexperienced group were significantly wider.

Five mathematical methods of curve fitting were applied to one set of data points, with the resultant average range in predicted life being 1·4:1. This variability arises mainly from the subjective choice of a functional form for the S/N curve. The added variability due to other arbitrarily-chosen constraints such as weighting, the non-intersection of curves within a family, and the choice of a fatigue limit, is also discussed.

Many factors associated with the determination of fatigue data influence the resultant S/N relationship and some of the more significant ones are considered. The specific data presented for these various factors give variations in S/N life, and hence in predicted life, ranging from 1·5:1 up to 10:1. Those factors examined include the loading accuracy of the testing machine, specimen manufacturing methods and the number of specimens tested, the definition of fatigue failure, variability between batches. The resulting differences in predicted lives demonstrate the need for considerable care in selecting and using S/N data for the purpose of life prediction.

1. INTRODUCTION

The acquisition of experimental information, whether to assess the validity of a hypothesis or to provide specific data for engineering design purposes, involves the conduct of tests in which studies are made of the response of samples to changes in a particular variable. Much of the information is presented in graphical form so that any particular features in the relationship can be more easily recognised and interpolations made between test points.

Experimentation involves uncertainties, and tests on nominally identical samples under nominally identical testing conditions will almost invariably give a different measured response. Observations are subject to experimental errors which can arise from a variety of sources which may be difficult or not economically feasible to adequately control. Although on a laboratory scale it may be possible to minimise the effects of errors associated with the testing process by introducing randomization techniques, a relatively large variability may remain which is inherent in the sample being investigated.

In the context of engineering materials, it must be recognised that standards and specifications allow relatively wide tolerances in chemical composition and that the strength requirements which are specified are usually minimum values. Providing the finished product meets the requirements of the specification, the manufacturer of the material can employ a variety of forming conditions and heat treatments in the various stages of manufacture: these may be dictated by plant capability or specific operational practices. The tolerances and limits imposed during production may differ significantly from one manufacturer to another in meeting an identical specification, or may differ between batches from the same manufacturer.

The net result is that quite wide variations in the strength properties of a material can occur both within a batch[1] and between batches and it is not unusual for the average ultimate tensile strength (UTS) of a batch to be 20% greater than the specification minimum value.[2] From a metallurgical viewpoint, such variations reflect differences in both the macro- and micro-structure of the material, although rarely is any attempt made to correlate these variations with resulting mechanical properties. Thus, variability in the behaviour or response of a material to an imposed loading condition must be accepted in engineering practice as the norm, rather than the exception.

In the field of fatigue it is common to measure the response of a specimen (in terms of cycles to failure) to an imposed alternating stress. Fatigue tests at different magnitudes of alternating stress allow a relationship between fatigue stress and cycles to failure (S/N) to be determined. The total numbers of specimens used to establish this relationship (which includes replicates at particular stress levels) have ranged from less than 10 to greater than 30. Among such replicates a scatter in endurance of one order of magnitude at any stress level is not unusual. It is common to adopt the average or median lives at the various alternating stress levels as the basis for graphically expressing the S/N relation.

In 1964 Buckland[3] stated that "in practice, however, the lines purporting to depict the relationship between S and N are frequently drawn by 'eye' and are usually intended to indicate some average fatigue performance". It is the author's opinion that the majority of published S/N curves—and most other graphs showing an experimental relationship between two variables —are still sketched "by eye" rather than derived mathematically. Statistical methods are, however, currently available for determining estimates of the distributions of endurance from which curves representing specific probabilities of failure may be established.

A major objective in much of the research associated with aircraft structural fatigue is to provide information which will allow a prediction to be made of the life of aircraft structures under a multi-load-level service history. S/N data are frequently used for this purpose. Such data should be obtained using both specimens and loading conditions which closely represent the particular structure or component of interest. The other major requirement for predicting fatigue life is, of course, the relevant service load spectrum for the item in question and, usually, this is also obtained experimentally. Two further steps, which are often based on somewhat arbitrary decisions, are then necessary to transform these data into a prediction of the mean service life. The first is to transpose the load spectrum into groups of cycles of constant amplitude. The

second is to define a "cumulative damage" rule which specifies how damaging is each of the transposed constant load amplitude cycles relative to the S/N curve which, itself, defines the life to failure for continuous cycling under such load amplitudes.

The aim of this paper is to consider the variations in predicted life which may occur as a result of differences in the shapes and positions of various estimated "mean" S/N curves. Two sets of data have been chosen for examination, both sets coming from comprehensive and well documented fatigue testing programmes, and two sources of variation are examined; that which comes from fitting a mean curve to a given set of S/N data points, and that which may arise from sources affecting the data points themselves (for example, the cyclic frequency used in the laboratory fatigue tests). To obtain data on the first source a canvass was conducted within the Structures Division of the Aeronatucial Research Laboratories (ARL) which provided a number of "best-fit-by-eye" mean S/N curves and also mathematically-defined mean S/N curves.

2. S/N CURVES

The basic fatigue test data supplied for the canvass were obtained during research investigations at ARL and are fully reported in References 1 and 4. Figure 1 shows results, taken from Reference 4, for axial load fatigue tests on circumferentially notched circular section specimens ($K_t = 1{\cdot}6$) of 2L.65 aluminium alloy which were tested at a mean stress of 66 MPa (9·5 ksi) in two Amsler "Vibrophore" machines at a cyclic frequency of approximately 115 Hz.* The information shown in Figure 2 was obtained from rotating cantilever tests on circular-section notched specimens ($K_t = 1{\cdot}45$) of D.T.D. 683 aluminium alloy at a cyclic frequency of 200 Hz,† but in this case data previously reported in Reference 1 for the stress level 172 MPa (25 ksi) (mainly runouts) were omitted. These two particular sets of data were chosen because their mean S/N curves were likely to be significantly different in shape.

Primary input S/N curves were obtained by providing technical and scientific staff within the Structures Division of ARL with fatigue data and asking them to construct what, in their opinion, was the best fit mean S/N curve: the fatigue data were the graphical plots shown in Figures 1 and 2 and the numerical data given in Table 1(*a*).

A survey was made of the results provided by those co-operating (46 persons), including persons whose interests and experience in fatigue ranged from virtually nothing to "very considerable", so that it was possible to assess whether variations in the range of predicted lives based on the S/N curves obtained, could be associated with the different fatigue experience. S/N curves drawn "by eye" were sought because, firstly, such curves are prevalent in published fatigue data and are generally used for current fatigue life estimations and, secondly, because many of the staff included in the canvass would not be in a position to produce precise mathematically defined curves. (Sufficient information (given in Table 1(*b*)) was, however, available for the derivation of mathematical curves which describe the mean S/N behaviour of the data shown in Figure 1.)

3. LIFE PREDICTIONS FROM S/N CURVES

3.1 Method of Prediction

When using S/N data to predict fatigue lives under a varying-load sequence the requirements are:

an S/N relation;
a service load spectrum;
a method of transposing the load spectrum into cycles of constant amplitude; and
a cumulative damage rule.

This Section briefly describes the procedures relating to the last three of these requirements which are relevant in the present context, while the following sections (3.2 and 3.3) present the various S/N relations provided by the canvass and the predicted lives which resulted from combining them with different spectra.

* The fatigue lives correspond to either complete fracture of the specimen or the development of cracks to a size where complete fracture would be expected in an insignificant number of additional load cycles.

† All specimens completely fractured.

Accumulation of service loads data over the years has enabled loading spectra to be expressed in a general form. One such presentation, given by Ostermann,[5] is shown in Figure 3. It is clear that spectrum D contains a larger proportion of low loads than do spectra A and B. Spectrum D may be related to positive gust loading on an aircraft whereas spectra A and B can typify positive manoeuvre loading. To give wide applicability to the S/N results, life calculations for each curve have been made using the four spectra shown in Figure 3. Several different spectra were used because, for a given cumulative damage rule, the proportion of calculable damage at any stress level depends upon the spectrum shape. Figure 4 shows the damage distribution for these various spectra when applied to one S/N curve.* (While the abscissa scale in Figure 3 is important, when predicting actual lives, it is not important when considering the ratios of lives.)

Since the present analysis uses a single S/N curve only, rather than a family of curves corresponding to various mean stresses, the spectrum shapes in Figure 3 have been taken, for convenience, as symmetrical about the mean stress level of the S/N data. Also, the stress axis in Figure 3 has been matched to the range of alternating stresses used to obtain the S/N data. Thus, the conversion of the load spectrum into constant amplitude cycles is unambiguous and is a straightforward matter.

The cumulative damage rule used (Step 4) was the usual Miner linear summation of cycle ratio ($\Sigma\, n_i/N_i = 1$). The subsequent transformation of various S/N curves into predicted lives used only those levels of stress employed in determining the S/N data points.

3.2 Eye-drawn Curves

Figures 5 and 6 are composites of all the "eye-drawn" curves for the data given in Figures 1 and 2 respectively. The scatter of predicted lives using such eye-drawn curves can be seen readily in the histograms of Figure 7 which are based on the S/N curves of Figure 5 and cover the four spectra A to D.

The standard deviation of predicted life has been estimated in each case, and by similarity of the histograms to a normal distribution, about 68% of predicted lives lie within one standard deviation from the average. Table 2 gives the average predicted life and its standard deviation for the four spectra and for both sets of S/N data. These statistics are given for the overall group (46 curves) and for the classifications "experienced" (16 curves) and "inexperienced" (30 curves).†

The point of interest in such results is the scatter and not the particular values of predicted life. Table 2 gives the scatter both in terms of the ratio highest/lowest predicted life, and in terms of the coefficient of variation (standard deviation divided by average life). The influence of the curve-fitter's experience on the dispersion of predicted lives can be seen in Table 2. The various curves of Figure 5 fitted by those of the experienced group led to a scatter of the predicted life characterised by a coefficient of variation of (when averaged over the four spectra) 27%, while fitted curves for the inexperienced group led to a corresponding figure of 38% (see Table 2(*a*)). A practically identical result was obtained using the S/N curves shown in Figure 6 (see Table 2(*b*)). An *F*-test showed that, when the coefficients of variation were pooled for all spectra, the experienced group gave less variability in predicted life than did the inexperienced group, at a significance level of 0·2%. This result did not apply to all individual spectra however. The *F*-test for spectrum D combined with the relevant curves from Figure 5, and for spectrum B combined with the relevant curves from Figure 6, showed the inexperienced group to have the smaller scatter in predicted life, but only at significant levels of 10% and 5% respectively.

Despite the smaller overall scatter in predicted lives for the experienced group, it is important to emphasise that their dispersions were 3 : 1 for the appropriate curves from Figure 5 and 2·4 : 1 for the appropriate curves from Figure 6.

3.3 Mathematically-defined Curves

It is clear from the results of the previous Section that personal bias influences the S/N curves (resulting in large variations in predicted life), and it may appear a simple matter to

* The curve used here was that defined by a least squares fit of a second degree polynomial to the data points shown in Figure 1, the points at each stress level being weighted by the reciprocal of the variance at that level. Since most curves are reasonably similar for the one set of data points, the damage curves are also similar.

† The experienced/inexperienced subdivision was made on the basis of answers to a question asked on "experience" in the canvass.

eliminate such bias by a mathematical approach. But mathematical analyses rely upon assumptions (which may involve subjective judgements) and it is the purpose of this Section to explore several methods of analysis, examine their variability, compare this with the eye-drawn variability, and discuss the assumptions inherent in such methods.

Five curve fitting methods were applied to the S/N data for the 2L.65 alloy (Figure 1). They all rely upon a least-squares best fit and are briefly described as:

(1) A polynomial function with the application of a significance test to determine the least degree giving a good fit.

(2) A simple power relation, $N = A \cdot S^B$ (A and B constants). This method has as its basis the knowledge that many fatigue data can be correlated by such a function (e.g., the well-known Coffin/Manson relationship[6,7]).

(3) The arbitrary fitting of consecutive straight lines (piecewise linear) on an S/log N plot, if judged applicable to the data. This, however, is not a universal method.

(4) A weighted polynomial. It is evident from the base data (Fig. 1) that the scatter of test lives (in terms of log life) varies from one stress level to another. It could thus be argued that a "better" fit will be obtained by weighting the test results at each stress level in the least squares analysis to favour those with less scatter; less scatter implying greater confidence in the position of the mean at any stress level. An additional S/N curve was provided by using a weighting factor of 1/variance of log life, appropriate to the stress level (a factor used by others[8,9]), in the fitting of a polynomial function.*

(5) A method of maximum likelihood with assumptions about the distribution of life at each stress level and the functional form of the curve. To compare the results of this method with those of the weighted polynomial, a polynomial functional form was used with the assumption of log life being normally distributed at each stress level. In practice this method follows an iterative procedure, with the first estimate of variance being that of the data points, and subsequent estimates being based on the position of the curve resulting from the previous estimate. In the present case, the method essentially is an iteration of the values of the variance used as a weighting factor for the method described above.

Figure 8 lists the five equations obtained by these various curve fitting methods and compares them graphically. It is clear that the weighted polynomial and the maximum likelihood method also using a polynomial have given practically identical results. As with the eye-drawn curves, lives were calculated from the same spectra and stress levels and the results are given in Table 3. Differences in predicted mean lives are again evident with an average coefficient of variation of 15%.

Although mathematically-derived curves supposedly eliminate personal bias, it is instructive to see whether or not this is so by comparing their resultant average and scatter in predicted mean life with the same quantities obtained from the analysis of the experienced eye-drawn group. Comparing Tables 2(*a*) and 3 it is clear that the average of the predicted lives of the mathematical group is neither consistently higher nor lower than the corresponding values for the experienced eye-drawn group over the range of spectra investigated. The mathematical group shows marginally less scatter in predicted life (significant at a level of 20% only) compared with that obtained from the experienced eye-drawn group. This is rather inconclusive because of the small sample taken for the mathematical group.

The foregoing has essentially examined one of the necessary assumptions in deriving a mathematical curve, namely, the assumption of the functional form of the curve. It is apparent that different curves (and hence different predictions of mean life in the present context) result from different functional forms. The power function is a rather rigid form, allowing little latitude, and in fact does not adequately represent all S/N data. Table 3 shows that the lives predicted using a power function for the S/N relation are somewhat different from those using other functional forms. The greater flexibility of the polynomial function may be expected to result in better fits, but this flexibility can lead to its rejection for either of two reasons. Firstly, most people familiar with fatigue data would accept one inflexion in an S/N curve, or in extreme cases two, but since polynomials of degree n may have $(n-2)$ inflexions, experience may limit the degree of the polynomial to three, or four at the most. Secondly, even with low-degree poly-

* It is noted that although fitting a polynomial involves no assumption about the distribution of the data points, the use of 1/variance as a weighting factor implies a normal distribution of log life.

nomials, curve fitting problems may arise from the common practice of testing groups of specimens at discrete stress levels. There is little constraint on polynomials *between* the data levels and positive slopes may occur, a result which, intuitively, is unacceptable. Thus, one has the option of using a rigid form which may not adequately suit all S/N data, or a more flexible form which may run into difficulties and force the user into further subjective judgements.

A possible solution, for any set of data, is to investigate a number of functional forms, all of which are considered acceptable (subjective judgement is required here), and to choose between them on the basis of some objective test, such as selecting that curve which has the least residual sum of squares.

Apart from the question of functional form, other assumptions may be inherent in deriving a mathematical expression to fit data points. Some methods require the specification of the distribution of lives at any stress level (e.g., the maximum likelihood method), and although a normal distribution of log life is often chosen, other distributions have been proposed.[8] Since scatter in S/N data is rarely independent of stress level, the use of a weighting factor may also appear necessary when using a least-squares analysis, as mentioned above. But the question of "what factor" may be open to judgement. Some idea of the effect of weighting on predicted life may be gained by comparing the polynomial function results shown in Table 3. The predicted mean life using a weighted curve decreased by an average of 10% when compared with that predicted using an unweighted curve.

This discussion has considered so far the specification of the S/N curve between the extremes of the data levels only. Often the impetus for a mathematical formulation lies in the need to extrapolate the S/N curve, particularly to lower stress levels where calculations may indicate that a significant proportion of the total damage could occur. Such extrapolations may indicate an unacceptably short fatigue life at zero stress. To overcome this problem the formulation of the curve may use not only the test data points, but the added constraint of infinite life at zero stress or at some *arbitrarily-chosen* endurance limit. This procedure is just as subjective as eye-drawn extrapolations.

The assumptions listed above all relate to the specification of a mean S/N curve through a specific group of test data, e.g. data at constant mean stress. But, in practice, life calculations often require a family of such curves, identified by some parameter such as mean stress or R-ratio. If the methods above are applied piecemeal it is possible for individual curves of the family to intersect. Such a possibility would be intuitively rejected. The only course then is to consider the data as a whole, under the constraint that curves of the family must not intersect.[23]

In concluding this Section it is emphasised that, irrespective of whether the S/N curves adopted are eye-drawn or mathematically-based, it is necessary to make subjective decisions in the treatment of the data. (A similar conclusion has been reached recently[10] in the fitting of curves to characterise fatigue crack growth.) The purpose of this paper is not to indicate which of candidate S/N curves is the best curve to adopt for a particular set of data, but rather to demonstrate the variability in predicted mean life which may result from the choice of different curves.

4. FACTORS INFLUENCING S/N DATA AND THEIR EFFECT ON LIFE PREDICTION

The foregoing discussion has centred around the determination of mean (50% probability of failure) best-fit S/N curves for particular sets of fatigue data. Apart from the use of weighting factors derived from the variance of the life data at different stress levels, no attempt has been made to assess the variability of the data or to determine S/N curves for lower probabilities of failure. Such curves would, when based on a statistically defined fatigue life scatter factor, be more appropriate to use in estimating safe lives. However, when S/N curves are published without individual or average test points being shown and without any indication of the variability in endurance, the reader cannot gauge the accuracy or reliability of the information presented. In fact, most published fatigue data will, at best, only allow an estimate to be made of the central tendency (average) behaviour and provide a statistically insignificant amount of information relating to variability. The question of the form of the distribution of fatigue life (whether, for example, log normal or extreme value) has not been emphasised in this paper as it is considered to be of only secondary importance in the current context.

When faced with the requirement to estimate the life of a component or structure under a multi-load-level spectrum, a basic problem is to choose the most appropriate fatigue data for the detail of interest. Careful consideration must be given to the selection and interpretation of S/N data for such a purpose, particularly when life estimates are required to a high degree of confidence

and the accuracy of the estimate could have serious ramifications in relation to safety and economy.

Very rarely would the analyst find in the literature, adequate data for the exact alloy, joint, notch geometry and K_t value, and mean stress, obtained on specimens of a size commensurate with his component and fatigue tested at about the cyclic frequency of his component in service. He is more likely to be faced with a rather inhomogeneous set of data embracing the results of fatigue tests carried out over a period of many years, in different laboratories and by a variety of experimenters, and he would probably overlook such matters as the testing method and type of testing machine (e.g. constant load, constant displacement) used to obtain the data, and its accuracy of alignment and load control, the definition of fatigue failure (e.g. a small fatigue crack or complete fracture) adopted by the experimenter, the procedures used in making the specimens, the number of specimens tested, and the influence of the fatigue test environment. These are all variables which can influence the fatigue lives of both individual specimens and groups of specimens, and hence the basic data from which S/N curves are derived.

Thus, in making the choice of one set of data compared with another for life estimation purposes, one must recognise the limitations of the data in order to assess its relevance for each situation. It is not intended to discuss each of the above variables individually as reference has been made to some elsewhere,[11] but simply to highlight several of these variables and indicate the magnitudes of the consequent variations in predicted fatigue lives in some cases and to emphasise that, in any practical situation, interpretation, extrapolation and subjective judgement of the data are inevitable at different stages of the life prediction process.

Fatigue testing equipment—accuracy of load calibration, setting and control. Fatigue data acquisition for aircraft structural design purposes has involved the use of many designs of testing machine ranging in load capacity from about 1 kN to over 2 MN, with the forces on the specimen being produced by mechanical, centrifugal, electro-magnetic, hydraulic or pneumatic actions. In addition, a variety of dynamic load measurement and control systems have been developed some of which are inherently more accurate than others. In a fatigue testing programme systematic and random errors in load measuring systems, variations within control circuits and differences between operators, can both increase the scatter in fatigue life and introduce undetected bias at particular load levels.

Little systematic research has been undertaken to compare the fatigue properties of "identical" specimens tested in different laboratories, but that which has indicates[12,13] that significant differences in the fatigue behaviour can occur.

The ISO Recommendation on Axial Load Fatigue Testing[14] states that "the mean load and the load range as determined by a suitable method of dynamic calibration should be known to within 3% of the maximum load of the cycle or 0·5% of the maximum load of the machine, whichever is the greater". Thus, taking the data in Figure 1 as the datum and using the polynomial unweighted S/N curve, a $\pm 3\%$ difference in load (stress) at an average life of 10^7 cycles would correspond to a variation in average life of from approximately 6×10^6 cycles to 16×10^6 cycles. Such a difference in average life would be quite possible from two identical fatigue machines whose load calibrations conformed to the ISO Recommendation. Considering this S/N curve to be displaced by $\pm 3\%$ in stress over the nominal alternating stress range from 103 MPa to 207 MPa, the predicted lives for the four spectra are as follows:

Spectrum	Predicted mean life (cycles) $\times 10^{-6}$		
	−3% S/N curve	Datum S/N curve	+3% S/N curve
A	0·1911	0·2649	0·3699
B	1·833	2·672	3·891
C	13·94	20·29	30·45
D	28·82	44·31	67·22

Definition of fatigue failure. The fatigue life corresponding to fatigue "failure" can, at the lower life extreme, represent the existence of a barely detectable crack whereas at the other extreme it represents complete separation of the component or specimen into two pieces. Between

these extremes fatigue crack growth under cyclic loading occurs, usually at an increasing rate. However, there is no unique value for the ratio $\frac{\text{life to crack initiation}}{\text{life to final failure}}$ as the actual ratio depends on the interaction of a number of quite independent variables including the severity of the stress concentrator at which the crack initiated and the severity of the load history. In specimens with moderately severe notches (K_t about 3), 50% of the fatigue life could be consumed by the crack propagating from a size detectable by conventional NDI methods to that completely fracturing the component. Again referring to Figure 1, if, for example, the basic fatigue data chosen for the life prediction under a multi-load-level spectrum had represented the average detectable-crack S N curve, with lives half those of the average S N curve to complete fracture, the lives predicted under each spectrum would have been halved also. This emphasises the need to know the criterion adopted for the end-point of fatigue tests when selecting data for life prediction purposes.

Fatigue loading conditions. For structural design purposes it is usually necessary to consider fatigue data covering a range of mean stresses. It has been common to use either plane bending or axial load (direct stress) loading conditions to obtain such data. However, these two loading conditions may indicate significant differences in fatigue performance because of the different stress gradients in the specimens. The following table gives the results of axial load and bending fatigue tests made on "identical" large butt-welded steel specimens[15]—the average life in bending is nearly nine times that in axial loading despite the nominal stress range being slightly greater. Under axial loading most failures originated at internal defects and inclusions; whereas under bending all failures originated at the surface where the maximum nominal stress occurs. These results underline the importance of selecting data obtained under load conditions matching those expected in service.

Comparison of Axial Load and Bending Fatigue Tests on Welded Steel Specimens

Endurance (cycles)	Location of failure
Axial load (0 to 80% yield strength)	
6,900	Failure in weld originating from internal weld defect.
17,700	
21,400	
70,000	Failed from weld.
114,000	Originated from junction of weld and parent metal.
Log. average life = 29,000	
Standard deviation of log. life 0·488	
Bending (0 to 100% axial yield stress)	
166,500	All failures originated at junction of weld and parent metal.
223,600	
269,400	
275,900	
415,800	
Log. average life = 258,000	
Standard deviation of log. life 0·145	

Specimen manufacturing methods. Machining operations, in addition to producing a surface finish whose roughness can be quantified by measurement, change the sub-surface structure of the material and the internal stress distribution. The number of variables and accepted techniques associated with machining and finishing are such that some variability in fatigue performance might be expected from specimens manufactured in different batches and from specimens made at different organisations.

Variability in the fatigue performance of aluminium alloys associated with differences in the drilling and reaming of stress concentrator holes has been discussed by Forsyth;[16] while some programme load fatigue tests on drilled and reamed notched specimens of D6AC steel

carried out at ARL have indicated a 30% to 50% difference in the mean life of specimens notched (using nominally identical procedures) by two different manufacturers.

Further evidence of the variability in fatigue performance associated with notching procedures is illustrated in Figure 9 which shows the S/N curves for two groups of circular-section circumferentially-notched specimens of DTD 683 aluminium alloy tested in rotating bending. At the lower alternating stress levels there are significant differences in mean lives (up to 5 : 1) for specimens notched using tool dwells at the notch root of zero and 200 revolutions.

Differences might also be expected between the fatigue performance of various batches of machined components, joints and structures because of uncontrolled differences in manufacturing and assembly techniques.

Frequency of cycling. A wide range of cyclic frequencies has been used to determine fatigue data. Although cyclic frequencies of about 1 Hz are quite common for the fatigue testing of full-scale aircraft structures and large components, most of the fatigue testing programmes to determine the fatigue behaviour of aircraft materials, joints and components have involved frequencies exceeding 10 Hz, and more particularly, between about 25 Hz and 150 Hz. In general, these frequencies greatly exceed those applicable to aircraft structures which, according to Schijve,[17] are 20–0·5 Hz for taxi loadings, 10–0·1 Hz for gust loadings, and 0·17–0·005 Hz for manoeuvre loadings.

Evidence has been presented[18,19] that both the fatigue life and fatigue fracture characteristics are frequency dependent and that the fatigue endurance increases with increasing frequency. Figure 10 illustrates two S/N curves for 2024 aluminium alloy,[20] obtained in rotating bending at cyclic frequencies of 3 and 24 Hz, which clearly indicate about a 2 : 1 difference in average life under these particular test conditions. Such a variation may be reflected in the prediction of fatigue life under a multi-load sequence.

Number of specimens tested. All fatigue testing programmes involve the selection of a small sample of specimens which are assumed to represent the population. A consequence, from the fatigue viewpoint, is that the estimated average S/N curve (and hence predicted life) could depend upon the number of specimens used to derive it. If, for example, the fatigue data in Figure 1 had been limited to the first two or the first four specimens, in order of testing, at each stress level, giving a total of 12 or 24 specimens tested compared with an actual total of 46, the predicted lives based on unweighted polynomial curve fits would have been as follows:

Number of specimens	Predicted mean life (cycles) $\times 10^{-6}$			
	spectrum A	spectrum B	spectrum C	spectrum D
12	0·1743	1·846	16·24	41·11
24	0·1723	1·739	14·39	34·73
46	0·2649	2·672	20·29	44·31

In this example, the predicted mean life for any one spectrum using the S/N curve based on 12 specimens is reduced substantially from that based on 46 specimens; the average reduction over the four spectra is about 25%.

Batch-to-Batch variations. The structural materials from which aircraft are built are available in a variety of product forms—sheet, plate, extrusions, forgings. These cover a wide range of physical sizes and shapes and heat treatments. Such products are available from a number of manufacturers and represent, in total, many casts of material. Acceptance of a batch of material for building into an aircraft structure is based, essentially, on its conformity with static strength properties, and rarely does it need to specifically meet a "fatigue performance" criterion.

Differences in static strength properties from batch-to-batch may also be reflected as differences in fatigue strength and fatigue crack propagation characteristics. Because of the large number of variables which affect fatigue life, rarely is it possible to isolate batch effects, as such, when comparing published fatigue data. The S/N curves illustrated in Figure 11, however, represent part of the results from a current ARL fatigue testing programme involving 13 different batches of extruded round aluminium alloy bar in diameters ranging from 16 mm to 25 mm

which were fatigue tested in rotating bending under identical conditions. They clearly show the effect on fatigue life to be quite sizeable.

Generalised data. This paper has been concerned primarily with the assessment and interpretation of particular sets of nominally identical fatigue data and has not considered the wider question of the use of generalised fatigue data obtained by combining information from different sources employing a variety of test articles and testing techniques. However, the recent generalisation of fatigue data for full-scale aircraft structures reported by Hangartner[21] provides some interesting information. Unlike less comprehensive generalisations of similar data of 10 to 15 years previously he has shown the need to separate aircraft structures of aluminium alloys into two groups on the basis of their structural materials--Al-Zn-Mg alloys or Al Cu-Mg alloys—because the average lives of structures using the zinc-bearing alloys appeared to be 3·5 to 4 times less than those using the copper-bearing alloys.

5. DISCUSSION

It is clear that, for the same set of S/N data points, differences can occur in the estimated *mean* curve, whether fitted by eye or mathematically, to the extent that predictions of mean service life can vary by a factor of two or three. Furthermore, even larger variations in predicted life can occur by selecting alternative fatigue test data, all of which might *appear* to be quite applicable to the case in hand.

Two important consequences follow. First, when calculating a safe operating life from the predicted mean life by the use of a fatigue scatter factor, it is unwarranted to specify such a factor too precisely--for example, it may not be justified to specify the factor to better than a whole number. Second, within the current techniques of data acquisition and manipulation, predicted mean lives (and hence estimated safe lives) can be specified legitimately only as a range—and this range can be quite wide. An illustration of this range for aircraft structural elements is provided by Ford.[22]

Thus there is little justification for any one life calculation based on a particular set of S/N data to be accepted as precisely specifying the predicted mean life. The confidence which one should place on such S/N data depends upon its applicability to the case under consideration, and also upon the confidence with which a mean curve can be fitted to the S/N points. The evidence in this paper suggests that, in some cases, service lives may not be predictable to better than a range of about 10 : 1.*

When multiple sets of fatigue data are available for the life calculation they should be weighted according to their relevance to the particular problem under consideration; and in order to assess the applicability of specific data it may be necessary to closely examine the original fatigue test conditions which were employed in their determination. Thus, considerable care must be exercised in the selection and manipulation of basic S/N data for life prediction under a complex loading sequence.

6. CONCLUSIONS

(1) The location of mean S/N curves fitted by eye to a given set of data points depends markedly on subjective judgement. Even among those experienced in drawing such curves the variability can be such that, when using the curves for life prediction under a multi-load-level sequence, the magnitude of predicted mean life may vary by a factor of three.

(2) Mathematical methods of curve fitting may eliminate some of the personal bias but are themselves open to subjective judgement. Arbitrary decisions about the functional form, the use of weighting, the non-intersection of curves within a family, and the likelihood of a fatigue limit, can contribute to variability in predicted mean life.

(3) In addition, the determination of fatigue data provides many other sources of uncertainty whose relevance must be considered in the selection of such data for life

* In addition to those problems associated with data selection and interpretation are those concerned with the subdivision of the load spectrum into cycles of constant amplitude and those concerned with the validity of any cumulative damage hypothesis which might be adopted. The uncertainties involved in these areas further compound the problem of accurately estimating a precise service life.

prediction purposes. These include the type of specimen, its method of manufacture and the number tested, differences in fatigue behaviour between batches of material, the loading accuracy of the testing equipment and the cyclic frequency of fatigue loading. It has been shown that differences associated with these factors can produce significant variations in S/N lives, and that predicted lives under a multi-load-level sequence can differ by up to 10 : 1.

7. ACKNOWLEDGMENTS

The authors wish to acknowledge the co-operation of those members of Structures Division, ARL, who took part in the canvass of S/N curves and for their many helpful suggestions. Particular thanks are extended to Dr. D. G. Ford for his advice on the statistical evaluation of the data, to Mr. A. S. Machin who was responsible for much of the computer analysis of the data, and to Mr. J. A. Lowes for his assistance with the basic data evaluation.

REFERENCES

1. Finney, J. M. — Abnormally High Fatigue Properties of DTD 683 Aluminium Alloy Extruded Bar. Aeronautical Research Laboratories, Report ARL/SM 287, Department of Supply, February 1962.
2. Mann, J. Y. — The Influence of Mean Stress and Stress Concentrators on the Fatigue Properties of 7178-T6 Aluminium Alloy. Aeronautical Research Laboratories, Report ARL/SM 327, Department of Supply, November 1970.
3. Buckland, W. R. — Statistical Assessment of the Life Characteristic. (See Chapter 4: Analysis of Fatigue Tests, pp. 101-119.) Charles Griffin and Co. Ltd., London, 1964.
4. Mann, J. Y., and Machin, A. S. — The Influence of Mean Stress and Stress Concentrators on the Fatigue Properties of Extruded 2L.65 Aluminium Alloy. Aeronautical Research Laboratories, Department of Defence (report in preparation).
5. Ostermann, H. — Fatigue Life Estimation under Special Loading Spectra by Means of Variable Amplitude Fatigue Strength Data Obtained with Standard Spectra. R. Aircr. Establ. Libr. Transl. no. 1357, May 1969.
6. Tavernelli, J. F., and Coffin, L. F. — A Compilation and Interpretation of Cyclic-Strain Fatigue Tests. Trans. Am. Soc. Met., Vol. 51, pp. 438-453, 1959.
7. Manson, S. S. — Behaviour of Materials Under Conditions of Thermal Stress. NACA Tech. Note 2933, July 1953.
8. Weibull, W. — Fatigue Testing and Analysis of Results. Pergamon Press, London, 1961.
9. Daniel, C., and Wood, F. S. — Fitting Equations to Data. Wiley-Interscience, 1971.
10. Pook, L. P. — Basic Statistics of Fatigue Crack Growth. Natl. Eng. Lab. Rep. No. 595, June 1975.
11. Mann, J. Y. — Fatigue Design - Data Requirements and Determination. SAE—Australasia, vol. 27, No. 6, pp. 219-224, November-December 1967.
12. Grover, H. J., Hyler, W. S., Kuhn, P., and Landers, B. — Axial-Load Fatigue Properties of 24S-T and 75S-T Aluminium Alloy as Determined in Several Laboratories. NACA Tech. Note No. 2938, May 1953.
13. Dunsby, J. A. — A Preliminary Analysis of the Results of Some Comparative Fatigue Tests Conducted by Eight Canadian Laboratories. Nat. Aero. Establ., Memo. ST-45, October 1962.
14. International Organisation of Standardization. Axial load fatigue testing. ISO Recommendation R 1099, July 1969.
15. Harris, F. G., Douglas, R. B., and Rowan, R. W. — Axial Load and Bending Fatigue Tests on Welded Normalised Manganese-Silicon Steel. Aeronautical Research Laboratories Tech. Memo ARL/SM 187, Department of Supply, June 1969.
16. Forsyth, P. J. E. — Microstructural Changes that Drilling and Reaming can Cause in the Bore Holes in DTD 5014 (RR58 Extrusions). Aircr. Engng, vol. 44, No. 12, pp. 20-23, November 1972.
17. Schijve, J. — Fatigue of Aircraft Structures. Israel J. Technol., vol. 8, No. 1-2, pp. 1-20, 1970.

18. Finney, J. M. — The Effects of Rate of Cycling on the Unusual Fatigue Behaviour of Two High-Strength Aluminium Alloys. J. Inst. Met., T.N. 118, vol. 92, pt. 11, pp. 380-82, July 1964.

19. Mann, J. Y. — Some Phenomenological Aspects of Scatter in Fatigue. Aeronautical Research Laboratories, Report ARL SM 342, Department of Supply, November 1972.

20. Mann, J. Y. — The Effect of Rate of Cycling on the Fatigue Properties of 24S-T Aluminium Alloy. Aeronautical Research Laboratories, Report ARL SM 188, Department of Supply, August 1954.

21. Hangartner, R. — Correlation of Fatigue Data for Aluminium Aircraft Wing and Tail Structures. Natl. Aeronaut Estab. Aero Report No. LR-582, December 1974.

22. Ford, D. G. — A Review of CA-25 Winjeel Fatigue Lives. Aeronautical Research Laboratories, Note ARL SM 387, Department of Supply, December 1972.

23. Ford, D. G., and Lewis, J. A. — Fitting Families of Polynomial S/N Curves to Fatigue Data. Aeronautical Research Laboratories, Report ARL SM 296, Department of Supply, April 1964.

TABLE 1
Canvass Numerical Data Provided for Fitting Mean S/N Curves

(*a*) Data for eye-drawn curves

Stress (Sa) (K.S.I.)	Median life		Log average life		Variance (of log life)
	Cycles (N)	Log cycles (log N)	Cycles (N)	Log cycles (log N)	
			2L65 aluminium alloy		
30	18,000	4·2553	20,900	4·3209	0·015
25	50,000	4·6990	67,900	4·8317	0·124
22·5	127,000	5·1038	151,600	5·1808	0·092
20	1,738,000	6·2401	1,071,000	6·0298	0·569
17·5	12.560,000	7·0990	6,215,600	6·7935	0·375
15	56,051,000	7·7486	46,166,200	7·6643	0·043
			DTD 683 aluminium alloy		
40	68,000	4·8325	65,900	4·8189	0·015
37·5	660,000	5·8195	412,000	5·6149	0·151
35	841,000	5·9248	849,000	5·9289	0·004
32·5	953,000	5·9791	1,024,900	6·0107	0·013
30	2,400,000	6·3802	2,956,600	6·4708	0·095
27·5	11,754,000	7·0702	10,235,600	7·0101	0·282

TABLE 1—continued

(*b*) Data for mathematically-defined curves

Alternating stress (Sa) (ksi)	Cycles to failure (N)	Log cycles to failure (log N)	Averages, variance
	2L.65 aluminium alloy		
30	16,000	4·2041	Median life (log cycles) = 4·2553
	17,000	4·2304	Log average life = 4·3209
	18,000	4·2553	Variance (of log life) = 0·0149
	18,000	4·2553	
	22,000	4·3424	
	26,000	4·4150	
	35,000	4·5441	
25	45,000	4·6532	Median life (log cycles) = 4·6990
	46,000	4·6628	Log average life = 4·8317
	46,000	4·6628	Variance (of log life) = 0·1243
	50,000	4·6990	
	52,000	4·7160	
	64,000	4·8062	
	419,000	5·6222	
22·5	88,000	4·9445	Median life (log cycles) = 5·1038
	96,000	4·9823	Log average life = 5·1808
	105,000	5·0212	Variance (of log life) = 0·0921
	127,000	5·1038	
	152,000	5·1818	
	158,000	5·1987	
	681,000	5·8331	
20	44,000	4·6435	Median life (log cycles) = 6·2401
	296,000	5·4713	Log average life = 6·0298
	298,000	5·4742	Variance (of log life) = 0·5693
	481,000	5·6821	
	1,738,000	6·2401	
	2,758,000	6·4406	
	5,066,000	6·7047	
	5,135,000	6·7105	
	7,966,000	6·9012	
17·5	411,000	5·6138	Median life (log cycles) = 7·0990
	1,073,000	6·0306	Log average life = 6·7935
	2,952,000	6·4701	Variance (of log life) = 0·3746
	10,077,000	7·0033	
	12,560,000	7·0990	
	14,071,000	7·1483	
	16,003,000	7·2042	
	18,221,000	7·2606	
	20,483,000	7·3114	

TABLE 1—continued

Alternating stress (Sa) (ksi)	Cycles to failure (N)	Log cycles to failure (log N)	Averages, variance
15	21,524,000	7·3329	Median life (log cycles) = 7·7486
	27,359,000	7·4371	Log average life = 7·6643
	45,731,000	7·6602	Variance (of log life) = 0·0425
	56,051,000	7·7486	
	59,614,000	7·7753	
	61,823,000	7·7912	
	80,344,000	7·9050	

Additional data

(i) Tensile properties obtained from standard tension specimens (unnotched):
0·1% proof stress = 69·4 KSI
0·2% proof stress = 70·3 KSI
Ultimate Tensile Strength = 76·0 KSI

(ii) Ultimate Tensile Strength of notched specimens ($K_t = 1·6$)—identical to specimens used in obtaining data tabulated above, equals 95·3 KSI.

(iii) All data points have been included; there were no runouts.

TABLE 2

Averages and Scatter of Predicted Lives Using Eye-Drawn S/N Curves

Spectrum	Overall group		Experienced		Inexperienced		Coefficient of variation $(s/\bar{N}) \times 100\%$			$\frac{\text{Maximum}}{\text{Minimum}}$ for predicted life		
	$\bar{N}$	s	$\bar{N}$	s	$\bar{N}$	s	Overall	Experienced	Inexperienced	Overall	Experienced	Inexperienced
					(a) *Curves for 2L.65 Aluminium Alloy – Figure 5*							
A	0·237	0·12	0·245	0·08	0·235	0·14	50	34	58	6·3	2·9	6·3
B	2·39	0·96	2·39	0·51	2·39	1·14	40	21	48	7·7	2·4	7·7
C	19·4	5·7	18·7	5·1	19·8	6·0	29	27	30	4·3	2·8	4·3
D	42·4	8·0	39·6	10·0	43·9	6·3	19	25	14	4·3	3·9	1·9
Average of the 4 spectra								27	38		3·0	5·1
					(b) *S/N Curves for DTD 683 Aluminium Alloy – Figure 6*							
A	1·33	0·87	1·26	0·23	1·37	1·1	66	18	80	11·5	1·9	11·5
B	4·02	0·83	4·07	1·1	3·99	0·63	21	28	16	2·8	2·6	2·0
C	8·61	2·1	8·41	2·1	8·73	2·0	24	25	23	3·1	2·5	3·0
D	10·2	2·9	9·91	2·9	10·4	2·9	28	29	28	4·0	2·7	4·0
Average of the 4 spectra								25	37		2·4	5·1

$\bar{N}$ = Arithmetic average of predicted mean life (cycles) $\times 10^6$.
s = Standard deviation of predicted mean life (cycles) $\times 10^6$.

TABLE 3

Averages and Scatter of Predicted Lives Using Mathematically-Defined S/N Curves for 2L.65 Aluminium Alloy (Fig. 8)

Spectrum	Predicted mean life (cycles) $\times 10^{-6}$					Average predicted life $\bar{N}$	Standard deviation s	Coefficient of variation $(s/\bar{N}) \times 100\%$	Maximum / Minimum for predicted life
	Polynomial function—unweighted	Power function	Consecutive straight line	Polynomial function—weighted	Maximum likelihood (using polynomial)				
A	0·2649	0·3964	0·2337	0·2379	0·2387	0·2743	0·07	25	1·7
B	2·672	3·448	2·549	2·372	2·379	2·682	0·45	17	1·5
C	20·29	17·90	20·03	18·16	18·19	18·91	1·1	6	1·1
D	44·31	29·88	39·18	40·30	40·30	38·79	5·4	14	1·5
Average of the 4 spectra								15	1·4

$\bar{N}$ = Arithmetic average of predicted mean life (cycles) $\times 10^{-6}$.
s = Standard deviation of predicted mean life (cycles) $\times 10^{-6}$.

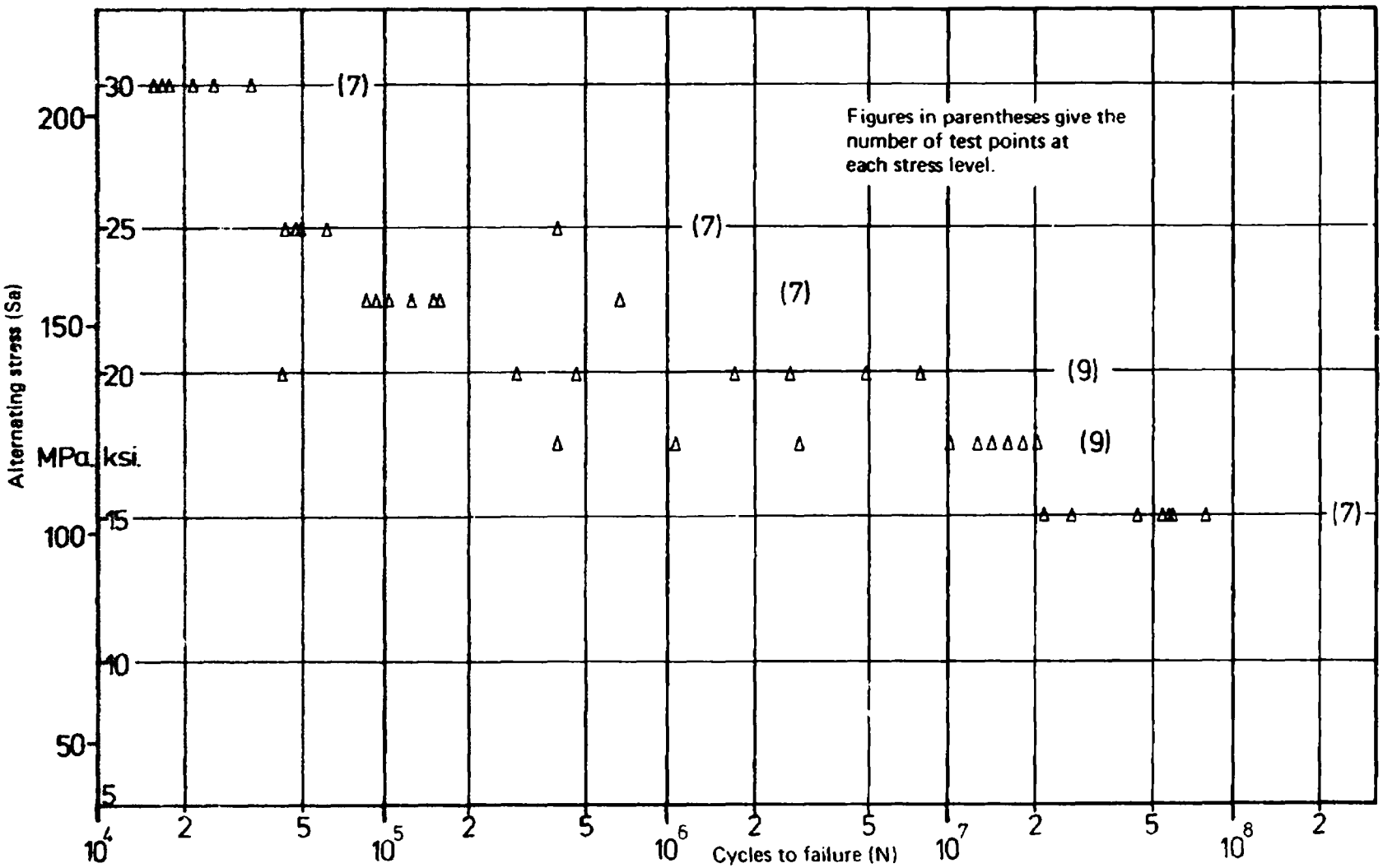

FIG. 1 FATIGUE DATA FROM 2L.65 ALUMINIUM ALLOY NOTCHED (K_t = 1.6) SPECIMENS TESTED IN AXIAL LOADING AT A MEAN STRESS OF 66 MPa (9.5 ksi).

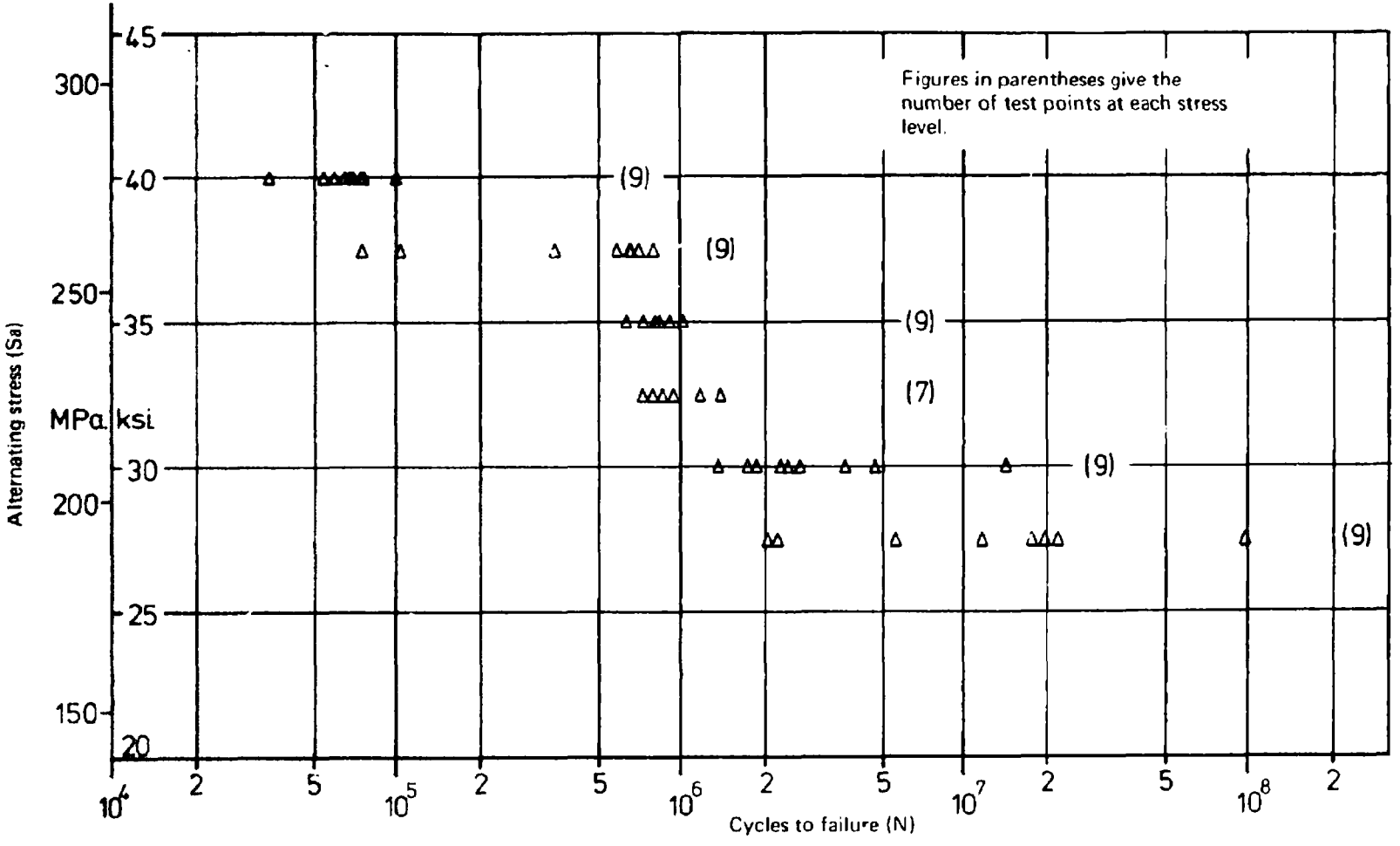

FIG. 2 FATIGUE DATA FROM DTD 683 ALUMINIUM ALLOY NOTCHED (K_t = 1.45) SPECIMENS TESTED IN ROTATING BENDING.

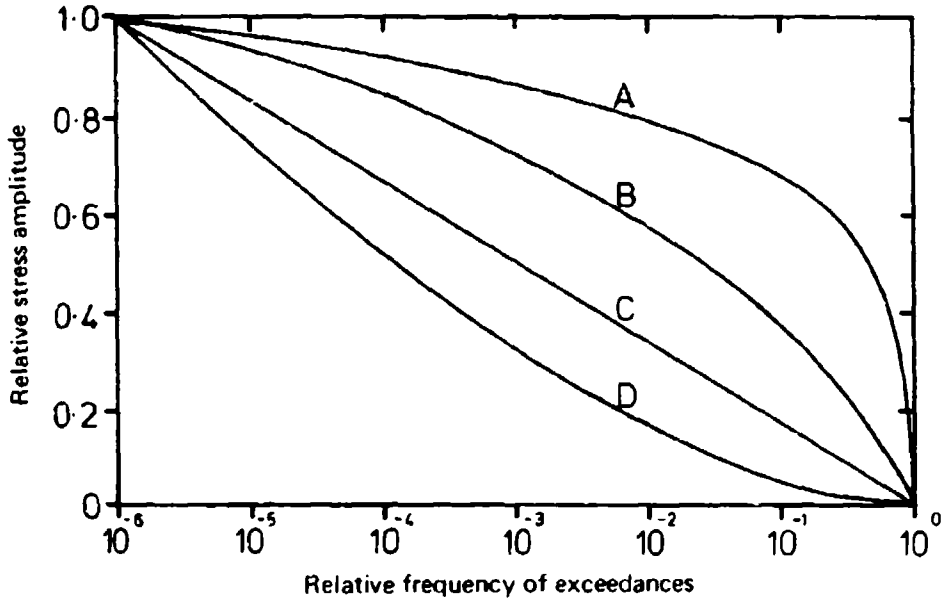

FIG. 3 GENERALISED LOAD SPECTRA (AFTER OSTERMANN (5)).

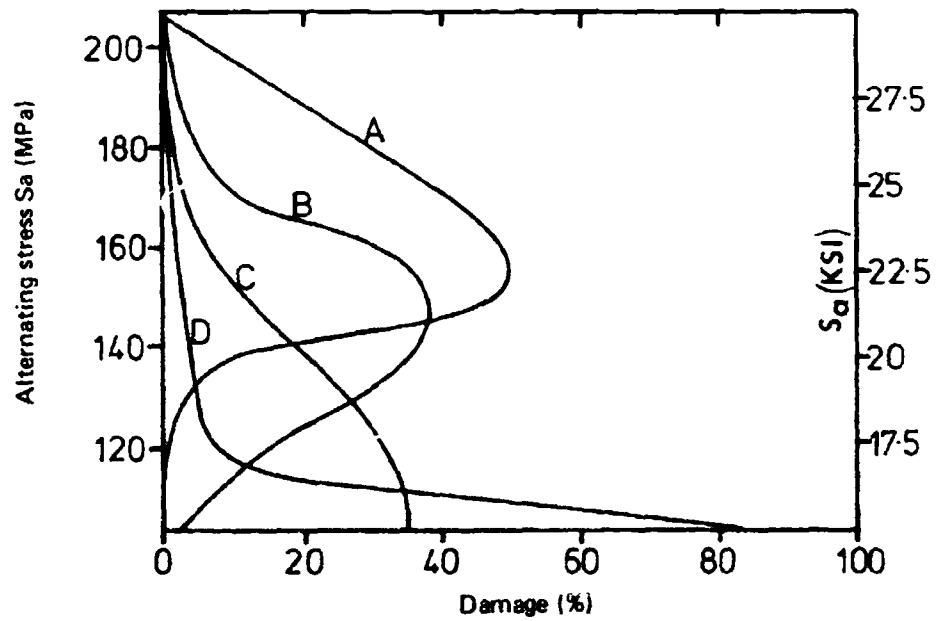

FIG. 4 DISTRIBUTION OF FATIGUE DAMAGE (NORMALISED) UNDER VARIOUS LOAD SPECTRA (AS SHOWN IN FIG. 3).

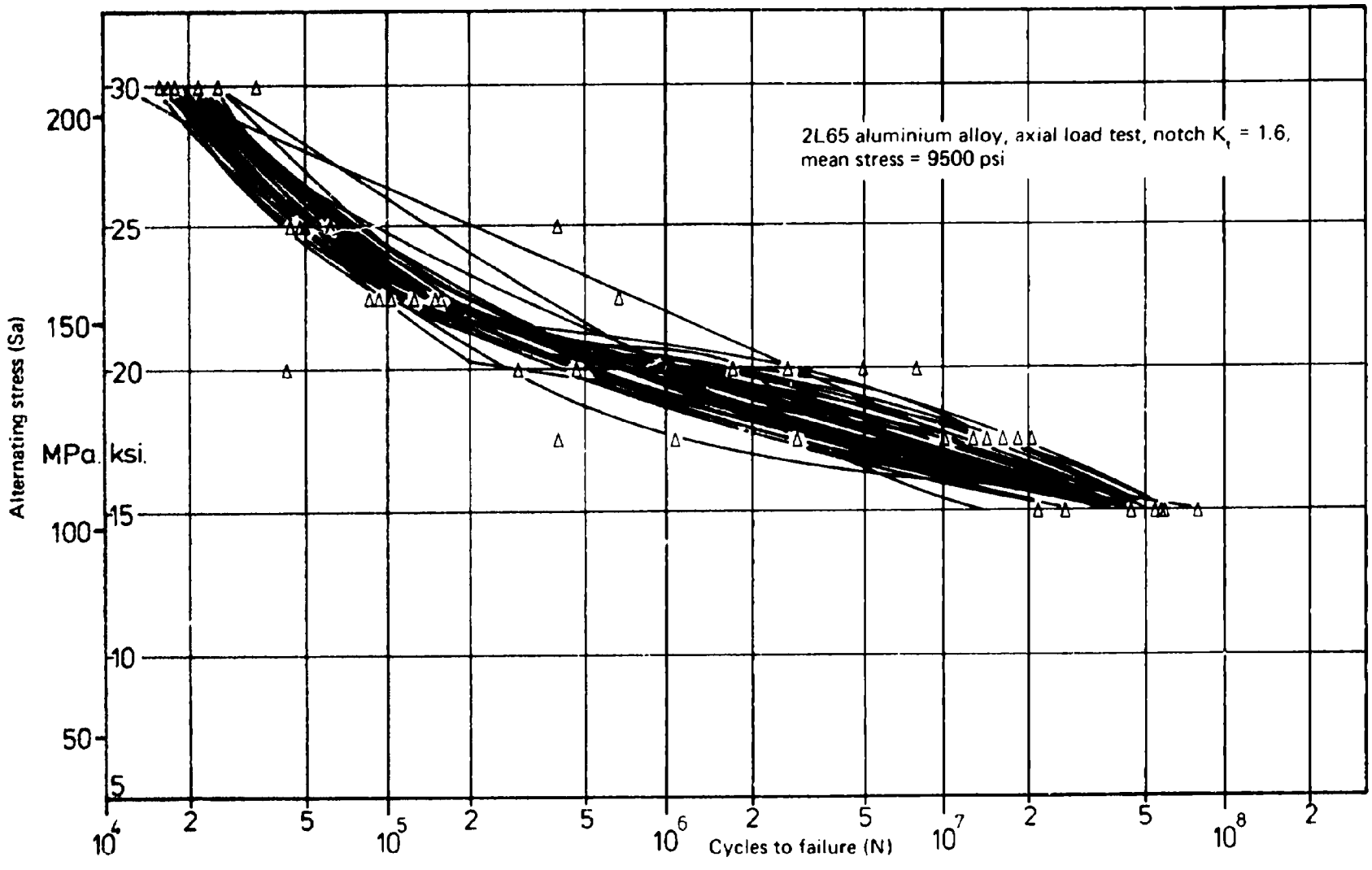

FIG. 5 COMPOSITE OF 46 S/N CURVES, EYE-DRAWN TO THE DATA SHOWN IN FIG. 1.

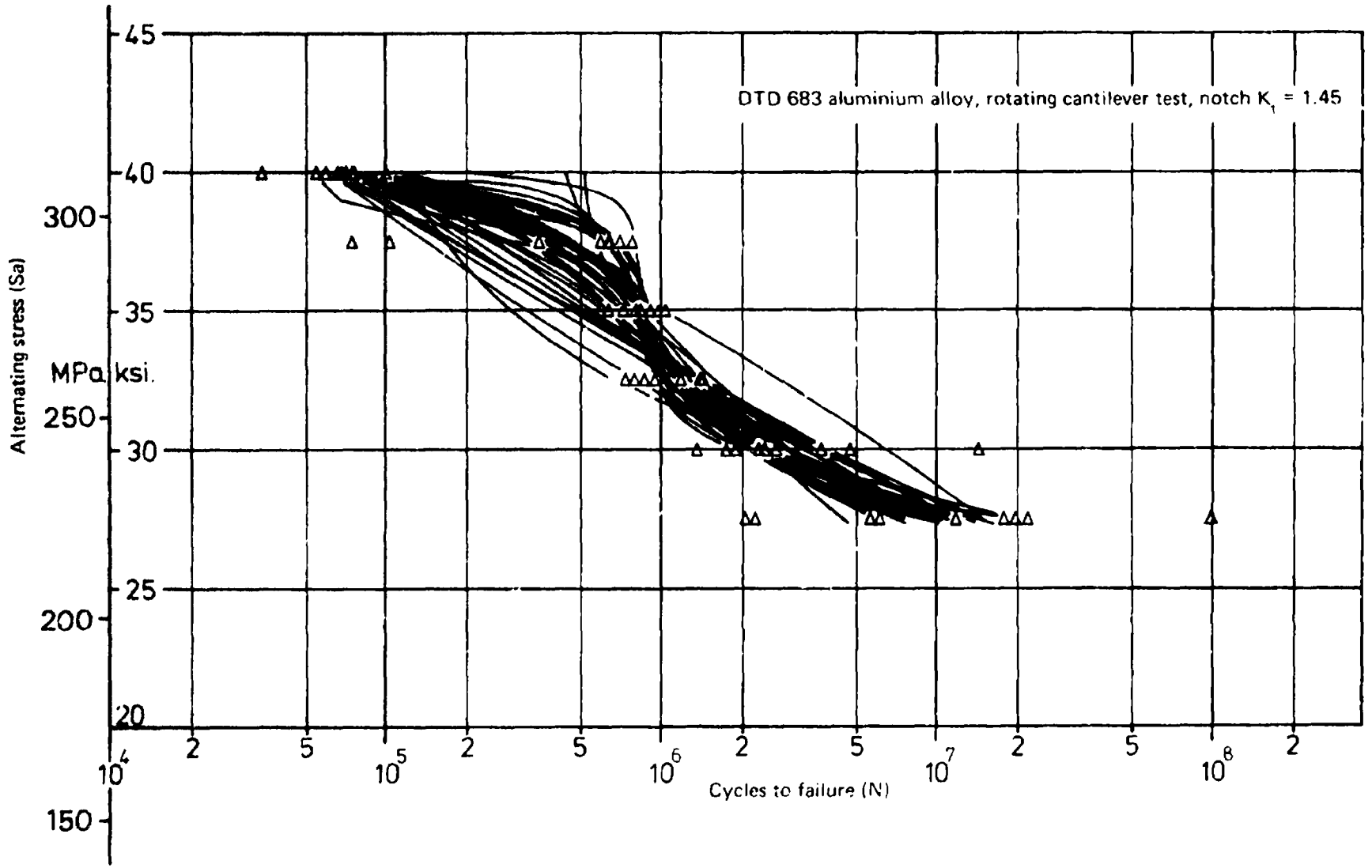

FIG. 6 COMPOSITE OF 46 S/N CURVES, EYE-DRAWN TO THE DATA SHOWN IN FIG. 2.

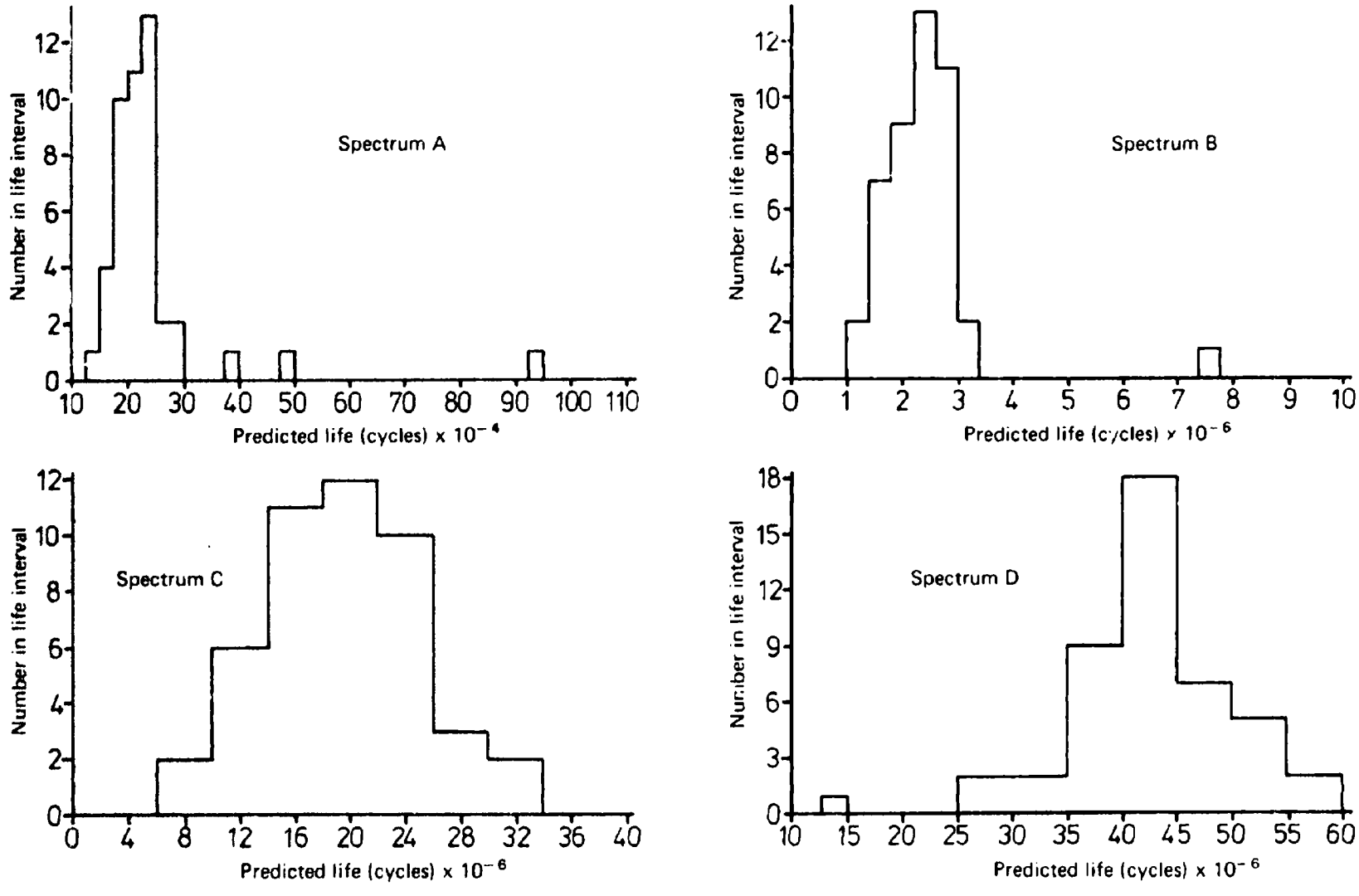

FIG. 7 HISTOGRAMS OF PREDICTED LIVES BASED UPON 46 S/N CURVES, EYE-DRAWN TO THE DATA SHOWN IN FIG. 1.

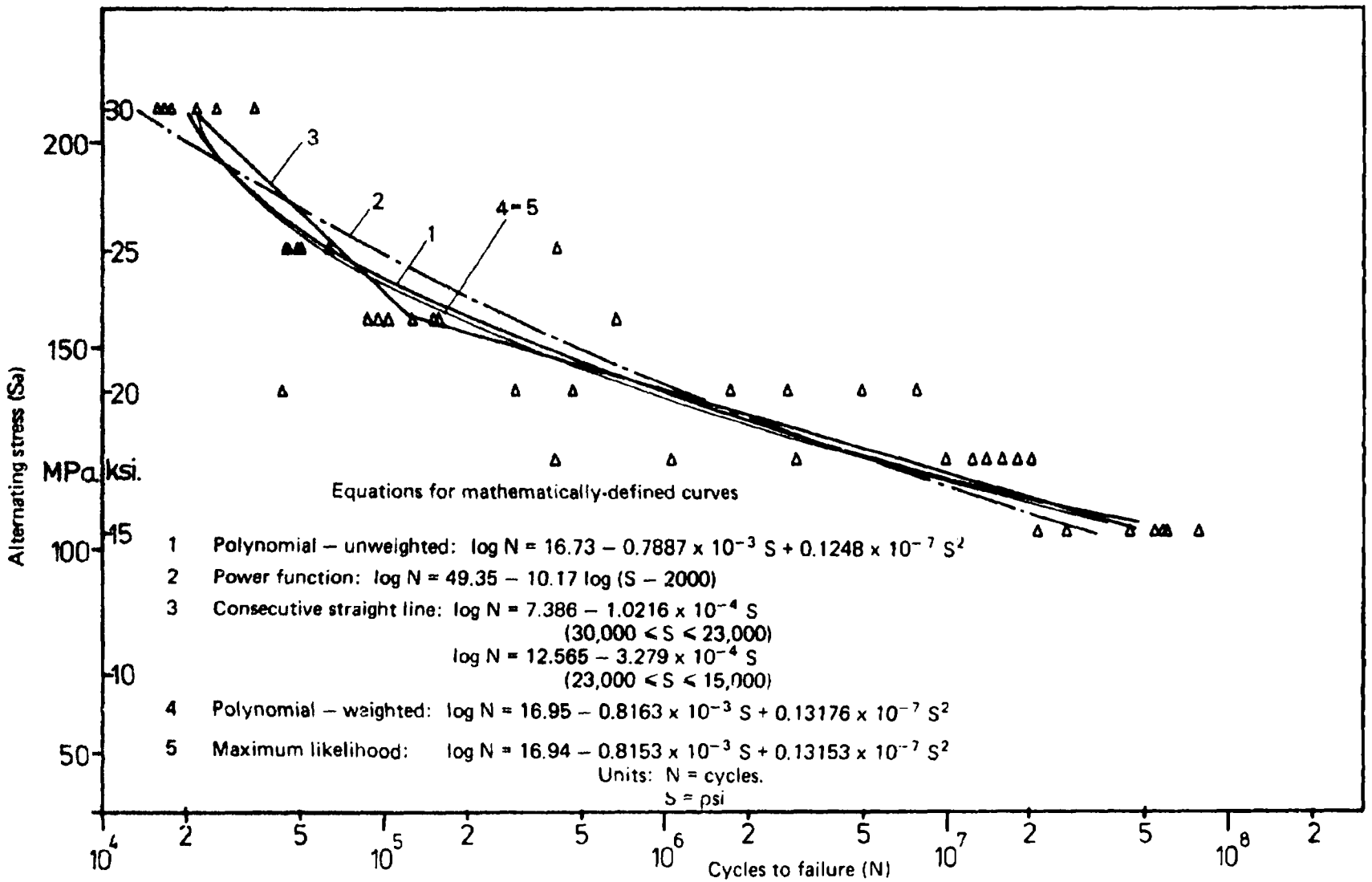

FIG. 8 S/N CURVES FITTED MATHEMATICALLY TO THE DATA SHOWN IN FIG. 1.

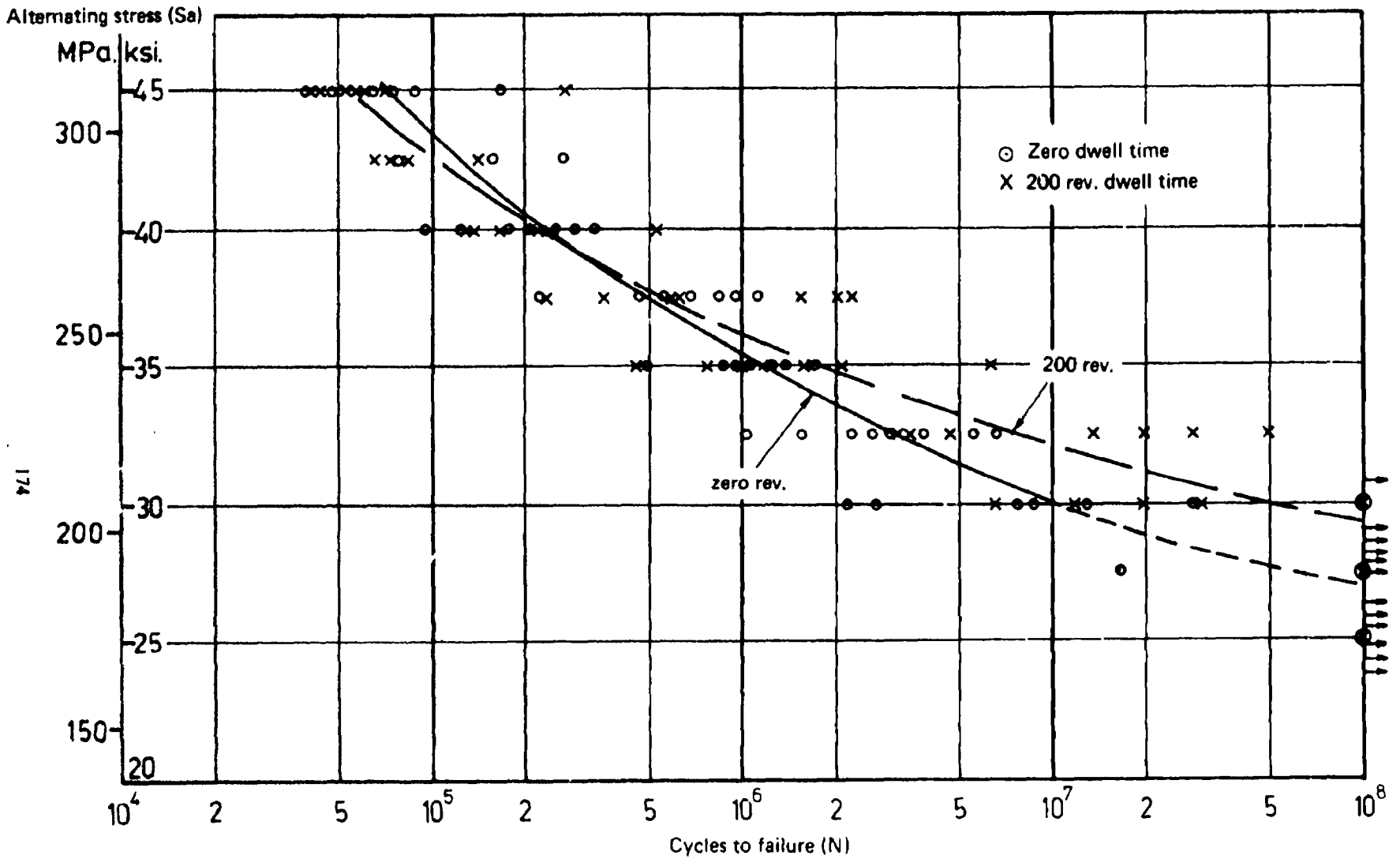

FIG. 9 EFFECT OF DWELL TIME FOR 0.185" (4.7 mm) RADIUS NOTCH (K_t = 1.2)

SPECIMENS OF DTD 683/3 ALUMINIUM ALLOY

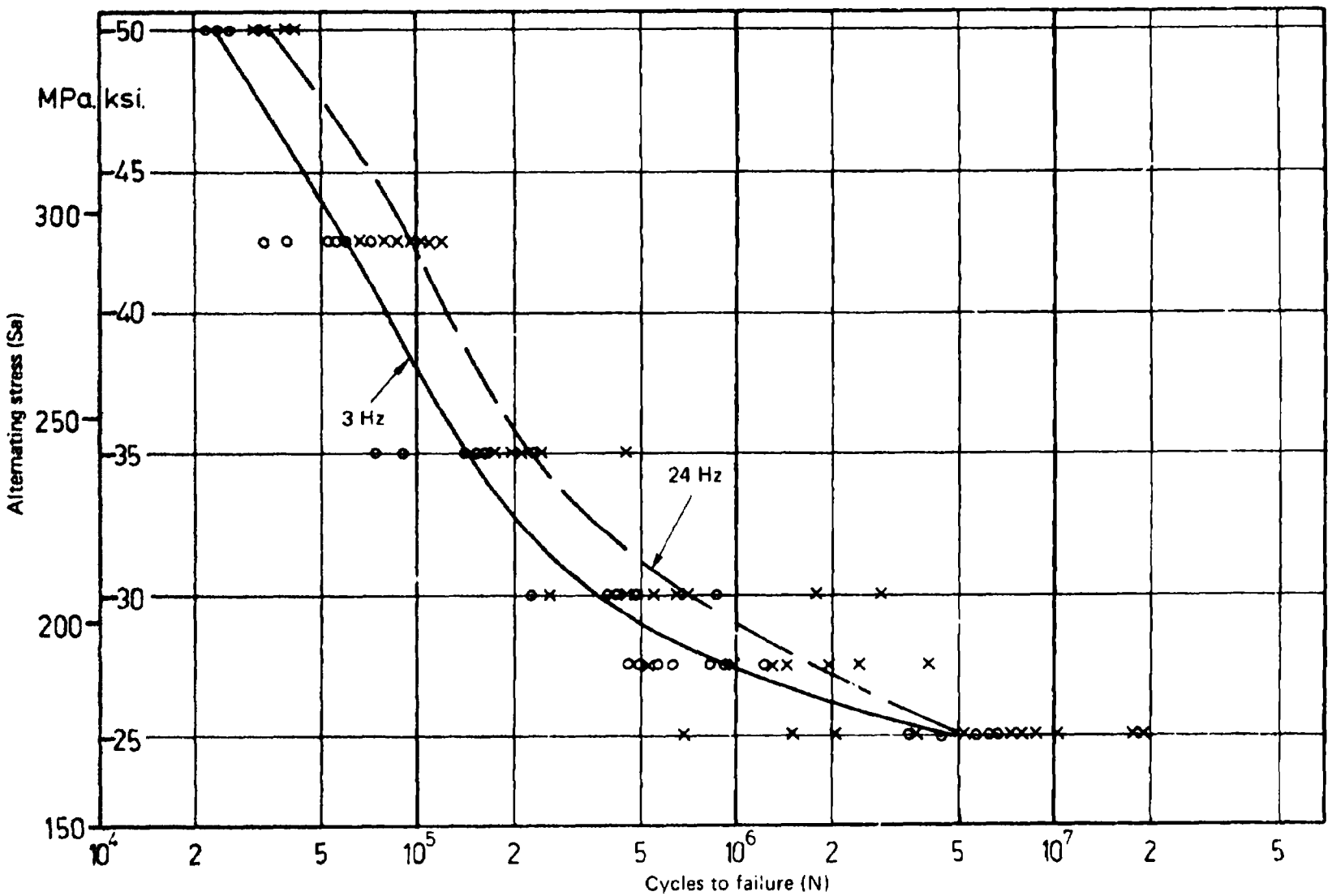

FIG. 10 EFFECT OF CYCLIC FREQUENCY - 2024 ALUMINIUM ALLOY UNNOTCHED SPECIMENS

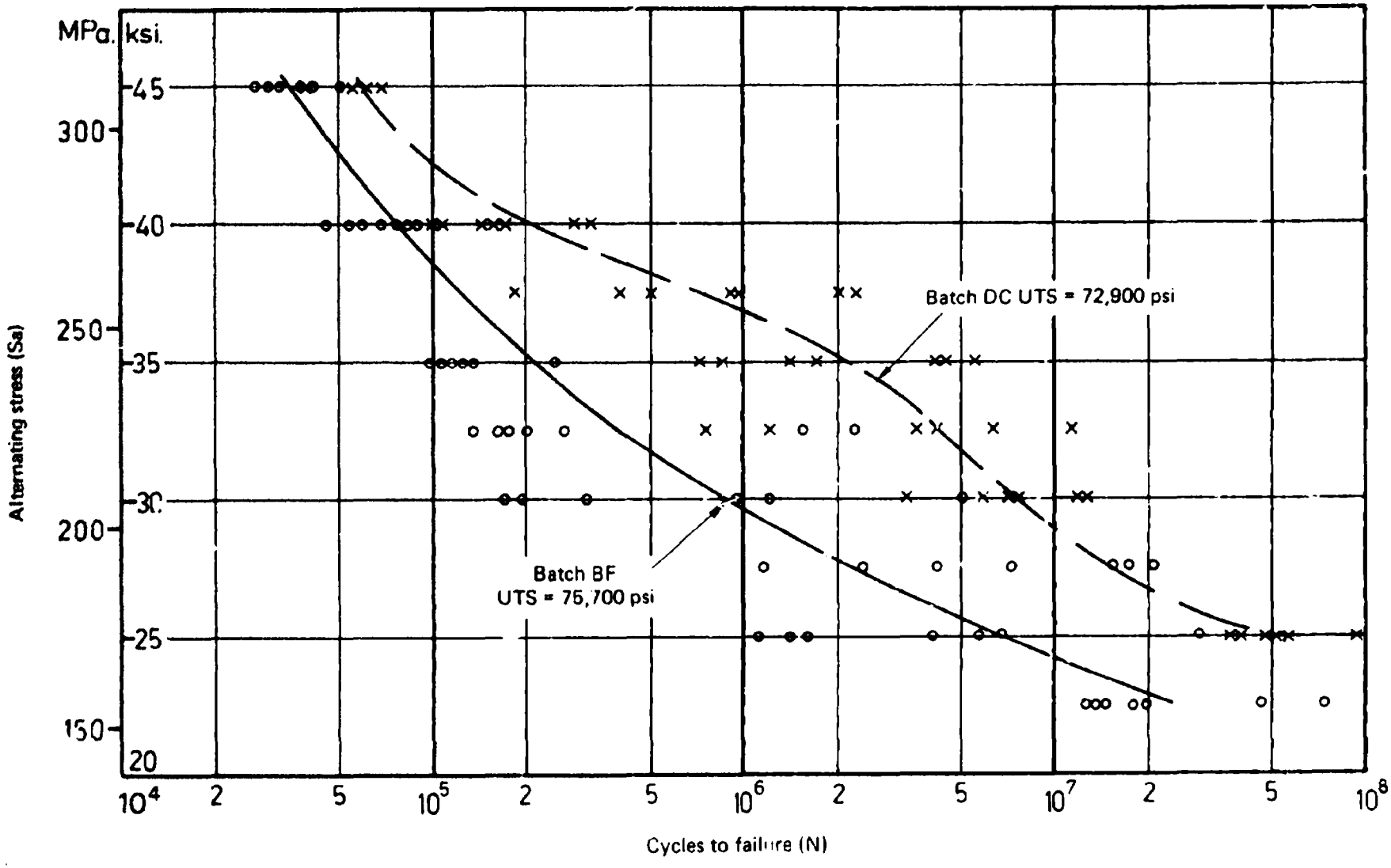

FIG. 11 BATCH-TO-BATCH EFFECT 2L.65 ALUMINIUM ALLOY UNNOTCHED SPECIMENS

DISCUSSION

QUESTION—*H. A. Wills (retired)*

What prospects are there for arriving internationally at agreed standards of specimen preparation and fatigue testing procedures—and for the analysis and presentation of the data?

Author's Reply

In view of the sensitivity of fatigue life to sometimes slight variations in material processing, test conditions and environment, the question of international standards on fatigue testing is quite a fundamental issue in fatigue. Some national and international standards in this field have been produced. The latest edition of the German DIN 50100 was published in 1953; five parts of the British Standard BS.3518 have been issued commencing in 1962; and various parts of the International Standards Organisation Standards and Recommendations have been available since 1964.

On the whole, these standards are more concerned with definitions, nomenclature and quite general procedures for fatigue testing, and leave considerable scope for individual fatigue testing programmes to be carried out under quite different environments, cyclic frequencies, etc. It is the responsibility of the individual who specifies or plans a particular investigation to select the testing conditions, etc., which are most appropriate to the end application of the test data.

In the past, fatigue test data have often been obtained simply by using any convenient test conditions in any available test machine. There is now, however, an increasing awareness of the effects of testing and environmental variables on fatigue life and of the need, in the laboratory fatigue test, to more closely represent service conditions if accurate indications of behaviour are to be obtained. One such example in the aircraft field, is the development of the standardised fighter load spectrum/sequence—FALSTAFF—which will enable fatigue data obtained in different laboratories to be directly interchangeable.

International standards on analysis and presentation of fatigue data have not yet been agreed and it should be clear from the paper why this is so. There is simply a lack of awareness of how sensitive are, say fatigue life estimates, to the interpretation of the basic test data. Although we have shown that fatigue data analysis requires judgements which can be rather subjective, it is hoped that papers such as the present one will focus attention on this area and ultimately lead to standardised procedures.

QUESTION—*Dr. L. H. Mitchell (ARL)*

Is there any justification for any of the types of mathematical curve fitting of S/N curves other than convenience? If not, why not use straight lines between the mean life at each load level tested? Because of the large standard deviation at each level more sophisticated approaches are probably not justified. It would be interesting to see the predicted lives with this approach for your comparative spectra. Also it would be interesting to see the standard deviations of these predicted lives if the standard deviation were assumed to vary linearly between each load level.

Author's Reply

In general, there is no particular reason for choosing any specific functional form. But if S/N curves are drawn in order to use interpolated values, there may be good reasons for rejecting some forms. For example, a high-degree polynomial may give an excellent fit through the mean points, but between the data levels the curve may deviate wildly from the general trend of the data and therefore the form would be rejected.

A similar argument, about interpolations, applies to the fitting of straight lines between average lives at adjacent stress levels. Interpolations are likely to be closer to reality by using curves shaped according to the general trend of the data rather than by using straight lines. Also, the use of a curve brings to bear the information from the data points at all levels in determining the mean position, as defined by the curve, at any one level; and further, a curve accords with the supposed physical relationship. Consecutive straight lines are weak on both of these points, although we do recognise some argument in their favour.

The use of a weighting factor is simply a recognition of the variation in scatter between stress levels. There is a tendency for scatter to increase with decreasing applied stress and a linear relation may be a reasonable approximation. We used the actual scatter at each stress level as a weighting factor, and for the data examined, the predicted mean life was reduced by an average of 10% over that using the data unweighted.

QUESTION - *Dr. N. E. Ryan*
(ARL)

You have presented a somewhat depressing picture of the very wide scatter in fatigue life that can arise even where simple test specimens and uncomplicated test methods are used. It is nevertheless obvious that these test procedures of themselves, contribute to the wide scatter. Can you indeed identify those factors which invariably lead to wide scatter?

Author's Reply

The scatter of fatigue lives at any stress level is simply a response of the material microstructure to the imposed test conditions. If these conditions are not adequately controlled from one test to the next, even larger scatter will ensue. For example, if the surface finish of the specimens was not controlled, or the test frequency was allowed to vary, or perhaps wide differences in the test atmosphere occurred, we may expect an increased scatter.

Our paper took the approach of examining the *variation in mean life*, for a limited number of cases, where only one test parameter was varied—such as load control, test frequency, material batch. The question of scatter about these mean lives was mentioned but not examined. The paper emphasises the need to choose S'N data, for any application, which have been obtained under conditions as close as possible to the case in hand, and it concludes that, in some cases, mean service lives may not be predictable to better than a range of about 10 : 1. The factor on mean predicted life to allow for scatter was not considered.

STRUCTURAL FATIGUE TESTING

by

R. A. BRUTON and C. A. PATCHING

SUMMARY

Fatigue testing of large assemblies and full-scale aircraft structures was for many years done only as part of research investigations into the fatigue behaviour of materials and methods of construction.

Difficulties in predicting fatigue behaviour of a structure from data obtained by testing materials and components, coupled with the economic need to extend the service life, have resulted in a steady increase in the number of full-scale tests.

Many aircraft designers do fatigue tests on components and assemblies for design and development, and then carry out a comprehensive fatigue test on a complete structure to demonstrate compliance with Airworthiness Requirements.

This paper discusses the various testing techniques available, selection of the test article, data obtainable from fatigue testing of components, assemblies and complete structures and the conclusions that have been reached based on experience from a large number of fatigue tests on aircraft wings at the Aeronautical Research Laboratories.

1. INTRODUCTION

Possibly the first full-scale aircraft structural fatigue testing was done in Germany by Gassner[1] on wings, followed after World War 2 by various research programmes to determine fatigue characteristics of aircraft structures, mainly at the Aeronautics Division of the Council for Scientific and Industrial Research, Melbourne, and to a lesser extent in English and American research laboratories.

Although lives calculated from these investigations showed a marked difference from lives obtained from tests on materials, components and assembles, full-scale testing was not universally accepted, mainly for cost reasons, until fatigue problems continued to occur unexpectedly in service involving aircraft from a number of countries.

Full-scale structural fatigue tests are now done either early in the service life to justify the airworthiness criteria, or towards the end of the predicted service life in order to obtain the maximum economic utilization of the airframe.

Laboratory representation of service conditions for both airworthiness and research investigations has resulted in the use of complex and expensive load control equipment: i.e. computer controlled and monitored servo electro-hydraulic loading systems.

2. TESTING TECHNIQUES

For many years two separate techniques were employed for loading structures, namely, hydraulic jacks (actuators) activated by a common oil pressure, or forced vibration near resonance of the structure; this latter technique was used for long endurance tests. There has been a continuing development of the hydraulic method culminating in electro-hydraulic servo operated actuators controlled and monitored by a computer, which has become the universal technique for fatigue testing of all structures.

2.1 Vibration Testing Method

This technique is particularly useful when large numbers of cycles at relatively low percentages of ultimate load are to be applied: it can be easily applied to the repeated loading of structures, especially wings and tailplanes. These structures can be subjected to a forced vibration in the fundamental symmetric mode at a frequency just below resonance.

In a wing test, the specimen must be suspended in an inverted attitude to take advantage of the structure weight, and to facilitate the application of mean loads. Mean load application can be achieved by suspending masses on low rate springs (see Fig. 1). This method apart from being cumbersome has a number of disadvantages. The major one is that the relatively heavy attachment fittings cause an unfavourable mass distribution near the tip, necessitating extra mass inboard, thus reducing the natural frequency and hence speed of testing.

Most of the problems can be overcome by using hydraulic jacks loading the structure through stiff springs: the jacks hold the fixed end of the springs essentially stationary.

The desired alternating load distribution can be obtained by modifying the mass distribution of the structure with the attachment of an appropriate array of added masses and springs, together with the provision of a finite wing suspension stiffness.

Various methods of excitation are possible, including:

(*a*) mechanical (out of balance) dynamic oscillator;
(*b*) crank and slider driving through a slipping clutch; and
(*c*) crank and slider driving through a spring.

The magnitude of the driving force is adjusted by controlling the frequency of excitation just below the resonant frequency of the structure to achieve the desired alternating load. Load control can be maintained by monitoring the amplitude of vibration, e.g. wing tip deflection, and the deflection indicator can form part of the frequency control loop.

Details of the design and application of this technique for the fatigue testing of aircraft wings can be obtained from References 2 and 3. A general view of a Dove aircraft wing under test is shown in Figure 2.

2.2 Hydraulic Loading Method

Until the advent of the closed loop servo electro-hydraulic loading systems, all previous hydraulic systems were open loop or "bang-bang". In other words the pressure increased at a rate depending on the output of the hydraulic power supply, until the desired load was reached when a solenoid or mechanically operated valve opened the supply line back to the reservoir. By careful design of the relief valve porting it was possible to produce a load cycle approximately triangular in shape.

Various load sensing and pressure control systems were successfully developed,[2,4] and by incorporating an electric resistance strain gauge cell which monitored the load on a large cathode ray tube, extremely accurate load control was achieved.[5] An hydraulic loading rig used for testing some 200 Mustang wings is shown in Figure 3.

The loading system utilized low friction hydraulic jacks of various areas connected to a common oil supply.

Fortunately for those concerned with structural testing, the era of guided missiles produced highly sensitive electro hydraulic servo valves which formed the major component of a load control loop having the capability of precisely controlling the load applied by a hydraulic jack. Furthermore, the control loop comprising either one jack or a combination of jacks can be commanded by a signal which can, for example, be obtained from a continuously recorded load parameter taken during actual flight. Since each jack can be individually controlled either independently or synchronised with a number of other jacks, it is possible to reproduce the variety of service load conditions in the testing laboratory.

The Aeronautical Research Laboratories (ARL) have equipped their structures fatigue testing laboratory with a system controlled by a small digital computer which will carry out the following functions:

(1) Provide independent control of a number of loading actuators (jacks).
(2) Store the load data for individual actuators for all turning points (peaks or troughs) in a load sequence.
(3) Apply the loads in the required sequence, changing the actuator loads smoothly.
(4) Synchronise actuator load changes to give a smooth change in total applied load.
(5) Measure the applied loads and strains at selected locations in the structure, and keep a permanent record of a number of these loads.
(6) Protect the test specimen from accidental damage.

The last function requires careful attention, since to maintain control of a closed loop electro-hydraulic servo system the hydraulic power supply, i.e. pressure and flow, must match the maximum demand. Hence there is an excess of power available and the specimen can be easily broken.

A typical set of protection circuits for a wing test is contained in Table 1. All of the circuits are connected to a central latch unit which provides independent display and storage of the condition of each circuit. The tripping of any circuit connected to the central latch causes hydraulic locking of all actuators; and special controls together with an auxiliary power system, are provided to permit removal of locked-in loads.

Further details of the ARL control system including the electronics are contained in References 6 and 7 and a view of a Mirage wing in the testing rig is shown in Figure 4.

The capability of locking the actuators means that damage to the test specimen is minimised at final failure, since it is virtually held in the deflected state, providing there are a number of actuators applying load to the structure. The fatigue fracture faces are held apart allowing the insertion of suitable material to preserve the markings for subsequent fractographic analysis.

3. LOADING CONDITIONS

In the early days of structural fatigue research for aircraft design and development programmes, constant amplitude loading was used. As test data accrued, it became obvious that the

mode of failure and fatigue strength of a riveted structure were dependent on both the maximum load and the load range of the applied load cycle. This led to the development of the programmed load sequence which can be used to represent a spectrum of service loads as proposed by Langford[8] for civil aircraft wings.

ARL investigations had shown that a well designed six load level programme, i.e. three load ranges, could produce the various modes of failure and fatigue lives predicted from a series of constant amplitude tests.

However, doubts about load sequence effects on the accumulation of fatigue damage led to tests where a small number of pre-selected load levels (representative of the loads experienced in flight) were applied in random order. This sequence had a finite number of load selections far in excess of that necessary to cause failure of the test specimen so no load sequence was repeated. A variation of this type of load sequence is to randomise the order of blocks of constant amplitude load cycles rather than individual load cycles.[9]

The introduction of the computer using a magnetic control tape has made possible the reproduction of actual flight-by-flight sequencing of loads. These load sequences are constructed from short periods of recorded flight data edited to remove small fluctuations. A typical control tape for a fighter type aircraft can be representative of various loading actions and service conditions as follows:

(*a*) Manoeuvre loads applied in a sequence obtained from continuous recording during actual squadron service.

(*b*) Gust loads applied in a random order but in selected flights. The number of gusts of a given magnitude for each flight hour is derived from measurements made during extensive flying in a wide variety of aircraft over a considerable range of geographic and environmental conditions.

(*c*) Landing gear loads (including wheel spin-up) applied between each flight sequence, representing significant load fluctuations recorded during take-off and landing trials.

(*d*) Pressurisation (by air) of the fuel tanks to normal working pressure during each flight.

(*e*) Variations in chordwise and spanwise loading resulting from movements in centre of pressure and variations in drag of external stores.

4. AIRWORTHINESS FATIGUE TESTING

Most aircraft designed in the past 20 years have been subjected to a full-scale fatigue test to establish a safe service life under a sequence of loads representing either projected or measured load history. There are two concepts currently accepted by airworthiness authorities throughout the world, these are "safe life" for non-redundant structures and "fail-safe" for redundant structures.

4.1 General Comments

Some airworthiness authorities rely upon the "safe life" concept when issuing a certificate of airworthiness where the safe life is based on a theoretical calculation entirely or a calculation supported by a full-scale fatigue test. This approach has proved to be wasteful, particularly with military aircraft, because each aeroplane experiences differing degrees of service loads and conditions, and hence has its own fatigue endurance.

The alternative approach is the "fail-safe" concept in which an aircraft is considered still safe to operate even though a crack may be present in the primary structure. Essential requirements of this concept are firstly that the structure has been designed to be redundant in the critical load carrying areas, and hence is well able to redistribute load; and secondly that a reasonable and economic inspection routine exists that can guarantee discovery of any crack before it has reached its critical length.

A recent development, not yet generally accepted by airworthiness authorities has been the "safety-by-inspection" procedure which permits continued operation of an aircraft with a crack in parts of critical structure that are non-redundant. This concept relies on Non-Destructive Inspection (NDI) techniques combined with established and proven data of crack growth rates, together with information on residual strength of the cracked structure. All this data is necessary to ensure that the strength, i.e. load carrying ability, of the structure will remain safe until the

next scheduled inspection. ARL have conducted airworthiness fatigue tests covering various approaches on the following aircraft: Dove,[3] Cessna,[10] Vampire[11] and Mirage.[12]

4.2 Fatigue Test Article

Selection of the fatigue test specimen is of prime importance; firstly it must belong to the same "family" as the aircraft in service, i.e. built on the general assembly line and all modifications incorporated. For economic reasons there is a strong desire to limit the specimen, e.g. by not installing control surfaces on wings and truncating the fuselage. Experience has shown that it is prudent to feed loads into the structure in the same manner as they would be in service, and to fit all items of secondary structure which could induce fretting corrosion or local stress concentrations.

Virtually all fatigue cracks leading to collapse of a structure originate through a detail feature, and by the presence of secondary bending stresses produced by local offsets or sharp changes in cross section.

In cases where the airworthiness fatigue test is done after the aircraft has been in service it is advisable to withdraw the oldest airframe from service and use it as the fatigue test specimen. This enables some of the effects of service environment to be taken into account, including major factors influencing crack initiation such as corrosion and fretting (produced by small loads which might not be applied in the test).

4.3 Pre-test Load Measurement

One of the major reasons for doing an airworthiness fatigue test is to reduce the number of uncertainties involved in the process of fatigue life estimation. The actual load distribution for particular loading cases may be ascertained by making flight strain measurements, preferably on the structure that will be used for the actual fatigue test. Such measurements are significant especially in the case of strutted wings where the influence of engine nacelles and fuselage on wing spanwise lift distribution is difficult to establish by other means.

4.4 Simulation of Service Load Spectrum

Prior to the introduction of load control by a computer using magnetic tape, it was necessary to represent the continuous service load spectrum by a series of discrete load levels. Although, as mentioned in Section 3, the number can be as small as six, for a symmetric spectrum (i.e. three load ranges), results have indicated that 12 load levels are preferable to adequately reproduce an asymmetric spectrum including a ground to air cycle as reported by Mann.[9]

There are numerous factors to be considered when determining truncation at both the high and low ends of the spectrum. At the high load end the infrequent positive loads should be included because they will cause static failure when the fatigue crack has reached the critical length for the applied load; however, in the case of work hardening materials they give a strengthening effect in areas of stress concentration. Schivje[13] in 1963 suggested that the maximum load imposed in a laboratory test on an aluminium alloy structure should be that load equalled or exceeded 10 times in the anticipated service fatigue life. Unless service load measurements indicate otherwise this load should not be closely followed by a large negative (compressive) load, otherwise the beneficial effect of the positive load is lost. In the case of airworthiness fatigue evaluation tests the various airworthiness authorities provide guidelines which will result in a fatigue life on test which has not been influenced either way by the large load cycles. Guidelines for small American airplanes are given in Reference 14.

At the low end of the spectrum it is regarded as essential that loads be included which theoretically produce no fatigue damage, since they influence crack initiation by fretting and loosening of joints. However, some compromise is necessary, as the rate of cycling of the test rig will generally place a practical limitation on the number of small loads that may be applied if the result is to be available in a reasonable time.

A comprehensive survey has been made by Mann[9] of the results of many investigations into the various factors that should be considered when designing a test load spectrum.

There is no rigid procedure for determining the intermediate load levels. One of the two following is usually adopted:

(*a*) each block of load cycles producing an equal amount of fatigue damage in the specimen;
(*b*) the peak load magnitude in each block differing by an equal amount to the preceding block.

4.5 Modification and Repair During Test

A full-scale structural fatigue test also provides data for the design of repair or modification schemes, and the opportunity to develop and prove these for incorporation if required during the service life of the aircraft. No changes should be made until the damage has reached a stage that can be confidently detected in service or, in the case where structural integrity is not impaired, until the normal overhaul period.

In those cases where the structure would not be repaired in service for economic or other reasons, e.g. a time consuming repair or the aircraft would have been in use for many years, it is possible to effect a repair on the test specimen to stop a fatigue crack developing in a known area in order to obtain failure in another region. This repair need not withstand design ultimate load as it will not be used in service. However, in all cases, care must be taken in the design of the repair not to introduce stress concentrations higher than those existing in the original structure.

4.6 Fail-Safe Substantiation

Fail-safe substantiation as mentioned in Section 4.1 is a concept adopted by airworthiness authorities[15,16] to ensure that should a serious fatigue fracture or crack occur, the remaining structure will withstand reasonable flight-loads, without excessive structural deformation, until such fracture or crack is detected by inspection.

The requirements to ensure these objects are:

(1) The structure must be designed with multiple load paths so that the load can be shared or shed when cracking occurs in a primary member, i.e. structural redundancy.
(2) The critical load carrying areas must be inspectable using techniques capable of finding cracks before they reach their critical length. The techniques and frequency of inspection should be such that if a crack that has already started is missed at one inspection, it is safe to permit growth until the next, i.e. the strength of the structure will not fall below a required minimum.
(3) The structure must be capable of tolerating damage, either by redistribution of load around a failed area, or by selection of design stress levels and material, permitting a relatively long critical crack length.
(4) In conjunction with structural redundancy there should be a combination of material selection, design stress levels, and crack stoppers to produce a controlled slow rate of crack propagation and hence provide a reasonable period between inspections.

With these requirements fulfilled a fatigue test can be carefully designed to reproduce service loads and hence cause cracking to occur in predicted critical areas of the structure. In such a test it is often difficult to know when to stop the investigation. Generally this stage is reached when it becomes no longer a viable economic proposition to repair fatigue cracks and proceed, or the factored test life has greatly exceeded that life which is required for the aircraft type. In this latter case the test should continue until fatigue cracks have been found in all critical areas.

When the test is halted it is often followed by further investigations into the ability of the structures to withstand proof load and/or into the residual strength of the structure. Most of these residual strength tests require further weakening of the structure by extending the crack length until a prescribed percentage of the load carrying tension area remains. Lengthening of the crack is usually done artificially by saw cutting from the crack tip. When this method is used it is mandatory that the tip of the critical crack be sharpened by further fatigue cycling of the structure.

The structure may then be statically tested to either failure or to a load just in excess of that necessary for an acceptable standard of safety.

A test article that has been loaded beyond the maximum load in the fatigue test loading spectrum for the purpose of residual strength investigation cannot be used any further as a fatigue specimen, because of the preloading effect on both crack initiation and propagation.

Thus fail safe fatigue investigations require the provision of another test article to establish the fail-safe characteristics of fatigue cracks as they occur in the test.

4.7 Safe-Life Testing

As previously mentioned in Section 4.1, when testing under a safe-life concept the criterion used to establish the safe service life is the actual fatigue life to catastrophic collapse divided by a factor of safety.

All aircraft with non-redundant structures automatically fall into the category of "safe-life", e.g. strutted wings and single spar attachments to the fuselage. Depending upon the results of the fatigue test it may be possible to extend the service life by monitoring crack growth, but this approach is yet to be accepted by airworthiness authorities.

The object of the test when applied to this type of structure is to establish, for the first and subsequent failures, the components involved and the corresponding fatigue lives using a load spectrum representing the average for the fleet. Similarly the test specimen is selected as being a normal average representative structure. Hence the safe life of type so obtained from the test covers all the operating fleet and each aircraft is removed from service when this life is reached.

Extensive major repairs should not be made to the specimen during the test, because the whole object is to obtain the life to catastrophic failure of the structure, from which a safe operating life is derived. However, normal scheduled servicing and inspections are done to maintain the test validity.

Progress of a safe-life test can be faster than a fail-safe test, since the detection of a fatigue crack may only require subsequent monitoring to determine rate of propagation. Similarly in service the aircraft is only subjected to routine inspections and minor repairs.

The main disadvantage of the safe-life concept is that it restricts the true serviceable life of better than average structures, and it allows "rogues" to exist undetected. Thus it is wasteful of the good structures while also harbouring the risk of non-detection of the weaker ones.

4.8 Development of NDI Techniques

Many aircraft owe their long service life to the fact that it was possible to design and develop non-destructive inspection (NDI) techniques during the full-scale fatigue test, e.g. Venoms operated by the Swiss Air Force.[17]

Some NDI techniques such as radiography rely almost entirely on prior knowledge gained during testing to give the exact location and shape of a fatigue crack to enable its detection during service. The application of other techniques using magnetic rubber, eddy current and ultrasonics has enabled crack propagation rates to be accurately determined during testing, such that an extension of life is obtained while the crack is growing to a critical size. This is the basis of the safety-by-inspection method of fatigue life monitoring.

5. TESTING OF ASSEMBLIES

The fatigue testing of large structural components or sub-assemblies is carried out using techniques as for full-scale structures. Some aircraft designers for many reasons, of which cost is a major one, have attempted to predict the fatigue behaviour of the complete structure from tests on components.

It has been conclusively shown that there are severe limitations in applying the data so obtained, and such tests are now confined to design and development of structural details and comparison of relative fatigue performance.[18]

Such tests can also provide other useful design data such as:

(i) scatter in fatigue life where new materials or fabrication techniques are introduced;
(ii) crack propagation data for reliability analyses; and
(iii) residual strength of structural elements.

The two main problems when testing structural elements to provide data for life estimation are:

(*a*) providing representative load distribution in the test specimen; and
(*b*) incorporating in the test specimen the manufacturing methods used in constructing the full-scale structure.

6. DATA AVAILABLE FROM FULL SCALE TESTING

Some of the information that can be obtained from a fatigue test that is representative of service conditions on a full-scale structure has already been covered. However, it and other information available from such tests are included in the following summary:

(1) Detection of areas of the structure liable to exhibit fatigue cracking during the service life of the structure, i.e. location and modes of failure.
(2) Life at which fatigue cracking may be expected to begin in each of these areas.
(3) A reliable value for the mean life to collapse or failure of the structure. A reliable mean life can only come from a well designed and planned test of a full-scale representative structure. Such a test also allows a reduction in the scatter factor used to determine the safe service life. There is a further reduction in the factor on statistical grounds if more than one specimen is tested.
(4) Rate of crack propagation in terms of service life. If not measured during the test, it is sometimes possible using fractographic techniques to analyse crack growth on the fracture faces at the completion of the test. This is done by relating the striations or markings on the surfaces to the load history.
(5) Residual strength of the fatigue cracked structure which provides additional data on the margin of safety of the structure.
(6) Design data on efficiency of repair and modification schemes, e.g. bonded fibre reinforced plastic repair patches.
(7) Determination of the inspectability of the structure, coupled with design and development of NDI techniques and equipment to be used during the service life of the aircraft.
(8) From tests on a number of identical structures, it is possible to produce data for subsequent design of similar structures and fatigue life estimation. ARL have produced such data from tests involving 20 Mosquito,[19] 28 Boomerang,[20] 21 Vampire,[5,11] and 222 Mustang[4,21,22,23,24] semi-span wing specimens. Data from these tests together with data from other investigations have been used in production of the aircraft design data sheets of the Engineering Sciences Data Unit sponsored by the Royal Aeronautical Society of UK.[25] The significant conclusions from full-scale fatigue tests done in ARL are given in the Appendix.

7. FACTORS RELEVANT TO FULL SCALE FATIGUE TEST PLANNING

The commitment of resources required to conduct a worthwhile full-scale fatigue test are of such a magnitude that the cost effectiveness of such tests must be considered. The following factors have to be considered before the most appropriate test can be formulated, and plans made for its execution:

(*a*) Cost—money, materials, and manpower.
(*b*) Timing—whether early or late in the life of the aircraft type.
(*c*) Load representation—use of complete airframe, flight-by-flight or programmed load sequences.
(*d*) Time scale of test—cycling rate of loads, shift work (continuous running).
(*e*) Inspection—frequency and techniques to be employed.
(*f*) Environmental factors—service flight conditions.

7.1 Cost

The costing of a test in terms of money, materials and manpower is a reasonably straightforward engineering task. The cost effectiveness of a test to determine the safe operating life of an aircraft is far broader, and involves some unknown factors, and evokes many more. In some cases it is easier to gauge the cost if a test is not done. This was highlighted by the cost to the United Kingdom of the fatigue failures in Comet and Viscount aircraft, which caused whole fleets to be suddenly withdrawn from service; unlike an accident from a cause peculiar to one aircraft, the presence of a fatigue failure affects equally the whole fleet.

Some years ago Harpur and Troughton[26] analysed costs and were able to show that fatigue testing can be justified on economic grounds alone.

7.2 Timing

For commercial aircraft, it is as important to know before the start of service the period of safe use as it is to know the scale and type of business that is predicted for the aircraft type. Hence fatigue tests are usually started prior to entry of the aircraft into service with the test staying well ahead of the service life.

The importance of knowing the safe operating life of a military aircraft is largely determined by the nature of the current threat. Fatigue is not a major factor in wartime, but during low threat or peacetime it affects training programmes, and the all important planning for and timing of replacements to meet the ever changing demands of preparedness. In many cases, fatigue tests of military aircraft are done towards the end of their theoretical predicted life in order to obtain a possible extension for the life of type.

7.3 Load Representation

The major consideration is how much of the actual aircraft is available as the test specimen, because the degree of load representation is directly related to both the aerodynamic complexity, size and cost of the structure, and its prime service role, e.g. sub- or supersonic, fighter or ground attack, aerobatic or non-aerobatic, etc.

The number of load cases required to encompass the various operational roles of the aircraft type depend mainly on its aerodynamic configuration, including fixed or variable wing sweep, flaps for STOL operation, tailless delta (which requires a large shift in centre of pressure over the mainplane), etc. Short range and agricultural aircraft have wide weight changes between the many landings which produce large and frequent ground to air cycles of load.

In general, if the whole airframe is to be tested, then the simulation of service conditions on wings, undercarriage, tailplane, flaps, engine reaction, cabin, and fuel pressurisation loads, will require many loading channels to ensure that the various fatigue critical areas are loaded correctly. These channels will require a comprehensive control system to apply the loads in the correct order and magnitude, and thus correctly represent the interaction experienced in flight-manoeuvres.

A test involving this degree of service load representation must have in-flight load data available for each channel in order to maintain a balance between the goal of the test and the considerable cost. The flight data should be edited to remove some of the small but numerous non-damaging loads, and to see that rare but known loads are included. The data are then arranged in flight-by-flight blocks, usually in arbitrary order. Modern test rig control systems permit the sequence of the load cycles within each block to be applied as recorded in service.

7.4 Time Scale of Test

The three main factors effecting the time to complete the test are the cycling rate of the loading system, the number of loads included to represent the lower portion of the test load spectrum, and the time taken to effect repairs to the test specimen.

Fatigue behaviour can be modified by variation in the rate of load cycling, but in the case of full-scale structural testing it is difficult to test faster than the natural frequency of the structure, e.g., about 12 Hz for wings of small aircraft, a rate which is reached in service from gust loadings.

As previously mentioned fatigue tests on aircraft structures are long term programmes, for example, testing of the Dove wing[3] which involved both airworthiness and research investigations spanned 10 years, while in the case of the Mirage wing[12] where the data were urgently required for extension of life of type and the test was run continuously, it still took nine months to simulate 33,000 flights.

Continuous test running is almost essential for full-scale fatigue tests and this will invariably involve shift work since it is unwise for safety reasons to leave servo hydraulic systems running unattended. Problems may arise in maintaining complex equipment outside normal working hours; however, this can be minimised with the use of reliable computer controlled and monitored systems.

It is most important that inspection periods for the specimen and testing equipment be carefully planned to make optimum use of available skilled staff and serviceable equipment. In this way the test proceeds as scheduled, and the test results are available sufficiently in advance

of service aeroplanes. However, a large amount of time can be consumed assessing the significance of fatigue cracks and determining repair procedures before resumption of the test.

For planning purposes it is prudent to assume that actual running of the test rig will occupy only 25% of the time allocated to conduct of the test, i.e. for an eight hour day the rig running time will be two hours per day with the remaining six hours being used for inspection, repair and unscheduled stoppages.

7.5 Inspection

One of the prime reasons for doing a fatigue test is to know when and where fatigue cracks are likely to occur in the structure. Hence an important objective for inspections in every fatigue test is to find all the cracks as soon as possible after initiation, and monitor their subsequent growth. In cases where this is not possible, fractographic techniques have been developed which enable growth data to be ascertained by an examination of the final fracture surface.

Techniques used and inspection periods chosen are mainly determined by the criteria adopted by the airworthiness authority. In tests conducted under fail-safe or safety-by-inspection criteria, the inspection and equipment used in these types of test to find cracks and monitor their growth are extensive and exacting because of, for one thing, changes of load with redistribution within the redundant structure.

The test is also used to develop the non-destructive inspection technique so that it can be confidently used to monitor the airframe in service.

Another essential factor to be determined from the test is the critical crack length for those areas of the structure liable to crack in service. Time must be spent on these inspections, and on the assimilation of the knowledge which they are revealing on the fatigue performance of the structure as the specimen advances toward final failure. Unless an adequate allowance of time is made for this vital aspect of a fatigue test it is more difficult to meet target dates and obtain the required data from the test.

Determination of both the timing of the inspections and the specialised equipment to be used for the various parts of the structure require considerable experience, skill and responsibility, because so much of the data cannot be obtained later—it must be recorded as it happens.

7.6 Environmental Factors

The effect of environment on fatigue behaviour has not been regarded as being significant for the majority of subsonic aircraft. Some tests have been done in the open rather than in the semi-protection of a laboratory, especially in the case of large aircraft where it is less costly and more convenient. It would be difficult to reproduce the changing conditions of rain, hail, icing, oil and fuel spillages, bird and lightning strikes, etc., that an aircraft experiences from flight-to-flight, and almost impossible in the laboratory to simulate the effect of ageing that is experienced by the structure during its service lifetime.

In the case of supersonic aircraft there are additional stresses imposed on the structure that can equal in magnitude those arising from manoeuvres, gusts, etc. These stresses are generated by the thermal gradient that the structure experiences when the aircraft accelerates to supersonic speed, causing heat to be generated in the boundary layer by compression and frictional forces. A reverse gradient occurs when the aircraft decelerates. In this latter case the internal structure is hot after the flight at supersonic speed, and the outside (of relatively low thermal capacity) is exposed to the cold atmosphere. The thermal stresses produced are proportional to the temperature gradient through the structure, and hence reduce to zero as the structure approaches uniform temperature. Structural temperatures of 120°C can be reached during flight at mach 2·2 (60,000 ft) which can also expose light alloy materials to the effect of creep and other temperature dependent phenomena.

In any fatigue life investigation on supersonic aircraft these thermal effects must be reproduced in the laboratory test even though their simulation adds tremendous cost to an already costly task.

8. FUTURE DEVELOPMENTS

Despite the continuing hopes that full-scale fatigue testing can be replaced by calculation and tests on components, experience has shown the continuing need for such tests.

Changes in materials of construction coupled with new or different manufacturing techniques can produce drastic reductions in fatigue life of new aircraft, a recent example being the General Dynamics F111 airframe.[27]

The computer controlled electro-hydraulic loading systems should be able to cater for all loading cases envisaged, although unfortunately the cost is high. However, the testing of supersonic aircraft structures still requires considerable research into the production of a laboratory representation of the thermal cycles, in a reasonable period of test time.

Certain materials such as the ultra high strength steels[28,29] are significantly affected by the atmospheric environment, and it may be necessary to control this aspect as well during testing.

The variation in service load history for individual aircraft has led to the formulation of fatigue life monitoring procedures in which fatigue damage for each aircraft is calculated using a number of significant parameters recorded in service.[12] The essential characteristics of laboratory tests in the future are that they will be conducted on a complete structure on which a flight-by-flight sequence simulating the service load history is applied, with the load distribution and environment varying according to the operating conditions pertaining to each flight.

9. ACKNOWLEDGEMENTS

The large and lengthy full-scale fatigue tests conducted at ARL have only been possible through the efforts of many persons and organisations who gave their full support and encouragement, particularly to the research programmes.

The collaboration of the Department of Transport (Air Transport Group), Australian airline companies, and the Royal Australian Air Force is greatly appreciated.

REFERENCES

1. Gassner, E. — Festigkeitsversuche mit wiederholter Beanspruchung im Flugzeugbau (Strength Tests with Repeated Loads in the Construction of Aircraft). Luftwissen, vol. 6, no. 2, pp. 61–64. February, 1939.
2. Kepert, J. L., Patching, C. A., and Robertson, J. G. — Fatigue Characteristics of a Riveted 24 S.T. Aluminium Alloy Wing. Part 1—Testing Techniques. Aeronautical Research Laboratories, Report SM 246, Department of Supply, Melbourne, October 1956.
3. Ellis, R., Graff, D. G., and Mitchell, B. J. — Dove Wing Fatigue Test. Aeronautical Research Laboratories, Note ARL/SM 408, Department of Supply, Melbourne, May 1974.
4. Mann, J. Y., and Patching, C. A. — Fatigue Tests on "Mustang" Wings and Notched Aluminium Alloy Specimens, With and Without Ground to Air Cycle of Loading. Aeronautical Research Laboratories, Note ARL/SM 268, Department of Supply, Melbourne, March, 1961.
5. Patching, C. A., and Mann, J. Y. — Comparison of an Aluminium Alloy Structure with Notched Specimens under Programme and Random Fatigue Loading Sequences. Fatigue Design Procedures, pp. 395–432. Pergamon Press, Oxford, 1969.
6. Ludowyk, C. J., and Moody, F. S. — Application of Electro-Hydraulic Control to Wing Fatigue Testing. Aeronautical Research Laboratories, Note ARL/SM 412, Department of Defence, Melbourne, November 1974.
7. Moody, E. S. — A Computer Based Instrumentation System for Structural Fatigue Testing. Aeronautical Research Laboratories, Note Structures 420, Department of Defence, Melbourne, January 1976.
8. Langford, P. S. — An Airworthiness Fatigue Requirement for Civil Aeroplane Wings. Australian Aeronautical Research Committee, AARC 35, November 1955.
9. Mann, J. Y. — Fatigue Testing—Objectives, Philosophies and Procedures. Aeronautical Research Laboratories, Report No. ARL/SM 336, Department of Supply, February 1972.
10. Benoy, M. B., Verinder, F. E., and Maddock, T. S. — Fatigue Tests on the Cessna 180 Wing and Strut. Aeronautical Research Laboratories, Report ARL/SM 318. Department of Supply, Melbourne, October 1967.
11. Bruton, R. A., and Patching, C. A. — Fatigue Testing of Twenty-Three Aircraft (Vampire) Wings. Aeronautical Research Laboratories, Department of Defence, Structures Report (unpublished).
12. Howard, P. J., Patching, C. A., and Payne, A. O. — Life Estimation by Parametric Analysis, Problems with Fatigue in Aircraft. Proceedings of the Eighth ICAF Symposium, ICAF Doc. No. 801, Swiss Federal Aircraft Factory, Emmen, June 1975.
13. Schivje, J. — Estimation of Fatigue Performance of Aircraft Structures. Fatigue of Aircraft Structures, Cleveland, ASTM S.T.P. No. 338, pp. 193–215.
14. Fatigue Evaluation of Wing and Associated Structure on Small Airplanes. Report No. AFS-120-73-2, Department of Transportation, Federal Aviation Administration, Washington, May 1973.

15. Design Requirements for Service Aircraft.
AvP. 970, Vol. 1, Chapter 200

16. British Civil Airworthiness Requirement, Section D, Chapter D1.

17. Branger, J. Life Estimation and Prediction of Fighter Aircraft.
International Conference on Structural Safety and Reliability, Smithson in Institution, Washington, April 1969.

18. Payne, A. O. The Fatigue of Aircraft Structures.
Engineering Fracture Mechanics, Vol. 8, pp. 157–203, Pergamon Press, 1976.

19. Johnstone, W. W. Static and Repeated Load Tests on "Mosquito" Wings.
Division of Aeronautics Report SM 104, Council for Scientific and Industrial Research, Melbourne, September 1947.

20. Johnstone, W. W., Patching, C. A., and Payne, A. O. An Experimental Determination of the Fatigue Strength of CA-12 Boomerang Wings.
Aeronautical Research Laboratories, Report SM 268, Department of Supply, Melbourne, 1959.

21. Payne, A. O., *et al.* Fatigue Characteristics of a Riveted 24 S-T Aluminium Alloy Wing: Part V—Discussion of Results and Conclusions.
Aeronautical Research Laboratories, Report SM 268, Department of Supply, Melbourne, 1959.

22. Jost, G. S. The Fatigue of 24 S-T Aluminium Alloy Wings under Asymmetric Spectrum Loading.
Aeronautical Research Laboratories, Report SM 295, Department of Supply, February 1974.

23. Payne, A. O. Random and Programmed Load Sequence Fatigue Tests on 24 S-T Aluminium Alloy Wings.
Aeronautical Research Laboratories, Report ARL SM 244, Department of Supply, Melbourne, September 1956.

24. Jost, G. S., and Lewis, Jeanette A. A Comparison of Experimental and Predicted Fatigue Lives of Mustang Wings under Programmed and Random Loading.
Aeronautical Research Laboratories, Report ARL/SM 300, Department of Supply, Melbourne, December 1964.

25. Data Sheets – Fatigue, Vol. 1, Sheet E.02.01.
Engineering Sciences Data Unit, London, June 1962.

26. Harpur, N. F., and Troughton, A. J. The Value of Full-Scale Fatigue Testing.
Fatigue Design Procedures, Pergamon Press, London, 1969.

27. Hinders, Urban A. F-111 Design Experience – Use of High Strength Steel.
AIAA Paper No. 70-884, American Institute of Aeronautics and Astronautics, New York, July 1970.

28. Kemsley, D. S. The Effects of Water Vapour Content and Temperature of an Air Environment on the Fatigue Behaviour of an Ultra-High Strength Steel.
Metallurgica, Vol. 10, pp. 421–24, Pergamon Press, United States, 1976.

29. Jost, G. S. Fatigue Tests on Ultra High Strength Steel Structures (Humphries Specimens).
Aeronautical Research Laboratories, Report ARL/SM 347, Department of Supply, Melbourne, March 1974.

30. Payne, A. O. Determination of the Fatigue Resistance of Aircraft Wings by Full-Scale Testing.
Full Scale Testing of Aircraft Structures, pp. 76–132, Pergamon Press, London 1960.

31. Parry-Jones, G. Fatigue Crack Propagation in Mustang Wings.
Report SM 289, Aeronautical Research Laboratories, Department of Supply, Melbourne, June 1962.

APPENDIX
Conclusions from ARL Full Scale Fatigue Tests

From the numerous experimental investigations involving fatigue testing of full-scale structures at ARL, it has been possible to arrive at a number of conclusions concerning techniques and the fatigue behaviour of riveted aluminium alloy structures.

The following is a brief statement of the more significant findings, not in any order of importance:

(1) The different methods of testing employed, viz. hydraulic and vibration, give appreciably the same results, e.g. life to crack initiation and collapse, modes of failures, etc., under identical loading conditions.[2]

(2) The types of failure which occur in separate areas of the structure under constant load amplitude testing are dependent on the load range and the peak load of the cycle. In the case of the Mustang wing, seven distinct types of failure were identified in four areas.[21]

(3) The continuous spectrum of service loads may, for testing convenience, be rationalised into programme blocks comprising a relatively small number of load ranges (from 3 to 6), or into random sequences of turning points at a number of levels (from 12 to 22). These sequences have proved adequate to establish the various locations of failure and their sequence.[11,30] In a well designed test on an aircraft structure there will usually be a number of failure regions. In the case of the Dove wing,[3] the structure cracked at approximately 27 locations, while on the Vampire wing[24] there were 12 failure regions.

(4) Riveted structures of 24 S-T or similar alloy show very similar fatigue strengths when compared on the basis of average stress in the critical areas. Such structures may be represented by a common alternating stress–mean stress diagram using a standard deviation in log life of $S = 0{\cdot}32$, which includes the effect of variation between structure types and the variation within structure types.[21] Such basic information is required when the need arises to make a cumulative damage summation for structures subjected to variable amplitude load-histories. Such a diagram has proved useful for making preliminary estimates of the safe life of 24 S-T structures.

(5) Fatigue failure in a riveted and bolted structure cannot be accurately predicted by tests on simple fabricated or notched fatigue specimens. The value of theoretical stress concentration factor required to give equivalent fatigue lives has ranged from 3·3 to 4·2.[5,21]

(6) The effect of a high preload, e.g. anything greater than 70% of the ultimate failing load in the tension mode, is to prolong considerably the life of the structure. However, in one experiment there was found an optimum value of approximately 85% of the Ultimate Failing Load, producing a maximum increase in life of about 300%.[21]

(7) The rate of crack propagation through a redundant 2024 aluminium alloy structure is reasonably constant for a large part of the total life (40% to 70%), then the crack rate progressively increases until failure occurs.[31]

(8) The assumption of linear cumulative damage shows reasonable agreement with the data for load levels of practical interest, provided a suitable procedure is adopted for replacing a fluctuating load sequence by equivalent load cycles.[23]

(9) The Laboratories have tested various ways of converting load histories to load cycles, as far as fatigue damage is concerned. None of the conversions has led to completely satisfactory predicted lives under random conditions, but they were fairly accurate for programmed loading.[24] Hypothesis H1 (load fluctuations determining fatigue damage are obtained by combining maximum "peaks" and minimum "troughs", irrespective of position in the sequence), known as the peak count method, gives, in general, predicted lives closest to those actually obtained and it is usually conservative; all other methods investigated produced optimistic lives. Hence for the purpose of con-

servatively estimating fatigue lives from basic S-N data the general use of Hypothesis H1 is recommended.

Considerable care is necessary in scaling S-N data so as to match total calculated fatigue damage to that observed in spectrum fatigue tests. In the case, for example, where linking manoeuvres are in significant numbers, or where the spectrum resolves itself into separate ground and air cycles, other methods, e.g. range pair counting, may prove preferable to H1 for scaling the S-N data.

(10) The variation in the transfer of load between removable panels and primary structure, i.e. panels such as fuel tank doors, attached with screws which may loosen, can greatly influence both the life and mode of final fatigue failure.

(11) It is essential in any full-scale fatigue test to continue the test until fatigue cracking occurs, i.e. until the fatigue critical component(s) or region(s) have been identified, and the way in which the fatigue failures develop. This applies especially to the "fail safe" type of structure. Progressive repairs to the fatigue cracked regions may be used to prolong the test.

(12) The estimation of fatigue life of a structure using existing data relating to similar structures or components is subject to a number of errors. Moreover the changing load distribution particularly in a redundant structure is so complex that fatigue testing of individual components does not in general well produce the actual loading conditions. Hence a fatigue test on the complete structure is necessary.

(13) The introduction of a large negative load, e.g. the ground-to-air cycle of loading, greatly reduces the fatigue endurance. In the case of the Mustang wing, specimens tested under a load spectrum representing a four engined turbo prop transport aircraft, gave a reduction in endurance of between 70% and 80% when the ground to air cycle was included.[4]

(14) The residual strength of a cracked structure is difficult to calculate since in the case of a relatively ductile material such as 24 S-T aluminium alloy the general yielding at failure is sufficient to redistribute the load across the cracked section.

(15) In many specimens the fatigue cracking leading to final failure of the structure was not detected until catastrophic collapse occurred, despite the application of a recommended non-destructive inspection technique. Hence it is essential to identify cracks in those full scale fatigue tests that are designed to allow for continued service of aircraft using the "safety by inspection" method of operation.

(16) The costs involved in a fatigue test programme are quite large and the technical problems associated with simulation of actual service conditions difficult to solve; hence the design of a fatigue test requires the application of considerable engineering judgment in order to achieve a cost-effective yet realistic test.

(17) Screw fastener tightening techniques can produce large variations in stress in primary structure, e.g. a range of 20% in the spar boom of a wing containing a number of large removable panels.[11]

(18) Radiographic inspection using X-rays was not found to be a reliable means for detection of cracks, even when the crack had been located visually.[10,11,12]

(19) Wooden aircraft structures have fatigue lives greatly in excess of those fabricated from aluminium alloy,[11,19] in the case of the Vampire tests two fuselages outlived 23 wings.

TABLE 1
Circuits for Loading System

No.	Name	Function/Description
		Protection Monitors
1	Pump Room Status	This circuit shows when hydraulic power is available, and will inhibit starting the system if pumps are off-line. Will stop all systems through main latch (lock-up systems) if hydraulic power fails.
2	PDP-11 Status	Shows computer is operating and on correct programme. Circuit is set by the computer, and when not set inhibits resetting the main latch. It shuts the system down through the main latch and solenoid valve supply if the computer fails.
3	Total Power	The circuit monitors system power supplies and inhibits reset of the main latch until all system electrical power is available at the specified voltage levels. It shuts the system down through the main latch if a power supply fails.
4	Smoke Detectors	All instrument racks are monitored for smoke. If smoke is detected the system is shut down through the main latch and a fire alarm is started.
5	Safety System Security	Indicates all protection printed circuit cards are correctly plugged into modules. Cards in the protection system carry shorting links which are all connected in series. If the loop opens the system is shut down through the main latch.
6	Manual Stop Buttons	Provides for emergency intervention by the operator. Buttons exercise direct control over the mechanical contactor in the electrical supply to the solenoid valves and as a secondary action trip the main latch.
7	Inertia Switch	Responds to violent motion of the wing, and will stop the system through the main latch unless inhibited by the computer. The switch is automatically reset whenever the inhibit signal is removed.
8	Wing Limits	Microswitches monitor travel of all actuators applying load to the wing. These switches can shut the system down through the main latch and through the mechanical contactor.
9	Undercarriage Limits	As for circuit 8, but monitors the travel of the undercarriage actuators.
10	LVDT Limits	Uses linear variable differential transformers to monitor the position of the wing. The circuit will stop the system through the main latch should the output voltage of the transformers exceed preset limits.
11	Rig Oil Pressure	When the rig oil pressure is zero prior to starting this circuit must be cocked by the operator before the main latch can be reset. Once the correct operating pressure is achieved the cocking circuit is automatically disabled, thereafter a fall in pressure below the set value will stop the system through the main latch.
12	Excess Error	Monitors error signal magnitudes in all servo-amplifiers, and shuts the system down through the main latch if the error exceeds a preset value on any servo-amplifier.
13	Excess Load	Monitors the load signal magnitudes in all servo-amplifiers, and shuts the system down through the main latch if the load exceeds its preset value in any servo-amplifier.

TABLE 1—continued

No.	Name	Function/Description
14	Slew Rate Limiting	Limits the maximum flow rate through the servo-valve by limiting the magnitude of the electrical signal which can be applied to it.
		Control Circuits
1	Main Latch to Computer	Carries a signal from the output of the main latch to the computer, and initiates a programme branch to the "Fault" routine.
2	Valve Supply to Computer	Indicates when electrical power is applied to the solenoid valve circuit, and in the READY and RUN states only, can also switch the computer programme to the "Fault" routine. In part this circuit duplicates the previous one.
3	Mechanical Contactor Control	Supplies electrical power to the hydraulic solenoid valve control circuits. It embraces emergency stop buttons, key switch, and microswitch limit switches. Circuit can initiate main latch action.
4	Key Switch	Operator's key switch must be closed before the mechanical contactor and thence the solenoid valves can be energised. Closing this key is the first step in the application of power to the test rig.
5	Servo-valve Isolator	When the main latch is tripped the base circuits of the transistors driving the servo-valve coils are opened. This reduces all servo-valve coil currents to zero and centres the valves.
6	Valve "V2" Switching	"V2" is made up of the two solenoid valves which together provide the main hydraulic control for the rig. The normal control circuits of these valves are fully duplicated, but when the main latch is tripped it de-energises only one of these valves directly. The other valve is de-energised by a combination of computer status and servo-amplifier status signals. The objective of this arrangement was to provide several possible paths for the shutdown signal.
7	Error Circuit Inhibit	During the application of "spring-back" load to the undercarriage this circuit inhibits all error signal monitors in the servo-amplifiers, and the inertia switch signal, to avoid spurious main latch shutdown. Without this inhibit signal the large transient signal would trip the main latch.
8	Inertia Switch Automatic Reset	The inertia switch may be tripped during the application of spring-back load. This circuit ensures the inertia switch is reset before the inhibit signal is removed.
		Protection (Miscellaneous)
1	Calibration Circuit Inhibit	Shunt calibration relays in the feedback amplifiers can only be energised when the key circuit is open. The application of electrical power to the solenoid valve circuit places an additional open circuit in the calibrate relay lines.
2	Barrier Condition	A system of light beams monitors movement of personnel into the inner test rig area. If the barrier circuit has been tripped the system cannot be started until the area is checked. If the barrier is tripped while the system is running a warning is sounded in the control room.
3	Voice Recording	Voices on the inter-com system are automatically recorded on a voice operated cassette magnetic tape recorder.

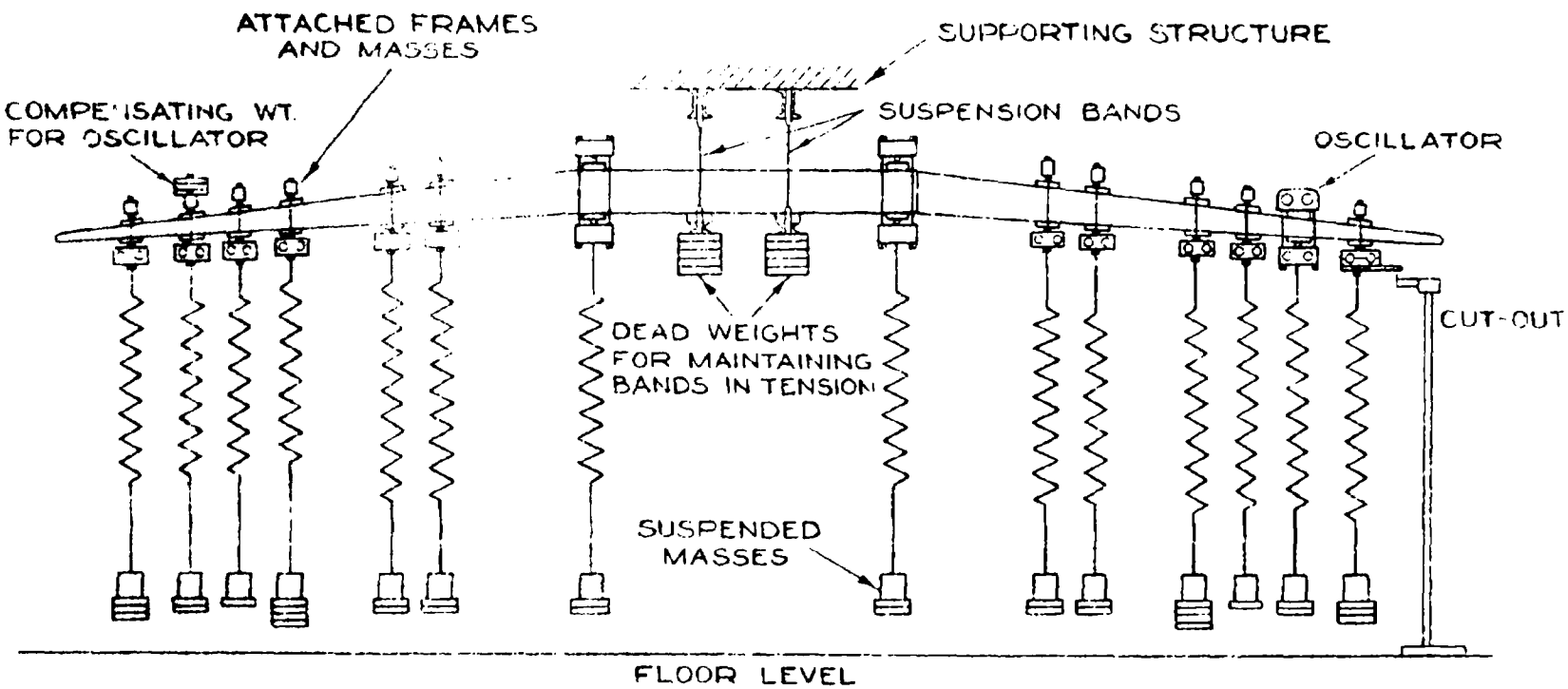

FIG. 1. VIBRATION TEST METHOD MEAN LOAD APPLIED BY SUSPENDED MASSES.

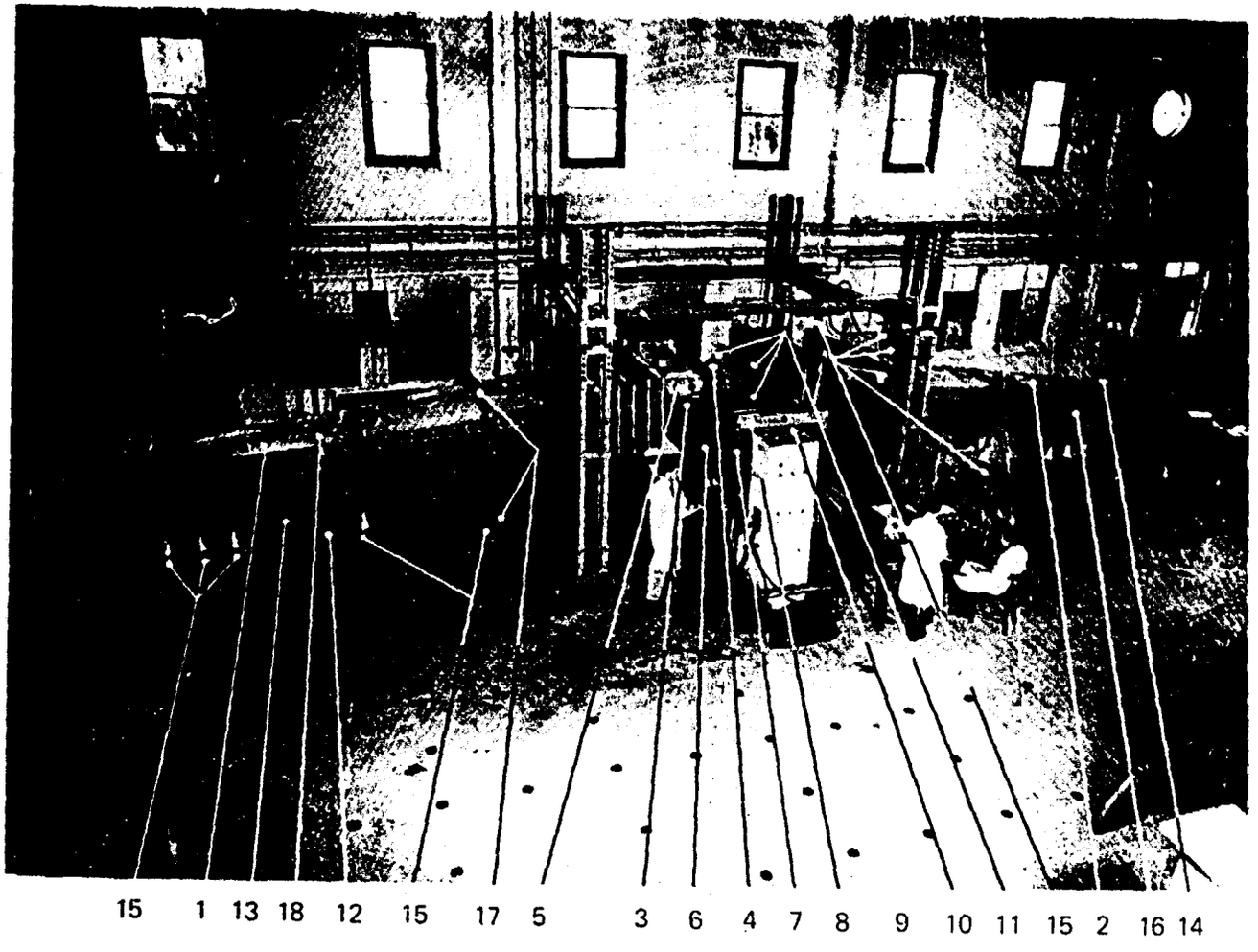

1. Port wing
2. Starboard wing
3. Dummy centre section
4. Centre section tension beam
5. Representative shear web
6. Support beams
7. Flexible steel links
8. Cross beam
9. Concrete column
10. Rubber buffer blocks
11. Wing attachment points 3
12. Stroking machine
13. D.C. motor
14. Deflection indicator striker plates (indicator not shown)
15. Mean load jacks
16. Attachment springs
17. Load attachment frames, including added masses
18. Stroking machine attachment frame

FIG. 2. VIBRATION TEST METHOD MEAN LOAD APPLIED BY HYDRAULIC JACKS.

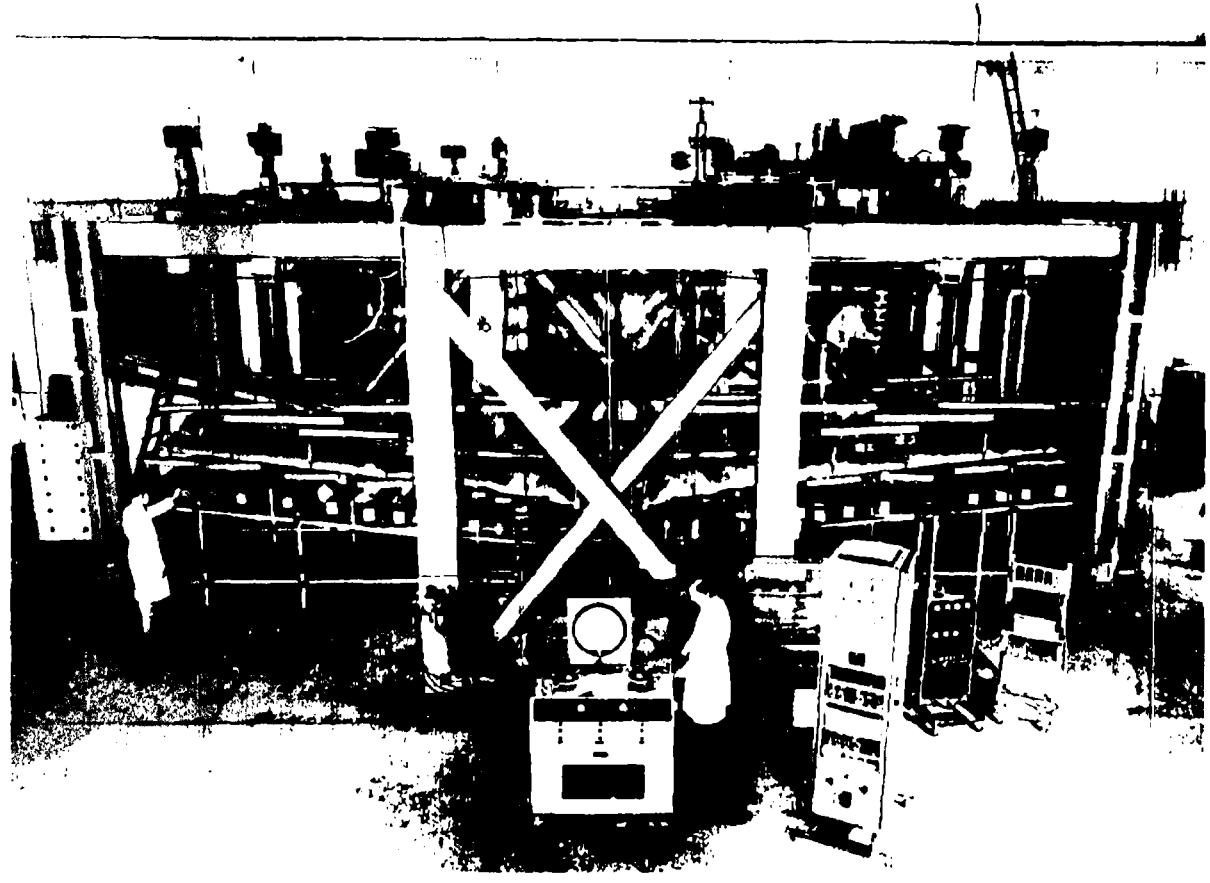

FIG. 3 HYDRAULIC LOADING RIG FOR TESTING MUSTANG WINGS

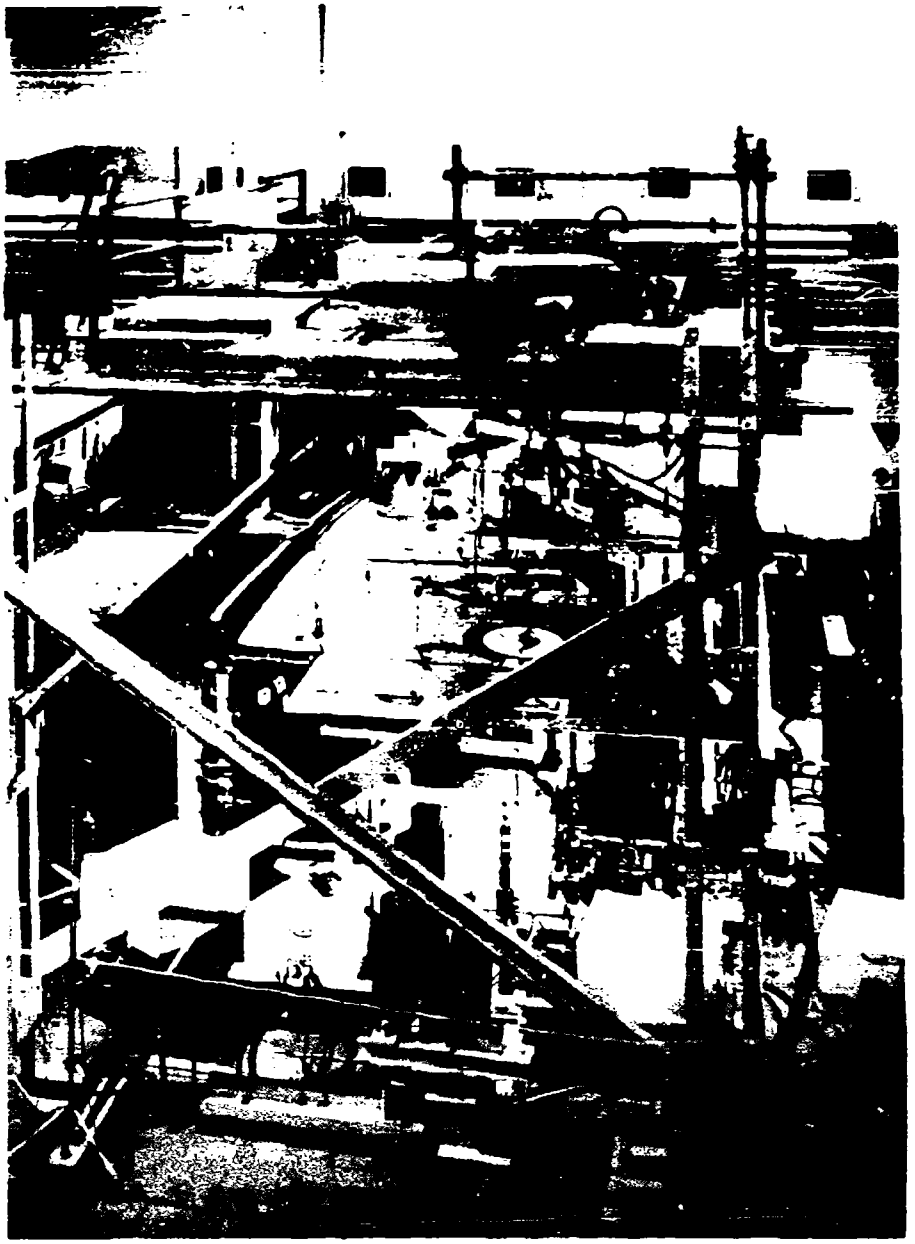

FIG. 4. ELECTRO HYDRAULIC FATIGUE LOADING RIG FOR MIRAGE WING FATIGUE TEST.

DISCUSSION

QUESTION—*I. M. McPherson*
(Engineering Development Establishment)

You mentioned that consideration had been given to the possibility of preloading a structure with the view to increasing its fatigue life. Just how serious is the possibility? What are the problems? Would you please expand on this matter?

Author's Reply

Preloading of a 24 S-T Al. alloy riveted structure to beyond 70% UTS will prolong the life under a much smaller fluctuating load. In experiments at ARL the optimum value of preload was found to be 80% which increased the life to failure by 300%.

The main problem is to load a structure to this high value so that all critical areas are preloaded, and other areas are not loaded beyond design limit stress. Large aircraft can have about 30% of wing area moveable, i.e. flaps, slats, spoilers, ailerons, etc., which influences the various loading cases to cover all flying conditions. When a loading case is defined, a rig has to be designed to apply and react the combination of these substantial loads.

If the structure were less complex and non-redundant, requiring say only one loading case to cover the major part of the flight envelope, there may be a strong case to take advantage of the pre-load effect.

During the early 1950s there was serious consideration given to subjecting new aircraft to design limit load during the production test flight. However, the idea was dropped because of the likelihood of exceeding the desired load and the fact that this could only apply 66% UTS which would be of doubtful value.

QUESTION—*J. G. Garlick*
(Defence Science Administration)

Would you comment on the application of your techniques to the field of helicopter flight loads and fatigue, as opposed to conventional airframe fatigue, which has been the principal concern of your paper.

Author's Reply

The techniques developed at ARL for fatigue testing of aircraft structures have been simple in concept; namely, to find means to simulate the "in-flight" loading conditions by distributing loads into the specimen in such a way as to not interfere with the structural integrity of the specimen. Before this can be done the magnitude, frequency, distribution and sequence of flight loads must be known.

Computer controlled servo-hydraulic systems have made it possible to apply any combination and sequence of loads that can be determined by instrumented flight tests, or from prediction. The only problem is time and money to design, construct, and commission these systems.

Considerable difficulty is met when these tried and proven techniques of fatigue testing are required to test a flying machine like a helicopter in which the lifting surfaces serve also as the propulsion device. This produces forces, i.e. "Tennis Racquet" moment, Coriolis force, etc., that can only be effectively produced by actually rotating the blades.

Other forces combine in forward flight to produce loads of small magnitude but high frequency (i.e. at natural resonance of the blade), and hence accumulate large n values. These forces must be included in the test because most current helicopter blades are made from aluminium alloy which has no fatigue limit. In addition, to simulate the interaction of all these blade loads on the drive gear would require a 6 degree-of-freedom servo hydraulic loading system.

The recording and analysis of helicopter flight load data are equally difficult because of the many forces that act and interact and do so on differing planes. However helicopter fatigue testing

can be done to a very high degree of simulation using the techniques of current flight load acquisition equipment and computer controlled servo hydraulic loading systems.

QUESTION—*Dr. Ford*
(ARL)

I query the appropriateness of maximum-peak minimum-trough type counting. The interpretation of ARL structural test results was made before there was much research on counting methods. For large excursions such as ground to air cycles the numbers of counts are almost equal.

As well as being as good an explanation, the range pair counting has more theoretical support which has been discussed by Japanese workers (Endo *et al.*).

Author's Reply

The proving of various methods of accounting for load cycles in a varying sequence has, to the authors' knowledge, not yet shown which method produces the most reliable estimate. Certainly the interpretation of ARL test results used only the five methods proposed at that time, and as yet the range pair counting has not been tested on that data.

However, any calculation of fatigue damage made for determination of safe life of an aircraft structure must be either correct or conservative, and the maximum-peak to minimum-trough type of counting was conservative in all cases checked.

QUESTION—*R. G. Noakes*
(Vickers Research Pty. Ltd.)

I was an engineering apprentice at the RAE, Farnborough—1934–38. It would be late in '35 or early '36 when some fatigue tests were conducted on a Fairey III F monoplane (if my memory serves me correctly).

The machine was mounted on a suspension and an electrically driven oscillator mounted on the wings. I assume these tests would have been reported in an RAE Tech. Memo presumably available from the Librarian.

Author's Reply

The authors are interested to learn of the early fatigue tests on the Fairey aeroplane; however, the reports of these tests, no doubt along with others, have not been released for publication. Our reference for reports has been the bibliography on the fatigue of materials, components and structures 1838–1950 compiled by J. Y. Mann and published by Pergamon Press, and the tests referred to are not listed there.

QUESTION—*R. B. Douglas*
(Department of Transport)

The authors have described "safety-by-inspection" as not having been accepted by airworthiness authorities. Could they please explain how this differs from "fail safe based on partial failure of non-redundant structures" which is accepted by some airworthiness authorities?

Author's Reply

The fail-safe concept envisages a redundant structure capable of experiencing a relatively large fatigue crack or even failure of a component part, which could be easily found during a routine inspection, while the structure still retains sufficient strength and stiffness for safe operation. As far as the authors are aware this requirement is still applicable, and furthermore, when such a crack is detected in a fail safe structure it may be either repaired or retired.

However, "safety-by-inspection" is being used to extend the service life of cracked non-redundant structures by monitoring the growth of extremely small cracks, e.g. less than 1 mm long. The detection of such small cracks in structures which are not easily inspected requires the use of very costly and time consuming inspection procedures.

These inspections are made at intervals derived from calculations based on a thorough knowledge of the crack propagation characteristics of the critical area. Currently at ARL structural reliability theory is applied to the calculation of these intervals.

This approach has been used only in those situations where life of type cannot be obtained by other proven means.

QUESTION—*Air Vice Marshal R. Noble*
(Department of Defence—Controller Service Labs. and Trials)

(1) Are there trends towards standardisation of flight load spectra throughout the world?
(2) Is there a trend to wider use of fatigue monitoring recorders and techniques in individual aircraft?

Author's Reply

Standard fatigue loading proposals were made in 1973[1] when it was considered desirable to test transport type aircraft using a common loading sequence.

In May 1975 proposals for a Fighter Aircraft Loading Standard for Fatigue (FALSTAFF)[2] based on the operation of four different aircraft types flown by European air forces were presented for examination by the member countries of the International Committee on Aeronautical Fatigue (ICAF).

Although there is considerable merit in using a standard loading spectrum, there is still some uncertainty in effecting the transformation from test life into flying life for the particular service load spectrum. Hence, airworthiness authorities are still inclined to require a test loading which closely represents the conditions for the structure under consideration.

Peacetime economies dictate that aircraft are operated to the maximum possible service life. Fatigue lives estimated on the basis of average operating conditions are of necessity conservative. Furthermore, data collected from various countries has shown quite a range in the severity of loads experienced by different aircraft of the one type both during flight and on the ground.

Hence, there is an increasing use of fatigue monitoring equipment and many fleets carry recorders in every aircraft.

The wider range of operating conditions for some aircraft, such as variable swept wing types has led to the introduction of multi-channel recorders which obtain data on a number of operational parameters and these are being fitted to a significant percentage of the fleet.

References

1. de Jonge, J. B., Schutz, D., Lowak, H., and Schijve, J. — A Standardised Load Sequence for Flight Simulation Tests on Transport Aircraft Wing Structures. LBF-Bericht FB-106/NLR, TR 73029U, March 1973.
2. — Description of a Fighter Aircraft Loading Standard for Fatigue Evaluation. ICAF Document No. 839, March 1976.

STRUCTURAL LIFE PREDICTION

CURRENT DEVELOPMENTS IN THE LIFE OF AIRCRAFT STRUCTURES

by

A. O. PAYNE

SUMMARY

Current procedures for fatigue design and fatigue life estimation, substantiation and monitoring of aircraft structures are reviewed. Major gaps in the present state of knowledge are identified and further research directed towards filling these gaps is discussed.

It is shown that the fatigue assessment of modern aircraft structures is a very complex problem for which no general method of solution has yet been established despite the extensive research programmes being conducted on various aspects of the subject.

There is, however, a well developed trend for basic studies of the various aspects of fatigue behaviour to find increasing application and reference is made to the major fields of structural fatigue research.

1. INTRODUCTION

The fatigue of airframes became a serious problem of air safety in the 1950-1960 era; it has since received not only a great deal of attention from aircraft designers and airworthiness authorities, but it has also been the subject of extensive investigation by aeronautical research establishments throughout the world. As a result, the safety aspect has been overcome but with considerable economic and operational penalties. Because of these penalties and the continuing trend towards high performance aircraft, fatigue is one of the most important design and operational considerations for both military and civil aircraft, and there is a continuing effort to develop more refined methods of fatigue design and analysis. Despite the large amount of research there is still no final solution from the engineering point of view and none of the current fatigue design and life monitoring procedures has become universally accepted.[1]

This paper reviews the field of fatigue of aircraft structures with the objectives of:

(*a*) presenting a general picture of the state-of-the-art,

(*b*) assisting the formulation of a more unified approach to the problem,

(*c*) indicating areas where research is needed to achieve a satisfactory solution.

2. SERVICE ENVIRONMENT

Throughout its service life the aircraft structure is subjected to a complex sequence of loads ranging from very frequent fluctuating loads of small amplitude up to very large loads approaching the ultimate strength. It may also be subjected to a considerable range of temperatures and atmospheric conditions.

2.1 Loading Actions

The basic load environment consists of manoeuvres characteristic of the aircraft type and its missions and of gusts characteristic of the atmosphere and the structural response. The applied loading can be derived from a knowledge of the flight parameters and the aircraft configuration (i.e. the details of each mission) and the member loads or stresses in the structure can then be calculated.

In some aircraft the loads applied during landing, taxying and take-off are comparable in severity to the flight loads and must be considered in estimating fatigue damage.

In the design stage, representative data must be relied on but during the life the load history can be obtained from measurements within the fleet. This may be done either by sampling to estimate the average spectrum or preferably by recording in each individual member of the fleet.

2.1.1 Manoeuvre Loads

Recording programmes have been carried out, particularly on military aircraft to obtain data on manoeuvre accelerations. In the US the Vgh recorder has been extensively used and although the continuous record from this instrument presents a formidable problem of data analysis it allows the separation of manoeuvre loads from gusts loads. In the UK, Europe and Australia, the RAE fatigue meter has been widely used to record vertical acceleration and this direct reading instrument has provided a great store of data. The gust counts are established either from civil aircraft operation under corresponding conditions (where manoeuvre loads can be neglected) or by consideration of the negative loads which are nearly all due to gusts.

Representative data on manoeuvre loads are presented in military specifications,[2,3] and in the general literature.[4,5]

2.1.2 Turbulence

Investigation of flight loads at very low altitude over various types of terrain have given detailed information on low level gusts.[6,7] A spectrum of gust velocities in clear air and in

thunderstorms has been obtained for various altitudes in an extensive programme by NASA.[8]

Information on flight loads, primarily due to gusts, has been obtained on nearly all the civil airline routes of the world. As a result of these investigations much information has been obtained on atmospheric turbulence and is presented in various references.[9,10]

Unlike a manoeuvre, a gust applies a dynamic load to the aircraft and the elastic response of the structure has a major influence on the resulting load. This problem has been investigated analytically and relationships between gust velocity and the consequent aircraft response have been published. The techniques of power spectrum analysis have also been applied and while they are more complex they can help relate the random load history of the structure to a random applied load input

2.1.3 Landing Load Cycles

In transport and bomber aircraft, the load cycles applied during landing, taxying and take-off (referred to as landing load cycles) may do appreciable fatigue damage because the overhung weight of the wings, particularly with full fuel tanks, produces a bending-moment comparable with that under flight loads. This increases not only the effective amplitude of fatigue loads, but produces the tensile stresses in the upper wing surface which may lead to fatigue failures there also.

Data have been collected on landing load cycles and some load spectra are available in the literature.[2,5,11]

2.1.4 Composite Mission Analysis

In the military field, there are many different mission categories for the various aircraft types, and a Composite Mission Analysis is often the best or even the only realistic approach to adopt. This is a basic approach which identifies "mission segments" or parts of the mission for which the relevant flight parameters are substantially constant.

The characteristic environmental spectra of the mission segment given in terms of these parameters, can be applied to give the corresponding spectra for any aircraft operating in the mission segment. In this way the environmental spectra for a mission can be built up from its components or mission segments.

This comparatively recent approach has been developed by the USAF[2] and with the compilation of the appropriate data it should provide a powerful method for establishing environmental spectra.

2.2 Other Factors

As aircraft become more complex, the effects of environment begin to assume more importance. Thus the introduction of jet aircraft led to problems of sonic fatigue; supersonic aircraft introduced effects related to kinetic heating which combined with mechanical load cycles presents a potential fatigue problem. Jet engines and aerodynamic buffeting at high speed have introduced vibration problems. Development of higher strength materials has accentuated the effects of corrosion.

2.2.1 Sonic Effects

Sonic fatigue may arise where fluctuating air pressures (usually associated with jet noise or turbulent boundary layer fluctuations) cause resonant vibrations of structural panels. The stress and strain levels so induced may be sufficient to cause fatigue cracking. The input energy is commonly broad-band random, and the resulting vibration has either a single mode or a small number of modes. Therefore the structure behaves as a filter, responding only to the resonant frequency components present in the exciting noise spectrum.

2.2.2 Temperature Effects

The greatly increased speeds of modern aircraft produce heat in the boundary layer due to adiabatic compression and skin friction, and this presents potential problems. The increased temperature of the structure may cause long term deterioration of the material properties; this

can be countered by the introduction of materials with good performance at elevated temperatures such as titanium and stainless steel. Creep deformation at the higher operating temperature does not appear to be a serious problem since the sustained mean stress is not large compared to the ultimate strength. Thermal strains arising from non-uniform temperature distribution are potentially serious in relation to static strength as well as fatigue. High temperature testing of structures to meet the critical static strength condition is becoming more widely adopted, but some investigation into the effect of repeated thermal cycling is required.

2.2.3 Vibration

The flexible structures in large aircraft may have pronounced dynamic effects under gust loads and landing loads, and the resulting vibration of the structure may cause considerable fatigue damage. Extensive research is in progress on aeroelastic effects such as occur when a structure in flight is subjected to a rapidly applied gust load, but theoretical analysis is difficult until ground resonance tests are done on a prototype structure. With the continuing trend towards large aircraft in which these dynamic effects can be important, there is a need for further research in this area.

2.2.4 Corrosion

Corrosion has proved to be a serious problem in some materials such as the zinc bearing aluminium alloys and the low alloy ultra-high strength steels; it can cause a marked decrease in fatigue strength and it is a factor subject to considerable variability. The intergranular cracking characteristics of stress corrosion can be particularly serious in areas where there are in-built assembly stresses or internal stresses due to interference fit connectors.

The development of modern inspection techniques has provided some measure of safety against intergranular cracking but repair schemes are usually difficult and costly.

2.3 Further Research Needed

More accurate prediction of aircraft service loads under specified operating conditions is required particularly in the design stage before flight measurements are available. For this purpose, it is necessary to establish those parameters in the load history which affect the fatigue life of the structure. These parameters must be related to any theory for accumulation of fatigue damage discussed in the next section. However, it is relevant here since the factors significant in fatigue are the essential data to be obtained in the flight recording programme.

2.3.1 Pool of Representative Flight Data

A co-operative programme is required for the collation and pooling of data by various countries to obtain characteristic representations of operating conditions and load histories for various aircraft.

Compilation of representative load spectra is being carried out by many establishments as referred to in Section 2.1 but there is a dearth of information on asymmetric loads. The major requirement is to obtain data defining representative load histories for various aircraft types.[12]

2.3.2 Aircraft Response

Further research is required into the elastic response of aircraft structures to a random load input,[13,14] particularly as regards techniques for determining mode shapes and frequencies. Attention should also be given to the more accurate determination of the stresses induced by the elastic response of large civil and military transport aircraft to both gust loads, and landing and taxying loads.

2.3.3 Turbulence

Increasing attention is being given to the development of a model of atmospheric turbulence.[15] In addition to providing a fuller understanding of the variability of turbulence, this would meet the practical requirement of providing representative gust load spectra for various altitudes and areas of operation.

2.3.4 Taxying Loads

Research into the prediction of taxying loads from the aircraft response characteristics is required, particularly as regards the non-linear characteristics of the landing gear.[16]

2.3.5 Load Alleviation

Various proposals have been made for both gust and manoeuvre load alleviation, and this subject has great potential value in combatting the fatigue problem. The usual method of gust alleviation is to use accelerometers to sense the aircraft response, and fast acting servos to operate the appropriate control surfaces which are used to apply "direct lift control" rather than to produce changes in aircraft altitude. Proposals for manoeuvre load alleviation have been made which use symmetrical movements of the elevons or ailerons to produce an inboard movement of the centre of pressure on the wings.[17]

Research is required into the application of load alleviation and gust alleviation techniques in the fatigue design of aircraft structures.

2.3.6 The Effect of Temperature

Further work is required into the effect of temperature. There is a need for research into heat transfer by conduction and convection on fabricated structures, and the stresses arising from the resulting thermal gradients. For the present generation of supersonic aircraft which operate below Mach 3, the effect of radiation is slight. The effect of convection is also small at high altitude, except for integral fuel tanks which include a large part of the modern aircraft structure.

Research into the effect of temperature and thermal fatigue of aircraft materials should be continued, especially welded ultra-high strength steel and diffusion bonded titanium construction.

3. FATIGUE LIFE CALCULATION AND SUBSTANTIATION

From the aircraft load history, the fatigue performance is calculated in the design stage, then usually substantiated by test and continuously monitored throughout the service life. Three major design philosophies have been developed, designated safe life, fail safe and reliability based procedure.

3.1 Safe Life Procedure

In this method the average life is estimated and divided by a safety factor or scatter factor to give a safe life after which the structure or component is retired from service.

3.1.1 Fatigue Design

The fatigue performance of the design is estimated from the design stress analysis and from fatigue data relating to the design. Since in general there is no prospect of obtaining fatigue data for the particular service load history, fatigue life data under cyclic loading for various mean load alternating load combinations (the A-M diagram) is normally used. The fatigue life under the service load history is then calculated according to some appropriate cumulative damage hypothesis. An appropriate safety factor is then selected to give a safe life.

The steps in the procedure are as follows:

(i) *Identify Critical Areas*—The potentially fatigue critical areas must be identified from the design stress analysis, design drawings and possibly wooden models showing the structure in three dimensions.

(ii) *Derive Relevant Fatigue Data*—From the design analysis, establish the member or component load in terms of flight loading and hence obtain the load spectrum for this component or member. An A-M diagram relevant to the component or member is then obtained from one of the following sources—

(*a*) Data on similar structures or components of the same or similar material such as the ARL A-M Diagram for aluminium alloy structures,[18] or the data on notched materials, structural components and complete structures published in the Royal Aero. Society Data Sheets,.[19] The assumed equivalence between the particular

structure or component and that represented by the data is one major source of possible error—the estimate of the corresponding stress or load is yet another.

(*b*) Fatigue tests on individual components of the structure. The actual component is tested in this case but the fatigue performance in the structure may differ considerably from that in a testing machine due mainly to difficulties in reproducing the same loading conditions. This method is widely used in the design stage to give the relative performance of different designs.

(*c*) Fatigue data from notched specimens of appropriate K_t value. The differences in stress gradient, combined stresses and surface finish between the notched specimen and the actual component may have a considerable effect. S-N curves for different notch configurations of the same K_t value differ from each other and often differ markedly from the S-N curve of the structure.

(*d*) Basic fatigue data on the component material. Investigations have been made into the problem of defining some basic equation relating the local stresses and strains of the stress concentrator[20] such as that due to Neuber:

$$K_t = (K_\sigma \, . \, K_\epsilon)^{\frac{1}{2}}$$

where K_t is the theoretical stress concentration factor for the notch and K_σ and K_ϵ are the local stress and strain concentration factors respectively. This equation together with the stress-strain curve for the material enables the local stress and strain of the stress concentrator to be found and the corresponding life can be obtained from the S-N curve of the material.

There are a number of difficulties with this method however: the local stress–strain relationship is a function of the strain history and this is particularly so in the small plastic zone ahead of the advancing crack during the crack propagation phase; in a fabricated structure the effects of load redistribution, fretting, etc., further complicate the situation. The method is therefore still under development and would seem to be most suited to the crack initiation phase in a monobloc structure.

(iii) *Estimated Average Fatigue Life*—From the basic data in (ii) and the known load history for the part, the life to initiation of a macroscopic fatigue crack is calculated; for a safe life structure, this is taken as the life to failure. Theories for calculating the accumulation of fatigue damage have been put forward, and their accuracy investigated. For the continuous load spectrum applying to aircraft structures, none of these theories shows any advantage for general application over the simple linear cumulative damage theory.[18,21–23]

(iv) *Selection of the Scatter Factor*—The scatter factor is selected from consideration of the structure and the loading conditions. It takes account of uncertainties in the life estimate as well as the variability in fatigue performance, and is often greater in the design stage than after fatigue substantiation of the structure. Since it is based on the acceptable safety level, there is also an essential input from previous experience.

The factors contributing to the inherent variability in fatigue performance are much more complex than those governing variability in ultimate strength, and no serious attempt has been made to quantify these on theoretical grounds as yet. Present methods usually rely on reference to relevant data on similar structures.

(v) *Safe Life Estimate*—A safe life is calculated by dividing the average fatigue life by the scatter factor to obtain a safe life for each critical area. This information is used to indicate the adequacy of the fatigue design and is a basis for any fatigue life substantiation programme undertaken after the structure has been manufactured.

3.1.2 Fatigue Life Substantiation

Research on the fatigue performance of structures showed that, in a complex structure under a wide ranging load spectrum, local yielding occurs causing stress redistribution and changing material properties in the region of fatigue nuclei.[18] In a fabricated structure this process is even further complicated by progressive "working" of the connectors causing galling and fretting and progressive load redistribution between members. Mainly because of these factors, the identification of critical areas is extremely difficult and there are many well-known cases where unsuspected failure areas have appeared even under the well-defined conditions of a fatigue test.

(Valiant, DC9, Boeing 727, Caravelle, F-111, etc.) These factors complicate identification of critical areas discussed in (i) of Section 3.1.1, the derivation of adequate fatigue data in (ii) and the problem of calculating fatigue damage as described in (iii). These difficulties are all overcome by a well-designed full-scale fatigue test which is now widely adopted, and is virtually mandatory under US and UK military specifications,[2,3] to confirm the investigations under (i), (ii) and (iii) above. The final selection of the scatter factor is then made to give a safe life for the various critical areas that have been established by the test.

3.2 Fail Safe Procedure

This procedure is applied to structures in which fatigue cracks or component failures can be found before the strength falls to an unacceptable level. It basically consists in establishing an adequate inspection procedure and demonstrating that a specified residual strength of the cracked structure is maintained between inspections. The only relevant military specification at present is Av.P 970[3] which essentially specifies that the inspection period shall be one third of the interval between the life at which a crack can be detected with certainty and the life at which the residual static strength has been reduced to 80% of the ultimate design load, as determined in a full-scale fatigue test.

3.2.1 Fatigue Design

At the design stage in addition to predicting the initial life, a crack propagation curve and a residual strength calculation are required.

The major steps are:

(i) Prediction of life to initial cracking (as in Section 3.1).

(ii) Calculation of the crack propagation curve. Comparison with previous designs provides valuable information. Semi-empirical methods have been proposed using relevant data in conjunction with stress analysis by matrix methods. An approach has been developed recently to predict the crack propagation from the basic crack growth properties of simple specimens of the same material using a stress intensity approach. In a monobloc structure where the effects of fretting and load redistribution are absent, this method has some prospect of success. The conditions in the small plastic zone ahead of the crack in the structure can be expected to be comparable with the corresponding conditions in a simple specimen. However, factors such as differences in stress gradient, and the effect of triaxial stress components have a major influence and attempts to allow for the geometry of the part and shape of the crack front have not been successful. A study of the crack propagation process may provide an insight into this problem

(iii) Calculation of residual strength in the cracked condition. Stress analysis by matrix methods in conjunction with other representative data can be used in the design stage.

3.2.2 Fail Safe Substantiation

The difficulties in Section 3.1 apply in this case with the additional complication of the requirement to establish reliable inspection procedures, and determine the crack propagation rate and residual strength of the structure throughout the inspection interval.

It is essential to the fail safe approach that *all* potentially fatigue critical areas are identified and inspected. The full scale fatigue test has now come to be universally accepted in the military and civil transport field to identify critical areas and establish reliable inspection procedures. The residual strength requirement and the crack propagation rate are then substantiated.

The role of the full-scale fatigue test in the fail safe philosophy is aptly described by Maxwell —"the full-scale test is as important for fail safe structures as for the safe life type although the emphasis is different".

An important advantage claimed for the fail safe procedure is that any evidence of corrosion in the critical areas is likely to be detected during the inspection.

3.3 Reliability Based Procedure

As a fatigue crack progresses through the structure, the static strength of the structure decreases and there is an increasing risk of failure under the applied service loads. If the risk of

failure is calculated as a function of life, the inspection intervals to limit the risk to a specified value can be evaluated.[24] This is a quantitative approach, but it requires extensive data especially on crack propagation, residual strength and on the probability of crack detection.

3.3.1 Fatigue Design

Because of the difficulty in obtaining basic data the probabilistic approach is at present only used in a comparative way in the design stage to assist in studying the influence of various design parameters. It is finding most application in the fatigue life substantiation and monitoring stage.

3.3.2 Reliability Based Substantiation

The major steps in the reliability analysis approach are:

(i) determine all fatigue critical areas using full-scale fatigue test;
(ii) determine initial life and mean crack propagation curve using full-scale fatigue test;
(iii) determine residual static strength as a function of crack length by calculation from representative data in conjunction with results from component tests and full-scale fatigue test;
(iv) development of inspection procedures and estimation of probability of detection from a full-scale fatigue test and component tests;
(v) determine variability in initial fatigue life and in crack propagation rate from representative data;
(vi) determine variability in residual static strength at various crack lengths from representative data;
(vii) determine any environmental effects, e.g. corrosion or temperature, from comparative tests on components;
(viii) carry out a reliability analysis to calculate inspection intervals to maintain a specified safety level.

3.4 Further Research Needed

There is a need to establish more uniform safety standards and improved design criteria; to further these aims, there are several important aspects requiring investigation as follows.

3.4.1 Specification of Safety Standards

The methods of specifying the safety levels and the values to be adopted are basic questions, and the long standing lack of uniformity should be overcome if possible. This would require international agreement.

3.4.2 General Approach to Fatigue Design

It is suggested that the reliability approach could be developed to incorporate into one design procedure, safe life, fail safe and reliability based inspection procedures. The application of reliability theory to the problem has been dealt with by a number of research workers. The essential requirement is to obtain the great amount of data needed and if possible develop simplifying assumptions to reduce the data requirement.

3.4.3 Adoption of Standards of Crack Detection

There have been major advances in inspection techniques but their reliability is a vital question; detection probabilities associated with different cracks should be established for each of the various inspection procedures. This is an area in which collaboration between various laboratories should be established.

3.4.4 Calculation of Fatigue Damage

There is a need for the study of the metal physics aspect of the accumulation of fatigue damage in the monobloc construction for both crack initiation and crack propagation. This could be done in conjunction with detailed stress analysis of the part using matrix methods.

Subsequently the influence of environmental effects on the crack propagation process should be investigated and quantified if possible.

4. FATIGUE LIFE MONITORING IN SERVICE

In monitoring according to safe life, fail safe or reliability based inspection procedures, the accumulation of fatigue damage is calculated from the flight load history, to enable scheduling of inspections or replacements.

4.1 Monitoring by Tail Number

In military aircraft particularly, substantial changes can occur in the load spectra for different aircraft in the fleet and this, together with the increasing requirements for extensions to the service life, has led to fatigue life monitoring by tail number, in which each aircraft is fitted with its own recording instrument.

4.2 Repetition of Fatigue Calculations

Data accumulated on the loads environment, on stress versus load relationships and on any fatigue problems observed during inspections are put into the original fatigue analysis and the calculation of safe life or inspection intervals is continually reiterated. If necessary, adjustments are made in the fatigue life monitoring procedure. This process enables uncertainties in the calculations to be progressively eliminated, and allows changes in missions to be taken into account.

4.3 Further Research Needed

4.3.1 Development of the Fatigue Gauge

A reliable fatigue sensing device, if it could be developed, would be a great advance for both safe life and fail safe structures. The most likely development would seem to be a sensor which would relate the fatigue performance in service to that in a full-scale fatigue test under a closely representative load history or would closely monitor lead the fleet aircraft. Extensive testing in a variety of situations would be essential to prove such an instrument.

4.3.2 Development of Flight Recorders

There is a real need for a reliable compact and low cost instrument recording in several channels and providing rapid data processing. Some current developments are the ARL Range Pair Counter,[25] the RAE Cycle Counter[26] and the NASA–ARDC Eight Channel Recorder.[27]

REFERENCES

1.	Payne, A. O.	The Fatigue of Aircraft Structures. JI Eng. Fracture Mechanics, Vol. 8, pp. 157-203. Pergamon Press, 1976.
2.		Airplane Strength and Rigidity, Reliability Requirements. Repeated Loads and Fatigue. MIL-A-8866. Department of Defense, Washington, D.C.
3.		Av P. 970, Vol. I, Icaflet 200.
4.	Mayer, J. P., and Hamer, H. A.	Applications of Power Spectral Analysis Methods to Manoeuvre Loads Obtained on Jet Fighter Airplanes During Service Operations. NASA TN D-902, May 1961.
5.	Taylor, J.	Manual on Aircraft Loads (chapter 5). Pergamon Press, Oxford, 1965.
6.	Saunders, K. D.	B-66 Low Level Gust Study. Technical Analysis WADD TR 60-305, Vol. I, 1961.
7.	Bullen, N. I.	Gusts at Low Altitude in North Africa. RAE Technical Note Structures 304, 1961.
8.	Tolefson, H. B.	Summary of Derived Gust Velocities Obtained from Measurements within Thunderstorms. NACA Report 1285, 1956.
9.		British Civil Airworthiness Requirements. Air Registration Board, Section D2.
10.	Hooke, F. H.	Operating Loads and Safe Life Estimation. JI I. E. Aust 36 (1-2), 1-8, 1964.
11.	Weibel, J. P.	Undercarriage Loading of Three Aircraft: Porter PC6, Venom DH-112 and Mirage 111S. ICAF Symposium, Melbourne, May 1967.
12.	van Dijk, G. M.	Introduction to a Fighter Aircraft Loading Standard for Fatigue Evaluation. "Falstaff", 8th ICAF Symposium, Lausanne, 1975.
13.	Cox, R. A.	A Comparative Study of Aircraft Gust Analysis Procedures. Aeronaut, J. Royal Aeronaut. Soc. 74, 807-813, 1970.
14.	Rider, C. K., Sparrow, J. G., and Thompson, M. R.	Fin Strains in Mirage A3-76 During Flights in Severe Turbulence. ARL Note SM407, 1974.
15.	Sherman, D. J.	The Cumulative Exceedence Distributica for Accelerations Due to Turbulence Encountered by a Mirage. ARL Tech. Memo. SM228, 1975.
16.	Hall, A. W., Hunter, P. A., and Morris, G. J.	Status on Research on Runway Roughness, Conference on NASA Aircraft Safety and Operating Problems. Vol. 1, NASA SP-270, pp. 127-142, 1971.
17.	Long, G., and Farrell, P. A.	Use of Load Alleviation to Extend the Fatigue Life of Mirage. ARL Tech. Memo. SM223, 1974.
18.	Payne, A. O.	Determination of the Fatigue Resistance of Aircraft Wings by Full-Scale Testing. ICAF Symposium, Amsterdam, 1959.
19.	Royal Aero. Society	ESDU Data Sheet E-02-01.
20.	Impellizeri, L. F.	Cumulative Damage Analysis in Structural Fatigues. ASTM STP 462, 40-68, 1970.

21. Finney, J. M., and Mann, J. Y. — Fatigue Behaviour of Notched Aluminium Alloy Specimens under Simulated Random Gust Loading with and without Ground-Air Cycle. Proc. of ICAF Symposium on Fatigue of Aircraft Structures, pp. 151-77. Pergamon Press, London, 1963.

22. O'Neill, M. J. — A Review of Some Cumulative Damage Theories. ARL Report SM326, June 1970.

23. Williams, J. K. — The Airworthiness Approach to Structural Fatigue. ICAF Symposium, Munich, June 1965.

24. Diamond, P., and Payne, A. O. — Reliability Analysis Applied to Structural Tests. Proc. of Symposium on Advanced Approaches to Fatigue Evaluation, Miami Beach, May 1971. NASA SP-309, pp. 275-332, 1972.

25. Ford, D. G., and Patterson, A. I. — A Range Pair Counter for Monitoring Fatigue. ARL Tech. Memo. SM195, January 1971.

26. Goodwillie, A. G. — A Comparison of Flight Loads Counting Methods and their Effect on Fatigue Life Estimation Using Data from Concorde. ARC Current Paper CP1304, 1974.

27. Taylor, J. P. — Structural Integrity Program for High Performance Aircraft. Proc. Symposium Fatigue of Aircraft Structures. WADC, 1959.

APPENDIX

Development of Reliability Approach to Fatigue of Aircraft Structures at ARL

by

A. D. GRAHAM, J. M. GRANDAGE and A. O. PAYNE

Research has been carried out at ARL for some years[1-6] which has led to developments in the fatigue life substantiation and monitoring of aircraft structures.

The evaluation of the risk function using data from a full-scale fatigue test on the structure in conjunction with representative data from other sources has enabled a reliability based safety-by-inspection procedure to be developed.[3,4]

This led to the proposal suggested in Section 3.4.2 for a more general approach to the fatigue safety of aircraft structures which includes both the fail safe and safe life approaches.[3,5]

The method has been applied to provide a quantitative basis for establishing inspection intervals for some aircraft fleets in service with the RAAF so as to extend their safe operating life.[7] The computer program for calculation of inspection intervals to ensure a specified safety level has been transferred to the RAAF to operate on the CYBER 76 computer in Canberra.

At the request of the Department of Transport (DOT), ARL is investigating the application of these techniques to the problem of aircraft such as the Fokker F-27 and the Boeing 707 and 727 which are reaching very long service lives in the neighbourhood of the life they have been tested to in the full-scale fatigue test.

Following this it was decided to hold a Symposium on structural reliability in Melbourne under the auspices of DOT and ARL to consider all aspects of this important problem. There were a total of 48 attendees including five senior representatives from the Boeing company and leading engineers from the RAN, RAAF, ANA, QANTAS, TAA, Singapore Airlines and National Airways of New Zealand.

The Boeing Co. "95/95 Concept"[8] for fatigue life monitoring of large fleets of civil transport aircraft was presented and compared with the reliability based approach.[9] The proceedings of the Conference are reviewed in Reference 10.

As stated in Reference 3 the ARL procedure involves an extensive body of data and a number of assumptions which warrant some development and testing of the procedure in practice.

In a move to set up a data bank ARL has proposed within the Technical Co-operation Programme a reliability questionnaire which would draw information from aeronautical establishments within the member countries (UK, USA, Canada, Australia, New Zealand). A pilot survey of the replies to a questionnaire has been carried out[11] to investigate the problem of processing and storing consolidated data from various sources.

A research programme is also current to investigate the significance of the major assumptions involved in the ARL reliability based safety-by-inspection procedure.

This is described below by reference to the derivation of the risk function and consideration of assumptions involved.

The ARL Reliability Approach developed in References 4 and 7 considers a structure in service subjected to repeatedly applied loads S from the service load spectrum $F_x(S)$. There will be a period during which the process leads to the formation of a macroscopic crack at a fatigue critical area. This is called the life to initial failure N_i and it marks the beginning of the wear-out process in the structure. As the life continues the fatigue crack extends with a progressive reduction in residual strength as shown in Figure 1.

During this period there is an increasing probability at each successive application of a service load, that the structure will fail statically and this type of failure is termed here "static fracture by fatigue". However, if the structure continues to survive this risk the crack will eventually reach, at a life N_F, some length l_0 at which it will collapse under the steady mean load and this is defined as "fatigue fracture".

Assumptions:

(*a*) Static and fatigue strength are independent.

(*b*) The fatigue life N_l at any crack length l has a logarithmic normal distribution $p_z(z)$ with variance independent of l.

It then follows that for any structure the life N_l bears a constant ratio z to the median life $\tilde{N}_l$ at the same crack length l.

$$N_l = z \cdot \tilde{N}_l$$

(*c*) The median crack propagation curve is known.

$$l = g(\tilde{N}_l)$$

(*d*) The residual strength $R(l)$ expressed as a ratio of the mean value $\mu_R(l)$ by the variate $x(l) = R(l)/\mu_R(l)$ has a characteristic distribution $p(x)$ for all values of l.

(*e*) The mean strength $\mu_R(l)$ is a known function of the crack length l.

$\mu_R(l) = \mu_0 \cdot \Phi(l)$, where μ_0 = mean strength uncracked.

(*f*) For the small probabilities of failure considered the effect of losses from the population on the probability distribution of residual static strength (x) and fatigue life (z) can be neglected.

Derivation of the Risk Function

It follows[3,4] from the assumptions that:

$$r_s(N_s) = \int_{l=0}^{l=l_a} \int_{x=0}^{x=\infty} F_s[x \cdot \mu_0 \cdot \Phi(l)] \cdot p_z(x) \cdot p_l(l) \cdot dx \cdot dl \tag{A1}$$

$$r_s(N_s) = \int_{z=\frac{N_s}{\tilde{N}_a}}^{z=\frac{N_s}{\tilde{N}_F}} \int_{x=0}^{x=\infty} F_s(x \cdot \mu_0 \cdot \Phi[g(N_s/z)]) \cdot p_x(x) \cdot p_z(z) \cdot dx \cdot dz \tag{A2}$$

and

$$r_F(N_s) = 1/\tilde{N}_F \cdot p_z(N_s/\tilde{N}_F) \tag{A3}$$

and the total risk of fatigue failure at N_s,

$$r_{FT}(N_s) = r_s(N_s) + r_F(N_s) \tag{A4}$$

and the probability of survival

$$L_{FT}(N_s) = e^{-\int_0^{N_s} r_{FT}(N) \cdot dN} \tag{A5}$$

where $r_s(N_s)$ and $r_F(N_s)$ are the risk of static fracture due to fatigue and the risk of fatigue fracture respectively at any service life N_s.

The importance of some of the major assumptions is being investigated by studying the influence of the following factors using static and fatigue strength data applicable to an actual structure:

(i) *Variance of Fatigue Life at Different Crack Lengths* (related to Assumption (*b*))

The major assumption in (*b*) that the variance in fatigue life is constant is investigated by studying the effect on the risk when a linear variation in variance of log life between initial and final life is assumed.

$$\sigma_l = b - a \log \tilde{N}_l$$

By a suitable choice of a and b this case can be made to approximate any prescribed relationship of the crack propagation curves taking

$$\log \tilde{N}_l - \log N_l = u \cdot \sigma_l = u(b - a \log \tilde{N}_l) \tag{A6}$$

where u is the standardised normal deviate $u \sim N(0, 1)$

$$u = \frac{1}{\sigma_l} \log \frac{\tilde{N}_l}{N_l} \tag{A7}$$

$$\tilde{N}_l = \text{antilog}\left[\frac{u\,b + \log N_l}{u\,a + 1}\right] \tag{A8}$$

Transforming in equation (A1) from the variate l to the variate u with

$$u_1 = \frac{\log \dfrac{\tilde{N}_l}{\tilde{N}_s}}{b - a \log \tilde{N}_l} \quad \text{at } l = 0$$

and

$$U_2 = \frac{\log \frac{\tilde{N}_F}{\tilde{N}_s}}{b - a \log \tilde{N}_F} \quad \text{at } l = l_0$$

$$r_s(N_s) = \int_{x=0}^{x=\infty} \int_{U_1}^{U_2} F_x\left(x, \mu_0, \Phi\left(g\left(\text{antilog}\left[\frac{ub - \log N_s}{ua - 1}\right]\right)\right)\right) \cdot p(u) \cdot p(x) \cdot du \cdot dx \qquad \text{(A9)}$$

(ii) *Form of the Distribution of Fatigue Life* (related to Assumption (*b*))

The assumption that the distribution of fatigue life is log normal is investigated by comparing the corresponding risk functions with those calculated from the Weibull distribution

$$P(N_l) = \exp\left[-\left(\frac{N_l - \epsilon_l}{V_l - \epsilon_l}\right)^k\right] \qquad \text{(A10)}$$

The Weibull distribution is applied using the assumption

$$\epsilon_l / V_l = \text{Constant } C_\epsilon \text{ for all } l.$$

Then

$$P(N_l) = \exp\left[-\left(\frac{N_l/V_l - C_\epsilon}{1 - C_\epsilon}\right)^k\right]$$

and it follows that N_l/V_l is constant for constant P at all crack lengths l. In particular for the median structure taking $V_l/\tilde{N}_l = C_\mu$.

Then

$$\epsilon_l/\tilde{N}_l = C_\epsilon \cdot C_\mu = \epsilon_\mu$$

and with

$$z = N_l/\tilde{N}_l$$

$$P(N_l) = \exp\left[-\left(\frac{N_l/\tilde{N}_l - \epsilon_l/\tilde{N}_l}{V_l/\tilde{N}_l - \epsilon_l/\tilde{N}_l}\right)^k\right]$$

$$= \exp\left[-\left(\frac{z - \epsilon_\mu}{C_\mu - \epsilon_\mu}\right)^k\right] \qquad \text{(A11)}$$

Hence the expression for $r_s(N_s)$ in equatoin A2 for the log normal distribution may also be applied for the Weibull distribution with

$$p(z) = d(P(z))/dz$$

where

$$P(z) = \exp\left[-\left(\frac{z - \epsilon_\mu}{C_\mu - \epsilon_\mu}\right)^k\right]$$

as above.

To simplify the comparison the two parameter Weibull distribution is used taking $\epsilon_\mu = 0$, and the dispersion parameter k and characteristic value C_μ are calculated from the mean and variance of the log normal distribution of life.

(iii) *Effect of Variability in Residual Strength on* r_F (related to Assumption (*d*))

It is assumed in *A*3 that failure under the mean load will always occur at the same crack length l_0. In fact because of the variation in structural resistance $p(x)$ the crack length at static fracture will vary with x.

$$r_F(N_S) = Pr\{R = \alpha\mu_0\} \text{ where } \alpha\mu_0 = \text{mean load}$$

$$= 1/\tilde{N}_f \int_{x=a}^{x=\infty} p_z\left(\frac{N_s}{\psi^{-1}(\alpha/x)}\right) \cdot p(x) \cdot dx.$$

where

$$(\alpha/x) = \Phi[g(N_s/z)]$$

$$= \psi[N_s/z]$$

$$N_s/z = \psi^{-1}(\alpha/x)$$

This can be calculated in comparison with $r_F(N_s)$ in A3.

(iv) ***Modification of Probability Distribution of x and z by Losses from the Population*** **(related to Assumption (*f*))**

As losses in the population due to failures increase, x and z are no longer independent variates but have a joint distribution which varies with the life N_S, $p_{x,z}(x, z|N_S)$.

Considering structures in the element (dx, dz) at an initial life $N_I = z \cdot \tilde{N}_F$ at any subsequent life N_S, the probability of survival in this element is

$$\exp\left[- \int_{N_I}^{N_S} F_S(x \cdot \mu_0 \cdot \Phi(g[N \cdot z])\, dN \right]$$

Hence

$$p_{x,z}(x, z|N_S) = p_{x,z}(x, z|N_I) \exp\left[- \int_{N_I}^{N_S} F_S(x \cdot \mu_0 \cdot \Phi(g[N \cdot z])) dN \right]$$

$$= p_0(x) \cdot p_0(z) \exp\left[- \int_{N_I}^{N_S} F_S(x \cdot \mu_0 \cdot \Phi(g[N \cdot z]))\, \cdot dN \right]^*$$

where $p_0(x)$, $p_0(z)$ denote the probability distribution of x, z in the original population.

Hence to investigate the effect of losses in the population, both risk functions can be calculated using the distribution $p_{x,z}(x, z|N_S)$.

$$r_F(N_S) = 1 \cdot \tilde{N}_F \int_{x=a}^{x=\infty} p_{x,z}\left(x, \frac{N_S}{\psi^{-1}(\alpha/x)}\right) \cdot dx$$

and

$$r_S(N_S) = \int_{x=a}^{x=\infty} \int_{z=a}^{z=\infty} \sum_{N_I}^{N_S} F_S(x \cdot \mu_0 \cdot \Phi(g[N_S \cdot z])) p_{x,z}(x, z|N_S)\, dz\, dx$$

(v) *Accuracy of Numerical Integration*

The success of the ARL safety-by-inspection procedure has been largely dependent on the numerical evaluation of the multiple probability integrals.[1,2] A technique has been developed in which the functional relationships are not required in analytical form but the basic data is put directly into the computer.

The integration employs an adaptive routine using a Simpson or a Gaussian approximation according to the accuracy required and constraints on computer time, and represents an advance in the current techniques. The accuracy and performance of this procedure is being tested using integrable functions including functions with a singularity representing the sharply peaked integrands that usually occur in the reliability integrals.

A practical example of the application of the ARL safety-by-inspection procedure is shown in Figure 2. Inspection intervals are established to extend the safe life of the structure while maintaining a required safety level expressed as an acceptable risk of failure per hour.

When the risk per hour rises to the maximum allowable an inspection is carried out and the risk is then reduced to the continuous inspection value (which is the risk of failure due to undetected cracks). Thus the risk of failure will vary between the continuous inspection value and the specified maximum risk r_{max} as illustrated in Figure 2. The corresponding probability of survival is shown in Figure 3.

---

* Strictly a normalising factor should be applied to allow for the total losses in the whole population but for the small probabilities of failure considered this is a second order effect which is omitted to reduce the computation.

References

1.	Payne, A. O., and Grandage, J. M.	A Probabilistic Approach to Structural Design Paper presented at the International Conference on Application of Statistics and Probability to Soil and Structural Engineering. Hong Kong, September 1971. (Also published as ARL SM Report 337, February 1972.)
2.	Ford, D. G., and Grandage, J. M.	The Approximate Life Distribution of Cracked Structures with Random Risks. ARL Structures Tech. Note SM 363, March 1971.
3.	Payne, A. O.	A Reliability Approach to the Fatigue of Structures. ASTM STP511, 1974.
4.	Payne, A. O., and Diamond, Patricia	Reliability Analysis Applied to Structural Tests. Paper presented at ICAF Symposium, Miami Beach. May 1971. (NASA SP-309, 1972.)
5.	Hooke, F. H.	A Comparison of Reliability and Conventional Estimation of Safe Fatigue Use and Safe Inspection Intervals: Advanced Approaches to Fatigue Evaluation. ICAF, 1971. (NASA SP-309, 1972.)
6.	Hooke, F. H.	Probabilistic Design and Structural Fatigue. The Aeronautical Journal, June 1975.
7.	Grandage, J. M., and Diamond, Patricia	A Proposed Inspection Procedure for the Macchi Centre Section. ARL Note SM394, 1973.
8.	Thompson, P. A.	A Procedure for Estimating the Demonstrated Fatigue Life of Airplane Structure from Fleet Service Experience. Boeing Co. document No. D6-41246TN presented at DOT ARL Symposium, December 1975.
9.	Payne, A. O., and Grandage, J. G.	Structural Fatigue and Reliability. Presented at DOT-ARL Symposium, December 1975.
10.	Payne, A. O., and O'Brien, X. X.	Review of Symposium on Structural Reliability held at ARL, December 1975.
11.	Gratzer, L. R.	Pilot Survey of a Questionnaire for Obtaining Reliability Data. Presented to Panel H3-TTCP.
12.	Mallinson, G. D.	Note on the Numerical Evaluation of the Risk Function. ARL Structures Internal Report, 1970.
13.	Mallinson G. D., and Graham, A. D.	A Report on the Numerical Evaluation of Multiple Probability Integrals. ARL Structures Internal Report.

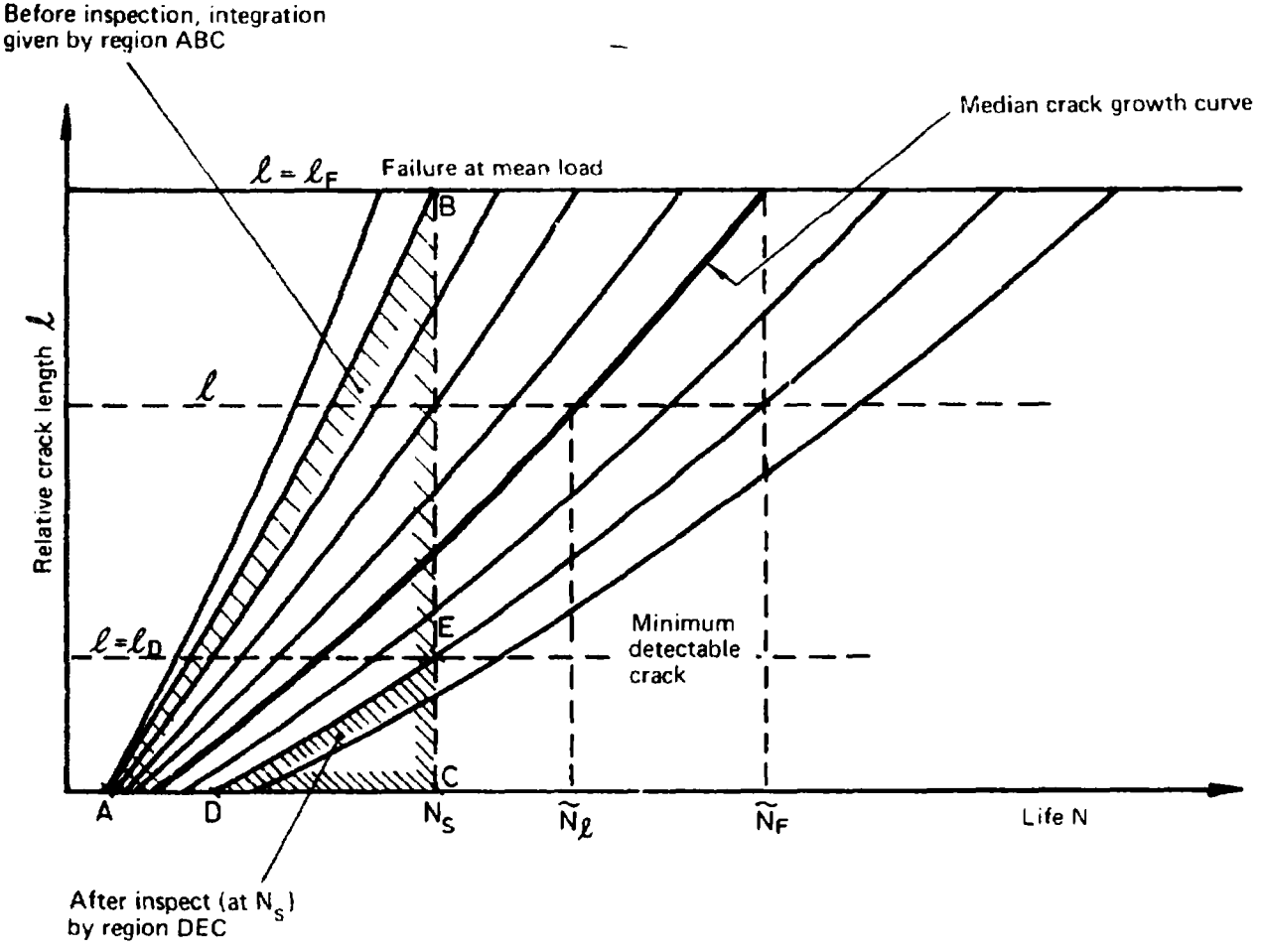

FIG. 1 MODEL OF THE FATIGUE PROCESS

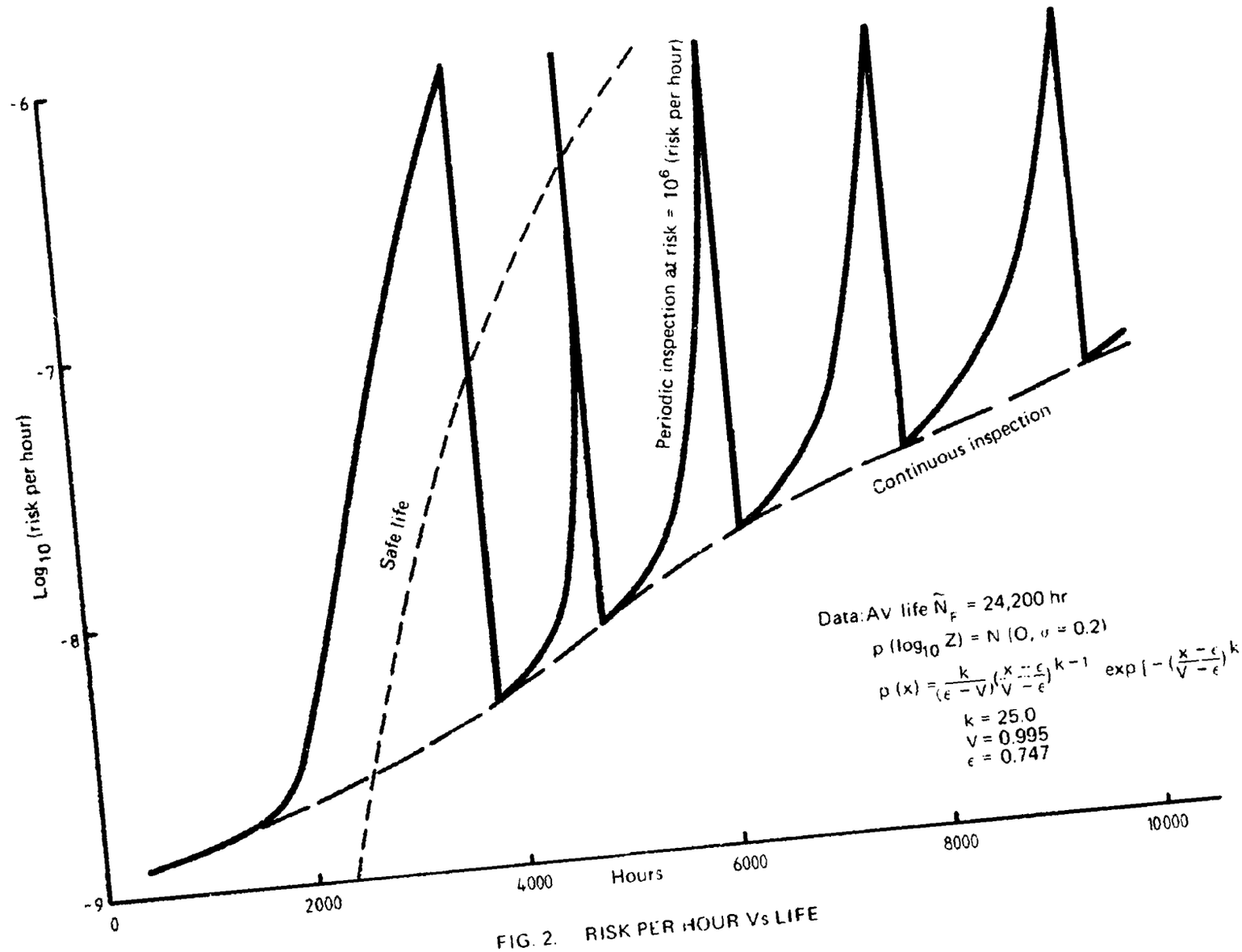

FIG. 2. RISK PER HOUR Vs LIFE

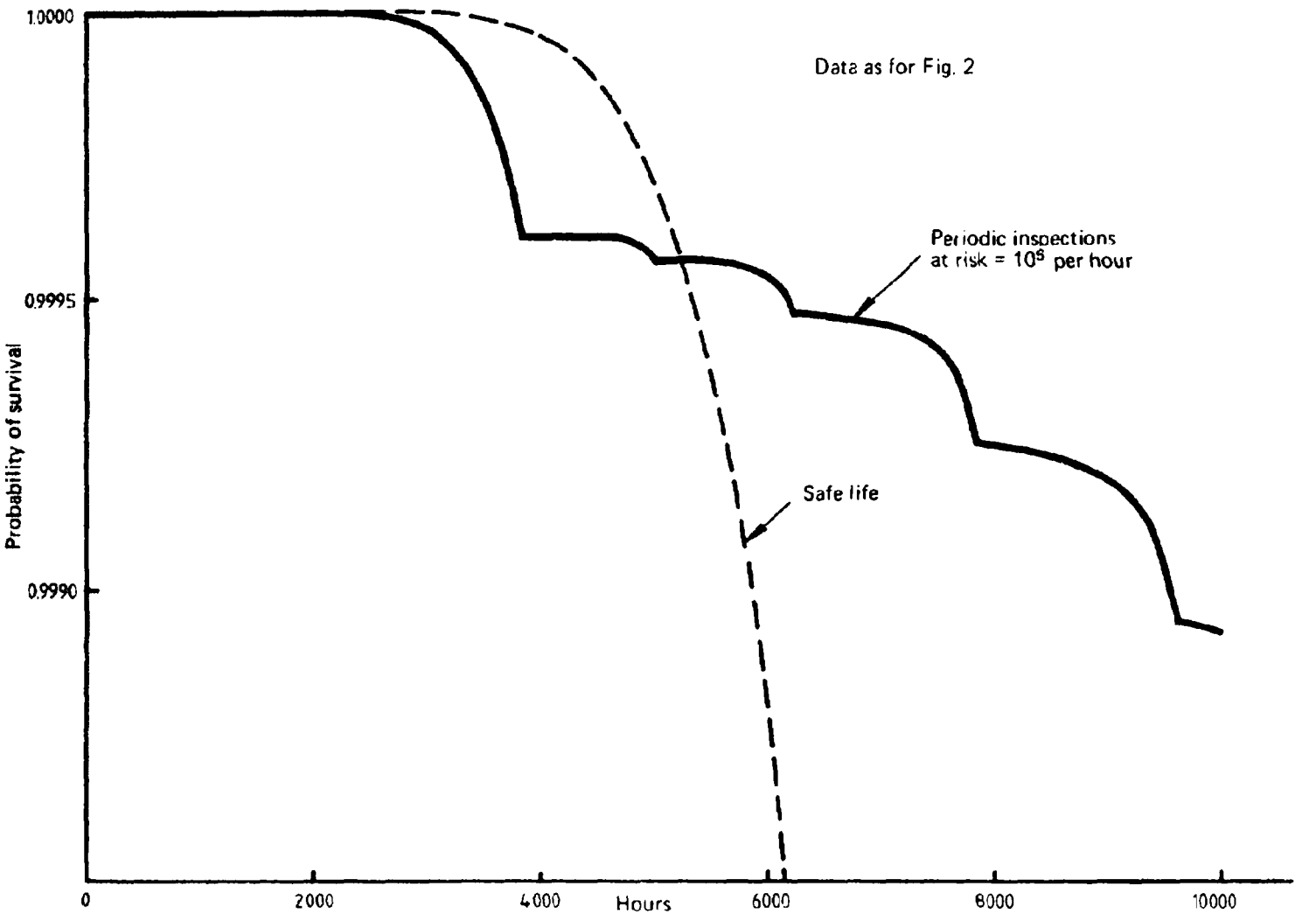

FIG. 3 PROBABILITY OF SURVIVAL Vs LIFE

DISCUSSION

QUESTION *J. Visick*
Ansett Airlines

Hooke, in his review (Tech. Memo. 253), on page 3 warns against unwittingly attributing too much reliability to the precision of the mathematics in estimating fatigue lives.

Mann agrees with this quoting life factors of between 0·1 to 10·0. It appears that in spite of these statements both speakers (Hooke and Payne) are producing more and more precise mathematics in an attempt to deal with a highly random and unpredictable subject.

In practical aircraft operating environment, fatigue testing—no matter how carefully applied —is not considered to provide meaningful data beyond about 30,000 hours flying time. This is due to the influence of other factors—corrosion, manufacturing errors (e.g. Viscount VH-RMQ), noise and small loads which are omitted from the fatigue test, etc. The only manner in which the behaviour of an aircraft fleet can be predicted is by observing the behaviour of that fleet in actual service. One procedure that has been put forward in this respect is the so-called 95/95 approach proposed by Boeing aircraft. This technique appears to have been almost totally ignored at this Symposium. Is this due to the fact that the speakers consider the technique invalid —if so what alternative do they offer for life prediction of a fleet in a real, as opposed to a laboratory, environment?

Author's Reply

Regarding Mr. Visick's comments concerning fatigue life monitoring by inspection, he and I are, in fact, in agreement on what should be done and why it should be done; we disagree on the question of how it should be done.

There is agreement as to the inaccuracies that can arise in representing the service conditions of an aircraft by a full-scale fatigue test, although I do not think there is any basis for assuming that the relevant factors such as "corrosion, manufacturing errors, noise and small loads" only become important beyond a life of 30,000 hours.

There is agreement on the difficulty in obtaining valid data and the need to develop simplifying assumptions as stated in Section 4.3.2 of my paper.

There is agreement on the advantages of using an inspection procedure for fatigue life monitoring wherever possible: in establishing the fatigue life by these procedures we both favour a quantitative approach which it is hoped employs precise mathematics.

The area of disagreement is on the fatigue life monitoring-by-inspection procedure to be adopted. At ARL we have studied various approaches to this problem including the 95/95 concept. As mentioned in the Appendix to my paper this was featured at a Joint Reliability Symposium held by ARL and the Department of Transport at which representatives of the Boeing Airplane Co. were invited to attend and they presented a detailed account of the 95/95 concept and its application to a number of their fleets.

From these investigations of the problem we have been led to develop a Reliability Approach based on data from a full-scale fatigue test which are progressively updated by the results of fleet inspections:

The advantages seen for this approach are:

(*a*) The inspection procedure (which is vital to the success of this type of approach) can be established on the test specimen under controlled conditions.

(*b*) It provides a quantitative criterion for establishing the inspection intervals based on the fundamental condition of the safety level.

(*c*) It enables a structure or part thereof, which it is not possible to inspect (such as many safe life structures) to be also embraced by the philosophy: using the reliability analysis such a structure can be operated to the prescribed safety level.

Its major disadvantage as stated in the paper is the extensive data required on the fatigue and static strength characteristics of the structure.

The particular feature of the 95/95 concept is that although the probability distribution of life is assumed as in the other approaches, the mean life is estimated with a specified degree of confidence (95% in fact) from the results of fleet inspections. It therefore has the advantage that the mean is estimated from the performance of the structure under service conditions. (An excellent feature of the Boeing policy is the complete "Tear Down Inspection" carried out on long life aircraft from a large fleet but this feature could be included in any other fatigue life monitoring-by-inspection procedure.)

The 95/95 concept has the disadvantages that:

(*a*) It is only applicable to fail safe structures—arbitrarily defined in the Airworthiness Specifications as structures that have some specified strength capability with detectable cracks present.

(*b*) There is no opportunity of developing and establishing an inspection procedure for each failure before it is found in service.

(*c*) It assumes that the whole fleet is subjected to the same service load spectrum. While this may be a reasonable assumption for some civil aircraft, it is quite untenable for many military aricraft types.

QUESTION—*F. G. Blight*
ARL

Fatigue is now recognised as a major consideration in design of aircraft. It has been suggested that there will therefore be no need for any Australian full-scale fatigue tests of imported aircraft and that the recent full-scale test on the Mirage wing will be the last of its kind. Would Dr. Payne please comment on this thesis?

Author's Reply

As Mr. Blight has pointed out aircraft designers have come to recognise the importance of fatigue and as a result, the fatigue design of aircraft structures has improved considerably and fatigue certification for a design service life, usually based on a full-scale fatigue test, is now carried out by the manufacturer.

However, I believe a requirement for fatigue substantiation by full-scale testing in this country will continue for the following reasons:

(a) As a result of the good flying conditions and the large area of the Australian continent the utilisation rate of both civil and military aircraft types tends to be much greater than in most overseas countries.

(*b*) In the military role, Australia often requires and achieves an economic life-of-type greater than that guaranteed by overseas designers.

(*c*) Operations in Australia can produce problems not encountered and not catered for by overseas designers, e.g. frequent operation from rough airfields.

Because of these factors I think there will continue to be occasions in which Australia will find it cost effective or even essential to carry out a fatigue investigation which includes a full-scale fatigue test of the structure or a major component.

QUESTION—*D. M. Turley*
MRL

I would like to follow up Mr. Blight's question concerning the possibility that the Mirage may well have been the last full-scale fatigue test to be done in Australia at ARL since these days most manufacturers are now doing their own full-scale fatigue testing. With regard to the Nomad aircraft have such full-scale tests been done in Australia or are they intended to be carried out, and if not, why not?

What is the design criteria for the Nomad—safe life,
fail safe, or
safety by inspection?

Author's Reply

GAF are carrying out a full-scale fatigue test on the Nomad wing, stub wing and wing to fuselage assembly, to certificate the aircraft in both civil and military roles. The test has been

designed to establish the fatigue performance under these two types of load history using data on flight and ground loads from an instrumented aircraft which was flown to simulate both military and civil operations. The investigation is a collaborative programme involving GAF, RAAF, DOT and ARL.

GAF have designed the Nomad on the safe life criterion.

AIRCRAFT STRUCTURAL LIFE MONITORING AND THE PROBLEM OF CORROSION

by

L. M. BLAND

SUMMARY

The principles of fatigue design, and related structural maintenance, are briefly described for two essentially different philosophies of structural fatigue life. In once case, it is assumed that no crack is present in any structural component at the beginning of service and that the components should remain crack-free throughout the service life. In the other case, it is conservatively assumed that cracks are present in all components when service begins but that these cracks, growing slowly, can be tolerated for the required service life. The relevance of the chemical and physical environment in which the structure exists is discussed for the two cases.

The role of structural service monitoring in ensuring safe and economic operation of aircraft is considered and the place of environment and corrosion monitoring in the general monitoring scheme is identified. The importance of non-destructive inspection in corrosion monitoring is also considered, with an assessment of the applicability and adequacy of various inspection methods in the monitoring task. Indications are given of the limitations of these methods and of the requirements for improved planning of the corrosion monitoring process.

1. INTRODUCTION

A primary concern in the design of the structure of high performance aircraft is the achievement of the lowest structural weight consistent with adequate static strength and endurance. Endurance, in the context where the possible effects of corrosion are disregarded, is the resistance of a structural component to crack development by the mechanical process of fatigue. This resistance, measured in terms of service time to failure, depends upon factors arising in, or effective through, the design, manufacture, service and maintenance of the structure. Failure by fatigue may be defined by either crack initiation or growth to critical size.

If the processes of manufacture, including quality control and assurance, are assumed to be prescribed in the course of design, then adequate endurance will depend upon the design being in accord with the service conditions which are experienced and the maintenance processes which are applied. Variation of the service from that assumed in the design and in the maintenance planning will change the endurance. Similarly variation of the maintenance from that required by the design, for the given service conditions, will also affect the endurance.

As part of the design process, an estimate is made of the service fatigue life on endurance which may be expected from the structure.[1,2] The initial analytical life estimate is verified or adjusted according to the results of full-scale component and airframe tests carried out subsequently. However, the assumptions made, and the data used, in the early estimates of fatigue life may not correspond to what is eventually experienced in service, at least by some of the total fleet. Where high levels of safety, and optimization of usage are to be achieved, flight tests and service monitoring programmes must also be carried out to establish more accurately the values of the parameters of service* which may affect the service life.[3] Using this information the estimate of life (both total and residual) may be continually revised, either for the existing circumstances, or to take account of a change in the mode of operation.

The possibilities of a detrimental influence of the service environment, directly or through corrosion, on fatigue performance are considered in aircraft design and maintenance planning. Preventative measures are accordingly taken, including the provision of corrosion protection systems (see Section 4.2). Notwithstanding the protection provided, however, a corrosion factor may be introduced into the fatigue life estimation process[2] to account for the detrimental effects which the chemical environment may have on fatigue crack initiation or growth.

There is always a likelihood of discrepancies between the assumptions made regarding corrosion in the fatigue design and the maintenance planning stages and the conditions and effects actually encountered during service. The resulting inadequacy of the corrosion prevention measures and/or the life factor is evidenced by the high proportion of fatigue cracks, which start at regions affected by corrosion (Fig. 1).[4,5] There is clearly a need for close monitoring of aircraft structures during service, to detect corrosion which may affect the fatigue life. Ideally, the environmental influences which are encountered in service should also be monitored. Where discrepancies are found between what was assumed in the design and what exists in actual service (and maintenance), adjustment of preventative measures should be made and the endurance re-estimated.

In this paper, the tasks of corrosion and environment monitoring are discussed, and their place in the general scheme of service monitoring of aircraft structures is considered for two essentially different philosophies of fatigue lifeing. These philosophies differ in their assumptions about the pre-service condition of the structural components and the implied criteria of failure. For one, the structural component (Type I, see Figure 2) is assumed to be crack-free at the beginning of service, and failure is considered to have occurred when a detectable crack forms.

In normal circumstances the component remains crack-free throughout its service life.[1,2] Such components are considered as damage-resistant, and no inspection for cracks during their

* Since endurance is dependent upon maintenance, as well as on design and service, there is a similar need for monitoring of the manintenance process. However, maintenance monitoring is not considered further in this paper.

service life is prescribed. However, it is specified that they shall be replaced, or their condition exhaustively reviewed, after a substantial, predetermined period of service—their safe life. For the second philosophy, the structural component (Type II, Figure 2) is conservatively assumed to be cracked at the beginning of service; the defect size, which is assumed, depends upon the effectiveness of the pre-service non-destructive inspection (NDI).[5,6] It is further assumed that the crack starts to grow immediately upon the beginning of service and it is required that a life substantially in excess of the specified service life should be achieved before the crack reaches critical size.[7] Such components are considered as damage-tolerant but periodic inspection of them, to detect developing cracks and determine their size, is prescribed; repair or replacement of the component is then undertaken as necessary.

In the following sections, the essential elements of the process of design and maintenance are described for these two philosophies of fatigue lifeing and certain basic parameters of concern in the fatigue-monitoring of aircraft structures are discussed. Special reference is made to environment and corrosion monitoring and to their place in service minitoring. The role of NDI in corrosion monitoring is also discussed and the adequacy of the available NDI methods for this task is assessed.

2. DAMAGE-RESISTANT (TYPE I) STRUCTURES

2.1 Fatigue Design and Analysis

A preliminary activity of basic importance in fatigue design is the determination of the spectrum of loads, i.e. the magnitude and frequency of load variations, to which each load-carrying structural component will be subjected during service.[8] From the load spectra, estimates are made of the sequence of maximum and minimum stresses which will occur at various locations within the various components with their nominated sectional dimensions, their individual stress-concentrating geometries and the associated critical areas.

Where an initial crack-free condition is assumed, the fatigue life of a structural component is initially estimated using Palmgren-Miner's linear cumulative damage rule.[9,10] According to this rule, fatigue damage, which culminates in the initiation of a crack is equal to the sum of n/N, expressed as $\Sigma n/N$; here n is the number of cycles experienced of a given amplitude of stress fluctuation and N is the number of cycles of that amplitude which cause failure of the given material. Component failure, which marks the completion of component life, is considered to have occurred when $\Sigma n/N = 1{\cdot}0$. Values of N (fatigue data) are obtained from fatigue tests on specimens representative of the given structural component or the critical area of the component.

A distribution of values of N is obtained in a comprehensive test programme for determining S/N data (Fig. 3*a*). In the estimation of aircraft structural life, appropriately conservative (low) values in the distribution of N are taken at each of the relevant levels of stress, S.[2]

The physical and chemical environment in which structural materials exist may affect their mechanical performance, including their endurance (Figs. 3*a* and *b*).[11,12] The spectra of variations in temperature and chemical composition of the environment should ideally be determined for each component and an estimate made of the contribution of cumulative corrosion damage to fatigue crack initiation.

Some cognisance of component temperature is taken in the fatigue analysis of sub-sonic aircraft.[5,13] However, although the chemical environment greatly influences the S/N characteristics of unprotected test specimens, it seems often to be assumed that, because of the corrosion protection systems applied to aircraft components, the environment will not have effective access to the structural material. Nevertheless, as has been noted, part of the factor of safety generally applied to the estimated life may be intended to allow for chance access of the chemical environment to the structure where a probabilistic (rather than a deterministic) approach is used in the fatigue analysis, a scatter factor corresponding to a certain percentile of the assumed statistical distribution of values of fatigue life is used (rather than a simple factor of safety) and no account is then taken of the possible influence of the corrosive environment on the fatigue behaviour.[14,15,16]

2.2 Ground and Flight Tests, and Service Monitoring

Substantiation of the design fatigue analysis (by full-scale testing) and verification of the

design assumptions (by close monitoring of actual service experience) are essential to the assurance of structural integrity.[17,18]

2.2.1 Ground (Laboratory) Tests

Full-scale static and fatigue testing in the laboratory allows verification of the stress analysis, by measurement of local strains with strain gauges. Fatigue testing of the full aircraft structure may also identify fatigue-critical areas not indicated by the stress analysis[19] and, of course, it demonstrates the fatigue life of the structure under the test conditions. Usually no attempt is made in such fatigue tests to simulate the thermal/chemical environmental spectra which might be encountered in service—notwithstanding the significant effect the environment may have on fatigue cracking. However, as for the analytical estimate of fatigue life, the factor of safety may be sufficient to account for additional variability resulting from environmental influence. Where a probabilistic scatter factor is used, no allowance is again made for the effect of the environment.

2.2.2 Flight Tests

The utilization of various recording instruments on flight test vehicles, early in the development phase of an aircraft, allows verification or more accurate establishment of the flight loads for given operating conditions[8,13] and, in some areas, direct verification of the stress analysis through the use of strain gauges. Flight testing also affords opportunity for accurate determination of the thermal spectrum of the components during operation. Generally, in these tests when Type I structures are involved, no attempt is made to collect detailed information regarding the chemical environment in which the aircraft will operate.

2.2.3 Service Monitoring

The service usage of many high performance aircraft very often differs significantly from that assumed in the fatigue design analysis, the associated maintenance planning, and in the early flight testing. Therefore, there is a general need to record, on a continuing basis, a representative sample of those actual operating conditions which affect the fatigue life of the structure.[20] In the traditional approach, these conditions are identified as those which determine the successive variations in load; the process of recording them may be described as load monitoring. The spectra of environmental influences (of a chemical kind) which the aircraft experiences in its service are generally considered to be of secondary importance, even though a high proportion of fatigue cracks in aircraft structural components initiate in areas affected by corrosion.

Using the recorded load information, the estimate of the total fatigue life may be continuously revised (life monitoring). Similarly, there may be a continuous assessment of the accumulation of fatigue damage for a group of aircraft undergoing identical service, or for individual aircraft being used in a unique way (damage or usage monitoring). The service usage of the aircraft may then be modified accordingly, and/or the maintenance schedules and procedures adjusted, so as to attain the optimum or required life. Alternatively, with unchanged operation and maintenance, the expectation of service life is changed. This process of service monitoring is usually considered to be essential for Type I structural components. Here fatigue damage is considered to comprise the cumulative effects of load variations only which result eventually in the initiation of a crack.

2.3 Service Monitoring and Corrosion (Type I Components)

2.3.1 Possible Approaches

Reference has been made to the use of a safety factor to allow for variability in fatigue life. The proportion of this factor intended, in the initial design analysis and subsequent full-scale tests, to allow for the corrosive effects of the environment is usually not defined. Thus, in the context of service monitoring, the operator and the airworthiness authority have to consider whether or not that part of the factor meant to cover the effects of corrosion on fatigue life is adequate for the environmental conditions actually encountered in service. Where it is not there will be, of course, a corresponding inaccuracy in the estimate of fatigue damage on life.

There are several possible approaches to making accurate allowance for the effects of corrosion on fatigue damage and life estimates for Type I structural components. Measurement

and recording of the physical and chemical environment spectra for nominated components could conceivably be done by a test aircraft flying representative missions and undergoing relevant experience on the ground over an adequate period, but at present considerable practical difficulties remain to be overcome. This process of measurement and recording, which might also eventually be carried out for aircraft in service, may be described as environment monitoring. However, reliable estimation of the adjustment factor, that would more accurately account for the effect of the environment on fatigue damage and life using such data, and the requisite analytical methods are beyond existing competence. There are presently no cumulative corrosion damage laws analogous to the Palmgren-Miner rule by which such recorded data might be readily utilized.[21]

On an empirical basis, if some simulation of the real environment could be made, laboratory tests on simple notched and unnotched specimens would produce S N data for comparison with similar data from tests in ordinary laboratory air. This comparison would give some indication of the adequacy of the factor being used.

Further insight into the likelihood and possible magnitude of corrosive effects detrimental to endurance could be gained by systematic compilation of information on the incidence, location, nature and extent of corrosion in the structures of the given aircraft-type during its service life. Observation and recording of the deterioration of, and damage to, the structural corrosion protection systems may also provide relevant information. The collection of such information is properly part of the maintenance process. Utilized in an appropriate way, with resort to statistical procedures, information of this kind (Fig. 4) could serve as the basis for estimating the probable effect of corrosion on fatigue performance[21] and, thus, for deciding the adequacy of the factor used to allow for this effect. However, because of the complexity of the processes of corrosion and its influence on fatigue crack initiation[22,23,24] analytical determination of this factor, even from a comprehensive data base cannot be made in the present state of understanding. An intuitive process of judgment, informed by the empirical observations -may be used to estimate the factor for both the deterministic and probabilistic approaches to fatigue damage and life estimates.

The activities of

(i) inspecting for corrosion,

(ii) recording its occurrence, and

(iii) estimating the corrosion factor to be used in damage and life calculations on the basis of these observations,

constitute the process of corrosion monitoring for Type I (and Type II -see Section 3.3) structures.

Both corrosion monitoring and environment monitoring, ideally, are essential parts of aircraft service monitoring.

2.3.2 Structural Maintenance, Inspection and Corrosion

2.3.2.1 Structural Maintenance

In the general context, structural maintenance comprises

(i) the inspection of a component (possibly after some associated disassembly),

(ii) the assessment, measurement and recording of its condition with respect to damage or incipient deterioration, and

(iii) its refurbishment,* repair or replacement as required.

Generally, the maintenance process[25] is undertaken on a precisely scheduled basis; unscheduled maintenance is sometimes required as a result of unforseen events or circumstances.

Only limited maintenance is carried out on damage-resistant structural components of aircraft, i.e. those components designed to remain in a crack-free condition for a specified service life. Where maintenance is undertaken, its purpose is

(i) to ensure that no material deterioration has taken place, or

(ii) to repair any deterioration either at the component surface or internally,

which might affect the mechanical fatigue resistance under the given loading conditions. Similar attention is given to the corrosion protection systems applied to accessible structural components.

* Refurbishment comprises cleaning and/or re-establishing of a specified surface —or other— condition. Repair comprises removal and/or re-constituting and/or replacement of affected material

Common forms of deterioration are mechanical damage, caused by accidental (abnormal) forces unrelated to the flight operation, and corrosion, resulting from chemical/electrochemical interaction of the structural material with the environment. When such deterioration is found, it is remedied by refurbishment, repair or component replacement.

Normally, with Type I structural components, no inspection for fatigue cracks is made in the course of scheduled structural maintenance.[20,26] Furthermore, structural disassembly is generally limited and many component surfaces remain inaccessible during even the most extensive scheduled servicing. However, inspection of some of these surfaces is often feasible, even without disassembly, by non-destructive methods which may then be appropriately used as part of the maintenance activity.

2.3.2.2 Inspection and Corrosion

As noted earlier, inspection during maintenance of Type I structures, may provide valuable information regarding corrosion of components during service and deterioration of corrosion protection systems. Inspection of accessible (or partly accessible) regions, particularly those suspected (through past experience or other reason) to be susceptible to corrosion, may be undertaken at various times by all operators. Ideally, the designer/manufacturer would collect all the information so obtained,[25] collate and analyse it as appropriate and then redistribute the consolidated data, together with a clear statement of its practical implications back to the operators.

The various inspections which may be undertaken as part of the corrosion monitoring process are:

(1) Systematic, scheduled inspection of all aircraft at the time of major overhauls (e.g. RAF/RAAF "E" Servicings) for evidence of corrosion and/or deterioration of corrosion protection systems, using specialised NDI methods and procedures (see Section 4.4).
(2) Systematic specially-scheduled inspection of a representative sample of aircraft, often with limited special disassembly, in areas particularly suspect because of recent experience.
(3) Limited inspection at random times, as opportunity occurs, e.g. when repair or modification work is required for reasons which may not be related to corrosion.
(4) Exhaustive, and eventually destructive, analytical inspection of aircraft specially selected from the total fleet on the basis of their particular experience and at an appropriate service life time (e.g. USAF Analytical Condition Inspection—ACI).

3. DAMAGE-TOLERANT (TYPE II) STRUCTURES

3.1 Fatigue Design and Analysis

In the fatigue design of damage-tolerant aircraft structural components, definition of the planned aircraft missions, and the associated component load and stress spectra, is of the same basic importance as for damage-resistant (crack-free) components. Similarly important are the identification of fatigue critical regions (i.e. regions of maximum stress) and, for this type of component, minimum critical crack size (in individual components).

When an initially cracked condition is assumed, the fatigue life of the component is taken as the time for the crack to grow by slow, stable propagation to critical size (Fig. 2),[27,28] whereat under a normal load, probably at the higher end of the spectrum, it would extend catastrophically through the remainder of the component section by the process of fast, unstable fracture. Such components are operated on the basis of periodic, scheduled inspection of critical regions for evidence of predicted and unpredicted crack development.

To estimate the fatigue life, it is first necessary to establish, or assume, the form, size and orientation of the crack which is considered to be present at the beginning of service. These characteristics are determined by complex interplay between

(i) the quality of the initial, stock material,
(ii) the control of the subsequent processes of fabrication, and
(iii) the sensitivity and reliability of the NDI methods (Fig. 5)[29] and procedures used on the finished component.

For a given material and component geometry, the time taken for the growth of a crack to critical size is a function of the physical and chemical environment in which the component is operating, as well as the sequence of load variations.[30,31,32] The *chemical* environment is

generally expected to have its predominant influence on the fatigue life of Type II structural components[33] by accelerating the rate of fatigue crack propagation (Fig. 6). *Physically*, however, the environment determines the critical crack size (Fig. 7), for a given material and given spectrum of service loads, through its influence on the temperature of the component. The chemical environment may also have some influence on critical crack size,[7] but, in the usual aircraft environments, this effect is probably of minor significance.

Corrosion protection systems are provided for Type II structural components, to prevent general access of the environment to the components and the occurrence of corrosion which might assist the initiation of fatigue cracks additional to those assumed to be present. However, access of the environment to the cracks considered to exist at the beginning of service is assumed.

Because of the influence which the environment, in both its physical and chemical aspects, may have on fatigue crack growth (and thus on the endurance of crack-tolerant structural components), accurate definition of the spectra of component temperatures and environment compositions is of basic importance to the adequate design and safe operation of Type II structures.[5] Currently, however, a simple definition of the expected common chemical environment, based on past general experience, together with minimum expected component temperature is all that is usually given to the designer. An example of the environmental exposure of a particular structural component, defined in this way is given in Table I. Related fatigue crack propagation rate data ($da/dn\ V\ \Delta K$, See Figure 6) are used accordingly in the crack propagation calculations.

Complex load sequence/environment interaction effects are neglected, or considered to be accommodated by a general conservatism introduced into the calculations. Component temperatures, determined largely by environment temperature in sub-sonic aircraft, are usually defined simply as minimum values conservatively chosen with regard to fracture toughness and critical crack size.

In the deterministic approach to the fatigue design of a crack-tolerant structural component, the flight time (calculated on the above basis) for the growth of the assumed crack from its initial size to the critical size for the given temperature, and under a specified high load, in the service load spectrum is the estimated fatigue life of the component. If the overall degree of conservatism in the calculations is high, this life may be taken as the appropriate safe operating period between scheduled inspections undertaken to monitor possible crack development in nominated critical regions. More usually, a period of operation equal to a half, or a quarter, of this time is taken as the inspection interval. The factor of 2, or 4, is introduced to cover uncertainties in the life estimation process. Possible unconsidered effects of the chemical environment on crack growth are of particular relevance in this respect.

In the probabilistic approach to the determination of safe inspection intervals,[34] the probability distribution of initial defect sizes, the variability of crack growth rates and the probability distribution of service loads—and of critical crack size and residual strength—are all considered. The need for inspection and, thus, the times of inspection or inspection intervals are derived from the calculated risk of failure associated with the progressive increase in size of the assumed crack and associated decrease in residual strength (i.e. the critical load for a crack of given size). Possible effects of the environment on the fatigue life or inspection interval, through enhanced crack growth and varied critical crack size (fracture toughness) or residual strength, are included but, again, only in a general and approximate way.

3.2 Ground and Flight Tests and Service Monitoring

3.2.1 Ground (Laboratory) Tests

Full-scale and static fatigue tests are made for crack-tolerant, as for crack-resistant, structures to:

(1) substantiate the design analysis,
(2) complement the analytical process of identification of fatigue-critical areas,
(3) verify the crack growth and residual strength predictive procedures, and
(4) give a more comprehensive base for maintenance planning and prescription of inspection techniques and procedures.

Simulation in the fatigue test of the full service spectra of variations of the chemical and physical environment would give a more realistic test result. However, both the exact determination of these spectra in actual service and their correspondingly precise simulation in the test

laboratory on a large scale are largely beyond existing economic technological competence. Consequently, the result of the fatigue test will inevitably be somewhat inaccurate.[5,35]

An attempt may be made to account for possible deleterious effects of the environment by applying a safety factor to the fatigue test result, on the basis of the judged unrepresentativeness of the test conditions. Some experimental indication of the appropriateness of the factor, or that part of it which relates to environmental influence, may be obtained from tests on smaller components in ordinary laboratory air and in an environment simulating, to some degree, that to be encountered in service.

3.2.2 Flight Tests

Flight loads survey, with the actual aircraft-type operating in a representative sample of realistic missions, are necessary for the verification of the component load and stress spectra assumed in the initial design of damage-tolerant structures, as for damage-resistant components. Also, the sensitivity of the fracture toughness of the structural material (and, thus, of its critical crack size and residual strength) to component temperature requires for Type II structures, accurate measurement of temperature–time profiles to be attempted in the flight test programme. Furthermore, because of the marked deleterious effect which the chemical environment may have on fatigue crack propagation in Type II structures, there is growing acknowledgement of the need for detailed assessment of that environment in the test programme.[5,28,32] However, as already noted, considerable technical difficulties remain to be overcome before environmental monitoring can be adequately carried out, even in special flight test vehicles.

3.2.3 Service Monitoring

As for Type I structural components, a difference may exist between the aircraft service assumed when designing Type II (damage-tolerant) components and the actual service experienced by production aircraft of the given type. There is therefore a similar need to closely monitor the load spectra to which Type II components are subjected in service and to confirm or adjust the estimated safe inspection interval.[36] Alternatively, the aircraft usage may be changed to give a more acceptable rate of growth for the assumed crack. Again, as for Type I structures, this process may be performed for groups of aircraft undergoing common service or they may be a continuous estimate of fatigue, i.e. crack growth, for components in individual aircraft whose service experience is unique.

The same difficulties of accurately and comprehensively monitoring the chemical environment exist for aircraft in service as for flight test aircraft. However, the larger service fleet and the longer period over which they are kept under observation affords valuable opportunity for indirect monitoring of the environment by the observation and recording of its general corrosive effects.

3.3 Service Monitoring and Corrosion (Type II Components)

The effect of chemical environment on fatigue crack propagation is more fully understood than its effect on crack initiation.[37–41] However, as has been indicated, there is still a considerable lack of understanding of the effects on crack growth of the complex interactions between the succession of variable component loads and the accompanying sequential variations in the detailed constitution of the component environment. Thus, even if an accurate record of the chemical environment of a structural component were obtained over a significant period of time, reliably accurate estimates of crack growth in that time could not presently be made by a wholly analytical procedure. (Testing of representative components in an environment simulating the measured one, however, could give useful results—see Section 3.2.1.) Resort therefore, must be made, for Type II (and Type I) structures to indications from the corrosion monitoring process in order to assess the aggressiveness of the environment and so to judging the appropriate factor for use in calculating safe inspection intervals for Type II components (see Section 3.1).

The processes of observation, recording, and assessment of corrosion in the course of scheduled structural inspections, and upon other opportunities, thus have a twofold purpose in the case of Type II structures (as for Type I). On the one hand, the need for refurbishment or repair is established and, on the other, an indication is given of the appropriateness of the factor used in the calculation of the intervals at which scheduled inspections are made (for evidence of excessive crack growth).

Specification of the areas to be inspected in the corrosion monitoring of Type II structures (100% inspection not being feasible), and the formulation of the methods of inspection are functions of the maintenance planning process as for Type I structures.

Concern with deterioration of the corrosion protection systems in the inspection of Type II structures, in so far as it might affect fatigue performance, is related to the initiation of fatigue cracks, during service, additional to those assumed to exist when service began. As noted in Section 3.1, the protective systems are assumed to be ineffective in preventing the chemical environment gaining access to the pre-existing cracks.

4. INSPECTION FOR CORROSION IN SERVICE MONITORING OF TYPE I AND TYPE II STRUCTURES (CORROSION MONITORING)

The inspection of structural components for evidence of corrosion; the determination of the nature, extent, prevalence and precise locations of such corrosion as may exist; and the recording and statistical assessment of the relevant data (i.e. the process of corrosion monitoring), in the present state-of-the-art, have been identified as an essential part of the service monitoring of both Type I and Type II aircraft structural components. Inspection and assessment of the corrosion protection systems used for both types of components form part of the fatigue oriented corrosion monitoring process only for Type I structures, where crack initiation denotes failure.

4.1 Relevant Characteristics of Corrosion

Corrosion[42] is a surface phenomenon in which the chemical composition of a material is changed by chemical/electrochemical interaction and combination with one or more elements of its environment. Physical effects of this process of relevance to the endurance of aircraft structural components[42,43,44] are (Fig. 8):

(1) *One-Dimensional, Local Irregularity*

—Local pitting (pitting corrosion, crevice corrosion)

This effect predisposes the material to the initiation of cracks by the stress-dependent processes of fatigue and stress-corrosion cracking.

(2) *Two-Dimensional Discontinuity*

—General surface roughening (uniform corrosion, filiform corrosion, fretting corrosion)

—Intergranular and transgranular cracking (corrosion cracking, stress-corrosion cracking)

Surface roughening also predisposes the material to the initiation of cracks by fatigue (and stress-corrosion cracking).

Cracking of the listed kinds, which in severe form may in itself cause a significant reduction in component strength, constitutes a nucleus for crack growth by fatigue and thus comprises, in effect, the initiation of a fatigue crack.

(3) *Three-Dimensional Bulk Reduction*

—Larger scale transformation of metallic material (galvanic corrosion, exfoliation corrosion)

Extensive reduction in bulk of the material comprising a structural component, with associated decrease in material cross-section and consequent decrease in stiffness and strength. (Corresponding increase in stress, for given load and in strain.)

4.2 Corrosion Protection Systems and Corrosion Monitoring

Measures taken by aircraft designers and manufacturers to prevent corrosion include the selection of material of low susceptibility[44] in the given environment; avoidance of detrimental galvanic combinations of material; and the avoidance of structural geometries conducive to the entrapment and retainment of fluids. Generally, however, the application of appropriate corrosion protection systems and procedures to the structural materials is of principal importance. All of these measures, and particularly the last, are of relevance to the purposeful planning and execution of the corrosion monitoring process.

Corrosion protection—the prevention of the interaction of a reactive environment with a sensitive structural material—is achieved in aircraft, where water is of primary importance, by (see also Figure 9)

(1) Exclusion of moisture by physical barriers, i.e. surface films (inorganic and organic),

electrodeposited coatings, chemically reacted coatings, jointing compounds, sealing compounds, anti-fretting compounds, water-displacing compounds, etc.

(2) Preferential electrochemical (anodic) sacrifice of electrodeposited metallic films.

(3) Chemical passivation of surface layers of the base metal and chemical inhibition of the corrosion process through the presence of coatings of inhibitor.

Gradual deterioration of corrosion protection systems occurs with time, under the effects of the physical and chemical environment and of the normal stresses and strains of service. Accidental mechanical and other, damage may also be a cause of deterioration. These processes, together with inherent deficiencies and inadequacies in the protection systems corresponding to the current state-of-the-art, may lead to at least the beginning of corrosion. In many instances onset of corrosion is accompanied, and thus marked, by an acceleration or concentration of the processes of deterioration of the protection system. The detection and assessment of such effects, during scheduled, or unscheduled inspection or those carried out on an opportunity basis, is part of the corrosion monitoring process. As already discussed, awareness of this kind allows a more appropriate adjustment, to account for possible environmental influence, to be made to the expected life for which a Type I component can be operated in the uncracked condition.

The detection and assessment of evidence of corrosion protection system deterioration or inadequacy is part also of the corrosion control process. Maintenance of the integrity and adequacy of the protective coatings, films, etc., which are used to separate the susceptible structural material from the corrosive environment, or to otherwise prevent or inhibit corrosive reaction, is achieved by frequent inspection and assessment supplemented by washing, cleaning, restoration and refinishing. These activities, and the inspection for, and removal of, any corrosion which might have occurred, followed by repair (reinforcing) of the structural material and restoration, perhaps with modification, of the protection systems is usually all that can be done to prevent or minimize corrosion of the structure of an aircraft after it enters service. For a given aircraft (i.e. one for which the materials of construction have been selected, the structural components designed and the corrosion protection systems specified), the above procedure comprises the essential process of corrosion control. It, in turn, is part of the general maintenance process. This subject is not discussed further in this paper.

4.3 Inspection, and the Accessibility of Surfaces

Because corrosion is a surface phenomenon, its detection and assessment is most readily and accurately carried out when the inspector has direct access to the surfaces of the component. Similarly, because corrosion protection systems are applied to the surfaces of concern, their inspection is greatly influenced by the accessibility of the component surfaces.[46]

Potentially, corrosion may occur at any surface and the surfaces of the components of aircraft structures have various degrees of accessibility. The accessibility of a given surface thus largely determines the particular corrosion monitoring procedures which are followed. Four classes of surface accessibility may be identified (Table 2) with respect to the *in situ* inspection of structural components, viz:

(1) *Direct Access* which allows the inspector to examine the surface visually at close range, to bring to the surface various inspection devices and materials, and to conduct at the surface a variety of non-destructive inspection procedures.

(2) *Indirect Access, Class I* where inspection of the surface of interest can be made only through the medium of the component material itself. Visual examination is not possible and only a limited number of other NDI methods are applicable, with larger component section thickness further limiting that number.

(3) *Indirect Access, Class II*, where the inspection must be carried out through the medium of one intermediate material, which is solid but may or may not be metallic.

(4) *Indirect Access, Class III*, where the inspection must be carried out through the media of two or more intermediate materials, one or more of which may not be metallic and may even be gaseous (air). In the latter case, applicable inspection methods are severely limited.

Direct Access and Indirect Access, Classes I and II may be achieved via specially-provided access hatches for components which otherwise would be of Indirect Class III. Limited Direct Access may also be available through fortuitously positioned openings of restricted size.

Where there is only indirect access, of one class or another, accurate identification of the kind of corrosion which has occurred, and assessment of the extent and degree of damage, often initially requires some destructive disassembly and examination for at least one structural unit. On the basis of this investigation, the fleet maintenance procedures for corrosion damage detection, removal or repair and protection system restoration are established. Subsequent fleet inspection is done with minimum disassembly and destruction. Repair, restoration, and replacement generally require, however, more extensive disassembly; sometimes, destruction (and hence repair or replacement) of undamaged structural sections adjacent to the corrosion-damaged region is necessary.

4.4 Inspection Methods used in Corrosion Monitoring

Corrosion monitoring has been defined as the process of component inspection conducted to detect, identify and assess corrosion of the structural material and/or deterioration of corrosion protection systems applied to such material. More specifically, the immediate purposes of the monitoring inspection may be stated as:

(1) Detection of any surface-connected inhomogeneity or discontinuity, and/or surface irregularity of significant dimension.
(2) Identification of the inhomogeneity, discontinuity or irregularity as corrosion of a particular form and/or as the effects of deterioration of the corrosion protection system.
(3) Assessment of the degree (the extent and severity) of the corrosion damage and/or protection system deterioration.

The non-destructive inspection methods appropriate to these tasks are determined by the accessibility of the surfaces of interest and by the nature of the information required.

A classification of surfaces on the basis of accessibility for inspection has been given in Section 4.3 and Table 2. NDT methods commonly used in corrosion monitoring of aircraft structures, or which presently seem to be of significant promise[48-50] are:

(1) *Visual Examination*—Direct
Replica
(2) *Radiography*—X-ray
Gamma-ray
Neutron
(3) *Penetrants*—Liquid
Radioactive gas
(4) *Magnetic Particle*—Conventional
Magnetic rubber
(5) *Ultrasonics*
(6) *Eddy Currents*
(7) *Thermography*—Non-contact
(8) *Acoustic Emission*

Table 2 lists the applicability of these NDI methods for the given classifications of accessibility of component surfaces of interest in aircraft structural corrosion monitoring. More than one inspection method is applicable to each class of surface, but not all methods can be used in each case. For example, magnetic particle inspection is applicable, of course, only to magnetic materials; moreover, its use is limited to the detection, and assessment, of corrosion damage in the form of cracking. Table 2 also lists the judged adequacy, in the present state of development, of the non-destructive inspection methods nominated for each of the surface classifications with asspect to the detection of corrosion, its identification, the assessment of its severity and the resessment of its prevalence. The performance of an NDI method, may be affected by numerous factors, some of random influence; comments on these are included in the table. However, generally, the capabilities of the operator, which depend largely upon his experience, understanding and diligence, are considered to be most important.

5. DISCUSSION AND CONCLUSIONS

Corrosion monitoring is one of several distinctive monitoring processes which may be identified in the general area of the service monitoring of aircraft structures.

These processes are: Flight Load Monitoring
Fatigue Life Monitoring
Fatigue Damage or Usage Monitoring
Environment Monitoring
Corrosion Monitoring
Maintenance Monitoring

Ideally, in estimating the fatigue life of aircraft structural components or the fatigue damage they may have incurred, exhaustive reference should be made to the full record of environmental conditions experienced in service. However, as has been stated, neither the means for economic and precise acquisition of the basic information nor its subsequent analytical treatment are yet available. Similarly, determination of the fatigue life by a programme of laboratory testing suffers from the same lack of relevant basic information; even if it were available, the very considerable cost in achieving an accurate simulation of the environment may limit its application.

Corrosion monitoring - that is, the detection, identification and assessment of the corrosion (and deterioration of the corrosion protection systems) which occurs in an aircraft structure -- has a twofold purpose, one part of which, in the present circumstances, is directly relevant to the estimation of fatigue life or damage. It is undertaken mainly, however, to reveal where and how action should be taken to prevent further corrosion. In this way, corrosion monitoring contributes to the process of corrosion control. At the same time, it may provide a data base (in the form of statistical records of the incidence, nature and extent of corrosive effects, and of corrosion protection system deterioration), from which an intuitive assessment of the aggressiveness of the environment to the given materials and its probable influence on fatigue crack initiation and growth may be derived. Using this assessment, an adjustment may be made, where necessary, to the estimate of fatigue damage accumulated in a given period of service, or of the expected safe life of a component, or of the period of service which may be safely performed between inspections. In both these ways, corrosion monitoring contributes to the maintenance of the airworthiness of the structure and to the optimization of its usage.

Clearly, adequate monitoring of aircraft structural corrosion is highly dependent upon effective inspection methods and procedures. The planning and execution of a satisfactory corrosion inspection programme, however, may be a difficult and costly task. Aircraft structures are generally complex, and the surfaces at which corrosion may occur are often highly inaccessible. Furthermore, corrosion often occurs at unexpected locations, usually as the result of some factor not considered in the design or in the maintenance planning. Accidental damage to a corrosion protection system during assembly of the structure is a common, random, causal event.

Presently, the achievement of satisfactorily effective, and acceptably economic, monitoring of the corrosion of aircraft structures depends largely upon improvement of NDI capabilities. In this respect, for example, the potential of the acoustic emission inspection method appears to be very high.[51] There is also an important need for imaginative development, in the context of maintenance planning, of general programmes and procedures of corrosion monitoring through and in which the inspection techniques are applied. There appears to be a particular need in this connection for a greater cognisance of the numerous and various factors which determine the effectiveness of the environment in causing corrosion of structural components. Of special sigficance in this regard are the inherent inadequacies, the instability and the vulnerability of the measures taken by the designer/constructor to protect the structure from corrosive processes, and the influence which the fabrication and assembly processes may have on their eventual effectiveness.

REFERENCES

1.	Advanced Approaches to Fatigue Evaluation. NASA SP-309 (Proc. Sixth ICAF Symposium). Washington, DC, 1971.
2. Stone, M.	Fatigue and Fail-Safe Design of a New Jet Transport Airplane. Proc. Fourth ICAF Symposium, pp. 1-66, Pergamon Press, London, 1969.
3. Howard, P. J., Patching, C. A., and Payne, A. O.	Life Estimation by Parametric Analysis. Proc. Eighth ICAF Symposium, Pre-print, 1975.
4. Cohen, B.	Corrosion Fatigue in the Aerospace Industry. Proc. NACE International Conference on Corrosion Fatigue, pp. 65–83, 1971.
5. Coffin, M. D. and Tiffany, C. F.	New Air Force Requirements for Structural Safety, Durability and Life Management. J. Aircraft, vol. 13, no 2, pp. 93-98, February 1976.
6. Gibson, C. M.	B-1: USAF Priority Number One. Flight International, vol. 106, no. 3432, pp. 911-19, 26 December 1974.
7. Bland, L. M.	Aircraft Structural Life Prediction and Considerations of Chemical Environment. Proc. Third Tewksbury Symposium on Fracture, pp. 235–51, University of Melbourne, 1974.
8. O'Brien, K. R. A., Benoy, M., and Douglas, R.	Fatigue Certification of General Aviation Aircraft in Australia. Society of Automotive Engineers, Paper 720311, March 1972.
9. Edwards, P. R.	Cumulative Damage in Fatigue with Particular Reference to the Effects of Residual Stresses. Royal Aircraft Establishment Technical Report 69237, November 1969.
10. Matolesy, M.	Thoughts on Miner's Fatigue Damage Rule. Royal Aircraft Establishment Library Translation 1609, October 1974.
11. Uhlig, H. H.	The Role of a Critical Minimum Corrosion Rate on Fatigue Damage. Proc. NACE International Conference on Corrosion Fatigue, pp. 270–78, 1971.
12. Lee, H. H., and Uhlig, H. H.	Corrosion Fatigue of Type 4140 High Strength Steel. Metallurgical Transactions, vol. 3, pp. 2949–57, November 1972.
13. Lowndes, H. B., Jnr., and Miller, W. B.	The US Air Force Weapons Systems Fatigue Certification Program. Proc. Fourth ICAF Symposium, pp. 139–60, Pergamon Press, London, 1969.
14. Payne, A. O.	The Life Estimation Process for Aircraft Structures. Unpublished Note, ARL, 1974.
15. Hoskin, B. C., and Ford, D. G.	Scatter Factors in Aircraft Fatigue Life Estimation. ARL Note SM350, April 1970.
16. Mann, J. Y.	Some Phenomenonological Aspects of Scatter in Fatigue. ARL Report SM342, November 1972.
17. Payne, A. O.	Discussion of Reference 2. Proc. Fourth ICAF Symposium, pp. 61–65, Pergamon Press, London 1969.

18. Harpur, N. F., and Troughton, A. J. — The Value of Full-Scale Fatigue Testing. Proc. Fourth ICAF Symposium, pp. 343–373, Pergamon Press, London 1969.

19. Murnane, S. R. — Northrop/United States Air Force F-5E Aircraft Fatigue Structural Integrity Program. Northrop Corporation, California, May 1975.

20. Payne, A. O. — The Fatigue of Aircraft Structures. Engineering Fracture Mechanics, vol. 8, pp. 157–203, 1976.

21. Clementson, A. — Corrosion in Aircraft. British Journal of NDT, vol. 17, no. 2, pp. 40–45, March 1975.

22. Laird, C., and Duquette, D. J. — Mechanisms of Fatigue Crack Nucleation. Proc. NACE International Conference on Corrosion Fatigue, pp. 88–117, 1971.

23. Duquette, D. J., and Clarkin, P. A. — Initial Process—Chemical Aspects, Critical Introduction. Proc. NACE International Conference on Corrosion Fatigue, pp. 183–84, 1971.

24. Grosskrentz, J. C. — The Effect of Surface Films on Fatigue Crack Initiation. Proc. NACE International Conference on Corrosion Fatigue, pp. 201–10, 1971.

25. Langford, P. S. — The Principles and Practice of Airworthiness Control. Lawrence Hargrave Memorial Lecture, Royal Aeronautical Society, 1975.

26. Hooke, F. H. — The Fatigue Life of Safe Life and Fail Safe Structures, a State-of-the-Art Review. ARL Report SM 334, June 1971.

27. Wood, H. A. — The Use of Fracture Mechanics. Principles in the Design and Analysis of Damage Tolerant Aircraft Structures. AGARD Lecture Series No. 62, Fatigue Life Prediction for Aircraft Structures and Materials, Chapter 4, 1972.

28. — Report of the Committee on the Application of Fracture Prevention Principles to Aircraft. National Materials Advisory Board, Washington, DC, February 1973.

29. Pettit, D. E., and Hoeppner, D. W. — The Influence of Non-Destructive Inspection Parameters on the Preproof and Postproof Fatigue Crack Detection Limits for Fracture Mechanics Applications. Proc. Ninth Symposium on NDE, pp. 434–41, San Antonio, April 1973.

30. Knott, J. F. — Fundamentals of Fracture Mechanics. Butterworths, London 1974.

31. Hardrath, H. F. — Fatigue and Fracture Mechanics. J. Aircraft, vol. 8, no. 3, pp. 129–42, March 1971.

32. Buntin, W. D. — Concept and Conduct of Proof Test of F-111 Production Aircraft. Aeronautical Journal of Royal Aeronautical Society, vol. 3, no. 1, pp. 45–57, July 1971.

33. Barsom, J. M. — Effect of Cyclic Stress Form on Corrosion Fatigue Crack Propagation below $K_{I\,s.c.c.}$ in High Yield Strength Steel. Proc. NACE International Conference on Corrosion Fatigue, pp. 424–36, 1971.

34. Payne, A. O. — A Reliability Approach to the Fatigue of Structures. ASTM STP511, Probabilistic Aspects of Fatigue, pp. 106–55, 1972.

35. Anderson, W. E. — Corrosion Fatigue—or How to Replace the Full-Scale Fatigue Test. AGARD Lecture Series No. 62, Fatigue Life Prediction for Aircraft Structures and Materials, Chapter 5, 1972.

36. — Design Against Fatigue. AGARD Conference Proceedings No. 141, 1973.

37. Pelloux, R. M., and Latanision, R. M. — Fatigue Crack Propagation—Critical Introduction. Proc. NACE International Conference on Corrosion Fatigue, pp. 279–80, 1971.

38. McEvily, A. J., and Wei, R. P. — Fracture Mechanics and Corrosion Fatigue. Proc. NACE International Conference on Corrosion Fatigue, pp. 381-95, 1971.

39. Gallagher, J. P., and Wei, R. P. — Corrosion Fatigue Crack Propagation Behaviour in Steels. Proc. NACE International Conference on Corrosion Fatigue, pp. 409-23, 1971.

40. Kemsley, D. S., Ryan, N. E., and Jost, G. S. — Environmental Effects on Fatigue Crack Initiation and Propagation in Ultra-High-Strength Steels. Eighth ICAF Symposium, Pre-print, June 1975.

41. Crooker, T. W. — Basic Concepts for Design Against Structural Failure by Fatigue Crack Propagation. Naval Research Laboratory (NRL) Report 7347, Washington, DC, January 1972.

42. Uhlig, H. H. — Corrosion and Corrosion Control: An Introduction to Corrosion Science and Engineering. Wiley, New York, 1971.

43. Payer, J. H., and Staehle, R. W. — Localized Attack on Metal Surfaces. Proc. NACE International Conference on Corrosion Fatigue, pp. 211-269, 1971.

44. Hoeppner, D. W. — Corrosion Fatigue Consideration in Materials Selection and Engineering Design. Proc. NACE International Conference on Corrosion Fatigue, pp. 3-11, 1971.

45. — Corrosion. Lockheed Field Service Digest, no. 49, December 1965.

46. Bond, A. R. — Corrosion Detection and Evaluation by NDT. British Journal of NDT, vol. 17, no. 2, pp. 46-52, March 1975.

47. Meister, R. P., Randall, M. D., Mitchell, D. K., Williams, L. P., and Pattee, H. E. — Summary of Non-Destructive Testing and Practice. NASA CR-2120 Washington, DC, 1972.

48. Gardner, C. G. (ed.) — Non-Destructive Testing. NASA SP-5113, Washington, DC, 1973.

49. Vary, A. — Non-Destructive Evaluation Technique Guide. NASA, SP-3079, Washington, DC, 1973.

50. O'Brien, K. R. A., Hollamby, D. C., Bland, L. M., Glanville, D. W., and Scott, I. G. — Crack Detection Capability of Non-Destructive Inspection Methods in Relation to the Airworthiness of Aircraft. Eighth ICAF Symposium, Pre-print, June 1975.

51. Rodgers, J. — The Use of Acoustic Emission for Detection of Active Corrosion and Degraded Adhesive Bonding in Aircraft Structure. Twenty-fourth US Defence Conference on Non-Destructive Testing, Pre-print, 1975.

TABLE 1

Environmental Exposure Data for Given Structural Component

Environment	Flight time %	Ground time %
50–70% relative humidity	—	35·2
75% relative humidity	45·8	—
75–100% relative humidity	—	34·1
Condensation	3·7	19·7
Rain	0·7	11·0
Dry air	49·8	—

Reference 32.

Table 2. Surface Accessibility, Applicability, and Adequacy ; of NDI Methods

SURFACE ACCESSIBILITY

Direct Access

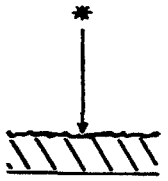

* = Observer

—— = Surface of interest

CORROSION EFFECT (dimensional representation)

(Local)

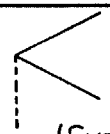

(Surface)

(Cracking)

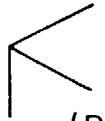

(Bulk)

INSPECTION METHOD	(Local) APPLICABILITY	(Local) ADEQUACY: Detection	(Local) ADEQUACY: Identification	(Local) ADEQUACY: Assessment of Severity	(Local) ADEQUACY: Assessment of Prevalence	(Surface) APPLICABILITY	(Surface) ADEQUACY: Detection	(Surface) ADEQUACY: Identification	(Surface) ADEQUACY: Assessment of Severity	(Surface) ADEQUACY: Assessment of Prevalence	(Cracking) APPLICABILITY	(Cracking) ADEQUACY: Detection	(Cracking) ADEQUACY: Identification	(Cracking) ADEQUACY: Assessment of Severity	(Cracking) ADEQUACY: Assessment of Prevalence	(Bulk) APPLICABILITY	(Bulk) ADEQUACY: Detection	(Bulk) ADEQUACY: Identification	(Bulk) ADEQUACY: Assessment of Severity	(Bulk) ADEQUACY: Assessment of Prevalence
VISUAL																				
Direct	X	A	A	B	A	X	A	A	B	A	X	B	B	C	B	X	A	A	A	A
Replica	X	B	C	C	C	X	A	B	C	C	X	C	C	C	C					
RADIOGRAPHY																				
X-ray																				
γ-ray																				
Neutron																				
PENETRANTS																				
Liquid	X	C	C	C	C						X	B	B	C	B					
Gas	X	A	B	B	A	X	A	B	B	A	X	A	A	B	A					
MAG. PARTICLE																				
Convent.											X	B	B	C	B					
Rubber Soln.											X	A	A	C	A					
ULTRASONICS											X	B	C	C	B					
EDDY CURRENTS											X	A	B	C	B					
THERMOGRAPHY	X	B	B	C	B	X	B	B	C	B										
ACOUSTIC EMISSION	X	A	D	C	B	X	A	D	C	B	X	A	D	C	B	X	A	D	C	B

A good
B satisfactory
C fair
D poor

Notation for statement of Adequacy of inspection method, corresponding to general expert application.

COMMENTS

With optical and other aids, including devices for accessible but more remote areas.

Krypton gas applicable only where evacuation can be carried out and radioactivity hazard can be adequately managed.

Applicable only to magnetic materials.

Heat applied from observers side. Performance variable, so confidence level lower.

Adequacy assessment assumes corrosion active at time of inspection.

Table 2 (contd)

SURFACE ACCESSIBILITY

Indirect Access

Class I

- through the medium of the material itself.

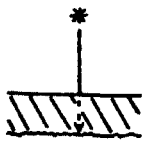

* = Observer

—— = Surface of interest

CORROSION EFFECT (dimensional representation)

(Local)

(Surface)

(Cracking)

(Bulk)

INSPECTION METHOD	APPLICABILITY	ADEQUACY: Detection	Identification	Assessment of Severity	Assessment of Prevalence	APPLICABILITY	ADEQUACY: Detection	Identification	Assessment of Severity	Assessment of Prevalence	APPLICABILITY	ADEQUACY: Detection	Identification	Assessment of Severity	Assessment of Prevalence	APPLICABILITY	ADEQUACY: Detection	Identification	Assessment of Severity	Assessment of Prevalence
VISUAL Direct Replica																				
RADIOGRAPHY X-ray	X	C	C	D	C	X	C	C	C	C	X	C	B	B	C	X	B	B	B	B
RADIOGRAPHY γ-ray	X	C	C	D	C	X	C	C	C	C	X	C	B	B	C	X	B	B	B	B
RADIOGRAPHY Neutron	X	A	A	B	A	X	A	A	B	A	X	B	A	B	A	X	A	A	B	A
PENETRANTS Liquid Gas																				
MAG. PARTICLE Convent. Rubber Soln.																				
ULTRASONICS	X	B	D	D	C	X	B	C	C	C	X	B	C	C	B	X	B	B	B	B
EDDY CURRENTS	X	B	D	D	C	X	B	D	D	C	X	B	B	C	C	X	B	C	C	B
THERMOGRAPHY																				
ACOUSTIC EMISSION	X	A	D	C	B	X	A	D	C	B	X	A	D	C	B	X	A	D	C	B

- **A** good
- **B** satisfactory
- **C** fair
- **D** poor

Notation for statement of Adequacy of inspection method, corresponding to general expert application.

COMMENTS

Applicable only if sufficient accessibility to vicinity of remote side of section for placement of recording film (or x-ray source). Reference standards useful.

No non-metallics present.

For sections up to 10 cm, with phase-sensitive low frequency system.

Adequacy of assessment assumes corrosion is active at time of inspection.

Table 2 (contd)

SURFACE ACCESSIBILITY
Indirect Access
Class II – through the medium of one intermediate material (metallic or non-metallic).

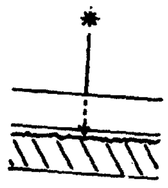

* = Observer
—— = Surface of interest

A good
B satisfactory
C fair
D poor

Notation for statement of Adequacy of inspection method, corresponding to general expert application.

CORROSION EFFECT (dimensional representation)

INSPECTION METHOD	(Local) APPLICABILITY	(Local) ADEQUACY Detection	(Local) ADEQUACY Identification	(Local) ADEQUACY Assessment of Severity	(Local) ADEQUACY Assessment of Prevalence	(Surface) APPLICABILITY	(Surface) ADEQUACY Detection	(Surface) ADEQUACY Identification	(Surface) ADEQUACY Assessment of Severity	(Surface) ADEQUACY Assessment of Prevalence	(Cracking) APPLICABILITY	(Cracking) ADEQUACY Detection	(Cracking) ADEQUACY Identification	(Cracking) ADEQUACY Assessment of Severity	(Cracking) ADEQUACY Assessment of Prevalence	(Bulk) APPLICABILITY	(Bulk) ADEQUACY Detection	(Bulk) ADEQUACY Identification	(Bulk) ADEQUACY Assessment of Severity	(Bulk) ADEQUACY Assessment of Prevalence	COMMENTS
VISUAL																					
Direct																					
Replica																					
RADIOGRAPHY																					
X-ray	X	C	C	D	C	X	C	C	C	C	X	C	B	B	C	X	B	B	B	B	Applicable only if sufficient accessibility to vicinity of remote side of section for placement of recording film for x-ray sources. Reference standards useful.
γ-ray	X	C	C	D	C	X	C	C	C	C	X	C	B	B	C	X	B	B	B	B	
Neutron	X	A	A	B	A	X	A	A	B	A	X	B	A	B	A	X	A	A	B	A	No non-metallics present.
PENETRANTS																					
Liquid																					
Gas																					
MAG. PARTICLE																					
Convent.											X	C	C	D	C						Where intermediate material is thin film e.g. paint coating and underlying material is magnetic.
Rubber Soln.											X	C	C	D	C						
ULTRASONICS	X	C	D	D	C	X	C	D	D	C	X	C	D	D	C	X	C	D	D	C	With low frequency equipment and good coupling between layers.
EDDY CURRENTS	X	C	D	D	C	X	C	D	D	C	X	B	C	D	C	X	B	D	D	C	For sections up to 1 [illegible] mm, with [illegible] low frequency system
THERMOGRAPHY						X	C	D	C	C						X	C	D	C	C	With heating from remote side of section, close contact between layers and thin outer layer
ACOUSTIC EMISSION	X	B	D	C	B	X	B	D	C	B	X	B		C	B	X	B	D	C	B	Dependent on acoustic matching of materials and thin contact or coupling.

Table 2 (contd)

SURFACE ACCESSIBILITY

Indirect Access
Class III
- through the media of two or more intermediate materials (one of which may be non-metallic)

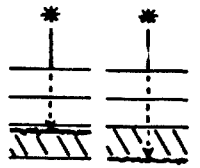

* = Observer

~~~ = Surface of interest

CORROSION EFFECT (dimensional representation)


(Local)

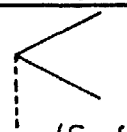
(Surface)

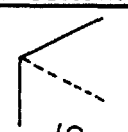
(Cracking)

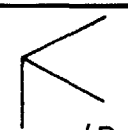
(Bulk)

INSPECTION METHOD	APPLICABILITY	ADEQUACY: Detection	Identification	Assessment of Severity	Assessment of Prevalence	APPLICABILITY	ADEQUACY: Detection	Identification	Assessment of Severity	Assessment of Prevalence	APPLICABILITY	ADEQUACY: Detection	Identification	Assessment of Severity	Assessment of Prevalence	APPLICABILITY	ADEQUACY: Detection	Identification	Assessment of Severity	Assessment of Prevalence
VISUAL Direct Replica																				
RADIOGRAPHY X-ray	X	C	D	D	C	X	C	D	D	C	X	D	D	D	D	X	C	D	D	C
γ-ray	X	C	D	D	C	X	C	D	D	C	X	D	D	D	D	X	C	D	D	C
Neutron																				
PENETRANTS Liquid Gas																				
MAG. PARTICLE Convent. Rubber Soln.																				
ULTRASONICS																				
EDDY CURRENTS	X	D	D	D	D	X	C	D	D	C	X	C	D	D	D	X	C	D	D	C
THERMOGRAPHY																				
ACOUSTIC EMISSION																				

A good
B satisfactory
C fair
D poor

Notation for statement of adequacy of inspection method, corresponding to general expert application.

COMMENTS

Applicable only if sufficient accessibility to vicinity of remote side of section for placement of recording film (or x-ray source). Reference standards useful.

Non-metallics almost certainly present

Not more than 10 cm total section thickness, all metallic. Phase sensitive low frequency equipment.
~~~

TABLE 2—continued

Inspection method	General comments
Visual	Adequacy of method highly dependent upon knowledge and experience of operator. For Indirect Access, Class II, where intermediate layer is non-metallic, effectiveness of method may depend upon fortuitous effect, such as blistering of paint film, caused by corrosion of underlying metal.
Radiography	Ideally 2% variation in thickness can be detected with X-radiography but generally the technique is limited to "coarse filter" type performance. All radiographic methods are influenced by the presence of such materials as paints, sealants, corrosion products and dirt. Neutron radiography is particularly sensitive to hydrogeneous materials, such as corrosion products—and paints, sealants, etc.
Penetrants	Successful use of liquid penetrants for corrosion cracking, stress corrosion cracking and corrosion fatigue cracking depends upon the cracks being free from corrosion products and other filling.
Magnetic particle	Sometimes a useful sensitivity can be achieved to corrosion cracks underlying paint films—particularly with the magnetic rubber technique.
Ultrasonics	The adequacy of ultrasonics in corrosion monitoring and other fields, is highly dependent upon the knowledge, experience and skill of the operator.
Eddy currents	Affected by a number of factors; therefore there is an important need for the use of accurate reference standards, with constant careful standardization of equipment.
Thermography	Affected by a number of factors, with consequent need for careful exploration of the actual suitability of the method in each case where its application appears possible.
Acoustic emission	Sensitive to the low-level energy release which accompanies the corrosion process. The potential of the method is considered to be very high, for numerous applications, and it is currently the subject of much development effort.

Scanning electron microscope photograph of crack surface showing corrosion pit "A" and fatigue markings "B"

Metallographic section through corrosion pit showing associated fatigue crack.

FIG. 1. FATIGUE CRACK ORIGINATING AT A CORROSION PIT IN AN ALUMINIUM ALLOY AIRCRAFT STRUCTURAL COMPONENT

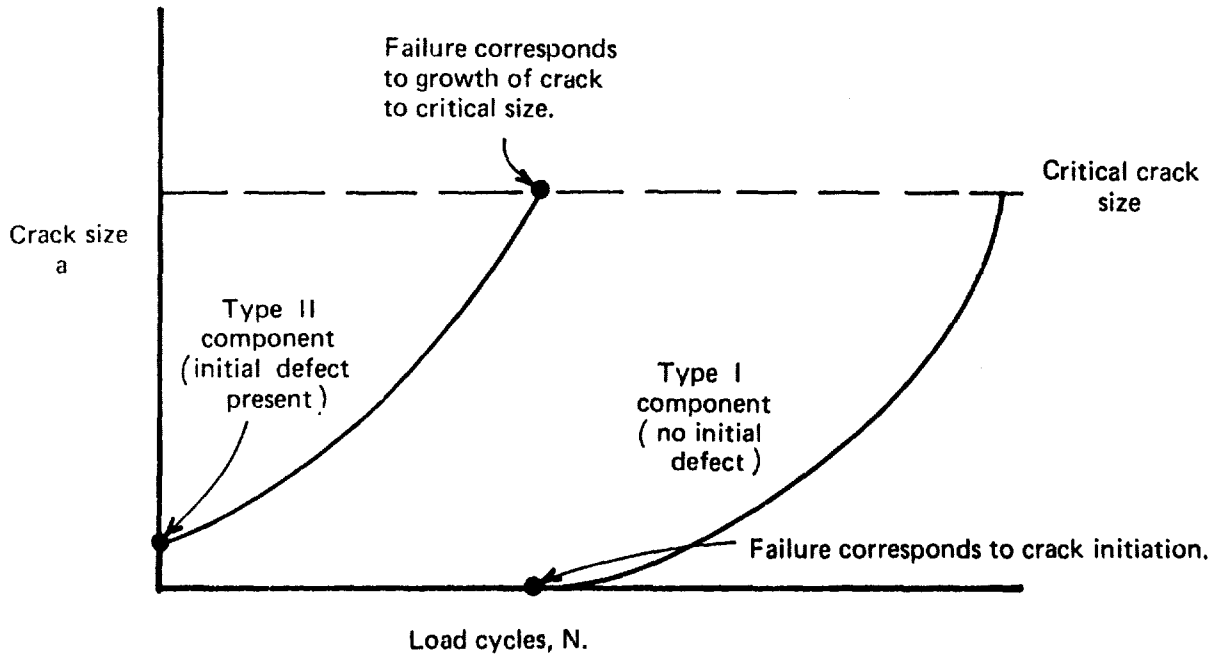

FIG. 2. SCHEMATIC REPRESENTATION OF FATIGUE CRACK DEVELOPMENT FOR COMPONENTS (TYPE I AND II) WITH DIFFERENT INITIAL DEFECT CONDITIONS.

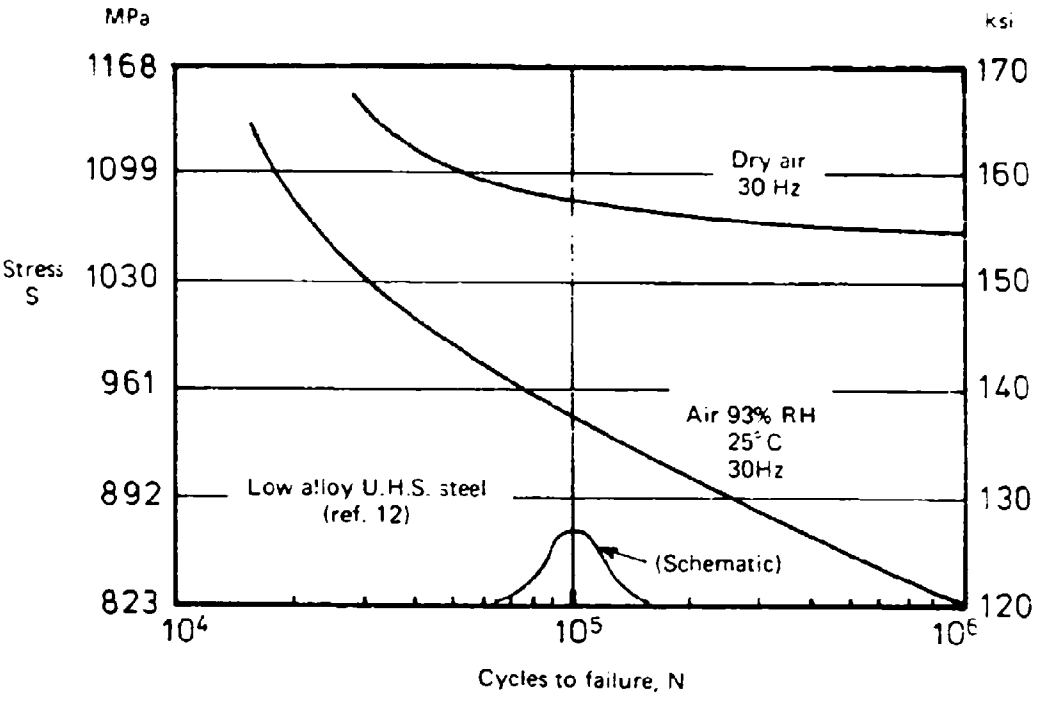

(a) S–N FATIGUE DATA FOR HIGH STRENGTH STEEL SHOWING EFFECT OF AGGRESSIVE ENVIRONMENT ON FATIGUE LIFE.

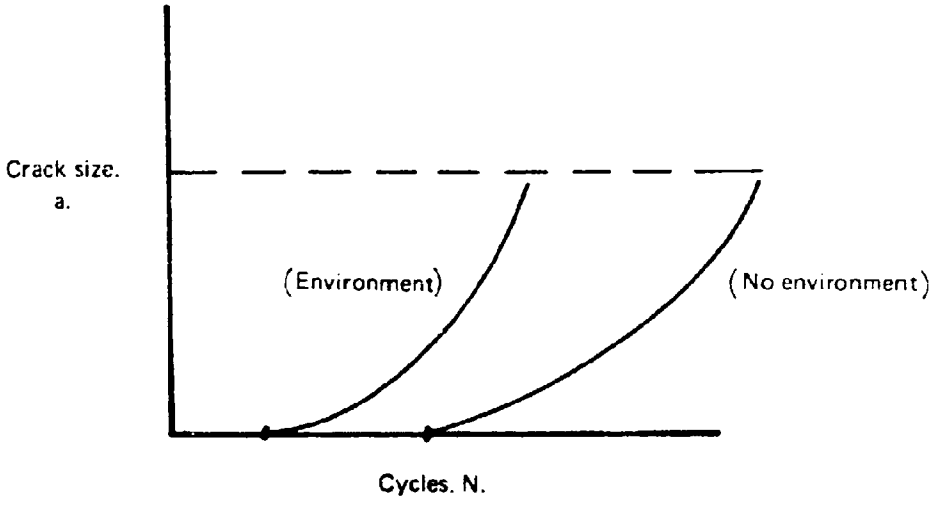

(b) SCHEMATIC REPRESENTATION OF EFFECT OF AGGRESSIVE ENVIRONMENT ON TIME TO FATIGUE CRACK INITIATION AND SUBSEQUENT CRACK GROWTH IN TEST SPECIMENS REPRESENTING TYPE I STRUCTURAL COMPONENTS.

FIG. 3 EFFECT OF CHEMICAL ENVIRONMENT ON FATIGUE PROPERTIES OF AIRCRAFT STRUCTURAL ALLOYS.

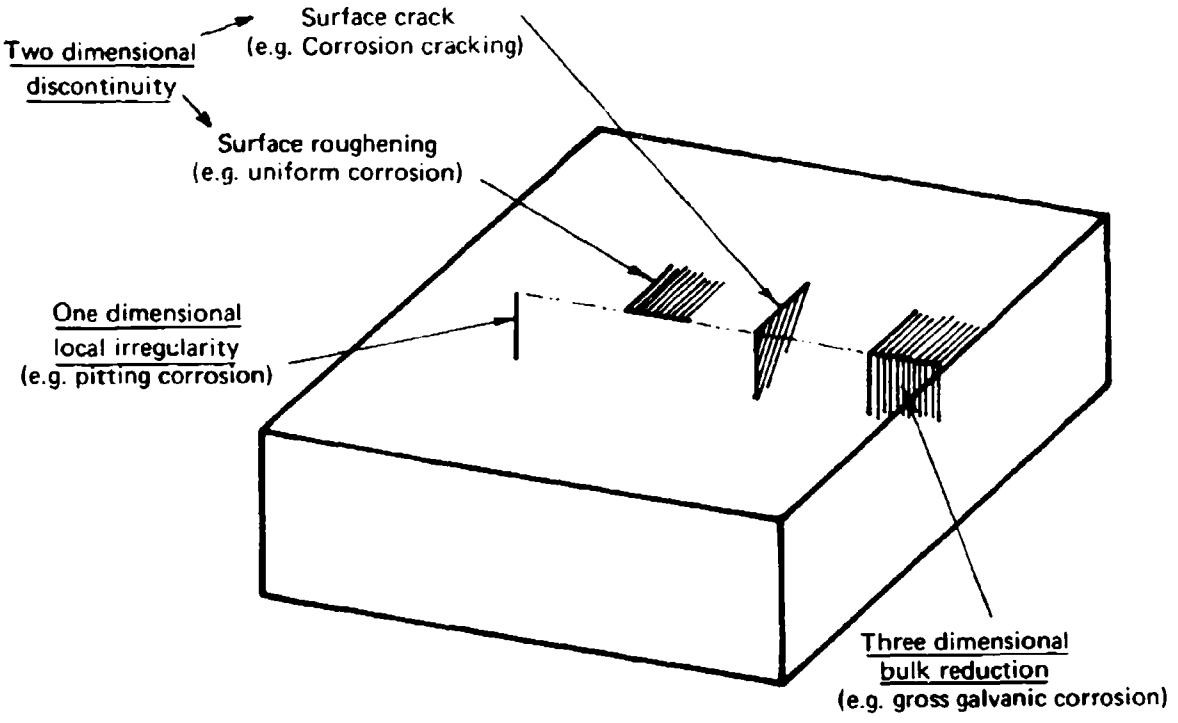

FIG. 8. SCHEMATIC REPRESENTATION, IN DIMENSIONAL FORM, OF PHYSICAL EFFECTS OF CORROSION ON AIRCRAFT STRUCTURAL MATERIALS.

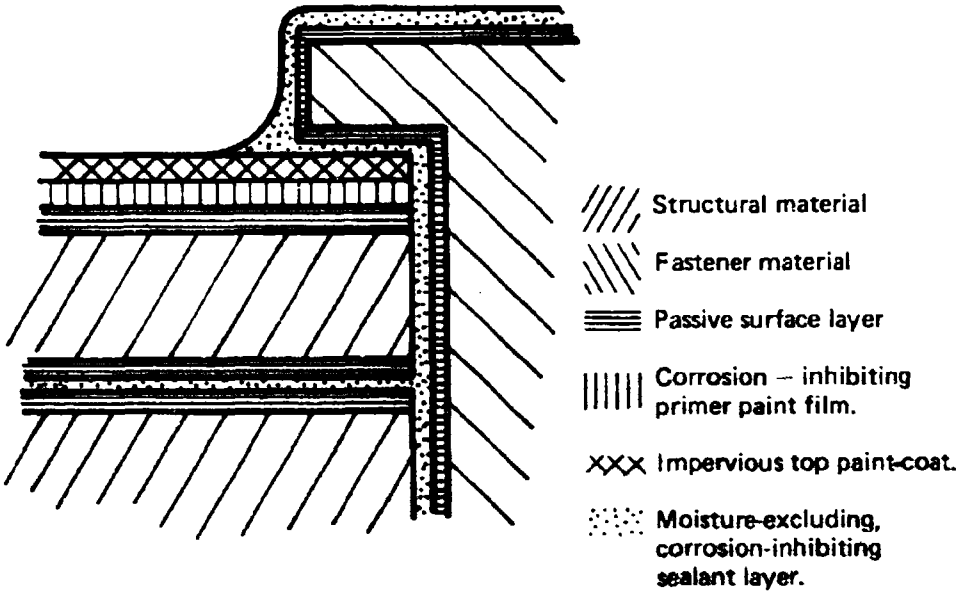

FIG. 9. SCHEMATIC REPRESENTATION OF TYPICAL CORROSION PROTECTION SYSTEM USED IN AIRCRAFT STRUCTURAL ASSEMBLY.

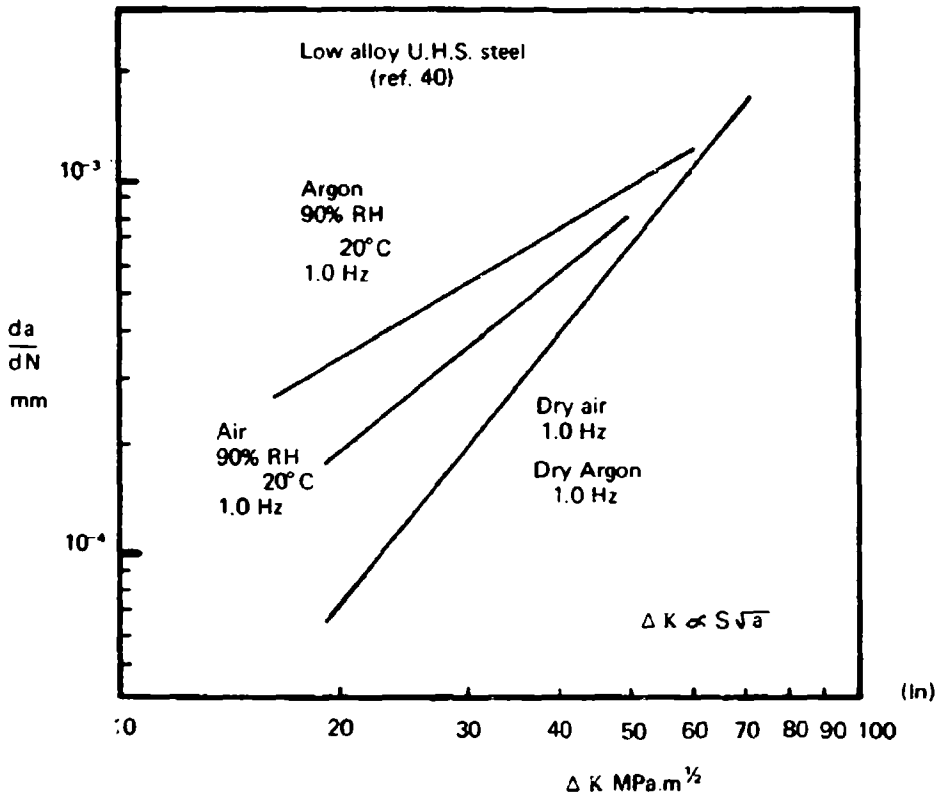

FIG. 6. EFFECT OF AGGRESSIVE ENVIRONMENT ON FATIGUE CRACK GROWTH RATE OVER MEDIUM RANGE OF VALUES OF STRESS AMPLITUDE.

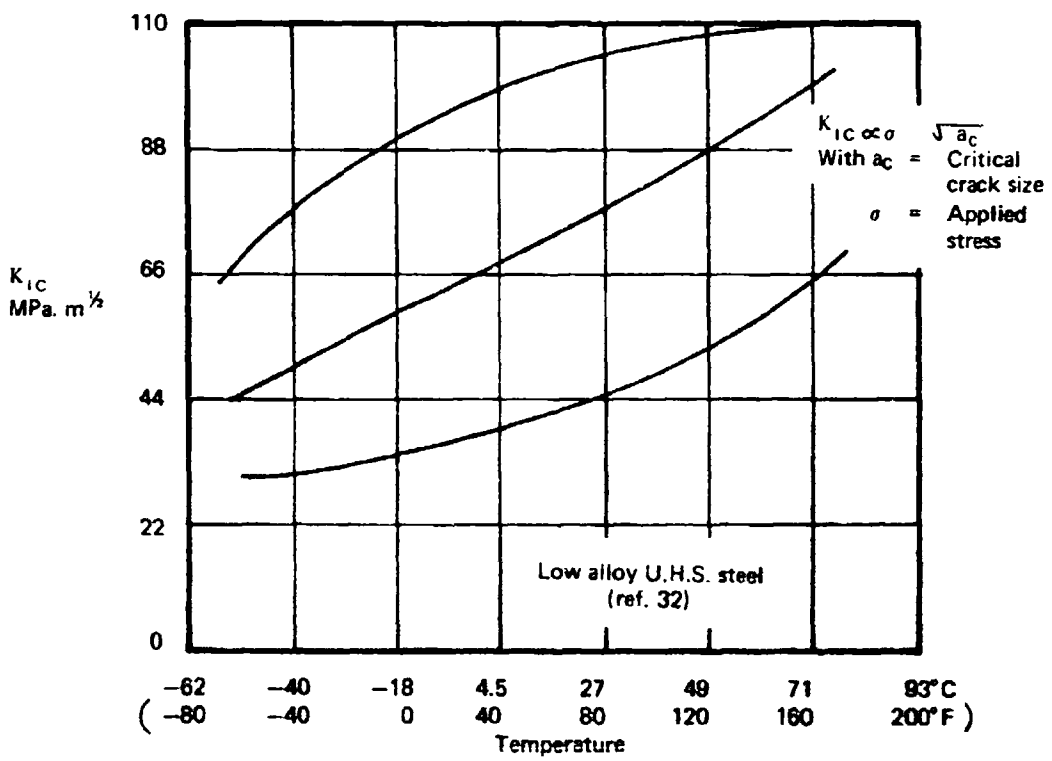

FIG. 7. VARIATION OF CRITICAL CRACK SIZE, EXPRESSED IN TERMS OF FRACTURE TOUGHNESS, WITH TEMPERATURE.

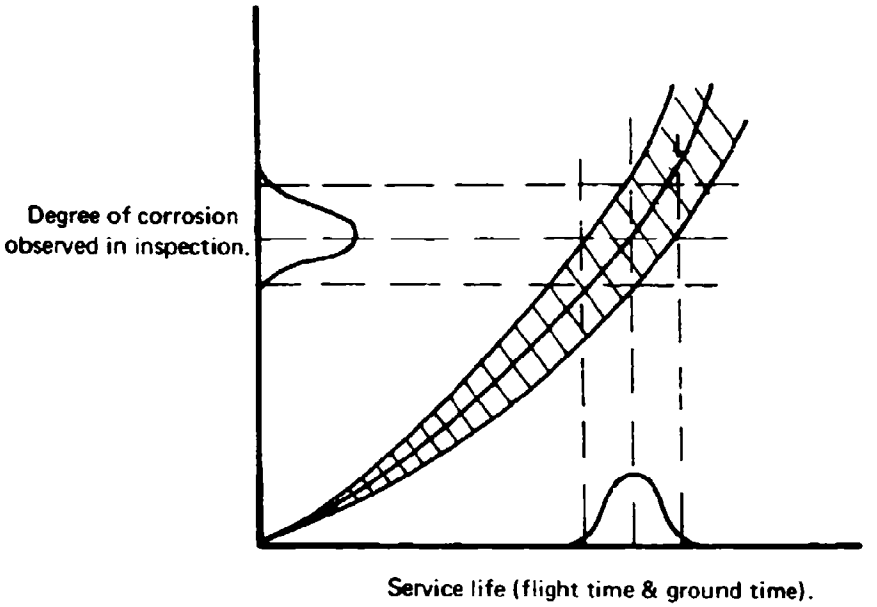

FIG. 4. SCHEMATIC EXAMPLE OF REPRESENTATION OF STATISTICAL DATA ON OCCURRENCE OF CORROSION IN STRUCTURAL COMPONENT.

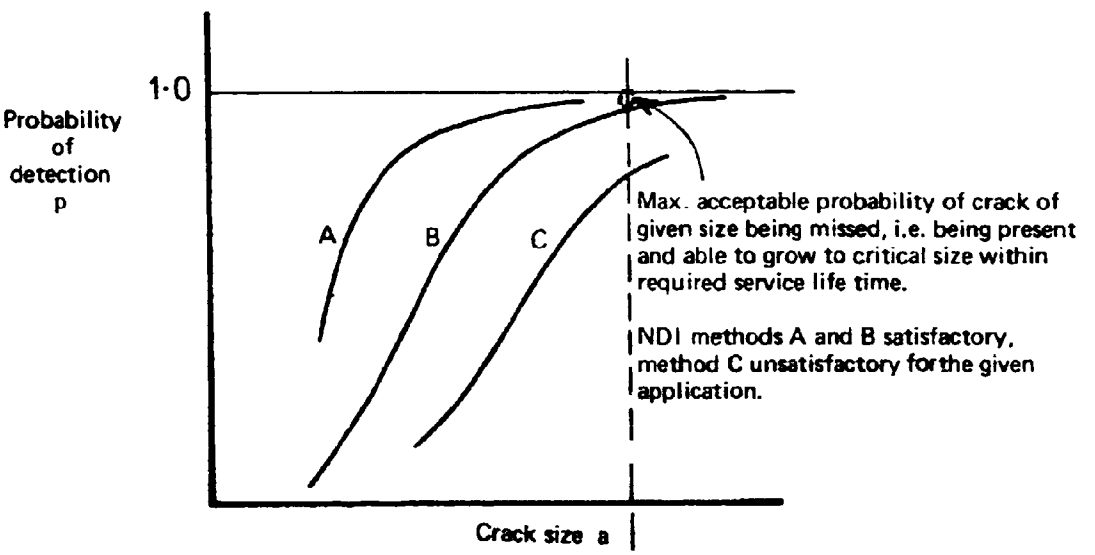

FIG. 5. NON DESTRUCTIVE INSPECTION AND CRACK DETECTION PERFORMANCE.

DISCUSSION

QUESTION –*B. R. Jackson*
(Royal Melbourne Institute of Technology)

Has ARL done any research on the effects of corrosion preventative compounds (penetrants) on the fatigue properties of riveted components?

Author's Reply

Work has not been done at ARL on the effects of corrosion preventative compounds of the penetrant type on the fatigue properties of riveted components. However, a comprehensive investigation is in progress at ARL on the fatigue behaviour of bolted joints of aluminium alloys, titanium alloys and high strength steel alloys in the "dry" condition and with one of two water-displacing corrosion-inhibiting liquids applied to the joint surfaces.

RAE, Farnborough, have done work on riveted aluminium alloy sheets to which similar corrosion-inhibiting liquids have been applied. The reference to this work is:

O'Neill, P. H., and Smith, R. J. A Short Study of the Effects of Penetrant Oil on the Fatigue Life of a Riveted Joint. RAE Technical Report 73174, 1974.

QUESTION—*G. E. F. Young*
(Ansett Airlines of Australia)

In your viewgraph of aircraft monitoring, should not an item be included for production monitoring?

We have had examples of: Incorrect bushing of holes,
Incorrect drilling or de-burring,
Incorrect plating process (non-baked), etc.

Author's Reply

The processes of quality control and quality assurance as applied during aircraft construction are monitoring functions which may be denoted by the general term "production" monitoring proposed by Mr. Young. This monitoring task would properly be included in a comprehensive list of all the monitoring activities the performance of which is of relevance to aircraft structural life. However, since this monitoring is undertaken before the service life begins, it is not properly to be classed as part of the service monitoring. (Where such procedures, e.g. the bushing of holes, are carried out as part of the maintenance function, during the service life of the aircraft structure, then the monitoring of these procedures is part of the maintenance monitoring process, which in turn is part of service monitoring considered in the broader connotation.)

NDI AND THE DETECTION OF FATIGUE

by

I. G. SCOTT

SUMMARY

The problems of monitoring fatigue cracks by NDI are discussed and recent developments in the methods and techniques are reviewed. Three aspects of work at ARL are considered in some detail, viz.

(i) the part played by the operator in NDI,

(ii) applications of acoustic emission to fatigue studies,

and (iii) future trends in NDI.

Some new philosophies in fatigue testing are also considered.

1. INTRODUCTION

A fatigue crack is usually tightly-closed, multi-branched and open to the surface; it may or may not be associated with corrosion. Dangerous fatigue cracks can be very small and difficult to find. Various NDI techniques are available which permit rapid scanning of a suspect area; all use some form of crack enhancement.

Although direct methods of examination (e.g. hand lens or microscope) can be used to find small defects, these methods are likely to be very time-consuming. As well, they are inapplicable to hidden surfaces. Consequently various indirect methods are used—these include penetrant, magnetic particle, eddy current and ultrasonic methods. In all cases, the presence of a crack is enhanced by some means—in penetrants, by the concentration of fluorescent chemicals in the region of the crack, in magnetic particle and eddy current techniques, by the distortion of a magnetic field and in ultrasonics, by the amplified echo of a sound wave reflected from the defect.

Although a great deal of time in Materials Division, ARL, is spent in direct application of NDI to specific problems, the importance of research in NDI has not been overlooked. For example, the development of fracture mechanics has increased the need to know more than just the presence and location of cracks. Hence, an active research programme is maintained wherein improvements to existing techniques and the developing of new techniques are being studied.

This paper first considers current methods of monitoring fatigue cracks and the significance of the operator with regard to the reliability of crack detection. The development of acoustic emission for detecting and monitoring cracks is then discussed, and future trends are reviewed.

2. MONITORING THE PROGRESS OF FATIGUE CRACKS

The progress of comparatively large fatigue cracks can be monitored fairly easily. Most of the common NDI techniques can be used, although simple radiography is fairly insensitive unless shapes and directions of cracks are known. The extremities of cracks can be located with reasonable accuracy and the sub-surface depth estimated by studying specimen shape and conditions of loading. Cracks are sometimes opened by application of a suitable directed load with consequent enhancement of detection capability. Cracks under the heads of fasteners are harder to locate. Ultrasonic techniques in which the transducer is rotated round the bolt head or in which phased transducer arrays are employed, have been used but they have not been particularly popular. If the fastener can be removed, then the magnetic rubber technique can be used to obtain a replica of an internal defect—provided that the specimen material is magnetic.

A simple surface-wave technique can be applied to map accurately crack-front geometries for a propagating crack. Ho *et al.*[1] used a plastic wedge to generate surface waves from a compression type PZT transducer, at the comparatively low ultrasonic frequency of about 0·5 MHz. Whittingham[2] describes an electronically switched linear scanner, comprising 39 piezo-electric elements of which four contiguous elements are in use at any instant. Reed relays, activated by the initial ultrasonic pulse, are used to advance the four-element array, one element at a time. The simultaneous use of four elements helps to smooth out variations in element characteristics and provides a narrow ultrasonic beam. Griffiths *et al.*[3] found that by moving a transducer in discrete steps and suitably processing the read-out, a synthetic phased array could be built, which was much cheaper than conventional phased arrays. Up to 60 elements could be synthesised. Sugg and Kammerer[4] described an on-board ultrasonic structural surveillance device used to monitor structural areas for fatigue-crack growth. The system sequentially pulsed and interpreted echoes from 10 transducers using a multiplexer. Transducers were bonded permanently in carefully chosen locations on the test structure.

Although ARL has always made extensive use of electrical strain gauges little use has been made of these resistance gauges as fatigue monitors. Provided the gauge and crack front can be suitably aligned, individual elements extend and are broken as the crack front passes beneath. Special gauge shapes and hardened foils are often used in this application. Harting[5] used a

gauge made from a fully annealed constantan foil which progressively work-hardened when subjected to cyclic strain and underwent a change in resistance. Large permanent changes in resistance were noted, which related to the integrated load-frequency history of the gauge, but difficulties were experienced in calibration. There were also problems in matching gauges to chosen materials but Kowalski[6] claimed that use of a dual element gauge overcame many of the matching difficulties. As well, Harting's gauge becomes unreliable once a crack starts either nearby in the specimen or within the gauge itself. Blackburn[7] used these gauges in comparative tests on a group of fighter aircraft. Dally and Panizza[8] have proposed the use of conducting polymers (graphite particles in an epoxy matrix) to replace the foil, and claim that a greatly increased strain range results.

In situations where growing cracks are accurately located (e.g. in single-edge-notched specimens), their progress can be monitored by means of electric potential methods. These methods are readily applicable to laboratory specimens of regular shape, but not to large specimens or those of irregular shape (e.g. aircraft components). Furthermore, the attachment of electrodes (both current and potential) is made by a variety of surface-damaging means (including welding) which would not be permitted on aircraft. Theoretical analyses of potential methods are confined to specimens of regular and simple shape and have been confirmed experimentally. Users prefer to adopt experimental calibration based on simulated cracks (e.g. saw cuts). However, it is agreed that the method is sensitive largely to geometrical effects and is independent of variations in material parameters such as chemical composition, heat treatment, etc. Sensitivities are adequate and similar to those obtained by the best NDI methods. There are obvious problems with crack branching, the formation of multiple cracks and non-linear crack fronts. Scott[9] reviewed the method in 1969 and Clark and Knott[10] in 1975.

3. THE OPERATOR AND NDI

It is one thing to find fatigue cracks in critical areas in aircraft under field conditions or quite small cracks in laboratory specimens undergoing testing. It is an entirely different matter when NDI operators are called on to find defects of unknown size and location under normal operating conditions. In such situations, the human operator becomes an element in a system which includes the chosen technique, the available equipment, the size and location of the crack and the working conditions.

The operator works under varied conditions - he may find the suspect surface is readily accessible or it may be hidden under layers of grease, corroding plating or flaking paint. He may be able to make measurements seated at a bench in an air-conditioned room or be called on to work on the tarmac or the hangar floor, frequently in a confined space. Most in-service fatigue cracks propagate from stress raisers, which usually occur in the most complicated parts of a structure. The need to find defects under the heads of fasteners has already been mentioned. In short, the operator may be given a difficult task and be expected to carry it out under difficult conditions. It is not surprising that his performance is variable.

Techniques and equipment are sometimes chosen for some non-technical reason (e.g. cost or availability of more suitable equipment) but, in most cases, suitable equipment is used. Provided equipment and technique are correctly applied, crack detection capabilities are probably adequate. However, some modern aircraft materials are quite intolerant of even small defects, and, with increasing application of philosophies based on fracture mechanics, some aircraft are permitted to fly with known propagating cracks. Consequently, it is no longer permissible to be vague about crack detection capabilities.

3.1 The Diagnostic* Nature of NDI

The NDI operator is called on to use equipment selected by someone else and to follow clearly defined instructions. He is required to undertake an important job but one which is likely to be quite tedious. Operator training usually comprises a short high-pressure course on a

* The diagnostic method of measurement is foreign to those of us who are used to dealing with measurements whose scatter can be described by a Gaussian or normal distribution. Herein, by making a large number of measurements, all of which are assumed to carry equal weight, it is possible to state not only the measured mean but also the measured spread and to predict the likely spread in later measurements.

very restricted subject. Often test results will simply be handed on to a senior officer for analysis. In the absence of feedback of results, the operator has no way of knowing whether he is doing a good or a bad job. Operators rarely come from professional ranks; they are often drawn from tradesmen who for some reason wish to change their field of work.

Partly as a consequence of this background and partly as a result of the nature of his work, the NDI operator adopts an unusual approach. Instead of making equally weighted measurements, excessive weight is given to the finding of a defect. A large number of unsuccessful attempts may be made to find a defect in a suspect area. However, immediately an indication of the presence of a defect is found, these earlier results are discarded and effort is concentrated on verifying what is now assumed to be a discovered defect. In some cases this may be done by using an entirely different method of NDI.

3.2 Crack Detection Capabilities

The effects on operator performance of nearby disturbances, an unhappy marital situation or the degree of importance of the task are likely to be quite considerable, but these lie in the realms of the psychologist or the human engineer. At ARL, other important factors have been identified which influence performance and which can be measured.

A series of tests was conducted at ARL to determine the ability of an operator to detect a defect in a laboratory specimen (Chin Quan and Scott[11]). Plate specimens ($50 \times 50 \times 13$ mm) were prepared, in each of which a fine slit was made about 13 mm from one corner. The ranges of slit sizes were different for the eddy current and ultrasonic techniques but generally conformed to "readily detectable" to "too small to detect". The probe and instrument setting remained constant for a test series, in the course of which up to six operators each made over 100 attempts to find the artificial defects; the operators were unable to see the defect which was covered in tape. Twelve specimens were used, two of which were free of defects and were designated controls. Specimens were presented to the operator in a random manner, until 10 readings had been made on each specimen.

In retrospect, many of the results were not surprising. Most operators had no difficulty in scoring 10/10 for large defects and 0/10 for small defects. For intermediate-sized defects, the scores fluctuated. However, there were a few "false alarm errors", i.e. claims to finding a defect in a control specimen. These seemed to come mainly from experienced operators. There was also some evidence of learning during progress of a test. Differences between the two techniques were mainly evident over the range of smaller defects. Using ultrasonics, the operators were quite definite in their inability to find small defects, whereas with eddy currents there was some doubt. Tests on the operator's ability to measure crack size, which is so important in modern NDI applications, were partially inconclusive. Although most operators were able to sort specimens into the correct order on a size basis, absolute size measurements were consistently high. Various factors could be defined but no single factor could be used to quantify completely operator performance.

Packman[12] conducted tests using specimens containing fatigue cracks and obtained similar results. Individual operator characteristics were similar but magnitudes of factors differed. However, his work was of major importance because it was extended and applied to real situations.

3.3 The Use of Confidence Limits

By quantifying the performance of the operator, a statistically based detection capability can be determined and used to ensure an increased reliability of NDI. Consequently, a fracture mechanics approach can be developed and efficient aircraft usage can be maintained (O'Brien *et al.*[13]). Klass[14] showed how these ideas could be applied to both construction and maintenance of modern high performance American aircraft.

In operator testing, detection sensitivity is frequently defined as the number of defects found expressed as a percentage of the number of defects known to be present, i.e. the probability of detection of a defect (P). In a binomial experiment, where n is the sample size, the probability of missing a maximum of r defects is the sum of the first $(r+1)$ terms of the expansion of $(P+Q)^n$, where Q is the probability of a failure. A confidence limit c can be introduced, where c is the proportion of succeeding trials with which a probability of P or better can be associated. It can be shown that to achieve a 90% probability at 95% confidence level, no misses are allowed in thirty tests. Similarly, if 90% of defects are found, then if batches of the same size are tested,

the probability of finding defects is 79%, with a confidence level of 95%. (False alarm errors are sometimes simply treated as failures. Davidson[15] showed how these errors could be treated separately using a Bayesian approach. The added complication is usually considered unnecessary.) Consequently, it is now possible to licence a factory or an operator in a quantitative manner - despite the use of a diagnostic approach to measurement. This represents one of the major developments in modern NDI with which ARL has had some association.

4. ACOUSTIC EMISSION

Few new concepts in recent years have received practical application in NDI, but one has been acoustic emission (AE).* The emphasis prevalent in other NDI techniques, on first finding defects and then analysing their importance has shifted to the immediate identification of malignant defects. AE is another modern technique of NDI which has been under study at ARL for some time, and is currently being evaluated and used.

Early attempts elsewhere to apply AE to fatigue studies met with mixed success. Unnotched titanium alloy specimens produced no significant AE until failure was imminent. Shinaishin *et al.*[16] claimed that this was a material characteristic, but were able to estimate the area of a fatigue crack from AE measurements on individual notched specimens. Hutton[17] tested specimens made from a high nickel alloy and a steel, and claimed that all three materials behaved in a similar manner. Peaks in the AE count rates were explained in terms of micro-crack initiation, the start of final failure, etc., and it was concluded that AE provided "a measure of remaining fatigue life in a given test specimen or component".

Tests on boron-aluminium and boron epoxy composite materials were conducted by Williams and Reifsnider.[18] Confusion resulted in early tests because inadequate instrumentation permitted fretting noises and AE to be measured together. Eventually, an excellent correlation between damage and total AE counts was established. In contrast, Fuwa *et al.*[19] used AE to establish that true fatigue processes do not apply for carbon fibre reinforced plastics and that fatigue deterioration is similar to that induced by tensile loading. In a typical low cycle test, no AE were recorded until the stress level exceeded 10–20% of the tensile fracture strength and further emissions only occurred when the load approached the maximum level reached in the previous cycle. No AE appeared during the unloading portion of the cycle and eventually the sample became silent. However, a fatigue limit was established below which no damage occurred; this was not based on the size of a measured defect but only on specimen behaviour under prolonged cyclic loading.

It was not until the importance of certain instrumentation requirements was realised that consistent results from AE testing were obtained. A gating technique was used to disable the AE system during those parts of the load cycle where machine noises were prevalent (Egle *et al.*[20]). Consequently, results were expressed as count rates per load cycle. In addition, testing-machine noise could be reduced by inserting high impedance joints in the noise path and using flexures rather than pins. Cross-correlation techniques are used either on the recorded results (Ono *et al.*[21]) or are applied during testing. (Smith and Morton[22] multiplied electronically the outputs from two transducers located equidistant from a growing crack. After further electronic conditioning very good rejection of spurious signals was achieved.) Crack closure AE was also identified. This type of emission reached a maximum for low maximum-to-minimum load ratio (R); for high R ($>0{\cdot}5$) crack surfaces tend to keep apart, signals are smaller and tend to vary. Hence, crack closure AE can be identified by its dependence on R or its effects eliminated by proper choice of gating times.

It has been shown already that different materials produce different AE under fatigue loading. Morton *et al.*[23] conducted tests on 2024-T851 aluminium alloy specimens and a single magnesium alloy specimen. The AE from the latter specimen was much greater than that from the aluminium alloy specimens. The primary deformation mechanism for magnesium alloys is twinning, whereas that for aluminium alloys is slip. Twinning processes are generally far noisier than slip processes. However, it was concluded that "the generic behaviour of AE of fatigue cracking is insensitive to" loading frequency variation (over the range 1 to 16 Hz and R ratio variations from 0·1 to 0·5). Harris and Dunegan[24] tested 7075-T6 aluminium and 4140 steel,

* AE refers to the detection and analysis of the stress waves resulting from extremely small energy redistributions within a specimen. These redistributions may arise from yielding, twinning, corrosion, etc.

finding that "data obtained at various band passes and gain settings did not show any large qualitative differences".* Hence, it was implied that the in-service testing of structures in hostile environments should be practicable. The AE rate per cycle was variable, from which it was deduced that crack growth was irregular. This result emphasises the need for continuous rather than sampled collection of data.

It can be demonstrated that the AE count rate (dN/dn = AE counts per cycle) during cracking is a function of the applied range of stress intensity ΔK. This is given by

$$\frac{dN}{dn} = C_1(\Delta K)\, C_2$$

where C_1 and C_2 are constants which change somewhat with load frequency, R and markedly from material to material. Attempted development of this simple approach generally fails. Morton *et al.* propose the addition of two terms—a term dependent on R along with a term dependent on both K_c (critical stress intensity factor) and K_m (maximum stress intensity factor). Harris and Dunegan prefer to introduce material specimen constants in the form of elastic modulus and specimen thickness. Clearly, an entirely satisfactory model has not yet been developed. Nevertheless, it is still possible to get many cycles warning of impending failure because the AE rate increases dramatically as failure approaches.

Developments in instrumentation are now permitting the application of AE to complex structures. Bailey and Pless[25] have conducted preliminary tests confirming that fatigue cracks growing from rivet fastener holes in an aircraft structure can be located and their progress monitored. Pollock and Smith[26] have monitored a military bridge during proof loading, in the course of which various noise paths were identified.

The concept of proof testing is relatively new, although it provides some of the earliest applications of AE (see e.g. Schofield[27] on pressure vessels). Corle and Schliessmann[28] have shown how AE, from specimens containing fatigue cracks of various sizes when loaded in tension, was characteristic of the material on a counts basis and was found to increase with increasing size of defect. Flaw-detection capabilities were claimed to be much in excess of those for conventional techniques. Dunegan,[29] in an excellent review article, describes how periodic overload testing can be conducted. Assume a structure containing a defect is loaded to a given magnitude and the AE during loading is measured. After a period of service, a malignant defect can be expected to grow and consequently on reloading the structure to the original magnitude, there will be an increase in the stress intensity factor. Consequently AE, dependent on stress intensity factor, will be observed. If no defect is present, or the crack has not grown, there will be no measureable increase in AE. It is possible, by making a number of simplifying assumptions, to determine the number of fatigue cycles at working load in terms of the AE observed during periodic overload.

In summary, AE can be used in three ways:

(i) to locate and follow the progress of a crack without providing indisputable evidence about crack size;

(ii) to follow the progress of a specimen or structure towards partial or complete failure without necessarily providing very much information about defect size; and

(iii) to differentiate between flawed and unflawed structures subjected to proof loading.

Work at ARL has been confined so far to assessing the potentialities of AE in following crack propagation in complicated structures. A load-operated gating technique has been used, crack-closure effects have been observed and the increase in signal strength close to failure has been compared with crack extensions measured by other techniques. A continuing programme is planned.

5. NEW CONCEPTS IN NDI AND FATIGUE

It is highly likely that the plastic zone associated with even a very small fatigue crack emits measurable AE; hence, the possibility of detecting fatigue cracks at a very early stage exists. For the engineer, the *existence* of a measurable crack is probably sufficient; but for the metallurgist, the idea of a fatigue crack *precursor* is attractive. Only a few modern NDI techniques show much promise as pre-crack indicators, possibly because the fatigue process is not sufficiently understood.

The behaviour of the breadth of the X-ray diffraction profile during fatigue has been studied. By using a micro-beam technique, Taira[30] measured parametric changes in the plastic

* Analysis of their results suggests that this is an optimistic interpretation.

zone ahead of the crack, i.e. the area wherein a crack is expected to propagate, and this method has been used to follow the progress of a fatigue crack. It appears to be best suited to study of the fatigue process in the laboratory. However, with the present rapid developments in technology, along with the possible use of the computer for control of scanning and for handling of results, field application does not seem to be an unrealistic prediction.

Photoelectron emission from freshly fractured surfaces has been observed but the process is not yet fully understood. By measuring localised exoelectron emission, Baxter[31] claimed to obtain reproducible results which provided very early indication of fatigue deformation and showed a relationship between emission and number of fatigue cycles. The specimen was mounted in a vacuum chamber and was systematically scanned by a light spot formed from a 1 kW mercury arc lamp. The electrons were detected by an electron multiplier, the input of which was held at 500 V DC with respect to the sample and a time rate was recorded. Tests showed that emission rates normally remained constant for up to 50 minutes under laboratory conditions. Tests were conducted on aluminium and steel specimens. Shortly after testing began, a point on the specimen showing a dominant peak count rate could be identified and this dominant peak was usually followed through to failure. (On one occasion the first dominant peak was joined by a second peak which eventually took over the dominant role.) It was found that emergence of a dominant peak was a very early precursor to final failure. It was assumed that the emission was associated with crack formation because it was extremely localised (beyond the 15 μ resolution of the equipment used). It was also assumed that the intensity of the localised emission provided a measure of fatigue damage. Baxter postulated the continuous generation of fresh fracture surfaces as the dominant source of the emission and emphasised its highly localised nature. The technique seems to be a highly sensitive detector of malignant cracks without giving strong indications of final failure. A more direct validation of fatigue-crack growth (say, metallographically) is awaited.

Specimens of 6061-T6 polycrystalline aluminium or cold rolled 1015 polycrystalline steel exhibited large changes in the attenuation of ultrasound prior to failure (Joshi and Green[32]). Typically, measurements of ultrasonic attenuation gave a strong indication of the onset of failure well before conventional measurements were able to detect a crack. Fifteen specimens of each material were used and in all cases changes in attenuation $>0{\cdot}4$ dB were observed before a crack was detected. It is postulated that, since dislocation motion is a prerequisite to fracture and ultrasonic attenuation is a very sensitive measure of dislocation motion, attenuation changes should be a good precursor of failure.

Bhattacharya and Schroder[33] found, for certain ferro-magnetic materials over a limited range of hardness, that AE signals could be readily detected as specimens were fatigued. These signals occur at the same time as Barkhausen type magnetic signals can be detected from an initially magnetically saturated specimen. It was suggested that the latter signals are a more reliable indication of progress of a fatigue crack than AE, which is strongly dependent on hardness.

Under fatigue loading conditions, materials dissipate heat energy because of hysteresis effects. The resulting temperature changes are small but can be detected using sophisticated techniques, e.g. scanning infra-red devices. Consequently, areas likely to suffer fatigue damage can be located and identified—frequently before the damage is visible as a crack. Charles *et al.*[34] claimed to be able to detect some fatigue cracks as early as 15% of fatigue life. Tests were conducted on mild steel and fibre-glass epoxy specimens using equipment having sensitivity better than $0{\cdot}1$°C in the 8–14 μ wavelength region. Analysis of a record using a densitometer permitted isotherms to be plotted and these patterns were particularly useful in following the propagation of a crack. Earlier, Attermo and Ostberg[35] had reported temperature rises as high as 30°C for PVC specimens, when heavy plastic deformation had occurred ahead of the propagating crack. For 18/8 stainless steel specimens, smaller temperature rises (14°C) were found. Reifsnider and Williams[36] showed that heat produced during fatigue comes from two sources—the first can be attributed to the phase difference between stress and strain brought about by the viscous nature of the material, while the second usually arises from mechanical damage. The most useful results were obtained from a 10-colour calibrated surface-temperature picture of the specimen using commercial thermographic equipment. Not only were areas of fatigue damage readily identified, but the coloured records lent themselves to further analysis. The specimens were made from boron-epoxy and boron-aluminium composite material and temperature changes of up to 36°C were recorded. The major temperature change appears to occur at the start of testing when other methods are particularly insensitive.

Microwaves have been used in various ways to find defects in poor conductors such as honeycomb structures, etc. Sound waves generated at microwave frequencies have wavelengths which are of the order of the wavelength of light and hence an acoustic microscope can be built (Young[37]) in which the contrast is acoustical rather than optical. Consequently, details may be seen which would otherwise be missed altogether. Andrew[38] described an imaging technique which is based on nuclear magnetic resonance (NMR) but it is in the early stages of development. Three alternating magnetic field gradients, of differing frequencies, are applied in orthogonal directions across the specimen and the intersection of the orthogonal planes defines a unique sensitive point at which the fields are constant. The signal from the sensitive point can be selected and used in scanning through thin slices of the specimen to prepare a three-dimensional image of the proton density in the specimen. Pullan[39] described X-ray imaging techniques which permit cross-sectional pictures of any part of the human body to be produced. An X-ray tube and scintillation detector scan across the body and measure X-ray transmission at frequent intervals. The system is then rotated through a small angle and the process is repeated. A complex Fourier transform analysis is used to produce a suitable image. Very small changes in density and atomic number can be detected. The apparatus is very expensive.

There are various methods whereby ultrasonic waves can be used to produce images of the interior of an optically opaque solid. In one commonly used technique, the received and amplified echoes from discontinuities in acoustic impedance are displayed as light spots on a CRT screen to produce a cross-sectional representation of discontinuities as the probe is scanned over the subject. The resolution of these ultrasonic devices is limited below frequencies of about 10 MHz, the limitation is due to wavelength while at higher frequencies, attenuation and absorption become excessive. There is an enormous literature on holography. Erf *et al.*[40] provide a good starting point. An interferometric technique is described whereby very small (half-wavelength) surface displacements can be detected by examining fringe patterns from photographic pairs. In a fatigue situation, surface distortion is often observed. Both phase and amplitude signals are accurately recorded before and after load application. Consequently, using continuous wave excitation, only extremely stable structures can be examined. However, Erf *et al.* overcame this problem by using pulsed laser systems, the duration of individual pulses being about 40 nanoseconds. Using a pulse separation greater than 20 microseconds, output energies approaching 3·2 joule pulse were realised. Detail of test techniques, along with some case histories, is given. Archbold and Eanos[41] proposed the use of laser photography to measure the deformation of weld cracks under load. Laser light was used to illuminate the crack area and double exposure photographs were taken before and after loading. Movements of the crack edges could be accurately measured from a speckle pattern. The method does not need the high stability required for holography. At ARL theoretical studies have been made concerning the use of Bragg diffraction imaging. The work on holography has not been done specifically for NDI application.

Many NDI techniques are wasteful of the information contained in the signal, using only a small portion and discarding the remainder. There is a host of techniques presently under examination or development in which more use is made of this information. Analysis techniques are used wherein flaw characteristics are determined on the basis of signal frequency content. Yee *et al.*[42] described how reflected ultrasonic signals were digitised before being transformed from time to frequency domain using a Fourier transform technique. Spectra were obtained for fatigue cracks, but these were very complicated and satisfactory interpretation has not yet been made. Defects in adhesive and braze-bonded assemblies were readily identified and the thickness of parallel-sided discontinuities was measured. Sachse[43] found spectra characterising a cyclindrical fluid-filled cavity were different from those associated with a flat circular surface. Hopefully, analysis will lead eventually not only to crack size determination but also perhaps to the nature of the crack or defect—in our case, whether it is a fatigue crack or not.

Zuckerwar[44] has proposed, and shown the feasibility of, a system whereby a specialised form of ultrasonic signal analysis is used to monitor defects in structures. Suitably chosen and located ultrasonic transducers are permanently attached to several points in the structure and one of the transducers acts as a transmitter. The cross-correlation function ("cross-correlogram") between the demodulated transmitted and received signal is established on-line by means of a fast-Fourier analyser. Random noise is largely eliminated by averaging a large number of cross-correlograms and, by subtracting the initial or reference cross-correlogram, a differential cross-correlogram is obtained having increased sensitivity. Tests were conducted on a plate containing holes of different size, a simple specimen with fatigue-induced defects and a rivetted specimen.

Little difficulty was experienced in detecting the presence of a small hole or the early stages of fatigue cracking. The detection of a crack under a rivet head was not truly tested because no observable cracks were produced. The system has yet to be tested on a complex structure and under field conditions on unknown defects. It serves to point the direction in which ultrasonic testing may well proceed. Cole and Reed[45] describe a somewhat similar technique. A structural signature based on the measurement of damping decrement of an excited structure is claimed to be invariant after conditioning but is closely related to the development of defects. It is a highly computerised technique which is at present very critical to measurement frequency, transducer location, etc. No real claim is made for its use as a flaw detection method but it is believed to constitute a feasible approach. In both of these techniques, it is implied that eventually a measure of structural deterioration will be obtained. A simpler specialised technique for defects around fastener holes was proposed by Schrooer.[46] The fastener under test was struck a sharp blow and the nearby vibrations were analysed. A crude analogy of the changed frequency of a sound and cracked bell was used. At the time, Schrooer found analysis of the waveforms too subjective but this may now be less of a problem because of recent developments in computing.

6. CLOSING REMARKS

It has been a primary objective of this paper to demonstrate that much work has been done in the past, is being done at present and is planned for the future, in connection with NDI and fatigue. The original idea of simply measuring crack lengths has been extended by studying the performance of the operator, by improving the capabilities of established NDI techniques and by an ever-increasing use of the computer not only to process and condition test results but also to control the progress of the test. It now seems possible that, with the aid of fracture mechanics concepts, measurement and prediction of crack growth rates will soon become relatively commonplace.

In areas where crack growth measurement is either not possible or is unpopular, other techniques for life prediction are being developed which involve entirely new philosophies. Proof testing has been used to validate the capabilities of high performance aircraft and may be used with or without the assistance of AE. The latter technique itself is developing as a viable new method for life prediction.

Finally, there are numerous laboratory techniques where either studies of the overall process can be made or the early stages (or precursors) of the fatigue process can be discovered. It is too early to predict which of these techniques will be developed to the stage of field application but, historically, many of them could be expected to reach this standard in the foreseeable future. To a large extent, the speed with which this is done will depend on obtaining a better understanding of the physical basis of the fatigue process.

REFERENCES

1. Ho, C. L., Marcus, H. L., and Buck, O. — Ultrasonic Surface-wave Detection Techniques in Fracture Mechanics. Proc. SESA, vol. XXXI, No. 1, pp. 42–48, 1974.

2. Whittingham, T. A. — A Hand Held Electronically Switched Array for Rapid Ultrasonic Scanning. Ultrasonics, vol. 14, No. 1, pp. 29–33, January 1976.

3. Griffiths, J. W. R., Szilard, J., and Ishaq, N. — Synthetic Phased Array for Non-destructive Testing. Ultrasonics, vol. 12, No. 6, pp. 246–47, November 1974.

4. Sugg, F. E., and Kammerer, C. C. — On-board Ultrasonic Structural Surveillance. Matls. Eval., vol. 32, No. 8, pp. 157–62, August 1974.

5. Harting, D. R. — The S N-fatigue Life Gauge: Response to Random Inputs. ISA TRANS., vol. 8, No. 1, pp. 62–70, 1969.

6. Kowalski, H. C. — Prospects of a New Method for Determining Cumulative Fatigue Damage. ISA TRANS., vol. 11, No. 4, pp. 358–68, 1972.

7. Blackburn, E. J. — Direct Measurement of Fatigue Damage in Aircraft. Strain, vol. 7, No. 1, pp. 25–30, January 1971.

8. Dally, J. W., and Panizza, G. A. — Conductive Polymers as Fatigue-damage Indicators. Proc. SESA, vol. XXIX, No. 1, pp. 124–29, 1972.

9. Scott, I. G. — A Comparison of Eddy-current and Potential or Conduction Techniques in Non-destructive Testing. Dept. Supply, ADSS, Aeronautical Research Laboratories, Report ARL MET 73, March 1969.

10. Clark, G., and Knott, J. F. — Measurement of Fatigue Cracks in Notched Specimens by Means of Theoretical Electrical Potential Calibration. J. Mech. Phys. Solids, vol. 23, pp. 265–76, 1975.

11. Chin Quan, H. R., and Scott, I. G. — Operator Effects in NDT. Non-destructive Tstg., vol. 8, No. 4, pp. 195–204, August 1975.

12. Packman, P. F. — Fracture Toughness and NDT Requirements for Aircraft Design. Non-destructive Tstg., vol. 6, No. 6, pp. 314–24, December 1973.

13. O'Brien, K. R. A., Hollamby, D. C., Bland, L. M., Glanvill, D. W., and Scott, I. G. — Crack Detection Capability of Non-destructive Inspection Methods in Relation to the Airworthiness of Aircraft. Paper 7-2, presented on 2 June 1975, at the Eighth ICAF Symposium, Lausanne, Switzerland.

14. Klass, P. J. — Non-destructive Evaluation Effort Grows. Aviat. Week & Space Technol., vol. 104, No. 7, pp. 59–65, 16 February 1976.

15. Davidson, J. R. — Reliability after Inspect
NASA Tech. Memo TM -71969, 1973.

16. Shinaishin, O. A., Darlow, M. S., and Acquaviva, S. J.
Acoustic Emission Detection of Fatigue Crack Initiation and Propagation in Notched and Unnotched Titanium Specimens. Paper presented at 35th National Fall Conference, ASNT, 13–16 October 1975.

17. Hutton, P. H.
Monitoring High-temperature Fatigue using Acoustic Emission Techniques. BNWL-SA-3989, December 1971.

18. Williams, R. S., and Reifsnider, K. L.
Investigation of Acoustic Emission during Fatigue Loading of Composite Specimens. J. Composite Matls., vol. 8, pp. 340–55, October 1974.

19. Fuwa, M., Harris, B., and Bunsell, A. R.
Acoustic Emission during Cyclic Loading of Carbon Fibre Reinforced Plastics. J. Phys. D: Appld. Phys., vol. 8, pp. 1460–71, 1975.

20. Egle, D. M., Mitchell, J. R., Bergey, K. H., and Appl, F. J.
Acoustic Emission for Monitoring Fatigue Crack Growth. ISA TRANS., vol. 12, No. 4, pp. 368–74, 1973.

21. Ono, K., Stern, R., and Lang, M.
Application of Correlation Analysis to Acoustic Emission. ASTM, STP 505, pp. 152–63, 1972.

22. Smith, S., and Morton, T. M.
AE Detection Techniques for High Cycle Fatigue Testing. Proc. SESA, vol. XXX, No. 1, pp. 193–98, 1973.

23. Morton, T. M., Smith, S., and Harrington, R. M.
Effect of Loading Variables on the Acoustic Emissions of Fatigue-crack Growth. Expl. Mechs., vol. 14, No. 5, pp. 208–13, May 1974.

24. Harris, D. O., and Dunegan, H. L.
Continuous Monitoring of Fatigue-crack Growth by Acoustic Emission Techniques. Expl. Mechs. vol. 14, No. 2, pp. 71–81, February 1974.

25. Bailey, C. D., and Pless, W. M.
Acoustic Emissions used to Nondestructively Determine Crack Locations in Aircraft Structural Fatigue Specimens. Proc. 9th Symp. on NDE, San Antonio, pp. 224–32, April 1973.

26. Pollock, A. A., and Smith, B.
Stress-wave-emission Monitoring of a Military Bridge. Non-destructive Tstg., vol. 5, No. 6, pp. 348–53, December 1972.

27. Schofield, B. H.
A Study of the Applicability of Acoustic Emission to Pressure Vessel Testing. Technical Report AFML-TR-66-92, November 1966.

28. Corle, R. C., and Schliessman, J. A.
Flaw Detection and Characterisation using AE. Matls. Evaln., vol. XXXI, No. 6, pp. 115–20, 1973.

29. Dunegan, H. L.
Using Acoustic Emission Technology to Predict Structural Failure. Metals Engng. Quarterly, vol. 15, No. 1, pp. 8–16, February 1975.

30. Taira, S.
X-ray Diffraction Approach for Studies on Fatigue and Creep. Proc. SESA, vol. XXX, No. 2, pp. 449–63, 1973.

31. Baxter, W. J.
The Detection of Fatigue Damage by Exoelectron Emission. J. Appl. Phys., vol. 44, No. 2, pp. 608–14, February 1973.

32. Joshi, N. R., and Green, R. E.
Ultrasonic Detection of Fatigue Damage. Engng. Fracture Mechs., vol. 4, No. 3, pp. 577–83, September 1972.

33. Bhattacharya, S., and Schroder, K.
A New Method of Detecting Fatigue Crack Propagation in Ferromagnetic Specimens. J. Testg. and Evaln., vol. 3, No. 4, pp. 289–91, July 1975.

34. Charles, J. A., Appl, F. J., and Francis, J. E.
Using the Scanning Infrared Camera in Experimental Fatigue Studies.
Proc. SESA, vol. XXXII, No. 1, pp. 133-38, 1975.

35. Attermo, R., and Ostberg, G.
Measurements of the Temperature Rise Ahead of a Fatigue Crack.
Int. J. Fracture Mechs., vol. 7, No. 1, pp. 122–24, March 1971.

36. Reifsnider, K. L., and Williams, R. S.
Determination of Fatigue Related Heat Emission in Composite Materials.
Expl. Mechs., vol. 14, No. 12, pp. 479–85, December 1974.

37. Young, L.
Microwaves.
Electronics & Power, vol. 22, No. 2, pp. 106–12, February 1976.

38. Andrew, E. R.
Spin Mapping.
Phys. Bull., vol. 27, No. 1, p. 15, January 1976.

39. Pullan, B. R.
Seeing Inside the Body: Medical Imaging.
Phys. Bull., vol. 26, No. 10, pp. 447–49, October 1975.

40. Erf, R. K., Gagosz, R. M., and Waters, J. P.
Holography: A New NDT Tool Comes of Age.
6th National SAMPE Technical Conference, Materials on the Move, pp. 97–109, October 1974.

41. Archbold, A., and Eanos, A. E.
The Use of Laser Photography to Measure the Deformation of Weld Cracks under Load.
Non-destructive Testg., vol. 8, No. 4, pp. 181–84, August 1975.

42. Yee, B. G. W., Chang, F. H., and Couchman, J. C.
Applications of Ultrasonic Interference Spectroscopy to Materials and Flaw Characterisation.
Matls. Evaln., vol. XXXIII, No. 8, pp. 193–9, 202, August 1975.

43. Sachse, W.
Ultrasonic Spectroscopy of a Fluid-filled Cavity in an Elastic Solid.
J. Acoust. Soc. Am., vol. 56, No. 3, pp. 891–96, September 1974.

44. Zuckerwar, A. J.
Application of Ultrasonic Signature Analysis for Fatigue Detection in Complex Structures.
NASA-CR-138113, February 1974.

45. Cole, H. A., and Reed, R. E.
A Method for Detecting Structural Deterioration in Bridges.
NASA-CR-137548, July 1974.

46. Schrooer, R.
The Acoustic Impact Technique.
Non-destructive Testg., vol. 3, No. 2, pp. 194–96, June 1970.

DISCUSSION

QUESTION—*Grp Capt. I. Sutherland*
(RAAF)

Several years ago we were aware that the problem with flying acoustic emission equipment was the range of extraneous noise and lack of discrimination. Can you enlarge on the application of acoustic emission in flying aircraft?

Author's Reply

In recent years our understanding of AE has greatly improved. Consequently, AE experiments are currently being conducted overseas (USA) in aircraft during flight. ARL believes it has the expertise to undertake such experiments in Australia. It should be possible to make equipment small enough to fit into aircraft and extraneous noise can be handled by choice of suitable transducer frequency, adequate filtering and a logic-based signal acceptance approach. Signal discrimination on an amplitude basis is likely to be sufficient but more sophisticated methods are available if required.

QUESTION - *Sqn. Ldr. L. Watts*
(RAAF)

As aircraft continue in service the structure "works", fasteners become relatively loose, modifications and repairs are carried out. Will these factors require continual revision of the structural noises which must be filtered out in order to make practical service use of acoustic emission?

Author's Reply

Some experimental work has already been conducted in this area. Although much of the structural noise can probably be eliminated by filtering, much useful information would thereby be lost. Changes in structural noise may well be a useful indication of the presence of fatigue.

QUESTION --*H. A. Wills*
(Retired)

Is there any possibility of using changes in electrical properties with load as a means of indicating the onset of fatigue?

Perhaps in a manner analogous with the electric resistance strain gauge.

Author's Reply

Measurements have been made, on laboratory specimens, of electrical conductivity. Changes in conductivity have been noted as fatigue testing progresses, and before a crack has been detected by conventional NDI. As described in the paper, strain gauges made from special foils have been used to monitor fatigue but there are unsolved problems with calibration.

THE DEVELOPMENT OF THE THEORY OF STRUCTURAL FATIGUE

by

D. G. FORD

SUMMARY

The relation of structural fatigue to other branches of fatigue is outlined by a brief historical survey which includes the main ideas of the theory and ends with some of the current problems and possible developments.

In the sections about cumulative damage and reliability, there are some minor improvements over previous formulations.

1. INTRODUCTION

Almost all the applications of fatigue are related to the probability distribution of life for structural or mechanical components, mostly those not amenable to simple stress analysis. In view of this fact, it is strange to tell newcomers to the field that no theory is used for the specific estimation of the probability densities of fatigue lives. Instead there are two empirical recipes for the separate estimation of mean fatigue lives and for their variance: the nature of the distribution is scarcely considered, except for a largely subjective allocation of either of the classical log-normal or Weibull densities. This allocation generally relies on results obtained from simplified small specimens, and, like the damage theories makes no allowance for the interaction of different fatigue prone parts of a component or structure; the very process that is the basic substance of stress analysis and design.

Since World War II this methodology has become so entrenched that "lips can scarcely frame the words" to properly pose the problems that arise from practical questions. What is lost on this occasion is the ability to incorporate advances in fundamental knowledge or to unify various branches of fatigue and the closely allied subject of fracture mechanics.

Nevertheless, several lines of theoretical development have contributed an essential part to a valid framework that is capable of incorporating any describable type of stress or strain analysis and almost all the suggested types of cumulative damage. Correct results of course depend on the correct choice of these two components. Such a choice can only be made after a comparison between theoretical and experimental results (in sufficient numbers) *provided* the latter are analysed by the application of the general theory with several (stress analysis)–(damage law) pairs. The pair of laws to be chosen is of course that which matches most closely the *probability distribution* of the experimental results, and for different cases the most appropriate pair may vary. Once the same pair of laws covers a wide range of cases we may safely mark an advance in our understanding of fatigue. Before this stage is reached the application of a rational theory will in principle lead to the accurate delineation of complex fatigue from data accurate for simple cases.

In this paper we avoid most proofs and briefly survey and outline a new discipline termed *structural fatigue*. We shall use a historical approach to indicate its relation to other fatigue studies including those where more knowledge is needed.

2. REVIEW OF FATIGUE

It is worthwhile here to restate some of the common or even trivial facts of fatigue in language appropriate to structural fatigue.

First of all one must start with a structure which we define as any object evincing a "stress" when acted upon by a "load", and also of course capable of fatigue. This definition includes anything from a simple tensile fatigue specimen to a large aircraft and the practical meaning is simply the object or class of objects of one's attention. The aim of structural fatigue theory is merely to relate the fatigue properties of simple structures to those more complicated but *not* to explain fatigue itself.

The meaning of "stress' is usually plain but in our abstract setting it could refer to strain or in general systems to entities such as voltage or pressure.[1] However, there is a difference in meaning between the stresses which cause the static collapse of a structure and the alternating or mean stresses which are important to fatigue. Structural fatigue theory incidentally allows a free choice of such entities.

The term "load" may be given a similarly abstracted meaning and in fatigue there is here some more definite controversy[2,3] which appears when it is necessary to count cycles from fatigue meters etc. to form Kollektivs or "spectra".

The result of fatigue is eventually failure of the structure and this occurs in three stages: precracking or damage followed by initiation and growth of cracks and finally by failure of the weakened structure under one of the loads.

Let us examine each of these stages more closely. During what we here call the damage stage, damage will be proceeding in a microscopic but finite volume of material. If this were happening in just one spot the macroscopic local stress response would be constant. If there were several critical regions the stress at a point suffering damage would be affected by the (macroscopic) cracks elsewhere but not by any damages elsewhere. However, the most general supposition is that damage is *self-affected* even when the nominal stress is constant.

We have been forced to partially describe crack growth by contrast to damage. A "crack" is a geometric parameter, not necessarily length, which can affect the stresses caused by loads at any critical point. Its rate of growth depends on cyclic variations in "stress", normally expressed as an intensity, which is affected by the crack itself, by any other cracks should they exist, but *not* by any damages. Both cracking and damages are most generally described by including historical effects but in the following these are summarised by the crack formulae and the damage parameters. After-effects are more likely with damage, since, by definition, this continually proceeds at the original critical location.

To describe the two stages (which may approximate several) it has been necessary to postulate critical regions or "control points" where the damage that eventually leads to cracking proceeds. In structural fatigue as developed so far the number of critical points is taken as countable and moreover finite but such simplification may not be enough to represent a plain specimen or even a shallow stress concentrator. Some work has been done here by McClintock[4] but not in the general setting of two-stage fatigue.

At the atomic level, all types and stages of fatigue proceed largely by the movements of dislocations. Since this is basically a matter of kinematics except for extremely high speeds of loading, fatigue, like plasticity, is not *per se* time dependent. Ultimately, plasticity also arises from dislocations so that fatigue may be regarded as a type of plastic shakedown on a microscopic scale. This simplified picture is of course complicated by the effect of chemical and electrochemical reactions which do depend on time, but quantitatively these may be regarded as perturbations to a process basically independent of time but not sequence. For this reason the structural theory subsumes such effects into the data.

From the mathematical point of view, fatigue—and doubtless other processes—may be regarded as a set of interacting (random) processes, one at each critical point, which proceed in two stages the second of which is capable of affecting either of the other stages proceeding elsewhere. This is the abstract picture; at the physical level each of these stages is driven by a sequence of generalised stresses modulated through a system or rule of counting. In further detail, the cycles counted are also a random sequence but it is convenient to imagine that the parameters measuring damage or cracking change so little in each cycle that two further approximations are possible.[5] These are that the vectors of damage or crack length after each cycle are points from continuous differentiable functions of a continuous number of cycles or equivalently of some pseudo-time. To complement this it is postulated that the derivatives of these depend only on averages of various functions of the random stress sequence. These assumptions allow one to set up differential equations for the growth of crack or damage vectors.

A practical prerequisite for these equations is that the damage rule at each single critical point is known and that the stress at or near critical points is predictable enough to calculate stresses and intensities in the presence of all the cracks with suitable accuracy. As described in Section 3.3 the appropriate stress is true local stress with allowance for plasticity, etc.

The final stage in fatigue is static failure of the structure, generally weakened by the preceding cracks, but not *by definition*, weakened by damage. This is merely an extension of the rule that the crack rate is not affected by the damage vector and it should be regarded, not as a restriction in generality, but as a test as to whether a given process belongs to the early or late stage of fatigue, i.e. whether it should be classified as damage or as cracking in the terminology used here. It is unfortunate that in the literature these terms are used interchangeably despite this fundamental difference.

Incidentally the term "static" is somewhat tautologous as used here. It distinguishes the load that fails the structure from all the preceding loads that allow its continued existence to suffer more fatigue in the form of either damage or further cracking. There is no suggestion, for example, that inertia loads need be absent. The distribution of the number of cycles to this final failure is a branch of the wider discipline of reliability theory though it does have some difficulties peculiar to fatigue.[6,7,8,9]

We shall now discuss these three aspects in more detail in a loosely historical approach.

3. DAMAGE THEORY

The earliest common reference to a quantitative theory of damage is Palmgren[10] in 1924 who stated the well known Miner-Palmgren hypothesis and applied it to estimate the lives of ball races, not merely simple specimens. In the time since then it has exerted a hypnotic attraction to all who need to average the fatiguing effects of differing stresses. Its attraction lies in the somewhat misleading sobriquet "linear damage" with which it is normally taken to be synonymous. It is a true theory of damage in a sense to be described later, retaining its original virtue of simplicity, and there is strong evidence that many of its failures are due more to misuse or the absence of supporting concepts. The linearity of the rule makes it almost automatic as a choice of damage for the fatigue monitoring of aircraft fleets and in fact the only serious competitor in the future is likely to be canonical damage which may be regarded as a linearization of any damage into probability.

The linear rule is normally written in the form

$$\Sigma n(S_i)/N(S_i) = C \tag{1}$$

where C is a constant adjusted by circumstances, but originally taken as unity (the limit for constant amplitude loading). The notation presupposes only a countable choice of loads, and not a continuous domain, and there is a similar vagueness in the choice of the strictly random fatigue life $N(S)$. For a fixed total number of applied loads (i.e. Σn fixed) the moments of this damage have been found[11] when $n(S_i)$ is the limit of a multinomial choice and $N(S)$ is log-normal with a given autocorrelation function. It was noted that independence of the lives N implied variance of order $1/(\Sigma n)(N(S_1)-N(S_2))$ where S_1, S_2 are typical loads. This arises through a situation basically similar to that holding for limit theorems in probability.

One of the obvious weaknesses of Palmgren damage was that with the vague definition of damage as either crack growth and/or precracking the rate of fatigue failure did not seem constant and the first allowance for this was made by B. F. Langer[12] in 1937 who postulated two stages of damage, corresponding to our damage and cracking, each obeying a linear law with different values $N_1(S)$ and $N_2(S)$ for the lives. Since only the current loads could do damage in each phase the rule also implies a type of sequence effect. The other innovation in the rule was that it was the first of many rules that required more testing for their parameters than would be needed for the corresponding programme test.

After Langer's paper the next milestone in damage theory was the development of programmed loading in 1939 by Gassner.[13] This has no direct relation to damage but it is important as the forerunner of wider experimental checks for damage theories and the full-scale fatigue tests which are now accepted as the most realistic means[14,15] of assessing fatigue in large structures.

After World War II, there was a proliferation of damage studies many being described in the reviews of Kaechele[16] or O'Neill.[17] However, most rules were *post hoc* from small specimen tests and had the disadvantage that the amount of testing required to establish parameters exceeded that involved in a series of programme or random load tests. Also after the War, there was renewed interest in the physics of fatigue but it is fair to say that none of this had much effect on the development of damage theory.

Thus the volume of investigation in the post war period has forced us in this short paper to confine attention to those events that the author finds important to the theory needed for structural fatigue. The first of these is the publication in 1945 of Miner's famous paper[18] in which the linear rule advanced by Palmgren was justified by assuming a constant input of energy in each cycle. This has proved to be wrong but the predictions of the rule were good enough to become and remain the basis of most practical life estimation systems.

It is important to note that Miner did test the linear rule[10] experimentally, considered statistical aspects of the tests and defined failure as the *first appearance* of a visible crack. The last two aspects were due to be ignored in the widespread use of the rule and indeed in the modifications to it that were introduced to overcome its deficiencies. The latter became apparent quite soon and one of the earliest failures of the rule was when it was applied to random noise data in 1956 by Head and Hooke.[19] However, the order of magnitude agreement and the simplicity of the rule have conspired to ensure its survival in the crude form in which it is generally used.

Bastenaire Damage

To appreciate the shortcomings of present means of applying damage rules it is perhaps quickest to develop Bastenaire damage which we now briefly do.

The concept of damage was first thought of by Kommers.[22] After Palmgren, French[21] related it to the state of the material. The axiomatic form was discussed by Bastenaire[23,24] in 1955 though the version presented here differs in some details.

Firstly, the damage at some critical point is in general a vector which specifies the *state* of the material there. Because the entire state is thus specified there is no question of sequence or historical effects in any deductions from the axioms; they are subsumed into the components of the vector state or damage. One way in which the state may be completely elucidated is through discovery of the *distribution* of the residual life at some reference stress. The functionally independent moments of the residual life distribution (to initial failure in our case) may then be regarded as damage parameters and the existence of Bastenaire damage ensures a one-to-one relationship between these moments and the damage vector. The state of the material then constitutes an equivalence class of all one-to-one transformations of the original damage vector or of the moments of the residual life distribution. Therefore there is no unique measure of damage; the physical reason for this is that damage is the same for a given specimen however it is specified provided that the space of damage has a high enough dimension.

If damage is a state of the material then it is reasonable to follow some other authors (e.g. Torbe[17a]) and say that the "state" of the material varies with the stress level during a cycle. Most investigators tacitly ignore this possibility but it should be considered in an axiomatic theory. Figure 1*a* represents a time history of load and "damages" during two possible fatigue cycles of the same range but different wave forms.

Because fatigue is independent of time or frequency to a first approximation, all the "damages" depend only on the current stress as indicated by the closed rectangle. In order to set up differential equations for damage the temporary aberrations of "state" caused by current stress must also be eliminated. In concept this is done by replacing such "states" by a differentiable damage which interpolates points of the "state" at some reference stress. In Figure 1*a* the dashed curve is such a function and we suppose that Bastenaire damage has this nature.

Note that the axioms framed in terms of a residual distribution of life presuppose a universe or population of specimens to which the particular type of Bastenaire damage applies. Thus the same individual specimen in the same physical state but which could be classified under two populations say would give rise to two different equivalence classes to describe its damage, i.e. the damage laws would differ according to the population being considered. One of the dangers of this is that conditional distributions of life must be treated carefully.[1] The probabilistic state of damage above must represent in the sense of mathematical expectation all paths or sequences of damage states leading to the damage in question in proportions appropriate to the original population of virgin specimens. Otherwise the notional test of residual life distribution is meaningless.

For a general abstract space of damage the existence of Bastenaire damage is assured by the fact that there is always some reference stress whose repetition will eventually fatigue the specimen. In the general case however the damage itself is equally abstract and has little practical use. However, it is natural to suspect that the residual life distributions, including those from zero time, depend largely upon just one or two parameters so that the damage may be similarly described. Because it is now agreed that the change of physical state of the material is gradual it is also natural to suppose some continuity of damage with respect to different load sequences. Such a concept requires nearness of different sequences to be defined, i.e. a topology is needed. Unfortunately for the sequences important to fatigue which are essentially discrete and time-free the choice of open sets is still unresolved.

This difficulty, however, allows one to take advantage of time-continuous approximations to load histories and their usual topology to set up differential equations for the growth of damage. As discussed by Ford[5] the pseudo-time is assumed proportional to the number of turning points and there is a possible ambiguity in mapping a discrete sequence of load cycles into a continuous one since in the physically discrete sequence there may be several small cycles completed during the passage of one large one. The axiomatic suppression of sequence effects reduces the error in this to the order of

$$(\Delta T)\,(\mathrm{d}D/\mathrm{d}t) \qquad \text{(Fig. 1}b\text{)}$$

where ΔT is the displacement of sequence order or pseudo-time caused by mapping the discrete sequence onto the continuous one.

This does not mean that noticeably different sequences always lead to the same damage merely because the Kollektivs or spectra are the same. Different sequence paths $S(n)$ to the same

Kollektivs as in (3) below lead to generally different damages $\mathbf{D}(n)$ despite the ultimate equivalence of spectra.

Having made the approximation of continuous cycles, suppose that damage at a critical point is also differentiable so that

$$\mathrm{d}\mathbf{D} = \mathbf{A}(\mathbf{D}, \mathbf{S})\mathrm{d}n + \mathbf{B}(\mathbf{D}, \mathbf{S})\mathrm{d}\mathbf{S} \tag{2}$$

where

$\mathbf{D}$ = Damage vector,

$\mathbf{S}$ = Load or stress

and

$\mathbf{A}$, $\mathbf{B}$ are vector functions.

This is simply the chain rule but the second term is an effect caused merely by a *change* of load rather than its application. It was therefore ignored by Bastenaire to produce

$$\mathrm{d}\mathbf{D}/\mathrm{d}n = \mathbf{A}(\mathbf{D}, \mathbf{S}), \tag{3}$$

an autonomous differential equation. This agrees with our viewpoint as depicted by Figure 1*a*.

Equation (3) appears abstract but it has been shown[17] that most of the proposed damage rules can be cast into this *Bastenaire form* by eliminating constants, one of the normal means of creating differential equations. This has been done by O'Neill[17] and the supposed sequence effects of many rules turn out to be just the complexities associated with the original formulation. Figure 2 shows the rule of Marco and Starkey[25] in the present and original formulation, the latter avoiding derivatives by the implicit use of D.

It has been stated that damage belongs to an equivalence class. Some members of this class contain the probability of failure as one of the components of the damage vector. The fact that damage applies only to a defined population allows this component to be unique so that this subset of functional transformations must exist. Any component, F say, which is the probability of failure shall be described as *canonical*. If one parameter suffices to represent the damage then such a component will be called *canonical damage*. Equation (3), with $\mathbf{D}$ replaced by F, then describes the life distribution for the given population of structures when the load history $S(n)$ is defined. In symbols

$$f(n) = \mathrm{d}F/\mathrm{d}n = A_F(F, \mathbf{S}). \tag{4}$$

When there are several components, (4) is replaced on the right by a scalar function (23) of some equivalent damage vector. This amounts to a simple selection of the appropriate component from the transformation to the damage containing the canonical component. Thus the equivalence

$$\{\ldots, F, \ldots\} \to \mathbf{D}$$

allows the multiparametric form

$$f(n) = A_F(\mathbf{D}, \mathbf{S}) \tag{5}$$

of (4).

In (3) let the right hand side depend only on $\mathbf{S}$ and let the average life to failure be $N(\mathbf{S})$ under the constant amplitude loads. If we put $D = 1$ at $n = N(S)$ then this recovers the linear Miner-Palmgren rule but with the added interpretation that the life distribution under constant amplitude,

$$F = F(D). \tag{6}$$

Because this is a functional relationship the distribution may also be found under other load sequences including random ones. Another consequence is that all the life distributions under constant amplitude are affine transformations of one another. Thus lives under constant amplitude have a single logarithmic variance. The result was first suggested by Yokobori in 1954,[26] before Bastenaire who did not consider it. For lives to final failure this is clearly contradicted by experimental evidence which therefore refutes the Miner-Palmgren rule for final lives. For initial failures there are too few results for any decisions as yet.

Ford[1,5] has used Equation (6) inversely to derive another rule from observed lives to failure under the assumption that the constant amplitude lives are log-Normal. Again, there is insufficient evidence relating to initial failures. One consequence of any Bastenaire rule is that damage in the colloquial sense can be done by loads below the endurance limit[1] since the presence of some failures there ensures the existence of canonical damage even though there may be runouts. Canonical damage in turn ensures the existence of any equivalent kind, and the physical mechanism of this cannot, by definition, be related to the presence of cracks but only to microprocesses local to the initial failure.

It has been shown that the existence of Bastenaire damage implies that of canonical damage, i.e. knowledge of the life distribution. Other components of vectors containing canonical damage

(not necessarily unique) can be interpreted in other physical ways. This has been briefly discussed by Ford[1] but not applied. It seems possible that each component of damage corresponds to a different physical mode of failure and this knowledge can be used to postulate multi-parametric damages from suitable experiments.

The most important result of formulating Bastenaire damage was that it allowed the distribution of initial failures under random loads to be calculated, at least implicitly. The simple fact that life to final failure was the sum of a random initial life and an approximately fixed time of crack growth allowed the revival of Langer's two stage structural theory. This has still been developed only for random loads, not necessarily "white", but this is by far the most important case.

In (5) let

$$\mathbf{S} \sim F(\mathbf{S}) \tag{7}$$

using F generically to denote the distribution function of its argument. Then the average density stemming from a given damage D

$$f(n) = \int A_F(\mathbf{D}, \mathbf{S})\, \mathrm{d}F(\mathbf{S}),$$

from (5),

$$= \hat{A}(\mathbf{D}), \qquad \text{say.} \tag{8}$$

If **D** is the consequence of a random load history then (8) may be regarded as another equation

$$\mathrm{d}/\mathrm{d}n\, F(\mathbf{D}) = \hat{A}(\mathbf{D}) \tag{9}$$

for the growth of average damage in pseudo-time including canonical damage.

Log-Normal Damage

To illustrate the applications of (3), (8) and (9) consider log-Normal damage.[1] Under constant amplitude let

$$F(\log n) = \Phi\{(\log n - \mu(S))/\sigma(S)\}G(S) \tag{10}$$

where Φ is the unit Normal distribution function. The runout probability $1 - G(S)$, which is similar to a probit function, may be regarded as part of the specification of the constant amplitude life distribution. Using $F = G(S)\Phi$ as canonical damage, ϕ to abbreviate the unit Normal density and Φ^{-1} as the inverse function or probit of Φ,

$$F = G(S)\,\Phi\{(\log n - \mu(S))/\sigma(S)\}$$

and

$$\sigma(S)\,\mathrm{d}F/\mathrm{d}n = G(S)\phi\{\Phi^{-1}(F/G(S))\}\exp\{-\sigma(S)\,\Phi^{-1}(F/G(S)) - \mu(S)\} \tag{11}$$

is the Bastenaire form for this type of canonical damage. It will be noted that (11) is almost in the form of an equation for the unit Normal deviate $\Phi^{-1}(F/G(S))$ so that this is equivalent to the convenient pseudo-damage

$$\frac{\mathrm{d}u'}{\mathrm{d}n} = \frac{\mathrm{d}F}{\mathrm{d}n}/G\phi(u')$$

$$= \sigma(S)^{-1}\exp(-u'\sigma(S) - \mu(S)) \tag{12}$$

This is a pseudo-damage since the inclusion of $G(S)$ in the transformation means that the interpretation depends on the current load cycle. However, it does hold if $G = 1$ when it follows that the rule (12) resembles a Miner-Palmgren rule with linear damage weighted by a factor $1/(\sigma(S)\exp(u\sigma(S))$. The true deviate damage is actually

$$u = \Phi^{-1}(F)$$

for which

$$\frac{\mathrm{d}u}{\mathrm{d}n} = \frac{G(S)\mathrm{e}^{-\mu(S)}}{\sigma(S)} \cdot \exp(-\sigma(S)\Phi^{-1}(\Phi(u)/G(S))) \cdot \frac{\phi(\Phi^{-1}(\Phi(u)/G(S))}{\phi(u)} \tag{13}$$

This reduces to (12) when $G = 1$ but otherwise the first factor approximates damage done below the endurance limit, when $G \leqslant 1$. The terms Φ^{-1} vanish when $\Phi(u) \to G(S)$ and then cease to be real. This represents a failure of the one parameter theory but the conservative approach

would be to make $du\,dn$ zero in such cases. From such a time onwards, if all the loads were small enough there would be a probability

$$1 - \Phi(u)$$

of runouts.

To illustrate (9), let the cycles be distributed $F(S)$ so that (11) averages to

$$f(n) = \int_0^{S_{ult}} \frac{G(S)\,dF(S)}{\sigma(S)\,e^{u(S)}} \cdot \phi\left\{\Phi^{-1}\left(\frac{F}{G(S)}\right)\right\} \cdot \exp\left\{-\sigma(S)\,\Phi^{-1}\left(\frac{F}{G(S)}\right)\right\} \tag{14}$$

The form of this distribution obviously depends on the Kollektiv as expressed in $F(S)$. Since this has followed from a simple type of Bastenaire rule it seems likely that the query "what is a typical type of life distribution in random load fatigue?" is fatuous. Equation (14) is effectively a first order differential equation for $F(n)$ since the load S is a dummy variable of integration.

In structural fatigue, densities like (9) or (14) are not solved alone but have their equations coupled with crack growth equations including generally those for cracks elsewhere. Thus in (14) S and hence $F(S)$ depend on the crack vector which in turn because of its randomness depends on $f(n)$. The exceptions to this are when there is only one critical point or when there is no interaction between cracks. Both of these cases are of course common and strictly the first is an example of the second. Before leaving this illustration, consider the analogue of (14) based on the equivalent damage u. This is merely a similar average of (13) and the same holds for any equivalent damages since the transformations cannot depend upon the load.

The experimental inputs to (13) or (14) are $\sigma(S)$, $\mu(S)$ and $G(S)$ all of which should be obtainable from suitable S-N tests to initial failure. Unfortunately there are no systematic test results known to the author because of the added requirement that all failures be the cycles to the first crack, suitably defined.

There is of course no reason why any of the Bastenaire rules cannot be applied to final failure but this negates their conceptual importance in structural fatigue. Bastenaire (ca 1960) has tested many steel specimens for IRSID in two step tests while Ford[27] has described some results (Fig. 3) of applications to data of Webber and Levy.[28] The agreement in each case was fair but it should be remembered that only final failures were considered. In Bastenaire's tests the damage function was taken to be a power law which is strange when one recalls that the canonical form of damage, which immediately suggests log-Normal damage, was first advanced by Bastenaire in his original paper.

Another damage of possible interest could be based on the observation[29] that the scatter of random or programme lives is similar to the scatter at the maximum amplitude.

Finally there is no reason why any canonical damage rule need only be applied to those cases where the constant amplitude density is known. For example, in log-Normal damage (11) becomes the axiom rather than (10) and afterwards the actual failure distribution is some function of F. However, the choice of a rule does restrict the life distributions. Thus the Miner-Palmgren rule can be applied to any data, initial or final, but it cannot be correct unless at least the constant amplitude densities are affine.

Damage and Residual Stress

The enormous number of programmed and random tests which cannot be applied to structural fatigue are mostly described in terms of the nominal stress and a stress concentration factor K_t. Because of this, the actual stresses at the notch roots have not been known, and useless rules have been compared on the basis of fictitious stresses or strains. Fortunately this situation has altered recently with the introduction of companion testing[30,31] and the spreading use of Neuber's rule[32] for a closer approximation of notch root stresses.

This rule states that

$$K_t^2 = K_\sigma K_\varepsilon \tag{15}$$

where the right hand quantities denote stress and strain concentration factors and K_t is the geometric factor. According to Topper *et al.*[33] K_f is prefereable to K_t and when K_σ is related to K_ε by the cyclic stress-strain curve or more correctly the one applicable at the time then (15) with K_f leads to notch root stress or strain. Equation (15) can also include changes in mean stress or strain[34] and the latest ESDU method uses this approach.

From our viewpoint, this is necessary to structural fatigue but (15) should not be regarded

as relating to damage but as part of the detailed stress analysis of the structure. In the use of (14) or similar equations, $F(S)$ refers to the notch root stress. The sequence of nominal stresses therefore has a marked effect on $F(S)$ and at present the only way to find the distribution of damage stresses is through simulation of the notch root conditions. This needs to be done often during a life distribution calculation and is likely to consume much computing time.

4. FRACTURE AND CRACK GROWTH

Fracture and Reliability

There is no need here to repeat the history of fracture mechanics except to state that the earlier papers of Griffith, Orowan, Wells and Irwin[35,36,37,38] bring us to the early 1960s when interest arose[39,40] in the application of reliability theory to the final fracture part of the fatigue process. At first sight, the various forms of fracture prediction are ideal partners to reliability theory and indeed they would be if they were accurate enough. Unfortunately, the life predictions from reliability are sensitive both to the accuracy of strength estimates and the scatter of these caused by variations of fracture toughness K_c. Because of this the practice at ARL has been to use numerical methods based upon experimental crack lengths.[41] Structural fatigue theory is outside this realm since its aim is to predict distributions of crack lengths which may then be used for the risk or hazard in a reliability estimate.

For completeness, we shall briefly outline reliability theory as applied to the failure of unmaintained structures. Other treatments[44,45,46] apply idealised assumptions to consider inspection intervals. There are also approximate analyses[45,46] of the case below.

Suppose that the length of cracks in the structure has the (possibly improper) density $f(\mathbf{a}|n)$ at n cycles and also that the strength for the crack vector $\mathbf{a}$ is distributed

$$R \sim f(R|\mathbf{a}).$$

Then the probability of failure during the nth cycle, the risk or hazard, is

$$h(n) = \int_0^\infty \int_0 \int_0^\infty \mathrm{d}F(S)\,\mathrm{d}F(R|\mathbf{a})\,\mathrm{d}F(\mathbf{a}|n) \tag{16}$$

It is convenient to split this integral into different parts according to the nature of the failure, noting first that $f(\mathbf{a}|n)$ is the solution of the standard problem of structural fatigue. The cracks may first be divided into those that do not affect the strength and, among the others, the runaway cracks for which $R = 0$. For simplicity the former will be equated with $\mathbf{a} = \mathbf{0}$ with the finite probability $\mathrm{d}F(\mathbf{0}|n)$ and the corresponding strength will be the fixed ultimate U. For runaway cracks $R = 0$ without loss of generality and the integral (16) reduces in order.

Thus

$$h(n) = \int_{\mathbf{a}_0}^{\mathbf{a}_u} \int_0^{R(\mathbf{a}_0)} \int_U^\infty \mathrm{d}F(S)\,\mathrm{d}F(R|\mathbf{a})\,\mathrm{d}F(\mathbf{a}|n)$$

$$+ \mathrm{d}F(\mathbf{0}|n) \int_U^\infty \mathrm{d}F(S) + \mathrm{d}F(\infty|n), \tag{17}$$

where the last term is the concentrated probability that there will be runaway cracks during the nth cycle. The second term is due to static load failures on an uncracked structure. In the first term, $\mathbf{a}_0$ is an initial crack which may be $\mathbf{0}+\epsilon$ although the evidence indicates finiteness. It will be important to discussions later.

Although (17) uses vector cracks, the loads there are scalar. The extension to several types of load or modes of static failure has not been seen by the author. It seems most natural to assume that each crack vector is associated with a random region in load space which is of course associated with static failure. The simplest description of such a region would be a functionally defined subset $B(\mathbf{R})$ of some abstract random vector $\mathbf{R}$, where

$$B(\mathbf{R}) \subset R_n,$$

the load space. For example, if $\mathbf{R}$ were scalar then it could represent a general scaling factor of all fracture toughness associated with the cracks. With this formulation the first integration of (16) changes to the region $B(\mathbf{R})$.

The dissection of (17) is now less obvious but if it is assumed that all of the crack lengths

and strength components of **R** are coupled, then the original strength should be associated with $\mathbf{a} = \mathbf{0}$, the absence of any initial failures. Similarly if any crack component becomes infinite then, because we have assumed that all load components load every critical region, failure must occur for any load that is applied except for cases of zero probability. The probability of runaway cracks then becomes harder to define. The simplest notation for the event is probably

$$1 - \int_{a_i < \infty} \mathrm{d}F(\mathbf{a}|n)$$

in terms of the complementary event. With these extensions

$$h(n) = \int_C \int_{R_s} \int_{B(R)} \mathrm{d}F(\mathbf{S})\, \mathrm{d}F(\mathbf{R}|\mathbf{a})\, \mathrm{d}F(\mathbf{a}|n) + \mathrm{d}F(0|n) \int_{B(U)} \mathrm{d}F(\mathbf{S}) + \{1 - \int_C \mathrm{d}F(\mathbf{a}|n)\} \tag{18}$$

where

$C = \{\mathbf{a} : a_0 \leqslant a_i \leqslant a_u\} \subset R_s$ with strict equality for at least one i,
$B(\mathbf{R}) \subset R_s$, the region for static failure defined by abstract strengths **R**,
a_u is a length defining runaway cracking, and
$U \epsilon R_R$ is the abstract ultimate when $\mathbf{a} = \mathbf{0}$.

Now $h(n)$ is a probability conditional upon the absence of prior failure whose probability may be written $1 - F(n)$. Hence, assuming continuous cycles,

$$Pr(\text{Failure at } n\text{th cycle}) = h(n|\text{No prior failure})\,(1 - F(n)) = \mathrm{d}F/\mathrm{d}n,$$

by definition, with $F(0) = 0$. The solution is

$$F(n) = 1 - \exp\{-\int_0^n h(n)\, \mathrm{d}n\}. \tag{19}$$

For the small probabilities of practical interest $f(n) \simeq h(n)$ and there is also a noticeable burning-in effect by which weaker structures are removed[47] more rapidly than others. This process also affects the average crack growth rates if it is assumed that failures are removed from the set of fatiguing structures. Reference 5 discusses this briefly but more investigation is still needed.

Crack Growth

After the almost unnoticed advent of the Bastenaire view of cumulative damage[23,24] the next breakthrough in fatigue theory was the publication in 1959 of a paper by Paris, Gomez and Anderson[48] which correlated constant amplitude growth rate with stress intensity. General confirmation has continued up to the present in the sense that improvements must be framed in the language of fracture mechanics. The empirical aspects of cracking have now shifted away from the growth of particular cracks to the relation $\mathrm{d}a/\mathrm{d}n$ vs. ΔK and its shortcomings. For most materials, this has the form shown in Figure 4 and the first suggestion of Paris[50] was that

$$\mathrm{d}a/\mathrm{d}n = c\Delta K^4$$

which was still reasonable when ΔK was taken as the rms. value of random noise.[53] In the study of non-dimensional growth data it was noticed by Ford[1] and independently by Roberts and Erdogan[52] that

$$\mathrm{d}a/\mathrm{d}n = c\Delta K^m K_{\max}{}^n = c(1-R)^n\, \Delta K^{m+n} \tag{20}$$

formed a good approximation to constant amplitude results for aluminium alloys. When $m = n = 2$ this may be interpreted as a model in which $\mathrm{d}a/\mathrm{d}n$ is proportional to the size of the plastic enclave and to the zone of reversed plasticity. This lends some theoretical support to the original fourth power law but it is too inaccurate in practice.

A frequently quoted growth relation is that first advanced by Forman, Kearney and Engle[53] which forces an infinite rate when $K_{\max} \to K_c$. Although this is intuitively appealing the rates indicated for high loads have little effect on averages and are actually overshadowed by retardation effects. There is no general agreement that the empirical fit is good[54] (see Fig. 5) and apart from this it has been noticed by Cheverton[55] that finite though rapid growth rates obtain even up to the point of failure.

The non-dimensional presentation of data[1] is based on the variables $\xi = \left.\dfrac{\mathrm{d}a}{\mathrm{d}n}\right/ r_n$, $\eta = r_{\max}/\rho_0$ and for thickness $\tau = t/r_{\max}$, where r_n and $r_{\max}$ are the nominal plastic zones associated with the intensities ΔK and $K_{\max}$ and ρ_0 is a characteristic length.

Convenience dictated the choice of nominal zones but the essential idea is that of geometrical ratios. In Figure 6 it may be seen that ξ varies between 10^{-3} and 1, corresponding to rates near the lattice spacing up to static failure which might be characterized by equality of the crack step and r_{max}.

The non-dimensional plotting highlights the now accepted fact that there are roughly three main regimes which correspond to different growth mechanisms. One of these is a type of pause above which the fatigue failure includes larger amounts of cleavage. This higher part also seems to be associated with transition to the 45° mode of propagation.[56,57] There is also some minimum ΔK needed for growth to start. Like the other parts of the crack rate relation this can be critically affected by environment.

Initial Length a_0

Because of the testing time the slow growth parts of ξ vs. η or da/dn vs. ΔK relations tend to be ill-defined but there is a clear suggestion that any crack must reach a minimum length to be "self-propagating". Reinterpretation of results for non-propagating cracks supports this and since Forsyth[60] it has been accepted that there are at least two types of crack growth in fatigue. The lengths at transition and of non-propagating cracks tend to have the same order of magnitude which in turn is similar to grain sizes and the range of surface residual stresses.

Thus with very small cracks there are many complications introduced among which is their interpretation as cracks at all. When it is also remembered that da/dn cannot be integrated from the singularity $a = 0$ of all known growth relations then the reasons for postulating a minimum crack length become overwhelming for any fracture mechanics (i.e. realistic) formulation of growth rate. However for the reasons above, the value of a_0 is extremely uncertain. Each of the phenomena mentioned suggest their own version of a_0 which may be loosely regarded as the diameter of the volume of material undergoing the damage before initial failure (whose definition depends on a_0). For maximum accuracy, it appears that a_0 should be chosen as that length above which fracture mechanics adequately predicts da/dn. Fortunately it can be argued (see below) that the damage rule can be modified to allow for changes in a_0.

In the fatigue of practical structures the sizes of notches, holes, etc., may also suggest an a_0 based on a typical dimension of these.[1,5] This would avoid calculation of intensity for awkward geometries but it retreats from the ideal of structural fatigue based on true phenomena back towards the present practice of adjusted comparative estimates of mean lives.

In the future it is most likely that the choice of a_0 will be aided by further investigation of transition form Type I to Type II cracking, testing the limits of applicability for stress intensity and simple *ad hoc* adjustments to fit predictions to test results.

Crack Closure and Retardation

It was first suggested by Elber[61] that during the growth of cracks under constant amplitude the faces of the crack start to touch before the minimum load is reached: this was supported by an approximate finite element type of model.[62] It has since been confirmed[63,64] and there are now methods of estimating the magnitude of the effect. The most plausible viewpoint is the model of Reference 65, in which natural elastic closure is prevented by plastic extensions around the lip of the crack. The faces are wedged apart by deformed material near the tips which means that even when the structure is unloaded there remains a residual intensity at the tip.

Under constant amplitude loading the effective intensity thus varies between this residual value and the nominal maximum so that the range is less and the mean greater, than one would otherwise expect. It follows that the removal of the residual intensity may allow faster propagation. Removal can be effected by either a period of low amplitude cycling or else by negative loads and after such procedures it has been observed that growth rates do increase.[65,66]

On the other hand, crack rates are dramatically decreased by preloading. This was first noticed by Hardrath and quantitative models have been advanced by Wheeler and Willenborg *et al.*,[67,68] which are both based on the relative sizes of the crack step and the current plastic zone. These models are empirical but there is a chance that extensions of crack closure studies will also elucidate retardation and acceleration.

In practice, it has generally been found for flight-by-flight sequences that the rate is fairly well estimated by straight forward summation of individual steps,[51,69] i.e. the various effects of randomness cancel. However, this rule of thumb is not absolute.[1]

Random Loads and Structural Fatigue

Detailed knowledge of cracking concerns individual striations or at most the effect of short

sequences. In structural fatigue, the need is to estimate lengths over several hundred hours or tens of thousands of cycles for many levels of average intensity. Thus the micro-steps above must be averaged over some hundred or thousand cycles after which these averages will form the derivatives in the partial differential equations for crack length densities. This implies the existence of crack growth and stress intensity subroutines in the package for their solution. Existing programmes for crack growth use cycle-by-cycle summation without regard for interactions. For the present this is adequate apart from the possible penalty in computing time but more knowledge of small scale statistical structure of the growth striations would be useful.

At present the theory of structural fatigue can allow for small scale randomness in da/dn but there is evidence[10] that each crack growth specimen has its own general crack rate as well as the small variations between successive cycles. The type of allowance in structural fatigue for such "random averages" is uncertain and the random or batch effects on da/dn need to be studied.

5. GENERAL THEORY

By 1961, all the ingredients for a rational theory were available namely differential equations for crack growth, cumulative damage for the distribution of initial failures and the given stress analysis. In the present discussion we have minimised the role of stressing by relegating it to the class of solved problems or, more accurately, those to be solved by others. The effect of stressing errors, which can include neglect of notch root strains, plasticity, etc., is similar to that of dimensional errors or of "random averages" for crack rates: outputs change but not the methods.

In 1967 the author presented a thesis[1] in which the two streams of canonical damage and crack growth were combined. The approach was to assume that da/dn was a deterministic function of crack length (on the macroscopic scale) and consider the growth of a crack whose randomness was entirely due to that of the initial failure, i.e. $f(\mathbf{t})$ ($\mathbf{t}$ = initial lives) was the derivative of canonical damage, and the crack vector at time n depended deterministically on the multipoint initial failures $\mathbf{t}$.

By analogy with the probability transformation in statistics it is useful to introduce the concept of fatigue as the sequence of transformations or mappings:

$$\mathbf{F} \to \mathbf{t} \to \mathbf{a}\,n \to h(n) \to f(n), \qquad N \text{ cracks},$$

where reliability spaces for $h(n)$ and $f(n)$ have been added to the original list. The first three terms are the damage hypercube $\{0 < F_i < 1\}$, initial lives in R_N, and crack lengths at n cycles, also in R_N. If it is assumed that the density of canonical damage in the hypercube is uniform, which amounts to independence between *damages* at critical points, then an almost immediate consequence is the independence theorem which states that

$$f(\mathbf{t}) = f_1(t_1) f_2(t_2) \ldots f_N(t_N), \quad \mathbf{t}_2 = (t_1 \ldots t_2\ \mathbf{o}). \tag{21}$$

The proof follows from the facts that the right hand side is merely the Jacobian of the transformation $\mathbf{F} \to f(\mathbf{t})$ and that $f(\mathbf{F}) = 1$. Obviously it depends upon the differentiability of the mapping and the number of cracks N but the truth of (21) is *not changed*. $f(\mathbf{F}) = 1$ means that each critical point is constructed from random batches of material.

Similar attempts by the author to construct a Jacobian for $\mathbf{t} \to \mathbf{a}\,n$ have been unsuccessful. Another approach is to choose many damage vectors $\mathbf{F}_j = \{F_{ji}\}$ say and integrate the damage equations from $\mathbf{F}(0) = \mathbf{0}$ until the components of damage reach F_{ji} in turn. The time of each occurrence is t_{ji} and subsequently this crack component, being non-zero may be "grown" so that the set of cracks $\mathbf{a}_j$ thus produced at time n is a mapping

$$\mathbf{F}_j \to \mathbf{t}_j \to \mathbf{a}_j n,$$

part of the fatigue of a particular specimen. The average over j of several $\mathbf{a}_j n$ s from such calculations is a Monte-Carlo solution for the average crack length and $f(\mathbf{a}\,n)$ is also estimated. Although this approach is potentially useful at least to check other methods it has not been pursued.

In the section about crack growth, the importance was stressed of the initial crack a_0. However, there was some latitude in its choice since errors here could be compensated in the canonical damage. Physically, the density of canonical damage is made to contain all the probability measure associated with cracks of length less than a_c which lie on the same trajectory

(Fig. 7). In practice this depends on having some knowledge of the propagation of such micro-cracks and the actual distribution of initial cracks, i.e. $f(a_0)$. However, experience with life prediction should enable direct adjustment of the damage rule and a_0 for best results. It is likely that the construction in Figure 7 could be elevated into an existence proof for canonical damage.

Crack-Damage Equation

Because the statistics of loads are either stationary or else known with regard to time and because crack rates are meant to be averaged over some hundreds of cycles, the differential equations for cracking take the form

$$\mathrm{d}\mathbf{a}/\mathrm{d}n = \mathbf{R}(\mathbf{a}), \qquad \mathbf{a}(n_*) = \mathbf{a}_*,$$

where one component of $\mathbf{a}_*$ is a_0. Similarly for damages

$$\mathrm{d}\mathbf{F}/\mathrm{d}n = \mathbf{A}(\mathbf{a}, \mathbf{F}), \qquad \mathbf{F}(0) = \mathbf{0}. \tag{22}$$

But these apply to a particular case. In the crack-damage theory of Reference 1, (22) was generalised to apply to *average* cracks and damages. This couples the two equations into a combined system of order $2N$ of the form

$$\begin{aligned} \mathrm{d}\mathbf{a}/\mathrm{d}n &= \bar{\mathbf{R}}(a) + a_0\bar{\mathbf{A}}(\mathbf{a}, \mathbf{F}), & \mathbf{a}(0) &= \mathbf{0}, \\ \mathrm{d}\mathbf{F}/\mathrm{d}n &= \bar{\mathbf{A}}(\mathbf{a}, \mathbf{F}), & \mathbf{F}(0) &= \mathbf{0}, \end{aligned} \tag{23}$$

the crack damage equations. It will be noted that the averaging has changed the original homogeneous equations into a single initial value problem with a forcing function coupling the two parts and proportional to a_0. Unfortunately the solution of (23) depends in turn upon solutions of $2^N - 1$ similar sub-problems stemming from the presence or absence of cracks at various critical points. This can be circumvented by approximation but the consequent algorithm is complicated and still approximate. However, one result that follows from (23) is that all moments of $\mathbf{a}(n)$ follow from linear differential equations which depend recursively upon the solutions for lower moments. One important conclusion is that much of the scatter in $\mathbf{a}(n)$ is caused by the presence or absence of the other cracks.

Markovian Formulation

After the crack-damage equations (23), the next breakthrough was the realisation that the system (22), exact within the present context, specifies a Markov process with the state vector $\{\mathbf{a}, \mathbf{F}\}$ in R_{2N}. For one crack, consider the probability density of a at times n and $n - \mathrm{d}n$ (Fig. 8), confining ourselves for simplicity to deterministic growth. For such cases

$$\begin{aligned} Pr(a \leqslant \text{Crack length} \leqslant a + \mathrm{d}a) &= f(a, n)\,\mathrm{d}a \\ &= f(a - \mathrm{d}a, n - \mathrm{d}n)\,(1 - (\mathrm{d}R/\mathrm{d}a)\mathrm{d}n)\,\mathrm{d}a \\ &- \left\{ f(a) - R(a)\frac{\partial f}{\partial a}\mathrm{d}n - \frac{\partial f}{\partial a}\mathrm{d}n \right\}\left\{1 - \frac{\mathrm{d}R}{\mathrm{d}a}\mathrm{d}n\right\}\mathrm{d}a \end{aligned}$$

which has for a limit the linear first order Chapman-Kolmogorov equation[71]

$$\frac{1}{f}\frac{\partial f}{\partial n} = \frac{R(a)}{f}\frac{\partial f}{\partial a} + \frac{\mathrm{d}R}{\mathrm{d}a} \tag{24}$$

where $\mathrm{d}R/\mathrm{d}a$ is a known function of a, because the crack growth law is an input to (22). The characteristics for (24) follow[72] from

$$\mathrm{d}n = \mathrm{d}a/R(a) = -\mathrm{d}f/f\,R'(a) \tag{25}$$

and the initial conditions for (24) from Figure 8 are

$$f(a_0, n) = f(n)/R(a_0).$$

The first equality in (25) indicates that the crack trajectories are base characteristics whilst the second with the initial conditions included shows that

$$f(a, n) = f(n_t)/R(a), \qquad a(n_t) = a_0, \tag{26}$$

along the crack trajectory. In (26) $f(n_t)$ is the initial failure density (or canonical damage) at n_t, the beginning of the crack through $a(n) = a$.

When there are several cracks (24) becomes

$$\frac{1}{f}\frac{\partial f}{\partial n}+\sum_{i=1}^{N}\frac{R_i(a)}{f}\frac{\partial f}{\partial a_i}=-\sum_{i=1}^{N}\frac{\partial R_i(a)}{\partial a_i} \tag{27}$$

where the ieft is the total derivative along the crack trajectory and the right hand side is a divergence or dilatation term. The alternative form of (27) is

$$D/Dn \log f = -\text{div } \mathbf{R}$$

which is analogous to the linearised equation of continuity for compressible fluid flow.

The initial conditions are complicated by the fact, that corresponding to the sub-problems in crack-damage theory, there are several subspaces of the crack-space with successively fewer cracks. During the fatigue process several of these are traversed in turn as more cracks begin and for each new crack there is a set of new boundary conditions which must arise from the solutions of canonical damage equations coupled with the growth of existing cracks.

6. FUTURE DEVELOPMENTS

Equation (26) can be applied immediately to reliability calculations,* and with change of variable it also applies to other less realistic crack models in use now. To complement this, the solution of (24) with various right hand sides has been programmed and a package for the more general (27) is being developed for $N = 3$.

In structural fatigue and reliability, the concept of runaway cracks needs to be included and generalised to cracks joining each other.

However, the most pressing need is for data that truly relates to the two stage fatigue process and its details. It is 15 years since Forsyth categorized crack growth and 40 years since Langer, on the evidence of his day, proposed that fatigue involved at least two stages. It is therefore disappointing to know that there is virtually no useable engineering data about initial failure for common alloys. Equally important, though less disappointing because this recent problem is attracting attention, is the need for a reliable engineering theory of crack growth under general load sequences.

Part of these deficiencies may be remedied by the inverse use of structural fatigue but provision of data is no more part of it than measurement of E or μ is part of elasticity theory. Successful application of theory requires data gathered for the purpose, that are preferably compatible with solid state physics; fatigue is now a large interdisciplinary subject whose further progress implies that those who actually and rightly specilize develop some appreciation of all its branches including structural fatigue.

---

* The addition of a reliability term to (24) has proved simpler and more significant.

REFERENCES

1. Ford, D. G. — The Analysis of Structural Fatigue. Ph.D. Thesis, Imperial College of Science and Technology, London, April 1967.
2. Schijve, J. — Analysis of Random Load time Histories with Relation to Fatigue Tests and Life Calculations. Fatigue of Aircraft Structures (eds. W. Barrois and E. L. Ripley). Proceedings of ICAF Symposium, Paris, 16–18 May 1961; Pergamon, 1963.
3. Matsuishi, M., and Endo, T. — Fatigue of Metals Subjected to Varying Stress. Paper presented at Japan Society of Mechanical Engineers, Fukuoka, Japan, March 1968.
4. McClintock, F. A. — The Statistical Theory of Size and Shape Effects in Fatigue. Journal of Applied Mechanics, Vol. 22, No. 3, pp. 421–26, September 1955.
5. Ford, D. G. — A Unified Theory of Structural Fatigue. ARL Report SM 338, May 1972.
6. Freudenthal, A. M., and Payne, A. O. — The Structural Reliability of Airframes. Technical Report AFML-TR-64-401, December 1964.
7. Birnbaum, Z. W., and Saunders, S. C. — A Statistical Model for Life-length of Materials. Journal of American Statistical Association, Vol. 53, No. 281, pp. 151–60, 1961.
8. Eggwertz, Sigge — Inspection Periods Determined from Data on Crack Development and Strength Reduction of an Aircraft Structure using Statistical Analysis. Proceedings of Symposium on Fatigue of Aircraft Structures, 1961; MacMillan, New York, 1963.
9. Payne, A. O., and Grandage, J. M. — Probabilistic Approach to Structural Design. Proceedings of First International Conf. on Application of Statistics and Probability to Soil and Structural Engineering, Hong Kong. Hong Kong University Press, September 1971.
10. Palmgren, A. — Die Lebensdauer van Kugellagern (The Life of Ball Bearings). Zeitschrift Vereines Deutsches Ingineurs, Vol. 68, No. 14, pp. 339–41, 5 April 1924.
11. Ford, D. G., and Lacey, G. C. — The Probability Distribution of Linear Cumulative Damage in Fatigue. Australian Aeronautical Research Consultative Committee. Report ACA-64, November 1962.
12. Langer, B. F. — Fatigue Failure from Stress Cycles of Varying Amplitude. Journal of Applied Mechanics, Vol. 4, pp. 160–62, December 1937.
13. Gassner, E. — Festigheitesversuche mit wiederholter Beanspruchen im Flugzeugbau (Structural Tests with Repeated Loads in the Construction of Aircraft). Luftwissenschaft, Vol. 6, No. 2, pp. 61–64, February 1939.
14. Payne, A. O. — Determination of the Fatigue Resistance of Aircraft Wings by Full Scale Testing. Proceedings of Symposium on Full Scale Testing of Aircraft Structures, Amsterdam 1959; Pergamon Press, 1961.
15. Schütz, D., and Loesk, H. — The Application of the Standardised Program for the Fatigue Life Estimation of Fighter Wing Components. Proceedings of 8th ICAF Symposium, Lausanne, June 1975.

16. Kaechele, L. — Review and Analysis of Cumulative Damage Fatigue Theories. Rand Corporation, Memo RM-3650-PR, August 1963.

17. O'Neill, M. J. — A Review of Some Cumulative Damage Theories. ARL Report SM 326, June 1970.

17a. Torbe I. — A New Framework for the Calculation of Cumulative Damage in Fatigue.
Part I -Historical Theory, USAA Report 106, Southampton, 1959.
Part II– Historical Theory, USAA Report 111, Southampton, 1959.

18. Miner, M. A. — Cumulative Damage in Fatigue. Journal of Applied Mechanics, Vol. 12, No. 3, Sept., 1945, pp. A159-64; Discussion, Vol. 13, No. 2, pp. A169-71, June 1946.

19. Head, A. K., and Hooke, F. H. — Random Load Fatigue Testing. Nature, Vol. 177, p. 1176, 1956.

20. Miner, M. A. — Experimental Verification of Cumulative Fatigue Damage. Automotive Industries, New York, Vol. 93, No. 11, pp. 20–22, 56–58, 1 December 1945.

21. French, H. J. — Fatigue and the Hardening of Steels. Transactions of the American Society of Steel Treatment, Vol. 21, No. 10, pp. 899–946, October 1933,

22. Moore, H. F., and Kommers, J. B. — An Investigation of the Fatigue of Metals. University of Illinois Engineering Experiment Station Bulletin 124, 1921.

23. Bastenaire, F. A. — Critical Discussion of the Nature of Cumulative Damage in Fatigue. IUTAM Colloquium on Fatigue (eds. W. Weibull and F. K. G. Odqvist). Julius Springer, Stockholm 1955.

24. Hooke, F. H. — Translation of Reference 23. University of Nottingham, Department of Mechanical Engineering Report, 1958.

25. Marco, S. M., and Starkey, W. L. — A Concept of Fatigue Damage. Trans. ASME Vol. 76, p. 627, 1954.

26. Yokobori, T. — Fatigue Fracture from the Standpoint of the Stochastic Theory. Journal of the Physical Society of Japan, Vol. 8, No. 2, pp. 265-68, 1953.

27. Ford, D. G. — Letter to F. Bastenaire.

28. Webber, D., and Levy, J. C. — Cumulative Damage in Fatigue with Reference to the Scatter of Results. United Kingdom Ministry of Supply S. and T. Memo 15/58, 1958.

29. Jacoby, G. H., and Nowack, H. — Comparison of Scatter under Program and Random Loading and Influencing Factors. Probabilistic Aspects of Fatigue. ASTM STP S11, pp. 61–74, 1972.

30. Stadnick, S. J., and Morrow, Jo Dean — Techniques for Smooth Specimen Simulation of the Fatigue Behaviour of Notched Members. Testing for Prediction of Material Performance in Structures and Components. ASTM STP 515, American Society for Testing and Materials, pp. 229-52, 1972.

31. Crews, John H., and White, N. H. — Fatigue Crack Growth from a Circular Hole with and without High Prior Loading. NASA TN D-6899, September 1972.

32. Neuber, H. — Theory of Stress Concentration for Shear Strained Prismatical Bodies with Arbitrary Non-Linear Stress Strain Law. Transactions American Society of Mechanical Engineering D. TASMA, pp. 544–50, December 1961.

33. Topper, T. H., Wetzel, R. M., and Morrow, Jo Dean — Laboratory Simulation of Structural Fatigue Behaviour. Journal of Materials, Vol. 4, No. 1, pp. 200–209; see also Effects of Environment and Complex Load History on Fatigue Life, ASTM STP 462, 1970.

34. Kirkby, W. T., and Edwards, P. R.
Cumulative Fatigue Damage Studies of Pinned-log and Clamped-log Structural Elements in Aluminium Alloy
RAE TR 69182, August 1969.

35. Griffith, A. A.
The Phenomena of Rupture and Flow in Solids.
Phil. Trans. Roy. Soc. *A*, Vol. 221, pp. 163–98, 1920–21.

36. Orowan, E.
Energy Criterion of Fracture.
Welding Journal, Research Supplement, Vol. 34, p. 157; also Trans. Inst. Engrs. Shipbuilders of Scotland, Vol. 89, p. 165, 1945.

37. Wells, A. A., and Roberts, D. K.
The Velocity of Brittle Fracture.
Engineering, Vol. 178, pp. 820–21, 1954.

38. Irwin, G. R.
Fracture Testing of High Strength Materials under Conditions Appropriate for Stress Analysis.
US Naval Research Laboratory, Report NRL 5486, July 1960.

39. Freudenthal, A. M.
Fatigue Sensitivity and Reliability of Mechanical Systems, especially Aircraft Structures.
Wright Air Development Center, WADD Technical Report 61-53, 1961.

40. Payne, A. O.
The Fatigue Characteristics of Structures and Their Fatigue Life Assessment.
Thesis for the Degree of Master of Engineering, University of Melbourne, 1961.

41. Diamond, Patricia, and Payne, A. O.
Reliability Analysis Applied to Structural Tests.
Proceedings of Symposium on Advanced Approaches to Fatigue Evaluation, Miami Beach, May 1971; NASA sp-309, 1972.

42. Ferrari, R. M., Milligan, I. S., and Weston, M. R.
Some Considerations Relating to the Safety of Fail-safe Wing Structures.
Proceedings of Symposium on Full Scale Testing of Aircraft Structures, 1959: Pergamon Press, pp. 413–26, 1963.

43. Shaw, R. R.
The Level of Safety Achieved by Periodical Inspection of Fatigue Cracks.
Journal of the Royal Aeronautical Society, Vol. 58, No. 526, pp. 720–23, 1954.

44. von Sydow, Lennart
Appendix A: A Statistical Method for Fail-Safe Design with Repsect to Aircraft Fatigue. Bo K. O. Lundberg and Sigge Eggwertz.
2nd International Congress ICAS, Zurich, September 1960; also as FFA Report.

45. Ford, D. G.
Appendix to Reference 44.

46. Ford, D. G., and Grandage, J. G.
Approximate Life Distribution of Cracked Structures with Random Risks.
ARL Structures Tech. Note SM-363, March 1971.

47. Hooke, F. H.
Probabilistic Design and Structural Fatigue.
Aeronautical Journal, Vol. 79, No. 774, June 1975.

48. Paris, P. C., Gomez, M. P., and Anderson, W. E.
A Rational Analytic Theory of Fatigue.
The Trend in Engineering, Vol. 13, No. 9, 1959.

49. —
The Cranfield Symposium on Fatigue Crack Propagation.
College of Aeronautics, Cranfield, 1961.

50. Paris, P. C.
The Growth of Cracks due to Variations in Load.
Ph.D. Thesis, Lehigh University, September 1962.

51. Paris, P. C.
The Fracture Mechanics Approach to Fatigue. Fatigue—An Interdisciplinary Approach.
Proc. of 10th Sagamore Army Materials Conf. (eds. Volker Weiss *et al.*), Syracuse University Press, 1964.

52. Roberts, R., and Erdogan, F.
The Effect of Mean Stress on Fatigue Crack Propagation in Plates under Extension and Bending.
Journal of Basic Engineering, Vol. 89D, December 1967; also Trans. ASME Series D, pp. 885–92.

53. Forman, R. G., Kearney, V. E., and Engle, R. M. — Numerical Analysis of Crack Propagation in Cyclic Loaded Structures. Journal of Basic Engineering, Vol. 89D, September 1967; also Trans. ASME Series D, pp. 459-64.

54. Wanhill, R. J. H. — Fatigue Crack Propagation Data for Titanium Sheet Alloys: Interim Report No. 5 IMI 318. National Lucht en Ruimtevaartlaboratorium, NLR-TR-74048U, April 1974.

55. Cheverton, K. E. — Crack Propagation in Flat Tensile Specimens of Light Alloy Sheet Materials Part I. UK Ministry of Supply Contract No. 6/Aircraft/12468/C8.10(6), June 1956.

56. Pook, L. P. — Fatigue Crack Growth Data for Various Materials Deduced from the Lives of Precracked Plates. National Engineering Laboratory, NEL Report No. 484, July 1971.

57. Harrison, J. D. — An Analysis of Non Propagating Fatigue Cracks on a Fracture Mechanics Basis. Metal Construction, Vol. 2, No. 6, p. 93, March 1970.

58. Greenan, A. F. — Fatigue Tests on Edge-cracked Magnesium Alloy Plate Specimens. National Engineering Laboratory, NEL Report No. 492, November 1971.

59. Paris, P. C., Bucci, R. J., *et al.* — Various papers in "Stress Analysis and Growth of Cracks". ASTM STP 513. Proceedings of the 1971 National Symposium of Fracture Mechanics, University of Illinois, 31 August–2 September 1971; published September 1972.

60. Forsyth, P. J. E. — A Two Stage Process of Fatigue Crack Growth. The Cranfield Symposium on Fatigue Crack Propagation, College of Aeronautics, Cranfield 1961.

61. Elber, W. — The Significance of Fatigue Crack Closure. Damage Tolerance in Aircraft Structures ASTM 486, pp. 230–42, 1971.

62. Elber, W. — Some Effects of Crack Closure on the Mechanism of Fatigue Crack Propagation under Cyclic Tension Loading. Ph.D. Thesis, University of New South Wales, Sydney, 1968.

63. Hanel, J. J. — Rissfortschreitung in ein-und mehrstufig Schwingbelasteten Scheiben mit besonderer Beruchsichtigung des Partiellen Risschliessens (Crack Growth in Sheets under Constant Amplitude and Programmed Loads with Regard to Partial Crack Closure). Report of Institut fur Statik und Stahlbau. ISSB TH Darmstadt, 1975.

64. Schijve, J., Jacobs, F. A., and Tromp, P. J. — Flight Simulation Tests on Notched Elements. NLR Technical Report TR 74033, 1974.

65. Schijve, J. — Fatigue Crack Growth under Variable-Amplitude Loading. Conference on the Prospects of Advanced Fracture Mechanics, Delft, The Netherlands, 24–28 June 1974; Noordhoff, 1974. Also Delft University of Technology, Department of Aeronautical Engineering, Report VTH-181, April 1974.

66. Schijve, J. — Prediction of Fatigue Crack Propagation in Aircraft Materials under Variable-Amplitude Loading. Delft University of Technology, Report VTH-193, March 1975; also ASTM Meeting, Montreal, 23–24 June 1975.

67. Wheeler, O. E. — Spectrum Loading and Crack Growth. Journal of Basic Engineering (Transaction of ASME, Series D), Vol. 181D, 1972.

68. Willenborg, J. D., Engle, R. M., and Wood, H. A. — A Crack Growth Retardation Model using an Effective Stress Concept. Report AFFDL-TM-FBR-71-1, 1971.

69. Goldsmith, N. — Private communication. 1975.

70. Donaldson, D. R., and Anderson, W. E. — Crack Propagation Behaviour of Some Airframe Materials. Proceedings of the Crack Propagation Symposium, Cranfield College of Aeronautics, Cranfield, September 1961.

71. Bailey, N. T. J. — The Elements of Stochastic Processes with Applications to the Natural Sciences. A Wiley Publication in Applied Statistics, Wiley, 1964.

72. Courant, R., and Hilbert, D. — Methods of Mathematical Physics. Vol. 2, Interscience. A division of John Wiley, 1962.

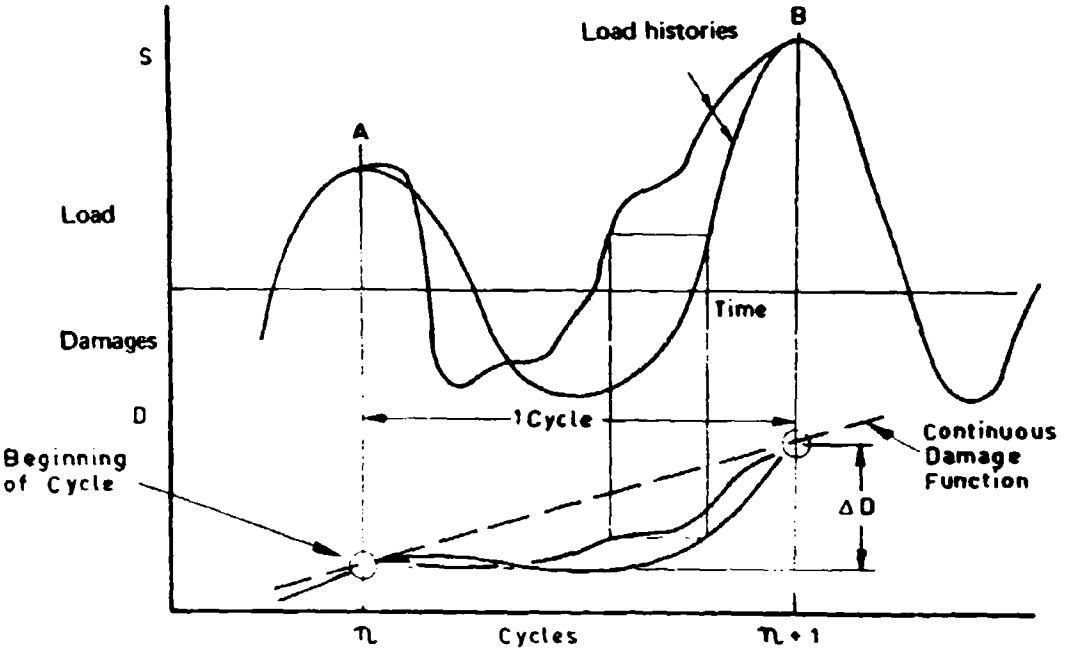

FIG. 1a DEFINING CONTINUOUS DAMAGE

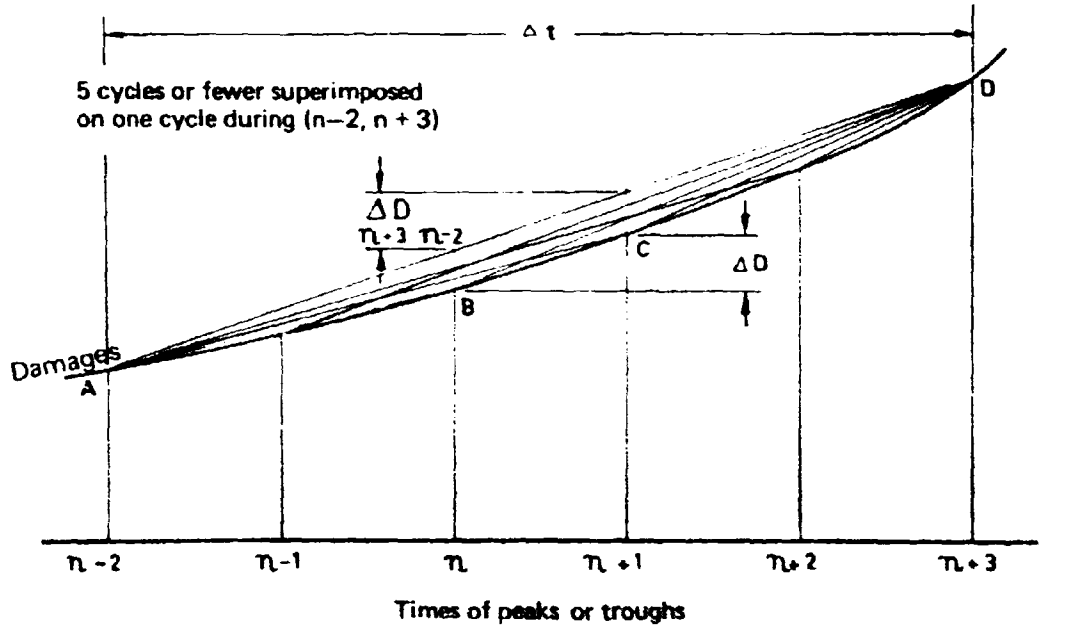

FIG. 1b DAMAGE DURING OVERLAPPING CYCLES

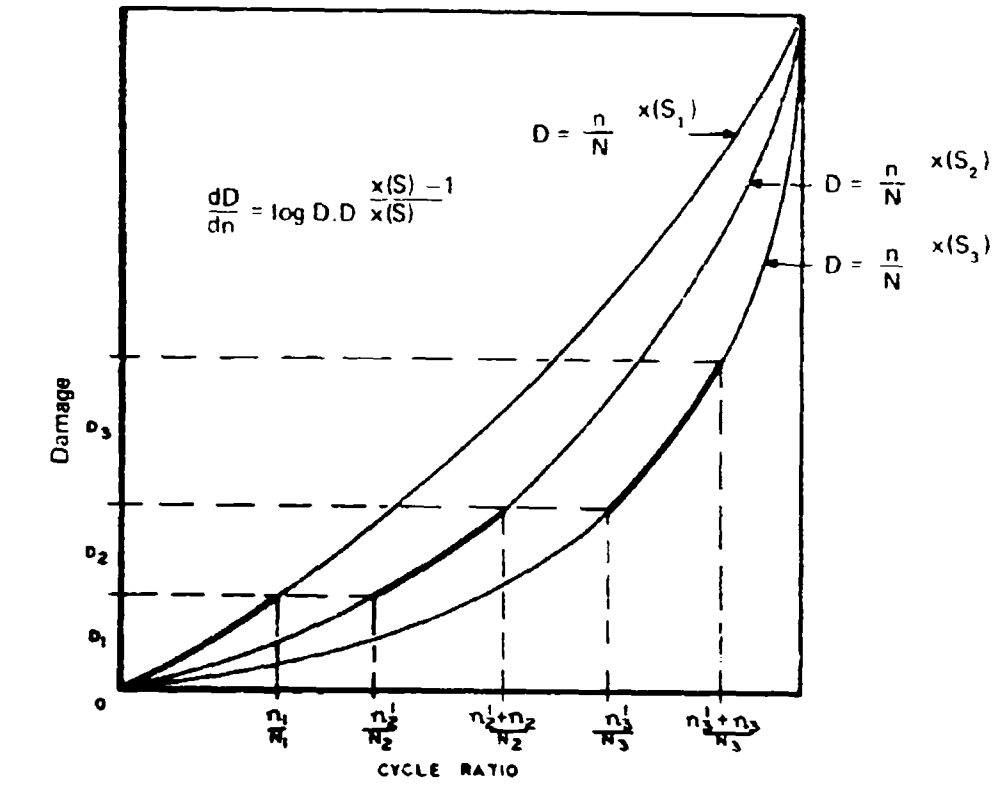

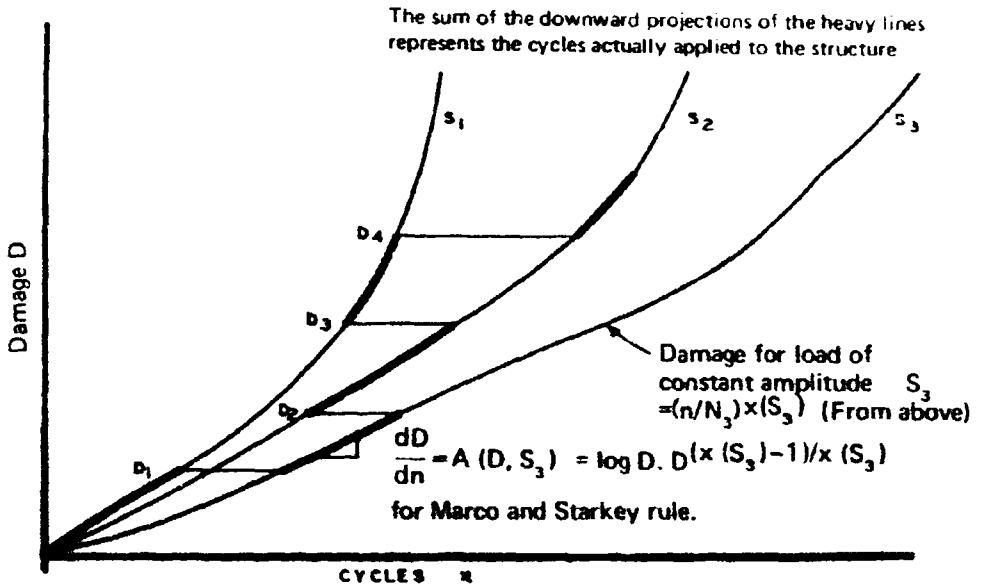

FIG. 2 BASTENAIRE FORM OF MARCO AND STARKEY'S RULE

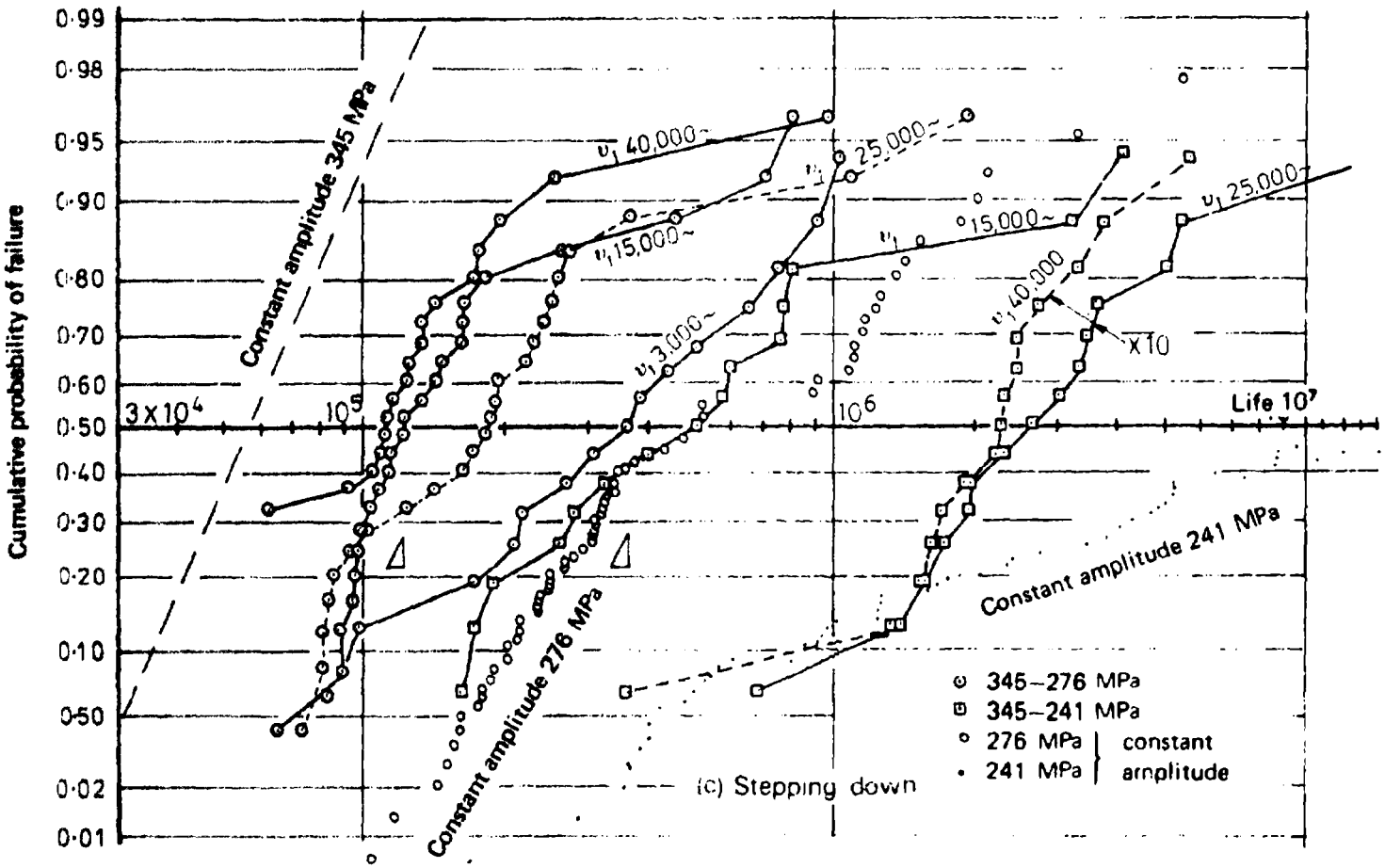

FIG. 3 CONTINUED

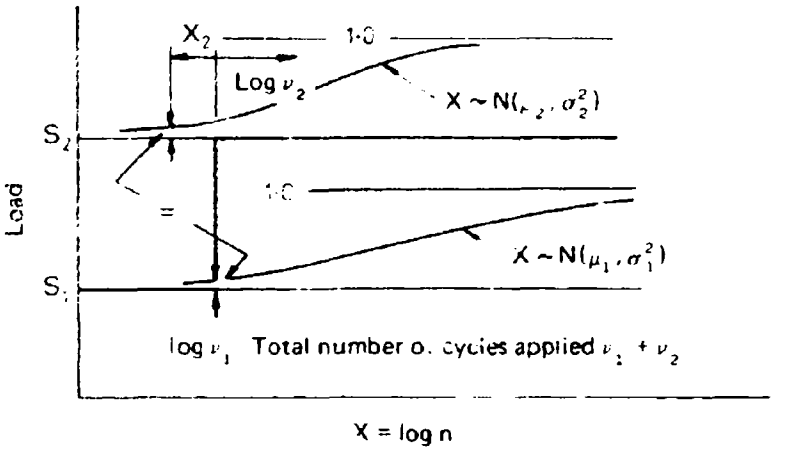

FIG. 3a STEP LOADING WITH LOG – NORMAL DAMAGE

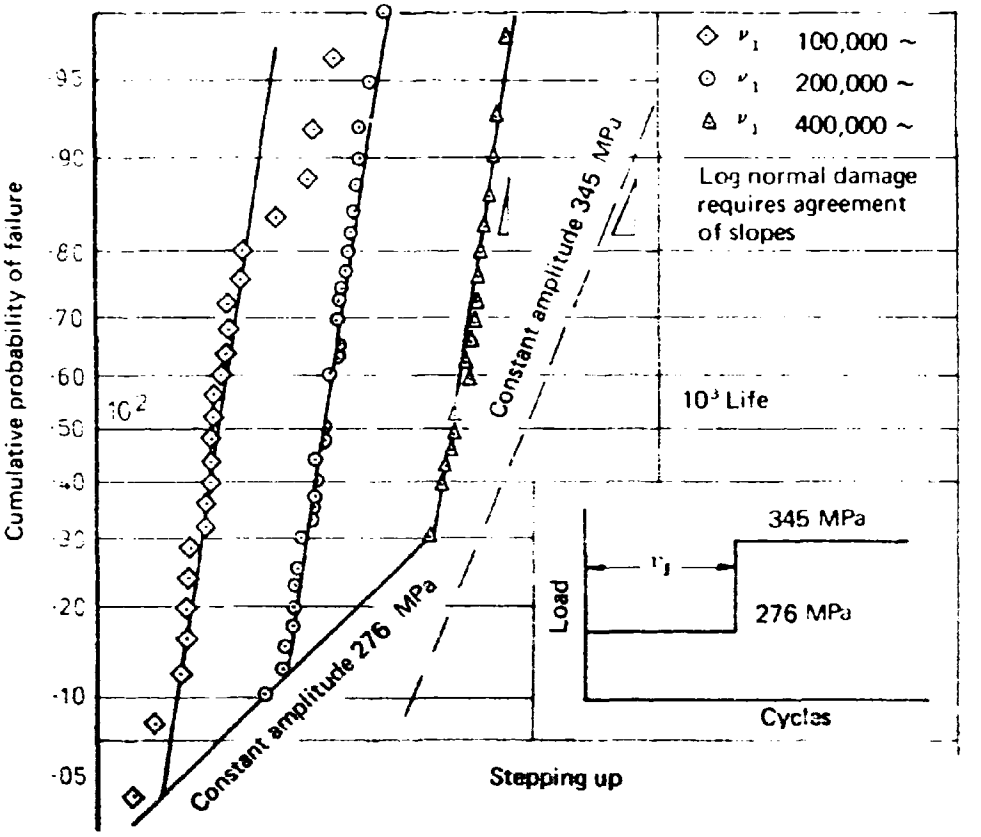

FIG. 3b RESULTS OF WEBBER AND LEVEY

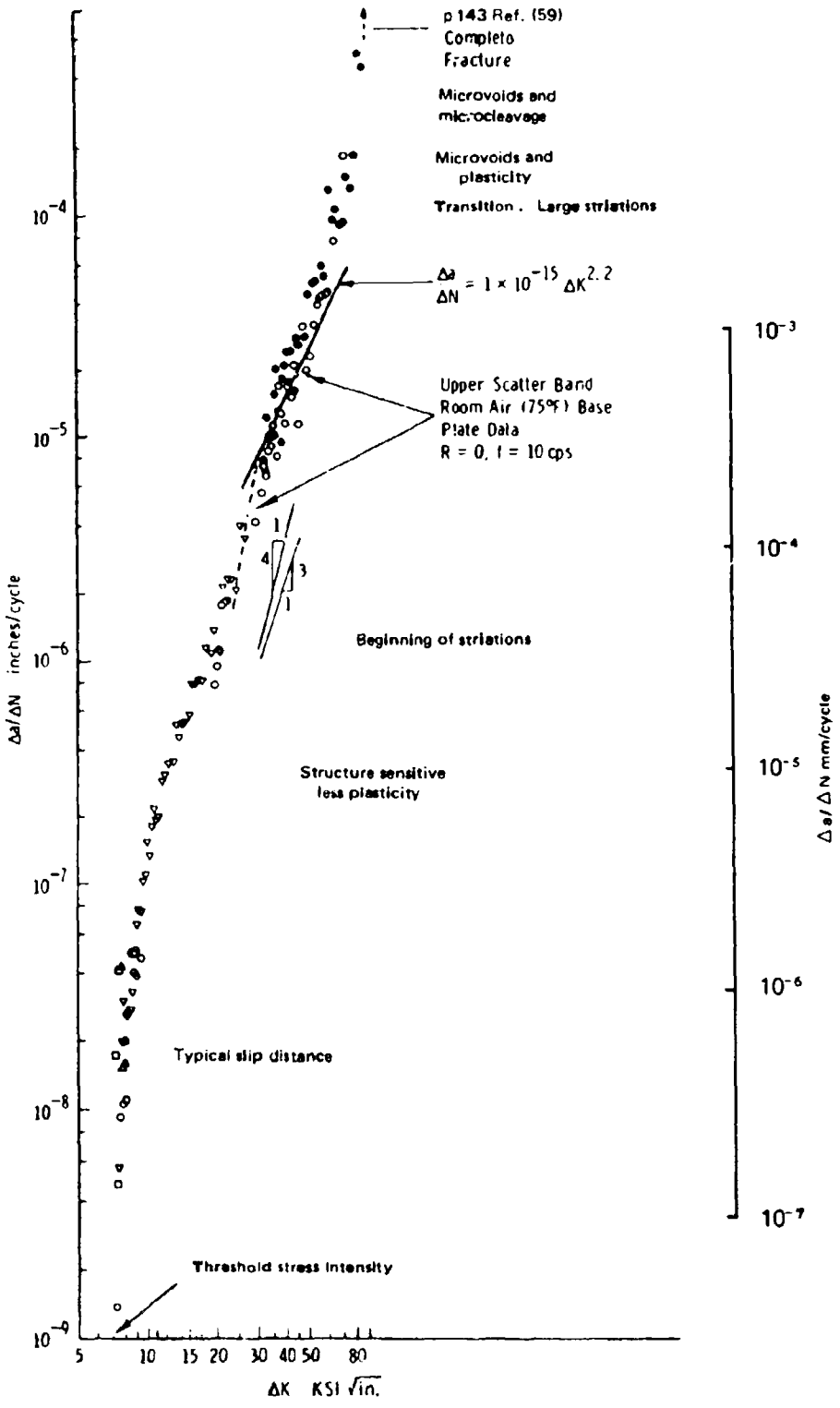

FIG. 4 TYPICAL CRACK RATE DATA
ASTM A533 B-1 steel — R = 0.10, ambient room air, 75F

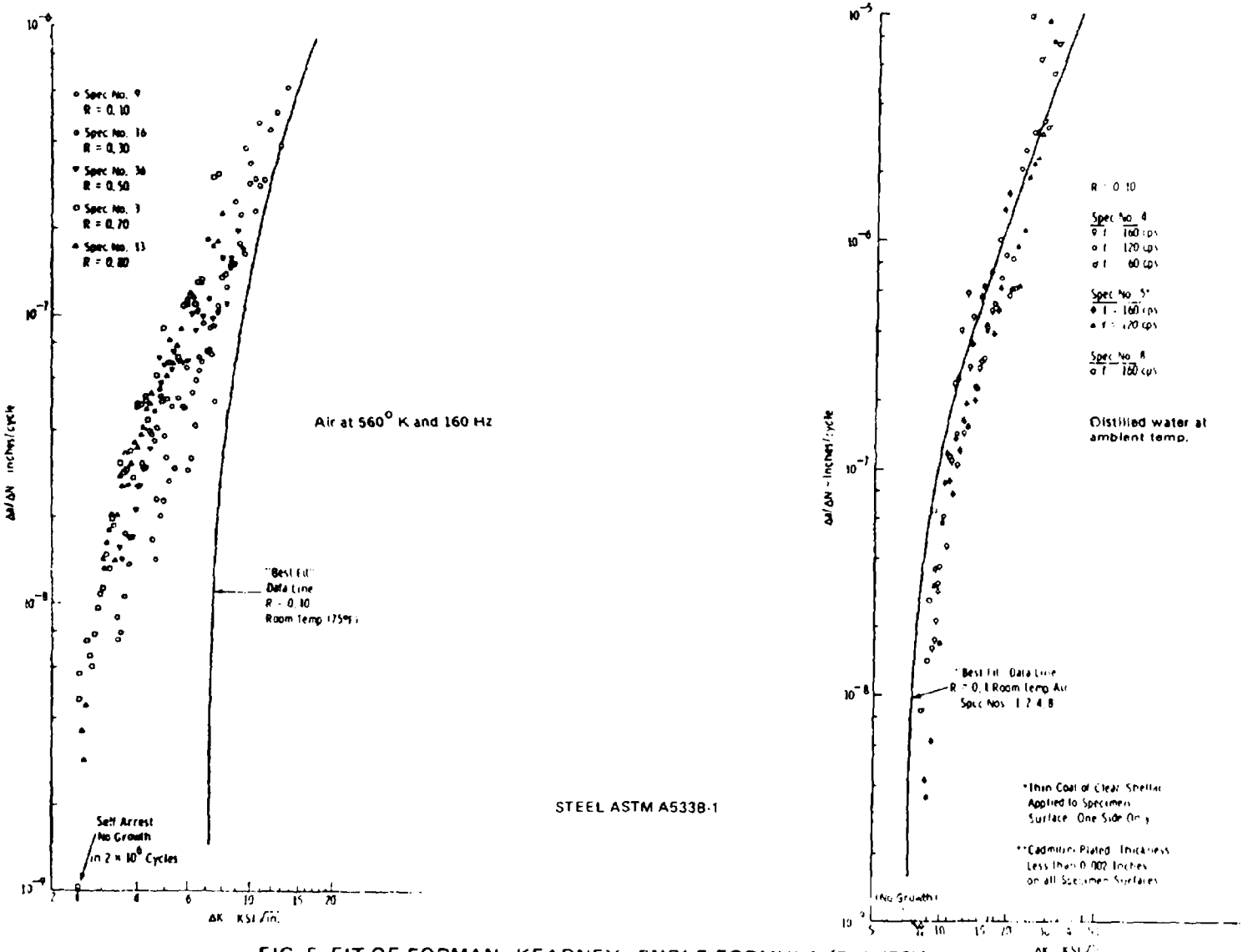

FIG. 5 FIT OF FORMAN–KEARNEY–ENGLE FORMULA [Ref. (59)]

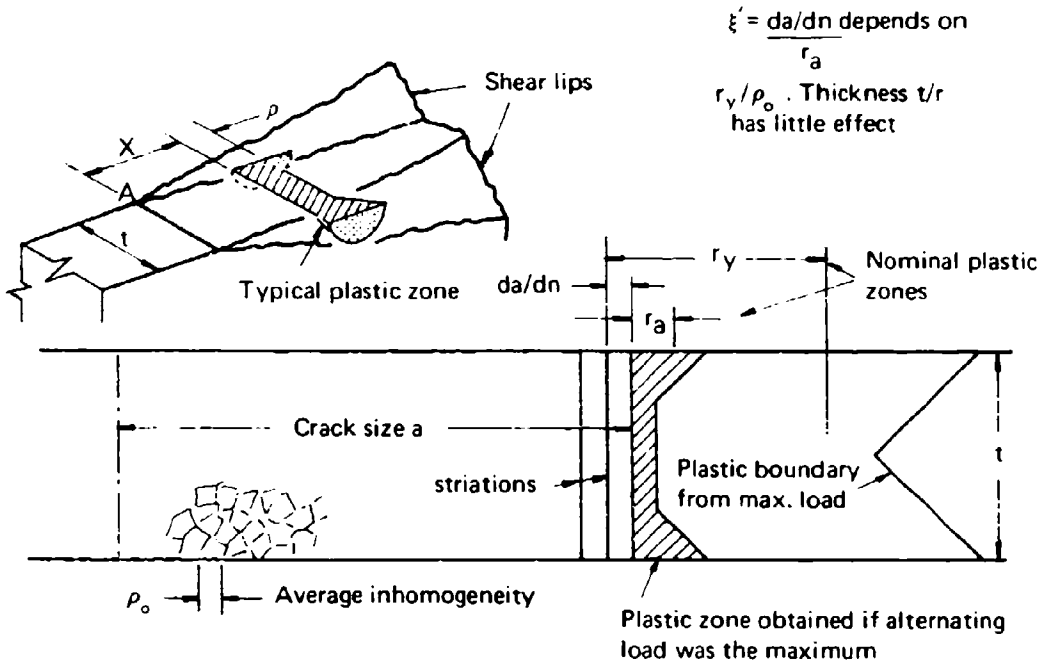

FIG. 6a CRACK RATE PARAMETERS

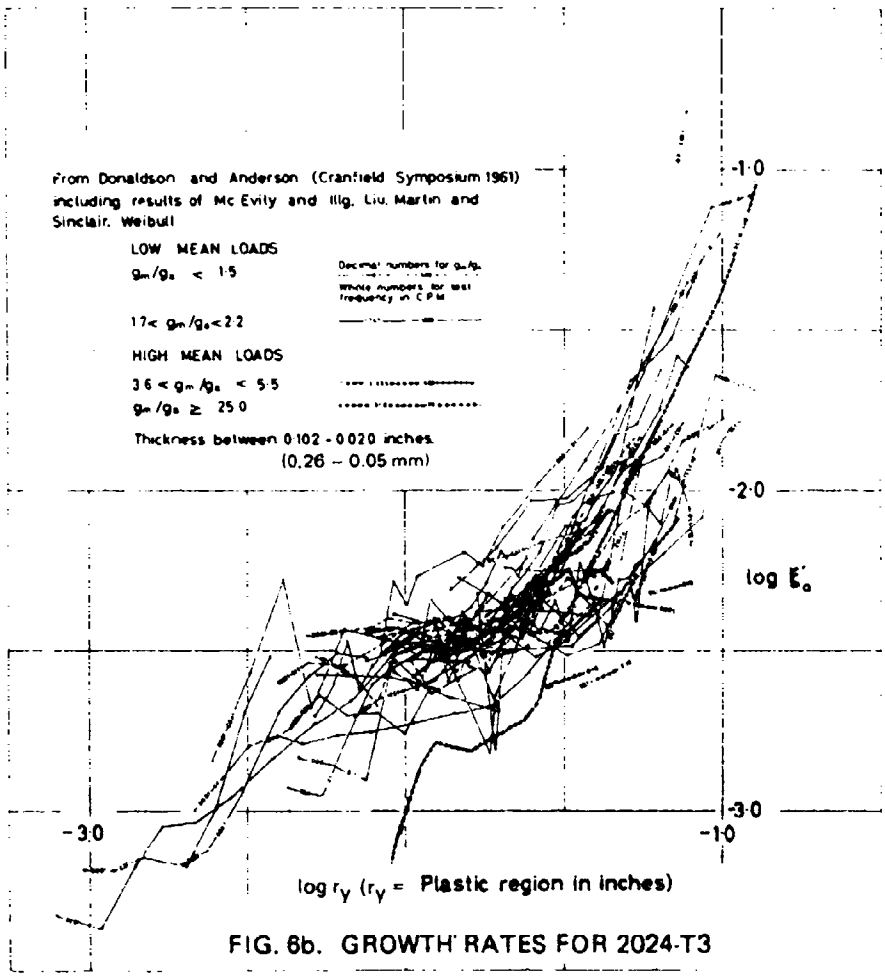

FIG. 6b. GROWTH RATES FOR 2024-T3

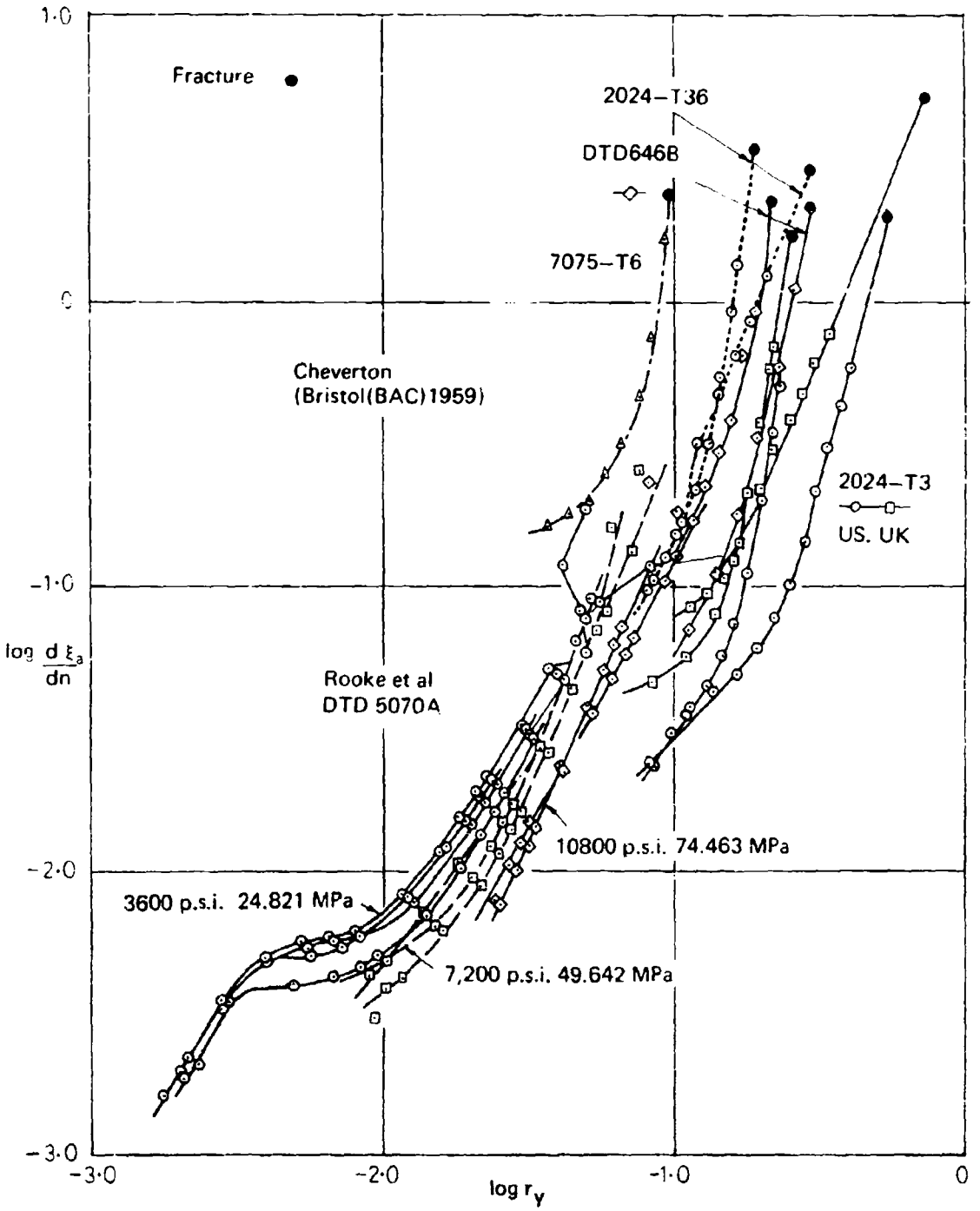

FIG. 6c CRACK GROWTH FOR HIGH STRESSES

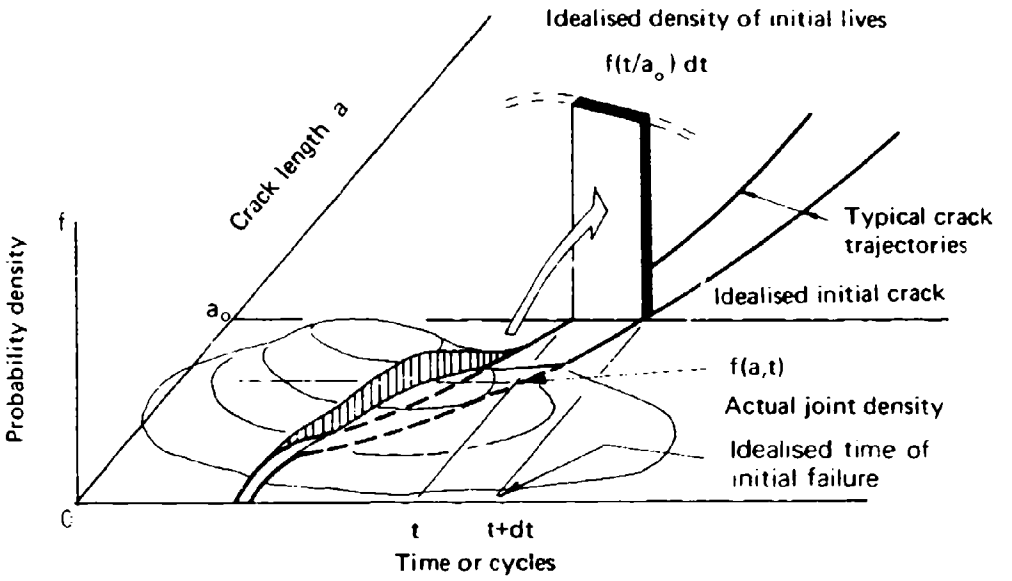

FIG. 7 RELATION OF ASSUMED AND ACTUAL INITIAL LIVES AND CRACK LENGTHS

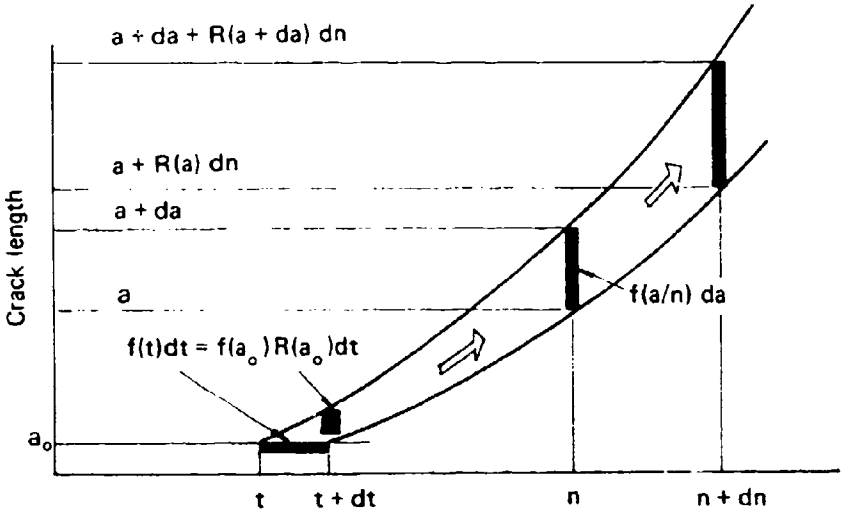

FIG. 8 DERIVATION OF CHAPMAN–KOLMOGOROV EQUATIONS AND INITIAL CONDITIONS FOR SINGLE CRACKS

DISCUSSION

QUESTION –*H. A. Wills*
(Retired)

What precisely is required as to the nature of *damage* and *crack propagation data* in order to make practical use of the unified theory?

What parameters are needed from the metallurgists to define crackless damage and crack growth?

Author's Reply

Because canonical damage is the distribution of initial life, once this is defined, any set of initial lives which allows estimation of the scatter at several load levels will allow the construction of a damage rule. If the data exists such rules may be extended to initial failure below the fatigue limit. For Miner damage only the mean S-N curve is needed but this involves some assumptions about the life distribution, as described in the paper. Naturally the more that is known about the initiation phase the better the rule that can be constructed. Although I have not investigated it in detail I also feel that the S-N data need not necessarily be couched in terms of constant amplitude loads; independent programmes or randomised loadings may also suffice. All these remarks apply to one-parameter damage. For higher dimensions, other dimensions of data are also needed and one must be closely guided by the metallurgists. Further investigations here should be interdisciplinary and include some statistical considerations.

Similarly, with crack growth simple da/dn data for various stress intensities is enough if simply additive rates are assumed but the outstanding problem here has probably been recognised as that of retardation and interaction generally. On the other hand the statistics of cracking have been neglected even at the level of differences between average crack growth curves for different specimens.

It is planned that the first implementation of the theory will use Miner damage for the initial life distribution and straight-forward da/dn data with simply additive rates. The next stage will then introduce retardation of crack growth and Neuber-Topper-Wetzel notch root analysis for improvement of stress analysis for initial damage.

However, the initial failure data obviously depends on how this is defined, which is related to the value of the initial crack length a_0. These are both the domain of the metallurgist but the choice must also be influenced by engineering and the mathematical convenience, which is one of the advantages of a two stage theory.

One approach to the idealized initial crack length is as a scale length for material or structural inhomogeneity. Another definition is that crack length above which fracture mechanics provides a reasonable description of crack growth. From Figure 7 it can be seen that the damage rule also depends on a_0 and it is possible that the primary choice will depend on metallurgists, what they can discover about crack initiation or, as some would have it, on the distinction between macro- and micro-cracking.

QUESTION—*J. M. Finney*
(ARL)

Mechanistically it is fairly clear that fatigue cracks both initiate *and* propagate by the local irreversibility of plastic deformation. Thus, in a real, physical sense, fatigue cracks initiate in the first cycle and there is no such stage as initiation. A major problem of course lies in quantifying the early rates of crack propagation, but the techniques of obtaining such data are not part of your theory.

With this concept, is it possible to simplify your theory by deleting the "so-called" damage stage?

Author's Reply

From a mathematical viewpoint, deletion of the damage stage is *not* a simplification. The idea of having two stages is that they can be described by two simple laws better than a more complicated one can treat the whole process.

Both of these stages certainly proceed by irreversible plasticity but this is not synonymous with cracking, in the engineering sense at least, and in the real physical sense the early stages of fatigue differ from the later ones. In crack growth itself there are several stages and it has been shown that there is much more scatter in the times to reach small crack lengths than there is in the subsequent growth times. The idealization of this situation is that there is a period to initial failure which randomises the system followed by cracking which couples the fatigue sites in the structure. It is mathematically convenient to dichotomise these and semantically useful to name them differently as successive stages of "fatigue".

Within this terminology "initial failure" may include microcracks in which case their quantification amounts to the derivation of equations governing "damage" as defined in the paper. As mentioned in the introduction, the best division between these is still a matter of research and experience. From Figure 7 it may be seen further that the damage law depends on the definition of initial failure; conventional analysis now postulates a single stage of damage with a_0 the size of the structure. Subdivision of this must be an improvement, but Dr. Finney's remarks should remind us not to tie it to convention.

QUESTION—*A. K. Head*

(Division of Tribophysics, CSIRO)

Most people think of damage as a one-dimensional measure by which the amount of "damage" in several specimens can be put in order.

The literature, however, contains many instances where ordering is not possible so that damage must at least be described as a vector. Is the set of damages you postulate simply the set of one-dimensional damages at each critical point?

Author's Reply

Not necessarily. The Bastenaire damage of Section 3 is most generally a vector for each critical point. Each damage vector leads to an initial failure probability which is a component of F later on. For simplicity however, this generality has not been maintained but it introduces no further difficulty.

Incidentally, the instances of multidimensional damage in the literature probably refer to final failures which combine our damage and cracking stages.

Dr. Head—Yes probably. Do you know of any work to establish the dimensionality of damage?

Author—No.

Dr. Head—Would you consider this to be one of the current problems of damage theory?

Author—Yes.

"AIRCRAFT STRUCTURAL RELIABILITY AND RISK THEORY—A REVIEW"

by

F. H. HOOKE

SUMMARY

Evaluation of the structural reliability and probability of failure during the lifetime is a statistical exercise based upon load history data and strength decay properties known or attributed to the structures in question. Reliability theory avoids the need for arbitrary decision regarding the level of strength deterioration assumed to render a structure unairworthy.

By defining failure to occur whenever a structure has imposed upon it a load larger than current strength, it provides a mathematically exact evaluation of the instantaneous risk of static ultimate failure and of fatigue failure, and of the long term reliabilities with respect to failure in either mode, on the basis of given data. The method dispenses with arbitrary scatter factors, though equivalent scatter factors may be determined from the relation between reliability and age if desired. The fatigue sensitivity of a structure is characterised by the relationship of fatigue failure risk to static ultimate failure risk. Structures initially ultimate-load-failure-sensitive tend to become fatigue-sensitive as they get older.

Fatigue risk is reducible in fail-safe and inspectable structures, but only in so far as cracking is within the range of in-service detectability. The variability of structural strength (whether present initially or resulting from variation in the rates of strength decay) causes a variation of the risk over the population, viz. a higher risk over weaker members and vice versa, which leads to a more rapid depletion of weaker members of the population. Risk averaging leads to over conservative estimates and to over frequent inspection requirements. Confidence in the efficacy of inspection in preventing catastrophic failures is related to the length of time, and the distribution of that length of time, during which a crack is inspectable and yet not unsafe. Time to first failure statistics are directly related to the expectation of finding a crack when inspecting at a nominated time.

Reliability of reliability estimates is examined, and is shown to be usually limited by sampling problems and arbitrary judgments concerning the attribution of properties to the population in question. The estimates are compared with those derived by semi-probabilistic or limit analysis methods.

SYMBOLS

A, B, C	Constants
Subscript o	Refers to virgin strength and constant strength, with the exception of m_o
Superscripts	Refers to mean or median
	Refers to time averages
$P(V), P(V \mid U_o)$	Probability that a load in the sequence will exceed V or $V \mid U_o$
H	Strength-decay-time parameter: time in which the member's virgin strength, U_o, falls to an arbitrary fraction, say $2U_o/3$
$\tilde{H}$	Median value of H
H_d	Time taken for a crack to reach detectable size
H_F	Time in which a member's strength falls to zero; is related to H
H_r	Crack growth time for component removal
H_w	Time taken for the crack in a member to reach the threshold size for strength deterioration
$m(V)$	Frequency per unit time of loads $> V$
m_o	Frequency of occurrence of loads greater than the load measuring threshold
n	Number of applied loads
$f(U_o), f(H)$	Density functions of U_o, H, etc.
$F(n), F(t)$	Probability of failure from zero to cycle n or time t
$r(t)$	Risk rate, instantaneous average risk rate
$\bar{r}$	Time averaged risk rate over a period of time
$r_o(t \mid U_o)$	Risk rate conditional on U_o, with strength preserved; i.e., risk on an element $f(U_o)dU_o$, whose strength remains at U_o
$r_o(t)$	Instantaneous average risk rate with virgin strength preserved
$r(t \mid U_o, H)$	Conditional risk rate, given U and H; i.e. risk rate on an element initially of size $f(U_o)f(H)dU_o dH$ whose strength is U at time t
$r_a(t)$	Approximate or erroneous instantaneous risk rate
$R(n), R(t)$	Total reliability at time n or t
$R(t \mid U_o, H)$	Conditional reliability given U_o and H; i.e., reliability at time t of an element $f(U_o)f(H)dU_o dH$
$R_o(t \mid U_o)$	Conditional reliability, given U_o constant; i.e., reliability at time t of an element $f(U_o)dU_o$ whose strength is preserved
$R_{\Upsilon_1}(t)$	Reliability at time t after an inspection at time Υ_1, as a fraction of original total
$R^1_{\Upsilon_1}(t)$	Reliability at time t after an inspection at time Υ_1, as a fraction of the survivors of the inspection
$R_a(t)$	Approximate or erroneous reliability
t	Time
$U, U_o, \tilde{U}_o$	Strength, virgin strength, median virgin strength
α_j	Fraction of a population having a risk r_j
Π	Product of similar terms
ψ	Crack growth function
ϕ	Strength decay function (of crack length)
ζ	Strength decay function (of time)
$N_i, \tilde{N}_i$	Crack initiation time, and median value
k_i	N_i/H, fraction of H concerned with crack initiation
k_d	H_d/H, fraction of H occupied by a crack reaching detectable size
k_w	H_w/H, fraction of H occupied by a crack reaching the size at which weakening commences
k_r	H_r/H, fraction of H during which crack is below size for component removal and replacement
$F_o(T, U_o)$	Probability of failure with virgin strength preserved
$F_F(T)$	$R_{U_o}(T) - R(T)$, probability of failure due to weakened structures

1. INTRODUCTION

In common parlance "reliability" means "trustworthy" or "dependable". in a person it implies that he may be counted on, that what he says is true, or what he says he will do will be done, without doubt and without fail. The confident expectation placed in a reliable person hopefully removes the outcome from chance, from luck or from risk. "Unreliable" describes one in whom it is a matter of chance whether or not what he says is true and what he says he will do, he does. Thus in the non-technical context reliability goes with expected certainty and unreliability goes with certain chance.

In engineering and structural contexts the shades of meaning are different. "Reliability" is applied not to determinate processes but to those involving chance: the "reliability" of a device is a quantified statement of the probability that it will perform its desired function for a desired period[1] (and often this period is its "life"): "unreliability" is the probability that it will fail to do so during the period: and "risk" is the probability that at one of the sequence of events comprising its life experience, or during a short elementary interval dt of its life, it fails to perform its function. "Reliability", "survivorship" and "probability of survival" are synonyms, and their complement is "probability of failure". "Hazard rate", "mortality rate" are synonyms for "risk".

Reliability theory ("risk analysis") is concerned with the inter-relationship between risk at each event or in each short interval in the life experience and probability of failure (and *ipso facto* of reliability) during the extended life period. The analysis may proceed from risk to reliability or vice versa, depending upon the purpose and data available. "Risk" may also be extended to include the probability that, at the next occurring event, there will be found signs of impending failure, though the member is not yet failed. If such a sign is observed, repair or replacement may precede failure: in this circumstance unreliability is not incompatible with safety.

In some cases, such as, for example, the game of roulette, the probability of a player's stake surviving over an evening's play can be calculated *a priori*, without any prior experiments, from only a knowledge of physical and geometrical constants which describe the conditions determining the risk, and the number of games he enters. More commonly future reliability is estimated upon observations of past performance. The reliability (in the normal sense) of an estimate is quite distinct from the numerical value of the estimate, and the use of the term "reliability" does not itself confer precision upon an estimated reliability.

In the field of electronic engineering, in which reliability theory, by that name, was developed, multitudes of actual components drawn directly from the production lines are regularly endurance tested to provide data on the risk of failure, as it varies with exposure time, and the sampling error of these data is small because of the largeness of the samples. By contrast, in engineering structures, and particularly aeroplanes, it has never been possible to take from the production line and test samples sufficiently numerous that the statistical properties of the total are well established; in the case of aircraft structures, commonly, only a single sample from the production line is tested; this provides a rather imprecise estimate of average performance while other statistical parameters such as variabilities in strength or endurance must perforce be attributed to the population on the basis of personal judgment, taking into account the results of tests on other structures whose resemblances to those in question may be sometimes close and sometimes "je ne sais quoi".

Much of electronic component endurance testing involves placing the component under constant stress (on normal electrical supply voltage, or perhaps a higher voltage, to accelerate the test) and observing the life to failure. Structural endurance testing is more complex, because it aims to reproduce more properly the timewise variations in load or stress which are known to occur in the service history. The service loads arise from a number of causes, but the most numerous ones acting upon civil aircraft are gust loads and on military aircraft are pilot induced manoeuvre loads. These loads have characteristics common to naturally occurring processes: they have no precisely definable upper limit (as for example the mathematical flea which at each jump jumps

half the dist ..e to his target). Their upper limits are more akin to the records of Olympic athletes: although the majority of athletes cannot reach record performance, the achievements of the extremes gradually increase with increasing time. It follows that whatever required strength values are set for design purposes there will occasionally be failures through the applied loads exceeding these values, and the service records of both civil and military aircraft confirm this fact. Customarily the compliance of a particular design with strength requirements is verified by a static virgin strength test programme, and its endurance is verified by a fatigue test programme of varying loads, the largest of which is never as high as the load level expected to occur once in the lifetime of a fleet—more often the largest load is at a level expected to be exceeded on the average about ten times in the lifetime of each aeroplane. It is generally considered that an endurance test limited at this level will not, through residual stress or retardation effects, favourably influence the life-to-failure result, so that it may be taken as a fair average estimator of fleet endurance.

Thus, on the assumptions that the static test strength is the population mean virgin strength, and that the probability distribution of strength and the load frequency distribution are known, reliability theory may be used to calculate the reliability under loads greater than the virgin strengths. Assuming also the strength decay properties of the set of structures, and assuming that a failure occurs whenever a structure suffers a load greater than its current strength, the theory may be used to calculate the total reliability allowing for above-virgin-strength failures and failures under loads less than virgin strength, whether these loads are higher or lower than the largest fatigue test load.

In the case of some electronic components the phenomenon of "burn-in" is exploited: components after manufacture may be subjected to a period of operation at higher-than-normal stress. Some may fail, but the survivors, when put into service at normal operating stress demonstrate enhanced endurance and greater reliability than those not so treated.

Comparable phenomena are autofrettage in gun barrels and preloading in structures, though engineers are wary of taking advantage of such an effect with structures in service because of the uncertainty that every member of the population will enjoy the benefit. Test programmes need to be most carefully examined to see that a test specimen is not thus benefited if the treatment is not to be later applied to the total production, otherwise reliability predictions will be totally falsified.

The criterion for a "safe" operating period will depend upon what is regarded as an acceptable probability of failure or an accepted reliability over that period. To accommodate widely differing operating periods the criterion may be expressed as an acceptable average risk rate per hour, and the criterion has sometimes been expressed in terms of acceptable instantaneous risk. Over the years various authors have proposed various levels for the reliability or risk, and the figures finally adopted usually involve some consensus of personal judgments.

Thus in any particular structural investigation, computed values of reliability or of risk, and corresponding safe operating periods, are estimates, uncertain because of the presence of sampling errors and of personal judgment. The field is one where it will never be possible to make estimates without sampling errors and personal judgments. Nevertheless it is appropriate that attention should be given to the reliability of these estimates, lest the user should unwittingly attribute the precision of the mathematics to the calculated estimates.

2. BASIC CONCEPTS OF RISK AND RELIABILITY

In matters of mortality, the risk rate ($r(t)$) is the ratio of the number of deaths per unit time, at time t, to the number of the population surviving at that instant. In matters of structural failures it is the ratio of the number of members of the population failing per unit time at time t to the number surviving unfailed to that instant, or, as in fatigue, where a specimen's age and endurance are expressed in numbers n of cycles of applied load, the risk rate $r(n)$ is the ratio of the number failing per load cycle at cycle n to the survivors at cycle n. It is the proportion of those surviving at cycle $(n-1)$ which is expected to fail at the nth cycle: thus also it is the probability of failure at the nth cycle of those then surviving.*

One may think of a biological population as it suffers the risk of death by contagious

* For a sequence of discrete cycles, the upper limit of the risk rate is obviously unity. For continuous time, if there are m_o cycles of load per unit time, the risk rate has an upper limiting value of m_o.

disease which attacks everyone regardless of age; in which case the population being studied does not need to be characterised by the age of each individual; the risk is only a function of the exposure time. Or, one may think of the risk of death from old age, in which the risk is associated with the age of each individual, i.e. both the risk rate and the proportion surviving are functions of age.

In the case of material failure through fatigue the risk of failure at the next cycle to be applied is a function of the load cycles endured since new. If, as in the case of aeroplanes, exposure to the load history is logged in hours and the load history is recorded as occurrences per unit time, the risk rate becomes a function of the individual's exposure time and its "endurance" or "fatigue resistance".

For reliability the symbol $R(t)$ or $R(n)$ is used herein, and $F(t) = 1-R(t)$, or similarly $F(n)$ is used for unreliability, viz. the probability of failure in the interval from time zero to time t or cycle n.

Let us consider a population of equal and constant strength $\bar{U}$ subjected to a sequence of random service loads V (i.e. the magnitude of loads in the sequence is a random variable) then there will be a certain probability r that the load occurring next will exceed $\bar{U}$, and therefore will cause failure at that event. The probability of survival is $(1-r)$ and the probability of survival of n such events is $(1-r)^n$, so

$$R(n) = (1-r)^n \tag{1}$$

and approximately

$$= \exp(-r\,n) \tag{2}$$

provided rn is small and n is large compared with unity.

If the risk is not constant but is a function of age n, i.e. at $n = 1, 2, 3 \ldots$ risk is $r(1)$, $r(2)$, $r(3) \ldots$

$$R(n) = \{1-r(1)\}\{1-r(2)\}\{1-r(3)\}\ldots$$

$$= \prod_{i=1}^{n}\{1-r(i)\} \tag{3}$$

where Π signifies the product of terms like $\{1-r(i)\}$
and approximately

$$R(n) = \exp -\{\sum_{i=1}^{n} r(i)\} \tag{4}$$

where, as above, $r(i)$ is small and n is large compared with unity.

Writing $f(n)$ as the fraction of the original population failing at load n,

$$f(n) = R(n-1)-R(n)$$

$$= \prod_{i=1}^{n-1}\{1-r(i)\}\,.\,r(n)$$

$$= R(n-1)\,.\,r(n) \tag{5}$$

And thus

$$r(n) = f(n)/R(n-1) = f(n)/\{1-F(n-1)\} \tag{6}$$

In the limiting case of large n, and $n = m_o t$, t being continuous, the RHS of (6) becomes the derivative of $ln\{1-F(t)\}$, whence

$$R(T) = \exp\{-\int_0^T r(t)\mathrm{d}t\} \tag{7}$$

It should be noted that, in (6), $f(n)$ is the probability density function of time to failure: $f(n)\mathrm{d}n$ is the proportion of the *original total* which fails in the interval $\mathrm{d}n$, while $r(n)\mathrm{d}n$ is the proportion of *survivors at cycle n* failing in the interval $\mathrm{d}n$. It will be appreciated that at early times during which the population is not significantly depleted, i.e. if $R(n)$ is sensibly equal to unity, one may approximately equate $f(n)$ and $r(n)$.

2.1 Mixed Populations with Different Risks

Many problems in textbooks of reliability theory concern populations on which the risk is uniform at any instant of time. In problems of reliability of structures, however, the strength at any time is not in general uniform but is randomly distributed, so that the risk is also random.

Suppose that the population consists of fractions $\alpha_1, \alpha_2, .\alpha_j., \alpha_q$ with risks $r_1, r_2, .r_j. r_q$, where $\sum_{j=1}^{q} \alpha_j = 1$.

The proportion of α_j surviving the first load is

$$R_{\alpha_j}(1) = 1-r_j \tag{8}$$

The total survivorship of the first load applied is

$$R(1) = \sum_{j=1}^{q} \alpha_j(1 - r_j) = \sum_{j=1}^{q} \alpha_j - \sum_{j=1}^{q} \alpha_j r_j \tag{9}$$

$$= 1 - \sum_{j=1}^{q} \alpha_j r_j \tag{10}$$

Now

$$\sum_{j=1}^{q} \alpha_j r_j = \bar{r}(1), \tag{11}$$

the average risk at load 1.

While, of course, the average risk conveys the idea of the fraction by which the whole population is depleted at the first load application, each element α_j is acted on not by the *average* risk but by its own risk r_j. To assume that all members are acted on by the (instantaneous) average risk would be to assume that all fractions α_j are equally depleted by the risk at the load cycle being applied, so leaving the probability distribution shape of the αs unchanged. It is clear, however, that the α_j subject to the greatest risk must be most depleted, and vice versa.

Similarly to (8), the proportion of the original element α_j surviving to immediately before the $(n-1)$th load is

$$R_{\alpha_j}(n) = (1 - r_j)^n$$

The total survivorship at the nth load is:

$$R(n) = \sum_{j=1}^{q} \alpha_j(1 - r_j)^n \tag{12}$$

The average risk at the nth load is:

$$r(n) = \frac{\sum_{j=1}^{q} r_j \alpha_j (1 - r_j)^n}{\sum_{j=1}^{q} \alpha_j (1 - r_j)^n} \tag{13}$$

In the above expression $R_{\alpha_j}(n)$ is the measure by which the original fraction α_j has been depleted by continued exposure to its risk; those members having the smallest risks will have been least depleted. As before, members are acted upon not by the average risk $r(n)$ but by their own risks.

If one had adopted risk averaging at each applied load in determining survivorship, the (erroneous) survivorship at the nth load is

$$R_e(n) = \{1 - \bar{r}(1)\}^n \tag{14}$$

If r and R are functions of continuous time then Equations (12) and (13) may be written

$$R(T) = \Sigma\, \alpha_j \exp\left\{-\int_0^T r_j(t)dt\right\} \tag{15}$$

and

$$r(T) = \frac{\Sigma\, r_j \alpha_j \exp\left\{-\int_0^T r_j(t)dt\right\}}{\Sigma\, \alpha_j \exp\left\{-\int_0^T r_j(t)dt\right\}} \tag{16}$$

3. STRUCTURAL MODELS AND RELATED FATIGUE RISK AND RELIABILITY ANALYSIS

Conventional semi-probabilistic analysis takes cognisance of ultimate load failure and of fatigue failure; the ultimate load failure risk is calculated from the frequency with which the estimated mean ultimate strength is exceeded, and the reliability and life are determined having defined the structures to be unsafe when their strength has fallen to some arbitrary level, for example, design limit strength[4] or some other fraction of limit strength.[5,6] Conventionally the mean endurance and the dispersion or "scatter" of endurance are estimated on the basis of tests, and it is the magnitudes of loads in the sequence defined for the test which determine to what level the strength will have fallen at the test "life". It is not hard to estimate the test life to any other reduced strength level.

By contrast, the reliability theory approach calculates reliability assuming failure to occur whenever a structure encounters a load greater than its current strength, whatever it may be. The risk of ultimate load failure is the risk of failure under a load greater than the virgin strength, and it can be estimated throughout the lifetime assuming that members retain their virgin strength throughout. The actual fall of strength arising from fatigue increases the risk (and decreases the

reliability). In this report the fatigue risk is taken to be the excess of total risk over the risk of failure with virgin strength preserved, and the unreliability due to fatigue is the excess of total unreliability over the unreliability with virgin strength preserved.

The calculation of reliability requires an applied loads frequency model and a structural model defining the distribution of virgin strength and its decay as crack growth occurs.

Aircraft load frequency information is usually available as "spectra" of frequency per unit time $m(V)$ with which load levels V are exceeded; a method of presentation which makes the data independent of the class intervals of the observations. Experimentally there is a lower limit to the size of loads measured and m_o is the frequency with which this level is exceeded. Smaller loads do occur, but their frequency can only be estimated by extrapolation. The data may be expressed as cumulative relative frequencies $P(V)$, where $P(V) = m(V)/m_o$. Clearly $P(V)$ is a probability - the probability that an applied load will exceed V, and it is therefore the risk of failure at one application of load upon a structure of strength V. Or, if the distribution of loads is defined by its density function $f(V)$, and $F(V) = \int_0^V f(V)\,dV$, then

$$1 - F(V) = \int_V^{\infty} f(V)\,dV \quad P(V)$$

In service usage the aircraft may undertake a variety of missions, and these may be included individually and representatively in the fatigue test history to determine structure mean endurance. For reliability and risk estimating these data are compounded into a single sequence-independent "spectrum".

In transport aircraft problems the wing load spectrum is usually available as an exponential expression similar to

$$m(V/\hat{U}_o) = \exp(A - B\,V/\hat{U}_o) \tag{17}$$

where $\hat{U}_o$ is the average or median virgin strength (see for example, References 2, 3, 7, 8, 9, 10). In combat aircraft the spectrum has sometimes been defined as exponential,[10] binomial[11] or by an empirical curve.[9]

A realistic model for the strength decay properties of a family of structures is less easy to categorise. In an early reliability analysis Ford[2] assumed uniform virgin strength and a general and constant decay rate of strength with time of the form $d\,d\sigma(U/U_o)/dt = -1/R$, immediately from time zero. Eggwertz[7] assumed uniform virgin strength and a log-normal crack initiation time, after which the strength decay rate was general and constant. One may surmise that his model was based on the research of Weibull[12] who showed that with mildly notched specimens scatter in initiation time far exceeded scatter in propagation time, while later work by Pook[19] and others has shown that in carefully made small laboratory specimens there was virtually no scatter in crack propagation rate.

Hooke[10] assumed uniform virgin strength, and a log-normal distribution of test life to failure (at an arbitrary test load) while Diamond and Payne[9] and Hooke[13] assumed that the structures had distributed virgin and residual strengths and a log-normal distribution of the life-time for the strength of structures of median virgin strength to decay to an arbitrary lower level, as it would in laboratory test. This log-normal distribution of lifetime was taken to apply to both initiation and propagation, and appeared to be more in accord with observations of crack propagation in aircraft structures tested under multi-level programme load tests.[14] Several crack propagation and strength-decay functions were investigated, representing ultra-high strength steel structures to which linear elastic fracture mechanics theory is assumed to apply, and aluminium alloy structures whose fracture and residual strength behaviour is nearer that of ductile materials.

This study will be concerned with a single critical location, and the structural modelling will be generally that of References 9, 10 and 13.

The assumptions are as follows:

(i) The virgin strength U_o is distributed as $f(U_o)$, with a distribution which may be normal, log normal or Weibull form. Normally a static strength test will provide an estimator of the population median virgin strength but the distribution shape and standard deviation will usually not be available for the structures in question: this lack may be alleviated by the selection and adoption from other test series[15,20,21,22,23,24] of test results from structures which are deemed to be the most similar to those in question. The standard deviations of various test series vary more than five fold. For the purposes of this report, the figure of 0·03 for the coefficient of variation of strength of metal structures has been adopted (after Reference 15). The shape of the distribution is uncertain, because of sample smallness. With a small value of the coefficient of variation

such as 0·03, three of the commoner distributions mentioned above are not very different.

(ii) The decay of strength of an individual with time cannot be measured, for its strength can only be measured once. The decay of strength of a population can be measured in a statistical sense, and a series of endurance tests will determine the mean, variability and distribution of the time for the strength to fall to the failing strength on test, which is often the highest load in the test programme. A single endurance test, as of a new structural design, will give an estimator of its life (to this critical strength level) but estimates of the scatter will need to be sought elsewhere.[24,25,26,27,3]

Strength decay is a function of crack growth, and crack growth is often measured by observation during the test or by fractographic examination afterwards. Although, in general, a member's strength decay rate is not scaled to its crack initiation time, this will be assumed in the analysis of this report.

Crack length as a function of time is expressed by the function

$$\ell/\ell_{cr} = \psi(t/H) \tag{18}$$

as shown in Figure 1*a*, where H is the time during which the crack length grows to the critical length, as defined above, viz. that at which the *structure of median virgin strength* has its strength fall to, say, limit strength or to the highest load in the test programme.* In accord with the results of tests on structures, H is a random variable, and an often adopted assumption is that it is log-normally distributed.

The decay of strength is a function of crack size, so we may write

$$U/U_o = \phi(\ell/\ell_{cr}) = \phi\{\psi(t/H)\} = \hat{U}/\hat{U}_o \tag{19}$$

as shown in Figure 1*b*.

Allowing for the variability of virgin strength about the median virgin strength $\hat{U}_o$ one may write

$$U/\hat{U}_o = U_o/\hat{U}_o\,[\phi\{\psi(t/H)\}] \tag{20}$$

or

$$U/\hat{U}_o = U_o/\hat{U}_o\,[\zeta(t/H)] \tag{21}$$

as shown in Figure 1*c*.

It will be seen that this model allows for any type of median crack growth, including one with a crack initiation period; ψ, ϕ, ζ, and the time $\hat{H}$ will be determined from test results: it also allows for variability of virgin strength U_o about the median $\hat{U}_o$: it does not allow crack propagation curves to cross (for a structure whose crack grows faster than another at one point in time will always do so) and it makes the residual strength of a structure at a variable time always to bear the same relationship to that of the structure of median strength as it did originally.

(iii) The limit to which any crack could grow is ℓ_F, the length of a crack right through the structure. The associated time is H_F. Because any structure with decreasing strength would have failed earlier as a result of a high load, the probability of a crack reaching ℓ_F is effectively zero.

3.1 Risk of Ultimate Failure

If the structure is assumed to have non-deteriorating strength (and *ipso facto*, it is assumed that fatigue cracks do not initiate), then the risk of failure concerns only the distribution of virgin strength.

For the load spectrum (17) the risk at time t on an element $f(U_o)\mathrm{d}U_o$ of the population whose virgin strengths are U_o, is

$$r_o(t/U_o) = m(U_o/\hat{U}_o) = \exp(A - B\,U_o/\hat{U}_o) \tag{22}$$

or in general,

$$r_o(t/U_o) = m_o\{1 - F(U_o/\hat{U}_o)\}$$

From (7) the reliability, conditional on U_o, i.e. of the element $f(U_o)\mathrm{d}U_o$, is:

$$R_o(t/U_o) = \exp\{-m(U_o/\hat{U}_o)t\} \tag{23}$$

and, averaged over the whole population, is:

$$R_o(t) = \int_0^\infty \exp\{-m(U_o/\hat{U}_o)\,.\,t\}\,f(U_o)\mathrm{d}U_o \tag{24}$$

---

* Mathematically, crack growth time may be characterised equally well by the crack initiation time N_i. Experimentally N_i is difficult to determine and is often not determined.

The initial average risk is obtained by averaging over the whole range of U_o, thus:

$$r_o(o) \quad \frac{\int_0^\infty m(U_o/\hat{U}_o) \cdot f(U_o)\mathrm{d}U_o}{\int_0^\infty f(U_o)\mathrm{d}U_o} \tag{25}$$

Since the element, which initially comprised a fraction $f(U_o)\mathrm{d}U_o$ of the population, comprises at time t only $f(U_o)\mathrm{d}U_o \cdot R(t\ U_o)$, the average risk at time t will be

$$r_o(t) = \frac{\int_0^\infty m(U_o/\hat{U}_o) \cdot R_o(t\ U_o) \cdot f(U_o)\,\mathrm{d}U_o}{\int_0^\infty R_o(t;U_o) \cdot f(U_o)\mathrm{d}U_o} \tag{26}$$

$$= \frac{\int_0^\infty m(U/U_o) \cdot \exp\left[-m(U_o/\hat{U}_o) \cdot t\right] f(U_o)\mathrm{d}U_o}{\int_0^\infty \exp\left[-m(U_o/\hat{U}_o)t\right] f(U_o)\mathrm{d}U_o} \tag{27}$$

$$= -\frac{\mathrm{d}}{\mathrm{d}t} R_o(t) \tag{28}$$

$$R_o(t)$$

It will be seen that the density function for strength conditional at time t is:

$$f(U_o\ t) \quad \frac{f(U_o) \cdot R_o(t\ U_o)}{\int_{U_o\ 0}^\infty R_o(t\ U_o) \cdot f(U_o)\mathrm{d}U_o} \tag{29}$$

This must be contrasted with the assumption sometimes made that "the probability distribution of structural resistance does not change throughout the life".

Had the load spectrum been expressed as probability of exceedance per cycle $P(U_o\ \hat{U}_o)$ where $\mathrm{d}n = n_o\mathrm{d}t$, then

$$R_o(n) = \int_0^\infty \exp\left[-P(U_o/\hat{U}_o) \cdot n\right] f(U_o)\mathrm{d}U_o \tag{30}$$

and the average risk is:

$$r_o(n) \quad \frac{\int_0^\infty P(U_o\ \hat{U}_o) \cdot \exp\left[-P(U_o\ \hat{U}_o)n\right] f(U_o)\mathrm{d}U_o}{\int_0^\infty \exp\left[-P(U_o\ \hat{U}_o)n\right] f(U_o)\mathrm{d}U_o} \tag{31}$$

3.2 Risk of Failure with Deteriorating Strength

In this case the structures are considered doubly distributed in strength according to assumptions (i) and (ii) above, i.e.

U_o and H are independently random.

If we consider an element $\mathrm{d}U_o\mathrm{d}H$, being a fraction $p(U_o)\mathrm{d}U_o p(H)\mathrm{d}H$ of the original population, whose strength at time t is $U = U_o\,\zeta(t/H)$, then its risk rate at time t is:

$$r(t\ U_o, H) = m\{U/\hat{U}_o\} = m\{U_o\,\zeta(t/H)/\hat{U}_o\} \tag{32}$$

and its reliability is, from Equations (7), (23), etc.

$$R(T\ U_o, H) = \exp\left[-\int_0^T m(U/\hat{U}_o)\mathrm{d}t\right] \tag{33}$$

The reliability of the whole is:

$$R(T) = \int_0^\infty \int_0^\infty \exp\left[-\int_0^T m\{U_o\,\zeta(t/H)/\hat{U}_o\}\,\mathrm{d}t\right] \cdot f(U_o)f(H)\,\mathrm{d}U_o\,\mathrm{d}H \tag{34}$$

and the average risk rate is

$$r(T) = \frac{\int_0^\infty \int_0^\infty m\{U_o\,\zeta(t/H)/\hat{U}_o\} \cdot R(T\ U_o, H) \cdot f(U_o)f(H)\,\mathrm{d}U_o\,\mathrm{d}H}{\int_0^\infty \int_0^\infty R(T\ U_o, H) \cdot f(U_o)f(H)\,\mathrm{d}U_o\,\mathrm{d}H} \tag{35}$$

$$= -\frac{\mathrm{d}}{\mathrm{d}t}(R(T))$$

$$R(T)$$

Equation (34) also includes the result of Equation (24) for static ultimate failure, with non-deteriorating strength. For, in Equation (34), the term $m\{U_o\,\zeta(t/H)/\hat{U}_o\}$ becomes $m\{U_o/\hat{U}_o\}$ and is no longer a function of H if the virgin strength is preserved, so that Equation (34) can be written

$$R_o(T) = \int_0^\infty \exp\left[-\int_0^T m\{U_o/\hat{U}_o\}\,\mathrm{d}t\right] f(U_o)\,\mathrm{d}U_o \cdot \int_0^\infty f(H)\,\mathrm{d}H \tag{36}$$

and as $\int_0^\infty f(H)\,\mathrm{d}H$ is equal to unity, and as $m\{U_o/\hat{U}_o\}$ is constant over all t, this degenerates to Equation (24).

$R_o(T)$ and $R(T)$ will thus change with time as shown in Figure 2. The ordinate of $R(T)$ indicates survival; the difference between it and $R_o(T)$ indicates probability of failure by loads less than virgin ultimate strength but larger than current strength, i.e. probability of failure in *weakened structures*, and the defect of $R_o(T)$ from unity is the probability of failure of unweakened structures.

It is perhaps not trivial to note that the latter component $P_o(T) = 1 - R_o(T)$ comprises the probability of failure of uncracked structures and of cracked but unweakened structures

(whether cracks are detectable or not), and that cracked structures are those in which cracks have initiated, i.e. $N_t < T$.

If the residual strength properties of the structure are, for example, of the "brittle type", in which, for larger crack sizes the residual strength is described by linear elastic fracture mechanics theory, whereas small cracks may exist up to a strength-degradation-threshold size without the strength being reduced, then there may be a considerable time period between crack initiation and the start of strength decay, so that, during this period any failures are ultimate load failures even though fatigue cracks are present. The reliability integral can be broken down into its components to analyse this: to do so requires that the population of structures be classified according as they are uncracked, cracked but unweakened, or cracked and weakened thus:

(i) Structures which are uncracked; failure is by loads exceeding virgin strength.
(ii) Structures which are cracked but to less than strength-degradation-threshold size; failure is by loads exceeding virgin strength.
(iii) Structures which are cracked and weakened; failure is
  (*a*) by loads above virgin strength,
  (*b*) by loads less than virgin strength.

Every structure will pass successively through these stages and the time in each stage will be as listed below:

(i) $0 < t < N_t = k_t H$ where $k_t = N_t/H$,
(ii) $N_t < t < H_w = k_w H$ where $k_w = H_w/H$,
(iii) $t > H_w$,

where N_t is the time to crack initiation and H_w is the time to the strength-degradation-threshold crack size.

The strength situation at time T for elements with various values of H is shown in Figure 4.

The reliability of the element while in the first regime is given by Equation (23)

$$R_0(T\,U_o, H) = \exp[-m(U_o\hat{U}_o)\,.\,T]^* \text{ for } T < N_t = k_t H \tag{37}$$

In the second regime it is, from Equation (33)

$$R(T\,U_o, H) = \exp\left[-\int_0^T m(U_t\hat{U}_o)\,dt\right]^\dagger \exp[m(U_o\hat{U}_o)N_t - m(U_o\hat{U}_o)\,.\,(T-N_t)]$$

for $N_t < T < H_w = k_w H$ (38)

and in the third regime it is

$$R(T\,U_o, H) = \exp\left[-m(U_o\hat{U}_o)\,.\,H_w - \int_{H_w}^T m(U\hat{U}_o)\,dt\right]$$

for $T > H_w = k_w H$ (39)

Now, for $T > H_w$, the reliability with virgin strength preserved (given U_o and H) is

$$R_0(T\,U_o, H) = \exp[-m(U_o\hat{U}_o)\,.\,T] \tag{40}$$

The probability of fatigue failure is obtained by subtracting $R(T\,U_o, H)$ of Equation (39), from $R_0(T\,U_o, H)$ of Equation (40),

$$\begin{aligned} F_f(T\,U_o, H) &= R_0(T\,U_o, H) - R(T\,U_o, H) \\ &= \exp[-m(U_o\hat{U}_o)T] - \exp\left[-\{m(U_o\hat{U}_o)\,.\,H_w - \int_{H_w}^T m(U_t\hat{U}_o)\,dt\right] \\ &= \exp[-m(U_o\hat{U}_o)T]\left[1 - \exp\int_{H_w}^T \{m(U_t\hat{U}_o) - m(U_o\hat{U}_o)\}\,dt\right] \end{aligned} \tag{41}$$

Now the reliability of the whole population can be obtained by integrating over the whole, allowing that those elements with $N_t = k_t\,.\,H > T$ only require to be expressed by Equation (37), those with $N_t = k_t\,.\,H < T$ but $H_w = k_w\,.\,H > T$ require to be expressed by Equation (38) and those with $H_w = k_w\,.\,H < T$ require to be expressed by Equations (40) and (41). This splits the integration with respect to the H variable into the three regimes mentioned above, viz., $H > T/k_t$, $T/k_t > H > T/k_w$, and $H < T/k_w$, and in the third regime the integral comprises the contributions from loads above and below the ultimate strength, thus

$$\begin{aligned} R(T) = &\int_{T/k_t}^{\infty}\int_0^{\infty} \exp[-m(U_o\hat{U}_o)\,.\,T]f(U_o)f(H)\,dU_o\,dH \\ &+ \int_{T/k_w}^{T/k_t}\int_0^{\infty} \exp[-m(U_o\hat{U}_o)\,.\,N_t]\,.\,\exp[-m(U_o\hat{U}_o)\,.\,(T-N_t)]f(U_o)f(H)\,dU_o\,dH \\ &+ \int_0^{T/k_w}\int_0^{\infty} \exp[-m(U_o\hat{U}_o)\,.\,T]f(U_o)f(H)\,dU_o\,dH \\ &- \int_0^{T/k_w}\int_0^{\infty} \exp[-m(U_o\hat{U}_o)\,.\,H_w]\{\exp[-\int_{H_w}^T m(U\hat{U}_o)\,dt] - \\ &\qquad \exp[-m(U_o\hat{U}_o)\,.\,\{T-H_w\}]\}f(U_o)f(H)\,dU_o\,dH \end{aligned} \tag{42}$$

Now, the probability of failure $F(T) = 1 - R(T)$, may be obtained from the above, and combining the first three terms within the limits $0 < H < \infty$:

---

* $m(U_o\hat{U}_o)$ is constant.

† $m(U\hat{U}_o)$ depends upon time.

$$F(T) = \int_0^x \int_0^x \{1 - \exp[-m(U_o/\hat{U}_o) \cdot T]\} f(U_o) f(H)\, dU_o\, dH + \int_0^{T-k_w} \int_0^x \exp[-m(U_o/\hat{U}_o) \cdot H_w] \{\exp[-\int_{H_w}^{T} m(U_o/\hat{U}_o)\, dt] - \exp[-m(U_o/\hat{U}_o)\{T - H_w\}]\} f(U_o) f(H)\, dU_o\, dH \quad (43)$$

In this equation, clearly, the first term is the probability of failure by loads above the ultimate strength, during the time $(0, T)$, in the whole population, whether an element be uncracked, cracked and unweakened or cracked and weakened. The second term is the probability of failure by loads less than ultimate strength, before the time T, on members which weaken during the period: it is therefore the accumulated result of the excess risk due to fatigue weakening in the period.

If all failures after initiation were accumulated as fatigue failures, the probability of failure by fatigue, viz., the second term of Equation (43) would be augmented by ultimate load failure contributions from the second and third terms of Equation (42) which would be:

$$\Delta F_f(t) = \int_0^{T-k_t} \int_0^x \exp[-m(U_o/\hat{U}_o) \cdot T] f(U_o) f(H)\, dU_o\, dH \quad (44)$$

and when $T - k_t$ is large compared with H, the effect will be to escalate the "fatigue risk"* and to decrease the probability of surviving the fatigue risk, over a period during which the total reliability and risk are scarcely changed from that with the virgin strength preserved. It actually takes the risk out of the ultimate strength failure category and puts it into the fatigue failure category. This effect may be negligible for load spectra in which the probability of ultimate load failure is negligible, and does not exist where weakening occurs contemporaneously with crack initiation. It is significant in cases where there is a significant risk of ultimate load failure or where there is a long period of relatively slow crack propagation without loss of strength.

In this report we thought it appropriate to link together all failures through loads greater than the virgin strength as "ultimate load failures", and to treat all failures of structures weakened through fatigue as "fatigue failures" or "failure of structures weakened by fatigue".

The "fatigue sensitivity"[17] of a structure is characterised by the ratio of the probability of failure in weakened structures to that under loads greater than virgin strength, i.e., by the ratio $\{F(t) - F_o(t)\}/F_o(t)$. It is a function of both the frequency of loads exceeding ultimate strength, the average rate of decay of strength, and the lifetime allowed. In 1967[18] it was reported that in a period of 20 years, Australia had had, in an advanced military trainer type two ultimate failures and no fatigue failure, in civil transport one catastrophic fatigue failure and one ultimate load failure and in agricultural aircraft two fatigue failures and no ultimate failure.

From this one would assert that agricultural aircraft were most fatigue sensitive, civil transports were partly fatigue sensitive, and advanced military trainers were not fatigue sensitive within the lifetime allowed. In general fatigue sensitivity tends to increase as t increases, so that it may be more factual to acknowledge that fatigue sensitivity for civil transports is controlled by effective life limitations.

This was done less satisfactorily in agricultural aircraft, and it either was not necessary or was most effective in the military advanced trainers in question.

3.3 Averaging of Instantaneous Risk

If the assumption were made that the probability distributions of strength and of H are unaltered "as a result of the very few structures which have failed between the commencement and time t",[16] this would be an assertion that, in Equation (33), the element reliability $R(T, U_o, H)$ is the same for every element $dU_0\, dH$ of the population as it is originally, and as it later becomes an element $dU(t)\, dH$ of the same population with degraded properties. Omission of the term $R(T, U_o, H)$ from numerator and denominator of Equation (35) leads to an erroneous expression for risk:

$$r_c(t) = \int_0^x \int_0^x m\{U_o \zeta(t/H)/\hat{U}_o\} \cdot f(U_o) f(H)\, dU_o\, dH \quad (45)$$

This expression represents a simple averaging of the element risk $r(T, U_o, H)$ of Equation (32), ignoring the element reliabilities $R(T, U_o, H)$. The effect of the element reliability $R(T, U_o, H)$ in the numerator of the correct Equation (35) is to reduce an element's contribution to the

* References 9 and 16 use a terminology "static fracture due to fatigue" for fatigue failures where the strength has not yet fallen to the mean or level flight load, and "fatigue failure" to define (quoting Reference 16), "failure by the fatigue crack extending either completely through the structure, or to the stage where final collapse is caused by the steady mean load".

The author does not favour the terminology unique to References 9 and 16, but uses "fatigue failure" and "fatigue risk" when failure occurs at a fatigue crack, regardless of its size, except when the load causing failure exceeds the virgin static strength.

instantaneous average risk $r(T)$ according as its survival probability has been depleted by prior exposure to the risk.

As Equation (45) does not itself place any lower limit on the magnitude of the strengths still present in the population at time T (in view of the degradation implicit in the expression $U = U_o\zeta(t/H)$), it has been proposed[16] at least to limit the integration to cover only those members of the population with crack size $\ell < \ell_F$, where $t = H_F$ and $U = 0$ at $\ell = \ell_F$. This may be expressed as $H > T/k_F$ where $k_F = H_F/H$. Or alternatively the limit has been proposed to be that crack length at which the strength falls to the steady mean or level flight load, and H_F is then attached to the time at which the crack reaches this length.

This makes the limits of integration of H to be ∞ and $H = T/k_F$, so that $r_e(T)$ becomes

$$r_e(T) = \frac{\int_{T/k_F}^{\infty}\int_0^{\infty} m\{U_o\zeta(t/H)/\hat{U}_o\} \cdot f(U_o)f(H)\,dU_o\,dH}{\int_{T/k_F}^{\infty}\int_0^{\infty} f(U_o)f(H)\,dU_o\,dH} \tag{46}$$

The erroneous reliability is thus:

$$R_e(T) = \exp - [\textstyle\int_0^T r_e(T)]$$

i.e.

$$R_e(T) = \exp - \left[\int_0^T \frac{\int_{T/k_F}^{\infty}\int_0^{\infty} m\{U_o\zeta(t/H)/\hat{U}_o\} \cdot f(U_o)f(H)\,dU_o\,dH}{\int_{T/k_F}^{\infty}\int_0^{\infty} f(U_o) \cdot f(H)\,dU_o\,dH}\,dt\right] \tag{47}$$

In some studies,[9,16] presumably in the interests of simplicity rather than accuracy, while the integration over H in the numerator of Equations (46) and (47) is confined only to $T/k_F < H < \infty$, that in the denominator still is over the range $0 < H < \infty$. This simplification reduces the integration in the denominator to unity, as a result of which $R_e(t)$ becomes

$$R_e(T) = \exp - [\textstyle\int_0^T \int_{T/k_F}^{\infty}\int_0^{\infty} m\{U_o \cdot \zeta(t/H)/\hat{U}_o\} \cdot f(U_o)f(H)\,dU_o\,dH\,dt] \tag{48}$$

and, of course,

$$r_e(T) = \textstyle\int_{T/k_F}^{\infty}\int_0^{\infty} m\{U_o\,\zeta(t/H)/\hat{U}_o\} \cdot f(U_o)f(H)\,dU_o\,dH \tag{49}$$

Equations (47, 48) and (46, 49) must be compared with the correct expressions in Equations (34) and (35) respectively.

4. RISK OF FAILURE WITH INSPECTABLE STRUCTURES

Users of structures have a deeply ingrained sense that structural integrity can be ascertained by inspection. For this sense to be substantiated, and because metal fatigue is a localised rather than an overall phenomenon, it must necessarily be ascertained where and how often to inspect; whether the structure is safe when the signs of failure are first detectable and whether incipient failure can be expected to progress sufficiently slowly that it can safely be found if inspections are scheduled regularly. Inspection merely divides the survivors into two, those having detectable cracks and those not. The former may safely be removed and are no longer at risk; the latter are returned to service. In the statistical model used here, as in all of the models described in Section 3, a member of the random bivariate population has its destiny determined by its initial values U_o and H, and knowing these one may determine whether this member will be detectably cracked or not at a subsequent time t, and how many such members survive up to time t, to be withdrawn if they fall into the detectably cracked class. So the dividing of the population depends upon a member's initial U_o and H; but strictly, upon its value of H.

The survivors at time t are given by $R(t)$ in Equation (34), and inspection divides the population as a member's crack growth time is shorter or longer than a critical value. The "detectable crack size" is ℓ_d, and H_d is the time in which it is reached.

From Equation (18),

$$\ell_d/\ell_{cr} = \psi(H_d/H)$$

Writing

$$H_d/H = \psi^{-1}(\ell_d/\ell_{cr})$$
$$H_d = H\psi^{-1}(\ell_d/\ell_{cr})$$
$$= k_d H$$

where k_d is the fraction of the lifetime at which the crack becomes detectable. All structures having $H < t/k_d$ have cracks which are detectable at time t; those having $H > t/k_d$ have not.

Suppose that an inspection is scheduled to be made at time $t = \Upsilon_1$. Then up to this time the risk upon and the reliability of the population will be exactly as given in Section 3.2. At $t = \Upsilon_1$, structures with $H < \Upsilon_1/k_d$ are found cracked and removed; these are denoted $F(\Upsilon_1)$, viz.

$$F(\Upsilon_1) = \textstyle\int_{H=0}^{\Upsilon_1/k_d}\int_{U_o=0}^{\infty} \exp -[\int_o^{\Upsilon_1} m\{U/\hat{U}_o\}\,dt]f(U_o)\,dU_o f(H)\,dH \tag{50}$$

while the remainder, $1 - F(\Upsilon_1)$, will continue in service and be subjected to service risk. Their reliability may be expressed either as the proportion of the original population remaining in service, viz:

$$R(T\ \Upsilon_1) \quad \int_{\Upsilon_1 k_d}^{\infty} \int_0^{\infty} \exp\ -[\int_0^T m\{U_o\, \zeta(t'H)\, \hat{U}_o\}\, dt] f(U_o) f(H)\, dU_o\, dH \tag{51}$$

(*note*: this differs from $R(t)$, Equation (34), only by the smaller range of integration, $\Upsilon_1 k_d < H < \infty$ instead of $0 < H < \infty$)

or as the fraction of those returned to service after Υ_1

$$R^1(T\ \Upsilon_1) \quad \frac{\int_{\Upsilon_1 k_d}^{\infty} \int_0^{\infty} \exp\ -[\int_0^T m\{U_o\, \zeta(t'H)\, \hat{U}_o\}\, dt] f(U_o) f(H)\, dU_o\, dH}{\int_{\Upsilon_1 k_d}^{\infty} \int_0^{\infty} \exp\ -[\int_0^{\Upsilon_1} m\{U_o\, \zeta(t'H)\, \hat{U}_o\}\, dt] f(U_o) f(H)\, dU_o\, dH} \tag{52}$$

The risk rate upon an element will remain as in Equation (32) for elements remaining in the population after Υ_1, and so, following Equation (35), the average risk rate will be found by limiting the range of integration of H to the range from $H = \Upsilon_1 k_d$ to ∞, thus

$$r_{\Upsilon_1}(T) = \frac{\int_{\Upsilon_1 k_d}^{\infty} \int_0^{\infty} m(U_o\, \zeta(t'H)\, \hat{U}_o) \,.\, R(T\ U_o, H) \,.\, f(U_o) f(H)\, dU_o\, dH}{\int_{\Upsilon_1 k_d}^{\infty} \int_0^{\infty} R(T\ U_o, H) \,.\, f(U_o) f(H)\, dU_o\, dH} \tag{53}$$

There is, of course, no option as regards the denominator, as by definition it is the survivorship at time t.

If inspection is continuous and the population is continually subject to withdrawal of structures with detectable cracks, then this happens when $t = t_d$, i.e., $H = t/k_d$. Clearly the reliability $R(\Upsilon_1\ \Upsilon_1)$ at (i.e., immediately after) an inspection at time Υ_1 is generally true whatever the value of Υ_1, so we may say that the reliability $R_c(t)$ with continuous inspection is, from Equation (51),

$$R_c(T) = \int_{T k_d}^{\infty} \int_0^{\infty} \exp\ -[\int_0^T m\{U, t'H\}\, dt] f(U_o) f(H)\, dU_o\, dH \tag{54}$$

The average risk is, following Equation (53)

$$r_c(T) = \frac{\int_{T k_d}^{\infty} \int_0^{\infty} m\{U, t'H\} \,.\, R(T\ U_o, H) \,.\, f(U_o) f(H)\, dU_o\, dH}{\int_{T k_d}^{\infty} \int_0^{\infty} R(T\ U_o, H)\, f(U_o) f(H)\, dU_o\, dH} \tag{55}$$

It is sometimes possible to distinguish by post mortem fractographic examination that failure had occurred in the presence of fatigue cracks of less than in-service detectable size. Whether the failure were one in service, or one occurring in a laboratory test, in which the failing load was measured, there would be little confidence that fail-safe principles could be used to achieve safety in this case.

The general effect of continuous inspections is (naturally) to deplete the population continuing in service more than it is depleted by the failure risks, so the reliability of the original population will be related to time as shown in Figure 3. If inspection is not continuous, then at each inspection the reliability falls by that fraction of the original population which is removed, as shown in Figure 5, and immediately thereafter the risk is lowered, only to rise again later. The more stringent are the inspections the more will fail to pass, and Figure 5 also shows how the reliability after inspection varies with limiting permissible crack length. After an inspection at any time Υ, the reliability will be the same as if there had been continuous inspection using the same limiting crack length.

5. COMPUTATIONS

Illustrative computations have been made including several cases which cover military and civil spectra, and structures with fatigue behaviour representative of materials with widely differing characteristics, the one with the failure ductility of aluminium alloy structures and the other with the "brittle" behaviour of high strength steel structures whose strength properties approximately obey the laws of linear elastic fracture mechanics up to the ultimate failure stress.

5.1 Change of Probability Distribution of Strength with Time, in the Absence of a Failing Load

The first case considered (denoted A(2)) is representative of a structure of aluminium alloy, acted on by a military manoeuvre type spectrum.

The parameter values applying in this case are given in column 2 of Table 1. The load spectrum adopted is a manoeuvre load spectrum identical with that used in References 10 and 13, and being a straight line closely fitting the curve used in References 9 and 16 within the range of loads above about 60% of the median virgin strength. The growth of crack length with time and the decay of strength with crack length were assumed linear, as in References 10 and 13, being reasonably representative of aluminium structures.

The decay of strength of the population by virtue of the relationship $U/U_o = \zeta(t/H)$, (i.e., by virtue of the fatiguing process, but in the absence of loads causing failure) is shown in fine line and denoted "undepleted" in Figure 6, at times of zero and 500 hours and then every 1000 hours to 5000 hours. The population, assumed initially Weibull distributed about a median value of $U/U_o = 1$ with a coefficient of variation of 0·03, gradually and continuously falls in mean strength, spreads out and becomes skewed in the opposite sense, as a result of the variability in H (age at which strength falls to $\frac{3}{4}U/U_o$).

By contrast, the second case, A(1), is representative of a structure of a "brittle" material, e.g., an ultra-high strength steel, subject again to a military manoeuvre spectrum, being that used in References 9 and 16. Parameter values applying in this case are also given in column 2 of Table 1. In this case the growth of crack length with time is assumed zero until initiation at time $H = 4·4$, it then rises with increasing acceleration as shown in Figure 1 of Reference 9. The fitted analytical expression is $\ell = \ell_{cr} = 0$ for $t < H/4·4$ and $\ell = \ell_{cr} = ((t/H)^{9·0} - 0·0000016)$ for $t > H/4·4$, differing by 0·0000016 from the expression adopted in Reference 10 in order to allow a crack initiation period as allowed in Reference 9.

The residual strength behaviour is assumed to be of "brittle type", in which general yield and ultimate failure coincide, and in which cracks smaller than a strength-reduction-threshold can exist without reducing the ultimate strength: above this threshold the laws of linear elastic fracture mechanics apply, and the failing strength is equal to $K_{1c}/\sqrt{\ell}$ where K_{1c} is the fracture toughness (equal to the failing strength times square root of crack length at which strength reduced with increasing crack size). Since, in this analysis, critical crack length ℓ_{cr} is defined as the crack length at which the strength of a structure of median virgin strength is reduced to limit strength, i.e., $\frac{3}{4}$ of U_o, the strength relationship is $U/U_o = 2\sqrt{\ell_{cr}/\ell}/3$ for $\ell > 4\ell_{cr}/9$, where $4\ell_{cr}/9 = \ell_{ic}$.

The decay of strength of the population (in the absence of loads causing failure) is shown in Figure 7. At 1000 hours there has been virtually no change in the population strength (even the 0·1 percentile of H is greater than 1000 hours). At successively later times the population does not gradually fall in strength: rather, the distribution deflates rather like a balloon leaking progressively more of its members to lower strength values, so that by 10,000 hours the strength of members is seen to be converging towards zero. It will thus be observed that the significance of crack initiation time has disappeared from the strength distribution; rather the time is significant at which the "fracture mechanics" strength-degradation-threshold crack length ℓ_{ic} is reached: only thereafter does the fatigue process increase the risk.

5.2 Reliability and Risk of Static Ultimate Failure with Strength Preserved

Calculation of the risk of ultimate failure (and of the reliability thereunder) for the case A(2) follows Equation (24), and the results are plotted as $R_{U/U_0}(t)$ in Figure 10. Obviously the risk is small, and the reliability falls to 50% only after $4·8 \times 10^5$ hours. The risk (i.e., the instantaneous average risk rate from Equation (26)), $r_{U/U_0}(t)$ is initially $r_{U/U_0}(0) = 4·61 \times 10^{-6}$; and its change with time is illustrated in Figure 9.

The risk rate changes with time as members of the population fail and these are more frequently those of lower strength; and thus by natural selection the survivors become stronger, and the risk smaller. The change in the probability distribution of strength with time (allowing only ultimate failure, and assuming strength preserved) is shown in Figure 8, the distributions being plotted at $t = 0$, 10^4, 10^5, 10^6 and 10^7 hours. It should be noted that for $t = 0$ the graph is of the density function $p(U/U_o)$, while later graphs show how this distribution is eroded by the risk (i.e., is factored by element reliability), leaving survivors whose average strength continues to increase. Had the initial risk continued to operate unchanged the reliability at longer times would have fallen significantly below $R_{U/U_0}(t)$, as is shown by the curve of $R_{U/U_{0_e}}(t)$ in Figure 10.

5.3 Reliability and Risk of Failure for "Ductile" Material under Manoeuvre Spectrum

The total reliability, allowing ultimate and fatigue failure $R(t)$ for case A(2), calculated from Equation (34) is plotted also on Figure 10. For small t it coincides with $R_{U/U_0}(t)$ and diverges perceptibly between 100 and 200 hours. The total usable fleet life, if every aircraft were used until it suffered failure, is represented by the area under this curve. The figure, highly hypothetical rather than practical, is in this case 3920 hours.

The instantaneous average risk rate (ultimate and fatigue) calculated from Equation (35)

is plotted as $r(t)$ in Figure 9. The instantaneous average total risk $r(t)$ at $t = 100$ hours is about 20% greater than the instantaneous average risk rate for ultimate failure $r_{U_0}(t)$, and it grows to twice $r_{U_0}(t)$ at about 350 hours, and to ten times the value at about 1200 hours. Crack initiation time does not enter explicitly into this calculation.

If the fleet were to be operated as a "safe life" fleet, under the acceptable fatigue risk conditions frequently adopted for military aircraft in Australia (viz. reliability not to fall below 0·999 in the lifetime), then the acceptable fatigue life would be reached when $R_{U_0}(t)$ exceeds $R(t)$ by 0·001, and this occurs for case A(2) at a little less than 500 hours (actually at $t = 500$ hours, fatigue probability of failure = 0·0015). This would correspond to a risk rate, if uniform from time $t = 0$, of $3·0 \cdot 10^{-6}$ which is about two thirds of the static ultimate failure risk in this case. In fact, this safe lifetime is rather short. Had the structures achieved the same probability of fatigue failure in, say, 5000 hours (reliability 0·9985), the risk rate, if uniform from $t = 0$, would have been $3·0 \times 10^{-7}$, one fifteenth of the initial risk rate for static ultimate failure alone.

The adoption of a limiting probability of failure during the lifetime as the criterion defining safe life thus penalises structures with good fatigue performance, since, the longer the fatigue lifetime achieved by the structure, the lower is the fatigue risk per hour demanded. More logical is the proposal by Lundberg[28] that the fatigue safety criterion should be specified as a limiting permissible average risk rate per hour, although the figure of 10^{-9} per hour which he proposes for civil aircraft is excessively severe for military combat aircraft.

The author considers that a more logical safe fatigue life criterion for military combat aircraft is one which would make the probabilities of failure during the lifetime from static ultimate and from fatigue failure equal. In Example A(2), this is seen in Figure 10 to occur at $t = 650$ hours when $F_F(650) = F_0(650) = 0·0029$. As the population is assumed to have a median life to failure on test of 5000 hours (failing at $2U_o$ 3) the corresponding safety factor is $5000/650 = 7·7$.

5.4 Change of Probability Distribution of Strength with Time, as Affected by Random Failure Loads

The effect of exposure to the risk over successively longer times, upon the probability distribution of strength of survivors, may be determined. Equation (33) determines the reliability at time t of an element $p(U_o)\,pH$ of the initial population, and its strength at time t is, of course, $U_o\zeta(t,H)$. These have been accumulated as a function of U/U_o for case A(2) in Figure 6, being shown in heavy line, and denoted "depleted", for $t = 1000$ hours to $t = 5000$ hours. This plot shows that as time passes and the population becomes more depleted it is most depleted in the members of lower strength (as would be expected): the average strength decreases progressively, but no members survive whose strengths are below approximately $U/U_o = \frac{3}{5}$. This study challenges the assumption frequently adopted that the probability distribution of strength (i.e., U/U_o) is unaltered with the passage of time. It also reflects upon the process of risk averaging of Equations (45) and (46), in which the integration with respect to strength is in the first case unbounded and in the second, extends to a lower bound which includes members whose strength is on the brink of reaching zero value, because, quite obviously, the probability distribution of strength is not limited at the level where member's strength falls to zero; it is limited by element survivorship at a lower bound approximating to, in this example, the limit strength. In addition it challenges the assumption sometimes used that the risk of fatigue failure consists of two components, a risk of failure r_S in structures whose strength has not yet fallen to the level flight stress or "mean stress",* and a risk of failure r_F in structures whose strength falls to the level flight stress or mean stress.* In this example, and in all practical cases, the alternating loads which are forcing the fatigue process are always sufficiently greater than zero that no structure can survive to fail at the level flight or mean stress. There is in fact only the one component of fatigue risk.

5.5 Reliability and Risk in "Safe-by-Inspection" Structures

"Fail-safe" or "safe-by-inspection" structures are inspectable, and cracks must be findable, and found, when exceeding some "detectable crack length" ℓ_d. Structures found cracked may or may not need to be withdrawn: the "crack size for component rejection" may be larger than ℓ_d, depending on the risk associated with its further operation.

In Example A(2), several exploratory calculations were made. In series Γ, it was assumed

* See footnote on page 310.

that inspections would be made at times $\Upsilon_1 = 100$ hours, $\Upsilon_2 = 200$ hours, $\Upsilon_3 = 300$ hours, etc., and that cracks could be detected and withdrawal made if $\ell \ell_{cr} > 0{\cdot}02$, i.e. $U U_o < 0{\cdot}994$. The reliability at a time t after an inspection at time Υ is calculated from Equation (42), and the risk rate from Equation (44). The results for $R(t)$ and $r(t)$ are plotted in Figure 9 and Figure 10 respectively. The curve labelled Inspection Schedule I in Figure 9 shows that during the first 300 hours the risk rate (on those surviving inspection) hardly exceeds $6{\cdot}0 \times 10^{-6}$ per hour, but the associated curve of Figure 10 shows a fall in reliability to 49·9% at 100 hours (i.e., 50% of the population is rejected at the inspection), and a fall to 3·99% at 200 hours, i.e., another 46% of the original population are lost at the second inspection. Thus 96% of the population has been rejected at the first and second inspections, in the interests of keeping the fatigue risk rate low, and at the same time a safe life of 500 hours without inspection would have been accepted. Clearly, the rejection criterion of $\lambda_d = \ell_d \ell_{cr} = 0{\cdot}02$ is too severe: it is probably easily achievable by modern techniques, but it throws away many cracked structures whose reliability is as good as many uncracked ones.

To further explore this point, an inspection schedule denoted A was investigated, in which one inspection was made at Υ = safe life of 650 hours, and structures withdrawn if cracks were found with $\ell > \lambda_d \ell_{cr}$, with values of $\lambda_d = 0{\cdot}05, 0{\cdot}01, 0{\cdot}20, 0{\cdot}50$. Reliabilities after time Υ were calculated, and plotted in Figure 10.

The calculations showed that, with $\lambda_d = 0{\cdot}50$, the largest value, the reliability was no different from that without inspection, i.e., the cracks tolerated were so large that inspection provided no safety. For successively smaller values of λ_d, the proportion surviving the inspection grew successively smaller, while the risk rate on those surviving grew smaller. For example, with $\lambda_d = 0{\cdot}10$, the proportion surviving inspection at $\Upsilon = 650$ was 24·9%, while the risk was reduced to $8{\cdot}9 \times 10^{-6}$ per hour (see Figures 9 and 10), a value which could well be regarded as acceptable. If, however, there were no further inspections, the reliability will eventually fall and become asymptotic to that resulting if there had been no inspection.

If it were desired to ensure that the instantaneous average risk of fatigue failure did not exceed the static ultimate failure risk, then the first inspection would need to be scheduled before the safe life. Calculations have been made for a third Inspection Schedule E, inspecting first at $\Upsilon_1 = 350$ hours and then at every 50 hours to 1000 hours using $\lambda_d = 0{\cdot}1$. The results for risk rate and reliability are also shown in Figures 9 and 10 respectively. It is interesting to observe from Figure 9 that this schedule with regular 50 hour periods between inspections keeps the average instantaneous risk to never more than $9{\cdot}6 \times 10^{-6}$ per hour over the first 1000 hours, while allowing 50% of the fleet to achieve a life of 550 hours, 30% to achieve 650 hours, 11% to achieve 850 hours, and 4% to achieve 1000 hours. This particular case provides an interesting example of the contrasts between operating the same structural fleet as safe life or as fail safe structures. In the two cases the total utilisation got from the fleet is not markedly different. As a safe life fleet all aircraft are retired at 650 hours: the safety criterion was satisfied (of a probability of failure by fatigue $\geq 0{\cdot}003$): the instantaneous average risk grew to a maximum value of $16{\cdot}2 \times 10^{-6}$ per hour at the end of life. As a fail safe fleet some structures, 68% in fact, were rejected before achieving the safe life, so as to keep the instantaneous average risk to a level, but others were operated *with equal safety* to well beyond the safe life, even to 1000 hours. Of course these remarks apply to the situation where load spectrum and fatigue properties are precisely known. When this is not so, the fail-safe treatment may well engender greater confidence in the user. It is also interesting to note from Figures 9 and 10, as might have been expected intuitively, that both the reliability and the risk rate immediately after the inspection at 650 hours are the same, whether this inspection were the first to be carried out, or whether it had been preceded by regular inspections at every 50 hours from $\Upsilon = 350$ hours or from the beginning.

Examination of the risk rate curve for Schedule E shows that from 650 hours to 1000 hours the instantaneous average risk was tending to rise, slowly but steadily. This effect results from the probability distribution of H; the risk will continue to rise (if there were any survivors) at least to the median value of H. With the risk gradually rising when inspection intervals are constant there is no justification for the practice sometimes adopted of increasing intervals between inspections. As structures are withdrawn it may be chosen to replace them with new. If the risk rate is calculated by averaging together the new and the old, and inspection intervals lengthened to keep the average risk constant, eventually all of the risk will be concentrated upon the oldest aeroplanes remaining in service. This is what might have been anticipated intuitively. It is preferable to keep the inspection intervals constant or even to reduce them

if this is necessary to avoid excessive increase in the risk on survivors of the original population.

6. ACCEPTABLE RISK

Every life experience involves risk. The estimation of the risk in any experience, and its weighing are highly subjective. Only in the courts of law does the fiction of "absolute safety" exist, and those (we) who are responsible for other people's safety may be tempted to argue "absolute safety" within those precincts, when in truth the chance of failure was "small" or "negligibly small". The question of safety becomes "safe for whom?" and negligibly small becomes "negligibly by whom?". A fighter pilot of a hypothetical service unit with one hundred pilots and aeroplanes, of which three of each are lost per year, may well consider the risk of his occupation acceptably small, and indeed his risk of death in any one year is no greater than that of a public servant on his retirement at age 65. If in our hypothetical example the average hours flown per year were 300, then the risk rate is 10^{-4} per hour. Actually, *structural* accident rates are much lower. Pugsley[30] has quoted $3{\cdot}2 \times 10^{-5}$ per hour as "a little above the average for modern (fighter) aeroplanes". Similarly, ultimate failures of the advanced military trainers referrred to in Section 3.2 above represent a risk rate of approximately $1 \cdot 10^{-5}$ per hour, while calculation example A(2) above gives an initial ultimate failure risk rate of $4{\cdot}6 \cdot 10^{-6}$ per hour. Taken altogether, these values of risk rate of structural failure (viz. 32×10^{-6}, 10×10^{-6} and $4{\cdot}6 \cdot 10^{-6}$ per hour) are regarded as acceptable because they are being accepted by the military authorities as a whole and by the individual personnel at risk, without there being imposed restraints on the operations or requirements enunciated for stronger structures.

In any activity in which the risk rate per hour monotonically increases with time, the risk will eventually reach an unacceptable level, by whatever subjective criterion the level is set: e.g., Maxwell[31] states, in the fail-safe context, "any damage arising from errors inseparable from normal operation is detected before the strength of the structure falls to an unacceptable level". Lundberg[29] pioneered the concept that this limit of acceptability is or should be measured by the accident rate. In considering the civil air transport field, where equally high risks would not be accepted by the general public, he observed that fatigue is the least excusable cause of accident, and "deemed it imperative to set the fatigue safety goal sufficiently high so that accidents due to fatigue are in practice never (or very seldom) heard of". By his comparison with an accident rate resulting from all causes of $300 \cdot 10^{-9}$ per hour, he proposed a fatigue accident rate goal of 10^{-9} per hour, and observed that, assuming an average lifetime of 10^4 hours, this would define an acceptable probability of failure of an aircraft during its lifetime of 10^{-5}. The accident rate from all causes of $3 \cdot 10^{-7}$ per hour seems to have been substantiated by some later studies (e.g. Table 5*a* of Reference 32) but in general, civil aircraft fatigue failure rates, whether for safe life or for fail-safe structures, have exceeded Lundberg's proposed target figures.

In ARL it has been the practice for many years to think of a figure of 10^{-3} as being an acceptable probability of fatigue failure during the lifetime for military aircraft, whether fighter, bomber, transport or maritime aircraft. In view of the differences in life of type of the aircraft of different roles, and indeed, the differences of risk known to accompany the various roles, it is now considered inappropriate to apply the same figure indiscriminately. A front line attack aeroplane, if it were employed for a life of type of 5000 hours would demand an acceptable fatigue risk of 2×10^{-7} per hour, which is 1/160, 1/50 and 1/25 respectively of the ultimate failure rates noted earlier as generally acceptable.

As the demanding of very low acceptable fatigue risks leads to retiring from service aeroplanes in which the risk of operation is *no greater or only marginally greater* than that of unfatigued structures, the fleet becomes rapidly depleted with only a marginal increase of safety, if any.

It is the author's view that for military aeroplanes used in a fighter role or any role in which the probability of ultimate failure is mensurable (e.g. say 5×10^{-6} per hour or greater) an acceptable average fatigue risk might well be chosen equal to the ultimate failure risk. On the other hand a fatigue risk of the order of 2×10^{-7} per hour seems not inappropriate for military transport aircraft, and for civil transport aircraft carrying fare-paying passengers, the fatigue accident rate goal of 10^{-9} per hour enunciated by Lundberg has never been challenged on grounds of being too low.

7. "RELIABILITY" OF RELIABILITY AND RISK ESTIMATES

It was pointed out in the commencement that in aircraft structural contexts, reliability and risk estimates must be based upon test data which are the product of sampling: the choice of data appropriate in representing the structure is a matter of judgement, as is the question of acceptable limiting values of reliability and risk. While personal judgement errors are not amenable to statistical analysis, sampling errors are.

The effects of sampling errors may be investigated by determining confidence regions for the parameters, and examining the range of reliabilities transformed from confidence regions. Although this might be done by a calculation combining the effects of every parameter's confidence range, this is considered inappropriate, and indicative methods are adopted here.

7.1 Confidence Intervals Related to the Sampling of H

Considering first the median endurance $\hat{H}$, this is usually determined from a single test, and is taken as an estimator of the mean value of the logarithm of endurance, $\mu_{\hat{H}}$. By normal sampling theory it may be shown that a 50% confidence interval for $\log \hat{H}$ is $\overline{\log H} \pm 0{\cdot}675\,\sigma_{\log H}/\sqrt{n}$ where $\overline{\log H}$ is the experimental test mean and n is the sample size. With a single test result for $\overline{\log H}$, and $\sigma = 0{\cdot}167$ adopted for the calculations of this report, we calculate the $\alpha = 50\%$ confidence region for H, viz. $(H/1{\cdot}296,\ 1{\cdot}296\,H)$: (the factor 1·296 is sometimes called the probable error). A region of 95% confidence (i.e., size $\alpha = 95\%$) is $(H/2{\cdot}12,\ 2{\cdot}12\,H)$.

To many, even to those familiar with fatigue and fatigue variability, it may seem questionable that a single test result is *likely* to be as much in excess of the population mean as 1·3 times the latter. An example of such an event happening was the testing of the first fatigue specimen of a Provost wing[32] in which port and starboard wings failed at 13,422 and 15,347 hours, which became the two largest values in a test series which was subsequently to grow to 41 wings; and these two values exceeded by factors of 1·42 and 1·62 respectively the mean life of the sample of 41. (Significantly, the first two results could not in any sense be regarded as "outliers".)

In general the lifetime T_β corresponding to a chosen probability of failure β or reliability $1-\beta$ is scaled directly to the value of $\hat{H}$. We may write $T_\beta = k_\beta \hat{H}$. Thus the confidence region for T_β becomes $(k_\beta \hat{H}/x,\ k_\beta \hat{H}\cdot x)$ where $x = 1{\cdot}296$ for a 50% confidence region and $x = 2{\cdot}2$ for a 95% confidence region.

7.2 Confidence Intervals Related to the Sampling of σ

Sampling errors in the standard deviation of $\log H$ should then be considered. An interval of 50% confidence for the variance is given by

$$\sigma^2_{75} < \sigma^2 < \sigma^2_{25}$$

where

$$\sigma^2_x = \Sigma(x-\bar{x})^2/\chi^2_x$$

Typically a test series such as Table V of Reference 24, with 44 specimens providing 34 degrees of freedom, has confidence regions

$$(\sigma_{75}, \sigma_{25}) = (0{\cdot}913s,\ 1{\cdot}100s), \qquad \alpha = 0{\cdot}5$$

and

$$= (0{\cdot}85s,\ 1{\cdot}21s), \text{ for } \alpha = 0{\cdot}95.$$

The pooled result of Table V of Reference 24 represented wings of four different aircraft and a built up panel. The largest unpooled standard deviation was $1{\cdot}20s$ and the smallest $0{\cdot}28s$. It is probably beyond the most intensive research to establish whether the four types of aircraft were sufficiently similar in construction, etc., that the pooled dispersion is more appropriate to any one than its own individual estimate (this being a criterion for valid pooling). It is probably even more beyond research to decide whether such data are relevant to modern aircraft of the 1970s.

Assuming these data are relevant, the effects on life for a nominated level of reliability may be examined. In Reference 10 it was observed that in general changes in σ produce no change in the life at which the reliability is 50%. It was shown in Reference 10 that the curve of reliability against life is bounded at high reliabilities by the ultimate failure risk (which is unaffected by σ) and below this, generally, by a line representing the reliability of the population against failure at the limit load, and Figure 10 of this report supports this view. The effect of changes in σ is to rotate this reliability curve about the point corresponding to T, $R(T) = 0{\cdot}5$, i.e., the life for a given probability of failure is altered the more that probability differs from 50%. Writing

$h = \log_{10} H$, i.e. $10^h = H$. $\mu_h = \log_{10} \tilde{H}$, etc., and σ is the s.d. Let us consider a fractile of the population given by

$$Pr\ (h < \mu_h - k_2\sigma) = \alpha$$

Then a region of 50% confidence for h is

$$\mu_h - k_2\sigma_{.5} < \mu_h - k_2\sigma < \mu_h - k_2\sigma_{.25}$$

So the 50% confidence region becomes

$$\log_{10} \tilde{H} - k_2\sigma_{.5} < \log_{10} \hat{H} - k_2\sigma < \ldots$$

or in terms of $\hat{H}$,

$$\hat{H} \cdot 10^{-k_2\sigma_{.75}} < \hat{H} \cdot 10^{-k_2\sigma} < \ldots$$

$$\text{or} \quad \frac{H}{10^{k_2\sigma}} \cdot 10^{k_2(\sigma - \sigma_{.75})} < \frac{H}{10^{k_2\sigma}} < \ldots$$

or writing $H_\alpha = \hat{H} \cdot 10^{-k_2\sigma} = H \cdot \varepsilon$

a 50% confidence region for H_α, the life to reliability α is

$$H_\alpha \cdot 10^{k_2(\sigma - \sigma_{.75})} < H_\alpha < H_\alpha \cdot 10^{k_2(\sigma - \sigma_{.25})}$$

$$\text{i.e.} \quad (H_\alpha \cdot 10^{k_2(\sigma - \sigma_{.75})},\ H_\alpha \cdot 10^{k_2(\sigma - \sigma_{.25})})$$

For example, if we are considering the lifetime for a reliability of 99·9%, viz. 0·999, we might have

$$Pr\ (h < \mu_h - k_2\sigma) = 0{\cdot}999,\ k_2 = 3{\cdot}09,$$

and, using as before, $\sigma = 0{\cdot}167$, with number of degrees of freedom = 34, the 50% confidence region is

$$(1{\cdot}08\ H_\alpha : 0{\cdot}88\ H_\alpha)$$

and the 95% confidence region is

$$(1{\cdot}25\ H_\alpha : 0{\cdot}69\ H_\alpha).$$

Comparison of this region of 95% confidence for H_α, allowing for sampling error of σ, with the corresponding confidence region for H_α allowing for sampling error of H, when based upon a single test, viz. $(2{\cdot}12\ H_\alpha : 0{\cdot}47\ H_\alpha)$, shows that the former is very considerably narrower than the latter. The same results are shown in a comparison of the 50% confidence regions of H_α, allowing for sampling errors of σ and H respectively. It is a fair deduction that if such a body of representative data are available for the estimation of σ, the uncertainty arising from sampling error of σ is very much less than the uncertainty arising from the sampling error of H.

7.3 Confidence Intervals Related to the Sampling of U_o

The mean static ultimate strength is normally estimated on the basis of a single test, and confidence levels are similar to those for H. Adopting the log-normal assumption, and $\sigma = 0{\cdot}03$ the 50% confidence region becomes $(1{\cdot}048\ \tilde{U}_o : \tilde{U}_o\ 1{\cdot}048)$ and the 95% confidence region $(1{\cdot}145\ \tilde{U}_o : \tilde{U}_o\ 1{\cdot}145)$.

The load spectrum for wings is often determined in terms of aircraft acceleration and is then defined in terms of ultimate strength. Confidence intervals for strength become confidence intervals upon the strength exceeded with a particular frequency m, thus, for example the manoeuvre spectrum $\log m = 6 \cdot 12U/\tilde{U}_o$ for A(2), becomes bounded by $m = 10^{6-12U/\tilde{U}_o \times 1{\cdot}048}$ and $m = 10^{6-12U/\tilde{U}_o \times 1{\cdot}048}$. At a representative level $0{\cdot}8\tilde{U}_o$, at which the depletion may be assumed, on the average, to be congregated, the 50% confidence interval for frequency becomes $(2{\cdot}75 \cdot 2{\cdot}51 \cdot 10^{-4} : 0{\cdot}35 \cdot 2{\cdot}51 \cdot 10^{-4})$. The 95% confidence region for m becomes $(16{\cdot}4 \cdot 2{\cdot}51 \cdot 10^{-4} : 0{\cdot}041 \cdot 2{\cdot}51 \cdot 10^{-4})$. One may assume as a first approximation that the lives are inversely proportional, thus giving a 50% interval $(0{\cdot}35\ H_\alpha < H_\alpha < 2{\cdot}75\ H_\alpha)$ and a 95% interval $(0{\cdot}041\ H_\alpha < H_\alpha < 16{\cdot}4\ H_\alpha)$. Thus errors in the relationship between the loads at which the frequencies of loads are measured, and the ultimate static strength of the wing are very critical, and considerable sampling error exists if the ultimate strength value is estimated upon the results of a single test.

7.4 The Effect of Variability in Virgin and Residual Strengths

The effects of variability in ultimate strength have not been directly investigated in this report, but may be deduced by comparison of the reliabilities calculated in this report, e.g. Figure 9 (the variability being included), with those calculated without variability in the virgin strength, as calculated in Figure 3 of Reference 10. This comparison shows that, at lifetimes where fatigue risk is significantly greater than that of ultimate failure, there is virtually no difference whether the population is assumed to vary in virgin strength or not. This might have been expected intuitively.

7.5 Confidence in Relation to Extrapolation of the Spectrum

Load spectra are of two sorts, those measured, and those predicted. A regular review of these two components is necessary as life proceeds. In fighter aircraft the predicted reliability is sensitive to the upper end of the load spectrum and those used in calculations (A1) and (A2) define approximately one exceedance of median ultimate strength per million hours. It is unusual for fighter aircraft to be lifed for more than 2000 hours and it is unusual for fleets to consist of 500 aeroplanes: for Australia a fleet of 100 aeroplanes is more realistic. So any load exceeding median ultimate strength is expected to occur less frequently than once in 100 lifetimes. In fact, the load expected once in the lifetime of 100 planes is nearer 94% of the median strength figure. It is therefore questionable whether such loads will occur. It will be noted that the initial risk of ultimate failure in case A(2) in approximately 5×10^{-6} which is once per fleet lifetime as above. Clearly the magnitude of this risk, and indeed of the permissible fatigue risk, cannot be precisely estimated: it is necessary to extrapolate the spectrum past the available data.

It should be remembered that habitual conservatism in the estimation of parameters when those parameters are known imprecisely (underestimates of strength and of population mean life to failure; overestimates of variability of endurance and of magnitudes of applied loads) will result in the risk and the probability of failure being greatly overestimated by comparison with the "best estimates", and thus the permissible life will be very much shorter than if estimated according to the methods of "best estimates".

In a typical example, an estimate was made of the life for a probability of failure of 10^{-3}, using the 97·5% confidence bounds for H, σ and $U/\hat{U}_o$. The resulting *best estimate* of the probability of failure in the lifetime was approximately $1 \cdot 56 \times 10^{-8}$.

The author considers it unreasonable to demand such a degree of safety, that, in aiming to achieve a probability of failure of 10^{-3}, a user actually adopts an ultra safe figure such that the best estimate of the probability of failure is five orders of magnitude smaller.

It must be remembered, however, that the data on H and $\hat{U}_o$ are obtained on a single test of one structure which belongs to the fleet, whereas the data concerning the standard deviation do not.

The above discussions render it clear that the safety of safe life structures is critically dependent upon the assumptions concerning the structural and endurance properties.

7.6 Confidence Related to Safe-by-Inspection Structures

Studies of fail-safe behaviour, in particular the investigations of instantaneous average risk after successive inspections, show them to be much less sensitive to the number of inspections during the time for strength deterioration. This confirms what has been deduced intuitively, that fail-safe structures can be continued in operation much longer and more safely than safe life structures—provided locations of potential failure are *all* known. If this is so structures may be continued in service with inspection for very much longer than their safe lives without the risk being significantly higher.

8. GENERAL DISCUSSION

Structural reliability in the presence of risks of ultimate failure and of fatigue failure is a function of the applied load spectrum, and particularly the high loads, and of the strength distribution and its rate of decay under the spectrum. We might describe these loads as "fatigue forcing" loads since many loads which help to initiate and to propagate fatigue cracks are too small in magnitude to be the final one which causes collapse. Crack propagation is an averaged effect and is not related to each individual successive load of the spectrum: the effects of crack retardation by single high loads, or crack acceleration by large loads of opposite sign or whatever, are not taken into account in current reliability approaches.

The structural behaviour of the material with time, when cracked, has a most marked effect on the reliability or risk at any time. Materials with "brittle-type" failure properties, such as ultra-high strength steels may support the initiation and growth of cracks for a considerable period without loss of strength, so that the reliability is unaffected until the strength-reduction threshold is reached, whereas with the more ductile behaviour of aluminium alloys strength decay and increasing fatigue risk commence together, immediately when crack initiation occurs.

Where there is a significant probability of ultimate failure (failure by loads greater than the ultimate strength), there is also a significant probability that structures which are fatigue cracked

will fail by loads greater than their ultimate strength, i.e., the structures would have failed at the particular time and applied load event whether they had been fatigue cracked or not. Reliability theory, properly applied, separates these possibilities. In this report we define fatigue failures as those where the failure load is less than the virgin ultimate strength. Ultimate strength failures can only be reduced by increasing the ultimate strength or by truncating the top of the load spectrum, perhaps by a placarded limit on the aircraft operation. Fatigue failures are capable of reduction by replacement with new components, or, in the fail safe area, by inspection. For structural problems the risk at an instant is not uniform over the population: it is greater on weaker members. It may be averaged, to indicate the population depletion by the next load; however, each structure, whether weaker or stronger, is acted upon not by the average but by its own risk. The adoption of instantaneous risk averaging for determining future reliability leads to underestimation of future reliability and over-estimation of future risk.

The distribution of strength of a population changes with time. With strength preserved, the survivors evolve to become, on the average, stronger with time, and the risk rate decreases with time. With a population deteriorating by the normal fatigue processes, the average strength falls with time, but again, weaker members are eroded more rapidly, so that the distribution becomes more and more positively skew, and no member survives to the point where its strength is zero, or falls to say, the level flight load. In one example, no members survived till their strengths had fallen below limit strength.

The safe life criterion of a probability of failure of 10^{-3} in the lifetime, when applied to fighter aeroplanes, may produce a fatigue risk comparable to the static failure risk if the lifetime is short; for a longer safe lifetime (say 5000 hours) the fatigue risk may well be an order of magnitude lower. Consideration is directed towards the adoption of a safe life criterion expressed as a time-average risk rate per hour, and to the adoption of a figure comparable with the static ultimate failure risk. For civil transport aircraft carrying fare-paying passengers, the fatigue risk goal proposed by Lundberg of 10^{-9} per hour has never been upstaged.

If a structure is inspectable and capable of being treated as fail safe, withdrawal from service when a crack is detected, however small, may be economically disastrous without significantly reducing the risk. Where crack growth rate between inspections is small, and its variability is confidently known, the intervals between inspections and the crack size for withdrawal from service should be mutually chosen to optimise the utilisation of survivors, while keeping the risk within bounds.

The estimation of reliability and of risk can be made with mathematical precision if the input data are precise. In any practical case the input data are never precise, since they involve sampling errors in the measurement of those parameters which are measured upon structures of the type in question, and personal judgements about parameters which are attributed to the structures in question but were measured on other structures: they involve estimations of the load spectrum, including at high loads where the frequency may be less than once in the lifetime of an aeroplane and even as low as once in the lifetime of a fleet: and the withdrawal from service of safe life or fail safe structures devolves upon the use of limiting acceptable values of the reliability and risk, which also are matters of personal and generally corporate judgement.

9. ACKNOWLEDGMENT

The author desires gratefully to acknowledge the assistance of Miss B. I. Green in making the computations.

REFERENCES

1.	Myers, R. H., Wong, K. L., and Gordy, H. M.	Reliability Engineering in Electronic Systems. John Wiley and Sons, Inc., 1964.
2.	Ford, D. G.	Appendix A to "Some Considerations Relating to the Safety of 'Fail-Safe' Wing Structures." Full Scale Testing of Aircraft Structures (eds Plantema and Schijve). Pergamon Press, 1961.
3.	Eggwertz, S.	Investigation of Fatigue Life and Residual Strength of Wing Panel for Reliability Purposes. ASTM Special Technical Publication 511, 1972.
4.	Anon.	British Civil Airworthiness Requirements, Parts D and K.
5.	Anon.	British Aviation Publication 970 (Av. P. 970). Ministry of Aviation, UK.
6.	Anon.	Federal Aviation Regulations of the USA, Parts 23 and 25.
7.	Eggwertz, S.	"Inspection Periods Determined from Data of Crack Development and Strength Reduction of an Aircraft Structure using Statistical Analysis." Fatigue of Aircraft Structures (W. Barrois and E. L. Ripley), p. 345. Pergamon Press, 1963.
8.	Schijve, J.	"Endurance under Program Testing." Full Scale Testing of Aircraft Structures (F. J. Plantema and J. Schijve), p. 45. Pergamon Press, 1961.
9.	Diamond, Patricia, and Payne, A. O.	"Reliability Analysis Applied to Structural Tests." Advanced Approaches to Fatigue Evaluation, p. 275. NASA SP-309, 1971.
10.	Hooke, F. H.	"A Comparison of Reliability and Conventional Estimation o Safe Fatigue Life and Safe Inspection Intervals." loc. cit., Ref. 9, p. 667.
11.	Gassner, E., and Schütz, W.	"The Significance of Constant Amplitude Tests for the Fatigue Evaluation of Aircraft Structures." loc. cit., Ref. 8, p. 14.
12.	Weibull, W.	"Basic Aspects of Fatigue." Colloquium on Fatigue, p. 289. IUTAM, Stockholm, May 1955.
13.	Hooke, F. H.	**Probabilistic Design and Structural Fatigue.** The Aeronautical Journal, p. 267, June 1975.
14.	Hooke, F. H., and Barnard, J. M. H.	Fracture Study as an Aid to Fatigue Evaluation. 37th Congress of AANZAS, Canberra, 1964; also ARL Tech. Memo SM 123, 1963.
15.	Atkinson, R. J.	Permissible Design Values and Variability Test Factors. ARC R&M 2877, 1955.
16.	Grandage, J. M., and Payne, A. O.	A Probabilistic Approach to Structural Design. ARL Report SM 337, 1972.
17.	Freudenthal, A. M.	Reliability Analysis Based on the Time to First Failure. 5th ICAF Symposium, 1967; Aircraft Fatigue, Design, Operational and Economic Aspects. Pergamon, 1972.
18.	Hooke, F. H.	Discussion on "Reliability Analysis Based on the Time to First Failure". loc. cit., Ref. 17.
19.	Pook, L. P.	Basic Statistics of Fatigue Crack Growth. NEL Report 595, June 1975.

20. Marmion, L., and Starkey, R. D. — Statistical Strength Tests of Typhoon Semi-span Tailplanes. ARC 8258, October 1944.

21. Starkey, R. D. — Interim Note on the Results of Strength Tests on 60 Master Tailplanes. RAE Tech. Note SME 155, June 1943.

22. Johnstone, W. W., and Patching, C. A. — Static Strength Tests on P.51D Mainplanes. ARL SM Note 185.

23. Freudenthal, A. M., and Payne, A. O. — The Structural Reliability of Airframes. Air Force Materials Laboratory Report, AFML-TR-64-401, December, 1964.

24. Jost, G. S., and Verinder, F. E. — A Survey of Fatigue Life Variability in Aluminium Alloy Structures. ARL Report SM 329, 1971.

25. Stagg, A. M. — Scatter in Fatigue: Elements and Sections from Aircraft Structures. RAE Tech. Report 69155, July 1965.

26. Stagg, A. M. — An Investigation of the Scatter in Constant Amplitude Fatigue Test Results in Aluminium Alloys 2024 and 7075. ARC CP 1093, 1970 (replacing RAE Tech Report 69075).

27. Bastenaire, F. — Etude statistique et physique de la dispersion des résistances et des endurances á la fatigue. Thesis, University of Paris, 1960.

28. Lundberg, Bo K. D. — "The Quantitative Statistical Approach to the Aircraft Fatigue Problem." Full Scale Fatigue Testing of Aircraft Structures. ICAF Symposium, 1959; Pergamon Press, 1961 (p. 393).

29. Ford, D. G., and Grandage, J. M. — Approximate Life Distribution of Cracked Structures with Random Risks. ARL Note SM 363, 1971.

30. Pugsley, A. G. — A Philosophy of Aeroplane Strength Factors. ARC R&M 1906, 1942.

31. Maxwell, R. D. J. — Fail Safe Philosophy, an Introduction to the Symposium. Proceedings of the 7th ICAF Symposium, London; RAE TR 73183, 1974.

32. Parish, H. E. — Fatigue Test Results and Analysis of 42 Piston Provost Wings. M o A S&T Memo 1 65, 1965.

TABLE 1

Constants Used in Reliability and Risk Calculations

Examples A(1), A(2) and A′(2) (military) and Examples B(1) and B(2) (civil transport) analyses

(1) Parameter	(2) Example A (military fighter type)	(3) Example B (civil transport)
$\hat{H}$ = Median population test life	5000 hours	16,667 hours
σ = Standard deviation of log H	0·167	0·167
$b\hat{U}_o$ = Highest test load	0·67 $\hat{U}_o$	0·5 $\hat{U}_o$
U_o is	Weibull distributed	Weibull distributed
σ_{U_o}	0·03	0·03
$\ell/\ell_{cr} = \psi(t/H)$ (i) Power fn. of t/H, with initiation at $H/4·4$ (ii) Linear fn. of t/H (iii) Piecewise linear fn. of t/H with initiation at $0·6\,H$	A(1): $(t/H)^9 - 1·6 \times 10^{-6}$ A(2): t/H	B(2): t/H B(3): 0 for $t/H < 0·6$ $t/H - 0·6$ for $0·6 < t/H < 0·97$ $-20 + 21\ t/H$ for $t/H > 0·97$
$U/U_o = \phi(\ell/\ell_{cr})$ (i) Inverse root fn. of ℓ/ℓ_{cr} (ii) Linear fn. of ℓ/ℓ_{cr}	A(1): 1 for $\ell/\ell_{cr} < 0·44$ $0·67\sqrt{\ell_{cr}/\ell}$ for $\ell/\ell_{cr} > 0·44$ A(2): $1 - \ell/3\ell_{cr}$	$1 - \ell/3\ell_{cr}$
$U/U_o = \phi\{\psi(t/H)\}$ $= \zeta(t/H)$	A(1): 1 for $t/H < 0·914$ $\frac{3}{4}[(t/H)^9 - 1·6 \times 10^{-6}]^{\frac{1}{2}}$ for $t/H > 0·914$ A(2): $1 - t/3H$	B(2): $1 - t/3H$ B(3): 1 for $t/H < 0·6$ $1·2 - 0·6t/H$ for $0·6 < t/H < 0·97$ $7·6 - 7t/H$ for $t/H > 0·97$
$m(U/\hat{U}_o)$ (i) Linear fn. of $U/\hat{U}_o$ (ii) Polynomial fn. of $U/\hat{U}_o$ matching Figure 2 of Reference 9	A(2): $10^{6-12U/U_o}$ A′(2): $10^{(A+BU/\hat{U}_o+\ldots}$ where $A = 24·4$ $B = -188·1$ $C = 528·1$ $D = -717·4$ $E = 467·1$ $F = -120·3$	$10^{4·3-15U/\hat{U}_o}$

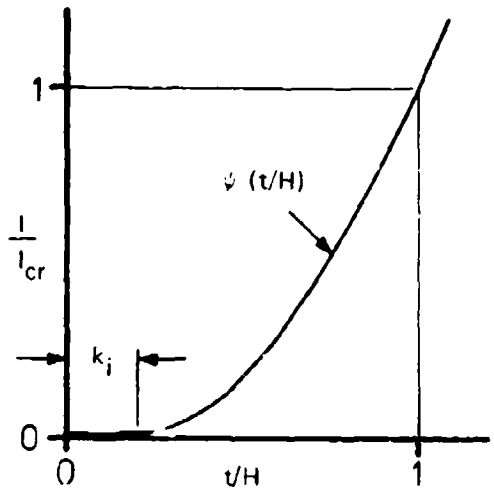

Fig. 1a

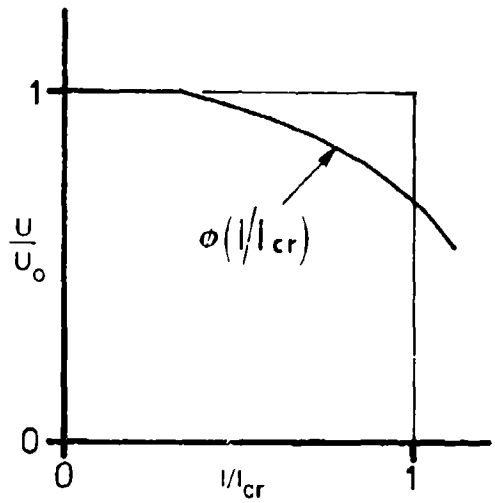

Fig. 1b

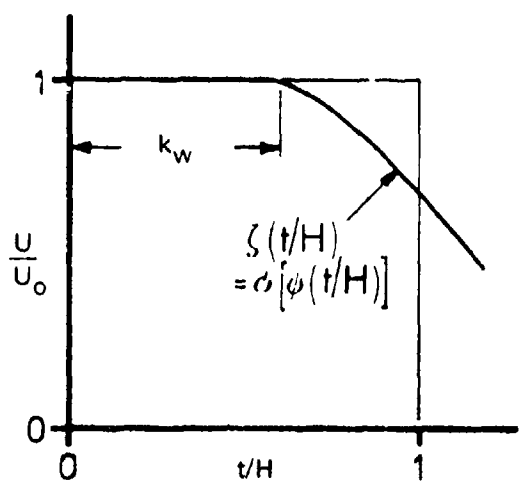

Fig. 1c

FIGS 1. a,b,c CRACK LENGTH – STRENGTH – TIME RELATIONSHIP

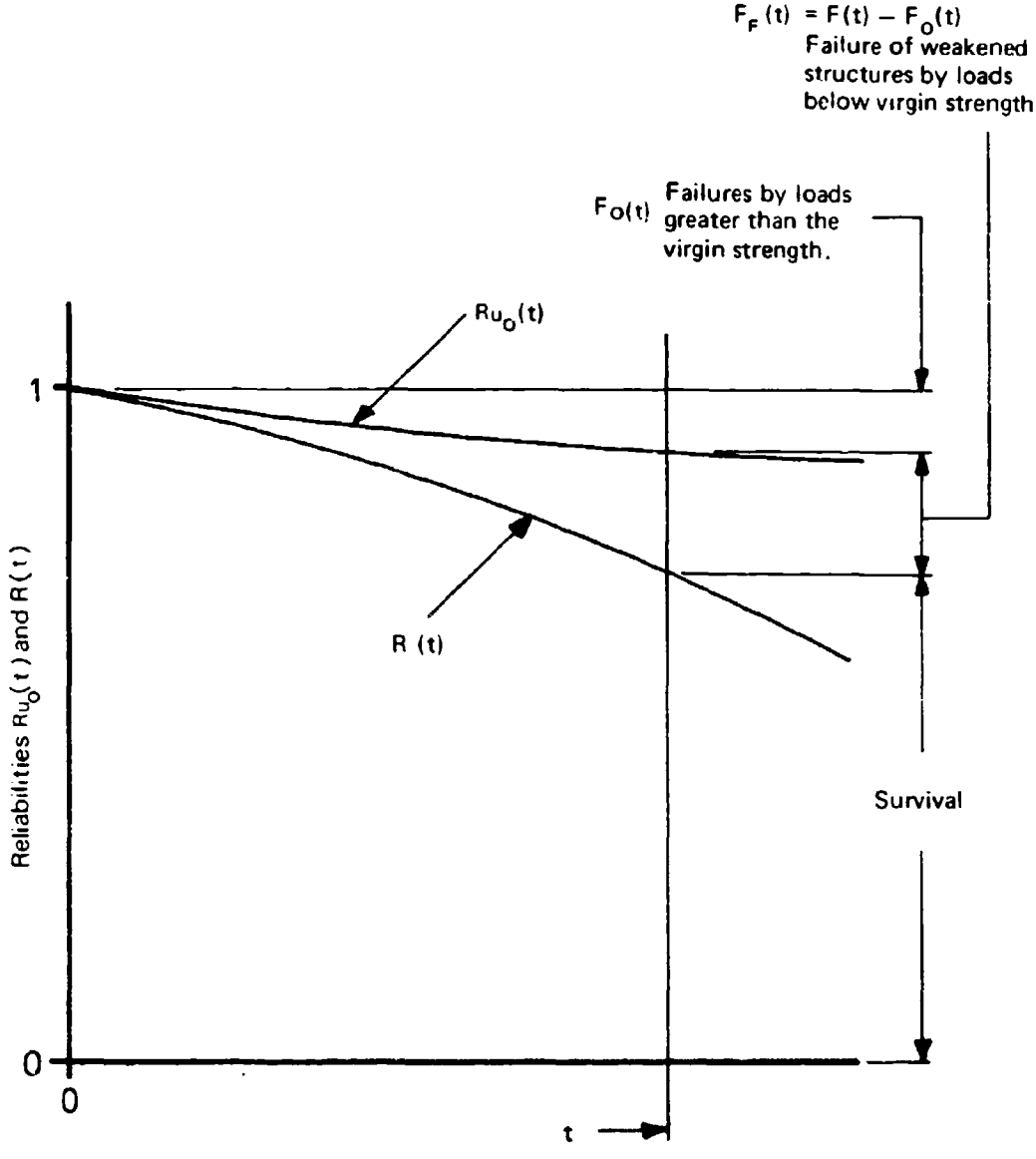

FIG. 2. FATIGUE AND ULTIMATE FAILURE RELIABILITIES.

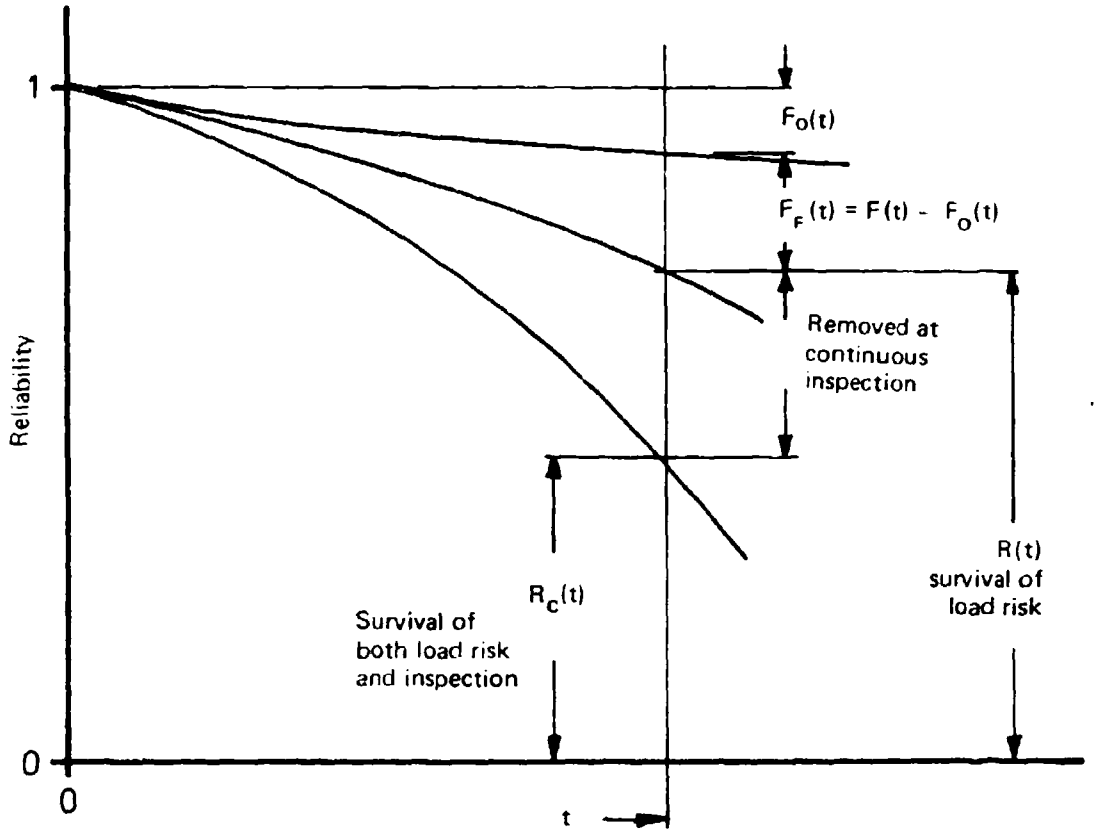

FIG. 3. SURVIVORSHIP OF FAILURE AND INSPECTION

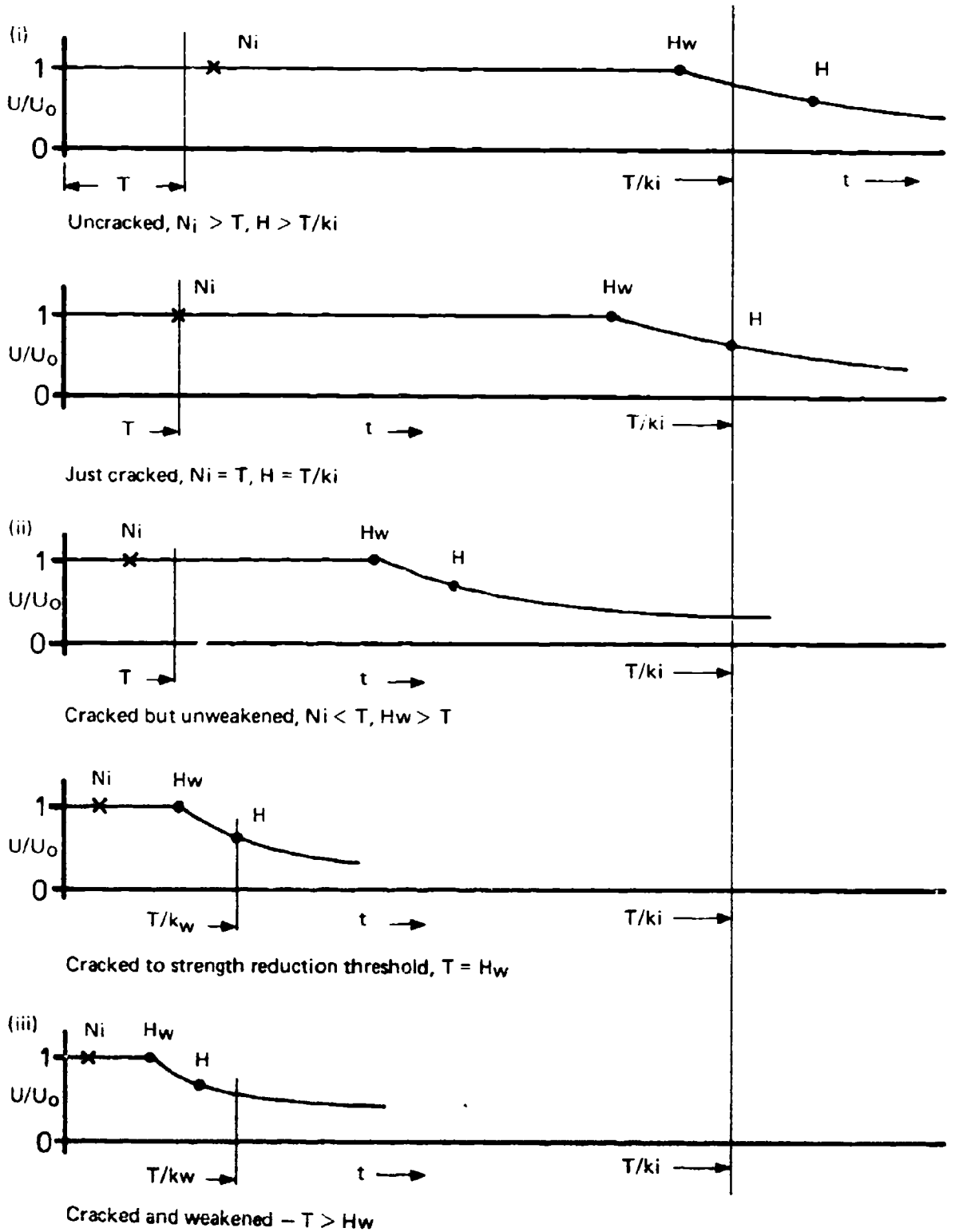

FIG. 4. STRENGTH SITUATION AT TIME T FOR ELEMENTS WITH DIFFERING H.

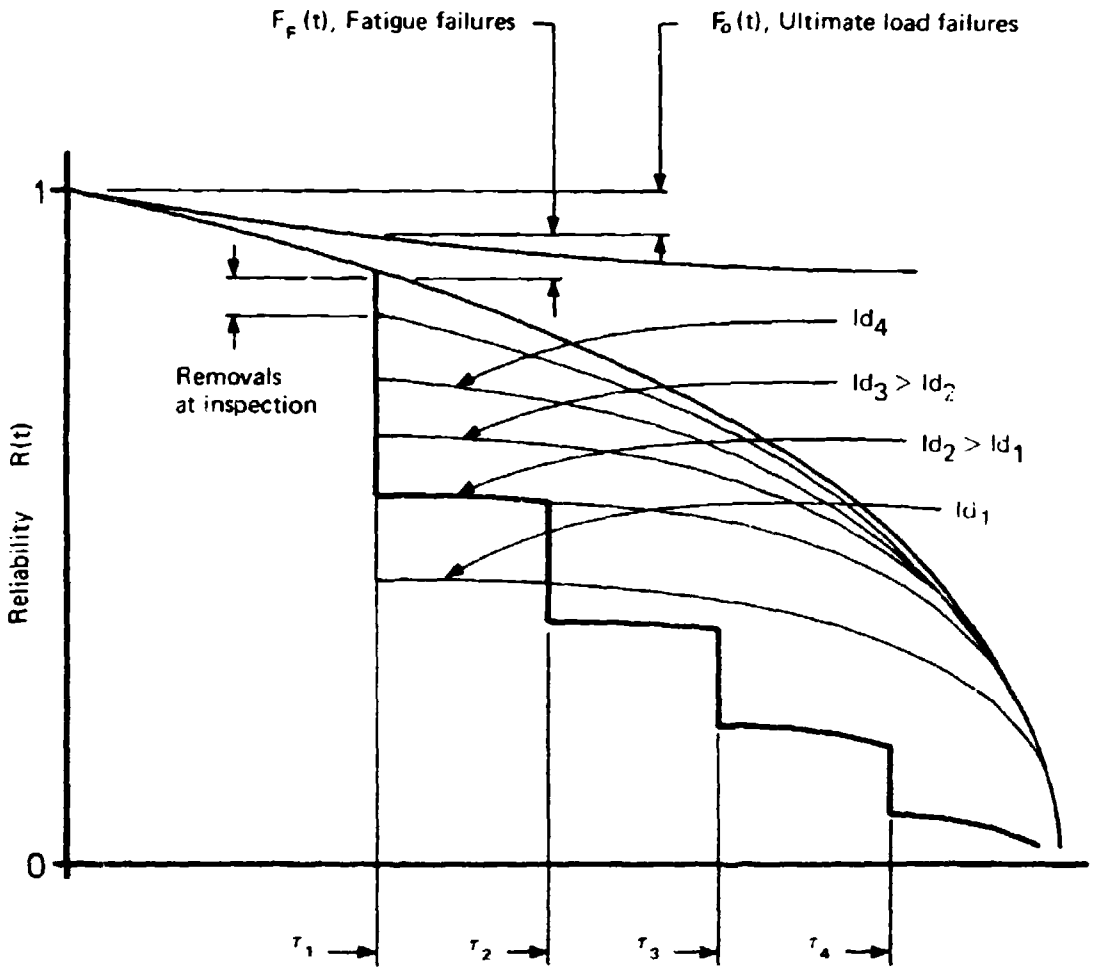

FIG. 5. RELIABILITY WITH INSPECTIONS, FRACTIONS REMOVED, ETC.

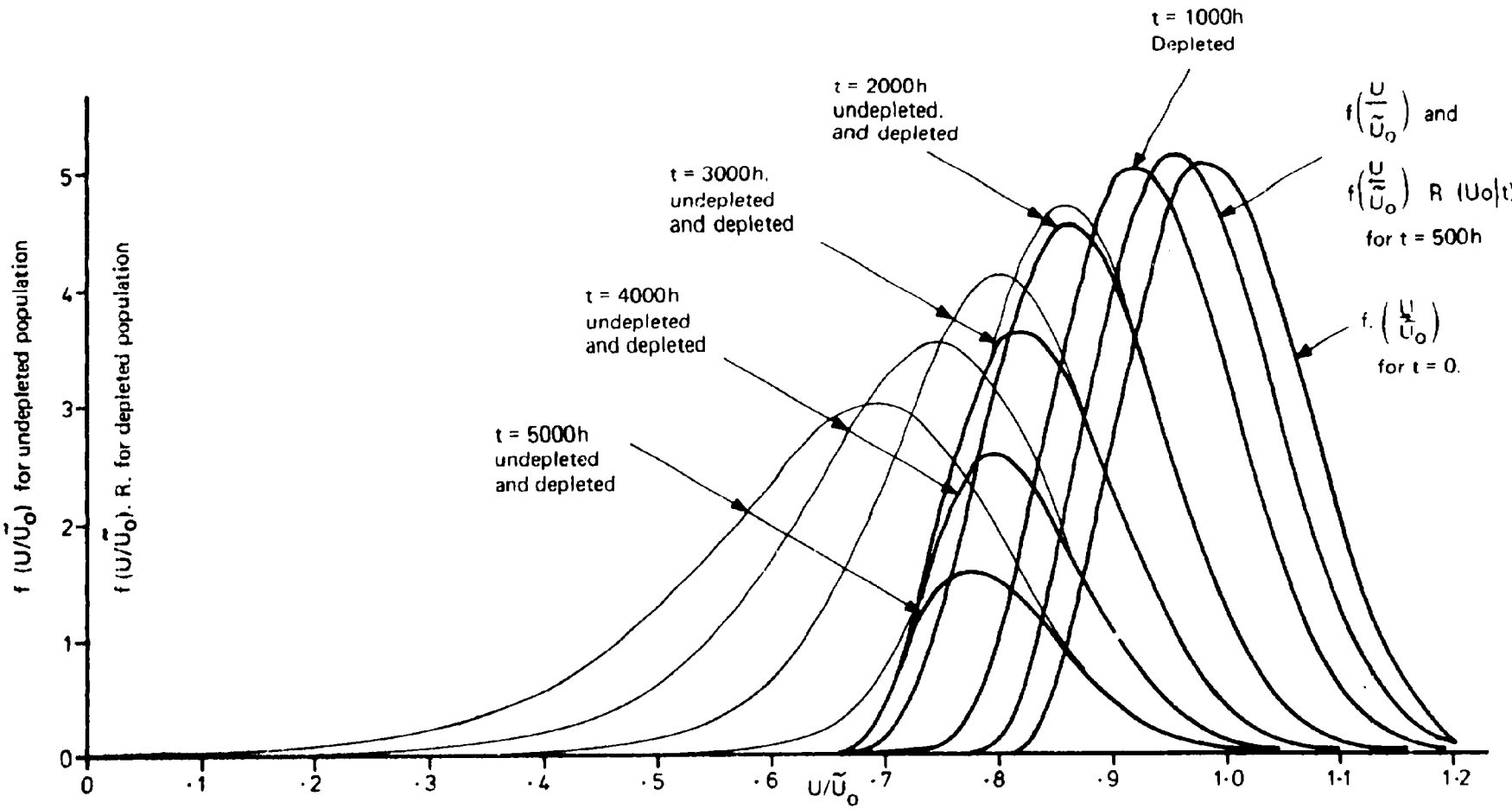

FIG. 6. PROBABILITY DISTRIBUTIONS OF STRENGTH, EXAMPLE A2 FOR UNDEPLETED POPULATION & POPULATION DEPLETED BY THE RISK.

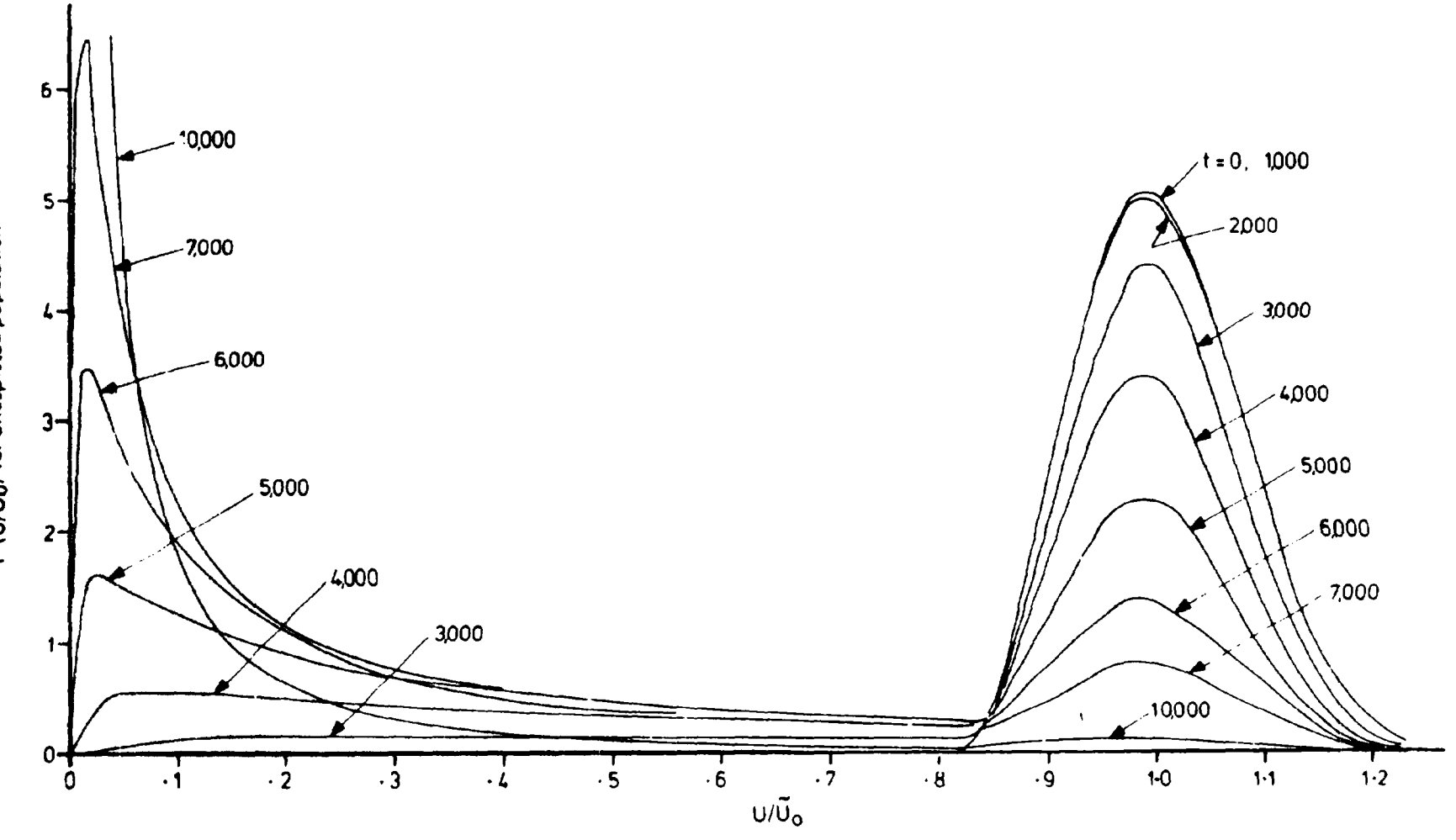

FIG. 7. PROBABILITY DISTRIBUTIONS OF STRENGTH -- EXAMPLE A 1 FOR UNDEPLETED POPULATION.

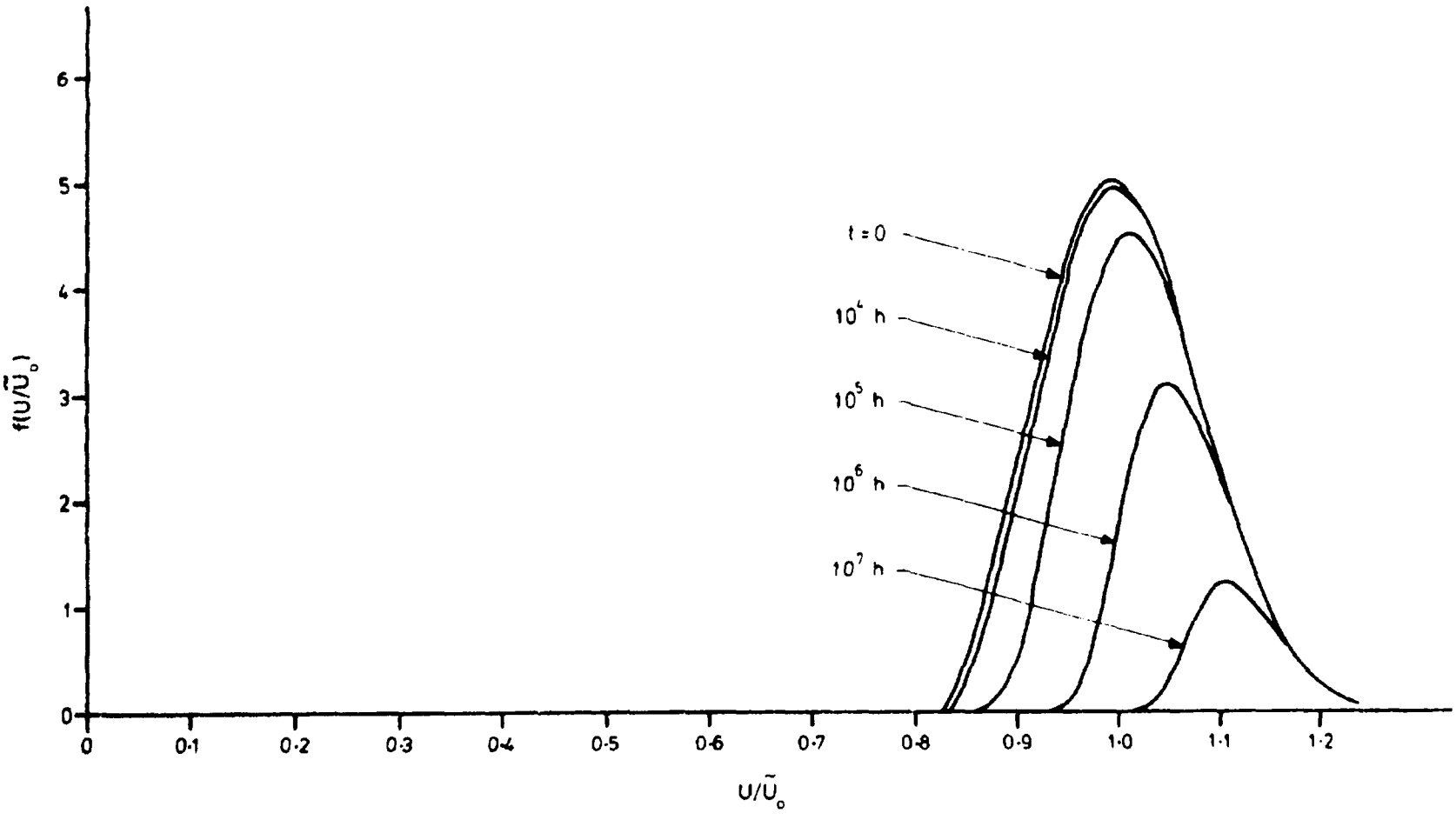

FIG. 8. PROBABILITY DISTRIBUTIONS OF STRENGTH – EXAMPLE A2 STATIC ULTIMATE FAILURE ONLY (POPULATION STRENGTH NON-DETERIORATING).

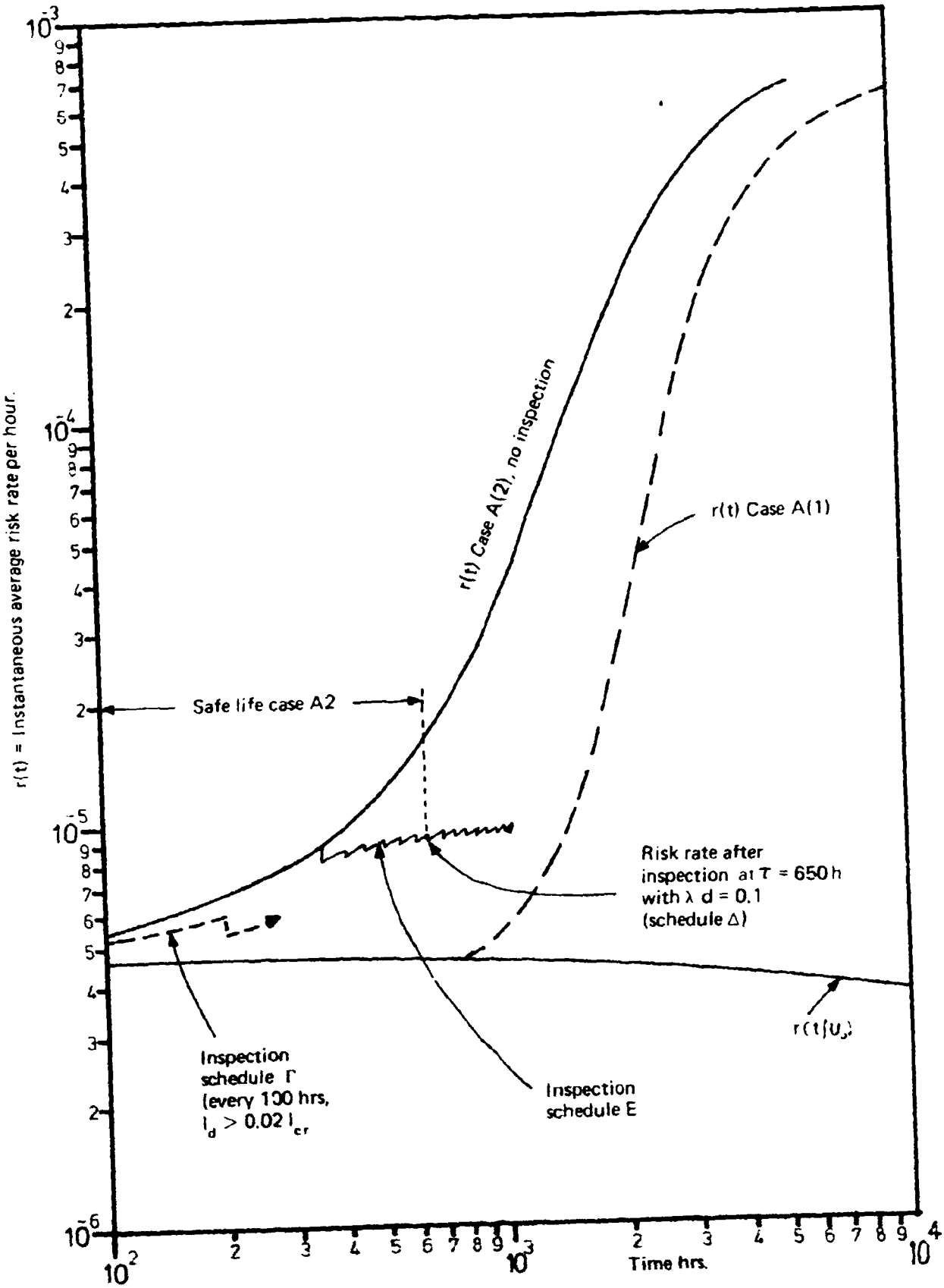

FIG. 9. INSTANTANEOUS RISK RATE WITHOUT & WITH INSPECTIONS – CASE A(2), & A(1).

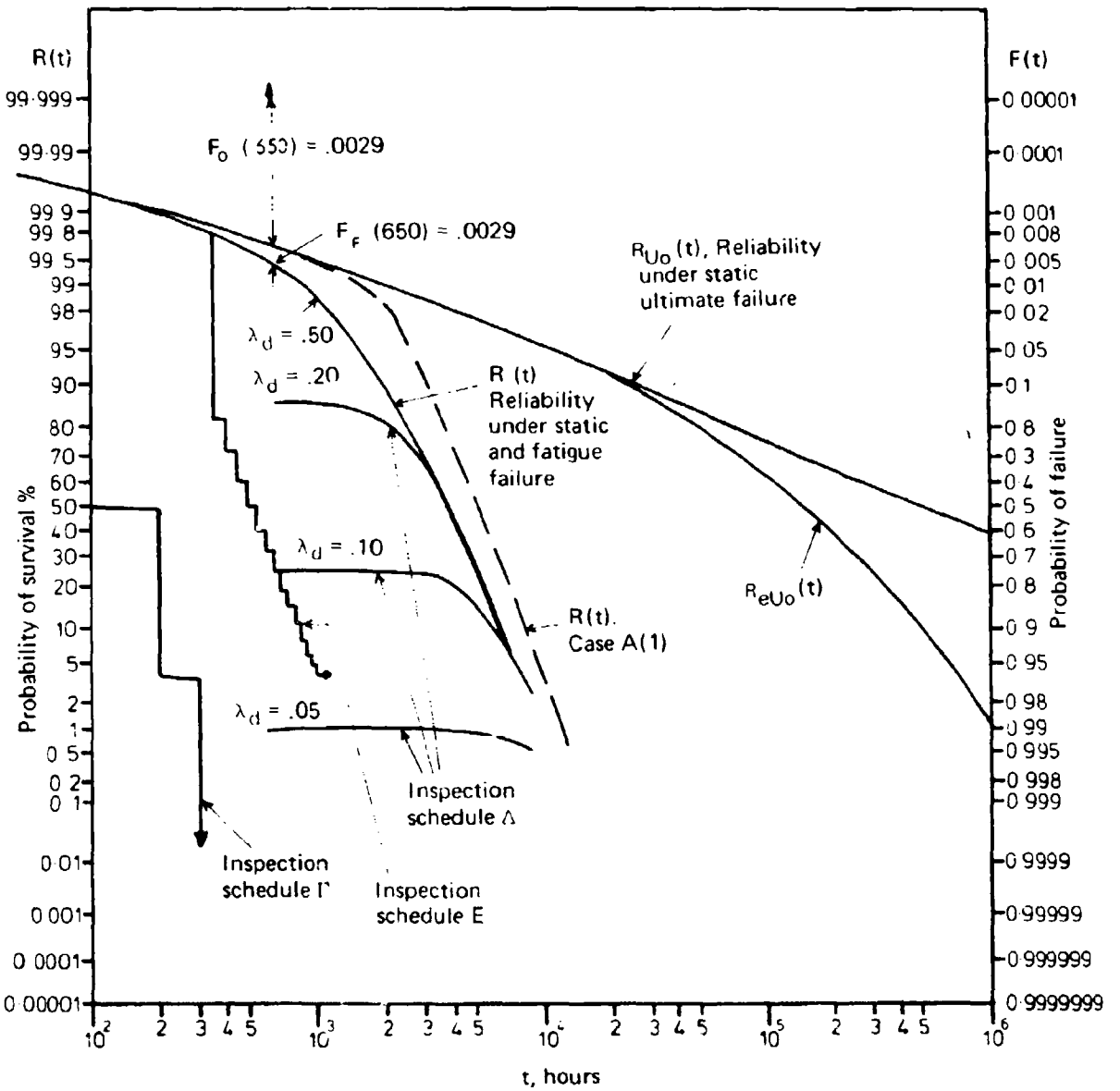

FIG. 10. RELIABILITY WITHOUT AND WITH INSPECTIONS, AND RELIABILITY ALLOWING STATIC ULTIMATE FAILURE ONLY – MANOEUVRE LOAD CASES A(2) AND A(1).

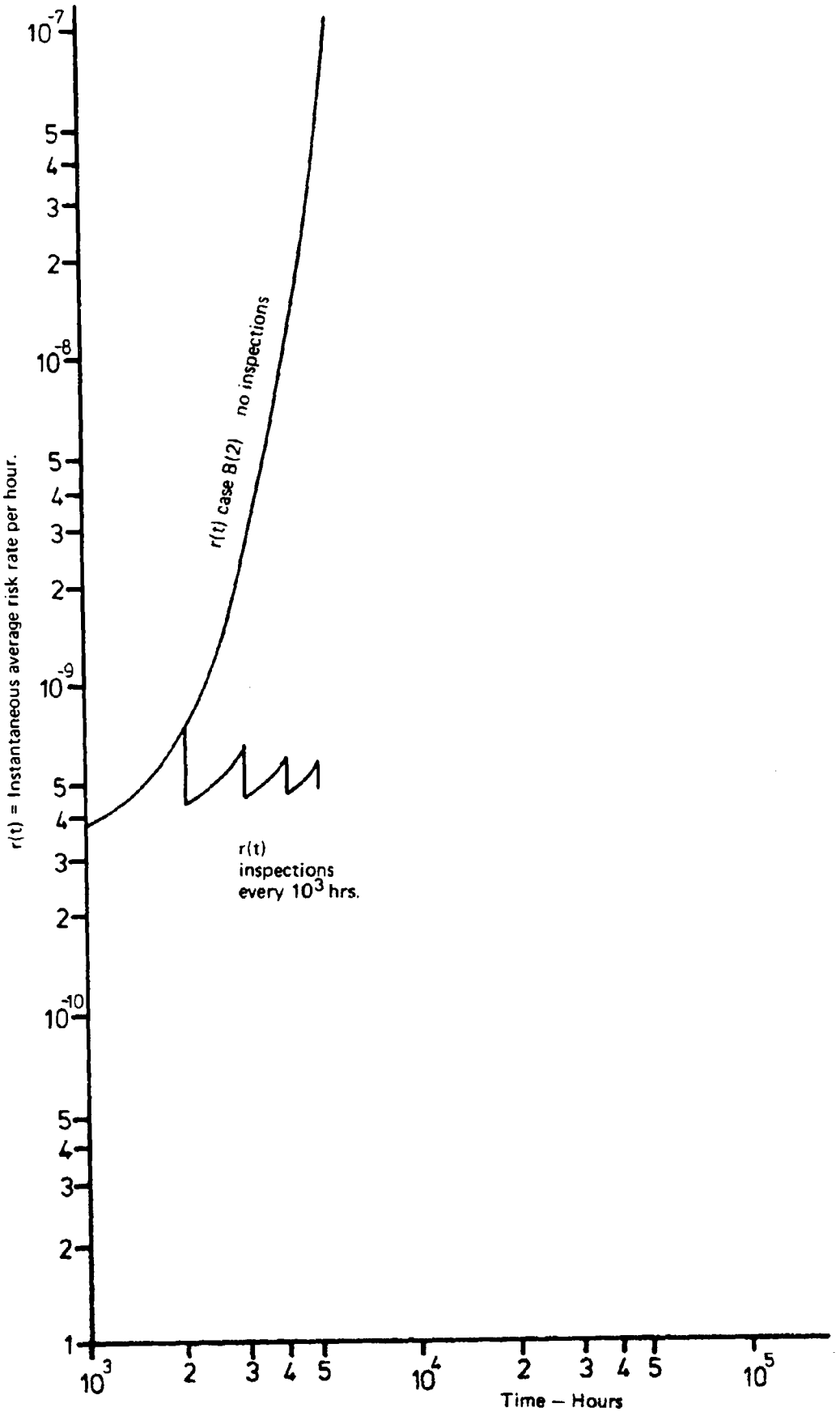

FIG. 11. INSTANTANEOUS RISK RATE WITH & WITHOUT INSPECTIONS – CASE B(2).

DISCUSSION

QUESTION *Wing Commander S. Woodbury*
RAAF

I would like to comment on one of the concluding remarks of your presentation and that is that for a fleet the maximum acceptable probability of failure due to fatigue should be about the same as that due to static overload. From a fleet operator's point of view this may not be appropriate because of the different implications of each type of failure.

A static overload failure implies that the structure has experienced a rare and chance event and hence all consequences of the failure are associated with that aircraft and this has little or no consequences for the remainder of the fleet. Whereas a fatigue failure implies a weakness in the fleet as a whole and can lead to grounding of the fleet. Operators should try to avoid this if at all possible hence the probability of fatigue failure should be kept as low as possible.

Author's Reply

It should be remembered that it was in respect of fighter type aircraft that the author proposed the adoption of an acceptable fatigue risk comparable with the ultimate static failure risk. Normally the armed service in question, the crew and the general public accept higher risks in fighter type aircraft than in passenger carrying vehicles.

The task of assuring fatigue safety in military aircraft was first addressed in Australia in respect of bomber, fighter and trainer aircraft (viz. Canberra, Vampire, etc.) and these were treated as "safe life" structures because their integrity could not be established by inspection. The criterion then adopted to determine the safe life was a probability of failure of 0·001 during the lifetime. This criterion is still used, although it now appears less than satisfactory because it penalises structures with long safe lives as compared with those with short safe lives. For the average risk rate per hour (which is, after all, the significant measure of risk), being the ratio of the probability of failure during the safe lifetime to that lifetime, will be smaller the longer the safe lifetime. Whether the structure of an aeroplane is "safe life" or "fail safe" or "safe-by-inspection" the author thinks that there is a need to examine critically the risk rate which is regarded as acceptable.

The static structural failure rate of fighter-type aeroplanes is of the order of 1×10^{-5} per hour (Pugsley,[30] quotes $3{\cdot}2 \times 10^{-5}$ per hour, Australian experience with the RAAF Sabre fleet was $1 \cdot 10^{-5}$, our Example A2, illustrated in Figures 9 and 10 gives $4{\cdot}5 \times 10^{-6}$ per hour). If we accept this failure rate, for aeroplanes with a life of type of 5000 hours, the probability of failure of an aeroplane during its life is 5×10^{-2}, and the expected number of failures in a fleet of 1000 aeroplanes is 50. If the life of type had been limited by the currently adopted Australian fatigue probability of failure, viz. 0·001, then the expected number of fatigue failures in the same fleet in this time is one.

If one were to require another 1000 hours of service from this type, either by buying a new fleet and pensioning off the old one, or by continuing to use the old fleet, the expected number of ultimate failures would be 10, while the expected number of fatigue failures in the old fleet would still be less than one.

This being the case it appears to the author ludicrous to pension off the fleet at 5000 hours, and ludicrous to adopt a fatigue failure rate of 10^{-3} in a fighter aircraft lifetime.

The time between the expected first fatigue failure in a fleet and the expected second failure is a direct function of the real scatter. If the real scatter is small then the second failure will follow hard on the heels of the first, or, as Wing Commander Woodbury has said, the expected first failure is a forerunner of imminent failure of many more of the fleet. If the structure is classed as "safe life" and the real scatter is small only a small scatter factor, *applied to the mean life*, will ensure a nominated safety level. If the structure is used past this safe life, the risk rate of ultimate failure will not change significantly, but the risk rate of fatigue failure will increase rapidly.

If the real scatter is large, the time between the expected first and the expected second failure is large, and the event of one fatigue failure does not presage an immediate second failure or imminent failure of many of the fleet. Continuing to use the fleet past the first failure event does not make an immediate significant change in the risk of either ultimate failure or of fatigue failure. If the real scatter is large, a large scatter is necessarily *applied to the mean life* to ensure a nominated fatigue safety level.

If the real scatter is small, but a large scatter factor is being applied to the mean life because the mean life is assumed highly uncertain, then the event of the first failure could be interpreted as presaging the rapid and unexpected approach to the mean lifetime: it could be used as a better guide to the mean value than the original estimate was. In these circumstances a first fatigue failure would be a logical justification for grounding the fleet.

In the case of "safety-by-inspection" the author doubts the wisdom of aiming to "keep the probability of fatigue failure as low as possible". In our example A(2), illustrated in Figures 9 and 10, the curves labelled Inspection Schedule Γ show the effect of removing structures with very small cracks. Four per cent of the population remains after 200 hours and none are left after the inspection at 300 hours. If the safe life had been declared to be that life at which the survivorship of fatigue and ultimate failure was 0·1% less than the survivorship of ultimate failure alone, the safe life so obtained is 440 hours, and in this lifetime the probability of ultimate failure is 0·2%. If Inspection Schedule E were adopted (in which the total risk never exceeds $9{\cdot}5\times 10^{-6}$), 50% of the population would survive past the inspection at 550 hours, and this would be the average fleet life available. If one were to use the fleet until the probability of fatigue failure became equal to the probability of static ultimate failure the life would be 650 hours, and the probabilities of failure in each mode would each be 0·0029 as shown. In this case the peak risk rate near 650 hours would climb to about $1{\cdot}6\times 10^{-5}$. Adopting this as a safe life, for a fleet of 100 aeroplanes, would still lead to an expectation of less than one failure in the fleet lifetime, and if such occurred, it would be equally likely to be an ultimate or fatigue failure. However, the author would prefer to be able to work with the example fleet as "safe-by-inspection", using, say, Inspection Schedule E, because the risk in this case is very little affected by the frequency of inspections, and it may be inferred that it is not greatly affected by the value of H, i.e. the mean time for the strength to fall to the arbitrary level by which H is defined.

QUESTION —*Sqn. Leader Bryce, RAAF*

According to the current ARL theory of reliability, the survivorship function always reduces throughout the aircraft's life. This approach may be appropriate for an artificial infinite fleet where the results of inspections are purely the calculated rejection rates. In the RAAF, however, the results of actual inspections may be used to modify the calculation of the survivorship function for a real aircraft. If an inspection has been carried out on the critical component of an aircraft, and no crack has been found, the operator may postulate that he now has as much information about that aircraft as he would have had, had the aircraft been continuously inspected throughout its entire life up to that point. Thus *post facto* the operator now knows that the actual risk which he has been sustaining has been far less than he had calculated while the possibility existed prior to the inspection that a crack had been growing in the critical structure. The risk has in fact been merely that under the risk function curve for continuous inspection.

Thus, while before the inspection it is quite logical to calculate the value of the survivorship function by integrating the entire area under the risk curve, and subtracting it from one, after the inspection it is not logical to do so.

After the inspection the area under the risk function curve, for that period prior to the inspection, which should be integrated is logically simply the area under the risk function for a continuous inspection situation. This results in an increase in the survivorship function after each inspection.

Calculation of the survivorship function in this manner is realistic from an operator's point of view, whereas the current method is not. It appears to be the logical way of transposing the infinite fleet situation to the individual aircraft situation. In fact this approach would enable, I believe, survivorship function for the unrejected Macchi fleet to remain above 0·999.

Author's Reply

Usually "reliability" or "survivorship" is taken as the probability of the original population surviving to a particular time t. After an inspection has been made, and some defectives have been removed, the reliability is usually expressed still as the proportion *of the original population* continuing to survive, as, for example, $R(T;\gamma_1)$ in Equation (51) of the paper, although one may evaluate it as the proportion of those *which survived the inspection*, as, for example, $R'(T;\gamma_1)$ in Equation (52) of the paper. In his calculations and in Figure 10, the author has used the former interpretation.

As far as the risk rate is concerned there is no option as to its interpretation, for it is, by definition, the proportion failing per unit time at time t, or the probability of failure at time t of survivors at time t. In the context of this problem the average instantaneous risk before an inspection is given by $r(T)$ of Equation (35), and after an inspection (when the population has been depleted by the defectives removed thereat) it is given by Equation (53).

It should be note that ARL theory of reliability is in a process of continued development and this paper is merely the most recent exposition of its current thought. Strictly, the survivorship is *not* the defect from unity of the integral from zero to t of the risk function: it is the negative exponential of the integral from zero to t of the risk function, provided the risk on all members of the population is uniform. Where this is not so, the negative exponential is summed over every element of the population, as in Equation (15) if the population consists of discrete fractions, or is integrated over the population, as in Equations (24), (34) and (51) if the population is continuously distributed.

In Equations (51), (53), etc., it is the limitation of the integration of H to the range $\gamma_1 k_a < H < \infty$ which, after an inspection, limits the survivorship and the risk functions to only those of the population which have survived the inspection, and it will thus be clear that the survivorship and risk immediately after an inspection at γ_1 are the same whether it was an isolated inspection or an instant in a period of continuous inspection. This is illustrated in Figure 9 where the risk under Inspection Schedule E (with inspections at 50 hour intervals) appears as a sawtooth curve at about $r(T) = 9 \times 10^{-6}$ per hour, commencing where the inspections commenced at $T = 350$ hours, and continuing to $T = 1200$ hours.

On this curve the risk after inspection at 650 hours is $8{\cdot}5 \times 10^{-6}$ per hour, and is identical with the figure under Inspection Schedule A, where the first inspection is at 650 hours, and the same crack size for component withdrawal is adopted.

On this diagram, Figure 9, curves have not been drawn for the risk under continuous inspection; however, the latter risk is the lower envelope of the sawtooth curve. Two other curves on this diagram are the risk under Inspection Schedule F, characterised by inspections every 100 hours and a more critical inspection procedure, with a crack size for component withdrawal of $0{\cdot}02\,\ell_{cr}$; and also the risk rate function $r(t;U_o)$, i.e. the risk for non-deteriorating strength.

It should be noted (and by example it can be seen from Figures 9 and 10) that inspection schedules which detect smaller cracks and reject the structures containing them will cause a more rapid depletion of structures left in service than inspections in which the detectable size, or the crack size for rejection of the structure, is larger.

If the user is considering the question of risk upon a single member of his fleet which has survived inspection with no detectable crack, then the user's fleet may be regarded as having been sampled from the infinite population assumed in the calculations, and the individual aircraft as one out of a fraction of that sample whose time for a crack to reach detectable size is longer than the time to that inspection. If at this inspection time the calculations showed a high probability that all structures are detectably cracked, while the individual structure was not, then doubt would be cast upon the assumptions of the calculation. Similarly, if at that time most structures were found cracked and the calculations showed a low probability of the structures being cracked, the assumptions might similarly be doubted.

If at an inspection time γ_1 a structure were found measurably cracked, and yet not cracked to the degree requiring removal, then knowledge of the crack size and the time γ_1 would permit an evaluation of the structure's characteristic time H. This would remove the need for integrating the reliability and risk functions over the variable H, and so the reliability and risk would become, after Equations (51) and (53),

$$R(T;\gamma_1) = \int_0^\infty \exp - \left[\int_0^T m\{U_o\,\zeta((t/H)/\hat{U}_o\}\,dt\right] f(U_o)\,dU_o$$

and

$$r_{\gamma_1}(T) \quad \frac{\int_0^T m\{U_o\, \zeta(t,H)\, \hat{U}_o\} \cdot R(T\,U_o, H) f(U_o)\, dU_o}{\int_0^\infty R(T\,U_o, H) f(U_o)\, dU_o}$$

where H has the characteristic value for the structure in question.

All of the above procedures are potentially applicable to the problem of the Macchi, mentioned by Sqn. Ldr. Bryce. However, as the author has pointed out in Sections 6 and 8, the adoption of an acceptable probability of failure in the lifetime of 10^{-3} (survivorship 0·999) equates to a risk of the order of 2×10^{-7} per hour which is so small in comparison with the ultimate static failure risk of fighter and trainer aircraft as to be unrealistically small. Also the author understands that the Macchi aircraft has a structure which is inspectable in parts and not inspectable in others. The consideration of the overall risk requires a combined approach, taking into account the risks in all relevant locations. The question of what is an acceptable risk also deserves reconsideration.

QUESTION – *Sqn. Leader A. J. Emmerson, RAAF*

The problem we face is the practical application of this approach. Aside from its use in general design or aircraft type evaluation, a primary application is in extension of an otherwise inadequate safe life on a safety by inspection basis. This requires hard numbers from the theory, and in particular hard numbers relating to the probability of survival of a nominated individual aircraft. Given that an individual aircraft has its own unique crack growth curve and measured flight load history, what are the prospects of expanding the theory to permit derivation of the probability of failure before next inspection for an aircraft in which the correct maximum crack size in the critical area is known?

The problem seems to lie in the assumptions lying behind your Figure 1*a*.

Author's Reply

It is the role of reliability theory as applied to the structural fatigue problem to provide formulae to calculate the probability of failure between one inspection and the next, for aircraft being treated as safe by inspection.

The survivorship (calculated on the basis of the size of the original population) immediately after an inspection at γ_1, and immediately before the next inspection at γ_2 may be described as $R(\gamma_1\,\gamma_1)$ and $R(\gamma_2\,\gamma_1)$ respectively, and may be calculated by putting γ_1 or γ_2 in place of T as the upper limit of the integration of the variable t in Equation (51) of the paper.

Subtracting $R(\gamma_2\,\gamma_1)$ from $R(\gamma_1\,\gamma_1)$ gives the probability of failure within the time interval from γ_1 to γ_2. Or writing $\{R(\gamma_1;\gamma_1) - R(\gamma_2;\gamma_1)\} \div R(\gamma_1;\gamma_1)$ gives the probability of failure of survivors of the first inspection. The above expressions are based on the assumption that at an inspection structures are divided into those which have or do not have cracks of a size appropriate for withdrawal from the fleet.

If at an inspection an individual aircraft is found to have a crack which is measurable and yet not as large as to require withdrawal of the aircraft from service, knowledge of its size and the time γ_1 permits evaluation of the structure's characteristic H value. It may then be treated as an individual with known crack propagation behaviour, but unknown residual strength. A question posed by Sqn. Ldr. Bryce amounted to the same thing, and expressions for risk rate and reliability in this case are given in the answer to his question.

QUESTION—*Sqn. Leader A. J. Emmerson, RAAF*

Would you please comment on the acceptability of the concept of calculating the mathematical expectation of a particular crack in a fleet for the purpose of predicting future aircraft losses caused by that crack?

Author's Reply

It would appear to me that the mathematical expectation of a crack (at a particular location) in a fleet is the defect from unity of the survivorship uncracked, i.e. the survivorship under continuous inspection as given by $R_c(T)$ in Equation (54) or under intermittent inspection as given

by $R(T|\gamma_1)$ of Equation (51) of the paper. When the instant T considered coincides with an inspection time γ_1 the expressions are identical.

If at some inspection time the actual survivorship uncracked of the fleet is found to be reasonably in accord with the calculated expectation, one may have confidence that the assumptions for calculating the expectation have been, if not individually proved, at least collectively supported, and confidence also that the assumption may be an adequate basis for the calculation of the survivorship, or of the risk rate of catastrophic failure at some later time, as given by $R(T|\gamma_1)$ of Equation (51) and $r_{\gamma_1}(T)$ of Equation (53) of the paper.

If there is no confirmation by inspection of the expectation of cracks (either because no inspections were made, or no cracks were observed) the prediction of future losses by failure can be no better than the prediction of present cracking. But of course, if the structures are "safe-by-inspection", future concern is primarily with the fraction of the fleet surviving inspection to some future life, and not with the expectation of catastrophic failures during the future life.

For a "safe-by-inspection" fleet, the size of the fleet surviving inspection at a particular time depends upon the crack length above which a structure is withdrawn from service. If the nominated crack size is very small the risk of catastrophic failure only grows slightly more than the risk of ultimate failure with non-deteriorating strength, but the population dwindles rapidly. If the crack length for withdrawal is larger the fleet will last much longer: the risk rate will in consequence be higher, though the risk of fatigue failure may still be no more than the risk of ultimate static failure.

Nevertheless it must be remembered that the occurrence or absence of cracking in members of a fleet which has accumulated a total hours H is no evidence concerning the integrity of an individual aeroplane when it shall have flown to a life of H hours.

QUESTION—*Sqn. Leader A. J. Emmerson, RAAF*

Conventional design procedures make some strength provision against the probability of failure under a single high load, by requiring that the structure be designed so as not to fail catastrophically under a load typically at least 1·5 times the highest load likely to occur in service (i.e. 1·5 times limit load).

To what extent would the procedures described in your paper unnecessarily duplicate this provision?

Author's Reply

It is true that the design strength requirements for aircraft require that they shall sustain without collapse a load 1·5 times the "limit load", and the latter is described as the "largest load likely to be encountered in service". Design strength requirements have to anticipate future experience by some extrapolation of the past. Some aircraft never encounter an event of limit load during their lives : others encounter more severe loads, albeit rarely. Some, more rarely still, encounter a load greater than design ultimate strength, and join the statistics of structural failures. The design strength requirements are set at a level which by past experience leads to a sufficiently small count of catastrophes that it is acceptable to users, whether they are a military service or the general public.

The procedures described in my paper permit calculation of the risk of ultimate static failure, knowing the applied load spectrum and the structural properties. They are not couched in a form particularly suitable as a design requirement, and the necessary data are usually not available at the design stage. Where the data are available the designer may use the procedures to estimate the risk of ultimate failure, and to upgrade his design if he thinks necessary.

QUESTION—*Dr. L. H. Mitchell, ARL*

At first sight it would seem that reliability has to do with infrequent events and therefore the tails of the distributions of the variables involved. Also I would have thought that the uncertainties regarding the tails would be much greater than the uncertainties in mean values. Could Dr. Hooke comment on the importance of the assumptions about the distributions assumed?

Author's Reply

The theory of aircraft structural reliability and risk has to do with both frequent and rare events, the former when dealing with the expected life to failure (of which a laboratory fatigue test life is an estimator), and the latter when dealing with a safe life or a safe interval between inspections. A safety factor relates the expected life to the safe life, and therefore the frequent event to the rare event.

One would expect the uncertainty in determining mean values to be less than that in determining extremes, but it is shown in Section 7 of the paper that, for example, estimation of the mean or median endurance H is fraught with considerable uncertainty when only a single fatigue test is carried out, and similarly the estimate of median virgin strength $\hat{U}_o$ is of dubious precision when derived from a single static strength test.

Nevertheless it is true that the risk of fatigue failure results primarily from the interaction of the upper tail of the applied loads distribution function with the lower tail of the distribution of residual strength, which lower tail is also related to the lower tail of the distribution of the life to critical crack size.

Of these three distributions it might be thought that the upper tail of the distribution function of applied loads is the most significant as regards variability, since loads of about the median virgin strength occur about once in the lifetime of a fleet, in fighter aircraft, and perhaps less often with transport aircraft. However, Figure 6, showing the distributions of residual strength at successive times reveals that structures whose strength is progressively decreasing, never survive past the point where their strength is reduced to about design limit strength, so that if every aircraft was used till it failed, the failing loads would be those lying between ultimate design load and limit load. There is less uncertainty about these than about the extreme tail. Similarly the shape of the distribution curve of virgin or residual strength has been investigated and proves to be not highly critical, but the value of the mean or median strength is critical. The lower tail of the strength-decay-time parameter is critical, and this is often determined by the application of a scatter factor to a laboratory-observed strength-decay-time, and here again the uncertainty is compounded from the sampling error intrinsic in a test on one component, and the uncertainty involved in applying a scatter factor derived from tests on other structures (possibly under different load spectra) than the one in question.

The uncertainties intrinsic in aircraft structural reliability analysis are at present perhaps the most important area of study.

QUESTION—*P. J. Howard,*
ARL

You say that aircraft remaining in an aged fleet have been selected for strength. Could they not also be selected for luck, in that they may be weak members who have fortunately avoided high loads?

Author's Reply

On the definition that "luck" is "that which happens by chance, fortune or lot", the sole concern of reliability theory is "luck". As with people, so with structures, life is a trial of strength, and the weaker are more likely to succumb to an event of stress than the stronger. In the spectrum of loads occurring on a fleet of aircraft, higher loads occur less frequently than lower loads, so that chance will cause the weaker, sooner than the stronger, to encounter and succumb to a load greater than each one's current strength. Considering all at the same "age", i.e. after the same number of hours or loads encountered, more of a particular strength will have survived (on the average) than of any lower strength. In the "fighter" example of the paper, and with the assumption that strength does not deteriorate with time, Figure 8 shows that, by "natural selection" the population of survivors acquires enhanced average strength, while, on the assumption that strength *does* deteriorate with age, Figure 6 shows that "natural selection" causes the survivors to have higher average strength than if the weaker had not been eliminated, though, of course, not as high as the average virgin strength. While an individual weak member may last longer than an individual strong member, this will not be so on the average. The survivors are selected *by* luck, rather than *for* luck.

QUESTION —*J. Visick,*
Ansett Airlines

Hooke in his review (Tech. Memo 253), on page 3 warns against unwittingly attributing too much reliability to the precision of the mathematics in estimating fatigue lives.

Mann agrees with this quoting life factors of between 0·1 to 10·0. It appears that in spite of these statements both speakers (Hooke and Payne) are producing more and more precise mathematics in an attempt to deal with a highly random and unpredictable subject.

In practical aircraft operating environment fatigue testing —no matter how carefully applied —is not considered to provide meaningful data beyond about 30,000 hours flying time. This is due to the influence of other factors—corrosion, manufacturing errors (e.g. Viscount VH-RMQ), noise and small loads which are omitted from the fatigue test, etc. The only manner in which the behaviour of an aircraft fleet can be predicted is by observing the behaviour of that fleet in actual service. One procedure that has been put forward in this respect is the so-called 95/95 approach proposed by Boeing aircraft. This technique appears to have been almost totally ignored at this symposium. Is this due to the fact that the speakers consider the technique invalid—if so what alternative do they offer for life prediction of a fleet in a real, as opposed to a laboratory, environment?

Author's Reply

It is the forte of reliability theory, as applied to structural fatigue, that, unlike conventional semi-probabilistic analysis, it does not regard a structure as unsafe when its strength has fallen to some arbitrary level, but it assumes that failure will occur whenever a structure encounters a load greater than its current strength. The theory applied to a structural and load frequency model, in which all of the relevant parameters are identified and specified, and its application leads to results which are, for the model, absolutely mathematically precise. It seemed to the author worthwhile to explore this problem.

In the Introduction the author has pointed out that the mathematical model may fail to represent accurately a particular real problem as a result of sampling errors arising from the smallness of samples, and of the personal judgments made in attributing properties (including such effects as environment) to the model, and also in deciding acceptable safety levels.

It is true that if the input data to calculation do not include the effects of corrosion which occurs in service, or of manufacturing defects made on one but not all of the fleet, then the result of calculation must be suspect. Where a structure is capable of being treated as "fail-safe" or "safe by inspection" it is agreed that observation of its behaviour in service is a good guide to establishing its safety.

Since inspection cannot be continuous, the application of reliability theory provides an indication of the required inspection frequency and the expected fleet total lifetime allowing for losses at inspections, as well as by attrition in service, and comparisons of service experience with theoretical prediction permit updating of the input data to correct for earlier errors and unrepresentative environments, etc. The author does not consider the 95/95 approach proposed by Boeing invalid, though time and space limitations prevented its consideration in the paper.

QUESTION *A. O. Payne*
(ARL)

Dr. Hooke has made a detailed presentation of risk equations for the case of a single type of failure in a population of structures. In this comment I would like to draw attention to certain aspects of the analysis illustrating what are in my opinion the essential problems in the successful adoption of the Reliability Approach in Structural Airworthiness

The reliability approach to fatigue is a rather complex procedure involving multiple probability integrals and requiring a very extensive body of data relating to the full scale structure particularly as regards the fatigue characteristics and the residual strength properties.

It is not possible to obtain all of these extensive data in the general case: recourse is had to using a physical model of the fatigue process to enable simplifying assumptions to be made, thus reducing the data requirement and enabling representative data from other structures to be used.

Evaluation of the integrals is usually not possible by analytical means and this difficulty is overcome either by making simplifying assumptions as regards the data functions in the integrand, to make the integration tractible, or by using numerical methods which again introduce difficulties with computing time and accuracy. It is important in my view to make realistic simplifications in the risk analysis where possible so as to reduce the computational difficulties and the data requirement rather than apply a more complex analysis which increases the basic approximations involved and the uncertainties in the assumed data.

On this aspect I disagree with Dr. Hooke. Referring to Section 5 of his paper for example, he has applied his analysis to the case of a fighter aircraft assuming linearity in residual strength and in crack propagation following References 10 and 13 of his paper, where the effect of these assumptions can be clearly seen.

In Reference 13 Dr. Hooke has calculated the risk of fatigue failure for a typical fighter aircraft assuming a log normal distribution of life about a median value of 8,000 hours with standard deviation s.d. = 0·2.

The risk function is calculated on the assumption of a linear reduction in strength from zero life to final failure. While it considerably simplifies the integrals in his complex expression for the risk function, this is an extremely conservative assumption for any aircraft structure. In Reference 10 a calculation has been carried out using the same load spectrum for a very similar case of a fighter aircraft (with a mean life of 8,000 hours and s.d. = 0·176, 2 = 0·24). However, in this case the risk function was simplified since the variability in strength was not included and a much more realistic assumption of a curvilinear crack propagation curve and corresponding residual strength versus life curve was used.

The basic input data for the two cases was therefore very similar giving safe lives according to current military airworthiness requirements[1] of 2,000 hours and 1,520 hours respectively (based on 99·9% Probability of Survival) but the results calculated by the reliability analysis for the two cases differ widely. The life to Reliability of 99·9% is 200 hours in the first case and 1,200 hours in the second. The result in the first case is so much lower than the safe life estimated by the currently accepted military airworthiness requirement as to indicate a completely overriding effect from the conservative assumption involved. This is in contrast to the second case where the simpler reliability equation with a physically realistic model of the fatigue process has given a realistic answer.

In the first case the advantage of the probabilistic approach as compared to the conventional airworthiness procedure of specifying an arbitrary residual strength requirement has been masked in my opinion, by the use of an unwieldy expression for the risk function associated with unrealistic assumptions concerning the basic data.

The difficulties in applying the reliability analysis become much more apparent in the general case of combined static and fatigue failure. In a complex structure static failure occurs by a different mechanism (often by compression buckling) and usually in a different area to fatigue failure and possibly under different loading actions (load spectrum).

These difficulties have been shown by recent work in the U.S.A., in particular in the comprehensive analysis by Bouton *et al.*[2] The reliability under static loading within placard limits and under conditions of high overload are both considered. The reliability in fatigue is included, based on the philosophy that the fatigue life can be estimated on the basis of an increasing risk of static failure with decreasing residual strength in the critical area. There are some similarities with the conventional procedure but the method considers failure in a probabilistic sense and allows for the variability in material properties and in the fabrication process: an allowance is also introduced for variation in the mean strength property due to inaccuracies in the design process.

The procedure has been investigated by application to the C141 transport aircraft.[3] The principal conclusion from that study was that the implementation of the complete system for static and fatigue strength would be premature at this stage since there is insufficient data available to establish the risk of failure in a complex structure under the various loading conditions that apply. However, it was considered that partial application to design could be done for testing and evaluation of the method.

I therefore suggest that the successful adoption of the reliability approach in structural airworthiness depends on developing a physical model of the structural failure modes which will reduce the data required and simplify the risk analysis as much as possible, paying due regard to the accuracy of the assumptions and approximations involved in evaluating the risk function.

References

1. –	British Airworthiness Requirements. Av. P. 970, vol. 1, Leaflet 200.
2. Bouton, J., Trent, D. J., Fisk, N., and McHugh, A. K.	Quantitative Structural Design Criteria by Statistical Methods, Vols. I-IV. AFFDL-TR-67-107, June 1968.
3. Campion, N. C., Hanson, L. C., and Morrock, D. S., *et al.*	Implementation Studies for a Reliability Based Static Strength Criteria System. Technical Report AAFDL-TR-71-178, vol. 1, February 1972.

Author's Reply

The author is completely in agreement with Dr. Payne that the reliability approach to fatigue of structures is a rather complex procedure, involving multiple probability integrals and requiring an extensive body of data. The author also agrees with Dr. Payne that the successful adoption of the reliability approach in structural airworthiness depends on developing a realistic physical model of the structural failure modes. On the other hand the author disagrees with Dr. Payne on two points, in that he (the author) contends that:

(1) a rigorous mathematical treatment of the problem does not present insuperable difficulty – it does not necessitate the use of simplifying assumptions either of the equations or of the functions or parameters; and

(2) "risk averaging" used by Dr. Payne is a significant departure from a realistic physical model of the problem.

In order to address the problem mathematically the population's structural properties must be expressed in mathematical or functional form, such as the parameters $\bar{A}$, σ, $\bar{U}_o$, σ_{U_o}, $\bar{\lambda}(U/I_{cr})$, $\zeta(t/H)$, $m(U/\bar{U}_o)$, listed in the author's Table 1. The constants and parameters are chosen to be those best fitting to the data available, and, where precise data are deficient, such data are *attributed* to the population. Thus is defined a structural model with properties which are the best descriptors of the real population which the model represents. In Section 7 of the paper is discussed the reliability of the results when the parameters cannot be defined precisely because of sampling error.

Once the properties of the structural model under study have been thus "optimised", the author treats it mathematically as having precisely defined properties, and the behaviour of this model (population) when exposed to the load spectrum can be determined with rigorous precision. The solution of the exact equations, e.g. Equations 35 and 34, 55 and 54, even though involving multiple probability integrals, is not of insuperable difficulty. In these Laboratories two approaches are used; in one case the functions are expressed as conjugate pairs of values of the function and its argument fitting the experimental data, and adaptive and interpolative integration routines are used, while the other approach is to fit the data plots with suitable analytical expressions (in the

author's paper, polynomials, piecewise linear and piecewise non-linear expressions) and use standard computer integration routines. In either method the accuracy of calculation has been demonstrated to be impeccable.

Regarding the second point, about risk averaging, the author sees it as basic to the structural reliability analysis that structures of differing strengths will fail at differing rates, suffer different risks and therefore have different survivorships. The mathematical equations must therefore permit the members of the population this liberty. When determining future reliability it is not valid to treat all members as though they suffered the average risk. The author therefore does not adopt the procedure of risk averaging, viz. writing the risk equation as

$$\bar{r}(t) = \int_H \int_{U_o} r(H, U_o|t)\, \mathrm{d}U_o\, \mathrm{d}H$$

and the reliability equation as

$$R(t) = \exp - \int_o^t \bar{r}(t)\, \mathrm{d}t,$$

approximations which are strictly correct only for $R(t) = 1$. Without solving the rigorous equations it is impossible to be confident concerning how far $R(t)$ may differ from unity and the approximation still remain acceptable, whereas the rigorous equations remain so down to any low level of survivorship. This may be needed if one is evaluating the risk on survivors of an original population after many have been removed at inspection, and replaced with new ones.

It is intellectually satisfying that use of the rigorous equations leads to results which match some of the subtle behaviours expected intuitively. One such is the "survival of the fittest" dealt with in Section 5.2 of the paper. Another is the observation that under the fighter-type load spectrum used to obtain the results in Figures 6 and 10, no member of the population can survive beyond the point where its strength has fallen to approximately limit load. These results do not follow if the instantaneous risk rate is averaged to derive population reliability, and the probability distribution of strength is assumed invariate with time.

Other subtleties are of interpretation, as, for example, the question dealt with at some length in Section 3.2, whether failure of a cracked but unweakened structure, under an applied load greater than its virgin strength, should be classed as a static ultimate or a fatigue failure. The question is not trivial, especially with structures of ultra-high strength steel, where the unweakened period may be as much as 95% of the life. In some treatments (not the author's) the fatigue failure probability is calculated not by differencing the total failure probability and the static failure probability, but by integrating equations for averaged total risk over all members of the population of H except those uncracked. The inclusion, in this integration, of static failure risk on all structures from those just cracked to those just beginning to be weakened produces a much larger answer (although the absolute values may be small), and leads to sigficant underestimation of the life at which the probability of fatigue failure reaches its limiting acceptable value. Where static failure risk is negligible (the civil aircraft situation) this error does not arise, but, on the other hand, limitation of the range of integration to only part of the population of H is then unnecessary. Similarly in some treatments the integration is limited to exclude members of the population of H whose crack length has reached or surpassed right through the structure. This is unnecessary where risk averaging is avoided, as the rigorous equations allow that none of such members will have survived so long—their individual reliabilities will have reached zero long before.

These subtleties have been exposed and others are being exposed by continuing research at ARL.

The two examples quoted by Dr. Payne from the author's previous work, though superficially similar, were chosen as illustrations with different structural properties. The earlier paper sought to investigate whether a reliability treatment gave results different from the conventional approach, and concluded that the differences in reliability resulted primarily from the former treatment's inclusion and the latter treatment's exclusion of static failure risk at the primary fatigue failure location. The example in the earlier paper was chosen to represent ultra-high-strength steel behaviour, with uniform virgin strength and a late fall-off in strength, while that in the later paper was chosen to represent a more ductile material's behaviour, with distributed virgin strength and an early and prolonged fall-off in strength. The results are not directly comparable with conventionally deduced safe fatigue lives unless the probabilities of static failure are subtracted. The earlier fall-off in reliability found in the later paper's example arises from its strength properties being more unfavourable than in the earlier paper's example.

If, as is sometimes, but not always, the case, static ultimate failure can occur earlier at another location than at the principal location for fatigue failure, the single-failure-location model is inadequate, and the risk of failure at the other location(s) must be computed and added

to the total risk at the first location, so that the survivorship of the population may be correctly assessed.

There has been, as Dr. Payne observed, an upsurge of interest in applications of structural reliability theory to aircraft problems in the USA, the UK and Sweden, and the work in Australia has not been slight. The spread of understanding of and expertise in the method is encouraging, and as far as Australia is concerned, applications are currently being implemented here which would have been regarded as premature five years ago. No doubt, as more experience is gained with, and a deeper understanding acquired of, the reliability approach to structural airworthiness, and predictions of the method are tested against experimental evidence of the life of aircraft structures, the differing views currently held among practitioners of the art will be progressively resolved.

CURRENT RESEARCH AND DEVELOPMENT

LOAD INTERACTION EFFECTS IN FATIGUE CRACK PROPAGATION

by
G. W. REVILL,
NINGAIAH,*
J. M. FINNEY

SUMMARY

A number of test parameters, including the relative magnitudes of loads, their precise sequence, cycle hold times, environment, and material thickness, influence the effect of load interactions on fatigue crack propagation in metals. Some experiments on the influence of material thickness are described. For 2024-T3 aluminium alloy specimens the delay in crack growth caused by a single overload was greater by a factor of about 8.5 for 1.6 mm thick specimens than for 6.4 mm thick specimens. The practical importance of this effect is emphasised.

Various proposed mechanisms of load interaction are described as well as models for quantitative predictions. The models all incorporate the extent of crack tip plasticity into the Paris formulation of fatigue crack growth. They do not accurately detail the course of crack growth through the interaction period.

It is concluded that satisfactory prediction of interaction effects will require some materials information, obtainable only by test. How close the generation of this information comes to replacing prediction by test remains to be seen.

* Now at the National Aeronautical Laboratory, Bangalore, India.

NOTATION

1, 2	Subscripts denoting first load applied, second load applied.
a	Current semi-length of crack
a_d	Increment of crack growth during retardation
a_p	Distance from crack origin to the elastic/plastic interface ahead of the crack tip
B, D	Constants
C	Paris equation constant
C_p	Wheeler retardation parameter
COD	Crack opening displacement
E	Modulus of elasticity
G	Shear modulus
K	Stress intensity factor
ΔK	Cyclic range of K
K_c	Value of K at fracture (fracture toughness)
K_{1c}	Plane strain fracture toughness
K_{eff}	Effective value of K
K_{max}	Maximum value of K
K_{th}	Threshold value of K required to propagate an existing crack
$K_{th(b)}$	Basic (constant part of) K_{th}
m	Paris equation exponent
n	Wheeler retardation exponent
N	Number of load cycles
N_d	Value of N involved in crack growth delay
p, q	Constant exponents
R	Cyclic stress ratio (equals minimum/maximum stress)
R_y	Length of plastic zone associated with cyclic load
r	Distance from crack tip
α	Constant exponent
β	Work hardening coefficient
γ	Plastic work term
ϵ_p	Plastic strain amplitude
ϵ_y	Yield strain
ϵ_F	Fracture strain
σ	Cyclic stress
σ_y	Yield stress
σ_u	Static ultimate stress
σ_m	Mean of cyclic stress range
ρ	McClintock process zone size

1. INTRODUCTION

The last 15 years of fatigue research has seen a marked shift in emphasis from earlier decades. The reasons are twofold. Solution of the elastic stress field around the tip of a crack[1,2] has led to the application of fracture mechanics to fatigue crack propagation[3] with some success. In addition, it has been more clearly recognised that the propagation of a crack to final failure could account for a major part of the total fatigue life, and that much useful service life could be obtained from cracked structures—including aircraft structures. A heavy emphasis on crack propagation research has followed.

The natural aim of much of this research is to generalize analytical expressions for crack propagation incorporating a minimum of test data, or at least incorporating data which are easy to obtain. Many expressions have been formulated which enable "reasonable" predictions of crack propagation rates under constant-amplitude cycling, but when such expressions are applied to a non-uniform loading sequence their predictive accuracy often suffers badly.

Load interaction effects in multi-level sequences are evident when the crack propagation rate during a cycle is different from that under constant-amplitude cycling. These effects occur in both block programmes and random load tests. Considered relative to the rate of crack propagation under constant-amplitude conditions, both accelerations and retardations in growth rates have been observed.[4,5] In a block programme accelerations normally occur when the preceding cycles are of smaller magnitude, and retardations occur when they are of larger magnitude. Accelerations are normally of shorter duration than retardations which can be so pronounced that, to all intents and purposes, a delay occurs in the growth of a crack despite the continued application of cyclic loads. Such a delay is illustrated and its magnitude defined in Figure 1*a*. Other patterns of retardation have also been observed and these are also illustrated in Figure 1. Figure 2 shows the acceleration phenomenon, and Figure 3 illustrates the symbols used in single peak overloading tests.

This paper describes methods currently available for coping with load interaction effects in predicting crack propagation rates, gives the results of an experimental programme to determine the effect of material thickness on delay period, examines other factors known to affect the delay, describes the various ideas already advanced to explain the effects, and finally examines the possibility of generalization.

2. THE BASES OF CRACK PROPAGATION LAWS

2.1 Propagation Under Constant-Amplitude Loading

To understand why load interactions occur, and why certain formulations have been proposed to account for their effects, it is necessary to appreciate the background of the variously-proposed constant-amplitude growth laws. It is intended simply to outline the bases of such laws with selected examples.

Strain hardening and fatigue damage models.

The first theoretical expression for fatigue crack propagation was derived by Head[6] who considered a model of rigid work-hardening elements representing the plastic zone at the tip of the crack. The fracture criterion is the fracture stress of each element and the following expression was obtained:

$$da/dN = \frac{\beta}{12E}\frac{\sigma^3}{(\sigma_u-\sigma_y)(\sigma_y-\sigma)^2}\frac{a^{3/2}}{l^{1/2}} \qquad (1)$$

where β is the work-hardening coefficient of the elements of original length l. Extensions of this type of model have used:

(i) an expression for the plastic strain amplitude ε_p at a distance r from the crack tip within the plastic zone of size R_y; and

(ii) a *fatigue* fracture criterion.

McClintock[7] applied the formula for the plastic strain distribution in mode III to mode I,

namely $\epsilon_p = \epsilon_y(R_y/r - 1)$, and used the Coffin/Manson law for low cycle fatigue as a fracture criterion. This yielded (using a Coffin/Manson exponent of $m = 2$)

$$da/dN = 7{\cdot}5\rho\,(\epsilon_y/\epsilon_p)^2(R/\rho)^2 \tag{2}$$

where ρ is a "process" zone size at the tip of the crack. The physical meaning of such a process zone leads to questions about the validity of this model.

A recent variant of this approach[6] applies the cyclic stress/strain properties determined on uncracked bulk samples to the material approaching the crack tip.

Theories using dimensional analysis

Using dimensional analysis and assuming that the factors controlling crack propagation are similar no matter what the crack length, Frost and Dugdale[9] showed that:

$$da/dN = f(\sigma)\,.\,a \tag{3}$$

By experiment Frost[10] determined $f(\sigma) = B\sigma^3$. Using the notion that failure occurs at a critical value of plastic work, Liu[11] determined $f(\sigma) = D\sigma^2$.

Models using crack tip geometries

A number of models are based on the idea that fatigue cracks extend because cyclic plastic flow enlarges the surface area of the crack tip, and the enlarged surface becomes the crack extension surface. The formulations of the various models depend upon the scale at which the details are considered.

Using a dislocation model, and suggesting that fatigue crack extension occurs at a critical crack tip displacement, Weertman[12] derived the equation:

$$da/dN = \frac{(\Delta\sigma\sqrt{a})^4}{2\gamma G\sigma_y^2} \tag{4}$$

where γ is a plastic work term.

Neumann[13] has shown that for a crack propagating by duplex slip, the average strains on both sides of the crack tip are dependent on the angle between the slip planes and also on material parameters which characterize slip inhomogeneity. For crack propagation to proceed under such a model the applied stress must produce crack tip strains of the order of one.

On a coarser scale, Tomkins[14] calculated the amount of crack tip "decohesion" using the known plastic cyclic behaviour of bulk samples, and equated this to da/dN. He obtained the relationship:

$$da/dN = B\Delta\sigma^3\sigma_m a \tag{5}$$

and demonstrated that this was similar to the Paris formulation (see following) at a particular mean stress.

Semi-empirical formulations

In the early 1960s Paris[3,15] applied the newly developed fracture mechanics formulations to fatigue crack growth and obtained the relation:

$$da/dN = C\,(\Delta K)^m \tag{6}$$

This formula has been the basis of most subsequent developments in fatigue crack growth relations and considerable theoretical and experimental effort has been devoted to establishing the constancy of the parameters C and m. Paris initially proposed $m = 4$ which results from the idea that the work absorbed per unit increase in crack length is constant. Assuming that all the plastic work is absorbed at the crack tip, the amount absorbed is proportional to the area of the plastic zone which is proportional to K^4.

All energy-based considerations give $m = 4$. However, Miller and Throop[16] found that $m = 3{\cdot}5$ with a standard deviation of 0·65 over 69 values. In recent years it has been recognised that a constant value for m does not apply over the whole range of growth rates that may be developed in a test. Crack propagation will not occur at ΔK values below a threshold value and there is a gradual transition to the Paris relation as ΔK is increased. Similarly, a progressive deviation from the Paris relation occurs as K approaches K_c. It has been suggested[17] that the wide variations which have been reported for the values of C and m are caused by deviations from the striation mode of fatigue crack growth.

2.2 Effect of Mean Stress

Except for the Tomkins model, the foregoing expressions for crack growth rates relate to the cyclic loading in terms of its amplitude only. A non-uniform stress sequence, however, will include "cycles" at varying mean stress levels, and since such variations affect the crack growth rate,[18] it is necessary to modify the expressions accordingly. A number of modifications to the crack growth equations have been proposed. Most are semi-empirical developments of the Paris

equation, empirical in the sense that they have been composed to fit certain crack growth data, although their credence lies in the use of fundamental materials parameters. Some formulations have been derived theoretically however, usually by considering the details of the plastic zone at the crack tip.

It is appropriate to examine several of these modifications because they demonstrate the approaches taken when formulations are extended beyond the simple zero mean stress constant amplitude case.

Forman *et al.*[19] modified the Paris equation to include the criterion; as $K_{max} \to K_c$, $da/dN \to \infty$, and in the process accounted for the effect of mean stress since $\Delta K = K_{max}(1-R)$. They suggested the relation:

$$da/dN = \frac{C(\Delta K)^m}{(1-R)K_c - \Delta K} \tag{7}$$

This equation has achieved only partial success in correlating experimental data.[18,20] It also has the limitation that K_c is not a material constant but is geometry and environment dependent.

Pearson[21,22] found that the Forman equation correlated the experimental data for high-toughness alloys only, but not at high ΔK values. He successfully correlated a large body of data by modifying the Forman equation to:

$$da/dN = \frac{C(\Delta K)^m}{\{(1-R)K_{1c} - \Delta K\}^q} \tag{8}$$

A further extension of the Forman equation has been given by Erdogan and Ratwani[23] to account for the threshold value of ΔK. They simply assumed that only part of the stress intensity range is effective in propagating a crack, and replaced ΔK by $(\Delta K - K_{th})$. Their resultant equation described their test data on 6061-T4 aluminium alloy obtained at a variety of mean stresses.

Erdogan and Roberts[24,25] proposed that the rate of propagation is related to the size of the plastic zone ahead of and in the plane of the fatigue crack, and this proposal led to:

$$da/dN = C(K_{max})^p (\Delta K)^q \tag{9}$$

Roberts and Kibler[26] compared this equation with the Forman equation and found that both adequately represented the effect of mean stress. They argued that, if the fracture modes in tension and bending are the same, and if the plastic zone size determines the growth rate, then rates of crack propagation due to bending could be calculated from data obtained in tension. These ideas led to a further modification of the Forman equation:

$$da/dN = \frac{C(1+\eta)(\Delta K_E)^3}{K_c - (1+\eta)\Delta K_E} \tag{10}$$

where $\eta = K_{mean}/\Delta K$, and, using K_T and K_B as the stress intensity factors for tension and bending respectively, K_E is defined as:

$K_E = K_T$ for plane extension,

$K_E = K_B/2$ for bending,

$K_E = K_T + K_B/2$ for combined loading.

Equation (10) gave a good fit to their crack growth data on 2024-T3 and 7075-T6 aluminium alloys.

Raju[27] has also related the rate of crack propagation to the size of the plastic zone within the framework of fracture mechanics by using an energy balance model and considering two sizes of plastic zone at the crack tip, an inner alternating plastic zone based upon ΔK and an outer pulsating plastic zone based upon K_{max}. From this model he deduced:

$$da/dN = \frac{C(1-R)^{4-m}K^4_{max}}{K^2_c - K^2_{max}} \tag{11}$$

Elber[28] took a different approach, demonstrating by experiment that a fatigue crack may be closed while the stress is still tensile. For 2024-T3 aluminium alloy he found by test that $\Delta K_{eff} = 0{\cdot}5 + 0{\cdot}4R$.

Three conclusions arise from considering the developments of fatigue crack growth laws to include loading conditions other than that of constant amplitude at zero mean stress.

(i) Formulations in the context of fracture mechanics now predominate for the good and practical reason that they have achieved some success in correlating test data.

(ii) The test data which have been correlated (often only to within an order of magnitude, however) are mostly constant amplitude data.

(iii) Extensions to the Paris equation (to cope with mean stress effects) are empirically based.

3. PARAMETERS AFFECTING LOAD INTERACTIONS

Although it is known that load interactions can drastically alter crack propagation rates, to quantify such effects for predictive purposes it becomes necessary to determine the dependence of their magnitude on the test conditions. For example, does the magnitude of any effect depend on specimen size and shape, frequency of cycling, environment, or testing mode? If so, we are approaching the position of actually doing the test under given conditions in order to obtain the data necessary for prediction under those conditions! It is necessary to investigate all factors which may affect crack propagation rates and then, hopefully, to generalize—a matter which is discussed later.

3.1 Effect of Material Thickness on Delay

The effect of specimen thickness on the magnitude of the delay in crack propagation which occurs after the application of a single high load has been determined as follows:

3.1.1 Test Requirements

Three requirements were considered important.

(i) For specimens of different thickness the nominal cyclic stresses should be identical and the high loads should be applied at specified crack lengths.

(ii) The range of material thickness should be sufficiently large to cover different stress states at the crack front. This requirement is counterbalanced by the need to use the one testing machine at a constant frequency to eliminate the possibility of variations in fatigue behaviour from this source. Load setting in fatigue testing equipment often becomes inaccurate in the lowest fifth of the load range thus limiting the range of thickness of specimens which may be tested at identical nominal stress levels. A thickness ratio of 4 : 1 was chosen, the actual thicknesses being nominally 6·4 mm and 1·6 mm.

(iii) Specimens of different thickness should have the same metallurgical structure, preferably homogeneous across the thickness, and come from the same batch of material.

3.1.2 Material and Specimens

2024-T4 aluminium alloy extruded bars of rectangular cross-section (108 mm × 11 mm) were rolled to either 6·4 mm or 1·6 mm thickness and heat treated to the T3 condition by solution treating, cold water quenching, stretching 5%, and precipitation hardening at room temperature. After this treatment average static tensile properties were:

Thickness (mm)	0·1% proof stress (MPa)	0·2% proof stress (MPa)	Ultimate tensile stress (MPa)	Elongation (%)
1·6	391	399	492	15·8
6·4	421	426	503	17·2

Plate specimens were made from this material to the dimensions shown in Figure 4. Photographic grids were reproduced on both polished faces of the specimens, one grid being used for recording crack propagation, the other for monitoring the length of the crack at which high loads were applied.

3.1.3 Test Procedure

All fatigue tests used a 600 kN hydraulic machine modified for cyclic loading, and a cyclic frequency of about 1 Hz. Specimens were cycled under the gross-area stress conditions shown in Figure 3 and the single high load was applied at total crack lengths ($2a$) of either 1·65 cm, 2·41 cm, or 3·18 cm. These crack lengths represent three different stressing levels although the ratio of high stress to alternating stress remained constant.

Table 1 shows the nominal stressing conditions (in terms of K values) at each of the three crack lengths. Automatic recording of the crack propagation was achieved by photographing on 35 mm film, each frame showing the cracks and reference grid and the cycle count.

3.1.4 Results and Discussion

Figure 5 shows the basic crack growth rates for the two thicknesses of specimen tested with and without high loads. Table 2 gives the delay periods for the two thicknesses and includes also the crack lengths over which the retardation was observed (see Figure 1 for definitions).

There is a large effect of specimen thickness on delay, the thinner specimens giving an average delay about 8·5 times greater than the thicker specimens. Similar trends have been noted recently by other workers. Shih and Wei[29] found a two-fold change in delay with 7075-T6 aluminium alloy specimens for a similar range of thickness to that covered by the present results. Mills and Hertzberg[30] covered a thickness range of 1·6 mm to 26 mm in 2024-T3 aluminium alloy and also noted larger delays with thinner specimens. A criticism of this work, however, is the use of different batches of material to obtain the thickness range. Shih and Wei do not report on this aspect of their work.

Table 2 shows the trend towards longer delays with larger crack lengths and also indicates the increasing proportion of the thickness taken up by plane stress fracture as crack length is increased. Since there was always some plane stress fracture at the surfaces, calculated plastic zone sizes (on the specimen surface) upon application of the high load were made using $R_y = \frac{1}{2\pi}\left(\frac{\Delta K}{\sigma_y}\right)^2$, where σ_y was taken as the appropriate 0·1% proof stress. These values are roughly comparable to the increment of crack growth (a_d) during the period of retardation (N_d) as shown in Table 2. This correlation was also noted by Mills and Hertzberg and indicates that the delay is the number of cycles needed for the crack to propagate through the plastic zone formed by the high load. The retardation models presented in Section 4 all use this correlation as a basis. Unfortunately, the correlation lacks sufficient precision to predict the effect of thickness on delay. This imprecision comes from uncertainty in the correct formula for R_y, as well as in the appropriate value for σ_y. Moreover, precise values of a_d are difficult to determine because of the shapes of the growth rate curves.

Figure 5 shows that, in some cases, crack growth does not cease immediately after the application of the high load, but the growth rate gradually decreases before accelerating to the original value. This effect has been termed "delayed retardation" and has been observed by others,[31–34] for example Figure 6 taken from Reference 34 shows the effect quite clearly. Delayed retardation is more evident in cases of higher overload stress intensity and occurs after the application of both single and multiple overloads.[31] It has been suggested[32] that the effect is caused by the crack gradually penetrating the plastic zone of the high load and becoming progressively influenced by the compressive stress which the surrounding material exerts on the plastic zone. However, it is not clear why the "clamp" should become stronger as the crack grows through the plastic zone; alternatively, it may be suggested that the effect is a result of changes in the shape of the crack front through the thickness. Since the retardation effect is likely to be greatest at mid-thickness, the crack growth observed on the surface may continue initially until a balance in degree of retardation is achieved across the section. It is interesting to note that in the work cited above, and in the present tests, all crack lengths were measured on the specimen surface only.

The results of the present investigation given above apply to specimens cycled at constant-load amplitude up to the predetermined crack length at which the single high load was applied. Many of the specimens then had further high loads applied at larger crack lengths. Each high load produced retardation and in some cases the retardations overlapped so that the unretarded growth rate was never again established. In these cases the plastic zones of the high loads also overlapped.

Early in the testing programme it was noticed that if the testing machine was stopped during a period of retarded growth and the load reduced to zero, the delay was shortened. For example, a 6·4 mm thick specimen, given a high load at a total crack length of 1·65 cm, and after a further 500 low-load cycles given a single excursion to zero load, the total delay was 5000 cycles compared with an average of 11,000 cycles for tests without the zero load excursion. This effect was shown to be predominantly dependent on the load history. Because of the influence of excursions to zero load, all results shown in Table 2 were obtained from uninterrupted tests.

Sharpe *et al.*[35] have reported recently on the effect of rest time at zero load on the magnitude of the delay. 2024-T581 aluminium alloy compact specimens, ranging in thickness from 6·4 mm to 25·4 mm, were tested for this purpose, using rest times of three minutes, one hour, and one day. There was virtually no change in N_d with rest time for a given thickness, and no effect of thickness on N_d under these test conditions. Unfortunately, no measurements of delay were reported without reducing the load to zero and their general results are therefore not irreconcilable with those given above.

Examination of replicas taken from the regions of high load failure of 6·4 mm thick specimens permits the sequence of failure to be described as follows (see Fig. 8). Briefly, upon application of the high load there is enlargement or stretching of the crack tip radius before the onset of tensile fracture as evidenced by the formation of dimples. In some replicas, though not all, quasi-cleavage, due to the subsequent lower magnitude cycling, followed the tensile fracture. Eventually fatigue striations were again formed although initially they occurred along a very irregular crack front and sometimes were much wider than normal. These features are similar to those observed by others.[30,34]

Although it appears, from the present results and those of others, that the mechanism of delay is gradually being understood (the present results are compatible with a number of mechanisms outlined in Section 4), two warnings must be noted in view of the large thickness effect. First, delay appears to be a three-dimensional problem, and the dependence of N_d on the degree of through-thickness constraint must be accounted for in any model. Second, and more practically, great caution should be exercised in extrapolating existing crack growth data to various design situations.

3.2 Other Observations

The effects of a broad range of loading variables on retardation have been investigated by other workers using a variety of materials and specimen configurations,[34,36–39] and those effects which appear general are listed below. These effects are for the case of a single overload followed by constant amplitude loading, except where noted.

(1) For a fixed value of ΔK_2, N_d increases rapidly with ΔK_1. There appears to be a limiting value $\Delta K_1/\Delta K_2 = 1{\cdot}7$ below which no delay occurs.
(2) Delay is a function of R_1, R_2. Increasing R_2 decreases N_d, but the effect of changes in R_1 appears variable.
(3) Delay is decreased, and may be zero, when compression loading is applied immediately after a high tensile load. (This finding is consistent with that given in the previous section on thickness effects, namely, that crack growth occurred immediately after the load was reduced to zero.)
(4) Delay increases with the number of consecutive high load excursions and is also increased when a further high load is applied during the delay period.
(5) Hold time at the minimum load decreases N_d.
(6) Increased holding time at the high load increases N_d.
(7) The effect of negative peak loads depends upon the subsequent cycling. If the R-value of the subsequent cycling is greater than zero, there is little effect on growth rate; but if $R = -1$, acceleration may occur.
(8) Low-high sequences have little effect on propagation rates at the higher load level; crack growth may be initially accelerated at the higher load level, but if so, it rapidly stabilizes.

The effects of environment, temperature, and frequency have received sparse attention. Irving *et al.*[40] attempted to measure crack tip closures in titanium alloys and suggested that closure occurred in air but not in vacuum. Cyclic frequency had little effect on this result. Chanani[38] found the amount of retardation to be similar, with respect to the appropriate baseline da/dN, for 7075-T6 aluminium alloy tested in air and salt water. However, for a given size of overload plastic zone, fewer cycles were required to grow the crack through this distance in salt water than in air. It was thus concluded that crack blunting did not govern the retardation.

Raju *et al.*[41] have annealed cracked aluminium alloy specimens for various times at various temperatures after the application of a high load. Progressive annealing continually reduced the subsequent delay. Crack blunting as such cannot therefore be a major factor in causing delay. Relief of residual stress is the most likely explanation of these results.

4. RETARDATION

4.1 Mechanisms

A number of concepts, listed below, have been proposed[28,34,42-44] as mechanisms controlling retardation:

(*a*) residual compressive stresses in the crack tip zone only;
(*b*) shape of crack tip—overloads enlarge the radius, requiring further cycles to sharpen it for additional growth.
(*c*) crack closure—if the crack closes on unloading from a tensile stress, the stress excursion felt at the crack tip is reduced;
(*d*) strain hardening in the plastic zone at the crack tip —making subsequent propagation more difficult;
(*e*) incompatible crack front orientations—the fracture mode can vary with stress and the overload may create a crack front orientation which is unfavourable for the lower stress cycling, thus suppressing propagation.

Some experimenters have claimed to demonstrate crack closure either by consistency with their experimental results,[34] by measurement of unloading COD slopes,[45] or by the potential drop technique of measuring crack areas.[40] However, Lindley and Richards[46] demonstrated that closure does not occur under plane strain conditions, although it may occur in regions of plane stress in both thin and thick specimens. They suggest, furthermore, that closure cannot explain the increase in crack growth rate with increase in mean stress observed at low alternating stress intensities in steels.

Other experimenters have claimed to demonstrate the insignificant contribution of blunting[38,41] or of strain hardening.[38]

Some of the proposals are not mutually exclusive although they have often been treated as such. For example, if the residual stress field produced by the overload is considered as a whole, and attention is not simply focussed on the plastic zone, closure can be envisaged. Which, if any, of the proposals has overriding importance is, at present, uncertain.

4.2 Models

It has been amply demonstrated that to achieve any degree of accuracy in predicting crack growth rates under random loading by using known constant-amplitude growth rates, it is vital to account for load interactions, and in particular for retardation. Three models have been proposed to specifically account for load interactions and, not surprisingly, all are based on the Paris law and all are empirically based. They commonly calculate crack growth increments cycle-by-cycle, the increment in each cycle being related to that which would have been obtained in a constant amplitude test at the same crack length.

The first retardation model was proposed by Wheeler[47] who multiplied the Paris constant C by a term C_p which was chosen to represent the interactions between the plastic zone due to the overload and that due to the lower stress level. Thus:

$$C_p = \left(\frac{R_y}{a_p - a}\right)^n \tag{12}$$

where R_y is the extent of the current yield zone at the lower stress level, $(a_p - a)$ is the current distance from the crack tip to the elastic-plastic interface caused by the peak overload, and n is a shaping exponent. The model therefore proposes the relation:

$$da/dN = \left(\frac{R_y}{a_p - a}\right)^n C(\Delta K)^m \tag{13}$$

The retardation is proportional to the distance the crack has progressed through the initial plastic zone, the retardation parameter C_p being bounded by zero and unity. The model requires the shaping exponent, n, to be determined experimentally.

As an alternative, Willenborg *et al.*[48] have operated directly on the crack growth driving function ΔK by computing a ΔK_{eff} from an assumed state of residual stress. Through the expression for the yield zone radius, $R_y = K^2/2\pi\sigma_y^2$, a reduction in stress is calculated from the distance between the extent of yield zones for the overload and subsequent cycles. The effective ΔK is then calculated for the subsequent cycles from

$$\sigma_{eff} = \sigma_{applied} - \sigma_{reduction}$$

If σ_{eff} is less than zero it is set equal to zero. Along with ΔK_{eff}, an effective value of R is calculated and normal constant growth rate data are then applied.

Lukáš and Klesnil[4] have experimentally determined a variety of transient growth rate effects and have satisfactorily correlated their test data by an alternative ΔK_{eff} approach. In the essence, their method uses the notion:

$$da/dN = (K^m - K_{th}^m) \tag{14}$$

where the threshold value, K_{th}, describes the condition of non-propagation and depends on a number of material constants. This equation incorporates a driving term for crack propagation (K^m) and a resistance term (K_{th}^m) which quantitatively describes the residual stress field. The crucial part of this formulation lies in the procedure for determining K_{th}^m which is not a constant but depends on the immediate value of K. Lukáš and Klesnil suggest:

$$K_{th} = K_{th_{(0)}}^{1-\alpha} K^{\alpha} \tag{15}$$

where α is a material constant (as they show for carbon steels by test[49]), and $K_{th(0)}$ is a basic threshold value, also a material constant, and equated to the fatigue limit of a cracked sample which must be determined by test.

Suppose there is a sudden change in load level, from level (1) down to level (2). The driving term will change from $K_{(1)}^m$ to $K_{(2)}^m$ but the immediate resistance term will remain unchanged at $K_{th(1)}$. The initial transient growth rate is then given by:

$$da/dN\,(\text{transient}) = C(K_{(2)}^m - K_{th(1)}^m) \tag{16}$$

The duration of this transient rate, in terms of the crack length, is calculated from the cyclic plastic zone size for the appropriate stress state and using the cyclic yield stress.

Lukáš and Klesnil suggested the simple procedure of assuming that the transient rate remains constant for the calculated crack increment, whereupon there is a sudden change in rate to the steady state level. Figure 7 shows the relation between their calculated and experimentally determined growth rates in a test which applied single overloads.

The three models should be recognised as first attempts to solve a practical problem. But since crack tip plasticity as such is considered as the sole cause of retardation, serious limitations arise. Briefly, these limitations are listed below.

(1) Most of the other possible mechanisms of retardation are not accounted for, yet there is experimental evidence that some of them, at least in particular cases,[34,44] are important.

(2) Consecutively-applied overloads increase N_d compared with that after the application of a single overload; yet all the models would predict no change in N_d. The experimental result appears to confirm the effect of cyclic hardening.

(3) The models do not account for effects such as delayed retardation.

But perhaps the major criticism of these models is that they make no attempt to predict the detailed course of crack propagation through the retardation period; they simply aim at giving a reasonable value for N_d. For example, within the detectability of measurement techniques, sometimes a crack will be completely stopped after a high load, and if the constants in the models are arranged to describe this behaviour, they cannot then predict any further crack growth which, in practice, may still occur. This being the case, and considering the fact that not all possible variables associated with retardation have been investigated let alone generalized, it is extremely unlikely that any of these models will be found universally applicable.

The Willenborg *et al.* model requires no information beyond the stressing history, the yield stress, and the steady-state crack propagation rates. The other two models require further experimental information (the Wheeler shaping exponent n, and the Lukáš/Klesnil threshold values of K) which is obtained by test under one set of conditions and then applied to the stress conditions at the crack tip. When the various mechanisms of retardation are considered it is clear that some materials information, obtainable only by test, will be a required input.

A further, more practical, problem arises when applying any of these models to the prediction of crack growth under random sequences. They all require cycle-by-cycle calculation of crack growth increments and this procedure has been found to be both cumbersome and to require the use of an extensive computer facility.[50,51]

Based upon the concept of crack-closure, Elber[50] has recently attempted to overcome this problem by modelling random load crack growth with an "equivalent constant-amplitude concept". This concept replaces the random sequence with a number of much shorter constant-amplitude sequences, each of which is selected to have the same total crack growth, crack-growth mode, and critical crack length as the corresponding part of the random sequence. The procedure hinges on choosing a crack-opening stress for the constant amplitude sequence which is the same as that for the equivalent random sequence (Elber had previously demonstrated that the crack-opening load remained essentially constant during crack growth under a random sequence

containing several thousand peaks). At present, crack-opening loads must be determined by test. The procedure is then to use constant-amplitude growth data with the modified Paris equation:

$$da/dN = C(\Delta K_{eff})^m \tag{17}$$

using data on the crack-opening loads to generate ΔK_{eff}. Elber claims reasonable prediction by this method.

No doubt various perturbations of the fundamental approaches to retardation will be tried. For example, Gallagher and Hughes[52] have generalized the Willenborg *et al.* ΔK_{eff} term to cope with the total arrest in crack growth observed at large values of $\Delta K_1/\Delta K_2$. Such generalizations of course require further test data. Whether generalized information will ever be adequate remains to be seen.

5. FUTURE PROGRESS

The basic description of crack geometry and mode of propagation appears clear from experimental evidence and theoretical argument; namely, that application of a tensile load of sufficient magnitude to a cracked sample induces preferential plastic flow at the tip of the crack, and this flow can have three consequences. First, it enlarges the crack tip profile; second, it can alter the properties of the material so affected (cyclic hardening/softening); and third, it induces a state of residual stress upon unloading. The magnitudes of some of these effects will obviously depend upon the general stress state. The state of stress, in conjunction with the metallurgical structure, will also be important in determining the macroscopic shape of the crack front.

From this description it is evident that parameters describing the cyclic behaviour of materials are necessary inputs to formulations which aspire to describe fatigue crack growth under non-uniform load sequences. The Wheeler exponent n is an attempt in this direction although it is not a material constant. The Lukáš and Klesnil K_{th} and α are claimed to be material constants but their universality has yet to be demonstrated. Other investigators[8] are attempting to apply the cyclic parameters obtained from tests on bulk uncracked specimens to crack propagation, but with only partial success.

These are steps in the right direction, but they are first steps only. A missing component is a realistic cycle-by-cycle description of the state of stress around the crack tip. The effect of thickness on delay, as shown in Section 3.1, highlights the need for this information. Although adequate descriptions should yield to both theoretical and experimental attack for reasonably homogeneous solids, it is not at all clear that this will be so for commercial alloys. Crack growth planes and crack front shapes in commercial alloys under fatigue loading are not yet predictable.[53,54]

Under fatigue loading the localized nature of plastic strain within the crack tip region presents a further problem. Since it is believed that fatigue cracks both initiate and propagate as a result of irreversibilities in the plastic strains induced by cycling,[55] a description of the localized degree of irreversibility would appear necessary. In addition, any crack growth model which describes the delays in growth observed under test, must also describe, during the delay, those micro-scale plastic movements which condition the crack for further propagation. A description of this conditioning requires knowledge of the localized plastic strain irreversibilities at the crack tip.

Future formulations of universal fatigue crack propagation laws will no doubt quantify many of the effects which can only be qualitatively described at present. Since satisfactory solutions using the approach will require many years of investigation, what can be recommended for the present and the immediate future? The recommendations depend upon the importance attached to accuracy. Fatigue crack growth rates under multi-level loading can be predicted currently within an order of magnitude using constant amplitude data and an interaction model. Where more accurate knowledge is required, actual tests under the desired load sequence are recommended. Such tests are now quite feasibile on a routine basis with the advent of computer-controlled electro-hydraulic fatigue machines.

6. CONCLUSIONS

(1) The quantitative effect of load interactions in fatigue crack propagation depends on a large number of test parameters, including the relative magnitudes of loads, their precise sequence, cycle hold times, environment, and material thickness.

(2) For 2024-T3 aluminium alloy specimens the delay in crack growth caused by a single overload was greater by a factor of about 8·5 for 1·6 mm thick specimens than for 6·4 mm thick specimens.

(3) Delay is thus a three-dimensional problem and the through-thickness constraint must be accounted for in any model. The large effect of thickness on delay also emphasises the need for caution in extrapolating existing growth data to various design situations.

(4) A variety of mechanisms of load interaction have been proposed but, so far, the models for quantitative prediction use the extent of crack tip plasticity only (as determined by fracture mechanics) as a factor on the Paris equation. The models also make no attempt to predict the detailed course of crack propagation through the interaction period.

(5) A satisfactory prediction of interaction effects will require some materials information, obtainable only by test. How close the generation of this information comes to replacing prediction by test remains to be seen.

(6) To obtain an accurate assessment of fatigue crack propagation under multi-load sequences, actual tests under such sequences are currently recommended.

REFERENCES

1. Williams, M. L. — On the Stress Distribution at the Base of a Stationary Crack. J. Appl. Mech., vol. 24, pp. 109–114, March 1957.
2. Irwin, G. R. — Analysis of Stresses and Strains near the End of a Crack Traversing a Plate. J. Appl. Mech., vol. 24, pp. 361–364, September 1957.
3. Paris, P. C. — "The Fracture Mechanics Approach to Fatigue." Fatigue—An Interdisciplinary Approach (eds J. J. Burke, N. L. Reed, and V. Weiss), pp. 107–132, Syracuse University Press, Syracuse, 1964.
4. Lukáš, P., and Klesnil, M. — Transient Effects in Fatigue Crack Propagation. Eng. Fract. Mech. (being published).
5. Ryan, N. E. — The Influence of Stress Intensity History on Fatigue-Crack Growth. Aeronautical Research Laboratories, Report ARL/Met. 92, Department of Supply, June 1973.
6. Head, A. K. — The Growth of Fatigue Cracks. Phil. Mag., vol. 44, ser. 7, p. 925, 1953.
7. McClintock, F. A. — "On the Plasticity of the Growth of Fatigue Cracks." Fracture of Solids, p. 65. John Wiley, New York, 1963.
8. Majumdar, S., and Morrow, J. — "Correlation Between Fatigue Crack Propagation and Low Cycle Fatigue Properties." Fracture Toughness and Slow-Stable Cracking. ASTM, STP 559, pp. 159–182, 1974.
9. Frost, N. E., and Dugdale, D. S. — The Propagation of Fatigue Cracks in Sheet Specimens. J. Mech. Phys. Solids, vol. 6, No. 2, pp. 92–110, 1958.
10. Frost, N. E. — A Note on the Behaviour of Fatigue Cracks. J. Mech. Phys. Solids, vol. 9, pp. 143–151, 1961.
11. Liu, H. W. — Fatigue Crack Propagation and Applied Stress Range—An Energy Approach. J. Basic Eng. Trans. A.S. M.E., vol. 85, p. 116, 1963.
12. Weertman, J. — "Rate of Growth of Fatigue Cracks Calculated from the Theory of Infinitisimal Dislocations Distributed on a Plane." Proc. 1st Int. Conf. Fracture, vol. 1, Japanese Society for Strength and Fracture of Materials, Sendai, Japan, pp. 153–164, 1966.
13. Neumann, P. — The Geometry of Slip Processes at a Propagating Fatigue Crack —II. Acta Met., vol. 22, pp. 1167–1178, September 1974.
14. Tomkins, B. — Fatigue Crack Propagation—An Analysis. Phil. Mag., vol. 18, pp. 1041–1066, 1968.
15. Paris, P. C. — The Growth of Cracks due to Variations in Load. Ph.D. Dissertation, Lehigh University, 1962.
16. Miller, G. A., and Throop, J. F. — Optimum Fatigue Crack Resistance. ASTM, 1969.
17. Richards, C. E., and Lindley, T. C. — The Influence of Stress Intensity and Microstructure on Fatigue Crack Propagation in Ferritic Materials. Eng. Fract. Mech., vol. 4, pp. 951–978, 1972.
18. Maddox, S. J. — The Effect of Mean Stress on Fatigue Crack Propagation. A Literature Review. Int. J. Fract., vol. 11, no. 3, pp. 398–408, June 1975.
19. Forman, R. G., Kearney, V. E., and Engle, R. M. — Numerical Analysis of Crack Propagation in Cyclic loaded Structures. J. Basic Eng., Trans. ASME, vol. 89, pp. 459–463, 1967.

20. Katcher, M., and Kaplan, M. "Effects of R-factor and Crack Closure on Fatigue Crack Growth for Aluminium and Titanium Alloys." Fracture Toughness and Slow-Stable Cracking. ASTM, STP 559, pp. 264-282, 1974.

21. Pearson, S. The Effect of Mean Stress on Fatigue Crack Propagation in Half-inch Thick Specimens of Aluminium Alloys of High and Low Toughness. R. Aircr. Establ. Tech. Rep. 68297, December 1968.

22. Pearson, S. The Effect of Mean Stress on Fatigue Crack Propagation in Half-inch (12·7 mm) Thick Specimens of Aluminium Alloys DTD 5050 and DTD 5090. R. Aircr. Establ. Tech. Rep. 69195, September 1969.

23. Erdogan, F., and Ratwani, M. Fatigue and Fracture of Cylindrical Shells Containing Circumferential Cracks. Int. J. Fract. Mech. vol. 6, No. 4, p. 379, December 1970.

24. Roberts, R., and Erdogan, F. The Effect of Mean Stress on Fatigue Crack Propagation in Plates under Extension and Bending. J. Basic Eng., Trans ASME, vol. 89, pp. 885-892, 1967.

25. Erdogan, F., and Roberts, R. A Comparative Study of Crack Propagation in Plates under Extension and Bending. Proc. 1st Int. Conf. Fracture, Sendai, Japan, 1965.

26. Roberts, R., and Kibler, J. J. Some Aspects of Fatigue Crack Propagation. Eng. Fract. Mech., vol. 2, pp. 243-260, 1971.

27. Raju, K. N. An Energy Balance Criterion for Crack Growth under Fatigue Loading from Considerations of Energy of Plastic Deformation. Int. J. Fract. Mech. vol. 8, No. 1, p. 1, March 1972.

28. Elber, W. "The Significance of Fatigue Crack Closure." Damage Tolerance in Aircraft Structures. ASTM, STP 486, p. 230, 1971.

29. Shih, T. T. and Wei, R. P. Effect of Specimen Thickness on Delay in Fatigue Crack Growth. J. Testing and Evaluation, vol. 3, No. 1, pp. 46-47, January 1975.

30. Mills, W. J., and Hertzberg, R. W. The Effect of Sheet Thickness on Fatigue Crack Retardation in 2024-T3 Aluminium Alloy. Eng. Fract. Mech., vol. 7, pp. 705-711, 1975.

31. Gardner, F. H., and Stephens, R. I. "Subcritical Crack Growth under Single and Multiple Periodic Overloads in Cold-rolled Steel." Fracture Toughness and Slow-Stable Cracking. ASTM, STP 559, pp. 225-244, 1974.

32. Rice, R. C., and Stephens, R. I. "Overload Effects on Subcritical Crack Growth in Austenitic Manganese Steel." Progress in Flaw Growth and Fracture Toughness Testing. ASTM STP 536, pp. 95-114, 1973.

33. Trebules, V. W., Roberts, R., and Hertzberg, R. W. "Effect of Multiple Overloads on Fatigue Crack Propagation in 2024-T3 Aluminium Alloy." Progress in Flaw Growth and Fracture Toughness Testing. ASTM, STP 536, pp. 115-146, 1973.

34. von Euw, E. F., Hertzberg, R. W., and Roberts, R. "Delay Effects in Fatigue Crack Propagation." Stress Analysis and Growth of Cracks. ASTM, STP 513, pp. 230-259, 1972.

35. Sharpe, W. N., Corbly, D. M., and Grandt, A. F. The Effects of Rest-time on Fatigue Crack Retardation. ASTM Symposium on Fatigue Crack Growth under Spectrum Loads, Montreal, June 1975.

36. Jonás, O., and Wei, R. P. An Exploratory Study of Delay in Fatigue Crack Growth. Int. J. Fract. Mech., vol. 7, pp. 116-118, 1971.

37. Corbly, D. M., and Packman, P. F. On the Influence of Single and Multiple Peak Overloads on Fatigue Crack Propagation in 7075-T6511 Aluminium. Eng. Fract. Mech., vol. 5, No. 2, pp. 479-497, 1973.

38. Chanani, G. R. Retardation of Fatigue-Crack Growth in 7075 Aluminium. Metals Eng. Quart., vol. 15, No. 1, pp. 40-48, February 1975.

39. Wei, R. P., Shih, T. T., and FitzGerald, J. H. — Load Interaction Effects on Fatigue Crack Growth in Ti-6Al-4V Alloy. NASA CR-2239, April 1973.

40. Irving, P. E., Robinson, J. L., and Beevers, C. J. — Fatigue Crack Closure in Titanium and Titanium Alloys. Int. J. Fract., vol. 9, pp. 105–108, 1973.

41. Raju, K. N., Ningiah, V., and Rao, B. V. S. — Effect of Exposure to Elevated Temperatures on Delay in Crack Growth due to a High Stress Cycle. Int. J. Fract. Mech., vol. 8, pp. 99–102, 1972.

42. Hudson, C. M., and Hardrath, H. F. — Effects of Changing Stress Amplitude on the Rate of Fatigue-Crack Propagation in Two Aluminium Alloys. NASA TN-D-960, September 1961.

43. Hardrath, H. F. — "Cumulative Damage." Fatigue—An Interdisciplinary Approach (eds J. J. Burke, N. L. Reed, and V. Weiss). Syracuse University Press, Syracuse, 1964.

44. Schijve, J. — Fatigue Damage Accumulation and Incompatible Crack Front Orientation. Eng. Fract. Mech., vol. 6, pp. 245–252, 1974.

45. Schijve, J. — Fatigue Crack Growth under Variable-Amplitude Loading. Delft Univ. Technology, Rep. VTH-181, April 1974.

46. Lindley, T. C., and Richards, C. E. — The Relevance of Crack Closure to Fatigue Crack Propagation. Mat. Sci. Eng., vol. 14, No. 3, pp. 281–293, June 1974.

47. Wheeler, O. E. — Spectrum Loading and Crack Growth. J. Basic Eng., Trans. ASME, vol. 94, No. 1, pp. 181–186, March 1972.

48. Willenborg, J., Engle, R. M., and Wood, H. A. — A Crack Growth Retardation Model using an Effective Stress Concept. AFFDL, Wright Patterson Air Force Base, Ohio, TM-71-1-FBR, January 1971.

49. Klesnil, M., and Lukáš, P. — Effect of Stress Cycle Asymmetry on Fatigue Crack Growth. Mat. Sci. Eng., vol. 9, pp. 231–240, 1972.

50. Elber, W. — An Equivalent Constant-Amplitude Concept for Crack Growth under Spectrum Loading. ASTM Symposium on Fatigue Crack Growth under Spectrum Loads, Montreal, June 1975.

51. Mann, J. Y. — Report on Overseas Visit to Europe and North America, May/June 1975, Embracing the 14th ICAF Meetings at Lausanne, Switzerland and Discussions Relating to the Fatigue of Materials. Aeronautical Research Laboratories, Tech. Memo. ARL/Struc. 234, Department of Defence, September 1975.

52. Gallagher, J. P., and Hughes, T. F. — Influence of Yield Strength on Overload Affected Fatigue Crack Growth Behaviour in 4340 Steel. AFFDL-TR-74-27, Wright Patterson Air Force Base, Ohio, July 1974.

53. Finney, J. M. — Stress Level at the Crack Front in Unnotched Rotating Cantilever Fatigue Specimens. Aeronautical Research Laboratories, Note ARL SM 283, Department of Supply, September 1963.

54. Anson, P. G., and Mann, J. Y. — Directionality Effects in the Fatigue and Fracture of Extruded 2024-T4 Aluminium Alloy. International Institute of Welding and Metals Technology Conference, Sydney, pp. 15-1-1 to 15-1-5, August, 1976.

55. Finney, J. M., and Laird, C. — Strain Localization in Cyclic Deformation of Copper Single Crystals. Phil. Mag., vol. 31, No. 2, pp. 339–366, February 1975.

TABLE 1

Cyclic Stressing Conditions

Crack length $2a$ (cm)	Stress intensity* K (MPa$\sqrt{m}$)		
	Minimum of alternating load	Maximum of alternating load	High load
1·65	9·92	24·82	42·68
2·41	12·20	30·53	52·50
3·18	14·36	35·94	61·80

* Correction factor for finite width is $\sqrt{(\text{Sec } \pi/2 \cdot 2a/w)}$, where w is width of specimen.

TABLE 2

Effect of Specimen Thickness and Crack Length on Delay Period

Crack length $2a$ (cm)	Thickness (mm)	Delay N_d (Cycles)	Average N_d (Cycles)	N_d(1·6 thick) / N_d(6·4 thick)	Crack growth during N_d a_d (mm)	Average a_d (mm)	High load plastic zone size* R_y (mm)	Proportion† of thickness with plane stress fracture just prior to high load (%)
1·65	6·4	11,000 10,500 12,000	11,000	8·6	2·0 1·7 1·7	1·8	1·64	10
	1·6	190,000 54,000 43,000	96,000		5·1 3·8 2·3	3·7	1·89	60
2·41	6·4	12,000 11,000 15,000	13,000	8·5	1·8 2·4 2·0	2·1	2·47	50
	1·6	115,000 109,000 99,000	108,000		6·2 — 6·2	6·2	2·87	100
3·18	6·4	24,000 45,000 32,000	34,000	—	— 3·3 —	3·3	3·43	70

* Calculated using the plane stress formula $R_y = \frac{1}{2\pi}\left(\frac{\Delta K}{\sigma_y}\right)^2$.

† Proportions only roughly determined.

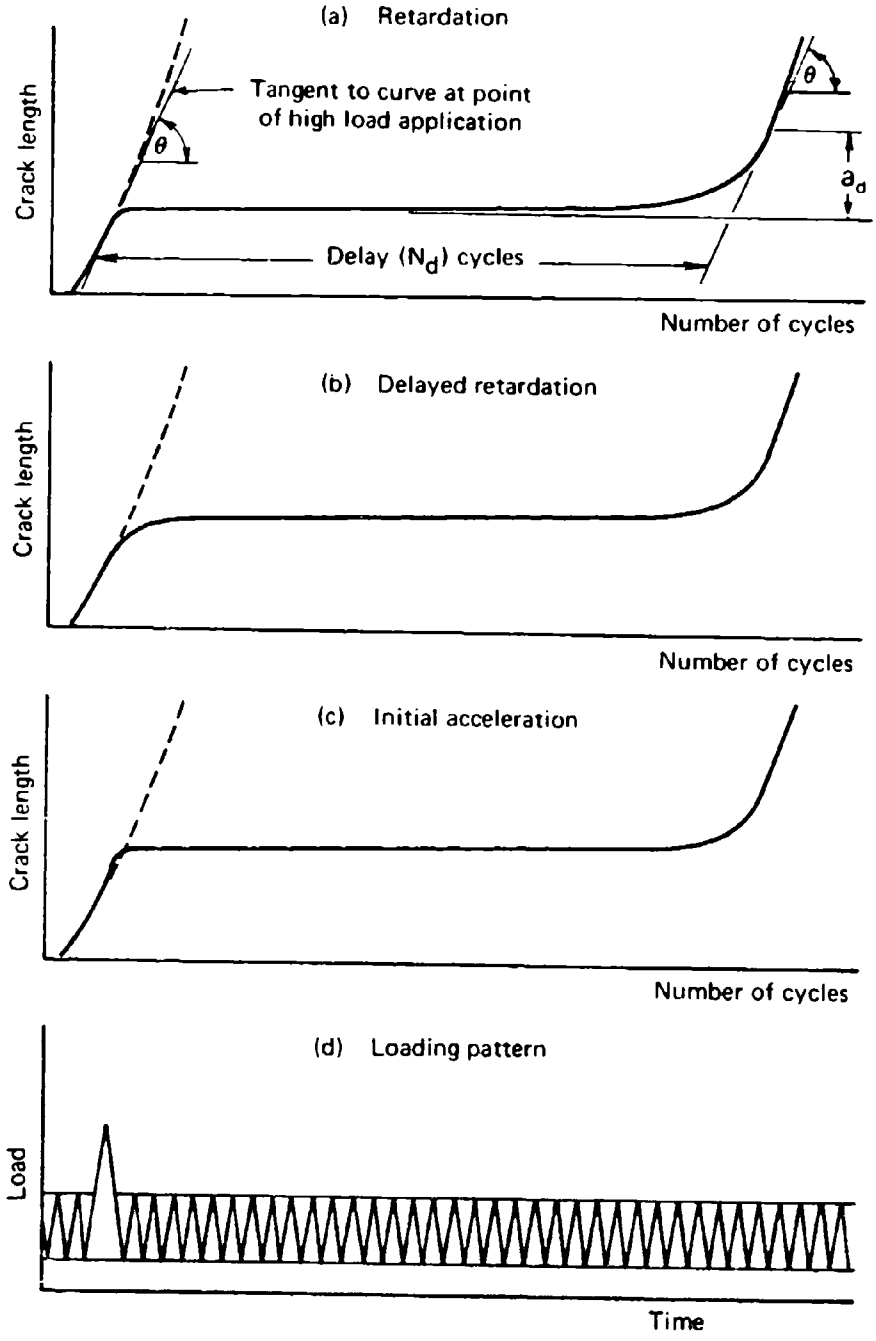

FIG. 1. SCHEMATIC DEFINING DELAY (N_d) AND ILLUSTRATING DIFFERENT CRACK GROWTH BEHAVIOUR AFTER A HIGH LOAD.

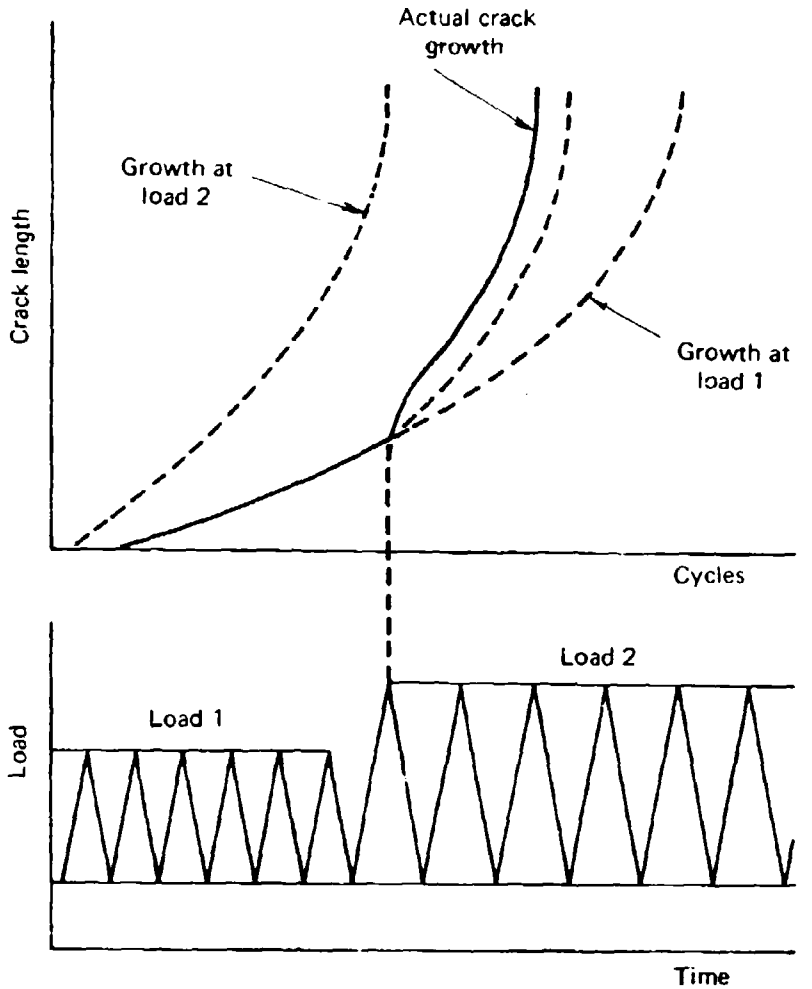

FIG. 2. SCHEMATIC SHOWING ACCELERATION IN CRACK GROWTH AT AN INCREASE IN THE LOAD RANGE

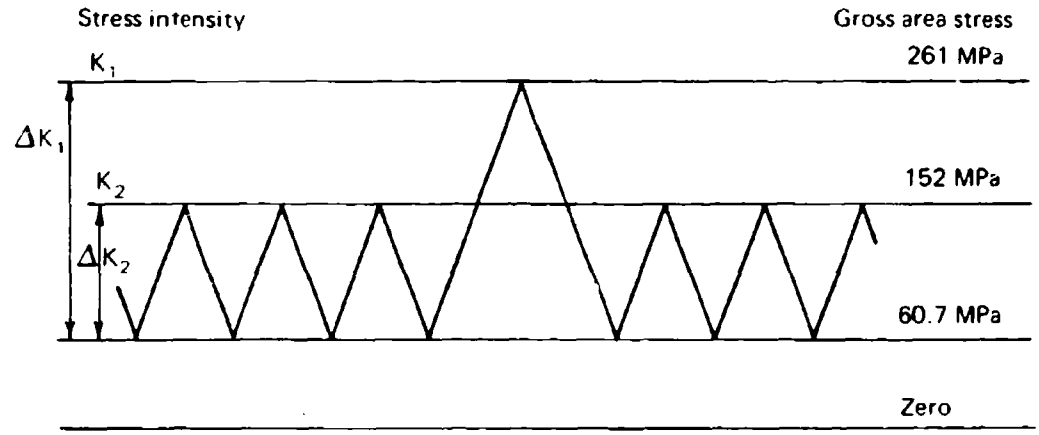

FIG. 3. LOADING PATTERN SHOWING A HIGH LOAD

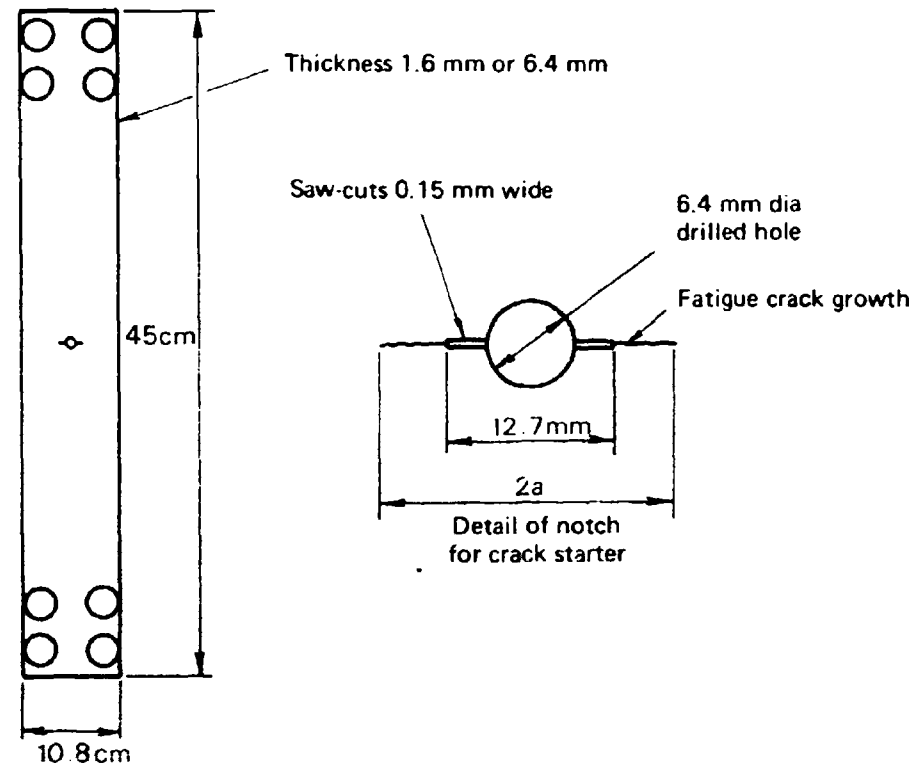

FIG. 4. DIMENSIONS OF 2024-T3 ALUMINIUM ALLOY SPECIMENS.

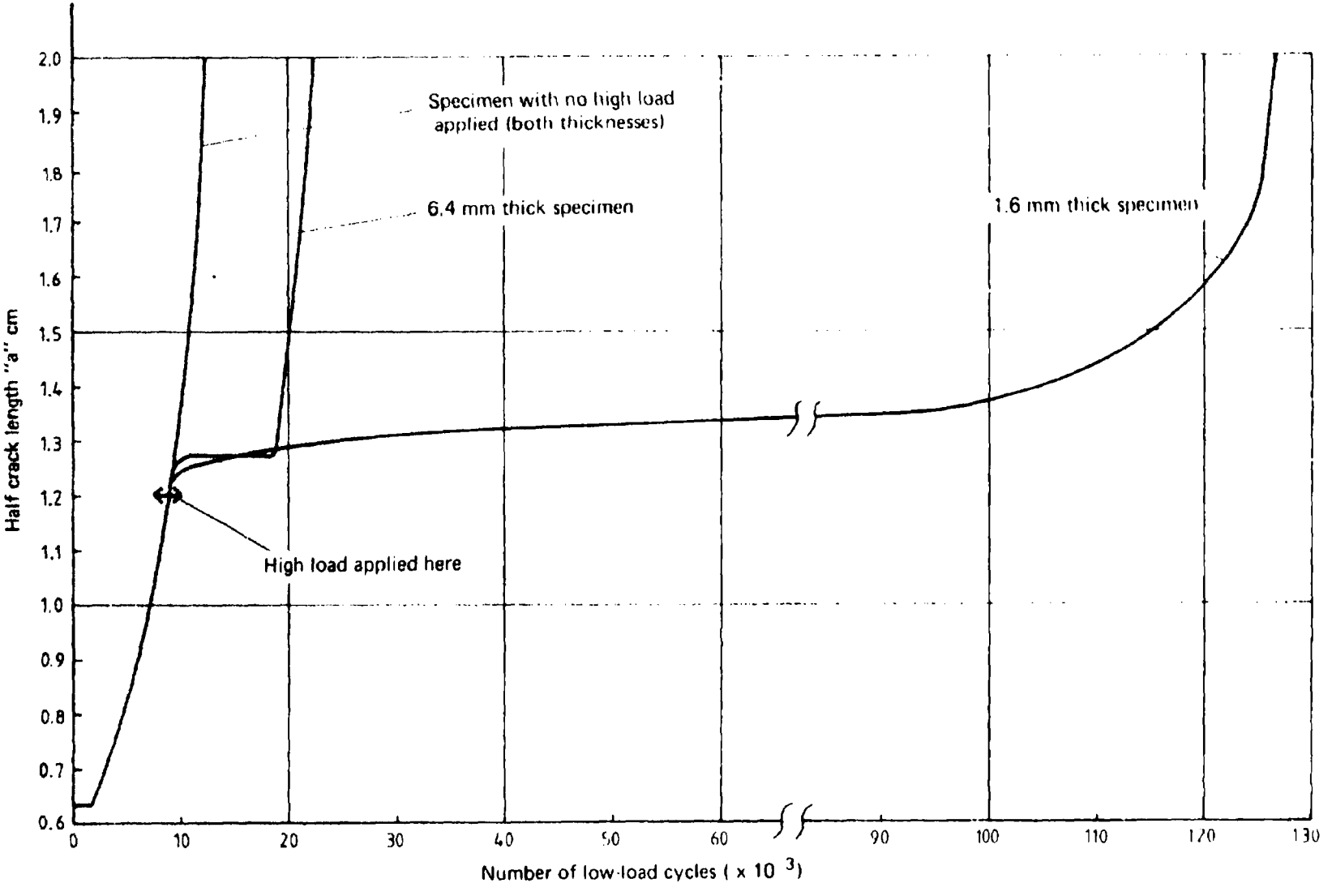

FIG. 5. EFFECT OF THICKNESS ON DELAY FOR 2024-T3 ALUMINIUM ALLOY SPECIMENS.

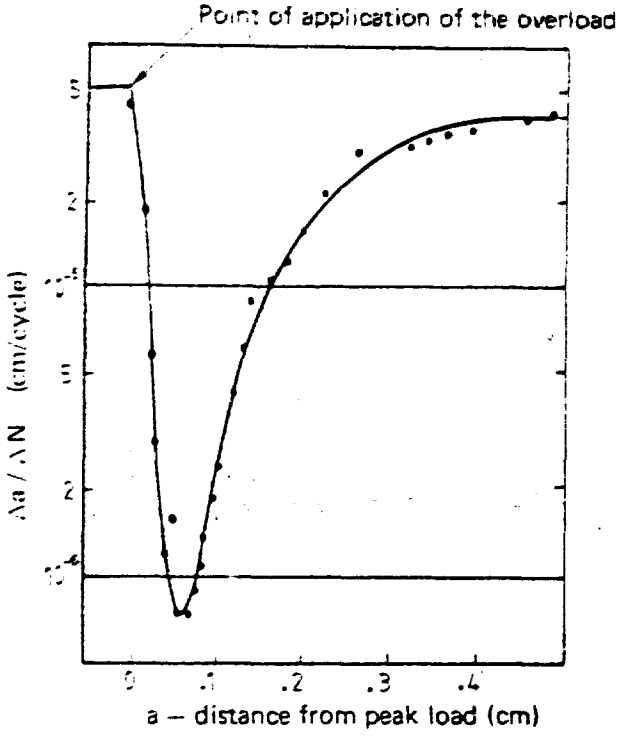

FIG. 6. GROWTH RATE THROUGH DELAY REGION IN 2024-T3 ALUMINIUM ALLOY (AFTER VON EUW, HERTZBERG, AND ROBERTS (34))

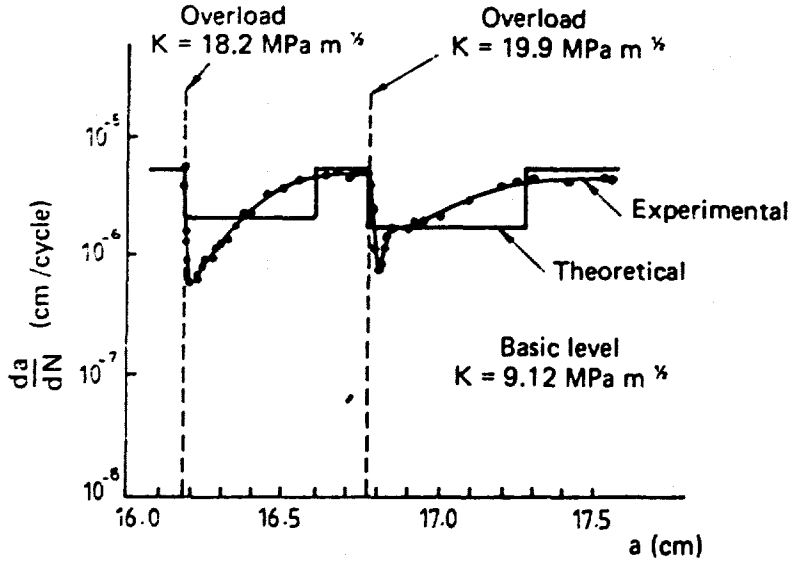

FIG. 7. EXPERIMENTAL AND THEORETICAL COURSE OF TRANSIENT CRACK PROPAGATION FOLLOWING SINGLE PEAK OVERLOADS (AFTER LUKÁŠ AND KLESNIL (4))

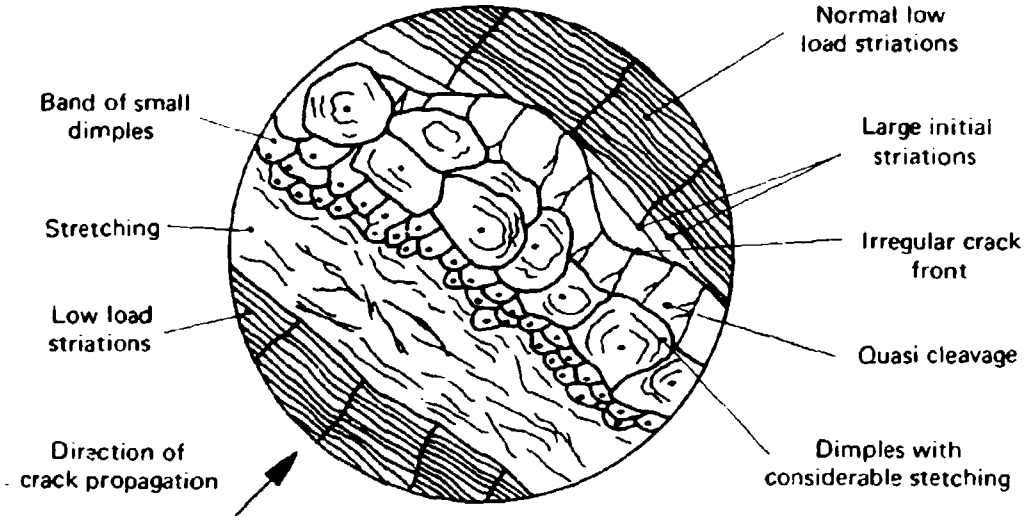

(a) Schematic of crack propagation sequence

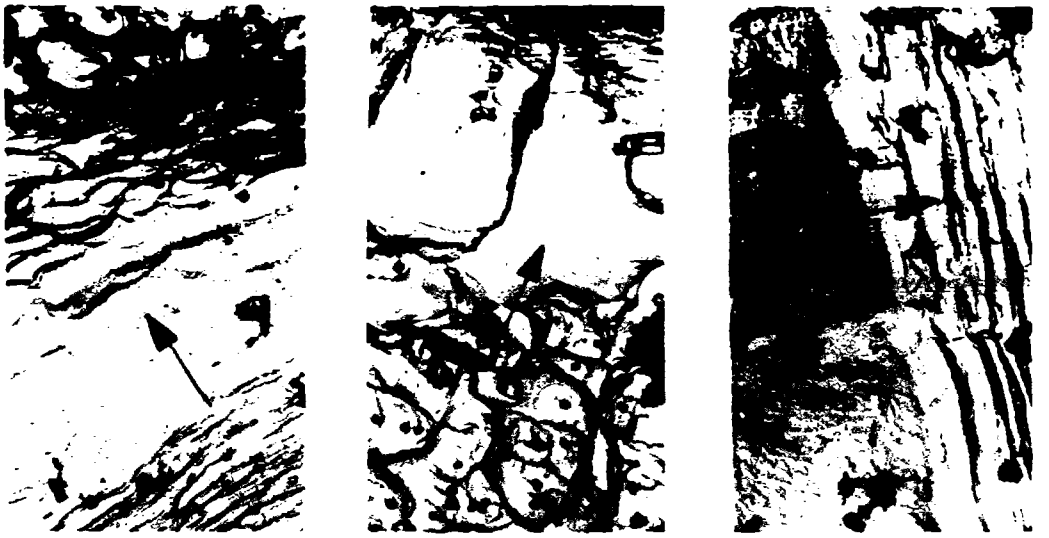

x 5000
(i) Transition from low-load striations to stretching to dimples as high load is applied

x 5000
(ii) Dimples with stretch marks as high load is applied

x8500
(iii) Quasi-cleavage followed by striations upon subsequent low-load cycling

(b) Electron fractographs of failure sequence (arrows indicate direction of crack propagation)

FIG. 8. SEQUENCE OF FAILURE AROUND THE APPLICATION OF A HIGH LOAD DURING CRACK PROPAGATION UNDER A LOWER LEVEL OF CYCLIC LOADS IN 2024-T3 ALUMINIUM ALLOY

DISCUSSION

QUESTION—*J. D. Newton*
(SEC, Victoria)

The experiments conducted on the centre cracked specimen indicated that the application of a highload delayed crack growth when the original load regime was resumed. It was further shown that increasing the specimen thickness reduced the extent of the delay after the high load application. I am not sure if the "high loads" applied were the same in proportion to gross specimen dimensions. However, by increasing the specimen thickness the situation at the crack tip is changed, by increasing the thickness the tendency is towards a plane strain condition. Therefore it would appear that the experimental conditions for the two specimens were not the same, rendering direct comparison of the results impossible.

Author's Reply

The high loads were applied at the same crack lengths and they gave the same nominal stress intensities in the two thicknesses. Even so, it is true that the three-dimensional stress conditions locally at the crack tip are different in the two cases because of different through-thickness constraint; but herein lies the explanation of the thickness effect on retardation. In this sense it is agreed that the experimental conditions are not the same for the two thicknesses; if they were, we are left with no variable at all to examine. It is legitimate to determine the effect of thickness on retardation, as we have done, and it is also legitimate to interpret the results as indicating the effect of changing through-thickness constraint, but we contest the notion that the results cannot be compared.

QUESTION—*P. D. Stewart*
(Swinburne College of Technology)

Could you comment on the effect of the hydrostatic component of the fatigue stress?

Author's Reply

Undoubtedly, as indicated in the reply to J. D. Newton, the effect of thickness on retardation is determined by the different three-dimensional stress states in the local crack tip region. These different stress states, upon application of an overload with attendant local yielding, will result in different local residual stress systems upon unloading, and subsequent lower-load crack growth rates will be affected accordingly. But at this stage even the initial stress states cannot be quantified adequately—the concepts of plane stress and plane strain are limiting cases only, and in addition there is the complexity of handling local yielding.

QUESTION—*P. J. Howard*
(ARL)

Do any of the models described include the effect of offset of mean stress caused by local plastic yielding?

Author's Reply

No. The three models described all use the fracture mechanics formula for calculating the extent of the yield zones resulting from the overload and from the lower-load cycles, and manipulate these values to alter either the constant C, the effective value of ΔK, or the exponent

m in the paris equation. The use of this formula is based on a particular stress distribution around the crack tip which depends on applied stress amplitude but is taken to be independent of cyclic history. Thus, effects such as cycle-dependent stress relaxation or creep are unaccounted for.

QUESTION *Dr. Keith R. L. Thompson*
(University of New South Wales)

Regarding the mechanism involved in the observed delay in crack growth following the imposition of single peak overload cycles, has the speaker observed any indication of a variation in the magnitude of this delay across the specimen thickness of the aluminium alloys investigated?

Such indications have been observed by the questioner whilst investigating the effects of single peak load impositions on sheet specimens (2·5 mm thick) of high strength AISI 4340 steels.* Following the imposition of single peak load cycles, continued crack growth under constant amplitude loading occurred initially at the crack front region adjacent to where stress relaxation during peak loading had occurred by through-thickness shear displacement. On the contrary at the interior of the specimen, stress relaxation at the crack front during peak loading had been achieved by microvoid coalescence which necessitated a re-initiation of the crack prior to its subsequent growth. On the basis of these fractographic observations it was concluded that the magnitude of the delay effect was dependent upon the prevalent stress state (i.e. plane stress or plane strain) across the crack front during peak load imposition. When the thickness of the specimen and the loading conditions are such that both stress states are operative across the crack front then the magnitude of residual crack tip opening displacement produced by the peak load cycle varies across the specimen thickness and as a result the magnitude of the observed delay effect.

Author's Reply

Our paper, Section 3.1.4, discusses the phenomenon of "delayed retardation" observed both by others and ourselves, and suggests that it may result from a dependence of the magnitude of the parameter causing retardation on distance from the surface. Moreover, the very result of our thickness experiments indicates a dependence of the degree of retardation on distance from the surface.

But these observations only indirectly bear upon your question of variation in the magnitude of the delay across the specimen thickness. We suggest also that the evidence given in your description, and in your references, is likewise insufficient to answer the question. The observation of different modes of plastic strain accommodation through the thickness, of itself, is not hard evidence of different degrees of delay.

QUESTION—*H. A. Wills*
(Retired)

It seems to me that there might be some advantage gained in "conditioning" all new structures by applying a high load of say 80% design ultimate (perhaps several times). This would ensure that most of the locally high elastic stress concentrations are reduced by local plastic deformation with a consequential improvement of endurance.

Even if it is established that large negative loads might have a detrimental effect on life, the "preloaded" structure would be commencing service with residual stresses such as to minimise to adverse effect of the negative load.

QUESTION—*Dr. N. Ryan*
(ARL)

Dr. Finney, your paper on load interaction effects and resultant retardation in fatigue-crack growth again highlights the advantages that might be obtained from periodic proof loading of large scale structures. Dr. Hooke indirectly alluded to such improvements in his introductory paper and Mr. Patching further amplified the potential benefits that could be obtained, for increasing fatigue life, in his account of fatigue testing of aircraft wing structures.

---

* K. R. L. Thompson. Ph.D. Thesis, University of New South Wales, 1972 (also Proceedings of International Institute of Welding and Metals Technology, Sydney, 1976).

The one factor which seems likely to negate the potential benefits to fatigue life from periodic high load levels are the compressive cycles introduced during air to ground (landing) or ground to air (take-off) procedures. Notwithstanding, should we not be giving greater consideration to applying the potential benefits from periodic high loads for the obvious practical advantage of increasing the fatigue life of aircraft structures?

QUESTION—*G. E. F. Young*
(Ansett Airlines of Australia)

I presume the discussion is based on tests on individual specimens. Could you please comment on additional effects when testing full-size structures?

Author's Reply

Two questions should be considered:

(i) What effect does an overload have on the rate of crack propagation in a full-scale structure?

(ii) Why are overloads not applied to aircraft structures to improve their fatigue life?

The first question is not easily answered because there appears to be a lack of data, but there are indications of a substantial decrease in growth rate. These indications come from the following:

(*a*) The marked increase in total life achieved in structures, as well as in joints and simple specimens, by applying an overload prior to testing.

Examples The Mustang wings referred to in the paper by R. A. Bruton and C. A. Patching.

A variety of specimens, joints and structures detailed by Heywood.*

The inflated test fatigue life obtained for the Comet aircraft by using the static test article for fatigue substantiation.

(*b*) The decrease in crack growth rate observed in structural assemblies as well as in specimens when a programmed load sequence is applied. For example, it has been found in these Laboratories that the crack growth rate in a large D6AC steel structural assembly was substantially slower in the descending phase of a programmed load sequence than in the symmetrical ascending phase.

(*c*) Following on the Comet experience, the fail-safe character of the Concorde structure, when cracks develop during the fatigue test, is being demonstrated by a static test on a separate article as mentioned by Mr. C. A. Patching in his talk.

The question of why overloads are not deliberately applied to aircraft structures is, also, somewhat difficult to answer from a research worker's point of view, but three reasons can be advanced.

(*a*) The magnitude of the benefit may be smaller in full-scale structures and in random load tests compared with simple specimens tested under constant load amplitude.

(*b*) The cost of applying periodic overloads to all aircraft in a fleet may outweigh the benefit margin.

(*c*) Operators apparently cope by using a patch and replacement scheme.

These answers are not entirely convincing. For example, overloads applied to Mustang wings gave a three fold increase in fatigue life—a substantial benefit. Moreover, the periodic cold-proof test for flaws in F-111 aircraft is obviously a cost-effective measure. The whole question of improving service fatigue life by deliberate overloads merits further investigation by operators, and perhaps further research.

---

* R. B. Heywood, Designing Against Fatigue. Chapman and Hall Ltd., London, 1962.

A MODEL OF CRACK-TIP BEHAVIOUR FOR FATIGUE LIFE DETERMINATION

by

F. P. BULLEN, J. A. RETCHFORD, C. B. ROGERS and B. J. WICKS

SUMMARY

Aircraft fatigue life estimation usually involves large-scale tests of complex structures, combined with fatigue data derived from standard tests on small specimens. Since the number of large-scale tests which can be performed is limited and the results from small specimens may not be directly applicable to the fatigue behaviour of structures, these estimates are necessarily subject to considerable uncertainty. The approach described here is directed at providing data which would improve the evaluation of fatigue life by simulating the performance of critically stressed areas of a structure using individual tests on small specimens.

The experiments which are presented in support of this approach have been carried out on polycrystalline copper, since the physical basis of crack-tip behaviour in this simple metal is also applicable to conventional aircraft materials. It is shown that, in these materials, cracks propagate under cyclic loading as a result of irreversible plastic strain, and a parameter describing the plastic strain at the crack tip is defined which is shown to be directly related to the rate of crack propagation.

A simple model of crack-tip behaviour is proposed using this concept, in which the elastic and plastic contributions from material around the crack tip can be isolated and recombined in varying proportions. This could allow the behaviour of a cracked component in a structure to be replicated on small cracked specimens, by superimposing on the specimen load spectrum a stress variation representing the effect at the crack tip, of the elastically deforming structure.

The model is validated under a wide range of load histories and the implications for practical aircraft materials are discussed.

1. INTRODUCTION

Fracture mechanics has provided a useful relationship[1] between the rate of crack propagation and the range of local stress intensity at the crack-tip during fatigue at constant amplitude. However, no satisfactory treatment of fatigue at variable amplitudes of loading has yet been developed. Much equipment is subject to repeated stresses of varying amplitude and assessment of its consequent rate of deterioration is required for estimation of economic life and to ensure reliability in service. Earlier papers in this Symposium dealt with the sophisticated analyses developed to predict deterioration in aircraft structures, where failure in service could be catastrophic. Such analyses are necessarily based on large-scale structural fatigue tests under selected load spectra. However, few such tests can be conducted, because of their cost and complexity, and hence the resulting predictions are subject to considerable uncertainty. Consequently, increased factors of safety are used in the design, maintenance and life-estimation procedures, with a resulting economic penalty. The penalty can be particularly severe in the case of aircraft.

If the scatter in fatigue characteristics typical of the airframe material and the conversion of characteristics from one load spectrum to another could be assessed with increased certainty from supplementary laboratory tests on small specimens, then much of the uncertainty in life prediction could be reduced. However, for reasons not yet established, the fatigue characteristics of small specimens under variable-amplitude loading cannot at present be directly related to those of structural components fabricated from similar material and subjected to the same stressing.

This paper describes materials research directed towards establishing a method for relating the rates of propagation of fatigue cracks in small specimens and in structural components. Modern reliability analyses recognize that even the best NDI methods have finite limits of resolution and, hence, that the schedule of inspection intervals should be based on the time taken for a crack of near-critical dimensions to develop from a microscopic defect. Accurate prediction of the time required for such crack growth can minimize the number of costly inspections which have to be undertaken. These considerations were the basis for choosing crack propagation in the present study.

2. METHOD OF APPROACH

At constant amplitude, the rate of propagation of fatigue cracks correlates well with the cyclic range of stress intensity.[1] However, there is strong evidence[2] that crack growth during fatigue results directly from the reversal of plastic flow near the crack tip. This apparent anomaly may not be significant in fatigue at constant amplitude, where the relationship between local stress and local strain is probably fixed. However, at variable amplitudes, the local stress strain relationship varies with load history.[3] The first stage of the present study was, therefore, to determine whether local stress or local strain controlled the propagation of fatigue cracks.

The next stage of the study was to develop increased understanding of the relationship (hysteresis loop) between crack-opening displacement (COD) and applied load during fatigue. It is apparent that, as load is first applied to a cracked specimen, the crack begins to open by elastic distortion of the surrounding material. In deformable materials, yielding then begins near the crack tip. On further increases in load, the crack opens further by increasing plastic flow in the growing plastic zone near the crack-tip and further elastic distortion of the surrounding unyielding material. As the load decreases (beyond peak load in the fatigue cycle), relaxation of the elastic distortion is resisted by the stretched material in the plastic zone (Fig. 1) and, when unloading is complete, the crack-tip region remains under compressive residual stress.

The role of the residual stress in opposing crack-opening on subsequent load applications warrants consideration, since it provides a means by which the crack can 'remember' its previous load history during variable-amplitude fatigue. The degree to which the residual stress is relaxed during unloading depends upon a balance between the elastic constraint and the stress required for reverse plastic flow of the stretched material. In particular, the degree of relaxation depends on:

(i) the relative proportions of elastic and plastic material in the specimen;
(ii) the geometrical configurations of the elastic and plastic material; and
(iii) the resistance of the deformed material to reverse plastic flow.

It follows from the above that a physical model of the load/COD relationship could be based on a summation of two component relationships, viz.

(i) an elastic component, dependent on the stiffness of the unyielded material, and
(ii) a plastic component, based on the stress/strain characteristics of the (uncracked) material.

The proposed model is illustrated schematically in Figure 2. Here, it is assumed that the elastic load/deflection relationship is linear and that the yielded zone does not increase significantly in size with increasing load. Both assumptions are only likely to be reasonable at small crack-openings. Experimental study of how well this model is followed in practice forms the second stage of the present investigation.

3. EXPERIMENTAL DETAILS

3.1 Specimens

Centre-notched fatigue specimens (Fig. 3) were machined from extruded bars of electrolytic tough-pitch copper. The short gauge length was of double concave section, in order to keep the plane of fracture normal to the load axis and to minimise crack-opening by hinging at the crack-tip. Thus, crack-openings measured in the central hole were reasonably representative of values near the crack-tip. Uncracked specimens of the same geometry, but without the crack-starting notches (Fig. 3) were used to determine the cyclic load/elongation characteristics of the copper. Identical central holes were used in both types of specimen to mount a clip-on strain-gauge extensometer.

After machining, the gauge lengths were electropolished with 'Opalu B' using the 'Ellopol System'. The specimens were then annealed *in vacuo* for three hours at 500°C and slowly cooled.

3.2 Test Procedures

Most tests were conducted in a servo-hydraulic machine at constant frequencies between 0·1 and 1 Hz using a sinusoidal waveform. Comparable results were obtained in some tests using an Instron screw-driven machine. Rates of crack propagation were determined from fatigue tests conducted by cycling between zero and given values of either COD or tensile load. In the former case, compressive loads closed the crack completely at the end of each cycle; due to 'stretching' of the material ahead of the crack-tip before fracture, occasional small adjustments of the COD zero were necessary to prevent excessive compressive loads being applied after meeting of the crack faces.

Tests at 'constant COD' showed fairly constant rates of crack growth throughout, apart from the very early and the late stages of propagation; this behaviour indicates a fairly constant amplitude of stress intensity. Tests at 'constant load' showed progressively increasing rates of crack growth corresponding to an increasing amplitude of stress intensity as the crack length increased and the area of uncracked section decreased. Rates of crack propagation were determined from measurements of crack length, made on the side surfaces of the specimens using a travelling microscope. Load/COD relationships were plotted autographically on an X-Y recorder. All tests were conducted in an air-conditioned laboratory. Specimens for tests at constant load amplitude were pre-cracked at constant strain amplitude.

4. EXPERIMENTAL OBSERVATIONS

4.1 Determination of the Parameter Controlling Crack Growth

Tests were conducted to determine whether local stress or local strain near the crack tip controls the growth of fatigue cracks. The effects of simple variations in amplitude were obtained by contrasting the rates of crack growth, under various test conditions, in cyclic tests at constant load amplitude and constant COD amplitude (Section 3.2). The effect of stress intensity on crack growth was assessed from the relationships between applied load and rate of crack growth at a given crack length; stress intensity is directly proportional to applied load at constant crack

length. The 'local cyclic strain' was taken as the plastic contribution to crack-opening and was given by the width ($\Delta\epsilon_p$, Fig. 2) of the load/COD hysteresis loop.

Plots of the rate of crack growth against

(*a*) the peak applied stress, and

(*b*) the plastic contribution to crack-opening

are given in Figure 4 and Figure 5. Figure 4 shows separate relationships between rate of crack growth and stress amplitude for each of the conditions used; each relationship is reasonably linear. Figure 5 shows a singular relationship between rate of crack growth and plastic contribution to crack-opening over the entire range of test conditions, which include variations of the following:

(i) Load history; by contrasting fatigue tests at 'constant load' and at 'constant COD' (Section 3.2).

(ii) Plastic constraint at the crack-tip; by varying the radius of curvature of the double concave profile of the gauge length from the usual 6 mm radius to 4·75 mm radius and 3·2 mm radius. This 'shortening' of the gauge length reduced the amount of plastic strain at the crack tip for a given load.

(iii) Metallurgical condition; by contrasting the behaviour of annealed and extruded copper.

On the basis of the above observations, it is concluded that the local plastic strain amplitude at the crack tip, the plastic contribution to crack-opening, determines the rate of growth of fatigue cracks in copper.

4.2 Analysis of Load/COD Hysteresis Loops

These tests were undertaken to develop a basis for predicting the plastic contribution to crack-opening during fatigue at variable load amplitude. The observations above suggest that this plastic contribution could be used to predict rates of crack growth, if its own behaviour could be predicted; it is not itself suitable as an engineering parameter. The present tests were based on the simple model described in Section 2 (Figure 2), relating the load/COD and load/elongation characteristics of cracked and uncracked specimens respectively. It is implicit in the model that the patterns and distributions of flow should be similar in the two cases. In the present work this objective was facilitated by

(i) using short gauge lengths of the same double-concave profile in both cases, and

(ii) by choosing this profile such that hinging at the crack tip during crack-opening was severely curtailed (Section 3.1).

However, the different amounts of material deforming still require consideration; in the cracked specimens, deformation is confined to small zones near the crack tips, while uncracked specimens deform over their whole cross-sections. Allowance was made for the different amounts of plastic material by load/scaling the load/elongation hysteresis loop for uncracked specimens, such that it intersected the load/COD loop for cracked specimens at the half-amplitude (of displacement) positions; in these tests, specimens were cycled between the same constant displacement limits.

The above procedure of load-scaling was based on the observation that, during tests at constant ranges of COD or elongation, the peak tensile and compressive loads usually became approximately equal after the initial cycles. This symmetry probably resulted because the initially soft annealed copper hardened during the initial cyclic deformation, such that its 'equilibrium' position was at the mean displacement. Accordingly, the elastic constraint opposing crack-opening would be relatively low at the half-amplitude position. The disparity of load-widths of the hysteresis loop at this position would then reflect the difference in the amounts of material deforming.

The results of tests using the above procedures were most encouraging and are detailed below.

4.2.1 Tests at Constant Amplitudes of Displacement

Comparison of the load/displacement hysteresis loops for cracked and uncracked specimens, using the procedures described above, shows that the 'difference' between loops obtained at low amplitude corresponds to a linear load/displacement relationship (Figure 6). Such linear relationships are consistent with an elastic component in the hysteresis loop relationship for cracked specimens, as proposed in our simple model (Figure 2). However, the difficulty of measuring plastic zone sizes precluded quantitative comparison of the slopes of these 'elastic' relationships with calculated stiffnesses of the unyielded portions of the specimens.

The rapid decrease in slope of the 'difference' relationship with increasing amplitude of

displacement and its departures from linearity and singularity at high amplitudes (Figure 6) are also qualitatively in accordance with the model. Here, the larger plastic zones produced at higher amplitudes considerably reduce the amount, and hence the stiffness, of the unyielded material in the cross-section. Thus, the elastic constraint opposing crack-opening reduces in stiffness with increasing COD in small specimens; this effect should not be as marked in larger specimens at these CODs. At high amplitudes, the progressive increase in size of the plastic zone, with increasing COD, during each load cycle should give a progressive decrease in the stiffness of the elastic constraint in small specimens. This progressive decrease in stiffness is consistent with the observed non-linearity of the difference relationship at high amplitudes. The loss of singularity at high amplitudes is attributed to differences in the COD/plastic-zone-size relationships during opening and closing of the crack.

4.2.2 Tests Involving Step-Changes in Displacement Amplitude

These tests were undertaken to determine whether or not the model could be used to interpret changes in the load/COD hysteresis loop after step-changes between two levels of (otherwise) constant COD. The same procedure, comparing the load/displacement relationships of cracked and uncracked specimens subjected to the same sequence of displacement amplitudes, was used.

Following downward step-changes in COD, the plastic contribution to crack-opening was less than the 'stable' value characteristic of a constant-amplitude test at the lower COD (Fig. 7). However, the plastic contribution increased rapidly to the stable value over a few cycles at the new amplitude. Measurements of crack growth, on the side surfaces of the specimens, were not sensitive enough to detect any transient changes in rate of crack growth during these few cycles. However, the excellent correlation between the plastic contribution and rate of crack growth (Figure 5) suggests that a transient retardation of crack growth probably does follow downward step-changes in amplitude. Such retardation is commonly observed in most materials.[4]

Following upward step-changes in COD, a transient increase in the plastic contribution to crack-opening is observed (Fig. 7); after a few cycles, the plastic contribution decreases to the stable value. The transient increase in the plastic contribution suggests that a transient acceleration of crack growth follows upward changes in amplitude.

Transient changes in the plastic contribution to crack growth (indicative of transient retardation and acceleration of crack growth), following step-changes in amplitude are of fundamental significance to the present study and the hysteresis loops for cracked and uncracked specimens were compared after step-changes in amplitude. After downward step-changes, the difference relationships were again approximately linear; the 'stiffness' decreased rapidly over the first few cycles after the step-change and then more slowly over about the next 100 cycles (Table 1). The significance of this behaviour is that the plastic contribution to crack-opening after the step-change is reduced, below that typical of continuous cycling at the new COD, because the material at the crack-tip has been fatigue-hardened to a greater extent by cycling at a higher amplitude (before the step-change). Hence, a small plastic zone, highly constrained by the surrounding hardened material, results during the first cycles after the step-change. However, with continued cycling, the small plastic strain produces cyclic-softening[5,6] of the hardened material so that the constraint decreases, the plastic zone increases in size and the 'memory' of cycling at the higher amplitude is lost.

The behaviour after an upward step-change is more difficult to follow than that described above because the modelling procedure is inadequate at high amplitudes, as explained earlier. Despite the non-linearity of the difference relationship, however, an obvious trend for its 'stiffness' to increase rapidly during the first few cycles can be discerned (Figure 8). Here, a specimen cycled at a low amplitude has a low level of hardening near the crack-tip, relative to one cycled continuously at a higher amplitude. Thus, after an upward step-change, an anomalously high plastic contribution to the COD will result until fatigue-hardening has reached its stable state ahead of the crack tip.

4.2.3 Tests at Variable Amplitudes of Displacement

In these tests, the amplitude of displacement varied from cycle to cycle and the hystreesis loops of cracked and uncracked specimens were again compared. The difference relationships were reasonably linear for each cycle at low amplitude but the model was again inapplicable for cycles of high amplitude (Figure 9).

Large amplitude changes commonly produced hysteresis loops which were not completely closed. The reason appears to be that the microstructural changes during each cycle are sufficient to ensure detectable changes in the pattern of residual stress around the crack tip.

5. DISCUSSION

The observations described here show that the plastic contribution to crack-opening controls the incremental growth of fatigue cracks. Evidence presented here also suggests that the model proposed for the load/COD relationships of cracked specimens could provide a basis for predicting the plastic contribution to the COD for various load histories. A most significant aspect of the model is that the plastic characteristics of the material in the plastic zone near the crack-tip can be evaluated independently of the degree of elastic constraint (subject to certain experimental requirements being met). This aspect appears particularly relevant to the important practical requirement (Section 1) of using the fatigue characteristics of small laboratory specimens to predict those of structural components.

Consideration of the problem above (in terms of the present model) indicates that, provided the crack-front and its plastic zone are entirely reproduced within the small specimen, the 'extra' material in the component will all be elastic and, thus, can only increase the elastic constraint on the plastic zone. Thus, it would seem to be feasible to predict the load/COD relationship of the component by summation of that determined for the small specimen and the stiffness relationship for the 'extra' material in the component. The plastic contributions to crack-opening, and hence the incremental growth of the crack, could then be determined for the component. An alternative means of accomplishing this end could be to use the capabilities of modern servo-hydraulic machines to add the elastic constraint of the 'extra' material to the load spectrum being used to test the small specimen.

The model also appears to provide the means to predict rates of crack-growth in different materials from a knowledge of their characteristics for reversed plastic flow. However, present studies have not progressed sufficiently to indicate how widely the model is applicable. The major limitation encountered in the present work was the failure of the model at large amplitudes. However, the limiting amplitude was relatively large, from the viewpoint of structural materials; the limited toughness of such materials usually results in unstable crack propagation at such CODs. Presently, the experimental difficulties of determining load/COD relationships accurately at very low amplitudes of COD have prevented direct assessment of the model on real materials at amplitudes typical of service conditions.

6. CONCLUSIONS

Tests on copper have shown that the plastic contribution to crack-opening controls the incremental growth of fatigue cracks. The behaviour of this plastic contribution during tests at variable amplitude cannot readily be predicted and would be difficult to monitor in service. A series of tests, under a variety of amplitude-sequences, has shown that the load/COD relationship for cycles of low amplitudes can be modelled from the characteristics of the material under reversed plastic flow and the stiffness of the unyielded material surrounding the crack. The additive nature of the model opens up the possibility of

(i) relating the fatigue characteristics of small laboratory specimens and structural components, and

(ii) relating the growth of fatigue cracks in different materials.

The approach proposed herein contrasts with the traditional mathematical approach to crack propagation. Traditionally, the plastic characteristics of the material are idealized to facilitate elastic/plastic analyses of the stress distribution, etc., around crack tips. However, the present study indicates that the 'width' of the load/COD hysteresis loop determines the increment of crack growth, at least in copper. This width depends primarily on the reversed plasticity characteristics of the material and, to a much lesser extent, on the elastic constraint from the unyielded material. Thus, it can be claimed that, when considering fatigue at variable amplitude, the reversed plastic characteristics should be incorporated precisely in any treatment, even if the elastic constraint then has to be idealized. Presently, the reversed plasticity characteristics under complex loading sequences can only be obtained empirically. Hence, experimental modelling of crack propagation (as proposed herein) may be preferable to the traditional elastic/plastic analyses when considering crack growth during fatigue at variable amplitude.

REFERENCES

1. Richards, C. E. and Lindley, I. C.	The Influence of Stress Intensity and Microstructure on Fatigue Crack Propagation in Ferritic Materials. Engineering Fracture Mechanics, Vol. 4, pp. 951-78, 1972.
2. Laird, C. and Smith, G. C.	Crack Propagation in High Stress Fatigue. Philosophical Magazine, Vol. 7, pp. 847-57, 1962.
3. Elber, W.	The Significance of Fatigue Crack Closure. American Society for Testing and Materials STP 486, pp. 230-42, 1971.
4. Ryan, N. E.	The Influence of Stress Intensity History on Fatigue Crack Growth. Aeronautical Research Laboratories, Metallurgy Report 92, 1973.
5. Feltner, C. E. and Laird, C.	Cyclic Stress-Strain Response of FCC Metals and Alloys. Acta Metallurgica, Vol. 15, pp. 1621-53, 1967.
6. Czoboly, E. and Sandor, B. I.	Cycle Dependent Softening in Notched Steel Specimens. Journal of Testing and Evaluation, Vol. 3, pp. 343-47, 1975.

TABLE 1

Relative Cyclic History	Saturation at 76 μm COD	Cycles following a step change to 25 μm COD						Saturation at 25 μm COD
		1	2	6	10	30	150	
Relative Elastic stiffness (Pa/μm)	$14{\cdot}0 \times 10^6$	$5{\cdot}3 \times 10^8$	$4{\cdot}4 \times 10^8$	$4{\cdot}2 \times 10^8$	$3{\cdot}9 \times 10^8$	$3{\cdot}2 \times 10^8$	$2{\cdot}8 \times 10^8$	$2{\cdot}6 \times 10^8$

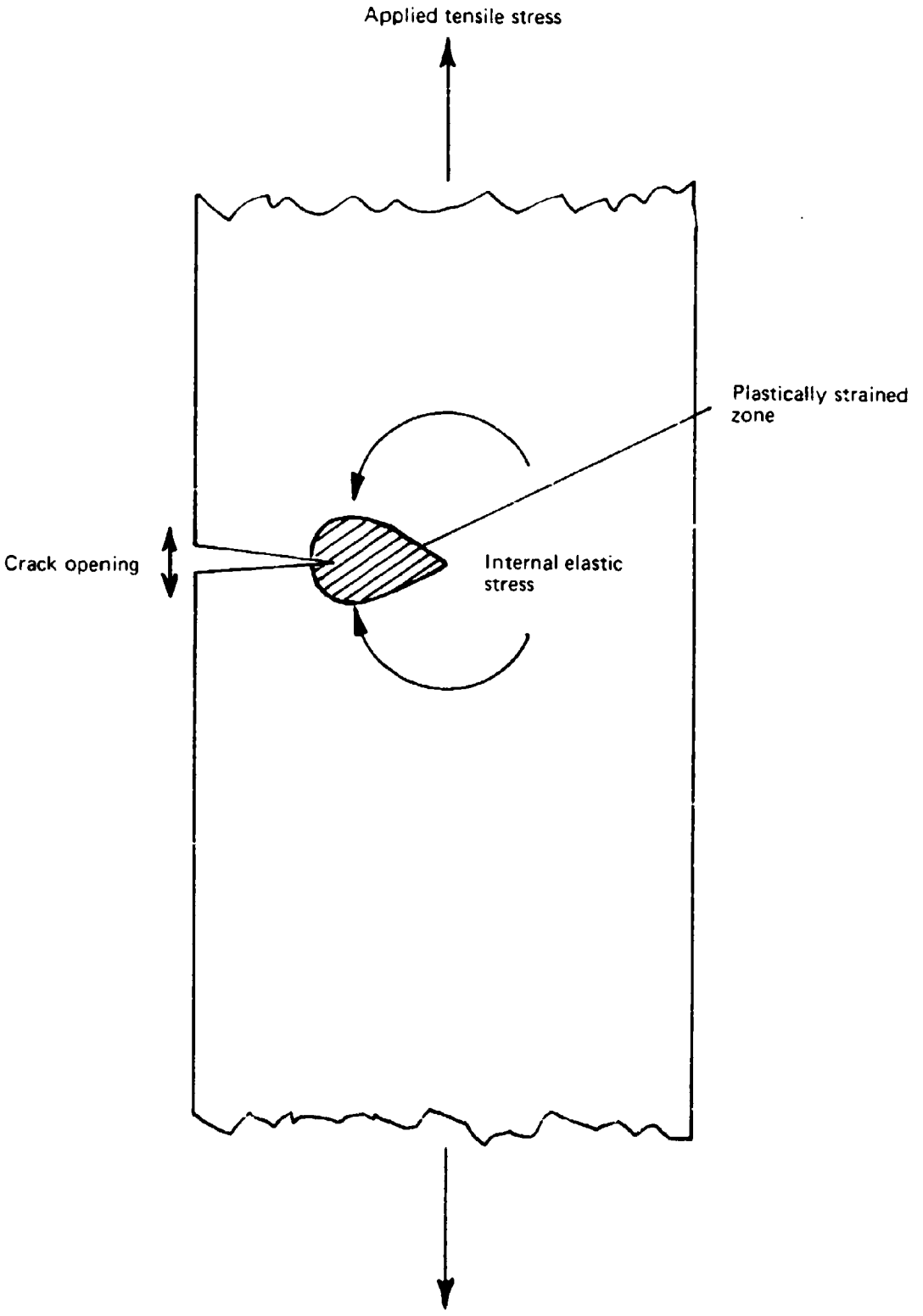

FIG. 1. SCHEMATIC REPRESENTATION OF A CRACK TIP PLASTIC ZONE AND THE SURROUNDING ELASTICALLY DEFORMED MATERIAL.

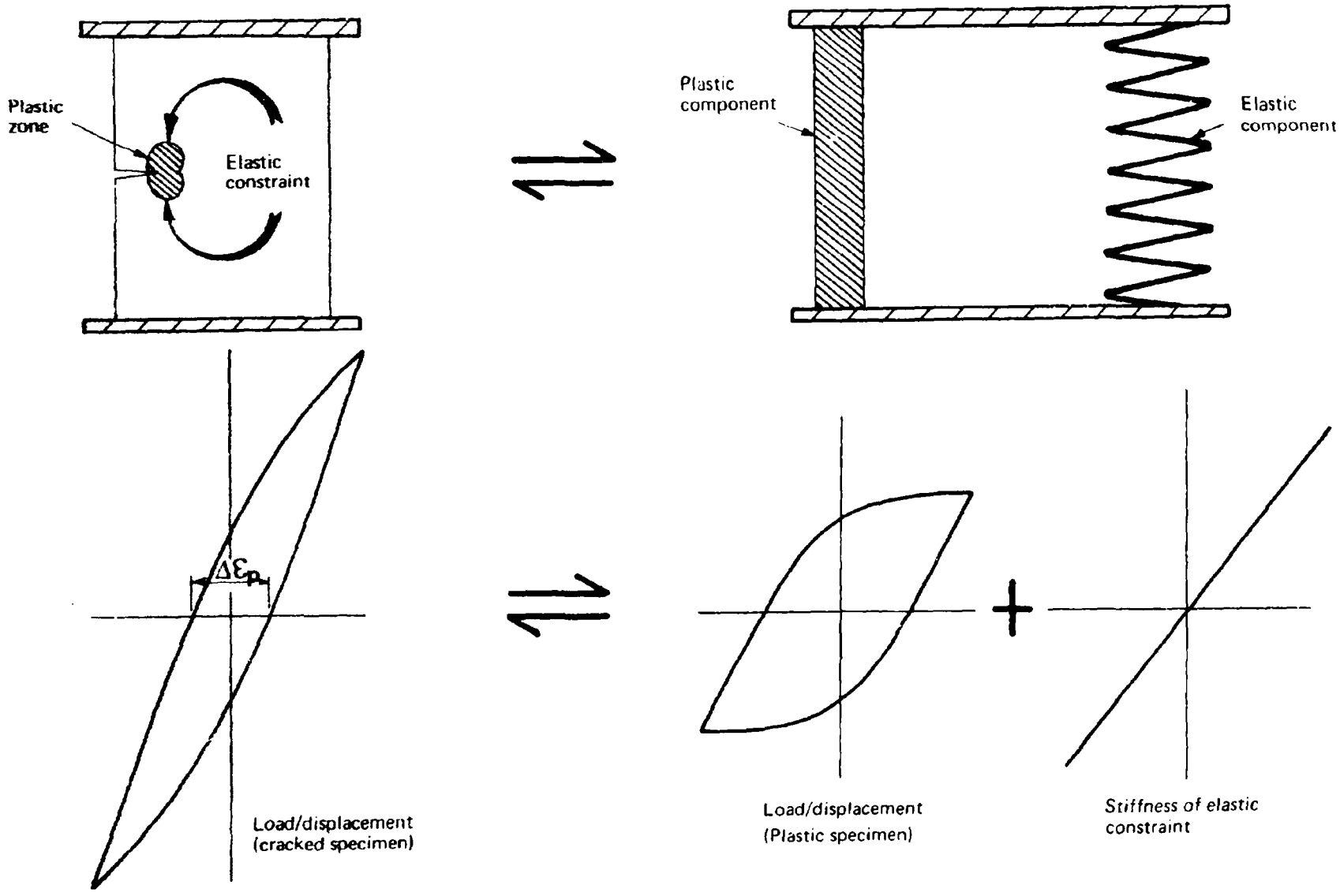

FIG. 2. A MODEL OF CRACK–TIP BEHAVIOUR USING A FULLY PLASTIC SPECIMEN AND AN APPLIED ELASTIC CONSTRAINT

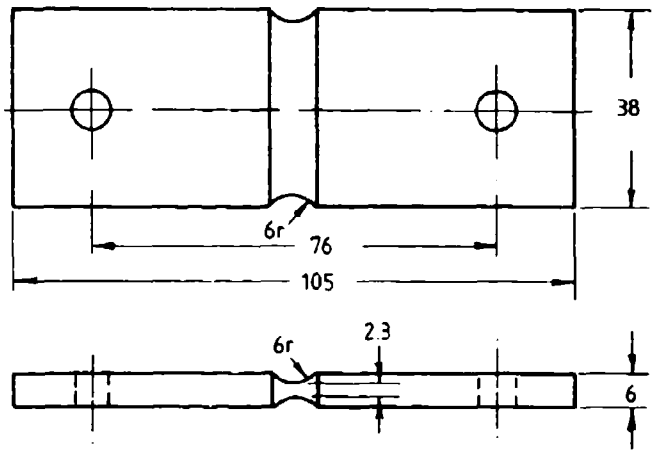

(a)

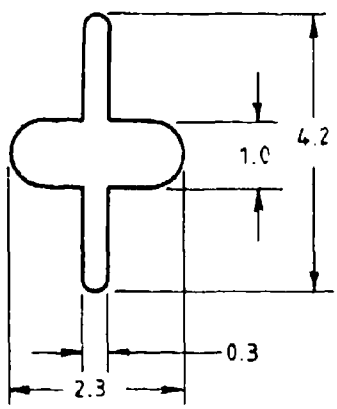

(b)

FIG. 3. SPECIMEN DESIGN USED IN THE CRACK–PROPAGATION STUDIES
(Dimensions in millimetres)

(a) Test specimen geometry

(b) Dimensions of the spark-machined centre notch

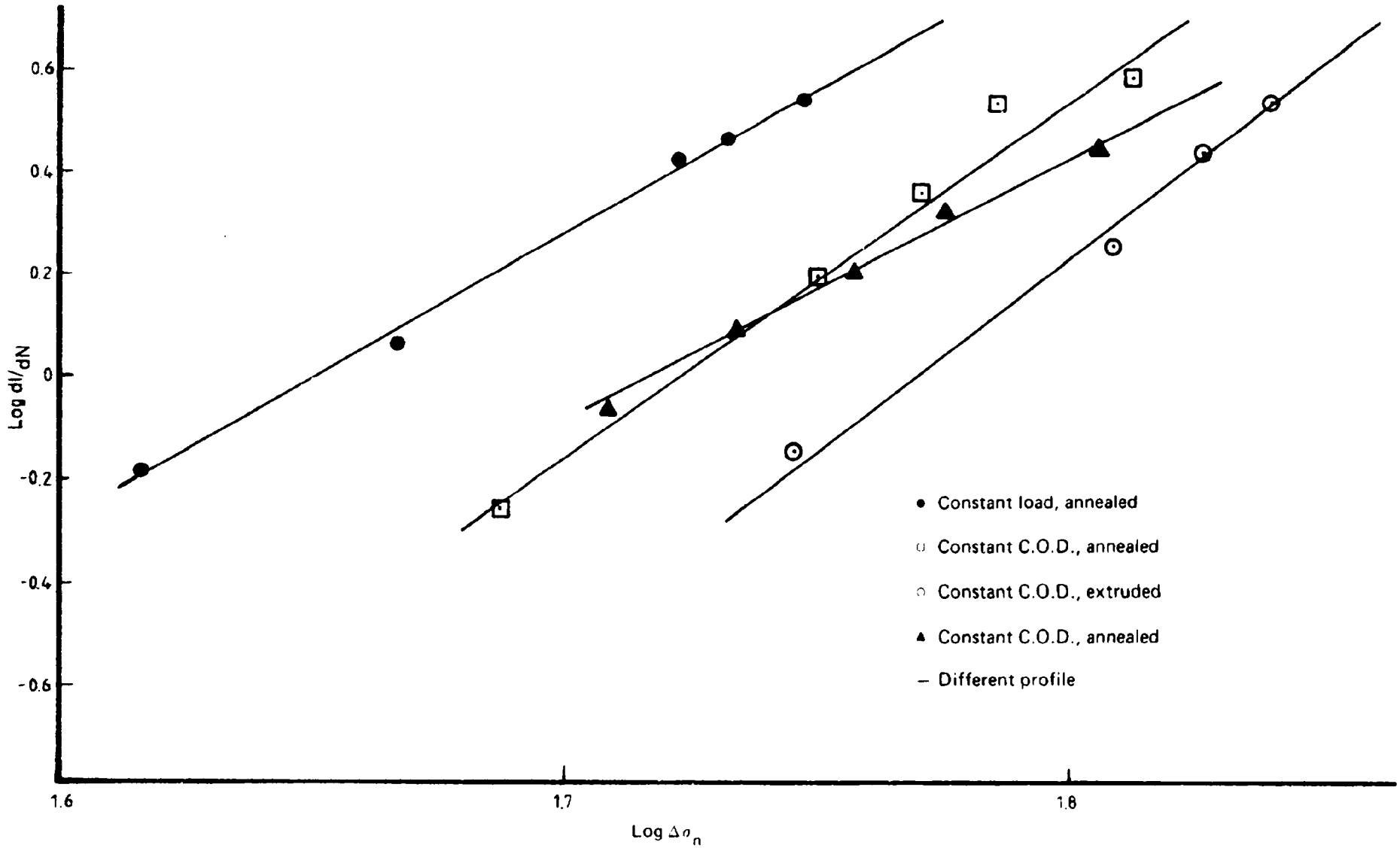

FIG. 4 RATE OF CRACK GROWTH AS A FUNCTION OF APPLIED CYCLIC STRESS

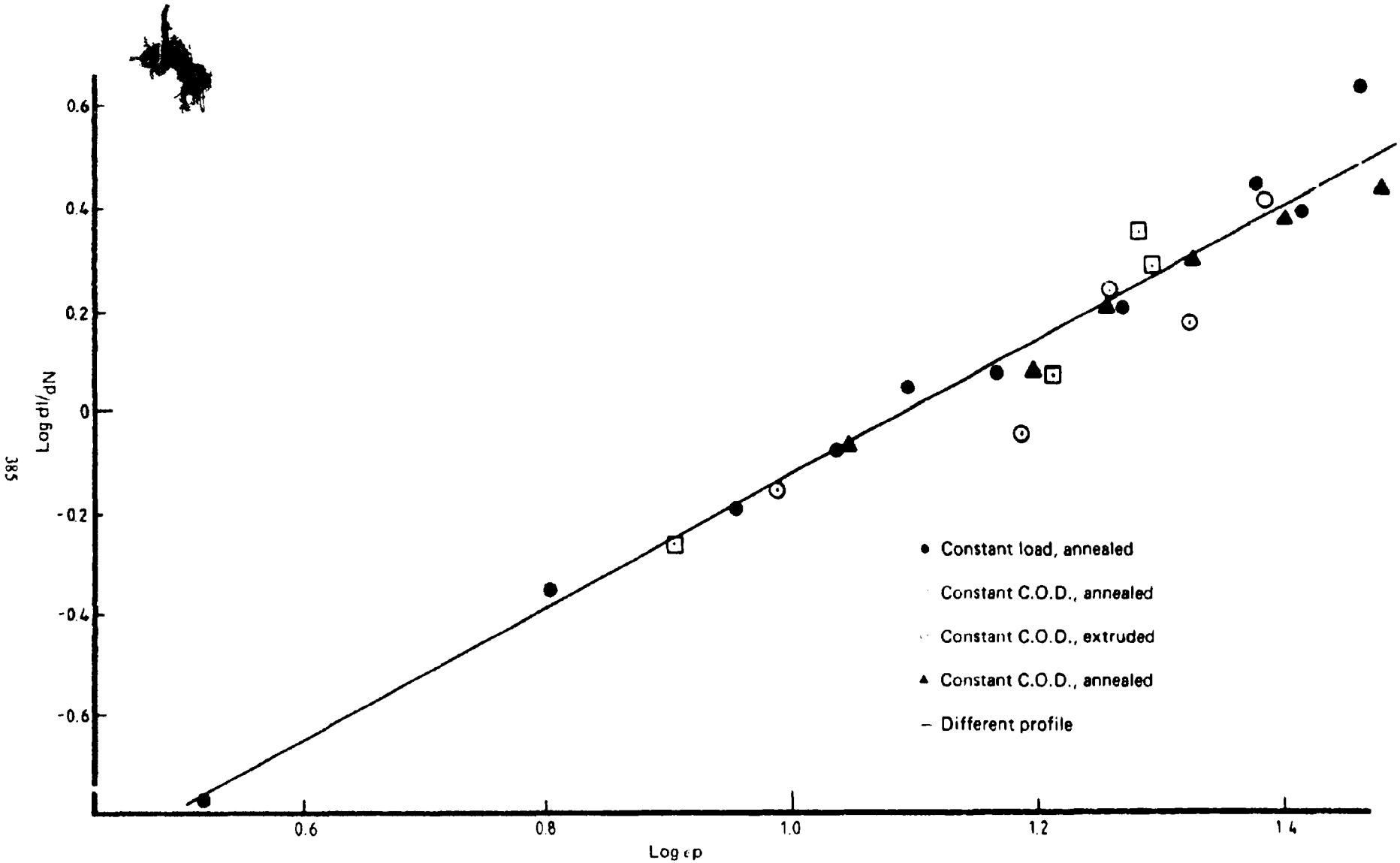

FIG. 5 RATE OF CRACK GROWTH AS A FUNCTION OF PLASTIC COMPONENT OF THE CRACK-OPENING-DISPLACEMENT

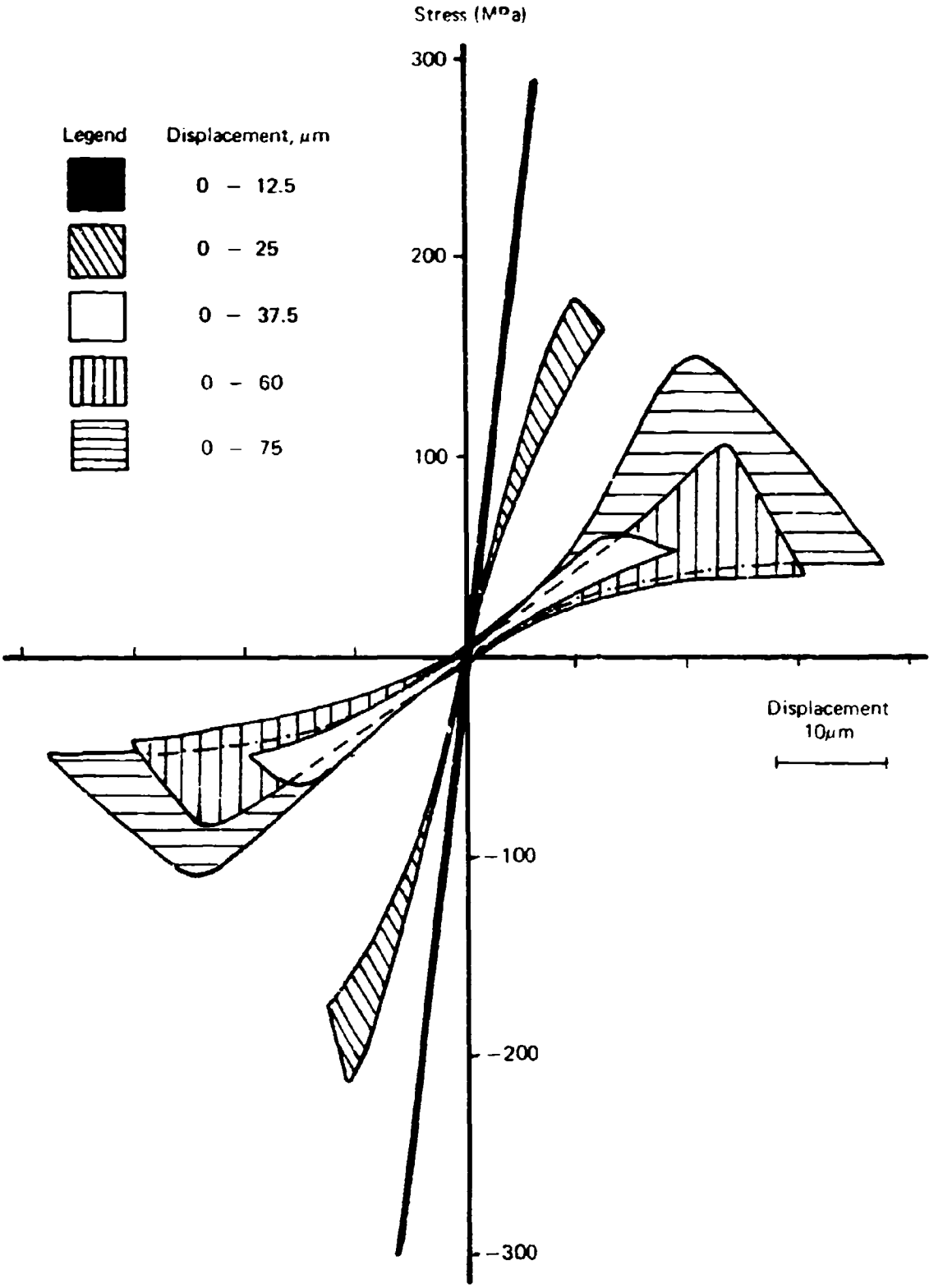

FIG. 6. DIFFERENCE RELATIONSHIP FOR CRACKED AND UNCRACKED SPECIMENS TESTED TO SATURATION AT VARIOUS DISPLACEMENT AMPLITUDES

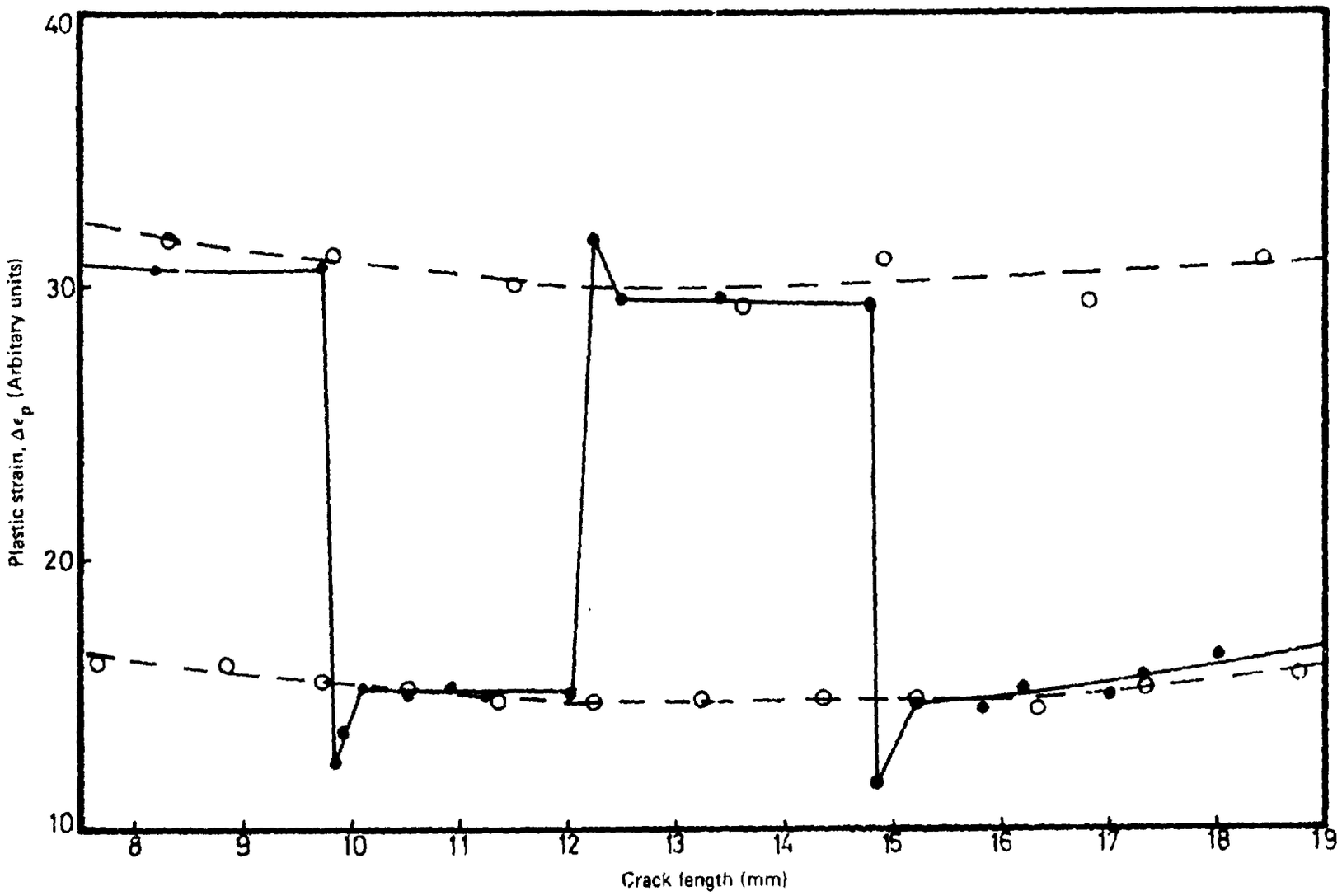

FIG. 7. THE EFFECT ON THE PLASTIC STRAIN COMPONENT OF C.O.D. OF STEPPED AMPLITUDE CHANGES FROM A C.O.D. OF 25μm TO A C.O.D. OF 76μm

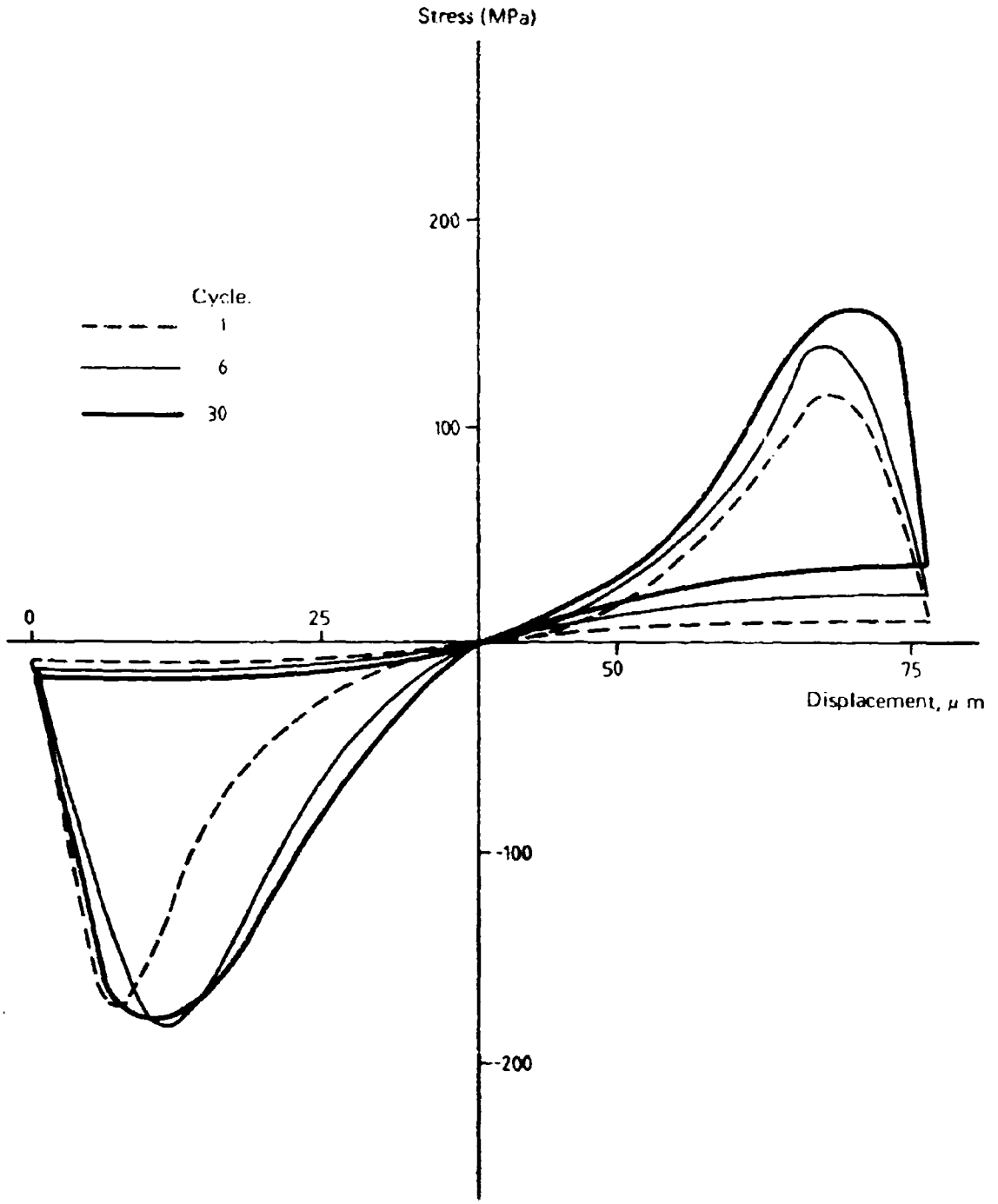

FIG. 8. DIFFERENCE RELATIONSHIPS BETWEEN THE STRESS–STRAIN CURVES OF CRACKED AND UNCRACKED SPECIMENS FOLLOWING A STEPPED INCREASE IN AMPLITUDE FROM 25μm TO 76μm

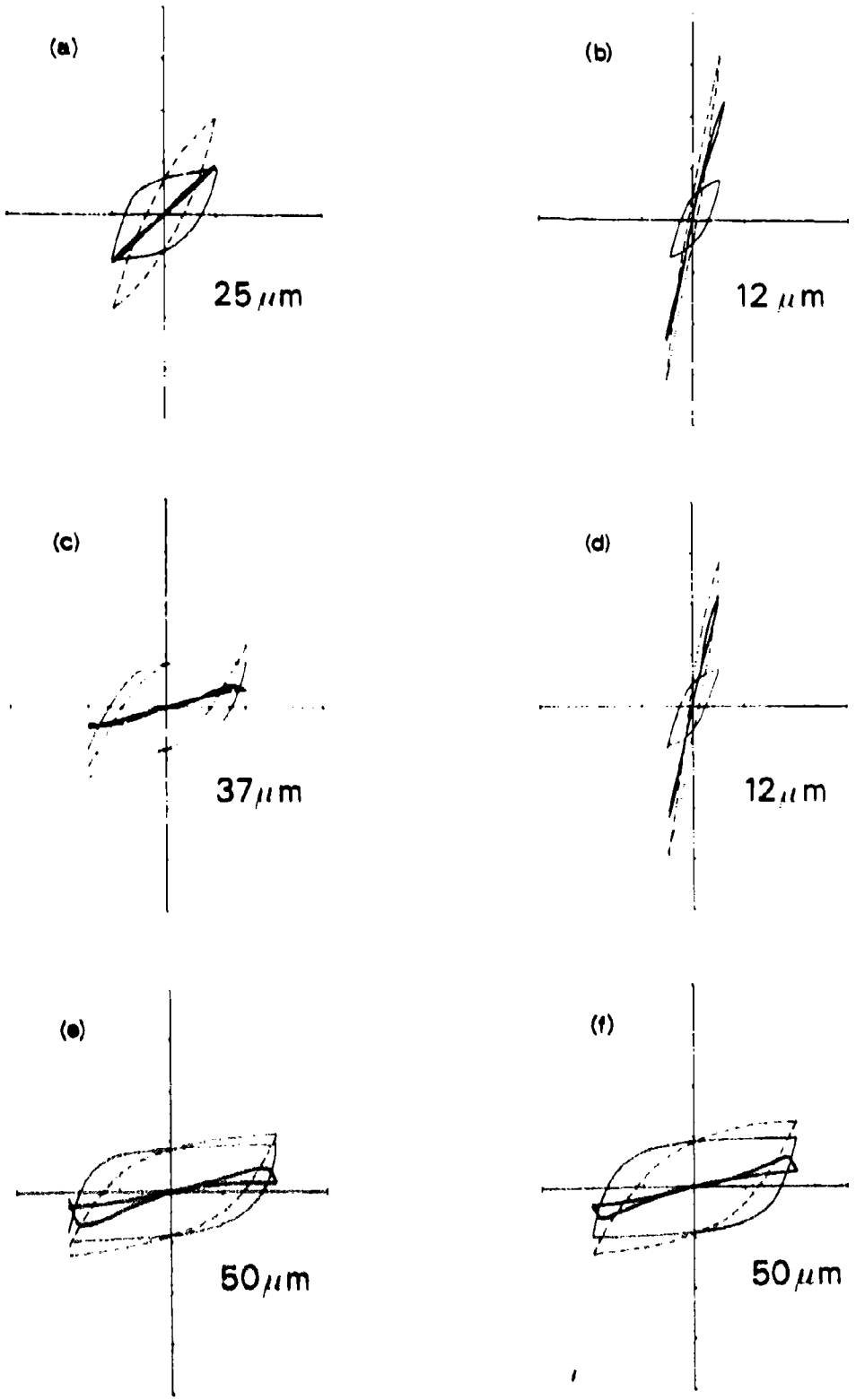

FIG. 9. DIFFERENCE RELATIONSHIPS BETWEEN THE STRESS–STRAIN CURVES OF CRACKED AND UNCRACKED SPECIMENS FOLLOWING A SERIES OF CONSECUTIVE CYCLES AT THE DISPLACEMENT AMPLITUDES SHOWN

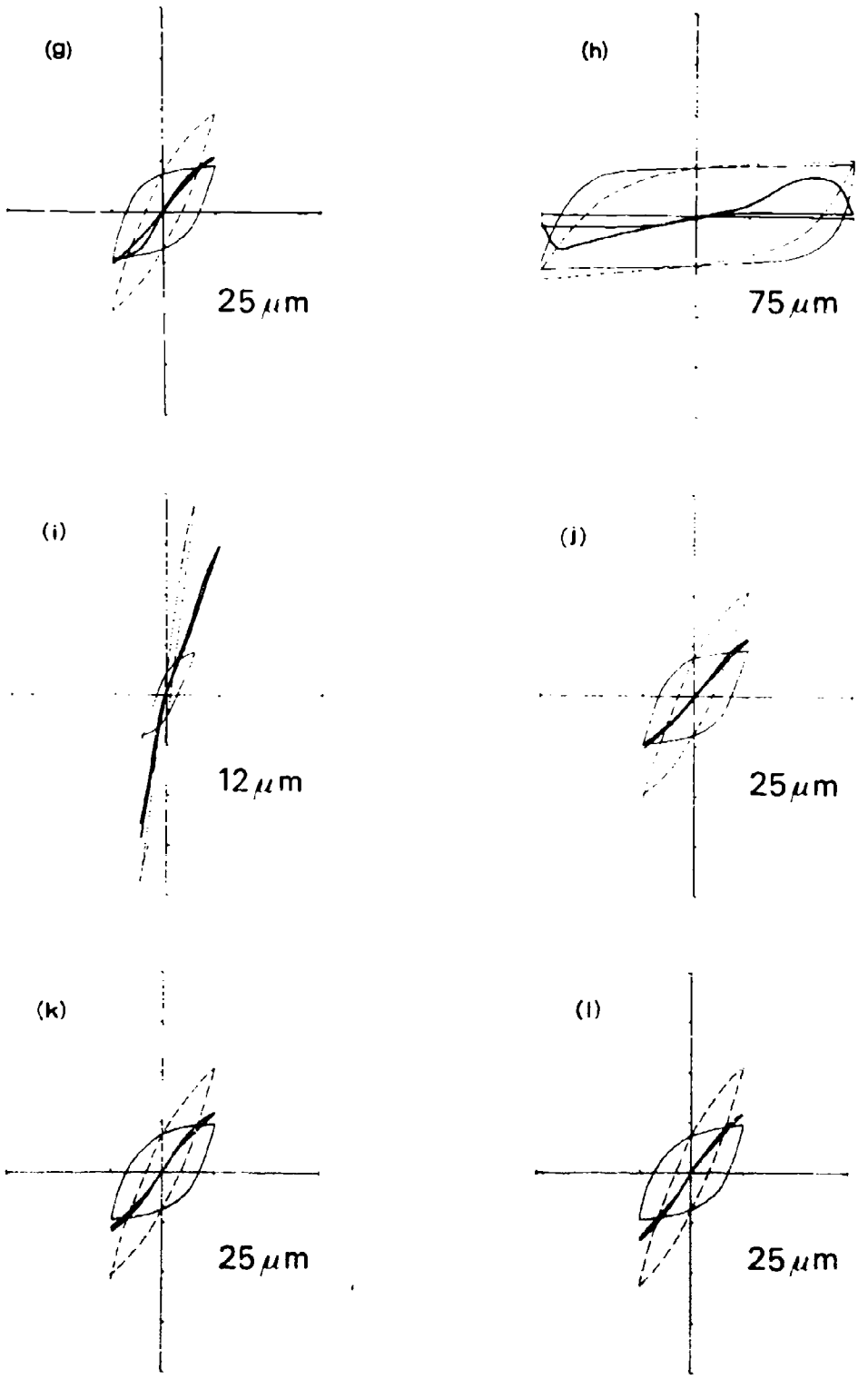

Fig. 9 Continued.

DISCUSSION

QUESTION – *P. J. Howard*
(ARL)

Has any consideration been given to simplifying the experimental model, e.g. by observing the variation with number of cycles of plastic strain range in a plain test piece cycled between fixed length limits?

AUTHORS' REPLY

Tests of this type, but using the specimen described in the paper, were performed to establish the relationship between crack growth rate and the plastic component of strain. The reasons for adopting the double concave specimen are given in Section 3.1.

Validation of the elastic-plastic model requires the comparison of data from cracked and uncracked specimens. The data from uncracked specimens provides the plasticity characteristics of the material undergoing reversed plastic deformation.

QUESTION – *J. C. Ritter*
(MRL)

It is reported in Section 4.1 that the radius of curvature of the double concave profile specimen gave a variation of plastic constraint at the crack tip. An increase in constraint means that the central region, i.e. interior of the specimen, will experience conditions closer to plane strain while the surface regions remain in plane stress. Besides reducing the amount of plastic strain at the crack tip, this shift toward plane strain might be expected to affect the processes of fatigue crack growth, leading to a deviation from the $\log(dl/dN)$ versus $\log(\epsilon_p)$ shown in Figure 5.

Have the authors found any evidence for such an effect?

AUTHORS' REPLY

Data from specimens with both the profiles seem to fit the same $\log(dl/dN)$ versus $\log(\epsilon_p)$ relationship. Thus, any effect could only be slight.

There is evidence, however, that the crack front is not straight (being more advanced at the centre), probably as a result of the variation from plane stress towards plane strain mentioned by Dr Ritter. We do not have any detailed comparison between the shapes of crack fronts in the two types of specimen. However, there appears to be no discontinuity in behaviour with increasing amplitude of plastic strain. Thus, to a first order, the predominance of plane stress or plane strain does not appear particularly significant in the types of test undertaken.

FATIGUE-CRACK GROWTH AND FRACTURE IN D6AC STEEL

by

N. E. RYAN

SUMMARY

Work at ARL on fatigue-crack growth and fracture in D6AC steel having differing tensile properties and fracture toughness values is reviewed. No simple correlation exists between tensile strength and toughness and, basically, fatigue crack-growth rates were independent of both these properties. The observations are interpreted in terms of the effects of variations of microstructure on deformation and fracture mechanisms. Some work using variable-amplitude loading showed transient effects after load changes.

Environmental factors were also studied and it was concluded that simple additivity of fatigue and stress-corrosion could not be used to account for crack-growth rates under corrosive environments. Various laws, developed from fracture mechanics concepts to express crack-growth rates on a function of stress-intensity amplitudes, are discussed.

1. INTRODUCTION

The design of high performance aircraft has led to an increasing need for materials with high specific strength, to minimize weight, and high elastic modulus, to provide the structural stiffness set by aeroelastic considerations. These requirements have led to an increased use of high strength steel in aircraft construction. With the development of high strength steels, the problem of their limited tolerance to cracks, i.e. their toughness, has arisen.

Fracture mechanics, based on linear elastic theory, has provided a quantitative measure of the toughness of materials through the concept of the stress intensity factor, K, which defines the state of stress at the tip of a crack in terms of the applied stress, σ, the crack length or depth, a, and the geometry of the structure: thus

$$K = M\sigma a^{\frac{1}{2}} \tag{1}$$

where M is a stress-distribution function involving the geometry of the structure and crack shape. The critical stress intensity (denoted by K_{1c} for tensile loading) at which unstable crack extension or fracture occurs under plane strain conditions is defined as the fracture toughness of a material.

The fracture toughness, K_{1c}, is a basic material property, substitution in Equation (1), the relation

$$a_{crit} = M(K_{1c}/\sigma)^2 \tag{2}$$

is obtained, which gives the critical crack size, a_{crit}, at which unstable crack extension will occur at a given load.

Crack extension can occur at stress intensities below K_{1c} (sub-critical crack growth) particularly under the cyclic loading experienced by aircraft, i.e. the process of fatigue. The stress intensity has been identified as the driving force for crack extension and the problem has been to define the rate of fatigue-crack growth as a function of the alternating stress intensity, $\Delta K = (K_{max} - K_{min})$ and to determine how the rate is influenced by material properties.

Fracture mechanics considers the crack tip as a singularity in an otherwise homogeneous continuum; however, in metals there is a zone of plasticity ahead of a loaded crack, illustrated in Figure 1. Provided that a condition of plane strain exists at the crack tip, the parameter K still adequately defines the state of stress. However, the nature and behaviour of this plastic zone determines the cracking behaviour and these characteristics are strongly influenced by microstructure.

D6AC steel can be heat-treated to give different microstructures with differing yield strengths and levels of fracture toughness. This paper presents ARL work on D6AC steel with particular consideration of:

(i) the relationship between microstructure, fracture mechanisms and fracture toughness;
(ii) the rate of fatigue-crack growth and various growth laws developed;
(iii) the influence of variable amplitude loading in fatigue-crack growth; and
(iv) the influence of environmental factors on fatigue-crack growth.

The composition of the D6AC, the heat-treatment schedules and the corresponding mechanical properties, are shown in Tables 1, 2 and 3, respectively.

2. MICROSTRUCTURE, TENSILE PROPERTIES AND FRACTURE TOUGHNESS RELATIONSHIPS IN D6AC STEEL

As the determination of fracture toughness, K_{1c}, requires a far more complex procedure than methods used for obtaining tensile properties, various attempts have been made[1,2,3] to relate fracture toughness with other, more easily determined, mechanical properties. These efforts have met with little success. The difficulties involved in such attempts have been demonstrated for D6AC steel, where different heat treatment procedures can lead to wide changes in fracture toughness without substantially changing the tensile properties.[4,5,6] In investigations at ARL, heat treatments A to D of Table 2 produce almost identical tensile properties but wide variations in fracture toughness (Table 3). Feddersson *et al.*[6] reported similar results;

their fracture toughness values in D6AC steel varied by a factor of 3 without any corresponding change in tensile strength properties.

Fractographic examination[4] shows that decreasing fracture toughness is associated with a progressive change in fracture mode, from micro-void coalescence at high toughness to predominantly quasi-cleavage with negligible shear lips, at low toughness values (Figs. 2 and 3). These decreasing values of fracture toughness, for the same tempering temperatures, correlate with decreasing quenching rates: high values of K_{1c} are obtained with oil-quenching and low values with air-cooling.

Microstructural changes, associated with differences in fracture toughness and in quenching rates, have been traced to the nature of the martensite formed during quenching. In oil-quenched material (heat treatment A, Table 2), which has the highest fracture toughness, a micro-twinned martensite is formed during the initial quenching. Subsequent tempering of this structure at 550 C introduces a fine, homogeneous distribution of carbide precipitate (Fig. 4).

Air-cooling from the intermediate quench, "Ausbay" at 520 C (heat treatment D, Table 2), produces a lath-type martensite with some evidence of bainitic carbide separation. Subsequent tempering of this structure at 550 C results in a heterogeneous distribution of carbide precipitate (Fig. 5) with an almost continuous distribution of carbide along the interfaces between the former martensite laths.

Quenching rates intermediate between air-cooling and oil-quenching (heat treatments B and C, Table 2), result in transitional microstructures, in which no large inter-lath carbide precipitates are present after tempering.

The wide variation in fracture toughness, independent of the tensile properties of the D6AC steel, has been attributed to the different responses of these microstructures to stress in the different testing procedures.[4]

In a tensile test, the tensile properties reflect the average response of the microstructure to increasing stress in a large volume of material. However, fracture toughness is determined by the response of the local microstructure in a minute volume of material - the plastic zone, to the complex stresses ahead of a loaded crack. Any difference in this response which leads to a change in the prevailing mechanism of fracture, e.g. from void formation and coalescence to particle-initiated cleavage, has a particularly significant effect on the fracture characteristics.

Thus, highly localized strain in a very small volume of material containing a heterogeneous distribution of particles favours low-energy cleavage fracture, and hence low K_{1c}, while uniform strain around a homogeneous distribution of fine carbide particles leads to high-energy ductile tearing by void-coalescence and, thus, to high K_{1c} values.

In D6AC steel, slow rates of quenching (e.g. air-cooling) promote a non-uniform distribution of carbide precipitates (Fig. 5) which favours cleavage fracture (Fig. 3) and leads to low K_{1c} values. Fast quenching rates (e.g. oil-quenching) promote a fine, homogeneous distribution of carbide precipitates (Fig. 4) leading to fracture by void formation and coalescence (Fig. 2) and high K_{1c} values.

3. FATIGUE-CRACK GROWTH AT CONSTANT AMPLITUDE LOADING

Early attempts to relate fatigue-crack growth to stress-intensity factors were made by Paris and co-workers,[5] who developed the relation

$$da/dN = C\,\Delta K^m \qquad (3)$$

where da/dN is crack growth per cycle, C, a materials constant, ΔK the range of stress intensity and m an exponent generally found to be about 4. However, it is now recognized that the relation between da/dN and ΔK is more complex, taking the sigmoidal form illustrated in Figure 6. In the centre, region II, $\log da/dN$ is proportional to $\log \Delta K$. In region I, as ΔK decreases, a threshold value (ΔK_{th}) is approached below which the rate of crack growth is negligible. In region III, at high values of ΔK, the growth rate accelerates at an increasing rate as K_{max} approaches K_{1c}.

Figure 7 shows the $da/dN - \Delta K$ data for D6AC steel with heat-treatments A, C, D and E (Table 2). The first three treatments produced similar yield stresses but different fracture toughnesses; the fourth gave a higher yield stress with an intermediate fracture toughness. The rates of cracking in the central linear section (region II) were the same for the four treatments. Below $\Delta K = 18\ \mathrm{MPa}\,m^{\frac{1}{2}}$ (region I), different values of ΔK_{th} were approached for the different heat-treatments. Positive deviations from the linear relation (region III) occurred at values of $K_{max} > 0{\cdot}7\,K_{1c}$.

Fractographic examination showed that the three regions of the $da/dN - \Delta K$ relationship could be identified with different fracture modes. In region I, a "specular or faceted" fracture surface predominated (Fig. 8), it has been suggested that the rate of crack-growth in this region is sensitive to microstructure.[8,9] In region II, between 18 MPa $m^{\frac{1}{2}}$ and $K_{max} < 0{\cdot}7\,K_{1c}$, crack growth occurred by the mechanism which gives rise to the familiar "striation" markings on the fracture surface (Fig. 9). In region III, the mode of cracking changed to either void coalescence or micro-cleavage (Figs. 10 and 11), depending on whether the fracture toughness was high or low, respectively. Similar fractographic observations have been made by Richards and Lindley,[10] Clark[11] and Ritchie and Knott.[12]

The mechanism giving rise to the striation markings is obviously unique to fatigue cycling and is apparently not closely dependent on bulk tensile properties and fracture toughness. While the precise details of fatigue crack extension by this mechanism are not fully understood, it is recognized that growth occurs by repeated cyclic strain at the crack tip. Theoretical considerations of Liu[13] and Lehr and Liu[14] indicate that the slope of the log da/dN - log ΔK relation in region II should equal 2. Richards and Lindley[10] found that, when growth occurred by the "striation" mechanism, the slope (for a large number of steels) varied between 2·5 and 2·9. In the present work with D6AC steel, a slope of 2·4 was obtained. The reason for values higher than the value of 2 predicted by Liu and Lehr is attributed to the occurrence of tensile fracture modes, even though the "striation" mechanism predominates.

The changes in fracture mode at low and high amplitudes of stress-intensity introduce difficulties in developing expressions to account for the relation between crack-growth rate and stress-intensity amplitude. Priddle[15] has shown that crack propagation at low values of ΔK is adequately described by introducing the threshold stress intensity amplitude, ΔK_{th}, in Equation (3), thus

$$da/dN = C^1 (\Delta K - \Delta K_{th})^m \tag{4}$$

Heald *et al.*[16] proposed the following modification of Equation (3) to describe crack growth at high ΔK values

$$da/dN = A\left\{\frac{\Delta K^4}{\sigma_y^2 K_{1c}^2 - K_{max}^2}\right\}^n \tag{5}$$

This equation predicts the effect of K_{max} as K_{max} approaches K_{1c} (region III), and further describes the effect of microstructure, principally through the parameter K_{1c}.

Richards and Lindley[10] proposed a combination of Equations (4) and (5)

$$da/dN = A^1\left\{\frac{(\Delta K - \Delta K_{th})^4}{\sigma_y^2 (K_{1c}^2 - K_{max}^2)}\right\}^n \tag{6}$$

for predicting fatigue-crack propagation, from very small values of ΔK to impending unstable failure.

Although Equation (6) is not accurate in detail (e.g. it does not reflect the independence of da/dN from K_{1c} and σ_y in region II), equations of this type show promise of predicting the fatigue-crack propagation rates to extreme stress-intensity regimes of a large number of materials, particularly steels.

Since the lowest rates of fatigue-crack propagation at ΔK values above region I were associated with the "striation" mechanism, and the rates were independent of tensile properties and fracture toughness, there does not appear to be much prospect of developing a steel which resists crack propagation under constant-amplitude cyclic loading. However, improved service life could be obtained by

(i) avoiding design conditions which would cause growth of cracks by mechanisms other than striations, and

(ii) developing high fracture-toughness values which extend the range of cyclic stress-intensity amplitudes over which the striation mechanism is maintained.

4. EFFECTS OF VARIABLE-AMPLITUDE LOADING ON FATIGUE-CRACK GROWTH

In service, aircraft structures experience a widely varying spectrum of fatigue loads, and this complicates the problem of predicting the rate of fatigue-crack growth. The simplest approach, based on fracture mechanics concepts, is to sum each increment of crack growth, determined from the da/dN versus ΔK relation, for each load cycle. Then, after N_1 cycles, a crack of initial length a_0 has a length a_1 given by

$$a_1 = a_0 + \sum_{N_1}^{N_1} f(\Delta K_1) \tag{7}$$

Numerous experimental studies—e g. Reference 17—have shown transient increases in cracking rate on increasing ΔK, and decreases on lowering ΔK. The effects of step increases and decreases in load on the rate of fatigue-crack growth in D6AC steel given heat treatment A have been studied by the author[18] and are illustrated in Figures 12 and 13. For the test results shown in Figure 12, a two-level spectrum was used. Before each sequential repetition of the load programme, 10,000 cycles of 4·5 kN load at 30 Hz were applied to provide fractographic markers (tide markings) for the initial positions of the crack front and to produce steady-state crack growth at the commencement of each succeeding programme. Figure 12 shows that, compared with "steady-state" constant-amplitude growth rates, step increases in load level abnormally increase the growth rate; descending changes in load abnormally retard growth. A detailed study of the effects (Fig. 13) illustrates their transient nature. After a step-increase in load, transient rates up to 7 times the steady-state rates were obtained; these decayed to the steady-state value after about 200 cycles. Following a step-decrease in load, crack growth stopped for about 2000 cycles and then rose to the equilibrium value after about 5000 cycles.

Elber[19] interpreted retardation and acceleration effects on rate of crack growth in terms of the effective stress range, $\Delta\sigma_{eff}$ at the crack tip, defined as the difference between the maximum applied stress, σ_{max} and the stress required to open the crack, σ_{op}.

$$\Delta\sigma_{eff} = \sigma_{max} - \sigma_{op}$$

The stress required to open the crack is a result of the constraint against crack-opening due to the plastic zone. The maximum radius of the plastic zone r_p, as given by Rice,[2] is (8)

$$r_p = \frac{1}{3\pi}\left(\frac{K_{max}}{\sigma_y}\right)^2 \tag{9}$$

The transient high rate of crack growth after an increase in cyclic load was attributed to the initially low constraint associated with the smaller plastic zone size produced at the lower load. The increase in constraint as the plastic zone size increased to the equilibrium value with continued cycling at the increased load was responsible for the decay of the transient acceleration. Conversely, crack retardation after decreasing the load was attributed to the high constraint of the large plastic zone produced at the high load level. Crack growth was arrested until the constraint was reduced by plastic relaxation due to cyclic softening in the plastic zone. The rate of crack growth then increased to the equilibrium value as the crack grew through the region of high constraint.

To date, no attempt has been made to incorporate stress-history acceleration effects into fatigue-crack growth laws. The neglect of the acceleration effect is probably not serious in view of the very rapid attenuation occurring over 200 cycles after a load increase. The retardation effect after a peak load, which persists for thousands of cycles, is of more practical importance. Wheeler,[21] using concepts similar to those of Elber,[19] introduced a retardation parameter, C_p, into Equation (7), so that

$$a_i = a_0 + \sum_{N_1}^{N_i} C_{pi} f(\Delta K_i) \tag{10}$$

The parameter C_p takes account of the strain state in the material at the crack tip and is related to the magnitude of the sequential plastic-zone sizes associated with the load changes. Wheeler's retardation parameter has the form

$$C_p = \left(\frac{R_y}{(a_p - a)}\right)^n \tag{11}$$

where R_y is the plastic zone size associated with the lower stress amplitude and $(a_p - a)$ is the distance from the tip of the crack, of length a, to the boundary of the plastic zone produced by the higher stress. The exponent n is experimentally determined and is characteristic of a given material and specified load spectrum; it is usually between 1 and 3.

A difficulty with interpretations based on plastic zone sizes is that, in the present work and in that of Amateau and Kendall[22] on D6AC steel, retardation persists over crack extensions that are three times the length of the maximum size of the plastic zone produced at the peak loads.

While it is not possible, at present, to account properly for retardation effects in fatigue-crack growth laws, their neglect does lead to conservative estimates of fatigue lives of structures; however, the benefits of the retardation effect after peak loads should be exploited in the future.

5. ENVIRONMENTAL ACCELERATION OF FATIGUE CRACK GROWTH-CORROSION FATIGUE

Although the influence of environment upon fatigue life has been recognized for over 40 years,[23,24] the practical significance of environmental factors has only been investigated as a serious problem over the last decade.[25-27] Environmentally enhanced (corrosion) fatigue cracking occurs as a consequence of the simultaneous influence of a cyclic stress and an aggressive environment. It can occur in environments which may not exhibit any corrosive action in the absence of the cyclic stress; the aggressive nature of the environment may not, therefore, be obvious. For instance, the absence of striation markings on fatigue-fracture surfaces, after testing in vacuum, suggests that atmospheric air makes an important contribution to the fatigue fracture mechanism.

The danger of neglecting corrosion-fatigue when assessing the service performance of structures is emphasised by the fact that water, which is almost always present in service environments, constitutes an aggressive environment under conditions of cyclic loading. Figure 14 illustrates the effects of moisture on the fatigue-crack growth rate in D6AC steel. At a cyclic frequency of 10 Hz, the rate of crack growth was not influenced by the presence of water or water vapour. However, when the frequency was reduced to 1 Hz, there was an effect, viz. increase in the rate of crack growth. The increase in rate was the same for distilled water as for argon–90% R.H. water-vapour atmosphere but was less in air with 90% R.H. water vapour. The significant effect of a decrease in cyclic frequency on the increase in rate in the presence of water was associated with a change in fracture mode. As shown in Figure 15, the crack path changed from transcrystalline (top) to intergranular (lower) on reducing the frequency.

One attempt to derive relations to predict fatigue-crack growth rates in aggressive environments has been that of Wei and Landes.[28] They considered the rate of crack growth by corrosion-fatigue as the algebraic sum of two components; one represents the rate of fatigue-crack growth in an inert reference environment, $da/dN_{(R)}$, and the other represents a time (or frequency) dependent (stress-corrosion) component. An attempt was made to compute the latter component by integration of the empirical relationship describing crack velocity under sustained loads, da/dt, for stresses and times corresponding to the load profile, K_t, over each cycle. Then, provided that these two contributing processes proceed independently without any synergistic interaction,

$$da/dN = da/dN_{(R)} + \int_{K_{min}}^{K_{max}} da/dt\,[K_t] \cdot dt \qquad (12)$$

A model of this type has the merit that, if it is applicable, the available stress-corrosion cracking data could be simply combined with fatigue data in inert atmospheres to predict crack-growth rates in various aggressive environments.

The Wei and Landes model was used to calculate crack growth rates for D6AC steel in distilled water, using the stress-corrosion data obtained by Pollock[29] for the same steel in distilled water. Pollock's data (Fig. 16), shows that the sustained-load cracking rate reaches a constant value of 0·05 to 0·1 μm per second over the stress intensity range of 20 to 50 MPa $m^{\frac{1}{2}}$. Calculations using Equation (12) gave values too low to account for the observed cracking rates (Fig. 14) by a factor of about 3.

A further difficulty with the Wei and Landes model is that increased fatigue-crack growth rates are obtained at K_{max} values below $K_{I.S.C.C.}$ (stress intensity below which stress corrosion is negligible). To overcome this problem, McEvily and Wei[30] substituted a new threshold stress-intensity amplitude $\Delta K_{th(f)}$, appropriate to corrosion fatigue, in Equation (4), to give the empirical relation

$$da/dN = C_1 (\Delta K - \Delta K_{th(f)})^n \qquad (13)$$

While this equation may adequately describe the behaviour of a particular material in one environment, the appropriate value of $K_{(th)}$ has to be determined experimentally for other materials in different environments.

Figure 17 illustrates the effect of hydrogen gas on the rate of fatigue-crack growth in D6AC steel. Two different loading wave forms were used, positive and negative sawtooth; the ratios of load-rise time to load-drop time were 9 : 1 and 1 : 9, respectively. Two cyclic frequencies were used, 1 and 0·1 Hz, so that the load-rise time for the positive sawtooth profile at 1 Hz was approximately the same as that for the negative sawtooth profile at 0·1 Hz.

With a sawtooth load profile, the Wei and Landes "addition" model predicts that the rate of corrosion-fatigue, crack growth at constant frequency should be independent of the ratio of

load-rise to load-drop time. Figure 17 shows that, at both 0·1 Hz and 1 Hz, da/dN is actually considerably greater with the positive sawtooth than with the negative. Furthermore, the rates are about the same for the positive sawtooth at 1 Hz and the negative sawtooth at 0·1 Hz. This latter result suggests that the environmental contribution of hydrogen in assisting crack growth occurs predominately during the loading portion of the cycle.

This sensitivity of crack-growth rate to load profile, the failure of the simple "addition" model to account for the rate of corrosion fatigue, and the change from a transcrystalline fracture path to a characteristic intergranular fracture mode associated with corrosion fatigue, suggests that corrosion fatigue should not be interpreted in terms of a simple super-position of environmental effects on the fatigue process in an environment. Thus, it should be analysed as a distinct fracture process that occurs as a result of complex interactions between the effects of the aggressive environment and the deformation resulting from the cyclic loading.

6. CONCLUSIONS

The present study of fatigue crack propagation in D6AC steel illustrates the complex nature of the process of fatigue in metals. It is shown that fatigue performance cannot be predicted solely from mechanical properties; microstructural effects on deformation and fracture processes play an important role, e.g. through their influence on the mode of fracture and, thus, on the fatigue behaviour.

Fracture mechanics, particularly through the concept of the stress intensity factor, provides the design engineer with a means of quantifying the tolerance of materials to cracks. The analysis of fatigue-crack growth data in terms of fracture mechanics concepts also provides quantitative measures of the complex effects of frequency, load profile, stress history and environment. While these data lend themselves to mathematical treatments which will ultimately be a basis for making predictions of fatigue performance, their principal role, at the present early stage of development, is, as an aid to the application of current conventional methods of lifing structures.

REFERENCES

1. Hahn, G. T., and Rosenfield, A. R. — Experimental Determination of Plastic Constraint Under Plane Strain Conditions. Trans. ASM 59, 909, 1966; also ASTM STP 432, 5, 1965.
2. Krafft, J. M. — Correlation of Plane Strain Crack Toughness with Strain Hardening Characteristics. Appl. Mat. Res. 3, 88, 1964.
3. Maklin, J., and Tetelman, A. S. — Relation Between K_{Ic} and Microscopic Strength. US Army Research Office Rept. No. 69-58, 1969.
4. Ryan, N. E. — Relationship Between Microstructure and Fracture Toughness in D6AC Steel. Aeronautical Research Laboratories, Met. Note 103, Aust. Department of Supply, 1974.
5. Peterman, G. L., and Jones, R. L. — Effect of Quenching Variables on the Fracture Toughness of D6AC Steel Aerospace Structures. Metals Eng. Q'ly, 15, 59, 1975.
6. Fedderson, G. E., Moon, D. P., and Hyler, W. S. — Crack Behaviour on D6AC Steel. Metals and Ceramics Information Centre, Battelle Memorial Institute MCIC 72-04, 1974.
7. Paris, P. C., and Erdogan, F. — A Critical Analysis of Crack Propagation Laws. Trans. ASME 85, 528, 1963.
8. Cooke, R. J., Irving, P. E. Booth, G. S., and Beavers, C. J. — Slow Fatigue-Crack Growth and Threshold Behaviour of a Medium-Carbon Alloy Steel in Air and in Vacuum. Eng. Fracture Mech., 7, 69, 1975.
9. Cooke, R. J., and Beavers, C. J. — Slow Fatigue-Crack Growth in Pearlitic Steels. Mat. Sci. and Eng., 15, 201, 1974.
10. Richards, C. E., and Lindley, T. C. — The Influence of Stress Intensity and Micro-Structure on Fatigue Crack Propagation in Ferritic Materials. Eng. Fracture Mech., 4, 951, 1972.
11. Clark, W. G. — Effect of Temperature and Section Size on Fatigue-Crack Growth in Pressure Vessel of Steel. J. of Materials, 6, 134, 1971.
12. Ritchie, R. D., and Knott, J. F. — Micro-Cleavage Cracking During Fatigue-Crack Propagation in Low Strength Steel. Mat. Sci. and Eng., 14, 7, 1974; see also Acta Met. 21, 639, 1973.
13. Liu, H. W. — Fatigue—An Inter-disciplinary Approach. Syracuse University Press, 1964; also Appl. Mat'l. Res., 3, 229, 1964.
14. Lehr, K. R., and Liu, H. W. — Fatigue Crack Propagation and Strain Cycling Properties. Int'l. J. Fracture Mech., 5, 45, 1969.
15. Priddle, K. — CEGB Rept. RD/B/N. 2233, 1972.
16. Heald, P. T., Lindley, T. C., and Richards, C. E. — The Influence of Stress Intensity and Microstructure on Fatigue Crack Propagation in a 1% Carbon Steel. Mat. Sci. Eng. 10, 235, 1972.
17. Corbly, D. M., and Packman, P. F. — On the Influence of Single and Multiple Peak Over-loads on Fatigue Crack Propagation. Eng. Fracture Mech. 5, 479, 1973.
18. Ryan, N. E. — The Influence of Stress Intensity History on Fatigue-Crack Growth. Aeronautical Research Laboratories, Met. Rept. 92, Aust. Department of Supply, 1973.
19. Elber, W. — Fatigue Crack Closure Under Cyclic Tension. Eng. Fracture Mech., 2, 37, 1970.

20. Rice, J. R.	Mechanics of Crack Tip Deformation and Extension by Fatigue. ASTM, STP 415, 247, 1966.
21. Wheeler, O. E.	Spectrum Loading and Crack Growth. J. Basic Eng. ASME, 94, 181, 1970.
22. Amateau, M. F., and Kendall, E. G.	Fatigue-Crack Growth Behaviour of a High Strength Steel. Aerospace Corp., Los Angeles, TR-0172 (2250-10)1, 1971.
23. Haigh, B. P.	Chemical Action in Relation to Fatigue in Metals. Trans. Inst'n Chem. Engs. 7, 29, 1929.
24. Gough, H. G., and Sopwith, D. G.	Atmospheric Action as a Factor in Fatigue of Metals. J. Inst. Metals 49, 93, 1932; 72, 415, 1946.
25. Bradshaw, F. J., and Wheeler, C.	The Effect of Environment on Fatigue-Crack Growth in Aluminium Alloys. Applied Mat. Research 5, 112, 1966.
26. Williams, D. N.	Environmental Corrosion-Fatigue Behaviour of Aluminium Alloys. Defence Metals Information Centre, Battelle Memorial Institute, DMIC Memo, 249, 1970.
27. Wei, R. P.	Some Aspects of Environment Enhanced Fatigue Crack Growth. Eng. Fracture Mech. 1, 633, 1970.
28. Wei, R. P., and Landes, J. D.	Correlation between Sustained Load and Fatigue-Crack Growth in High Strength Steels. Mat. Res. and Standards, ASTM 9, 25, 1969.
29. Pollock, W. J.	Aeronautical Research Laboratories, unpublished work.
30. McEvily, A. J., and Wei, R. P.	Fracture Mechanics and Corrosion Fatigue. Proc. Int'l Conf. on Corrosion Fatigue, NACE, Connecticut, 381, 1972.

TABLE 1

D6AC Steel—Chemical Composition
(AMS 6438)

	C	Mn	Si	P	S	Cr	Ni	Mo	V	Fe
Wt %	0·46	0·78	0·2	0·003	0·002	1·1	0·6	1·2	0·1	Rem

TABLE 2

Heat Treatment Schedules Applied to D6AC Steel

	Austenitizing Temperature °C	Intermediate "Ausbay" Quench C	Quenching Media	Tempering Temperature C
A	930	520	Hot oil – 60 C	550
B	930	520	Salt – 185 C	550
C	930	520	Salt – 210 C	550
D	930	520	Air – cool	550
E	930	520	Hot oil – 60 C	290

TABLE 3

D6AC Steel Mechanical Properties

Heat treatment	Yield strength MPa	Ultimate tensile strength MPa	Elongation %	Deduction in area %	Fracture toughness K_{1C}; MPa.$m^{\frac{1}{2}}$
A	1454	1620	16·4	50·2	105
B	1452	1618	15·2	49·0	95
C	1444	1622	15·1	49·8	85
D	1449	1644	14·4	47·5	46
E	1506	1900	10·5	39·6	60

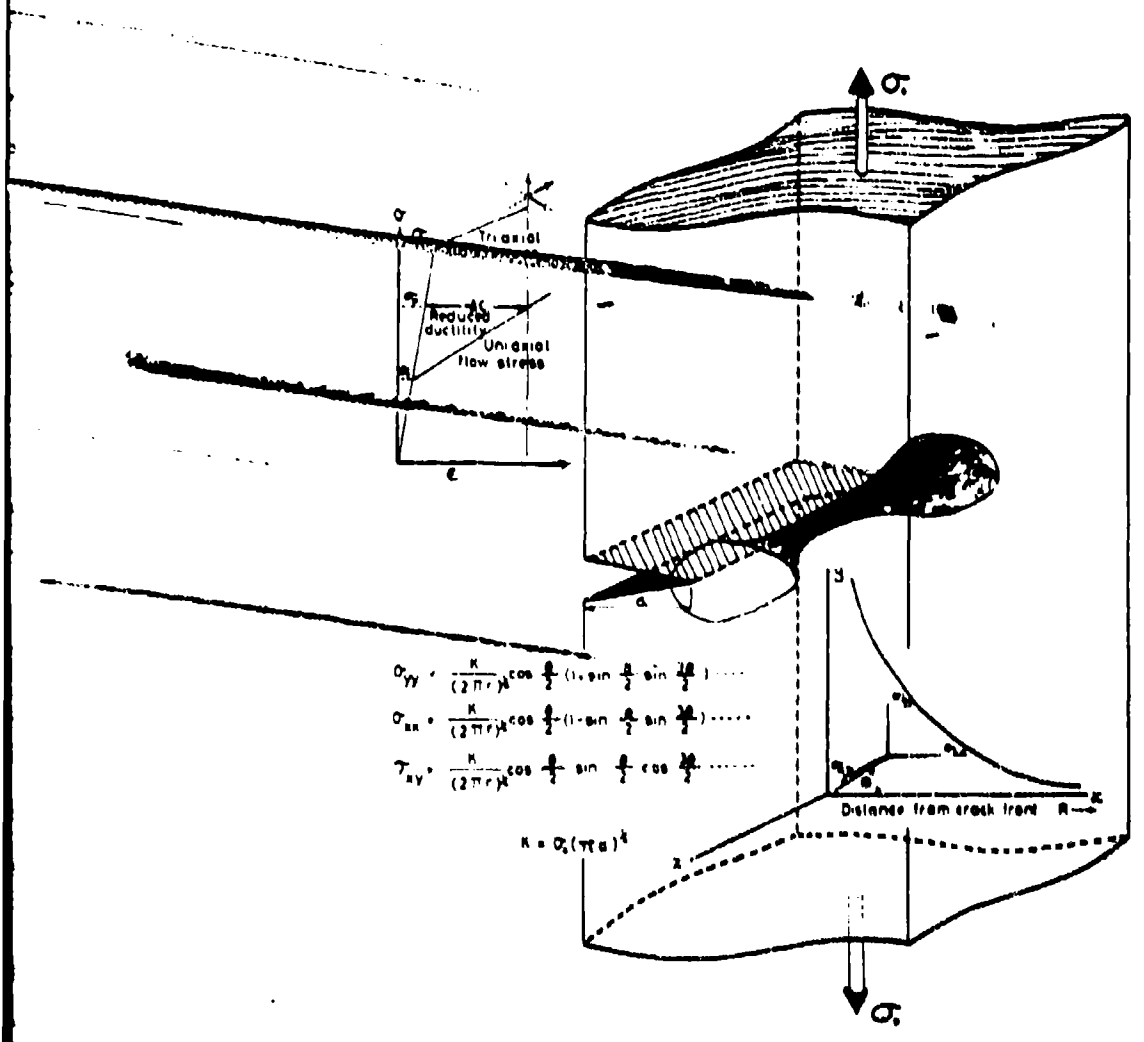

Fig. 1 Shows the characteristic plastic zone at the tip of a loaded crack and the identity of the stress intensity factor, K, as the coefficient of equations describing the state of stress in the region of the crack front.

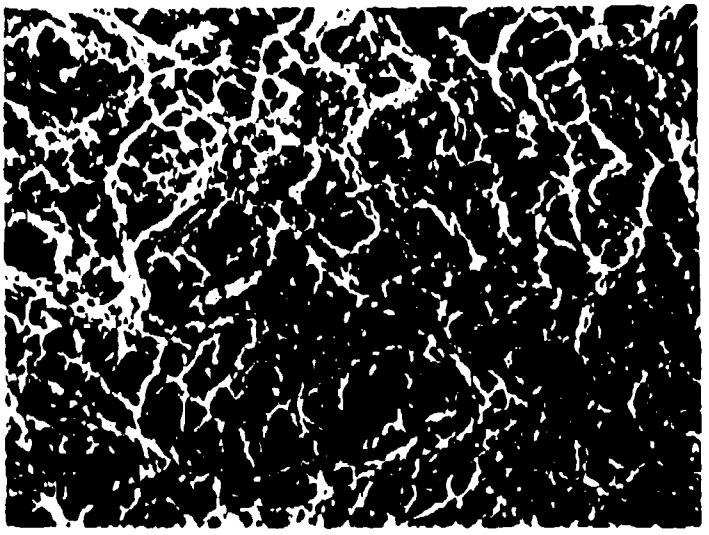

Fig. 2 Ductile, micro-void coalescence on the fracture surface of a high toughness, (K_{ic} ~ 100 MPa $m^{½}$) test specimen.

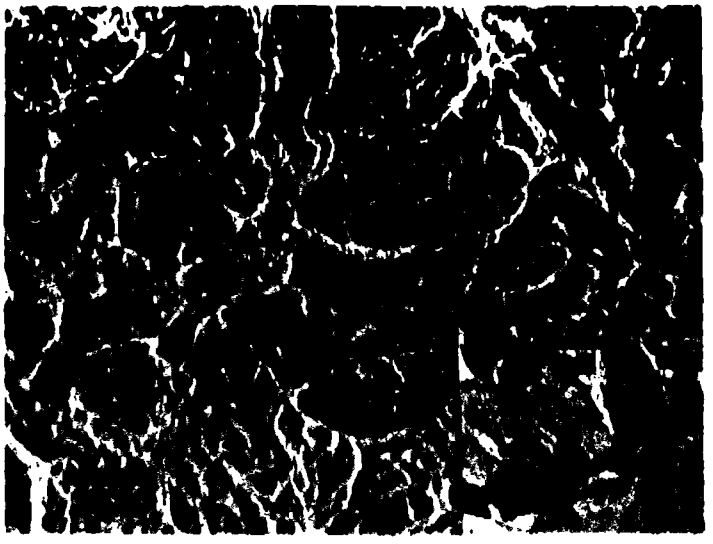

Fig. 3 Quasi-cleavage type of fracture surface of a low toughness (K_{ic} = 46 MPa $m^{½}$) test specimen. SEM

Inset: The same surface at higher magnification using a shadowed carbon replica. TEM

Fig. 4 Transmission-electron micrograph of the homogeneous distribution of fine carbides formed in the oil-quenched D6AC steel after tempering at 550°C. Inset shows the carbide distribution obtained using an extraction replica.

Fig. 5 Transmission electron-micrograph of the heterogeneous distribution of carbide formed in air-cooled D6AC steel after tempering at 550°C. Inset shows the carbide distribution using an extraction replica.

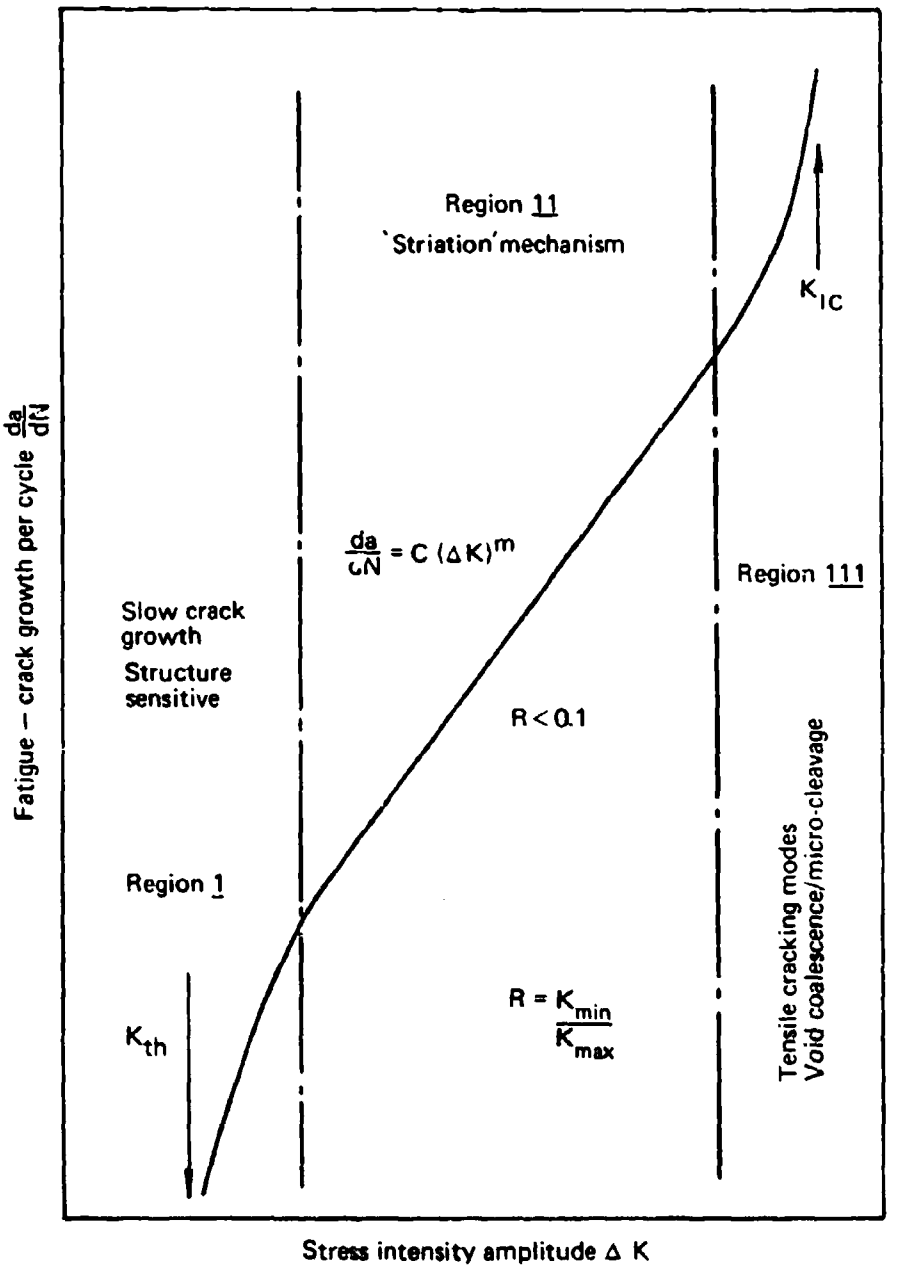

Fig. 6. A schematic illustration of the sigmoidal or three-stage relationship between the rate of fatigue-crack growth per cycle, $da/_{dN}$, and the cyclic amplitude of stress intensity, Δ K

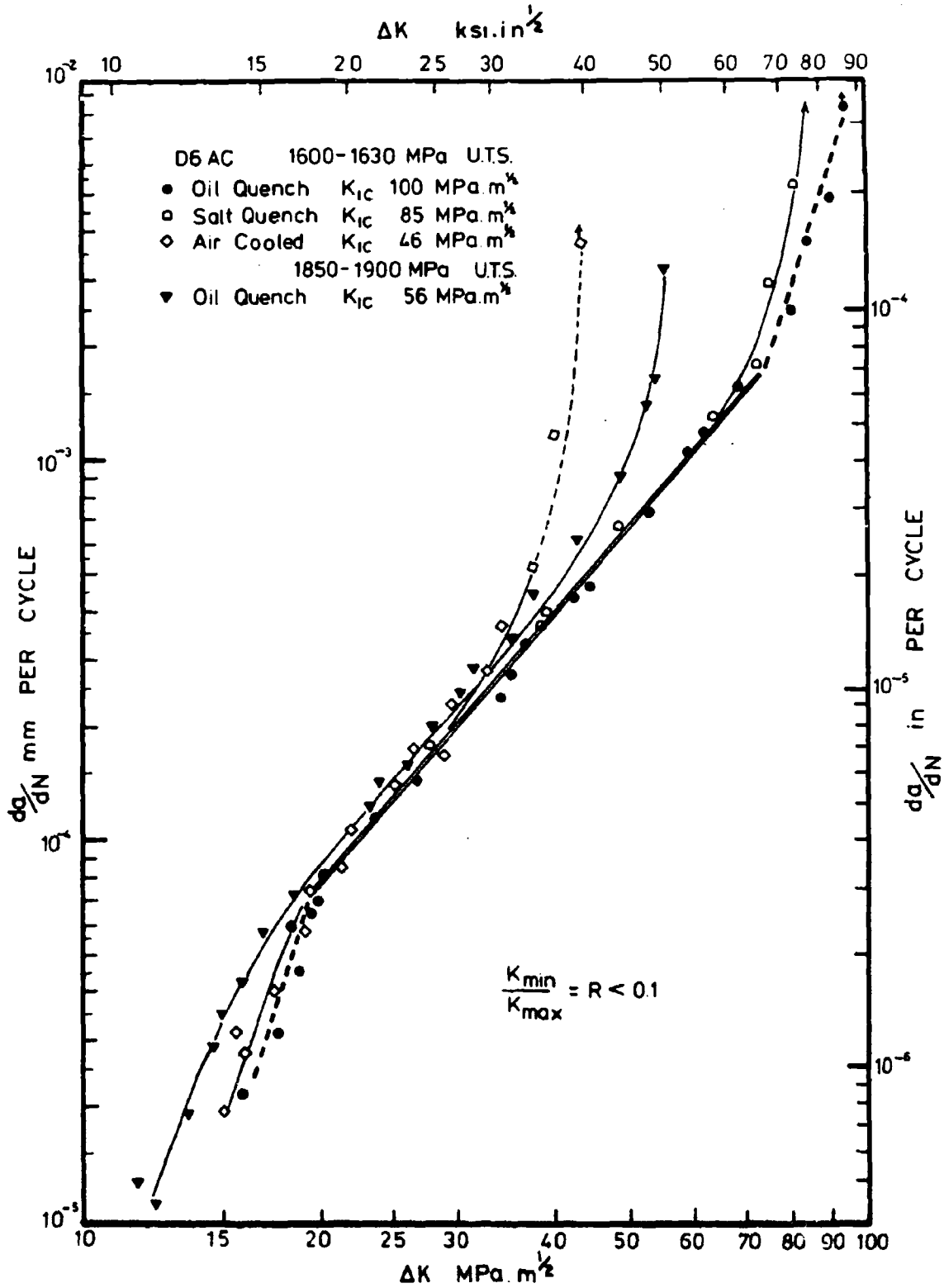

Fig. 7 The relationship between rate of fatigue-crack growth, $^{da}/_{dN}$, and stress intensity amplitude, ΔK, for D6AC steel heat-treated to different levels of fracture toughness, K_{IC}, and strength.

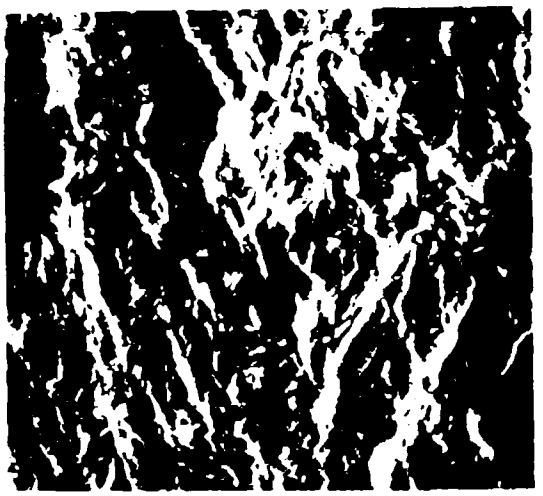

8a SEM
x 1000

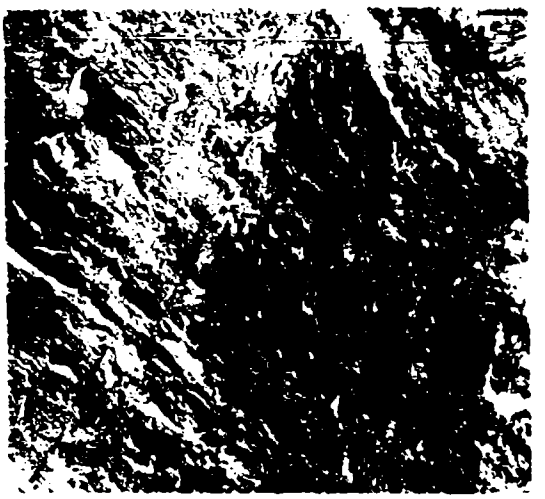

8b TEM
x 5000

Fig. 8 (a, b). Characteristic features on the fatigue-fracture surfaces of high toughness (100 MPa $m^{1/2}$) D6AC steel in region I, (low growth rate) of the $^{da}/_{dN} - \triangle K$ relationship. In region I the fracture surfaces of low toughness (46 MPa $m^{1/2}$) and high toughness steel is indistinguishable.

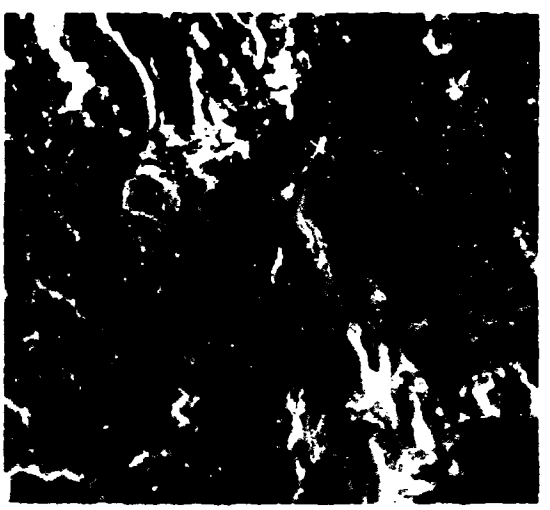

9(a) SEM
x 1000

9(b) TEM
x 10,000

Fig. 9 (a, b). Fatigue-fracture surfaces of high-toughness (100 MPA $m^{1/2}$) D6AC steel, from region II of the $^{da}/_{dN} - \triangle K$ relationship (where $^{da}/_{dN} \propto \triangle K^m$). Cracking in region II is characterised by the formation of striation markings.

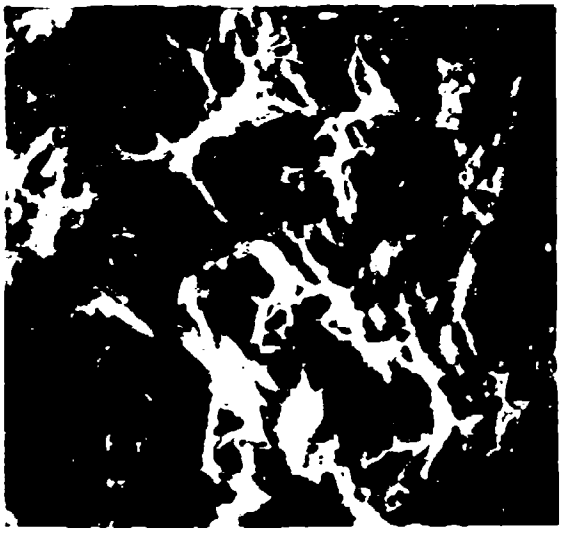

10(a) SEM
x 1000

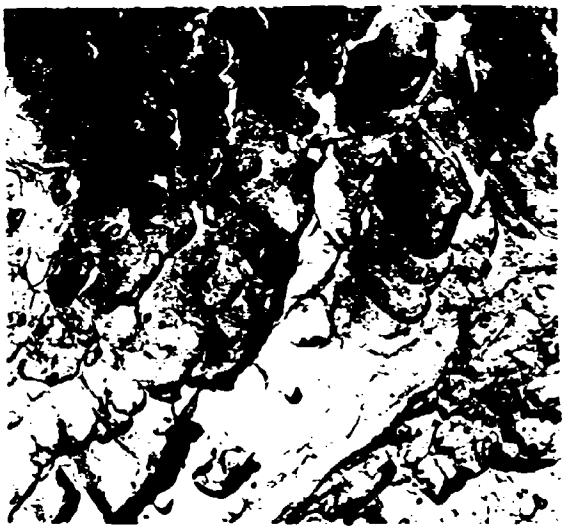

10(b) TEM
x 10,000

Fig. 10 (a, b). Fatigue-fracture surface of high-toughness (100 MPa $m^{1/2}$) D6AC steel from region III of the $da/dN - \Delta K$ relationship, where ΔK is greater than 0.7 K_c. Void formation and coalescence is noted.

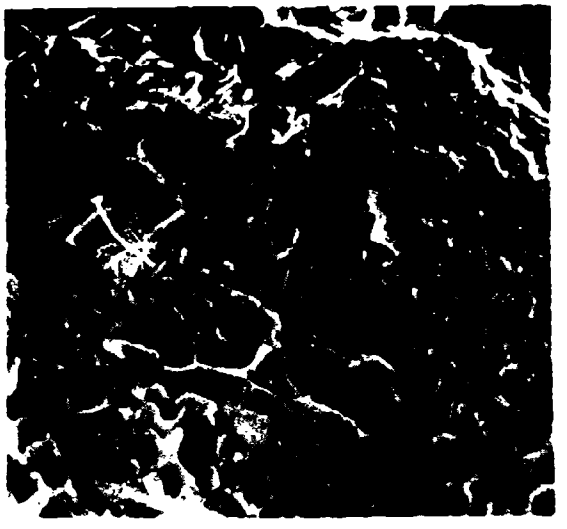

11(a) SEM
x 1260

11(b) TEM
x 10,000

Fig. 11 (a, b). Fatigue-fracture surface in low-toughness (46 MPa $m^{1/2}$) D6AC steel from region III of the $da/dN - \Delta K$ relationship. A micro-cleavage mode of fracture is noted.

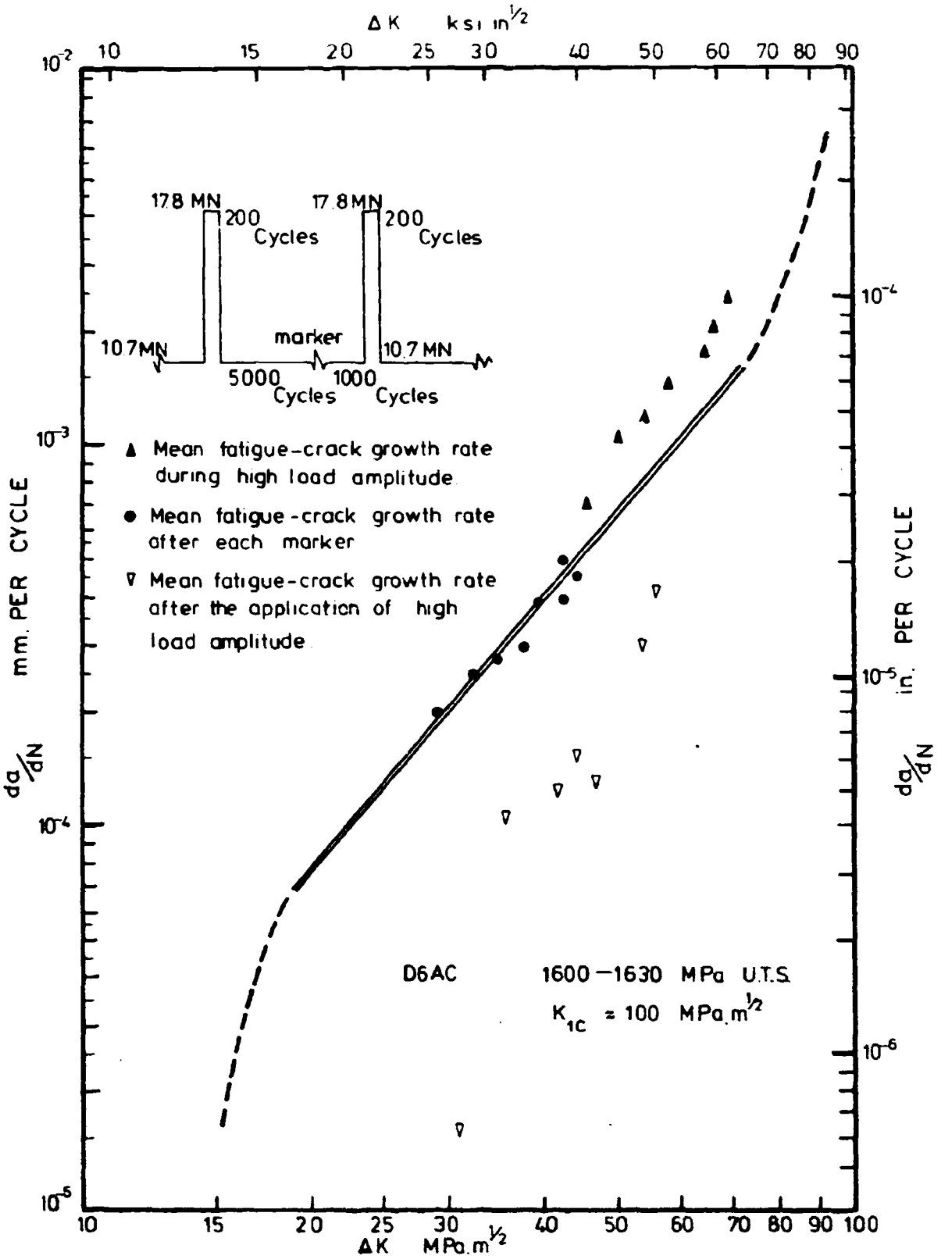

Fig. 12 Fatigue-crack growth rates per cycle $^{da}/_{dN}$ versus stress-intensity amplitude, ΔK, for the two-load level spectrum used in a detailed analysis of acceleration and retardation of fatigue-crack growth. Data points represent average rates of propagation for each succeeding load level for comparison with the continuous curve for constant-amplitude fatigue-crack growth.

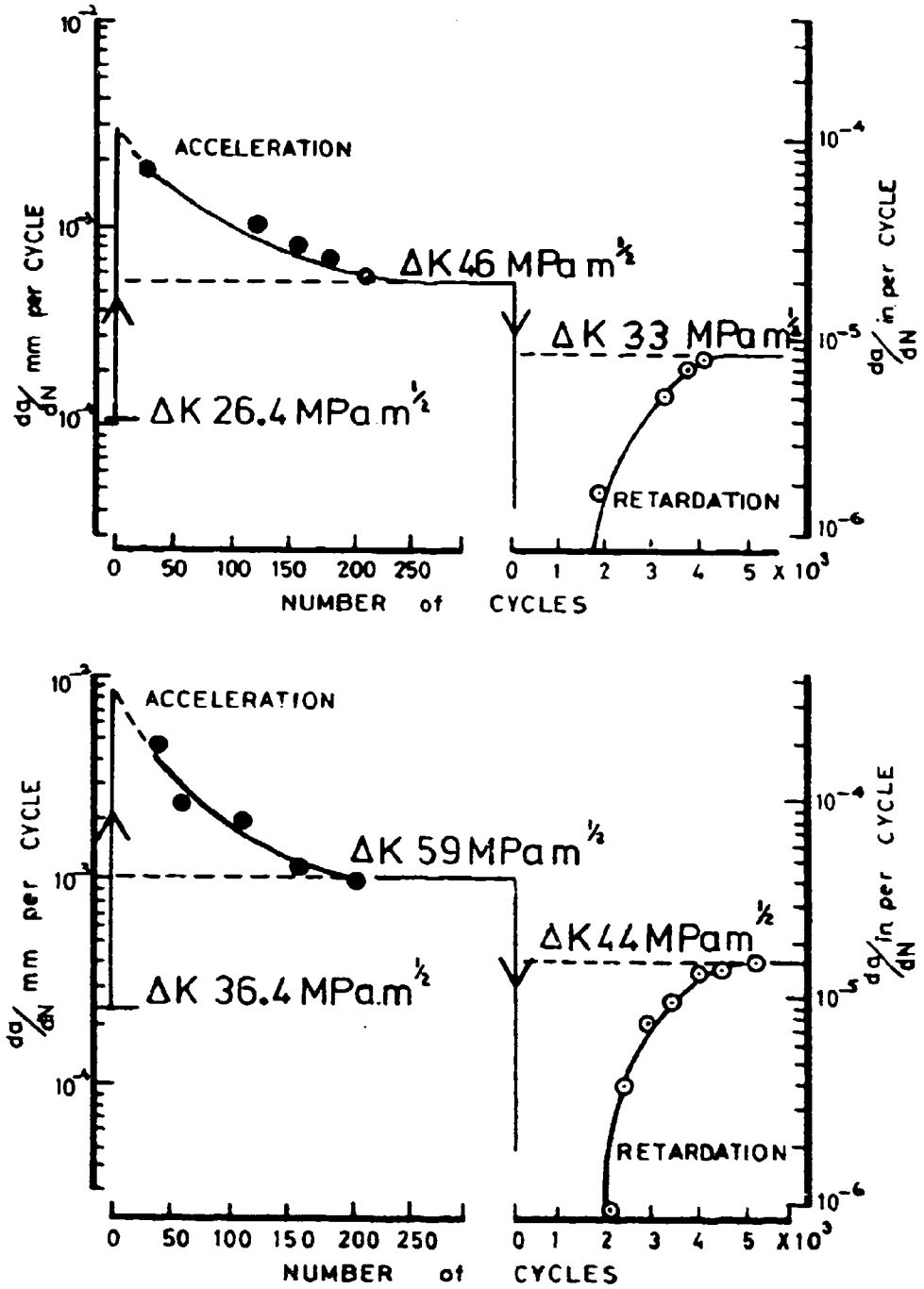

Fig. 13 Representative details of fatigue-crack growth rates in relation to numbers of cycles following step changes in cyclic load, according to the spectrum applied in Fig. 12. The acceleration or retardation in rate of crack growth, due to either an upward or downward change in cyclic load respectively, is shown relative to the growth rates (horizontal lines) normally expected for constant amplitude cycling, at equivalent amplitudes of stress intensity.

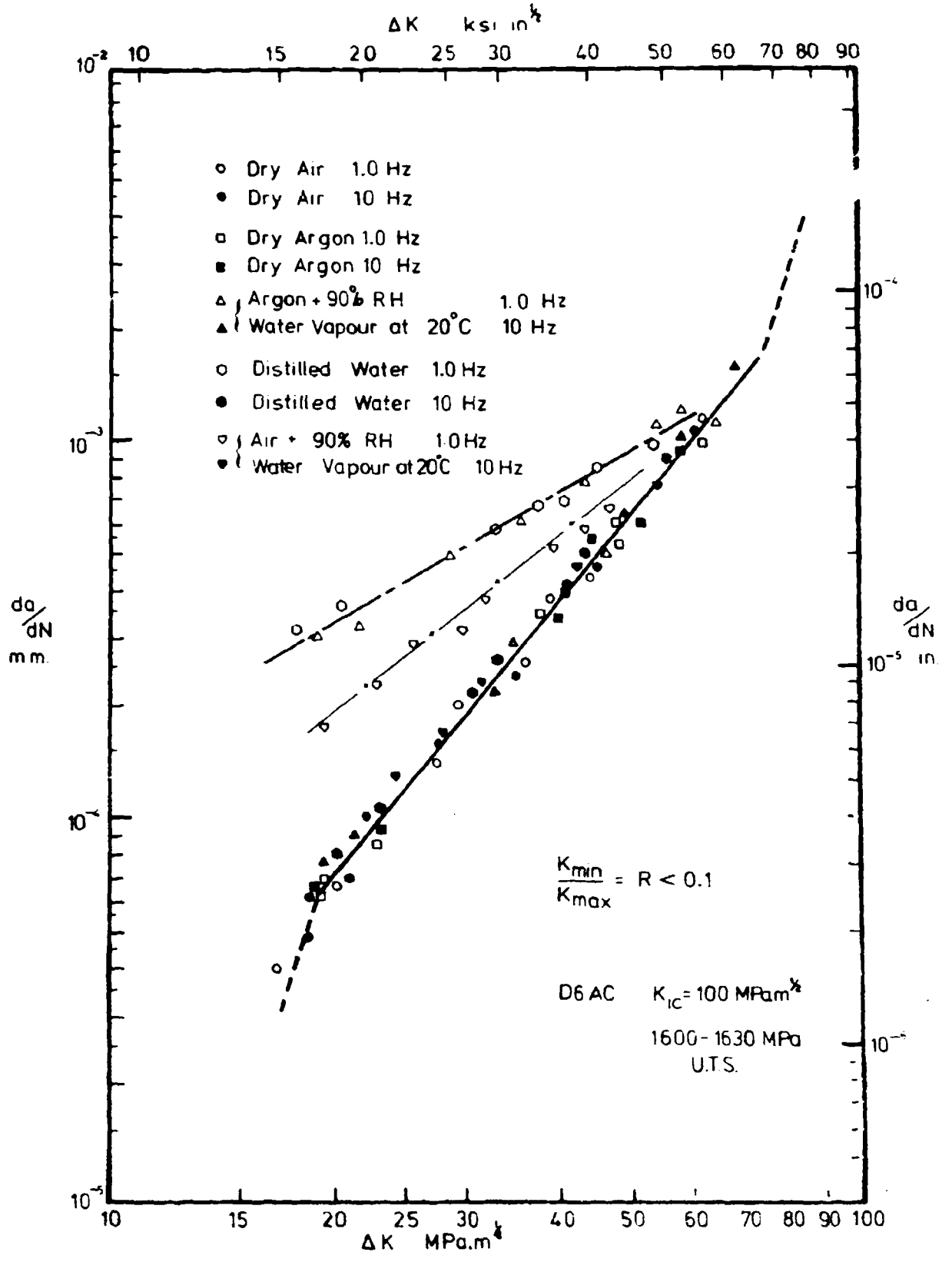

Fig. 14 Fatigue-crack growth per cycle, $^{da}/_{dN}$, versus the amplitude of stress intensity, ΔK, for fatigue cracking, in D6AC steel, in various environments containing distilled water or water vapour. The solid curve shows the rate of fatigue-crack growth in dry air or argon while the various data points relate to cracking in water-containing environments (listed) at either 10 or 1 Hz.

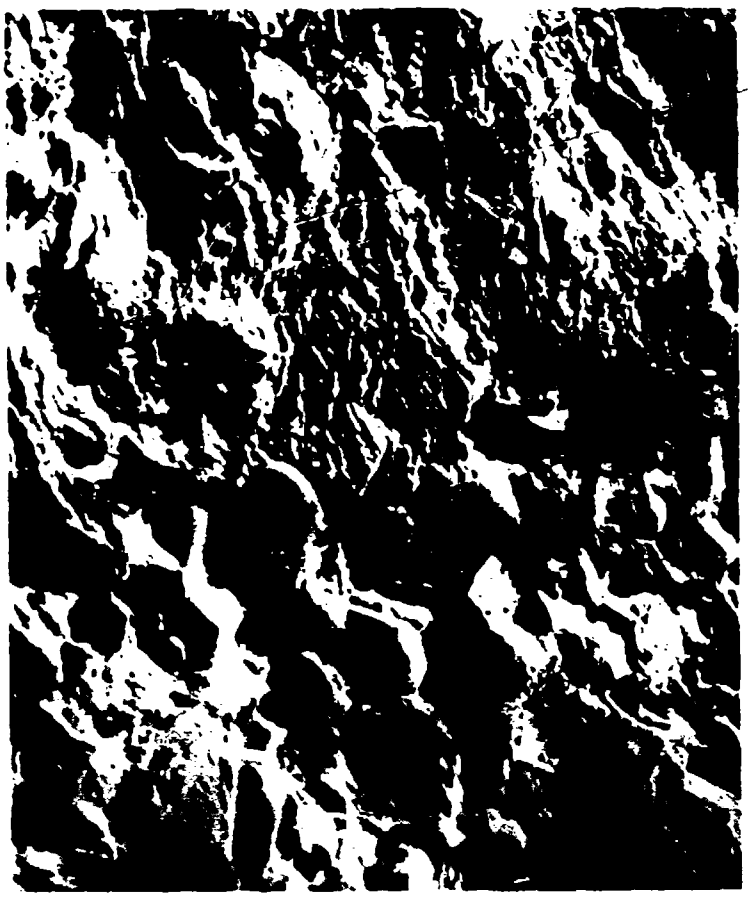

Fig. 15 Fracture surface of D6AC steel after cycling at 25 MPa $m^{½}$ in argon/water vapour. The transition from a trans crystalline (top) to an inter crystalline mode of cracking (lower) is induced by a change in cyclic frequency from 10 to 1 Hz. SEM x 750

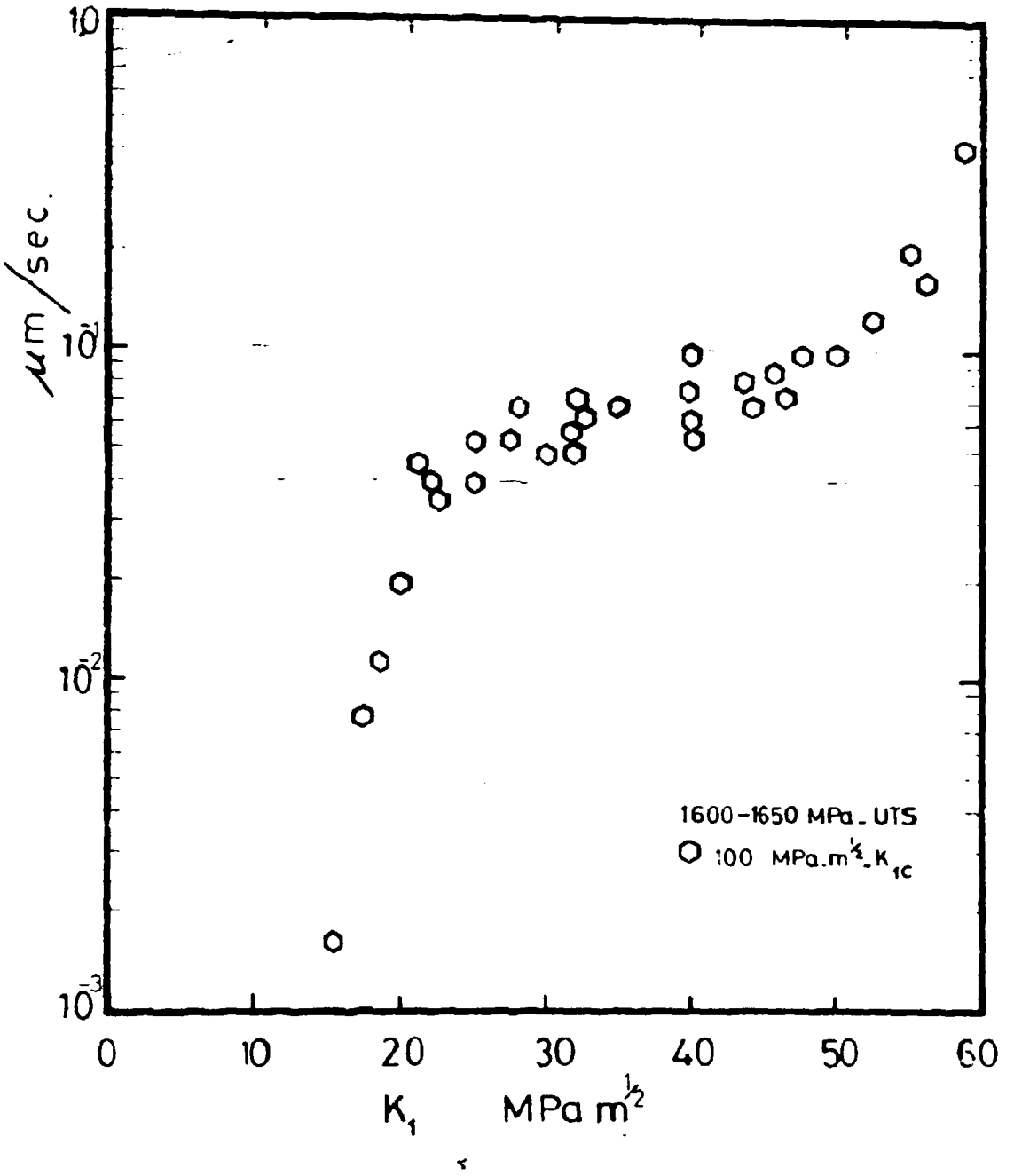

Fig. 16 Rate of stress corrosion cracking, $^{da}/_{dt}$, as a function of applied stress intensity K_1 for D6AC steel in distilled water.

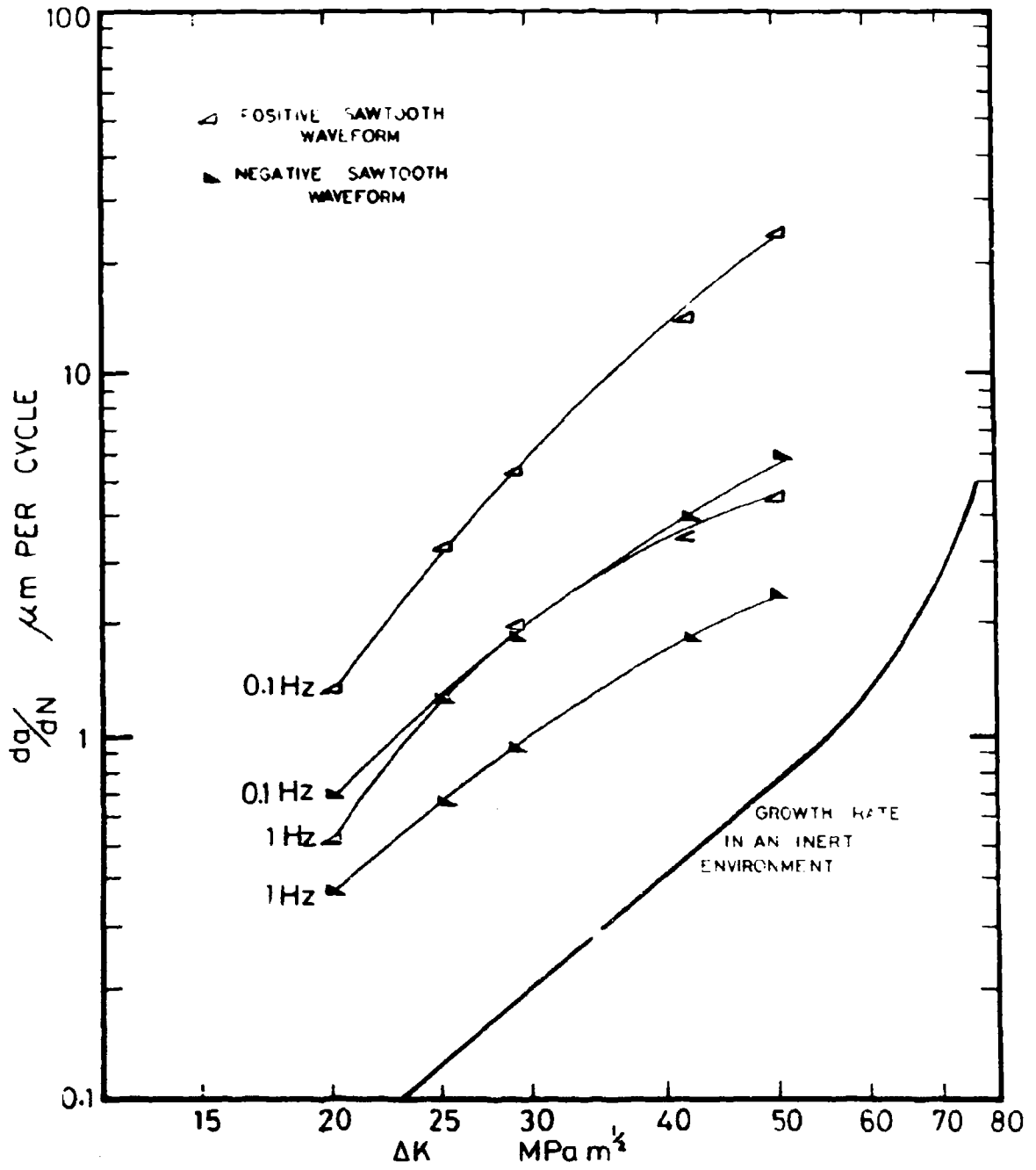

Fig. 17 Fatigue-crack growth in D6AC steel in low pressure (13.3 kPa, 100 Torr) hydrogen under positive and negative sawtooth cyclic load, wave forms. Rate of crack growth under a negative sawtooth wave form at 0.1 Hz is almost coincident with the growth rate under a positive sawtooth wave form at 1 Hz.

DISCUSSION

QUESTION—*Keith R. L. Thompson*
(University of New South Wales)

Has the speaker examined the effect of stress ratio R on the overall shape and the location of the inflexion points in the sigmoidal relationship shown in Figure 7?

The questioner has observed in high strength AISI 4340 steels that the first inflexion point in this relationship occurred at an essentially constant value of $K_{max}(K/1-R)$ and growth rate irrespective of R or material strength. Furthermore, the transition appeared to be related to both the commencement of shear lip development and a change in fracture mode from structure-sensitive to structure-insensitive. The second inflexion point in the highest strength level material used occured when K_{max} approached the plane strain fracture toughness of the material and was marked by the occurrence of elements of tensile crack growth on the normal fatigue crack growth mode. In the lower strength level material, the second inflexion point did not occur at a constant value of K_{max}, but it did appear to occur when crack growth occurred under essentially fully plane stress conditions.

Would the speaker like to comment on these observations?

Author's Reply

Your observations of fatigue-crack growth in 4340 steel are most interesting.

Our studies on fatigue-crack growth in D6AC steel have not included examination of the effects of mean stress or R. Your observations of the constancy of the lower inflexion in the $da/dN - K$ relationship is intriguing. However, I am not able to offer any explanation. An apparent change in fracture mode -or crack extension mechanism -is consistent with other observations which relate to this region of low growth rate.

Regarding the upper inflexion, it is well to recognise that change in growth rate can occur

(i) as a consequence of the intrusion of the tensile cracking mode, or

(ii) due to the transition from plane-strain to plane-stress conditions.

These processes are independent. The latter is unlikely to arise, even in low strength material, provided specimen thickness is adequate.

QUESTION—*J. C. Ritter*
(MRL)

I wish to make two comments:

Firstly, Dr. Ryan is correct in saying that the relationship (Fig. 7) between fatigue crack growth rate and stress intensity amplitude should apply to cases other than D6AC steel. Work at MRL, on high-strength gun steels of the 3½% NiCrMoV type, quenched and tempered to around 1300 MPa UTS has produced data which coincide exactly with those of the lower strength material shown in Figure 7. The common factor is the microstructure: a clean steel, rapidly quenched martensite, followed by tempering to give a uniform dispersion of fine carbide particles.

Secondly, the striation mechanism of crack growth (shown as Region II in Figure 6) is independent of microstructure only in the first approximation. Even when the contribution from tensile fracture modes, arising largely from the presence of non-metallic inclusions in the microstructure, is accounted for, there remains an effect of homogeneity of microstructure. This effect is seen when a very homogeneous steel achieved by electroslag remelting (ESR) is compared with a conventional molten ingot steel having the same, or even lower, inclusion content: the slope of the curve in Region II is lower for the ESR. This reduction is believed to result from the more uniform microstructure, down to a very fine scale, in the ESR.

Author's Reply

Your comment regarding the coincidence of fatigue crack growth rates in martensitic steels, independent of tensile properties, again emphasises the fact that no great improvements in resistance to fatigue cracking for tests at constant amplitude are likely to result from changes in alloy chemistry or heat-treatment.

The influence of alloy purity and non-metallic inclusions on fatigue-crack growth can be interpreted if we consider the mechanism of growth giving rise to "striations" as due to irreversible cycle strain, in which case theoretical predictions (References 13 and 14 of the paper) suggest that $da/dN \propto K^2$. Interfacial separation between hard precipitate, or inclusion particles, and the matrix introduces a perturbation in the crack growth process, leading to increased rates of growth. The slope of $\log da/dN$—$\log K$ is then almost always greater than 2 and increases with increasing particle size and impurity content.

QUESTION—*Sqn. Ldr. C. Giles*
(RAAF)

Tables 2 and 3 of your paper illustrate the effect of several high temperature heat-treatment schedules on the fracture toughness of D6AC.

What effect, if any, would you expect a simple bake cycle to have on fracture toughness? For example, a bake at 250°C followed by air cooling.

(This bake cycle is regularly used to relieve hydrogen embrittlement after stripping paint from D6AC components using paint stripper.)

Author's Reply

Changes in fracture toughness in D6AC steel are attributed to differences in quenching rate and their effect upon the initial, "as-quenched" martensite. The steel is subsequently tempered up to 550° to provide the desired tensile properties. Subsequent reheating for the purpose, say of removing hydrogen after cadmium-plating or paint stripping during maintenance, is unlikely to introduce any changes in fracture toughness, provided that the re-heating (or baking) temperature does not exceed the tempering temperature.

QUESTION—*N. T. Goldsmith*
(ARL)

The "intergranular" mode of cracking is presumably along prior austenite boundaries in the steel.

What then is the true path of the "structure-sensitive" fracture?

Could this be truly intergranular?

Author's Reply

Intergranular cracking resulting from environment-assisted (corrosion) fatigue cracking is clearly related to an almost continuous intergranular crack path, i.e. along prior austenite grain boundaries. However, faceted fatigue-crack paths in inert environments, in the slow crack growth region I (below 5×10^{-5} mm per cycle), also appear sometimes to follow across grain boundary faces. This, I believe, is largely due to the fortuitous incidence of grain boundaries oriented parallel to the direction of crack growth. The term "structure-sensitive" growth has loosely been applied to region I fatigue cracking where there is clearly some association between the rate of crack growth and microstructure; nevertheless, no unambiguous direct relationship has been demonstrated.

QUESTION—*P. J. Howard*
(ARL)

I think that what you have termed "acceleration" of crack growth is really retardation, and the observed decay in crack growth rate is due to the need for several stress cycles to set

up a steady state crack tip environment. This would also explain the effect, earlier described by Finney, that the retardation increases as the number of high loads increase.

Can "acceleration" be produced by treatments, e.g. annealing, other than pre-cycling at a lower stress?

Author's Reply

An initial (five-old) increase in rate of fatigue-crack growth, relative to the rate at constant amplitude for the same stress intensity range, is a consequence of a substantial step-increase in stress intensity range. The gradual decrease in rate of growth consequent upon further cycling at the new (higher stress) intensity range, is termed a growth rate decay or attenuation simply to distinguish it from the more commonly recognised "retardation" effect (described by Dr. Finney) following a marked step-decrease in stress intensity range. It is likely that the magnitude of the acceleration effect (relative to constant amplitude) would be greater the sharper the pre-crack, e.g. one introduced at a very low stress intensity. Further sensitizing of a sharp crack by annealing out the cyclic strain at the crack tip has been assessed in regard to the retardation effect, described in Dr. Finney's paper, but not in relation to the acceleration phenomena.

The terms "acceleration" and "retardation" are used to describe the transient changes observed in crack growth rates, relative to constant amplitude cycling at equivalent values of stress intensity range. It is true that the observed "attenuation" in an initially accelerated rate is also a progressive retardation. Nevertheless, changes in terminology could result in further confusion when discussing these phenomena. Both effects probably result from changes in the elastic and plastic constraints (residual stresses) developed around the crack tip. In the case of the decay following initial acceleration the constraint varied from a lower to a higher degree; in the case of "retardation", a change from a higher to a lower level of constraint is involved. However, extensive low level cycling, sufficient to induce the appropriate amount of plastic relaxation, can be required before further extension of the crack occurs after decreases in amplitude.

FIBRE COMPOSITE REINFORCEMENT OF CRACKED AIRCRAFT STRUCTURES

by

A. A. BAKER and M. M. HUTCHISON

SUMMARY

The fatigue performance of a range of commercially available adhesive materials has been examined to enable the selection of an adhesive system suitable for bonding of fibre composite reinforcements to cracked aircraft structures. Small constant stress cantilever 7075-T6 aluminium alloy fatigue specimens were used to evaluate the characteristics of the adhesives and also to examine the feasibility of using fibre composites to control crack propagation.

The adhesive selected for the repair application required curing at 130°C which, due to the low thermal expansion of the composite, induced residual tensile stresses in the aluminium at room temperature. Wedge-loaded, pre-cracked stress-corrosion specimens were used to show that these internal stresses do not significantly limit the practical usefulness of the proposed repair schemes.

Finally, two practical aircraft repairs are described which are currently being evaluated under operating conditions.

1. INTRODUCTION

Cracks initiate and propagate in many aircraft components due to factors which may include poor design, inappropriate choice of materials and/or unexpectedly demanding operating conditions.

Reinforcement of under-designed components before crack initiation is one solution (e.g. the bonded fibre composite doublers used on the wing pivot fitting of the F-111[1]) but, usually, components are reinforced after the discovery of cracks of sub-critical size. Repairs of this type are more often applied to light alloy components than to high strength steels since critical crack lengths are normally far larger in light alloys. Not all components can be strengthened or repaired but, where it is possible, a very cost-effective extension of the safe life of an aircraft can often be achieved.

Standard repair schemes to date have normally involved bolting or riveting strengthening members, made from the same type of material as the original component, to reinforce the cracked area. This procedure, although it introduces no electrochemical compatibility problems, can create undesirable stress concentrations at the point of attachment and also, by over-compensation of strength, can introduce fatigue problems at the ends of the reinforcement.

Recent technological advances in adhesive bonding and in fibre composite materials suggest the possibility of developing efficient repair schemes in which,

(i) the load is transferred from the component to the reinforcement without serious stress concentration, and

(ii) the properties of the reinforcement can be tailored to suit the particular application.

Table 1 lists the advantages and disadvantages of boron and carbon fibre reinforced plastics, compared to metals, for reinforcement (patch) material; these fibre composites probably have greatest potential value for this patching application, although other fibre composites based on steel wires, Kevlar fibres and glass fibres could also be important in particular applications.

This paper considers some aspects of work undertaken to evaluate various parameters associated with reinforcement of light alloys by fibre composites. Experience with two practical examples of this technique, for reinforcement of cracked aircraft components, is also considered.

2. BACKGROUND STUDIES

Successful reinforcement of metal components with fibre composites depends largely on efficient transfer of stress from the defective components into the composite material. Thus, the present background studies centered around the properties of adhesives and the adhesive bond achieved between 7075-T6 aluminium alloy and the chosen fibre composite. The three types of advanced fibre composites which were used (Table 2) all have advantages for the reinforcement of aluminium alloys:

(1) Carbon fibre reinforced plastic (CFRP) is comparatively inexpensive but can induce corrosion of metal in electrical contact with it because of its electrical conductivity and cathodic nature.

(2) Boron fibre reinforced plastic (BFRP) is more costly than CFRP but, since it is electrically non-conducting, presents no corrosion problems; in addition, thermal stresses are of less significance because boron fibres have a higher coefficient of thermal expansion than carbon fibres (see later).

(3) Boron fibre reinforced aluminium (BFRA) is the most expensive of the three; it was considered here mainly because its surface treatment for optimum bonding should be identical to that of the aluminium alloy to be reinforced.

Background studies were also undertaken to establish the feasibility of using bonded composites to prevent fatigue cracks from growing and to determine the influence of stresses introduced during bonding on the subsequent behaviour of the system.

2.1 Static Strength of Adhesives

A necessary pre-requisite to the study was a knowledge of the shear strengths of available adhesive materials; values of maximum shear strength were required, rather than the average values usually determined.

The development[2] of a step-lap sandwich specimen and calculation of the stress distribution within its adhesive layers enabled the determination of the maximum values of shear stress for several adhesives.[3] This specimen design (Fig. 1) virtually eliminates the two major causes of undesirable bending of the adherends which are common to most other test methods, viz.

(i) bending due to misalignment of applied loads, and

(ii) bending resulting from the differing mechanical properties of the adherends.

Other advantages over existing test methods include:

(*a*) close control of adhesive thickness,

(*b*) ability to measure adhesive thickness after testing, and

(*c*) reduced amount required of one adherend (the sandwiched material), which can lead to considerable economies of expensive materials.

Knowledge of the static strength, although useful as an initial guide, is not a sufficient basis in itself to allow the selection of adhesive materials for the present application. The behaviour under operational conditions, of cyclic stressing and environment in particular, is of paramount importance here.

2.2 Adhesive Behaviour under Cyclic Stressing

A comprehensive study was undertaken concerning the behaviour of selected adhesives under fatigue loading. This work is reported elsewhere in detail;[4] the most important features are outlined below.

2.2.1 Adhesives

The adhesive systems of greatest interest here are those which develop high fatigue strengths without requiring high curing temperatures, elaborate surface pre-treatment of adherends or high bonding pressures. Some capacity for stress relaxation could be advantageous as a means of reducing internal stresses, providing the rate of relaxation was low compared to the rate of cyclic stressing in applications involving fatigue. These requirements are very stringent and cannot be met by any currently available adhesive. The following range of adhesives (detailed in Table 3) was examined to enable the best compromise to be selected.

Ethyl cyanoacrylate was chosen because it is a solvent-free, one-component adhesive curing at ambient temperature without pressure; it is reported to be relatively rigid and to give high bond strengths with a very wide range of materials.

The flexible epoxies chosen are typical of the commercial low-pressure, twin-pack type which cure at ambient temperature; they are reported to bond a wide range of materials and to be resistant to fatigue.

The rigid epoxy cures at a relatively high temperature but little pressure is needed; it is reported to have given very high bond strengths.

Finally, the epoxy-nitrile film selected is typical of the advanced adhesives used to bond aircraft structures. It requires both a rather high temperature (however, lower than most comparable systems) and a high pressure; very high bond strengths are reported.

2.2.2 Method

Evaluation of the adhesive performance was based on measurements of the efficiency of strain transfer from the substrate to the adhesively bonded reinforcement; because of the analogous physical situations, strain-gauge theory was used for analyses of stress and strain. The efficiency of strain transfer depends on:

(*a*) the thickness and shear modulus of the adhesive,

(*b*) the substrate modulus, and

(*c*) the length, thickness and modulus of the reinforcing strip.

In a given system, the above parameters remain constant, except that

(i) the effective strip length changes if a fatigue crack grows in the adhesive layer, and

(ii) the effective modulus of the adhesive is reduced by any relaxation.

Consequently, the efficiency of strain transfer can be used to monitor changes from these causes.

Tests were carried out in bending using specimens (Fig. 2) consisting of 7075-T6 aluminium alloy constant-stress cantilevers (CSC) to which the reinforcing strips were adhesively bonded on one side; 7075-T6 reinforcing strips were used in some experiments instead of the composite. With the CSC specimen, the stress distribution in the adhesive layer closely approximates that produced by axially straining the substrate.

Various surface treatments were employed to prepare the CSC for bonding (Table 4). The BFRA and 7075 strips were given the same treatment as the CSC but alumina grit-blasting (with MEK degreasing before and after) was the only treatment found effective for CFRP and BFRP.

Changes in efficiency of strain transfer to the strip were determined by comparing the strain readings obtained during the test (e_s) with that observed at the beginning (e_s^o). Usually, instantaneous static strain measurements were made after loading the CSC specimens at their apex (Fig. 2); from these results the experimental parameter e_s/e_s^o could be evaluated. An important advantage of the bending method is that loading is fairly rapid so that errors due to strain relaxation in the adhesive layer are minimised; the 95% confidence limit on the mean of e_s/e_s^o measurements was estimated to be $\pm 0{\cdot}008$.

Relaxation measurements were made by loading the CSC specimen for five minutes, unloading, and then determining the compressive strain, e_u, which resulted.

Cyclic stressing of the adhesive layer was achieved by subjecting the CSC to reversed bending at 50 Hz in a laboratory environment at ambient temperature, the CSC being held at its fixed end in a strain-gauged dynamometer. The peak cyclic load was held constant during each test, giving approximately "constant-strain" conditions in the CSC. During the fatigue tests, readings of strain amplitude were taken from both the dynamometer and the strain gauge bonded to the strip. Measurements of changes in e_s during fatigue were usually made by periodically removing the CSC from the fatigue machine and carrying out a static measurement as described above.

The static method gives a precision much higher than could be obtained during fatigue because of errors introduced by slight movements in the gripping position. However, fatigue strain measurements were used for adhesives which showed a high degree of relaxation; since static measurements were then subject to large errors. In tests at high strain levels ($\sim \pm 1{\cdot}8 \times 10^{-3}$), gauge failures occurred which necessitated gauge replacement: the maximum error in e_s/e_s^o introduced by changing the gauge was estimated to be $\sim 0{\cdot}03$. After testing, all specimens were taper-sectioned along the strip length and metallographically polished to enable measurement of the thickness of the adhesive layer and to observe the nature and extent of fatigue-cracking.

2.2.3 Results

Relaxation measurements were used to estimate the effective shear modulus, G_L, of the adhesives after loading for five minutes. The results, normalised to an initial value for G_L of 1·1 GPa, are given in Table 5 together with the measured e_u/e_s^o ratio and the values of effective adhesive thickness, t_L.

Adhesives C and D relaxed comparatively slightly—the extent was acceptable for the present application. Adhesive A was also fairly resistant to relaxation; since A is cured at about room temperature, this resistance could have practical importance. In contrast, adhesives B and B′ suffered considerable reductions in their effective shear moduli, even though cured at ~90°C. The extent of these reductions indicates that these adhesives would not be of practical value for reinforcing applications.

When subjected to fatigue loading above a critical cyclic strain in the CSC, the strains in the strips decreased with increasing number of cycles (Fig. 3).* This fatigue damage in the adhesive layers was interpreted in terms of crack growth.[4] Adhesives C and D were the most resistant to fatigue damage. Adhesive C may be capable of even better performance than shown since the failures were mainly at the interface with the aluminium, despite the elaborate pretreatment of the aluminium surface. Failures in adhesives A, B and D were usually "cohesive" (Figs. 4, 5 and 6), suggesting that maximum strength levels were achieved in these adhesives. The favourable influence of the "Dacron" carrier fibres in adhesive D in inhibiting fatigue crack propagation is apparent in Figure 6. Adhesive A gave reasonably good fatigue behaviour when

* The terms "adhesive" and "cohesive" failures are used to denote failures at the adhesive/adherend interface and within the adhesive layers respectively.

used to bond BFRA to the CSC; in view of its low curing temperature and comparatively good relaxation properties, this adhesive may be of value for repairs where high temperature curing adhesives are unsuitable.

Since chemical surface pre-treatments of the aluminium are undesirable in many applications, simplified surface treatments were investigated for the most promising adhesives (A and D). Excellent fatigue results were obtained with adhesive D using the alumina grit-blast technique for the surface preparation of the aluminium; the failure was then cohesive (Fig. 3) and the cracking mode was similar to that in Figure 6. The trials using adhesive A with BFRA were disappointing. Poor results were obtained with both the grit-blast surface preparation and with a proprietary etching procedure used for mounting strain gauges with this adhesive.

The main conclusion resulting from this stage of the investigation was that adhesive D was suitable for practical repair applications using the simple alumina grit-blasting technique for surface preparation. The main disadvantage with this adhesive was the need for an elevated temperature cure.

During the above work, an interesting observation was made which could be of practical importance. Fatigue tests when $\frac{1}{2}e_s > 1{\cdot}8 \times 10^{-3}$ often resulted in failure of the strain gauges (by cracking of the grid). It was found that, on replacing the strain gauge using adhesive A, the initial strain reading was often much higher than the last reading of the old gauge. This effect naturally caused concern as to the significance of the results, even though, during subsequent continuation of the fatigue tests, e_s fell fairly rapidly to the expected value and then decreased at the normal rate. The behaviour appeared to be consistent with penetration and healing of fatigue cracks in the adhesive layer by adhesive A, which has an excellent wetting capability. In Figure 7 results confirming this view are shown; a BFRP/D specimen was fatigued to obtain a fall in e_s, plotted as e_s/e_s^o, and adhesive A was then flooded over the ends of the strip. The extent of recovery is shown by the vertical arrows (from crosses representing the fatigued state to full circles representing conditions after application of adhesive A). In the final part of the plot in Figure 7 the rate of decrease of e_s/e_s^o with N corresponds approximately with that expected if adhesive A alone had been used.

The above observations suggest that the technique could be important for field repairs of damaged bonded structures and of delaminated composite structures.

2.3 Crack Repair

Although both BFRP and CFRP bonded with adhesive D appeared promising for practical repairs, it was decided to concentrate, initially at least, on the use of BFRP simply because there is no danger of enhanced corrosion of the metal substrate. CFRP can be used for such applications providing simple precautions are taken, e.g. the inclusion of a glass cloth layer between the carbon fibres and the aluminium to act as an electrically insulating layer.[5]

A brief study was undertaken to demonstrate that the BFRP/D system could be efficiently used to inhibit fatigue crack propagation.

In principle, the problem of predicting the reduction in rate of fatigue crack propagation by patching reduces to that of finding the decrease in the cyclic range of stress intensity ΔK induced by the patch and then using the experimentally determined relationships between ΔK and the rate of crack propagation in the aluminium alloy, da/dN, to obtain the desired information. Typically, for metals under sinusoidal loading, $da/dN = A\Delta K^n$, where A and n are constants ($n \sim 4$ in many cases). Thus, small changes in ΔK strongly influence da/dN.

Detailed consideration of the theoretical aspects of patching have been given elsewhere;[6,7] a brief description of the salient parameters is presented here to aid further discussion. An analysis of the reduction in stress intensity by patching a centrally cracked infinite plate has been given by Takeshi Kanazawa *et al.*:[6] the assumed model is shown in Figure 8—the patches are assumed to be bonded only along the edges parallel to the crack. When the plate is subjected to tensile stress a reactive load P develops in the patches, producing an opposing stress intensity K_p in the plate. Since stress intensities can be algebraically summed, the effective stress intensity K_e is given by $K_e = K_a - K_p$ where K_a is the stress intensity that would have resulted in the unpatched plate. Typical results of the analysis, Figure 8, show that the compliance of the patch (revealed in this case by changes in L) and its position with respect to the crack determine the value of K_e; in general the patch should be close to the crack tip and be as stiff as possible.

As opposed to the end-bonded situation, for a patch of a given geometry maximum stiffness in the region of the crack can be obtained by

(*a*) bonding the patch over all its surface in contact with the plate, and

(*b*) using an adhesive with a high G_L, low relaxation characteristics and low t_L;

the theory proposed in Reference 6 has been extended to cover this case (Ref. 8). However, method (*b*) of increasing the effective stiffness of the patch also increases the local stress in the adhesive layer close to the crack, so that a compromise must be reached for fatigue crack-patching depending on the fatigue strength of the adhesive layer.

The influence of adhesively bonded patches on the rate of propagation of fatigue cracks in 7075-T6 aluminium alloy was studied using modified CSC specimens tested at 50 Hz in the laboratory environment at room temperature. A notch was cut in the edge of each CSC such that a fatigue crack would initiate and then propagate across the specimen at a level corresponding to the normal strain gauge position on the patch (Fig. 2). Fatigue cracks were then grown to a total crack length, from the specimen edge, of ~5 mm prior to patching. BFRP patches (0·15 mm thick) were bonded in corresponding positions on both specimen faces. Alumina grit-blasting was used to prepare the composite and metal surfaces for bonding in all cases except one. Here, for comparison, the aluminium was etched as listed in Table 3 (care being taken to prevent etchant from entering the crack).

Fatigue was carried out at constant applied bending moment and the crack length periodically measured microscopically after removing the specimen from the fatigue machine. In bending, there is a tendency for a crack on one surface to grow more rapidly than that on the other. This problem was avoided, at least in the stages of growth before the patch was reached, by setting a slight tensile bias in the fatigue machine and placing the CSC with the side initially having the shortest crack length under the tensile bias. Measurements of crack length could not be made when the crack front tunnelled under the patch, but the cycles to emergence were measured.

The rate of crack growth was much greater for unpatched specimens than for patched specimens, which was attributed to the general stiffening effect of the patches. Thus the efficiency of the patches in retarding crack growth cannot be obtained by direct comparison with the results of the unpatched specimen. This problem was overcome by comparing the rate of growth after the patched region with the expected rate in the same specimen. The expected rate was obtained by extrapolating the exponential regions of growth, as shown by the dashed curves in Figure 9.

A marked reduction in the rate of crack propagation occurred in all patched CSC specimens when the crack reached the patch position, Figure 9. Within the limits of experimental observation, the exponential form of the propagation curve appeared to be maintained until the crack actually tunnelled under the patch; this observation agrees qualitatively with the theory which suggests that the effect of a patch on K_ϵ is fairly short in range. An unexpected result was the gradual progressive reduction in the rate of propagation of the emerging crack. In the absence of the patch, the rate of propagation progressively increases, as shown by the dashed lines in Figure 9; the reason for this difference is not clear.

A measurement of the influence of the patch on crack propagation was made by calculating the effective range of stress intensity ΔK using the empirical relationship:

$$\Delta K = 275\,(\mathrm{d}a/\mathrm{d}N)^{1.4}\ MN\,m^{-3/2}$$

where $\mathrm{d}a/\mathrm{d}N$ is the measured rate ($m\,s^{-1}$) and the constants are taken from data on 7075-T6 valid for the rates observed.[9] Results for BFRP/D (Fig. 10) show a linear initial and extrapolated region (curves for unpatched specimens suggest that a linear extrapolation may be conservative) with a reduction in ΔK of up to 40%. Although the curves in Figure 10 initially show a qualitative similarity to the theoretical curves (Fig. 8), the region of negative slope after the patch is not predicted; of course the differences between the theoretical model and the experimental specimen are very large, making detailed comparison difficult.

In general, the apparent decrease in ΔK is not as large as may have been expected, considering that the patches were in the outer highly stressed regions. Unfortunately the specimens are complex so that no simple theoretical comparison is possible. However, the same method of effective ΔK measurement (e.g. from $\mathrm{d}a/\mathrm{d}N$ measurements) with specimens more amenable to analysis, such as that considered in Figure 8, may prove useful.

2.4 Influence of Residual Stresses from Patching on Stress-Corrosion Behaviour

Tensile residual stresses at room temperature can arise in a metal component on cooling after bonding fibre composite patches at elevated temperature. For a given geometry and bonding temperature, the magnitude of tensile stress depends directly on the difference in coefficients of

thermal expansion of composite and metal. This difference, based on data from the literature, is $\simeq 18 \cdot 10^{-6}C^{-1}$ for BFRP and aluminium, while a value of $\simeq 14 \times 10^{-6}C^{-1}$ was obtained from measurements of curvature of an aluminium strip at room temperature after bonding BFRP to one side at elevated temperature; these values are in reasonable agreement, considering the possible errors involved. For a composite/metal thickness ratio of 1 : 3, typical of much of the present experimental and practical work, an internal stress of $\simeq 60$ MPa would be expected. Tensile stresses of this magnitude in the aluminium alloy could adversely affect its fatigue behaviour and induce stress-corrosion cracking.

Work on reverse-bending fatigue of unnotched fibre composite reinforced aluminium beams[10] indicated that the stresses introduced by bonding with AF126 did slightly reduce the fatigue performance of the metallic component. The extent of this reduction was not of practical significance. Nevertheless, it was possible that the internal stresses could adversely influence the stress–corrosion behaviour of the aluminium (and, thus, possibly contribute to crack growth by corrosion-fatigue).

The approach taken to study the above stress–corrosion aspects was to select a system known to be prone to stress-corrosion, create a situation where stress–corrosion crack-growth was taking place, and then to monitor the influence of bonded reinforcing patches on subsequent growth of the cracks. It was assumed that, if patching prevented growth of the stress-corrosion cracks, then it was unlikely to initiate cracks in virgin specimens.

2.4.1 Materials

One of the practical reinforcements undertaken (c.f. Section 3.1) concerned cracks in ribs of an aircraft wing plank manufactured from 7075-T6 aluminium alloy, which is susceptible to stress corrosion. Due to the method of manufacture, the alignment of grain boundaries in the component favoured crack propagation parallel to the edge of the ribs. Ribs were cut from a discarded wing plank to make specimens (Fig. 11).

BFRP patches of dimensions 45 mm $\times$ 25 mm $\times \simeq 0{\cdot}45$ mm thick were made from four layers of pre-preg (100 μm diameter fibres in epoxy matrix) laid up with each layer of the boron fibres aligned in the same (25 mm) direction. After surface preparation using the alumina grit-blasting technique, the patches were bonded to the aluminium, with the fibre orientation at right angles to the cracks, using AF126 adhesive cured at 130°C.

Specimens were immersed at room temperature in an aqueous solution containing CrO_3 (36 g/*l*), NaCl (3 g/*l*) and $K_2Cr_2O_7$ (30 g/*l*); this solution is known to encourage stress corrosion in 7075-T6.[11]

2.4.2 Procedure and Results

A fine hacksaw cut (20 mm long) was made in the end of each specimen, into which was driven an aluminium wedge (7075-T6) to produce an overload crack extending for about another 30 mm. With the wedges still in place, the specimens were immersed in the aqueous solution and crack-growth was monitored visually. All specimens, except those used to establish crack-growth behaviour, were removed from the solution after crack-growth was well established (usually several days). This procedure avoided possible ambiguity due to the inclusion of the highly variable period for initiation of stress-corrosion cracking in the results. The desired patching or other treatment was then carried out before returning the specimens to the solution.

The position of the crack tips under the BFRP patches was monitored to ± 1 mm using an eddy-current technique.

Unpatched Specimens

The length of the overload cracks in the specimens varied considerably ($\simeq$45–65 mm). Thus, although the starting stress intensities at the various crack tips should all have been similar (K_{1c}), the simple specimen design would cause the stress intensity to change at different rates with subsequent increments of crack growth in different specimens. This effect, supplemented by variations due to slight material differences, accounts for the observed range of crack-growth rates in the reference specimens (Fig. 12); differences in incubation period have been omitted from the results. The general trend shown by these results is the same, viz. the rate of crack growth is initially high but decreases with time. Figure 12 also includes an "average" curve, representing the centre of the scatter band of the results for comparison with the behaviour of the other specimens.

The next step was to determine whether or not the thermal curing treatments had any influence on the crack-propagation rates. Specimens, in which active stress corrosion had been established, were subjected to the thermal treatments and returned (still wedge-loaded) to the aqueous solution. No significant change in cracking rate resulted (Fig. 13).

Patched Specimens

The location of the patches with respect to the crack tips could have significantly influenced subsequent crack propagation. The results of tests on specimens patched at three typical locations (Fig. 11) can be summarised as follows:

(*a*) When the edges of the patches were located 4 mm ahead of crack tips, the cracks grew until their tips were well under (up to 12 mm) the patches before crack-growth ceased (Fig. 14).

(*b*) When patches were located centrally over the crack tips, crack growth was prevented in all but a few instances, where a small amount of growth occurred (Fig. 15).

(*c*) When patches were located over the cracks with the cracks extending 4 mm beyond the patches, there was about the same amount of crack-growth as for case (*a*) before crack-growth ceased (Fig. 16).

2.4.3 Discussion

The above series of simple tests was designed to show whether or not the level of internal stress introduced into the aluminium by the chosen reinforcement scheme was sufficient to cause significant stress corrosion cracking in practical applications. The results show that no problem is likely to be encountered in practice, providing the patches are located over the crack tips.

The use of wedge-loaded specimens may be considered to be a rather demanding situation, since the stress encouraging crack-growth would be greater than that solely arising from the internal stress. However, this pre-loaded condition corresponds reasonably well to the practical situation where the reinforced components will be expected to sustain both the internal stresses and their normal operating loads.

For patches located ahead of the tip, crack-growth would be expected until the tip came close to, or reached, the edge of the patch. The observed crack-growth continued further, i.e. until the tip penetrated under the patch, possibly due to the influence of the internal stresses. Similarly, internal stresses could have contributed to the observed crack-growth in the specimens where the crack extended beyond the patches.

The most practically significant observation was that virtually no growth occurred when the patches were bonded over the crack tip and, even for the other patch locations, crack-growth eventually ceased.

Penetration of adhesive into the crack could occur during application of the patches over the cracks, thus isolating the crack tip from the corrosive environment. However, the action of the patches in stopping crack-growth was clearly demonstrated by those examples where patches were located ahead of the crack tips.

3. PRACTICAL REPAIR APPLICATIONS

In the preceding sections, it was demonstrated that bonding of fibre reinforced plastics to metallic components could be a practical method of repair or reinforcement. The next step was to apply this technique to actual components and to evaluate their subsequent performance.

The choice of suitable components is restricted because they must comply with the following requirements:

(*a*) the component must be amenable to repair;

(*b*) a conventional repair procedure must be either unavailable or less satisfactory for some reason;

(*c*) the aircraft operator has to be sufficiently interested to permit the subsequent evaluation inspections to be undertaken; and

(*d*) "fail safe" or closely monitored situations are necessary for initial evaluations, particularly in cases where no repair scheme has been developed previously.

This section describes the experimental schemes developed for the repair of two components which satisfied the above requirements.

Ideally, design expertise in repair schemes would enable the immediate selection of the optimum patch parameters (size, thickness, fibre orientation, patch taper, etc.) for each particular

problem. However, although work is currently under way to achieve this objective, such expertise was not available when considering the examples described herein. Thus, these repairs were developed on a basis which depended largely upon experimental verification of the choices made.

3.1 Hercules Wing Planks

The wing planks are machined from solid blanks to give wing skins with integral reinforcing ribs (Fig. 17). Internal wing structures, at a separation of about 450 mm, are riveted to the wing plank ribs. Stress-corrosion cracks commonly initiate in the ribs at the rivet holes and propagate along the ribs (parallel to the wing surface); the length of these cracks is regularly monitored. Various repair schemes involving metal reinforcement brackets riveted to the ribs and wing surface have been evolved but their application is very time-consuming and results in further regions of stress concentration (around the loaded rivet holes and at the ends of the brackets at the sudden change in section). Since essentially plane surfaces are involved, adhesive bonding of the metal reinforcement would be superior to riveting. However, even for these simple repairs it was economical to use BFRP, because of the small quantities required. Moreover, it was considered that the experience gained would be of considerable advantage for more complex future applications, where the abilities to mould BFRP into complex shapes and to tailor its mechanical properties (by variation of fibre orientation), combined with its low density, could be of paramount importance.

The patch thickness was chosen on the basis of restoration of tensile strength across the crack; the patch thickness chosen exceeded the minimum requirements by about 30%. The patches, 45 mm long × 25 mm wide × ~0·45 mm thick, were moulded from four layers of pre-preg; the length in the fibre direction (25 mm) was governed by the height of the wing plank ribs. Patches were bonded to both sides of the cracked ribs such that each crack tip was no more than half way under a pair of patches; further pairs of patches (reduced in length where necessary) were bonded to cover the cracked regions, where possible.

The assumption of pure tensile stress across the cracks is obviously an over-simplification. In practice, the loading cycle likely to cause further crack propagation involves compression along the length of the ribs, with a consequent tendency for buckling. This type of loading would lead to a peeling stress being applied to the bonded reinforcement in the fibre direction. The low stiffness of the patches transverse to the fibre direction could be an advantage with this type of distortion; since the longitudinal peeling stress and the danger of local stress concentrations in the metal at the patch ends should both be reduced.

Compression tests were carried out to gain an indication of the ability of the composite-patching technique to restore the original strength of cracked wing panels. Three specimens (~465 mm long and incorporating three ribs) were cut from a discarded wing plank (after ensuring that these areas were free from cracks). Two of these specimens then had simulated cracks introduced by spark-maching slots (~0·35 mm wide and 140 mm long) in all of the ribs. The slots were located mid-way on the width of the ribs (corresponding to the normal position of the cracks in the wing planks) and were centrally placed with respect to the specimen length. Overload cracks were then introduced at the ends of all the slots to give total crack lengths of ~150 mm. The length of the cracks and their location at the most critical region of the compression specimens (the antinodal position) were chosen to simulate the worst case which one would expect to encounter. BFRP patches were then bonded over the cracks in one specimen (Fig. 18*c*); the end pairs of patches were located so that the crack-tips were half way under the patches, and the space in between the end patches was then filled in with other pairs of patches. Woods-metal ends were cast on all the specimens and, finally, machining reduced the specimen lengths to 455 mm.

Dial gauges were used to measure deflections at twelve locations during the compression tests; the specimens, after testing, are shown in Figure 18. The relative behaviour of these panels is typified by the sideways deflection of an outer edge of a rib above the centre of the crack (Fig. 19). The cracks seriously degrade the properties of the panel; the maximum load sustained is reduced by ~30% but very significant decrease in panel stiffness, with initial distortion occurring at about 20% of that for an uncracked panel, is perhaps of even greater significance. However, in similar tests, the behaviour of patched panels was essentially identical to that of uncracked panels, within the accuracy of the test, the stiffness was the same, while the maximum load was only 2·5% lower. In addition, the patches did not debond during the test and, because there is little strengthening from the patches at right angles to the fibre direction (i.e., along the length

of the ribs), the general buckling behaviour of the ribs of the patched panel was very similar to that of the uncracked panel, with no evidence of stress concentration at the ends of the patches (Fig. 18).

Simple techniques had to be developed to allow the patches to be applied in the confined space within the Hercules wing. These included

(*a*) the use of a vacuum attachment to remove the abrasive during grit-blasting of the ribs,

(*b*) the application of the required pressure using hand-closed toggle clamps, and

(*c*) the use of silicone rubber heating tapes both to supply the required heating and to act as a compressible layer to help maintain the pressure during curing of the adhesive.

Using this procedure patches have been applied to reinforce many ribs containing small cracks (up to 25 mm from rivet holes) in one aircraft (Fig. 17) and, since then, NDI inspection has shown no further crack-growth during one year of normal operation.

Quite recently, examples of long cracks were discovered in another aircraft; these cracks were both about 280 mm long (extending ~140 mm either side of the rivet holes) and situated in corresponding positions in each wing. One crack was repaired using the standard procedure (Fig. 20) and the other using the fibre composite technique (Fig. 21). The former required about 5 man-days and the latter only 1 man-day. The repair of these two, essentially identical, cracks has given an ideal opportunity to compare subsequent performance of the two repair schemes, particularly in those regions at the ends of the two repairs where far greater stress concentration could occur with the standard repairs.

3.2 Macchi Landing Wheels

Problems have been encountered with cracking in service of magnesium alloy landing wheels—a typical example being those of the Macchi trainer. This is another situation where crack-length is carefully monitored; wheels are normally discarded when the crack approaches 25 mm in length; although wheels containing cracks many times this length have not failed catastrophically.

The thickness of the material in the cracked region is ≃15 mm. At the present stage of the reinforcing art, reinforcement of such thick material would not normally have been contemplated since the area available for bonding, and thus stress transfer into the patch, was rather limited. However, examination of the fracture surfaces showed that the cracks initiated at, or close to, the outer surface of the wheel and then propagated far more rapidly along the surface than through the thickness; even a crack of ~170 mm surface length had not fully penetrated the thickness of the wheel. Thus, the stressing situation was comparatively unusual in that the tendency for the crack to open obviously decreased rapidly with depth of penetration. Under these circumstances, the patching scheme was considered a feasible means of alleviating the problem. Since the number of fatigue striations on the fracture surfaces was only of the order of a few hundred, the failures were considered to result from high stress-low cycle fatigue with probably no more than one cycle per landing.

The experimental approach taken was to machine specimens (approximately 120 mm × 25 mm × 17 mm) from blocks of magnesium alloy supplied by the wheel manufacturer. Vee-notches of depth 2·5 mm were machined across the 25 × 120 mm faces and the specimens fatigued in four-point bending until cracks ~2·5 mm long were produced from the notches. The specimens were then machined to 14·5 mm thickness, to remove the Vee notches and to leave flat surfaces containing a sharp crack. A series of these specimens were then fatigue-loaded (again in four-point bending) at 6 cycles/min, to establish the loading conditions which would cause failure in about 400 cycles.

BFRP patches, 25 × 25 mm, were bonded onto the surfaces of two pre-cracked specimens with the boron fibres transverse to the cracks. The first patch was made from three layers of BFRP pre-preg. This specimen, when fatigue-loaded under the standard conditions for 1200 cycles showed no crack-growth. The load was then increased by 11% and a further 1000 load cycles applied, after which only 0·1 mm crack-growth had occurred. The second specimen was reinforced using a patch made from two layers of BFRP pre-preg. Here, the standard fatigue-loading conditions were applied for 3000 cycles, during which no crack-growth was observed. Although, from these results, the thinner patch appeared adequate, the safety factor was increased by using the thicker (3 layer) BFRP patches for reinforcing the wheels; the additional cost per wheel is less than $1.

Matched dies of mild steel were manufactured for production of patches with the three-dimensionally curved surface required to match the surface contour of the wheels. Such steel dies can be quickly and accurately made, particularly when numerically controlled machining facilities are available, and are cost-effective when large numbers of identical patches are required. However, cheaper means of making suitable dies are being investigated for applications requiring more complex shapes or a limited production of patches. Recently a method of moulding the patch directly from the surface of a similar component was developed; this technique will provide great cost savings in future applications.

The pre-formed patches were bonded to the wheels so that the ends of the cracks were covered (Fig. 22). The composite and metal surfaces were prepared by alumina grit-blasting and degreased with MEK. When curing the AF126 adhesive, pressure was applied by clamping a rubber-faced pad (contoured to the required shape); the bonding temperature was achieved by heating the whole assembly in a small oven.

One cracked wheel reinforced using this technique has been in service for several months, during which time the aircraft has landed ~500 times without further detectable crack-growth; without the reinforcement, sufficient crack-growth would have occurred for the wheel to be no longer serviceable.

4. CONCLUSIONS

This paper has reviewed a large part of the work directed towards using high performance fibre composites for the reinforcement of cracked aircraft structures.

The two practical repair schemes which have been attempted, one being an alternative to an existing procedure and the other a repair which could probably only be achieved using the fibre composite method, have been very successful, from the points of view of both cost-effectiveness and mechanical efficiency.

The undesirable residual tensile stresses introduced into the light alloy substrate during the patching procedure, due to the mismatch of thermal expansion, do not appear to have a major practical effect on the subsequent fatigue or stress-corrosion behaviour of the metal. The problem of internal stress could be avoided if a suitable adhesive curing at room temperature were available. However, of the adhesives examined, only those curing at high temperature had the properties required for the repair application. The requirement of a simple surface preparation for bonding, which is unlikely to encourage other problems such as stress-corrosion, restricts the choice of adhesive even further and, of those examined, the most suitable is AF126.

Further work is needed to obtain maximum benefits from composite reinforcements. Areas of such work include design, behaviour of adhesive systems under various environmental conditions and evaluation of new adhesives with particular emphasis on those with lower curing temperatures.

5. ACKNOWLEDGEMENTS

The authors wish to thank Mr. J. D. Roberts for assistance with the experimental work and the patching of Hercules wing planks, Mr. M. J. Davis for carrying out the evaluation tests and patching of Macchi wheels and Mr. R. Ellis for carrying out the compression tests on Hercules wing plank specimens.

REFERENCES

1. Dial, D. D., and Howeth, M. S. — Advanced Composite Cost Comparison. SAMPE, vol. 16, pp. 302-14, 1971.
2. Davis, M. J., and Baker, A. A. — Adhesive Strength Tests of Bonded Dissimilar Materials using a Step-Lap Sandwich Specimen. ARL Mat. Note 113, February 1976.
3. Davis, M. J. — Shear Stresses in Adhesive Layers of Bonded Step-Lap Sandwich Specimens. ARL Mat. Note 109, May 1975.
4. Baker, A. A. — Evaluation of Adhesives for Fibre Composite Reinforcement of Fatigue-Cracked Aluminium Alloys. ARL Mat. Report 97, July 1975.
5. Lumley, E. J. — Corrosion of Aluminium Alloys in Contact with Carbon Fibre Reinforced Plastic and with other Materials. ARL Mat. Note 108, February 1975.
6. Takeshi Kanazawa *et al.* — Some Basic Considerations of Crack Arresters, Parts I–V. Journal of the Society of Naval Architects of Japan, RAE Library Translation 1648, March 1972.
7. Mitchell, R. A., Wooly, R. M., and Chwirut, D. J. — Analysis of Composite-Reinforced Cutouts and Cracks. Journal American Institute of Aeronautics and Astronautics, vol. 13, No. 6, pp. 744-49, June 1975.
8. Coyle, R. A., and Baker, A. A. — Analytical and Experimental Investigation of the Influence of Bonded Patches on a Centre Cracked Panel. ARL Mat. Report (to be published).
9. Paris, P., and Erdogan, F. — A Critical Analysis of Crack Propagation Laws. Journal of Basic Engineering, vol. 85, pp. 528-32, 1963.
10. Baker, A. A. — Fatigue of Fibre-Composite Reinforced Metals. ARL Mat. Report (to be published).
11. Sager, G. E., Brown, R. H., and Mears, R. B. — Tests for Determining Susceptibility to Stress-Corrosion Cracking. Proceedings of Symposium on Stress-Corrosion Cracking of Metals, pp. 255–72, Symposium held December 1944—proceedings published by ASTM and AIMME, August 1945.

TABLE 1

Advantage and Disadvantage of the Use of Carbon and Boron Fibre Reinforced Plastics Compared to Metals for Patch or Reinforcement Materials

Property	*Advantage*
High stiffness and fatigue strength	Minimum patch thickness
Environmental stability	No need to coat patch
Non-conducting (boron fibres)	No danger of electrochemically induced corrosion of metallic component
Low density	Minimum weight patch and minimum balance disturbance on rotating components
Formability and tailorability of properties	Patches with complex curves and suitably orientated properties can be produced by a simple fabrication technology
	Disadvantage
High material cost	Limits use in large amounts – not usually a problem with patches
Low expansion coefficient	Can lead to undesirable tensile stresses in the metallic component
Limited storage life of raw material	May require refrigeration unless patches are preformed
Conducting (carbon fibres)	Can cause electrochemical corrosion of metallic component unless suitably insulated

TABLE 2

Materials Used for Fibre Composite Strips

Composite	Fibre			Matrix	Comments
	Diameter μm	Modulus GPa	Expansion Coefficient $\times 10^{-6}$ per C°		
CFRP	8	190	0·5	Epoxy Shell 828/DDS	Supplied as a sized warp sheet by Hyfil Ltd., U.K.
BFRP	100	390	5	Epoxy Bloomingdale BP907	Supplied as pre-preg tape with the fibres held on 25 μm glass cloth by Hamilton Standard, USA
BFRA	140	390	5	Aluminium Alloy 6061 annealed	Supplied as a mono-layer sheet by AVCO Systems Division, USA

TABLE 3

Adhesives Used and their Curing Conditions

Code	Type	Trade Name and Supplier	Curing conditions and composition
A	Ethyl-Cyanoacrylate	White Label Pearl Chemical Co., Japan	Ambient temperature set (+12 hours at 40°C optional) (one component)
B′	Flexibilized Epoxy (Polyamide cure)	AY 106/HV953U CIBA Ltd., U.K.	19 hours at 90°C (100 pbw 106 to 80 pbw 953)
B	Flexibilized Epoxy (Polyamide cure)	EC 2216 B/A 3M Company, U.S.A.	19 hours at 90°C (100 pbw base to 140 pbw hardener)
C	Rigid Epoxy (amine cure)	AY105/HY956 CIBA Ltd., U.K.	15 hours at 100°C (100 pbw 105 to 23 pbw 956)
D	Epoxy-Nitrile film (supported with a Dacron fibre mat)	AF 126 3M Company, U.S.A.	4 hours at 125°C under a pressure of 0·35 MPa (one component)

TABLE 4

Details of Surface Treatments

Surface Treatment	Adhesive	Details
Chromic Etch	A, B′	(*a*) Freon TF spray degrease. (*b*) Alkaline clean in TURCO 4215, 10 minutes at 60–70°C (*c*) Tap water rinse 5 minutes. (*d*) Deoxidise in sodium dichromate (33 gm *l*) sulphuric acid (310 g *l*) 15 minutes at 65°C. (*e*) Tap water rinse 10 min. (*f*) Dry 50°C.
Chromic Etch, Phosphoric Anodise	B, C, D	As above to stage (*e*) plus— (*a*) Anodic treatment in phosphoric acid solution (90 gm *l*) at 10V for 25 minutes. (*b*) Tap water rinse 15 minutes. (*c*) Dry 50°C.
Grit blast	C	(*a*) MEK degrease. (*b*) Alumina grit blast (50 μm grit). (*c*) MEK degrease

TABLE 5

Strain Measurements and Estimated Effective Shear Moduli after Five Minute Relaxation for a Number of Specimens

Adhesive	Strip	t_L mm	e_u/e_s^o	G_L GPa
A	7075	0·09	0·016	0·8
	CFRP	0·07	0·022	0·7
	BFRP	0·09	0·036	0·7
	BFRA	0·09	0·040	0·8
B′	7075	0·05	0·056	0·3
B	CFRP	0·11	0·400	0·2
	BFRA	0·09	0·140	0·5
C	7075	0·09	0·012	0·8
	CFRP	0·05	0·000	1·1
	BFRP	0·11	0·019	1·0
	BFRA	0·11	0·023	0·9
D	7075	0·07	0·010	0·9
	CFRP	0·09	0·007	1·0
	BFRP	0·11	0·017	0·9
	BFRA	0·11	0·022	0·9

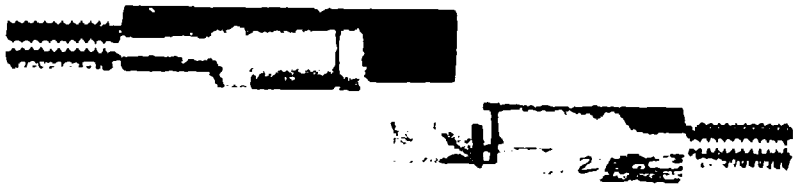

(a)

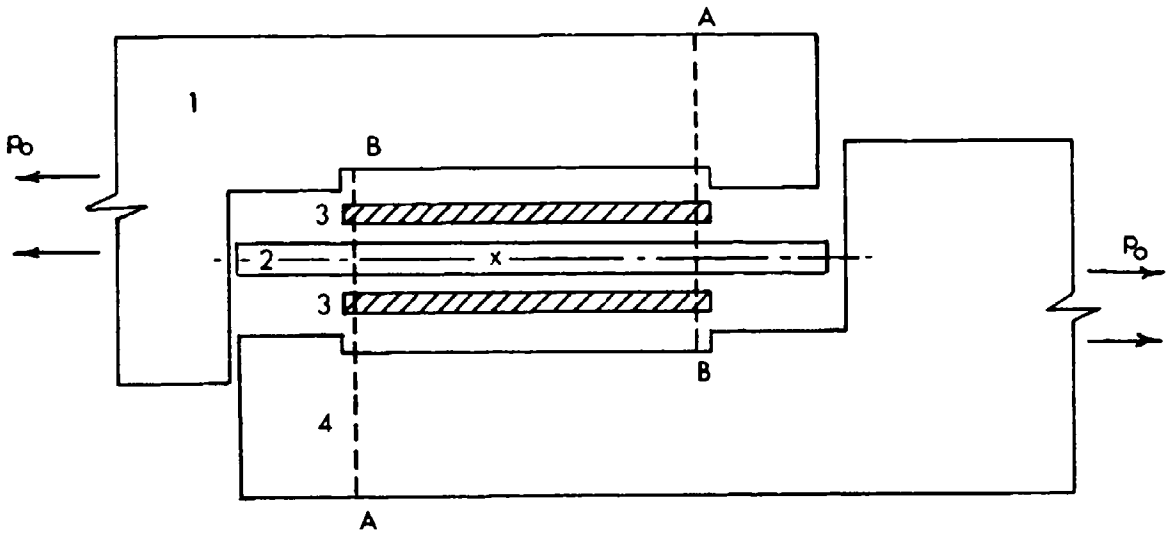

Regions 1 and 4 – Adherend A

Region 2 – Adherend B

Regions 3 – Adhesive

(b)

Fig. 1. Step-lap shear strength test specimen.
a. general view.
b. section of bonded region, cuts are made along the lines A B after bonding.

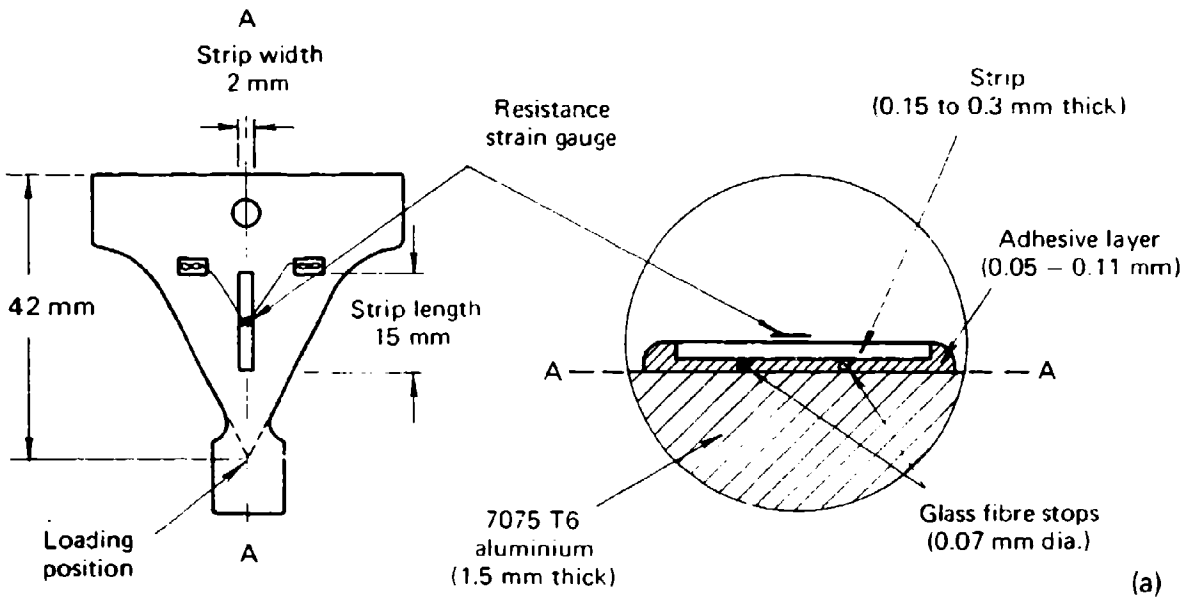

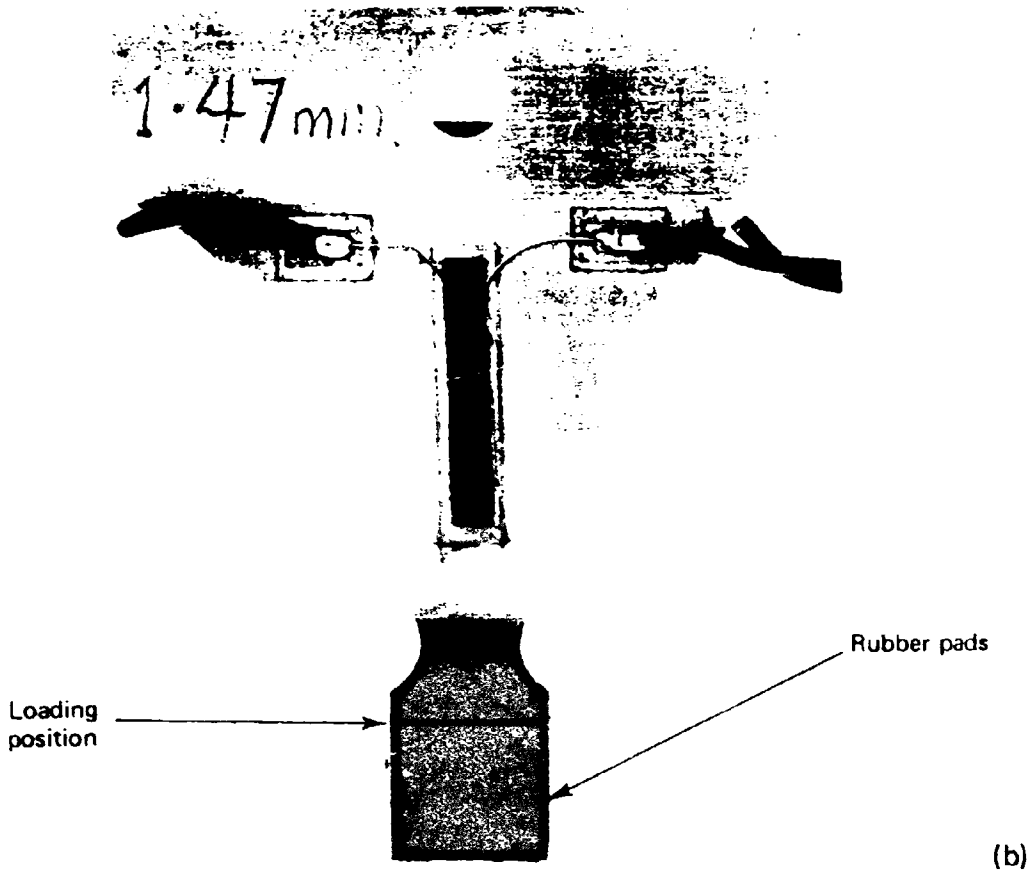

Fig. 2a. Schematic illustration of CSC specimens showing adhesive layer configuration

Fig. 2b. A CSC with a CFRP patch after fatigue.

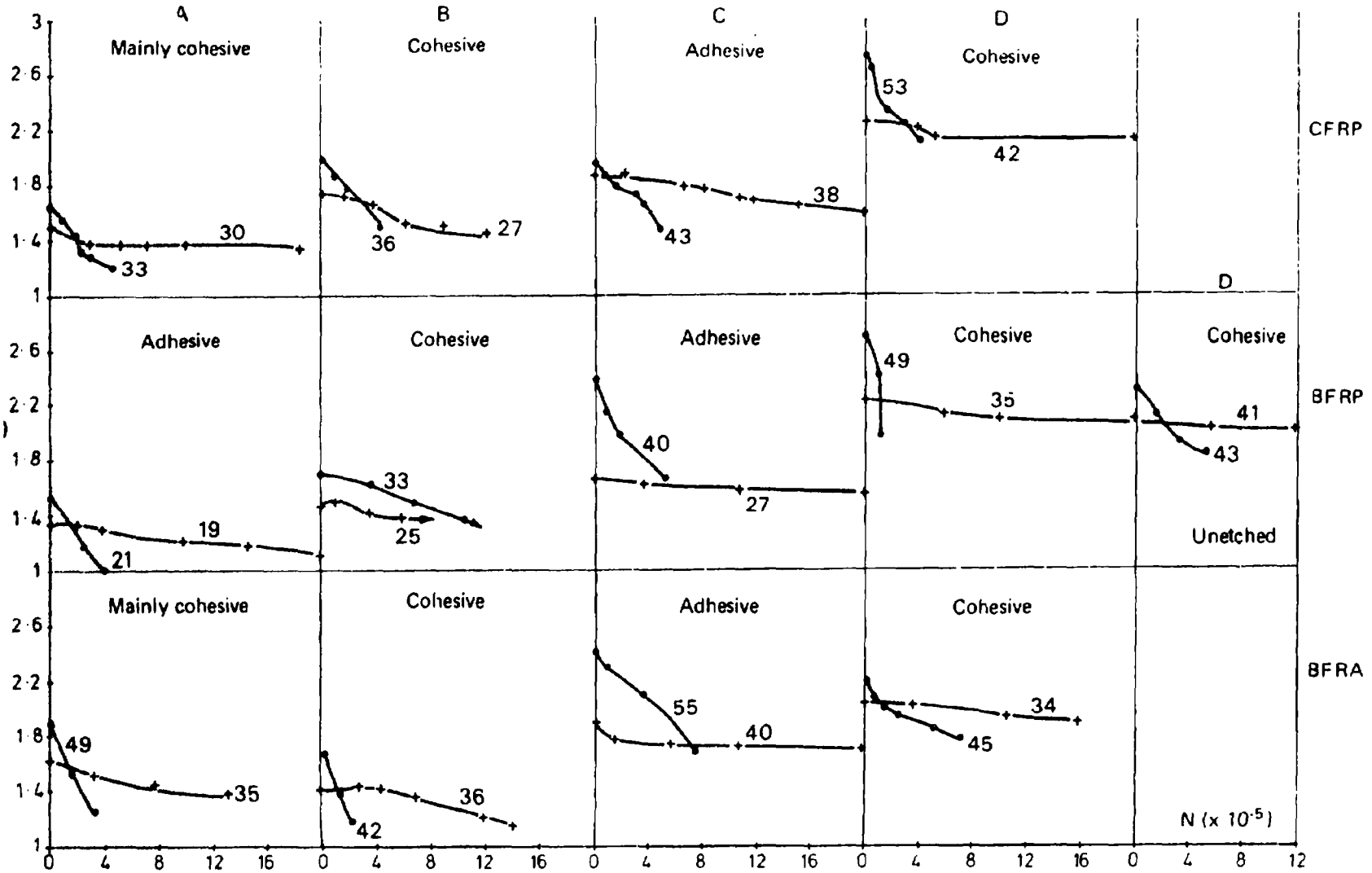

Fig. 3. *Plots of semi-cyclic strain range in the strip* ($\frac{e_s}{2}$) *versus number of cycles* (N) for the various strip/adhesive combinations. The numbers refer to the theoretical shear stress in the adhesive in MPa. The nature of the fatigue cracking observed is noted.

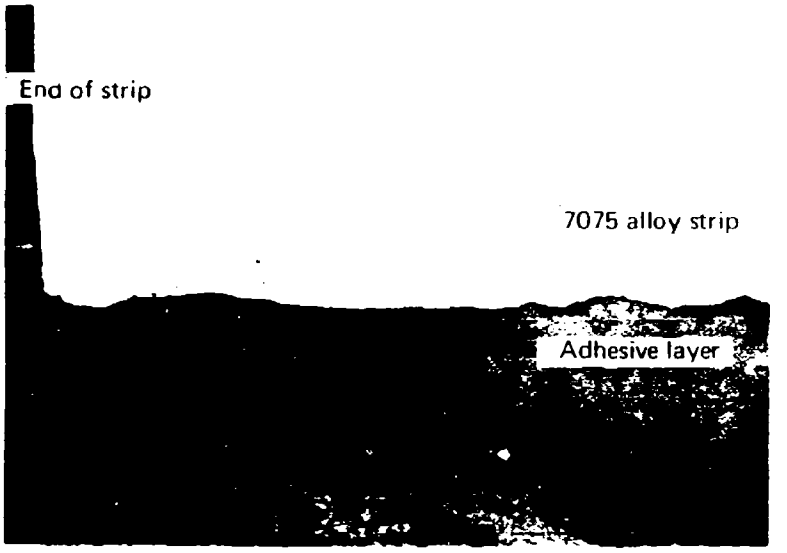

Fig. 4.

Micrograph of a 7075/A specimen fatigued at a nominal shear stress of ± 33 MPa, showing pronounced ± 45° fatigue cracking close to edge of strip, t_L = 0.05 mm

taper magnification x 3

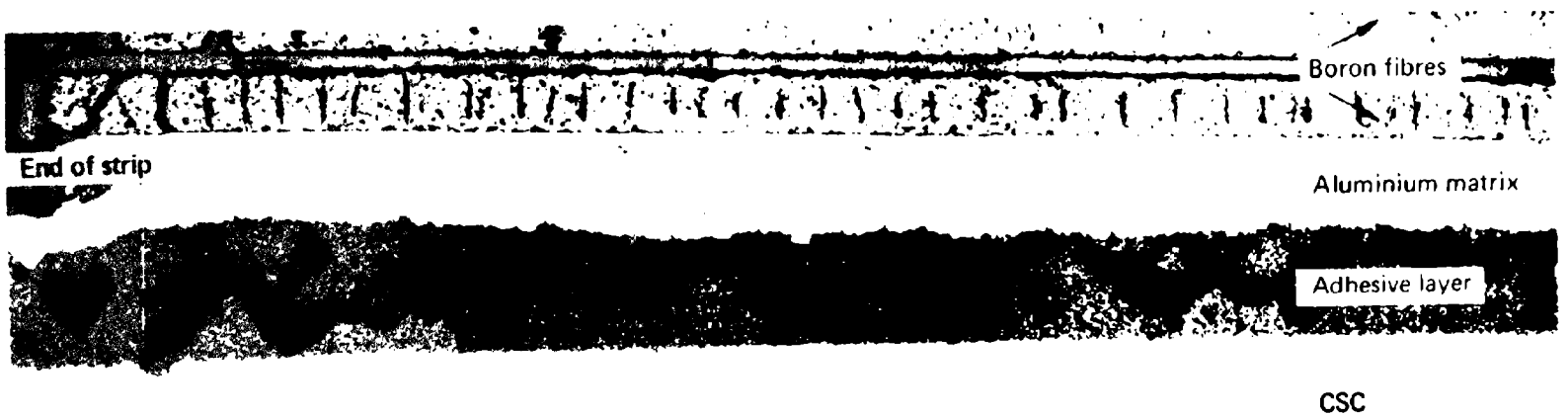

Fig. 5. Micrograph of a BFRA/B specimen, fatigued at a nominal shear stress of ± 36 MPa, showing cohesive failure by fatigue crack propogation on approximately ± 45° planes. t_L = 0.08 mm.
taper magnification x 3

Fig. 6. Micrograph of a BFRP/D specimen fatigued at a nominal shear stress of ± 40 MPa, showing that cohesive fatigue cracking is strongly influenced by the presence of polymer reinforcing fibres, t_L = 0.1 mm

taper magnification x 3

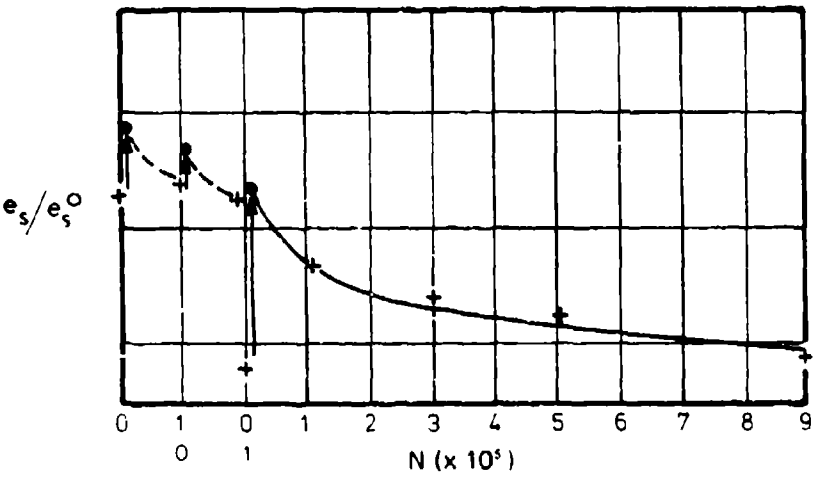

Fig. 7. Plot of e_s/e_s^o versus N for a B F R P/D specimen showing the effect of "repairs", at stages indicated by vertical arrows, effected by applying adhesive A to the patch area.

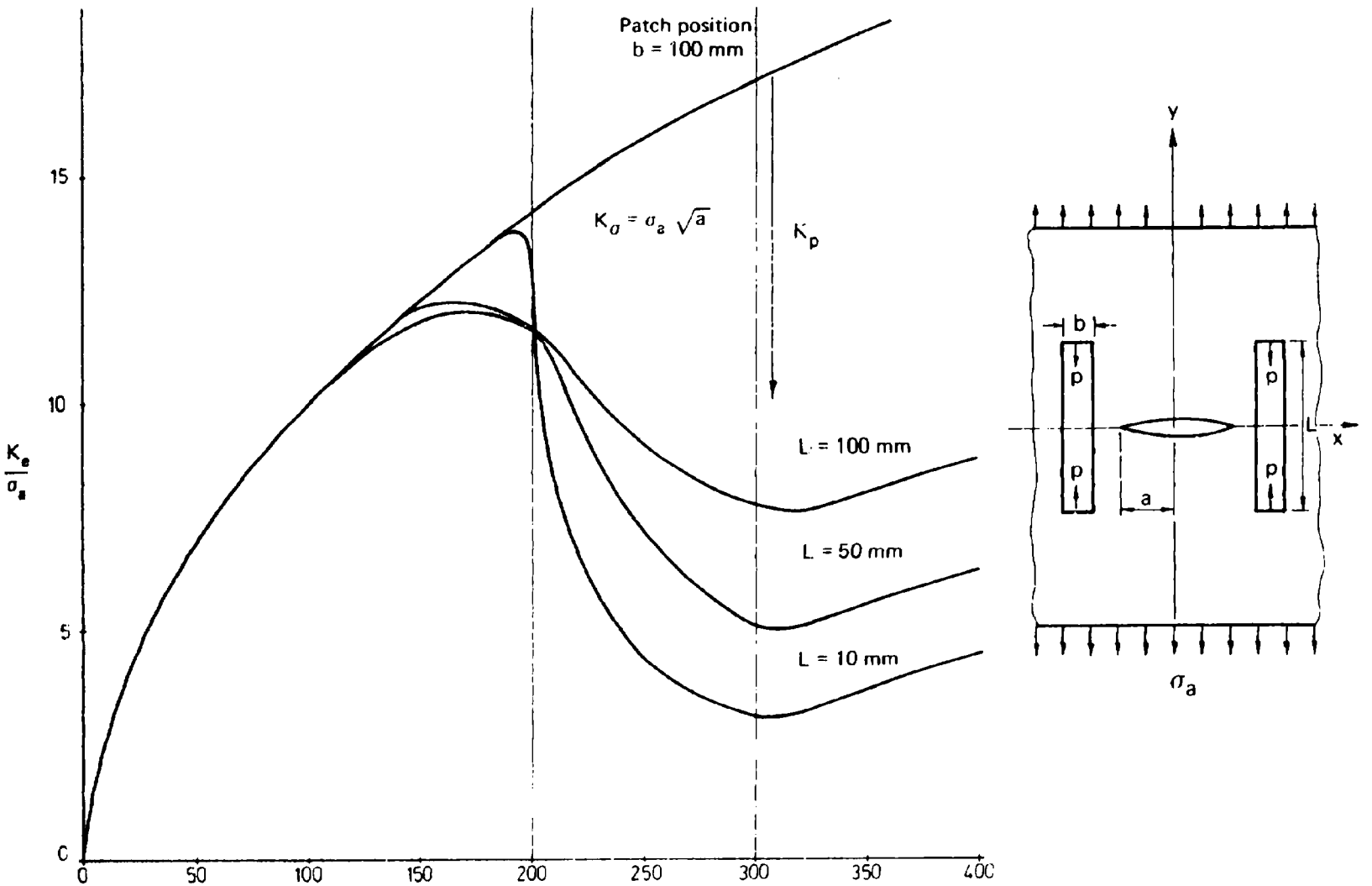

Fig. 8. Plot of theoretical effective stress intensity Ke versus crack length for a patched centre notched plate (shown schematically inset) with patches of various compliances at the position indicated.

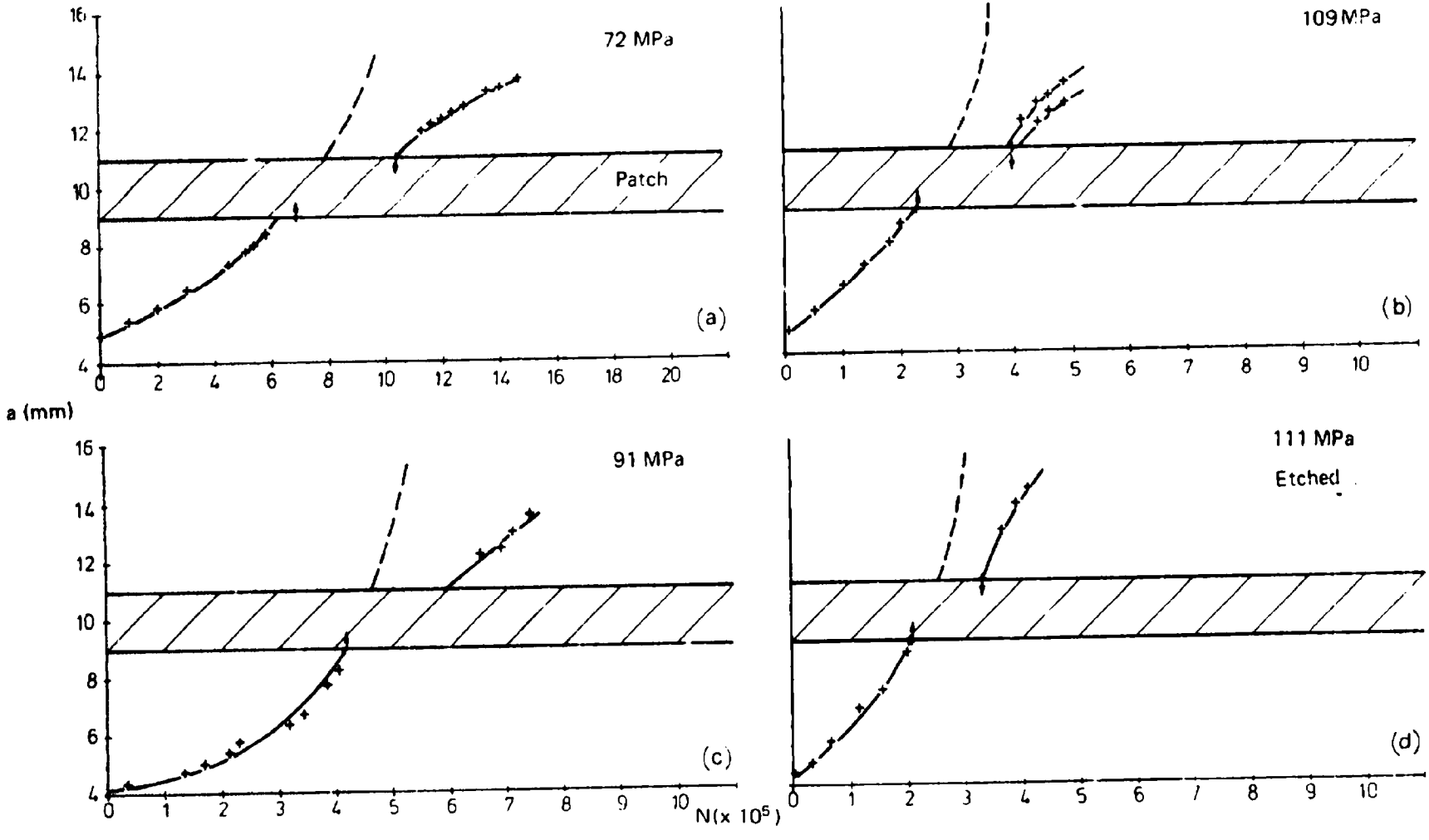

Fig. 9 Plots of crack length a versus N for BFRP patched specimens. Specimen for which results are plotted in (d) was given full etching treatment whilst the others were only grit blasted. Nominal stress levels are indicated on each plot. Dashed lines indicate the expected rate of crack growth in the absence of the patch.

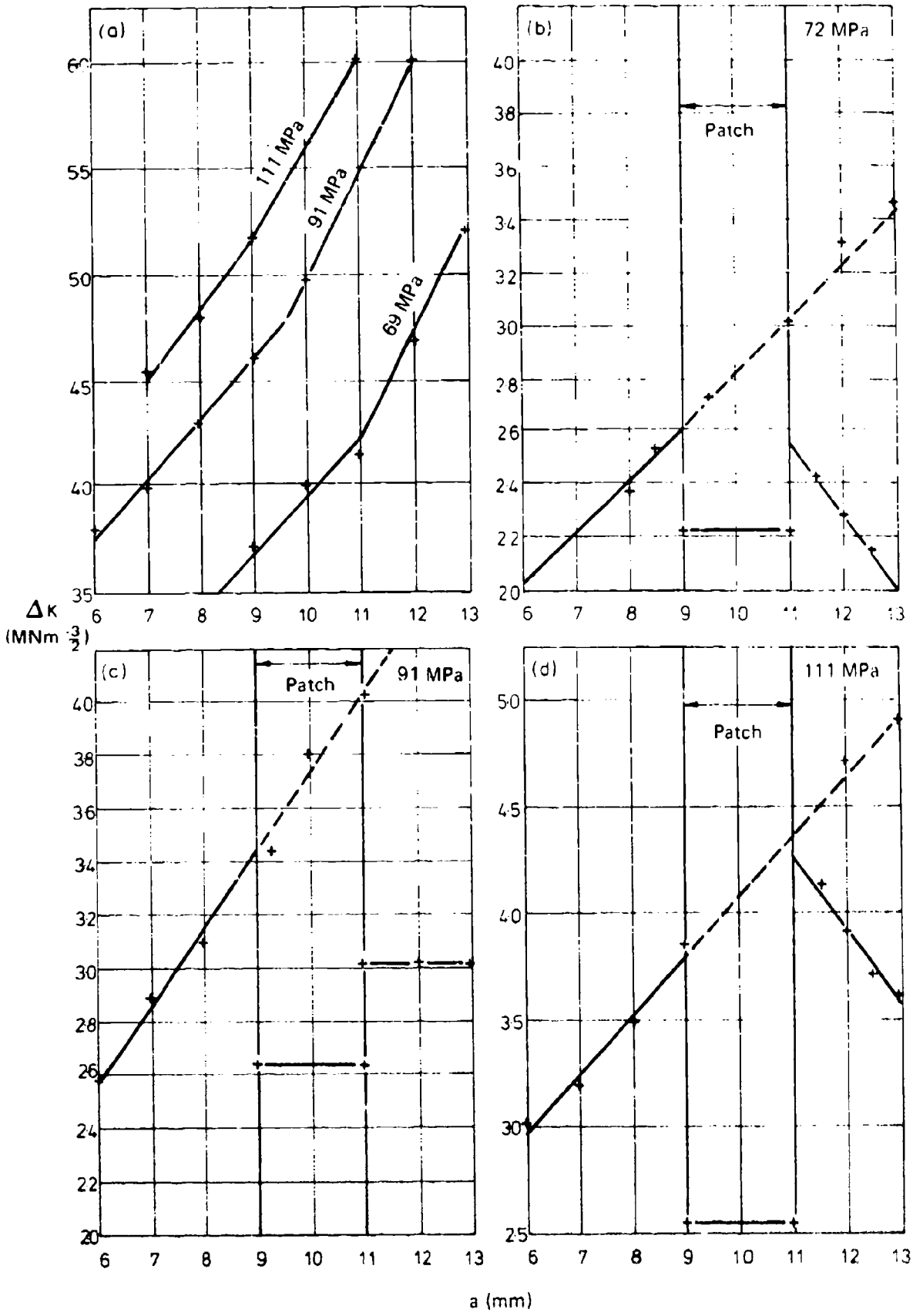

Fig. 10. Plots of stress intensity range ΔK (calculated from crack propagation rates) versus crack length,a, for (a) unpatched specimens and (b), (c), and (d) BFRP/D patched specimens. Nominal stress levels are indicated on each plot. Dashed lines indicate the expected relationships in the absence of the patch.

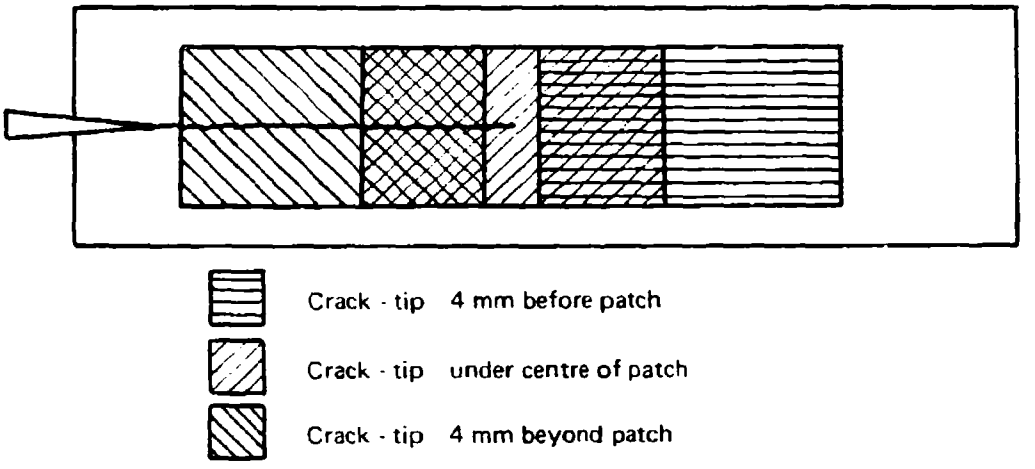

Fig. 11. Schematic illustration of specimen used for stress – corrosion studies showing the three patch locations.

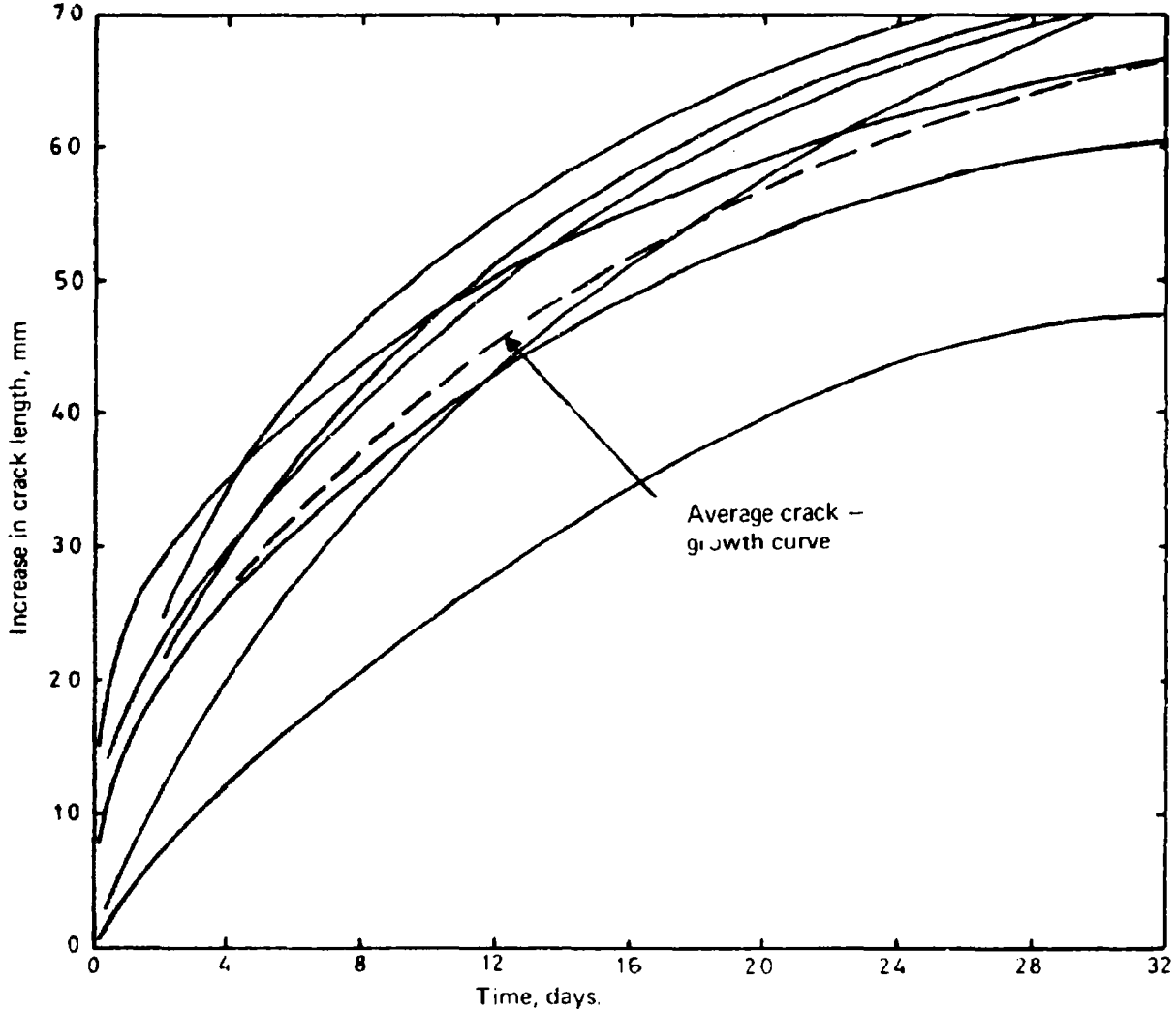

Fig. 12. Plots of crack growth versus time for wedge loaded stress-corrosion specimens.

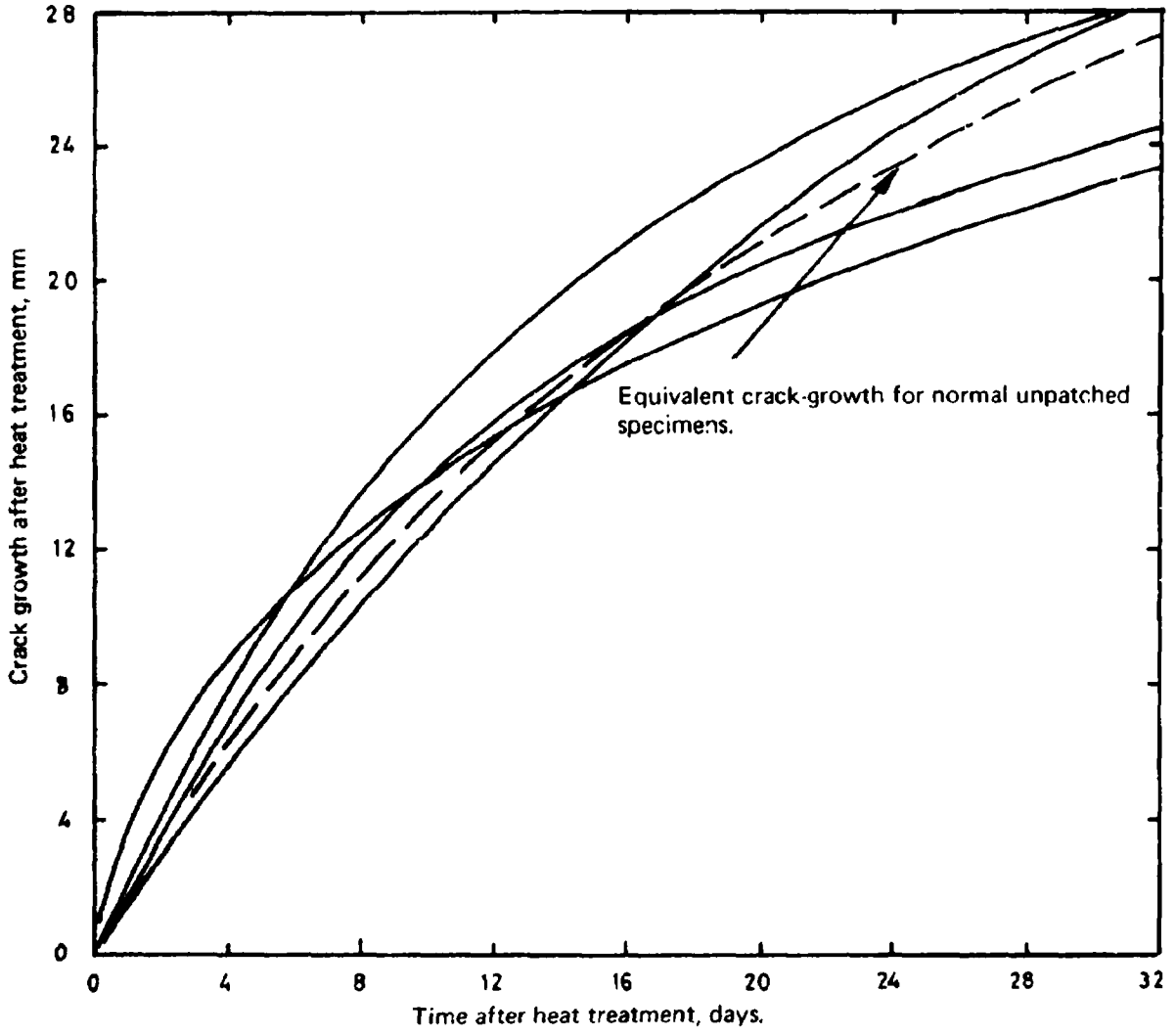

Fig. 13. Plots of crack-growth versus time for wedge loaded stress-corrosion specimens subjected to the thermal treatment used for patching.

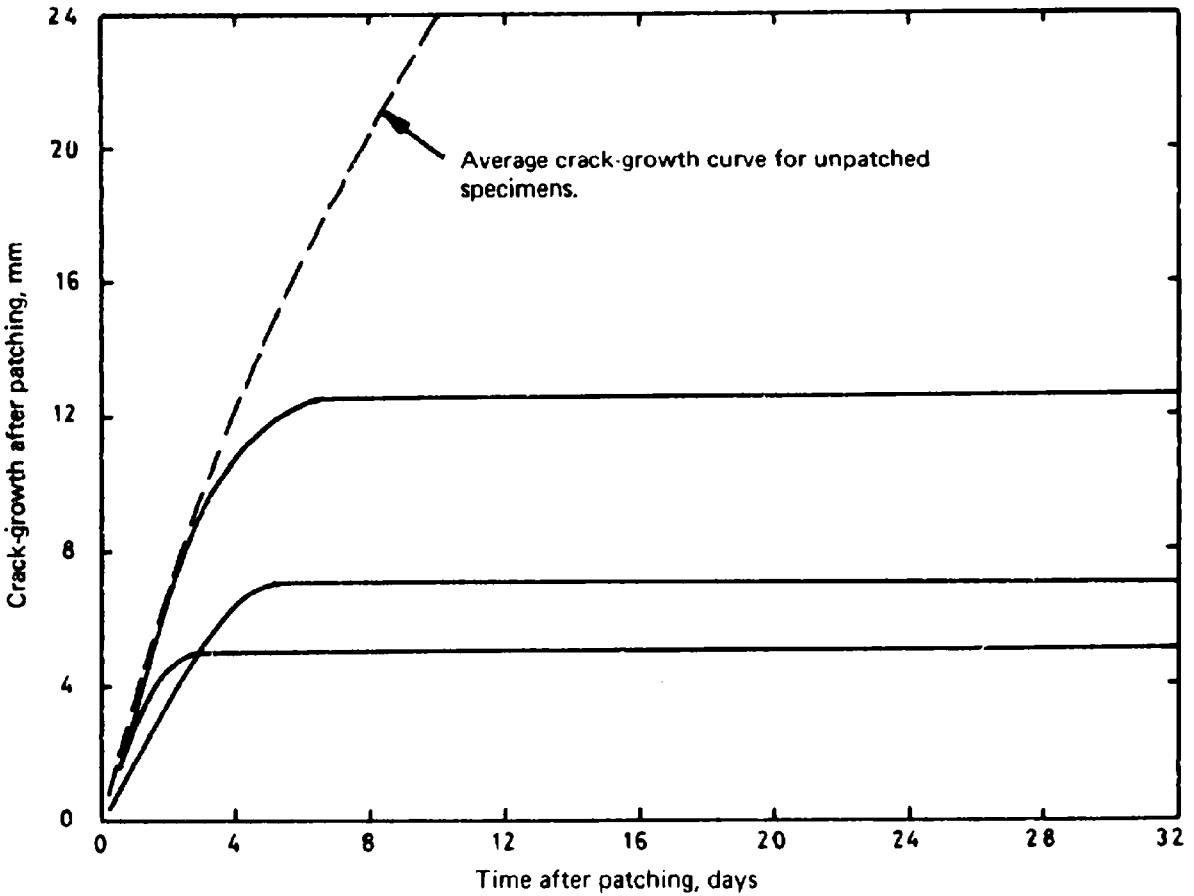

Fig. 14. Plots of crack-growth versus time for wedge loaded stress-corrosion specimens patched 4 mm ahead of the crack tip.

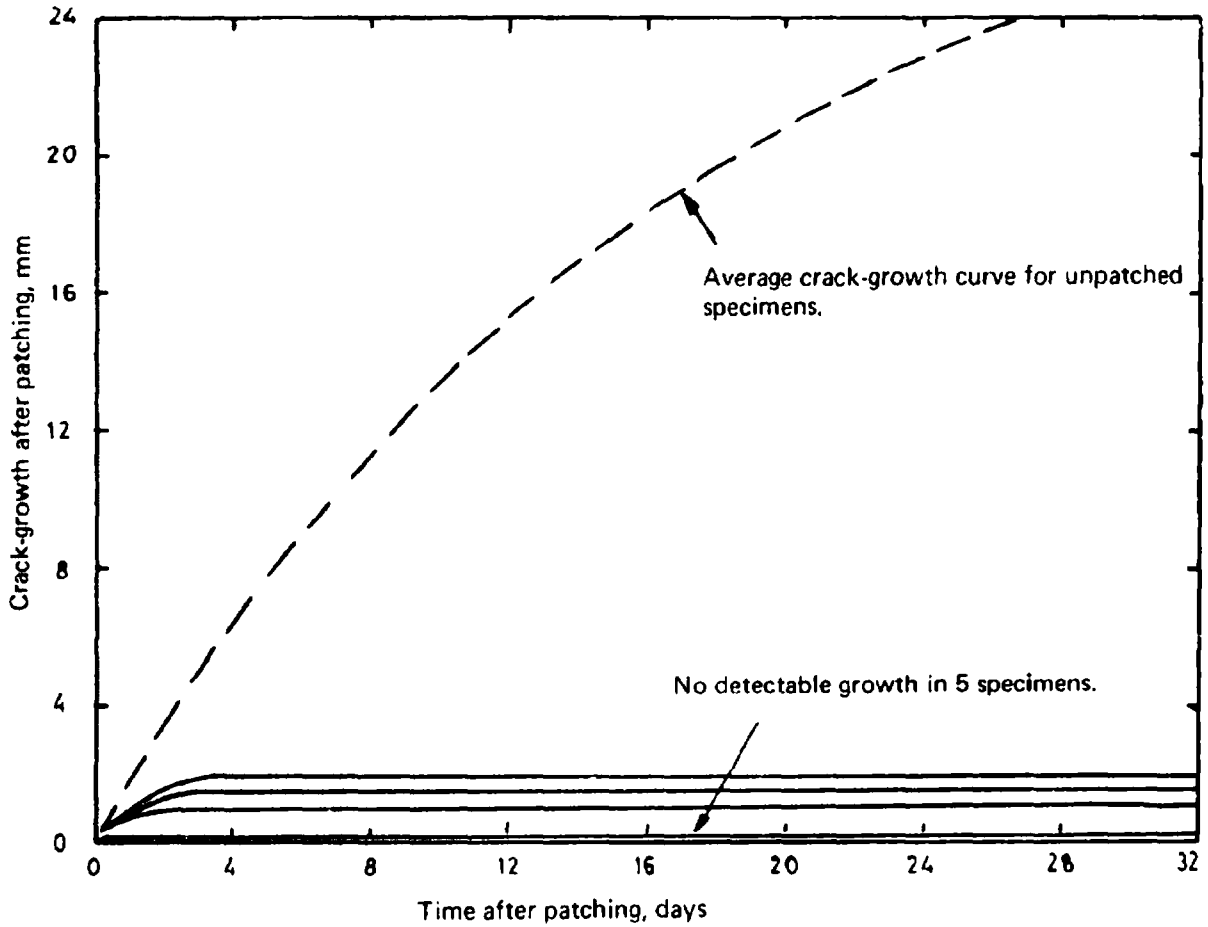

Fig. 15 *Plots of crack-growth versus time for* wedge loaded stress-corrosion specimens reinforced with the crack tip centrally under the patches.

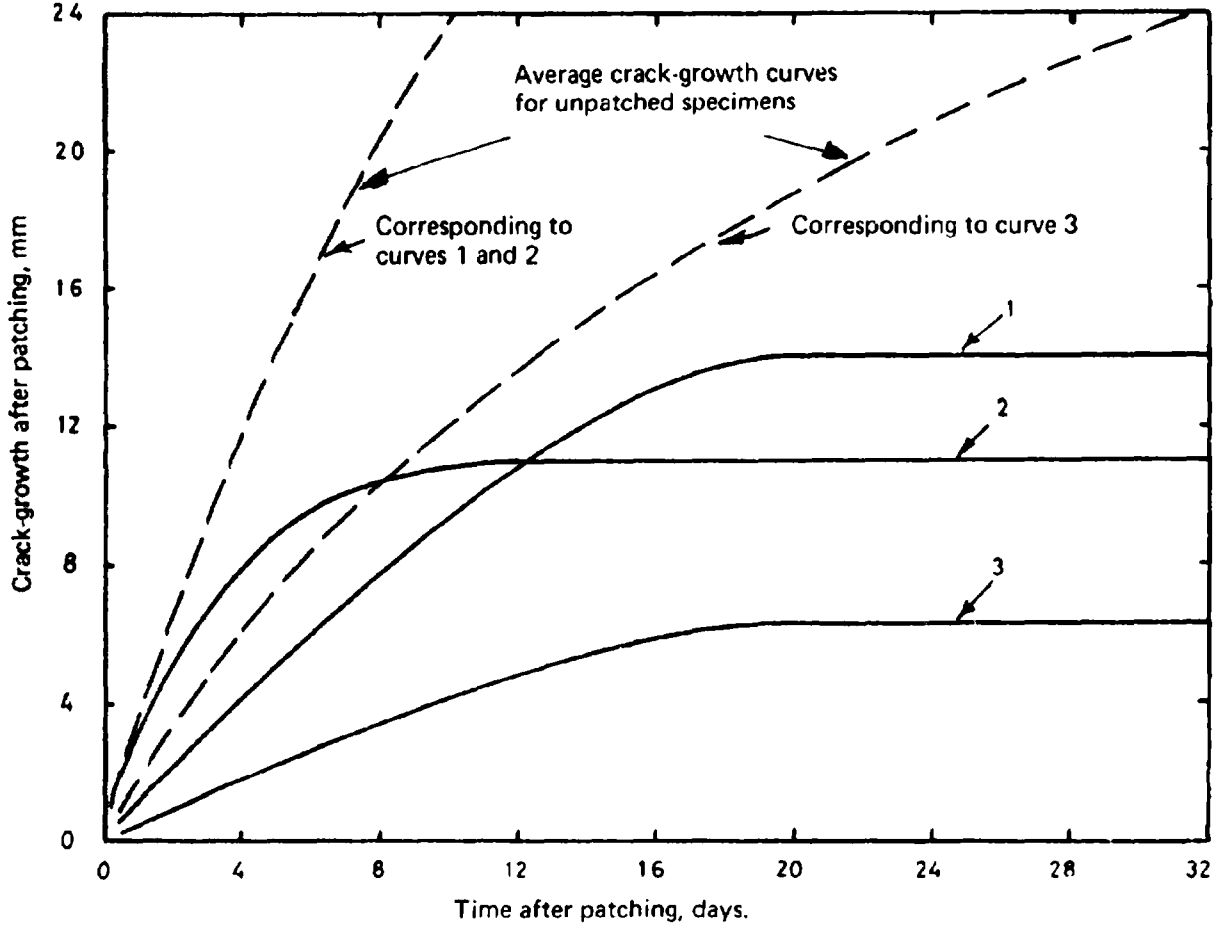

Fig. 16. Plots of crack-growth versus time for wedge loaded stress-corrosion specimens reinforced with the crack tip extending 4 mm beyond the patches.

Fig. 17. General view of underside of an upper Hercules wing plank showing examples of BFRP patches bonded over cracks. The repair, second from left, shows the coating of sealant (SR 1422A) which is applied after bonding.

Fig. 18. Three test panels constructed from Hercules wing plank material after testing under compression.
a. uncracked
b. cracked
c. cracked then reinforced with BFRP patches.

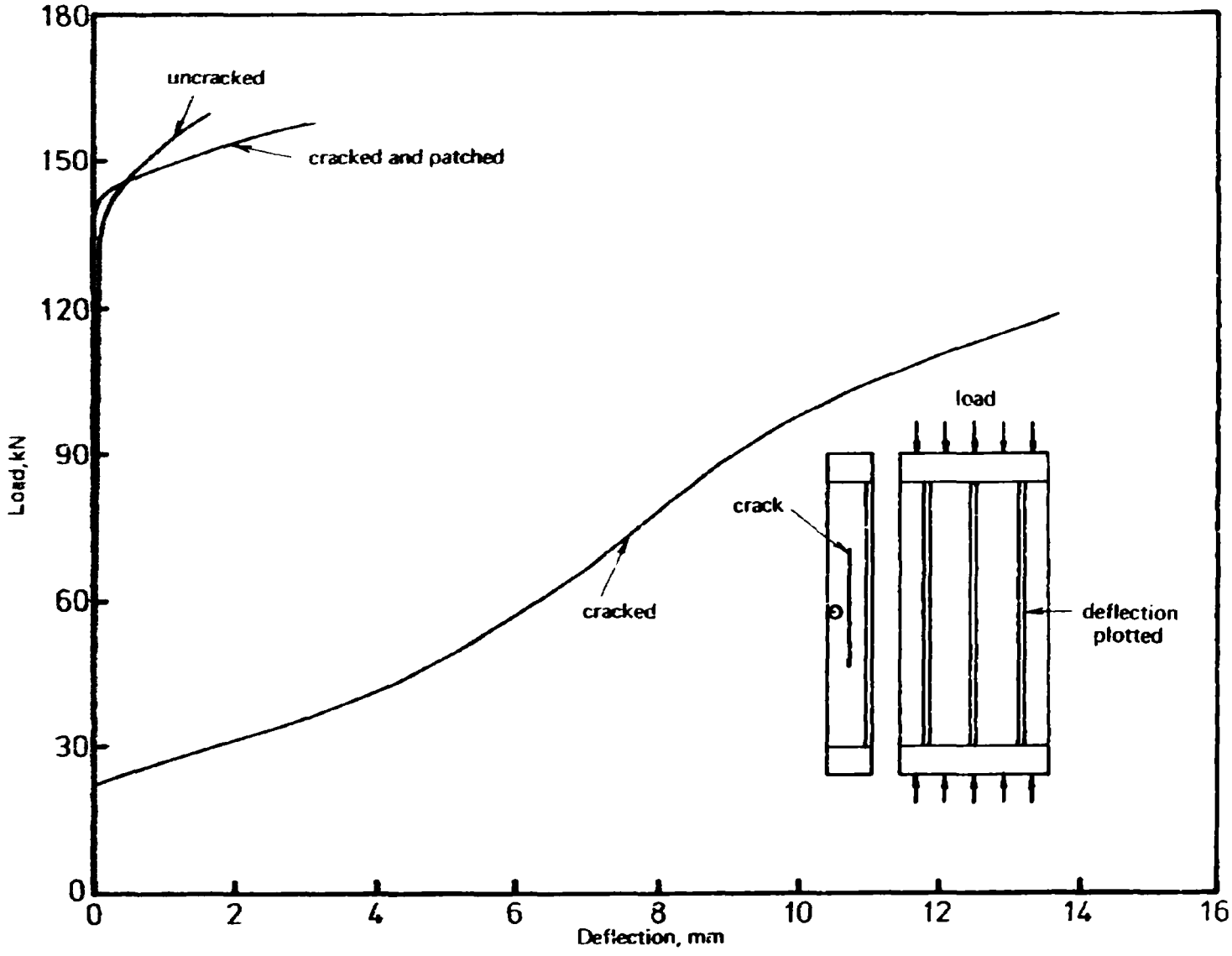

Fig 19 Load/deflection curves for wing plank compression test specimens; measurement positions are indicated in schematic diagram.

Fig. 20. Standard repair scheme used for long cracks in Hercules wing planks.

Fig. 21. BFRP composite repair scheme applied to a long crack in a Hercules wing plank.

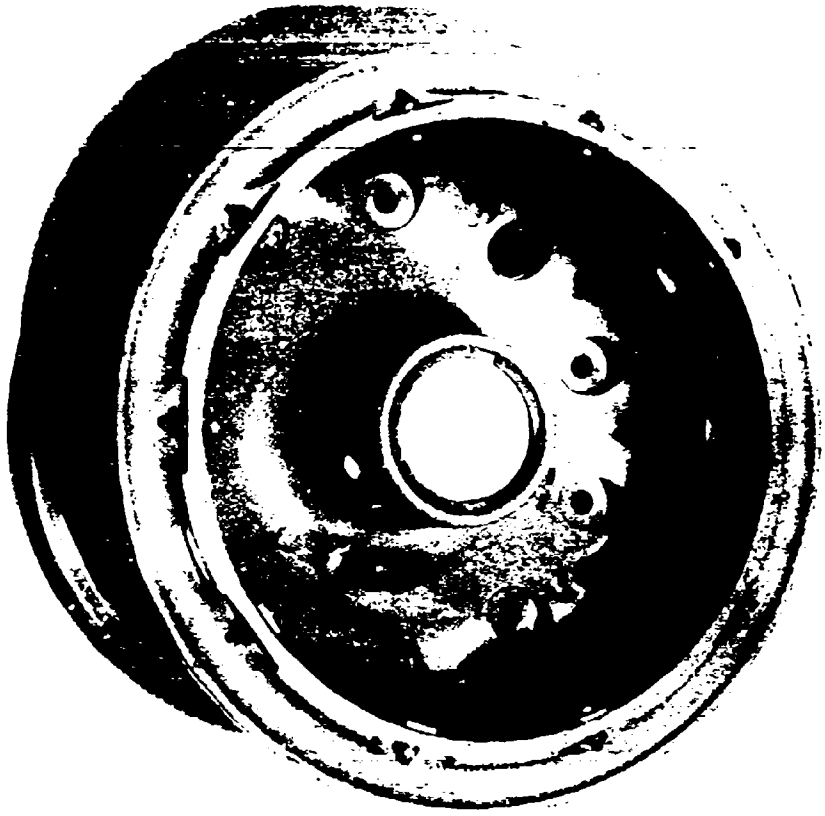

(a)

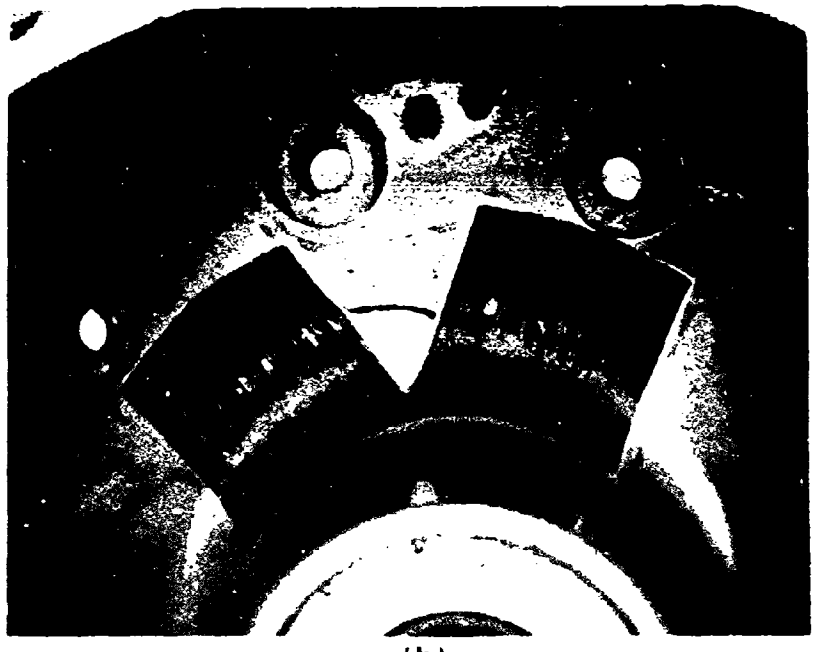

(b)

Fig. 22 Macchi landing wheel.
a. general view showing location of typical crack.
b. BFRP composite patches bonded over ends of crack.

DISCUSSION

QUESTION *Grp. Capt. I. Sutherland (RAAF)*

Concerning the practical application of these patches, since simple aircraft repairs are normally not "designed" as such but rely on replacement of lost material, would it not be possible to produce standardized repair patches on a material gauge size basis?

Authors' Reply

Design of the repair based only on the replacement of lost strength or stiffness in a cracked component may not be adequate, particularly if there is danger of serious failure should the crack propagate out of the repaired region. In general, some verification of the patching scheme would be necessary either experimentally, as for the two examples given in the paper, or theoretically based on the effective stress intensity in the component and shear stresses in the adhesive layer.

In a worn or corroded component, however, repair based on the replacement of lost material, on an effective gauge-size basis, should be satisfactory. The fibre composite material is most efficiently used for this purpose when replacing strength or stiffness in only one direction; however, biaxial reinforcement can be obtained by arranging the fibres, in the repair patch, at various angles. The need to tailor the form and mechanical properties of the composite patch for each type of repair may make the production of useful standard patches for a wide range of repairs difficult.

QUESTION—*B. A. Parker (Monash University)*

Bearing in mind what you said about the ease of application of patches by unskilled personnel, are there any difficulties in ensuring the quality of the adhesive bond (i.e. control of regularity and thickness of the adhesive film)?

Authors' Reply

It is most important that a very high level of cleanliness is maintained during the bonding procedure and the correct materials are used. However, we feel that the standards required for bonding the patches could be attained by any reliable operator after limited instruction.

With a supported film and low-flow adhesive, such as AF126, there is little danger of locally squeezing the adhesive out of any area, which would have regions with no bond. However, some variations in the thickness of the adhesive layer probably do occur when pressurising with Toggle clamps, as in the Hercules repair. These thickness variations, while not desirable, are not considered serious and must be accepted to maintain the simplicity of the repair technique.

QUESTION—*Grp. Capt. W. E. Sansum (RAAF)*

Most of the patches displayed were of simple shape or large radius of curvature. What is the ability to mould boron fibre patches to complex shapes and small radius fillets?

Authors' Reply

Boron fibres cannot be moulded to radii less than about 40 mm; however, carbon-fibre composite patches can be moulded to radii of less than 5 mm and would therefore be a better

alternative where patches with severe curvatures are required. Carbon-fibre patches would have to be insulated from the surface of the metal, in most cases, to avoid the danger of corrosion. A thin layer of glass-fibre reinforced plastic can be satisfactorily used as an insulating layer.

Patches with complex curvatures can easily be produced, provided the curvatures fall within the limits stated. However, reinforcement of regions with fillets of very small radius would be very difficult.

QUESTION—*K. G. Conlan*
(RAAF)

What procedures do you recommend for establishing the quality of the bond:
(*a*) when the patch is applied, and
(*b*) later when the repaired component undergoes scheduled or unscheduled maintenance?

Authors' Reply

At this time, for both initial and subsequent inspections of the adhesive bond, a high frequency eddy-current device has proved very successful. This technique, which was developed by Mr. Glanvill of these Laboratories, gives a go or no-go indication of the condition of the bond. Readings on the device are affected both by variations in adhesive thickness and by the presence of debonds; however, an experienced operator can distinguish between the readings from each source. The method used for the Hercules and Macchi patches is to be written up by Mr. Glanvill as an inspection procedure for the RAAF.

THE INFLUENCE OF THE WATER VAPOUR CONTENT AND THE TEMPERATURE OF AN AIR ENVIRONMENT ON THE FATIGUE BEHAVIOUR OF SAE 4340 STEEL

by

D. S. KEMSLEY

SUMMARY

Total fatigue lives, fatigue crack initiation and propagation lives, and fatigue crack propagation rates of notched ($K_t = 3{\cdot}15$) SAE 4340 steel specimens under program loading have been determined in air environments having 45 different water vapour content/temperature combinations. Forty-three of these involved unsaturated (less than 100% RH) conditions.

The maxima in total life and initiation and propagation lives, and the minimum crack propagation rate, did not occur in very dry air, but at 3% to 50% RH at 100°C to 40°C respectively (i.e. from 40°C to 100°C and water vapour contents of 20 to 30 g per kg of dry air). These results are not in conflict with previous work.

As the temperature of air of constant water vapour content is lowered, and the conditions change from an unsaturated to a saturated (100% RH, "fog") environment, a marked reduction in fatigue life occurs. This is due to the combination of a decrease in crack initiation life and a large increase in the rate of crack propagation.

These effects may be interpreted as being due to the production of various hydrogen contents in the specimens because of the various environments, and consequently as differences in the fatigue behaviour of various SAE 4340/hydrogen "alloys". The bearing of the results on the common concepts of "corrosion fatigue" and "atmospheric corrosion fatigue" is discussed.

1. INTRODUCTION

An environment of air saturated with water vapour results in a marked increase in fatigue crack propagation rate and a decreased fatigue life of ultra-high strength steels compared with the corresponding values in an unsaturated air environment at the same nominal temperature.[1-3]

However, the effects of variations in the humidity and temperature of *un*saturated air on fatigue behaviour are not at all clear. On the one hand, higher water vapour content has been associated by some workers with a faster fatigue crack propagation rate[4-6] or shorter total fatigue life,[7-11] while in the case of other workers, no effect has been observed, or was only sometimes present.[12-14] Only one of these studies[11] concerns high strength steel in an air environment of more than two water vapour contents, but it was limited to a single measured temperature of 25°C.

Again, the possible effects of humidity on fatigue crack initiation have apparently been neglected to date. Published experimental evidence is therefore insufficient to conclude that increasing water vapour content of air is always detrimental to fatigue life; in particular, the possible effects of such environmental variations on the fatigue behaviour of ultra-high strength steels are virtually unknown. The work to be described, involving 45 different water vapour content temperature combinations, provides some information in this field.

2. EXPERIMENTAL

2.1 Materials and Specimens

Keyhole-notched (K_t 3·15) fatigue test specimens of the form shown in Figure 1 were manufactured from SAE 4340 nickel–chromium–molybdenum steel of the following average composition: 0·4% C, 1·75% Ni, 0·84% Cr, 0·23% Mo. The specimens were rough machined to approximately 1·25 mm oversize and then heat-treated to the following schedule: austenitize at 816 ± 14 C, quench into warm circulating oil at 38 to 60 C, and temper twice at 355 ± 5°C for one hour. Specimens were then finished machined. The curved plane surfaces of the test section were polished longitudinally to a 600 grit finish, following which the two holes for the stress concentrator were drilled and reamed using high-speed steel drills and solid carbide reamers, and the connecting slot spark machined. Finally, a light 600 grit longitudinal polish was employed to remove any burrs developed during the machining of the keyhole notch.

The heat-treatment resulted in the following average static tensile properties: ultimate tensile strength, 1570 MPa; 0·1% proof stress, 1425 MPa; elongation, 8·4%.

2.2 Load Conditions

Each specimen was tested under repeated tension in a Losenhausen UHS 20 hydraulic pulsator using the four-stage program loading sequence illustrated in Figure 2, commencing with the lowest load range of the program. Most specimens were tested at a rate of 1·25 programs per hour, the remainder being tested at 0·8 programs per hour.

Under the particular machine control conditions used, the cyclic wave form was triangular (saw-tooth), with a faster rate of unloading per cycle than of loading. In a given test, the rates of loading and of unloading were constant during cycling at each of the four load levels in the program. Consequently, the cyclic frequency depended on the load level within a program, and on the rate of program load application, as shown in Table

TABLE 1

Cyclic Frequencies and Rates of Loading During Tests

Rate of program load application (programs/hour)	Rates of loading and unloading in each cycle (MPa/sec)		Cyclic frequency in each load level (Hz)			
	loading	unloading	Level 1	Level 2	Level 3	Level 4
0·8	290	1580	0·7	0·5	0·4	0·3
1·25	495	1580	1·1	0·7	0·6	0·5

Average cyclic frequencies at 0·8 and 1·25 programs per hour were 0·6 and 0·9 Hz respectively (2,594 cycles, i.e. 1 program, in 75 and 48 minutes respectively).

2.3 Environments

Air at constant pressure can contain water as vapour in amounts up to a saturation value which depends markedly on temperature. This dependence is shown by the saturation (100% relative humidity (RH)) line on the psychrometric diagram[15] for standard pressure (Fig. 3), in which all environments to the right of this line are unsaturated, and those to the left represent saturated ("fog") conditions. Curves representing any desired RH of unsaturated air may be constructed, those for 40, 10 and 1% RH being also shown on Figure 3.

At constant pressure, it is apparent that any two of the three variables, viz. water vapour content, RH or temperature, must be known if a particular environment is to be accurately defined and located on the psychrometric diagram. The specification of one or more RHs without the corresponding temperature or water vapour content does not permit meaningful comparisons between environments to be made.

In the present work, both the RH and the temperature of the air inside an environmental chamber which surrounded the specimen were monitored and controlled during each test. The test environments, including two in saturated air, are shown in Figure 3.

Specimen temperature was maintained to within ±1°C throughout each test in unsaturated air by means of a small electrical heating coil around the specimen test section. The coil had widely spaced windings to allow free access of the environment to the stress concentrator. The relative humidity of the air in tests involving unsaturated air was maintained by means of a heated water bath through which initially dry air was continually bubbled at constant rate; RH (or water vapour content) was controlled, within the limits indicated by the length of the vertical line at each environmental point in Figure 3, from a humidity sensor by feedback control to the heater in the water bath.

The saturated air environments were produced by increasing the water bath temperature and rate of airflow sufficiently to provide condensing conditions at the specimen at the required specimen temperature. The heating coil, although present, was not electrically connected in these environments.

The dry air used in all tests was commercial "medical dry breathing air" containing less than 25 parts of water vapour per million parts of air (less than 1 g water vapour per kg of dry air). This was supplied in standard compressed air cylinders which were connected to the environmental chamber by flexible hose through pressure-reducing valves and a flow-meter.

2.4 Observations

One specimen was tested under each of the environmental conditions in unsaturated air, and three under each of the two saturated conditions. Each fatigue test was terminated by complete fracture of the particular specimen, and the total life in programs was recorded.

The fracture surfaces of all specimens tested in unsaturated air exhibited well-defined program markings (Fig. 4*a*). The fatigue crack propagation lives in such tests were determined by counting these markings on enlarged (×20) photographs of the fracture surfaces from the

final markings of the most extensive crack backwards to within a standard actual distance of 0·1 mm from its origin. (Markings in the immediate vicinity of the origin were insufficiently delineated on the fracture surfaces to permit an accurate count-back to smaller crack lengths.) The fatigue crack initiation life was then obtained as the difference between the complete fatigue life and the number of programs counted on the fracture surface.

Measurements were made of the crack depth corresponding to each program marking of the longest crack in those thirteen specimens (1·25 programs per hour) in which the fatigue crack front had extended to the full width of the test section ("through" cracks). From these, the crack propagation rate per program, da/dN, was obtained. The corresponding stress intensity factors, K, were calculated using Newman's stress analysis for radial "through" cracks emanating from a circular hole in a rectangular plate.[16] Curves of da/dN against ΔK were then plotted using linear regression analysis, from which the crack propagation rates at a stress intensity range of 50 MPa $m^{\frac{1}{2}}$ were determined.

The nominal failing stresses of each of these specimens was calculated from measurement of the area of final failure and the record of the particular load stage at which that specimen had failed (assuming that failure occurred in each case at the maximum load of the stage concerned, and not while the load was increasing to that maximum).

The fracture surfaces of specimens tested in saturated air (Fig. 4*b*) showed no program markings, and were generally much rougher than failures in unsaturated air. Nevertheless, a region of fatigue crack propagation could be clearly distinguished from that of final sudden failure, and in some cases faint markings were also present.

Hydrogen determinations by hot extraction under vacuum were made on twelve unsaturated air (1·25 programmes per hour) specimens selected to cover the range of environments studied. Scanning electron microscopy was employed on 17 specimens, as indicated in Figures 5*a* and 5*b*, to ascertain to what extent, if any, intercrystalline failure was present.

3. RESULTS

3.1 Unsaturated Air

3.1.1 Total Fatigue Lives

The total fatigue life of each specimen is indicated in Figures 5*a* and 5*b* for 1·25 and 0·8 programs per hour respectively by the numerals against the corresponding environmental points.

A grouping of the unsaturated air results at 1·25 programs per hour into three temperature and three water vapour content ranges was made. A statistical analysis of the resulting nine groups of data indicated that fatigue lives as a function of both temperature and water vapour content are significantly different at the 2·5% level between corresponding groups and that there is no interaction between temperature and water vapour content over the ranges examined. The effects of these two variables therefore appear to be independent of each other.

Hence, the total fatigue lives in unsaturated air are dependent on both water vapour content and temperature. The general correlation may be described by contour lines of constant fatigue life, for example those at 20-program intervals which have been superimposed on Figures 5*a* and 5*b*. Although these contour lines must be regarded as indicative rather than exact with the currently available results, and although the maximum attainable total fatigue lives are not known, it can be seen that similar regions of relatively high total fatigue life exist at each rate of program load application. (This general similarity may extend to the more detailed shapes of corresponding contours, which have therefore been matched purposely despite the absence of experimental data in some areas). The regions of high total life involve relatively high water vapour contents (20 to 30 g water vapour per kg of dry air), and temperatures in the range 40°C to 100°C. It should be noted that, at both rates of program load application, the total fatigue lives in the driest environments (less than 1 g per kg) were only approximately 50% of the maximum total lives observed.

Total fatigue lives at 0·8 programs per hour may be somewhat less than at 1·25 programs per hour under identical environmental conditions. However, the relative paucity of results at the slower rate precludes a definitive conclusion.

3.1.2 Life to Crack Initiation

Figures 6*a* and 6*b* show these results, and contours of equal crack initiation life, for 1·25 and 0·8 programs per hour respectively. It will be seen that the life,environment relationship for crack initiation is similar to that for total life, i.e. crack initiation life is significantly greater in an environmental region of relatively high water vapour contents and temperatures than in very dry or much "wetter" air.

Calculation of the ratio of crack initiation life to total life in the various unsaturated air environments at the two rates of program loading shows that this ratio is more or less constant, averaging 0·64 at each loading rate, with standard deviations of 0·08 and 0·11 at 1·25 and 0·8 programs per hour respectively.

3.1.3 Fatigue Crack Propagation Lives

Fatigue crack propagation lives are plotted in Figures 7*a* and 7*b*, together with contours of equal life. Note that in this instance the contours are at 10-program intervals.

Although a somewhat similar dependence on environment to that for total and crack initiation lives seems to exist, the absolute differences in crack propagation life are less marked than those in total life or crack initiation life.

3.1.4 Fatigue Crack Propagation Rates

Crack propagation rates (μm per program) at a stress intensity range (ΔK) of 50 MPa $m^{\frac{1}{2}}$ are plotted in Figure 8 for those specimens in which the cracks extended the full width of the test section. Although a relevant stress analysis method was available for only this crack front shape, it is nevertheless apparent that the rate of fatigue crack propagation is least in the same environmental area in which total life and crack initiation and propagation lives are greatest, and that it is greatest in both the very dry and the highest water vapour content environments.

3.1.5 Failing Stresses

The nominal failing stresses of those specimens for which fatigue crack propagation rates were obtained are shown in Figure 9. It appears that failing stress may be dependent on both water vapour content and temperature, although not in the same way as other properties. In general, the failing stress appears to increase with increasing water vapour content.

3.1.6 Hydrogen Determinations

The hydrogen contents of all samples analysed were not statistically different from each other, and lay within the range 0·25 to 0·50 ppm. The analyses were not undertaken for some months after testing, and no special precautions were taken in storing the fractured specimens during this period. Since hydrogen is known to diffuse through steel at room temperature at an appreciable rate,[1] it cannot be discounted that the hydrogen contents of the various specimens may have differed at the time of fracture.

3.1.7 Scanning Electron Microscopy

All except three of the specimens examined (see Figures 5*a* and 5*b*) showed only transcrystalline fracture in the fatigue-cracked region. However, one specimen tested at 1·25 and two at 0·8 programs per hour also exhibited well-defined (30% to 50%) intercrystalline cracking in the high-load bands, the remainder of each fracture being transcrystalline. These three specimens are identified in Figures 5*a* and 5*b* by circles around the asterisks.

3.2 Saturated Air

The total fatigue lives for the six specimens tested under saturated air conditions were 9, 10 and 12 programs at 25°C and 7, 9 and 11 programs at 30°C. The corresponding mean total lives are 10 and 9 programs respectively, and are not significantly different. Taking the total life in very dry air (46 programs, Figure 5*a*) as unity, the presence of droplets of water on the test specimen surfaces has therefore reduced the total life to 0·2 of that in very dry air.

3.2.2 Fatigue Crack Initiation and Propagation

Assuming that the faint markings present on the fractured surfaces represent changes in load level within one program, it appears that the fatigue crack in each of these specimens has propagated completely in less than one program. This should be compared with the crack propagation life of 11 programs in very dry air (Fig. 7*a*).

The crack initiation life is therefore some 90% of the total life. Although this is a much higher ratio than the corresponding value in very dry air (76%), the absolute value of approximately nine programs is significantly lower than in any of the unsaturated air environments (Fig. 6*a*).

4. DISCUSSION

4.1 Saturated and Unsaturated Air Environments

Higher fatigue crack propagation rates and decreased total fatigue lives of ultra-high strength steels in a saturated compared with an unsaturated air environment at nominally constant temperature have been observed by others.[1-3] The present work extends these observations to two environments of constant water vapour content at various temperatures. In particular, at 1·25 programs per hour (see Figures 5*a*, 6*a*, 7*a*), the approximate ratios of average total, initiation and propagation lives in saturated air to the corresponding maximum observed values at the same water vapour content in unsaturated air are in the vicinity of 0·05 to 0·2. Fatigue crack propagation rates are consequently approximately 5 to 20 times greater in saturated than in unsaturated air of the same water vapour content.

These ratios demonstrate the marked detrimental effect of water in air when present as droplets, particularly on fatigue crack propagation behaviour, compared with an air environment containing the same concentration of water but entirely as vapour.

4.2 Water Vapour Content and Temperature of Unsaturated Air

The water vapour content and the temperature of an unsaturated air environment each influence the fatigue behaviour of SAE 4340 steel independently under the testing conditions employed. A region of water vapour content and temperature exists in which the total fatigue life and its components (crack initiation life and crack propagation life) each exhibit a maximum and the crack propagation rate (at constant stress intensity range, ΔK) reaches a minimum. That is, the fatigue lives are shorter and the actual crack propagation rate is faster in very dry and in relatively "wet" unsaturated air than in air of intermediate water vapour content (at least at 1·25 programmes per hour).

Dahlberg[6] and Neu and Fletcher[4] found that at "room" temperature, the fatigue crack propagation rate of SAE 4340 steel increased as the RH of a nominally constant temperature air environment changed from "dry" to approximately 10%, and then to approximately 80%. A similar result was obtained at 25°C for SAE 4140 steel.[11] The present results are not in conflict with these earlier findings, however, since the present experiments did not specifically include the environmental conditions used by these other investigators.

It is highly unlikely that the observed dependence of fatigue crack propagation on environmental conditions in unsaturated air is associated with capillary condensation of liquid water (as has been suggested elsewhere for crack propagation under static loading at 27°C and above approximately 60% RH[17]). The direction of the effect up to the water vapour content which gives maximum life is the opposite to that which would be expected, and also the rate of crack propagation and the fracture appearance in saturated air (when liquid water is known to be present) are entirely distinct from those in unsaturated air, even at water vapour contents greater than the optimum.

4.3 Possible Mechanism of Observed Effects

Atomic hydrogen is produced when iron is in contact with liquid water, and it can diffuse interstitially through iron and steel at room temperature.[18] The rates of production and diffusion depend greatly on deformation of the metal by abrasion or cold work before and during such contact.[19-23]. Hydrogen so produced may lead to hydrogen embrittlement, to which SAE 4340 steel is highly susceptible.[24-29] Hydrogen embrittlement is more marked the lower

the strain rate.[30] In addition, the fatigue life of this material is significantly reduced and the fatigue crack propagation rate increased by contact with water as liquid or as water vapour in air at relatively high RHs, and by processes which also produce hydrogen embrittlement (e.g. electrolytic charging and cadmium plating). Hence all of these effects on fatigue have been attributed to the presence of hydrogen in the material.[31-33]

In the present experiments, all variations in fatigue life and fracture characteristics are directly associated with variations in water vapour content and temperature, and similarly may be attributed to the presence of hydrogen in the specimens, derived from chemical reaction between the steel and water present as vapour only (unsaturated air) or as vapour and liquid (saturated air). The actual hydrogen content of a particular specimen during a test would thus be determined by the particular constant environment in which it was being tested, each resulting steel-hydrogen "alloy" then exhibiting its own particular response to fatigue. In the present experiments, the basic fatigue properties of hydrogen-free SAE 4340 steel in air at a particular temperature would be most closely approximated in the lowest water vapour content environment at that temperature. The maxima in fatigue properties probably reflect an environmental region in which the hydrogen content is an optimum (cf. similar optima of other interstitial alloying elements such as carbon and nitrogen in their effects on mechanical properties).

Although the common mode of fatigue failure in steels tested in either hydrogen or air is transcrystalline, a significant proportion of intercrystalline fracture is also sometimes present. The current explanation for this phenomenon is that intercrystalline fracture appears in significant amounts when the calculated diameter of the reverse yield plastic zone is equal to the prior austenitic grain size.[34,35] If this were the case, and assuming that the various environments in the present experiments give rise to various hydrogen contents in specimens during testing, then the observations of significant intercrystalline fracture reported here suggest that the size of this zone may depend on the hydrogen content of the steel and on the strain rate (cf. Ref. 36 for copper–beryllium alloys), being smaller at greater hydrogen contents and faster strain rates. It should be noted that in the present work intercrystalline failure is not associated with reduced fatigue performance, and that to interpret its presence as evidence of a detrimental environment would be incorrect.

4.4 Present Results and "Corrosion Fatigue"

It is commonly accepted that "corrosion and fatigue are mutually associated, and that fatigue is accelerated, and occurs under lower stresses, when the conditions tend to promote corrosion", and also that "the atmosphere, as well as fluid reagents, may act chemically upon the metal".[37]

The present results do not fit these generalisations readily. Conditions which would "tend to promote corrosion" in unsaturated air are increases in the water vapour content and/or the temperature, and one would therefore expect that the fatigue life would decrease with increasing water vapour content and temperature. In fact, however, increases in these variables (at least up to the optimum values) are associated with *increases* in fatigue life.

It is therefore of some interest to re-examine the origins of the accepted views on "corrosion fatigue", and "atmospheric corrosion fatigue" in particular. Haigh's original paper[37] was concerned with the effects of various corrosive media on the fatigue of brasses. He found that in several cases, corrosive environments reduced the fatigue lives of the different brasses to less than that in air at corresponding stress levels, but that the lives were unchanged in other cases, and in one circumstance (dilute hydrochloric acid on naval brass) they were actually increased compared with those in air. Since in this last case there would have been very little corrosion, Haigh reached the generalization reported above by arguing that in this instance, air must have been a more corrosive environment that dilute hydrochloric acid. This is the origin of the concept of "atmospheric corrosion fatigue".

Subsequently, many more examples of various metal/corrosive combinations in which the fatigue life is greater than that in air have been reported, and all have been taken as further evidence for the more corrosive nature of air.[38,39] They include 0·33% C steel in a sodium chloride solution at 96°C (6% increase in fatigue limit),[40] and lead in acetic acid (an increase of at least 75%).[41] In the latter case, the specimen surfaces were described as "deeply corroded".

As early as 1929, Haigh noted that "using chemicals which might be expected to provoke chemical action, the author has often been surprised to find that a beneficial rather than a harmful result would follow". He therefore modified his original statement on the mutual influence of

corrosion and fatigue reported above to the following: "the conjoint action of a chemical reagent and an alternating stress may be much more dangerous than either alone". He went on to deplore the use of the term "corrosion fatigue" (which had recently been introduced by McAdam[42]) as "ill-chosen and quite misleading".[43]

Unfortunately, however, neither Haigh nor others such as Gough and Sopwith[38] appear to have considered the possibility that the reported increases in fatigue life over that in air on which the whole concept of "atmospheric corrosion fatigue" is based need not be interpreted as indicating that air is more detrimental than those other environments. They may equally well be taken as evidence that those environments are beneficial compared with air. The latter interpretation is more readily applicable to the present results.

The fact that although many environments are detrimental, some are beneficial to fatigue life when compared with air - in the present case, very dry air—should stimulate the search for other beneficial environments, and for strengthening and weakening mechanisms.

5. CONCLUSIONS

(i) Both the water vapour content and the temperature of an air environment influence the fatigue lives of SAE 4340 steel specimens.

(ii) Within the environmental limits investigated, the total fatigue lives in unsaturated (less than 100% RH) air were approximately twice as long in an intermediate region as in very dry air or air of the highest RH. This intermediate region is approximately 40 C to 100 C, and 20 to 30 g water vapour per kg of dry air. These enhanced total lives involved crack initiation lives approximately twice, and crack propagation rates approximately half, those in the driest or "wettest" unsaturated air environments.

(iii) Total fatigue lives may be 20 to 25% lower at 0·8 than at 1·25 programs per hour under essentially identical environmental conditions.

(iv) A marked reduction in total life to only 10% of the maximum life occurs in air of constant water vapour content as conditions change from an unsaturated to a saturated state due to lowering of the temperature. This reduction is associated with a decreased crack initiation life (20% of the maximum in unsaturated air) and an increased crack propagation rate (estimated at approximately 30 times the unsaturated air minimum).

(v) The present results may be explained in terms of a hydrogen-"alloying" phenomenon, in which the hydrogen content of an individual specimen would be determined by the water vapour content and temperature of the particular environment in which it was being tested. The observed maximum fatigue lives and minimum fatigue crack propagation rates may occur at an optimum hydrogen content.

6. ACKNOWLEDGEMENTS

Thanks are due to J. F. Nankivell and L. Wilson, both of Materials Division, ARL, for carrying out the scanning electron microscopy and the hydrogen determinations respectively.

REFERENCES

1. Spitzig, W. A., and Wei, R. P. — Fatigue Crack Propagation in Modified 300-Grade Maraging Steel. Engng. Frac. Mech., vol. 1, pp. 719–26, 1970.
2. Hanna, G. L., Troiano, A. R., and Steigerwald, E. A. — A Mechanism for the Embrittlement of High Strength Steels by Aqueous Environments. Trans. ASM Qly, vol. 57, pp. 658–71, 1964.
3. Li Che-yu, Talda, P. M., and Wei, R. P. — The Effect of Environments on Fatigue Crack Propagation in an Ultra-High Strength Steel. Int. J. Fract. Mech., vol. 3, pp. 29–36, 1967.
4. Neu, C. E., and Fletcher, A. R. — Fatigue Crack Growth Behaviour of Four High Strength Steels in Two Humid Environments. Part I, US Dept. of Navy, Naval Air Development Center, Rpt. NADC-MC-7060, pp. 27, 29 January 1971.
5. Hartman, A., *et al.* — Some Tests on the Effect of the Environment on the Propagation of Fatigue Cracks in Aluminium Alloys. National Aerospace Lab., The Netherlands Rpt. NLR-TN M 2182, pp. 22, plus figs., May 1967.
6. Dahlberg, E. P. — Fatigue Crack Propagation in High-Strength 4340 Steel in Humid Air. Trans. ASM Qly, vol. 58, pp. 46–54, 1965.
7. Bennett, J. A. — Evidence Regarding the Mechanism of Fatigue from Studies of Environmental Effects. Acta Met., vol. 11, pp. 799–800, 1963.
8. Dunsby, J. A., and Wiebe, W. — Effect of Atmospheric Humidity on Aircraft Structural Alloy Fatigue Life. Matls. Res. and Stds., vol. 9, pp. 15–22, 1969.
9. Liu, H. W., and Corten, H. T. — Fatigue Damage under Varying Stress Amplitudes. Natl. Aeron. Space Admin., Rpt. NASA TN D 647, pp. 68, November 1960.
10. George, G. C. — The Effect of Environmental Relative Humidity upon the Ultrasonic Fatigue Endurance of an Age Hardening Aluminium Alloy. Corrosion Fatigue (ed. Natl. Assen. Corr. Eng.), Natl. Assen. Corr. Eng., pp. 459–67, 1972.
11. Lee, H. H., and Uhlig, H. H. — Corrosion Fatigue of Type 4140 High Strength Steel. Metall. Trans., vol. 3, pp. 2949–57, 1972.
12. Shives, T. R., and Bennett, J. A. — The Effect of Environment on the Fatigue Properties of Selected Engineering Alloys. J. Matls, vol. 3, pp. 695–715, 1968.
13. Paris, P. C., Bucci, R. J., and Little, C. D. — Fatigue Crack Propagation of D6ac Steel in Air and Distilled Water. Stress Analysis and Growth of Cracks (ASTM STP 513), Amer. Soc. Testing Matls., pp. 196–217, 1972.
14. Feddersen, C. E., Moon, D. P., and Hyler, W. S. — Crack Behaviour in D6ac Steel– An Evaluation of Fracture Mechanics Data for the F-111 Aircraft. Metals and Ceramics Info. Center, Battelle Memorial Inst., Columbus, Ohio, Rpt. MCIC-72-04, pp. 117, January 1972.
15. -- — ASHRAE Guide and Data Book – Fundamentals and Equipment for 1965 and 1966. Amer. Soc. Heating, Refrigerating and Air-Conditioning Engineers Inc., Charts 1–3, 1965.

16. Newman, J. C. — An Improved Method of Collocation for the Stress Analysis of Cracked Plates with Various Shaped Boundaries. Natl. Aeron. Space Admin. Rpt. NASA TN D6376, pp. 45, August 1971.
17. Johnson, H. H., and Wilner, A. M. — Moisture and Stable Crack Growth in a High Strength Steel. Appl. Matls Res., vol. 4, pp. 34–40, 1965.
18. Norton, F. J. — Diffusion of Hydrogen from Water through Steel. J. Appl. Phys., vol. 11, p. 262, 1940.
19. Choi, J. Y. — Diffusion of Hydrogen in Iron. Metall. Trans., vol. 1, pp. 911–19, 1970.
20. Swets, D. E., Frank, R. C., and Fry, D. L. — Environmental Effects on Hydrogen Permeation Through Steel During Abrasion. Trans. Met. Soc. AIME, vol. 212, pp. 219–20, 1958.
21. Namboodhiri, T. K. G., and Nanis, L. — Hydrogen Permeation and Embrittlement in Ferrous Materials. Univ. Penna. Tech. Rpt. No. UPH2-004, pp. 83, 1972.
22. Oriani, R. A. — The Diffusion and Trapping of Hydrogen in Steel. Acta Met., vol. 18, pp. 147–57, 1970.
23. Beck, W., *et al.* — Hydrogen Permeation in Metals as a Function of Stress, Temperature and Dissolved Hydrogen Concentration. Proc. Roy. Soc., vol. A290, pp. 220–35, 1966.
24. Johnson, H. H., *et al.* — Hydrogen, Crack Initiation and Delayed Failure in Steel. Trans. Met. Soc. AIME, vol. 212, pp. 528–36, 1958.
25. Steigerwald, E. A. *et al.* — The Role of Stress in Hydrogen-Induced Delayed Failure. Trans. Met. Soc. AIME, vol. 218, pp. 832–41, 1960.
26. Klier, E. P., *et al.* — Hydrogen Embrittlement in an Ultra-High Strength 4340 Steel. Trans. Met. Soc. AIME, vol. 209, pp. 106–12, 1957.
27. Beck, W., *et al.* — The Role of Absorbed CN-Groups in the Hydrogen Embrittlement of Steel. J. Electrochem. Soc., vol. 112, pp. 53–59, 1965.
28. Smith, J. A., *et al.* — Electrochemical Conditions at the Tip of an Advancing Stress Corrosion Crack in AISI 4340 Steel. Corrosion, vol. 26, pp. 539–42, 1970.
29. Morlet, J. G., *et al.* — A New Concept of Hydrogen Embrittlement in Steel. J. Iron and Steel Inst., vol. 189, pp. 37–44, 1958.
30. Brown, J. T., and Baldwin, W. M. — Hydrogen Embrittlement of Steels. Trans. Met. Soc. AIME, vol. 200, pp. 298–303, 1954.
31. Scheven, G., *et al.* — Effects of Hydrogen on Low Cycle Fatigue of High Strength Steel. Proc. ASTM, vol. 57, pp. 682–97, 1957.
32. Beck, W., *et al.* — Hydrogen Stress Cracking of High Strength Steels. US Naval Air Development Center, Rpt. NADC-MA-7140, pp. 213, 1971.
33. Beck, W. — Hydrogen and Fatigue. Brit. Welding J., vol. 15, p. 470, 1968.
34. Cooke, R. J., *et al.* — The Slow Fatigue Crack Growth and Threshold Behaviour of a Medium Carbon Steel in Air and Vacuum. Engng. Fract. Mech., vol. 7, pp. 69–77, 1975.
35. Frandsen, J. D., and Marcus, H. L. — The Correlation Between Grain Size and Plastic Zone Size for Environmental Hydrogen Assisted Fatigue Crack Propagation. Scripta Met., vol. 9, pp. 1089–94, 1975.
36. Scully, J. C. — Failure Analysis of Stress Corrosion Cracking with the Scanning Electron Microscope. Scanning Electron Microscopy, Part IV. Proc. Workshop on Failure Analysis and the SEM, IIT Research Inst., Chicago, Ill., pp. 867–74, April 1974.
37. Haigh, B. P. — Experiments on the Fatigue of Brasses. J. Inst. Metals, vol. 18, pp. 55–86, 1917.
38. Gough, H. J., and Sopwith, D. G. — Atmospheric Action as a Factor in Fatigue of Metals. J. Inst. Metals, vol. 49, pp. 93–122, 1932.

39.	Duquette, D. J.	A Review of Aqueous Corrosion Fatigue. Corrosion Fatigue (ed. Natl. Assen. Corr. Eng.). Natl. Assc. Corr. Eng., pp. 12-24, 1972.
40.	Lehmann, G. D.	The Variation in the Fatigue Strength of Metals when Tested in the Presence of Different Liquids. Aeronaut. Res. Cttee R. and M. No 1054, pp. 13 plus figs., 1926.
41.	Haigh, B. P., and Jones, B.	Atmospheric Action in Relation to Fatigue in Lead. J. Inst. Metals, vol. 43, pp. 271-81, 1930.
42.	McAdam, D. J., Jr.	Stress-Strain Cycle Relationships and Corrosion-Fatigue of Metals. Proc. Amer. Soc. Test Mat., vol. 26, pp. 224–54, 1926.
43.	Haigh, B. P.	Chemical Action in Relation to Fatigue in Metals. Trans. Instn. Chem. Engrs., vol. 7, pp. 29–48, 1929.

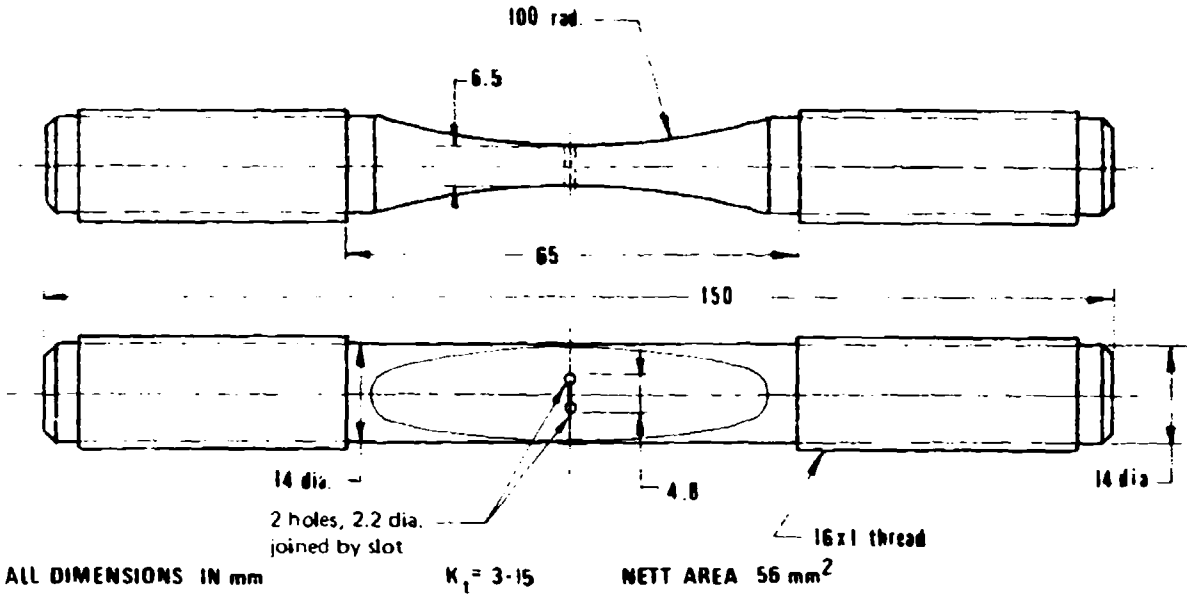

Fig. 1. Keyhole-notched (K_t = 3.15) Fatigue Test Specimen

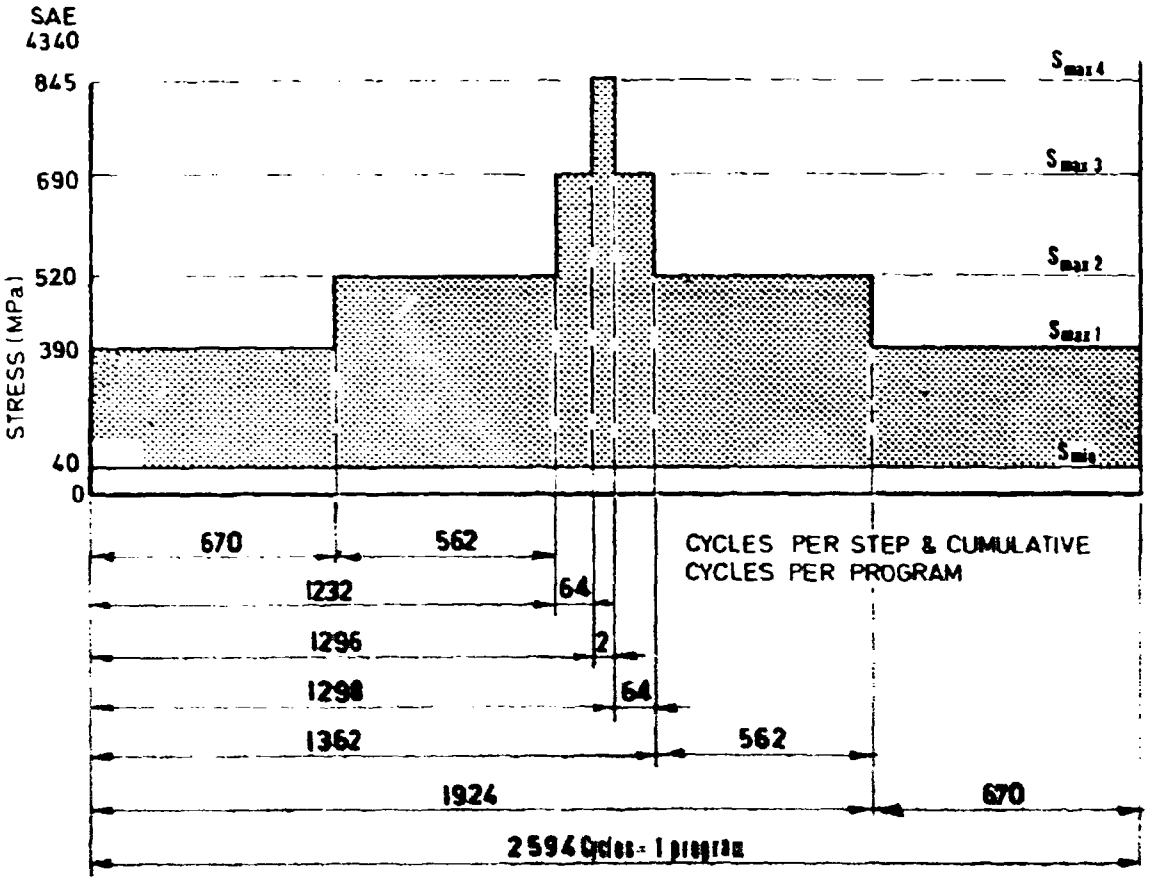

Fig. 2. Four-Stage Program Loading Sequence

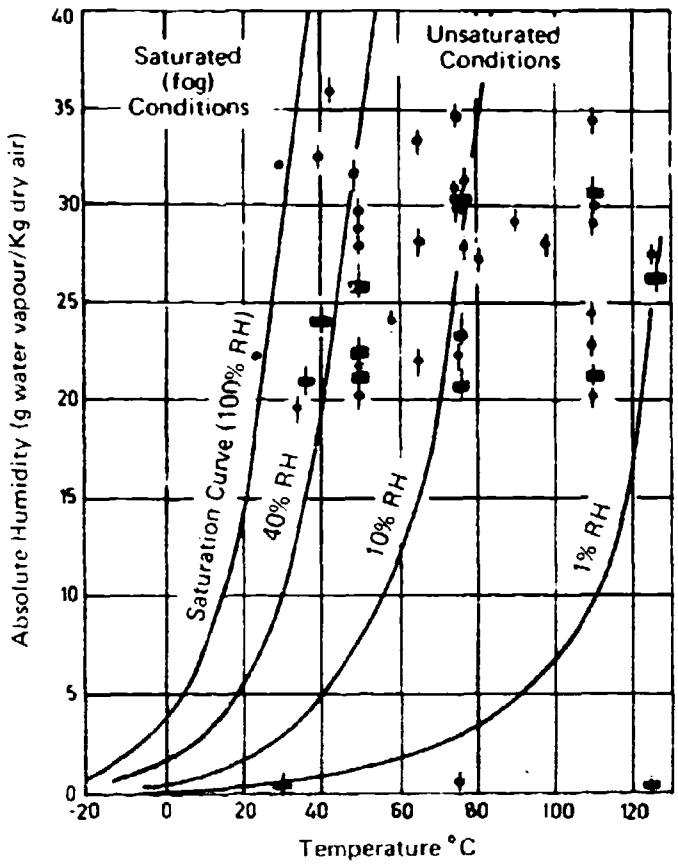

Fig. 3. Psychrometric Chart for Air at Standard Pressure (15) Showing Environments Used for Tests at 1.25 (♦) and 0.8 (◆) Programs per Hour.

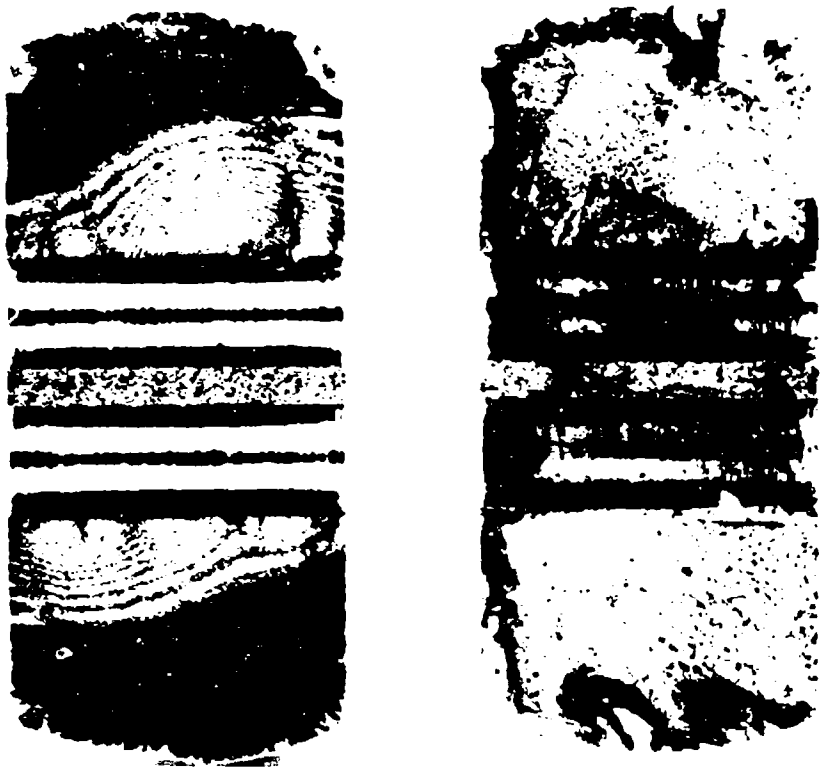

(a) (b)

Fig. 4. Typical Fracture Surfaces of Fatigue Specimens Tested in (a) Unsaturated Air, and (b) Saturated (100% RH) Air. x8.

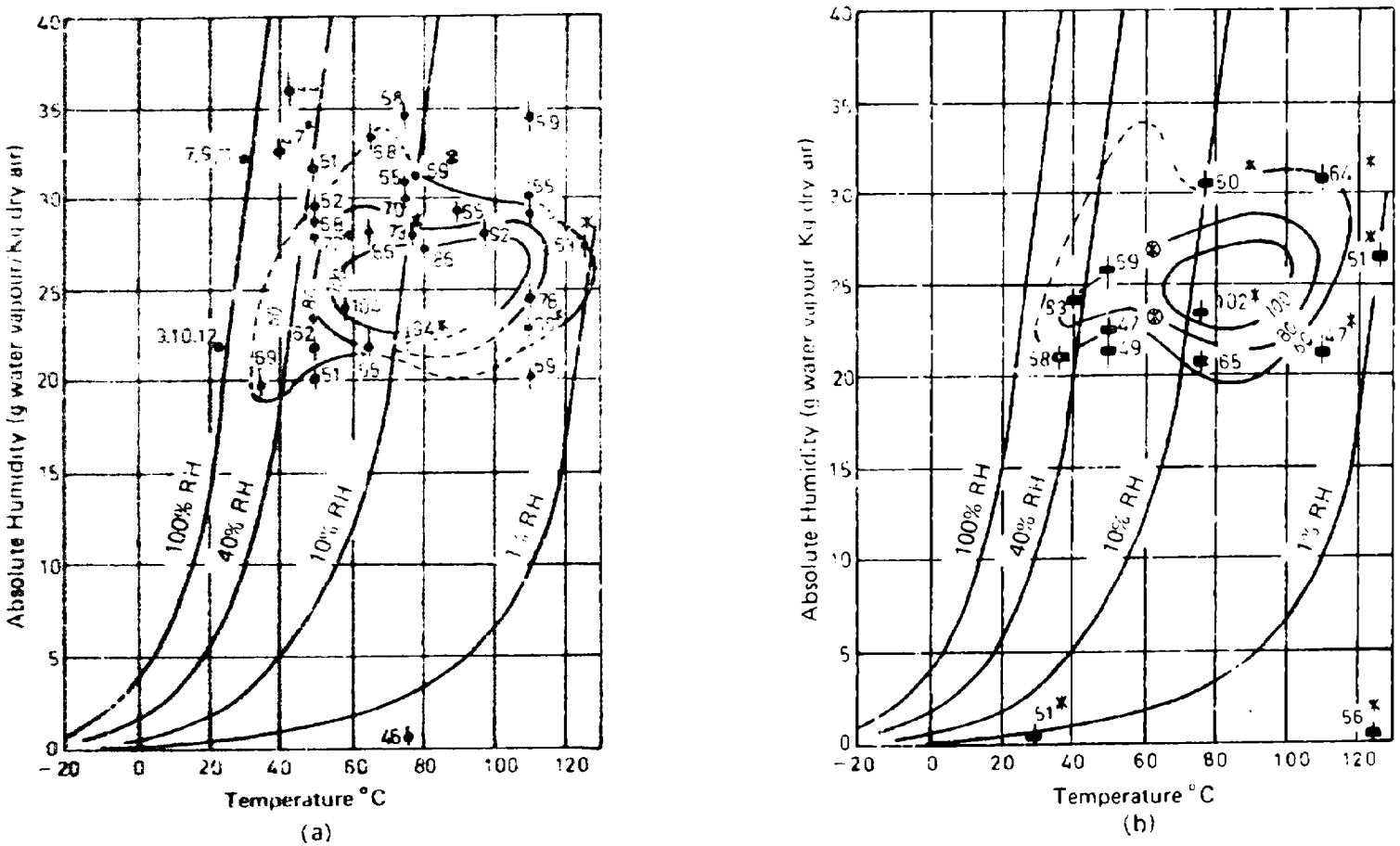

Fig. 5. Total Fatigue Lives in Air at Water Vapour Contents and Temperatures Indicated. (a) 1.25, and (b) 0.8 Programs per Hour. Contour Lines at 20 – Program Intervals of Constant Fatigue Life Superimposed.
*Specimens Examined by Scanning Electron Microscopy. ⊗ Extensive Intercrystalline Fracture Present

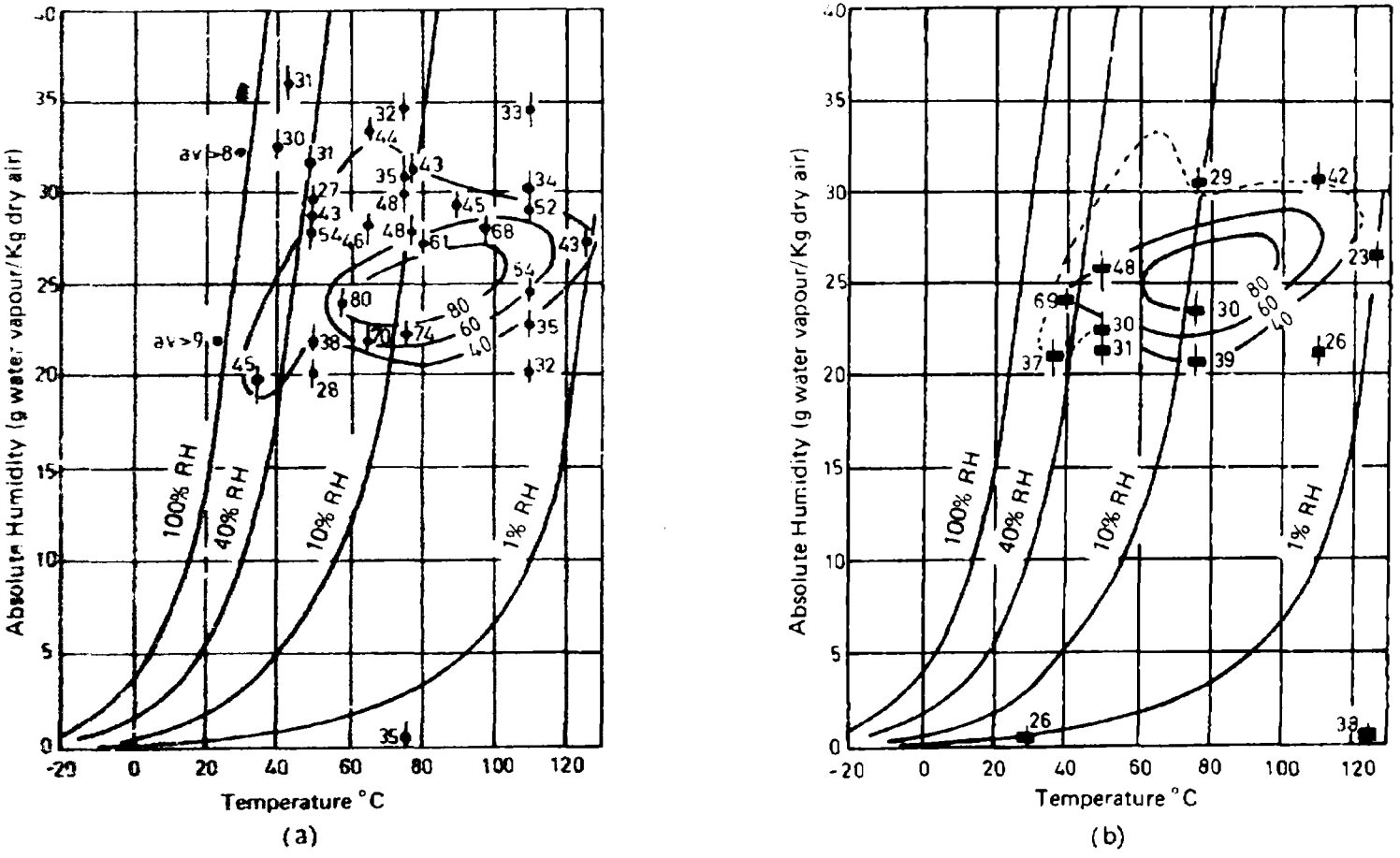

Fig. 6. Lives to Fatigue Crack Initiation in Air at Water Vapour Contents and Temperatures Indicated. (a) 1.25, and (b) 0.8 Programs per Hour. Contour Lines at 20 – Program Intervals of Constant Fatigue Crack Initiation Life Superimposed.

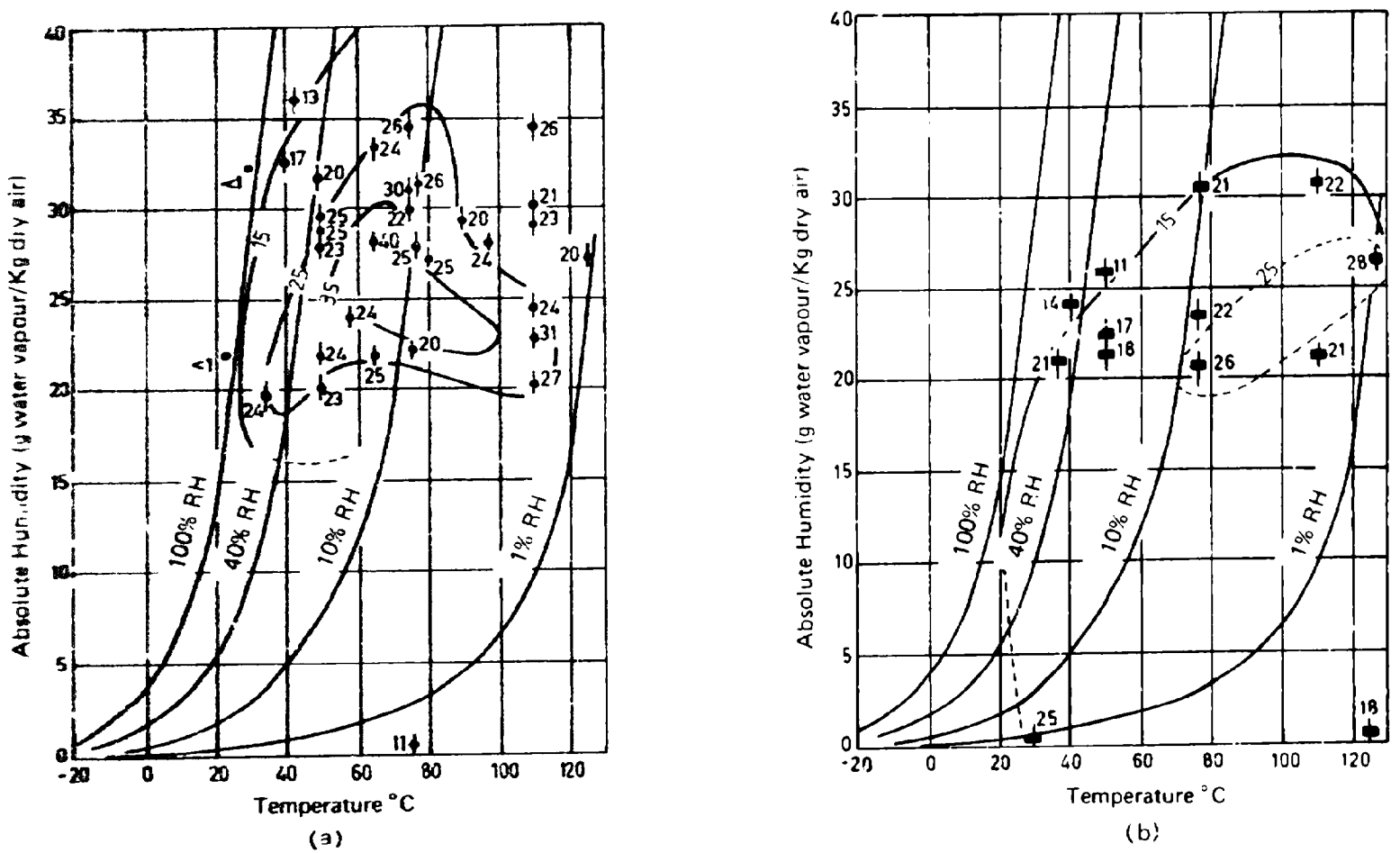

Fig. 7. Fatigue Crack Propagation Lives in Air at Water Vapour Contents and Temperatures Indicated. (a) 1.25, and (b) 0.8 Programs per Hour. Contour Lines at 10 – Program Intervals of Constant Fatigue Crack Propagation Life Superimposed.

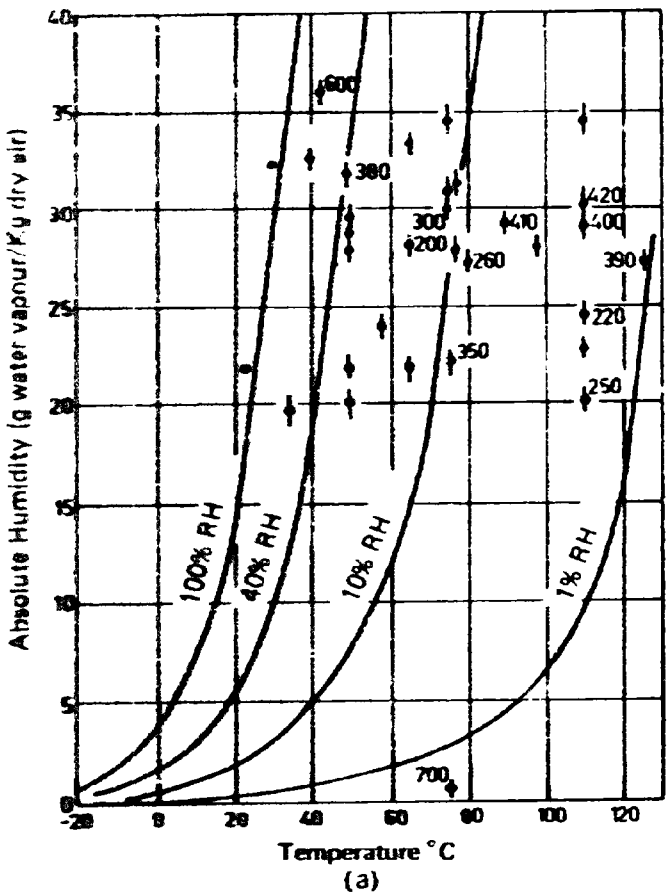

Fig. 8. Fatigue crack propagation rates, (da/dN) μm/program, at a stress intensity range (ΔK) of 50 MPam½, in the various environments indicated. Rate of program load application, 1.25 prog./hr.
(Where no result is given, the fatigue crack front shape was not amenable to analysis).

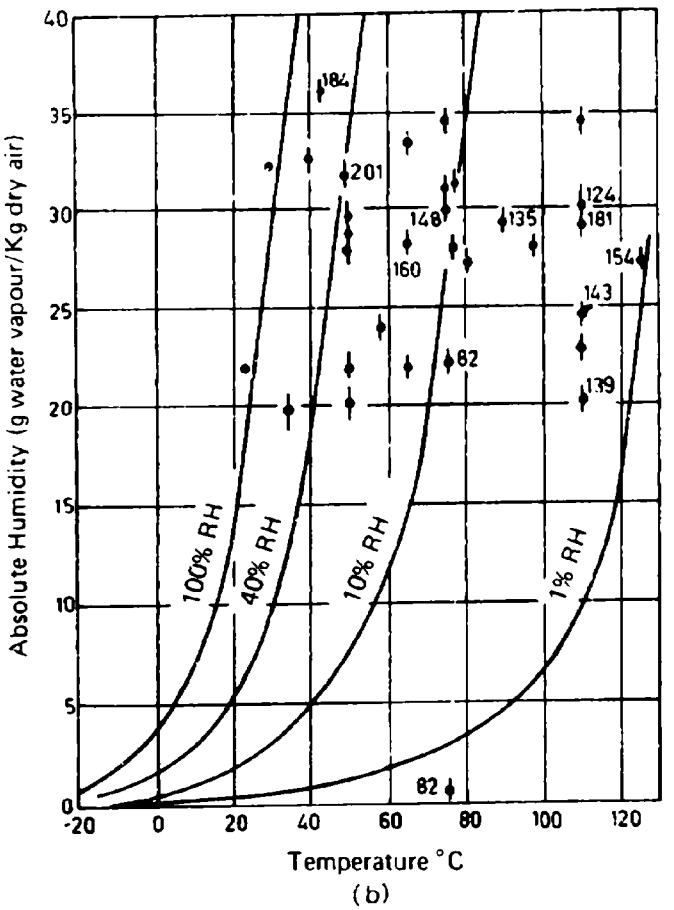

Fig. 9. Failing stresses, MPa, at water vapour contents and temperatures indicated. Rate of program load application, 1.25 prog./hr.
(Results presented for only those specimens for which fatigue crack propagation rates were calculated. See Fig. 8.)

DISCUSSION

QUESTION—*D. M. Turley*
(MRL)

For a given set of testing conditions, what is the reproducibility of your results?

Author's Reply

In saturated air, the total fatigue life has been found to vary by not more than two programmes either side of the mean in three tests under each of two separate environmental conditions (see Figure 5*a*). In later tests on D6AC steel specimens at 35°C in both saturated and very dry air, in which five specimens were tested in each of these two environments, the standard deviations were 0·05 and 0·04 for log mean lives of 19 and 59 programmes respectively. The effects reported in the paper may therefore be taken to be far in excess of overlap in scatter.

QUESTION—*N. T. Goldsmith*
(ARL)

In referring to fracture modes the term "intergranular" has been used. I take it that this refers to the prior austenite grain boundaries in the steel.

This then raises the question as to why the crack chooses this "intergranular" path, and conversely, what the actual path is when the crack follows a "transgranular" path.

Secondly, do the "grain" facets appear absolutely smooth, or do they show evidence of microscopic ductility being present as the crack grows through the metal?

Author's Reply

In the paper (Section 4.3, paragraph 3), I noted that intercrystalline fracture is believed to appear in significant amounts when the calculated diameter of the reverse yield plastic zone is equal to the prior austenitic grain size, and I then attempted to associate this with the present observations. No specific features of the transgranular paths, or evidence of microscopic ductility on the intergranular facets, were evident.

QUESTION—*Neil E. Ryan*
(ARL)

Dr. Kemsley, your presentation of the way a number of interdependent environmental factors influence fatigue life, particularly the interrelation between temperature and water vapour (or pressure) is indeed most challenging and thought provoking. Analysis of such data is, however, open to a multitude of speculative interpretations. To add to this speculation, I would venture to suggest that we could possibly start with the proposal put forward, at this symposium, by Dr. Lynch: namely, that crack growth processes are accelerated by the adsorption of various environmental species. Thus, in the case of liquid water we have only to contend with the adsorption of liquid water and its temperature dependence. While in the case of gaseous water–air mixtures, we have the competing processes for oxygen or gaseous-water adsorption, without any need to consider possible surface reactions leading to the formation of atomic hydrogen. Then, if gaseous water behaves in a manner analogous to that exhibited by hydrogen we are faced with interdependent and synergistic temperature and pressure dependencies, again without even having to consider the complications arising from competition with oxygen adsorption. With such a wide number of interdependent variables, the task of systematically determining the way in which environmental factors either increase or decrease fatigue life is indeed formidable.

THE USE OF ADHERENT ALUMINIUM FOILS FOR FATIGUE METERING

by

R. A. COYLE and M. E. PACKER

SUMMARY

Aluminium foils attached to fatigue specimens show an increase of intensity of the 311,333 X-ray diffraction line as a result of cycling and the increase is shown to arise from changes in texture. It is confirmed that this phenomenon can be used as the basis of a fatigue meter in certain situations. However, it is unlikely to be of general use in the aeronautical field because of its insensitivity to repeated-tension cycles.

1. INTRODUCTION

Miyata, Horisawa and Tashiro[1] bonded aluminium foils to fatigue specimens and showed that the integrated intensity of the 511,333 X-ray diffraction line from the aluminium foil had increased after fatigue testing. It was found that the intensity of this diffraction line depended on the number of cycles and the stress amplitude. They also used resistance-type fatigue gauges, and concluded that the integrated intensity could give a more sensitive measure of fatigue damage in the specimen.

Miyata *et al.* used test data to construct curves of constant integrated intensity for various load amplitudes and numbers of cycles for a particular set of test conditions (material, component geometry, test parameters, etc.). These curves were found to be closely parallel to the S/N curve (Fig. 1) and it was proposed that the integrated intensity from the foil could serve as a measure of the approach of the specimen to its S/N curve, i.e. to failure. In the practical situation, a component, with foil attached, was subjected to fatigue loading and when assessment was required the foil was removed and the integrated intensity of the diffraction line measured. The calibration curve for this particular integrated intensity was then prepared by interpolation. The number of cycles which could still be sustained by the component at some particular load level was then determined by plotting the horizontal line corresponding to this load level and reading off the number of cycles between the points of intersection of this line with the calibration curve and the S/N curve. Such a calculation can be made for any load level, regardless of the previous load history. For a variable load spectrum, they estimated upper and lower limits for the remaining life, corresponding to the maximum and minimum stress levels, respectively. This procedure implies that the foil can record damage for a variable load spectrum. In the service example they quote, for a rear axle shaft assessed after 5000 km under rough road conditions, they predicted a total life of 11 000–13 000 km for the left axle and 20 000–24 000 km for the right axle. These figures compared with an estimate of 45 000 km using Miner's rule. The actual lives of the axles are not clear from the paper but are simply reported as being in the range 10 000–20 000 km.

The investigations at ARL had two objectives: (*a*) to determine the reasons for the change in integrated intensity and (*b*) to assess the technique as a monitor of fatigue damage, particularly as applied to aircraft. The increase in integrated intensity seemed most likely to be caused by changes in preferred orientation or texture, although grain size and line-broadening effects were also considered. Details of the texture investigations are described only briefly here and will be fully reported elsewhere.

Another fatigue gauge has been recently described by Dally and Panizza[2,3]. This gauge, which consists of a thin film of polymer loaded with graphite flakes, measures fatigue damage as a decrease in electrical resistance. The gauge appears to be more sensitive than other fatigue gauges considered in this paper, but a detailed comparison has not yet been made.

2. EXPERIMENTAL

The Japanese workers used mild-steel fatigue specimens and in our earlier experiments mild-steel carrier specimens were also used. In most of our experiments, however, an aluminium alloy, 7075-T6, was used as the carrier specimen since this is more relevant to aeronautical applications. Qualitatively, the integrated intensity changes in the aluminium foil were the same for mild-steel and aluminium-alloy carriers.

The aluminium-alloy fatigue specimens were prepared by polishing on 600 grade wet-and-dry paper and deoxidising for 15 minutes at 65°C in a solution consisting of 32·8 g sodium

dichromate, 164 ml sulphuric acid and 1000 ml water. This treatment was found to improve the adhesion during fatigue tests.

The aluminium foil used is a commercial product 10 μm thick and is manufactured by a combined rolling and annealing process, full details of which are not available; the foil, although soft, is not fully annealed. One surface of the foil is much smoother than the other, apparently as a result of a pack-rolling process during manufacture. The rolling direction (RD), to which we refer at various points in the text, is apparent from roll marks on the surface of the foil.

Most of the experimental results were obtained from foil kindly supplied by the Mitsubishi Company of Japan (foil A). This foil meets the Japanese standard JIS H4191-1954 and the results should therefore be comparable with those of Miyata *et al.* Early results were obtained from foil of unknown origin (foil B) and some isolated results were obtained from foil kindly provided by Alcoa of Australia. The latter foils did not meet the Japanese Standard as regards purity, as their (Fe + Si) content exceeded 0·7%, but the three foils gave similar results and the choice of foil did not seem to be critical.

Foil specimens in the form of 10 × 20 mm rectangles were cut using a guillotine and were then deoxidised for five minutes in the dichromate solution. Early tests performed with smaller foils gave too much scatter in the integrated intensities.

To apply the foils, a drop of cyanoacrylate adhesive (Permabond N102—Pearl Chemical Company, Japan) was placed on the fatigue specimen. A foil was floated on the adhesive, located in position, and then pressed down with a glass plate covered with thin Mylar. Metallographic sections showed the resulting adhesive layer to be one third of the foil thickness, i.e. about 3 μm. The foils could be stripped off after soaking for 12 hours in dimethylformamide.

The integrated intensity measurements were made with a Philips PW1050 diffractometer using a proportional counter detector, a 2° incident beam and a 1 mm receiving slit. The foils were supported on a taut sheet of 5 μm Mylar stretched over the bore of the specimen spinner and a beam trap was used to eliminate extraneous back-scattered radiation. The 511,333 diffraction line from copper K_α radiation was measured with the detector fixed at 162° and with the specimen held perpendicular to the incident beam.

To check the effect of accidental damage to foils during preparation, mounting and removal, a foil was wrapped around a pencil and then flattened; the diffraction line profile and the integrated intensity were unaffected.

A pole figure displays the distribution of normals (or "poles") of a particular set of crystal lattice planes relative to specimen-based co-ordinates, using stereographic projection, and offers an experimentally convenient way of presenting information about preferred orientation in a specimen. For our texture studies, pole figures were prepared using the Schulz technique[4] with copper radiation. The pole figures were recorded out to 70° from the normal to the surface. No corrections were applied for absorption or defocusing because these are the same for all foils and are small for angles less than 40°.

Transmission electron microscopy was also used to study the aluminium foil. The foils were thinned by polishing in a solution consisting of 20% perchloric acid, 70% ethanol and 10% glycerol, the polishing cell being operated at 15 V and about −20°C. The window method was used but, in order to obtain uniform thinning over reasonable areas, it was found advantageous to mask the smooth face completely until the foil first perforated. The masking lacquer was then removed, a narrow strip reapplied around the edge, and thinning continued in the usual way. As a result, the foils examined in the electron microscope always came from very close to one surface of the original foil.

3. X-RAY DIFFRACTION MEASUREMENTS

3.1 Reversed-Cycle Fatigue

Foils were applied to constant-stress fatigue specimens of the 7075-T6 alloy, shaped as in Figure 2. These specimens were loaded in an electromagnetic reversed-bending fatigue machine which operated at 50 Hz. Two foils were mounted on each specimen, one with the rolling direction of the foil parallel to the direction of the applied fatigue stress and the other, perpendicular.

3.1.1 Diffraction Line Intensities

Integrated intensities of the type A foils were measured after cycling carriers at three levels of strain amplitude (Fig. 3). The intensity increased monotonically with the number of cycles

and reached a constant level after approximately 10^5 cycles for a strain amplitude of 0·002; this saturation has not been observed in the tests so far performed at the lower strain amplitudes.

3.1.2 Preferred Orientation

Transmission photographs were taken of the 111 and 200 X-ray diffraction rings from all the foils used to plot the 0·002 strain amplitude curves in Figure 3. Copper radiation from a 0·4 × 8 mm focal spot was used with a 1 mm collimator and a 30 mm film-to-specimen distance. The rings from the unstrained foil (Fig. 4*a*) show well-developed preferred-orientation arcs. As cycling proceeds, the density of these arcs decreases and new arcs are formed. The density of the new arcs increases with the number of fatigue cycles up to $1·2 \times 10^5$ cycles, beyond which there is no further significant increase. The positions of the new arcs depend not on the number of cycles, but only on the direction of loading relative to the rolling direction.

3.1.3 Grain Size

The rings in Figure 4*a* have the sharp spots indicative of annealed material. After cyclic loading to 10^4 cycles, the diffraction spots are small, but still sharp, and little further change occurs up to $9 \cdot 10^5$ cycles.

A microfocus tube with a 10 μm focal spot was used under similar experimental conditions to examine the diffraction spots more closely. Figure 5 shows portions of the rings which have been optically enlarged by a factor of 2. The unloaded foil (Fig. 5*a*) shows large, sharp spots; after 10^4 cycles most of the large spots have broken up into smaller sharp spots. After 9×10^5 cycles there is a range of spot sizes and it appears that the arcs in the original positions have a finer spot size than those in the newly-formed positions.

3.1.4 Line Profiles

Diffractometer traces were taken of the 511,333 line with copper radiation; no change in broadening was detected in foils after 9×10^5 cycles at a strain amplitude of 0·002.

3.1.5 Pole Figures

In order to study the effect of fatigue cycling on texture, 111, 200 and 311 pole figures were prepared from all the foils used to plot the 0·002 strain amplitude curves in Figure 3. Figure 6*a* shows the 200 pole figure of an unstrained foil and the texture can be identified from the pole figure as the standard "R" type texture[5]. After 2×10^4 cycles, the peaks nearest the centre show a distinct move towards the equator. When the rolling direction is parallel to the direction of cyclic stress, this change is seen as a coalescence of the peaks (Fig. 6*b*) and when it is perpendicular, it can be seen as a positional shift (Fig. 6*e*). Thereafter, there is no further movement of the peaks, but a redistribution of intensity from these peaks into a broad central band (Figs 6*c* and 6*f*).

Pole figures were also prepared of the carrier material before and after fatigue. The alloy was not strongly textured in the initial condition and while there were definite changes in the pole figure after fatigue, no systematic change could be measured.

3.2 Repeated-Tension Fatigue

Two tests were made in repeated tension using a flat mild-steel specimen as the carrier. The tests were performed on a Schenk machine between stress limits of approximately zero and 270 MPa. These limits were calculated to give a strain range of about 0·0013. The first specimen received $2·7 \times 10^5$ cycles and the second $7·5 \times 10^5$ cycles.

Transmission X-ray diffraction films of the foils showed that the diffraction spots had broken up into smaller sharp spots; neither these films nor pole figures showed any significant change in the texture. Diffractometer traces also revealed no change of profile or integrated intensity.

3.3 Simple Tension

A foil was mounted on a mild-steel specimen which was then deformed in tension up to a strain of 0·18. No change in the texture of the foil was detected (as expected for such a strain), but now both the X-ray diffraction transmission and diffractometer techniques showed the considerable broadening that would be expected from a uniaxially strained bulk specimen.

4. METALLOGRAPHIC OBSERVATIONS

4.1 Optical Microscopy

The proposition that an aluminium foil records a change in the carrier or substrate material proportional to fatigue damage, suggested that the foil under these experimental conditions was losing its identity and acting simply as an extension of the substrate. In particular, it seemed possible that slip activity in the foil might be severely modified to conform with slip activity in the substrate.

A careful attempt was made, therefore, to compare slip markings on the foils with those on the substrate. For these experiments, a mild-steel substrate was deformed by reversed bending. A typical pair of micrographs is shown in Figure 7; the two fields coincide to within 20 μm. The most heavily deformed areas on the aluminium foil correspond in general with the most heavily deformed areas on the substrate, but there is no correlation in detail, and there is no evidence that slip activity in the steel has forced any abnormal slip activity in the adjacent grain of aluminium.

In general, the surface markings on the aluminium foil were much more severe than those on the substrate. This was particularly apparent for one specimen tested at a low amplitude; there was virtually no damage on the substrate visible by optical microscopy, yet there was a substantial change in the appearance of the aluminium foil. It must be remembered, though, that any slip at the surface of the aluminium is rendered more obvious by the presence of oxide debris. This effect is particularly marked in the case of fatigue deformation.

Similar results were obtained from specimens tested in repeated tension (stress ratio $R = 0$). In the simple tension test, slip was not concentrated into bands and there was even less correlation between regions of slip activity on the substrate and on the foil. In this case though, there was very little difference in the severity of damage on the foil and on the substrate.

4.2 Transmission Electron Microscopy

The structure of the aluminium foil in the reference condition is shown in Figure 8—the as-received foil has been cemented to a substrate and removed, but there has been no fatigue cycling. This particular area shows substantial numbers of dislocations. In other parts of the foil, there were regions which were substantially free of dislocations. Precipitate particles are fairly common, both within the grains and at grain boundaries, but it has not been possible to identify them from diffraction patterns. In general, the grain boundaries in the initial material were steeply inclined to the plane of the foil so that they appeared on the viewing screen as sharp lines unless the foils were tilted at a steep angle to the beam.

Figures 9*a–c* show the structure of a foil which has been tested with the rolling direction perpendicular to the stress axis. The material is divided into sharply defined cells, the boundaries, in the main, consisting of polygonised dislocation walls. In this specimen, there were many regions of a hundred or more such cells, only slightly misoriented with respect to one another. There appeared to be no systematic trend in the orientation differences between the subgrains in a particular region, although dark-field images revealed regions in which clusters of subgrains could be imaged with a particular diffraction spot (Fig. 9*c*).

Dislocations were mostly confined to subgrain boundaries and there were few isolated dislocations within the cells. Precipitate particles were still present, but these did not appear to have interacted very markedly with the dislocation structure.

Figure 10 shows a foil tested with the rolling direction parallel to the stress axis. Once again the structure consists of heavily polygonised dislocation walls although there are more dislocations within the cells and a large number of dislocations loops are present. Grain boundaries in this specimen no longer tend to lie perpendicular to the foil.

Figure 11 shows a foil deformed by repeated tension. A few polygonised dislocation walls can again be seen, but many of the more ragged-looking boundaries are also polygonised (as could be seen by tilting) and it seems typical of this testing mode that the cell boundaries are more nearly perpendicular to the foil surface. There are many dislocations within the cells but the images are very short, indicating that few of these dislocations lie in planes close to the plane of the foil.

5. DISCUSSION

Our results show that a soft aluminium foil cemented to a carrier specimen undergoes changes in texture during reversed-cycle fatigue loading. The changes in integrated intensity seem to be due only to this variation in texture and the changes in grain size and shape, inferred from the diffraction spot studies, appear to have little direct effect. It seems unlikely that such a texture change occurs only in this pick-a-back experimental situation, although there are no known reports in the literature describing the effect of cyclic deformation on texture. Okubo[6] observed grain growth in copper electrodeposited on fatigue specimens and used the phenomenon to identify fatigue-critical areas. No attention was paid to possible changes in texture and the diffraction patterns he reproduces do not permit any conclusion to be drawn on this point. The substantial grain growth Okubo observed would, however, be unlikely to occur without changes in preferred orientation.

Our limited experiments were unable to detect texture changes in the substrate material. Since 7075-T6 is a precipitation-hardened alloy and the particular material we used had a poorly defined texture in the initial condition, this result is probably not significant.

The electron micrographs (Figs 9-11) show the very fine subgrains in the fatigued foils. The structures bear little similarity to the fatigue structures described by Segall and Partridge[7] in bulk specimens of polycrystalline, high-purity aluminium. In particular, Segall and Partridge did not observe the dislocation networks which are so characteristic of our foil specimens. The structures we observed were more like those observed by Weissmann, Shrier and Greenhut[8] in aluminium which had been fatigue-hardened to a saturation condition. Our networks are even more clearly defined than the ones they describe and it is inferred that our specimens, because they are supported by the substrate, have experienced a greater amount of fatigue deformation than they normally could before failure by cracking. That the aluminium foil has reached a saturation condition is consistent with the integrated intensity measurements.

The integrated intensity of the 511,333 diffraction line increases with the number of cycles over a range of strain amplitudes (Fig. 3). At all three amplitudes examined, the plot of integrated intensity against log (number of cycles) is approximately linear. At the highest amplitude, there is a saturation of the integrated intensity after about 10^5 cycles. It is presumed that saturation also occurs at lower amplitudes, but our tests have not been extensive enough to confirm this.

In Miyata's experiments (considering his Figure 3 for aluminium foil on a steel substrate), the maximum stress amplitude used corresponds to a strain amplitude of about 0·0015, at which amplitude lifetimes are less than 10^5 cycles. Comparing these test conditions with our own, we conclude that saturation would not have been reached in his foils. In our case, with aluminium foil on an aluminium alloy substrate, saturation has occurred well before final failure so that sensitivity is lost in the final stages. If the foil technique is to be used for predicting residual fatigue lives in aluminium alloys, a foil with a higher life will be required. It was perhaps a fortunate coincidence that the steel/aluminium combination used in the Japanese work gave satisfactory results. In general, the foil used on an arbitrary component will need to be chosen to match the properties of that component.

Considering that our main concern is to assess the aluminium foil technique for use in aeronautical applications, perhaps the most critical result is the apparent insensitivity to repeated-tension cycles. The implication is that the technique would be reliable only for fully-reversed stress cycles which would seldom occur in aircraft components. The conductive polymer gauge[2,3] may be more appropriate in these circumstances; it is certainly sensitive to repeated-tension cycles, but has not been assessed for fully-reversed cycles.

Although the aluminium foil gauge is insensitive to repeated-tension cycles, there may be some value in a technique which is able to distinguish between fully-reversed fatigue cycles and repeated-tension cycles. It is believed that fatigue crack propagation is dependent mainly on the stress-intensity amplitude, although the stress ratio R is also regarded as an important parameter in some quarters[9,10]. The significance of R in the initiation phase of fatigue is not known.

Miyata *et al.*[1] made certain claims regarding the suitability of the foil technique under variable amplitude conditions. We do not consider that their reported tests were extensive enough to substantiate these claims fully. Our own experiments were not designed to test this aspect and further experiments would be required to establish the relationship between cumulative damage and integrated intensity.

Certainly this foil technique should find application in cases where $R = -1$, but a better

understanding of the scatter characteristics would be required. In particular, it will be necessary to determine if the integrated intensity reading of a foil indicates the fraction of fatigue life expended in a particular specimen or the fraction expended in relation to the average S,N curve for the material.

The present procedures for application and removal of foils would present some difficulties in practical situations. Alternative methods of bonding and removing the foils have not been investigated and more convenient procedures may be possible.

6. CONCLUSIONS

(1) A soft aluminium foil cemented to a fatigue specimen undergoes changes in texture as a result of fully-reversed fatigue cycling.
(2) The texture change causes an increase in the integrated intensity of the 511.333 X-ray diffraction line.
(3) The integrated intensity increases almost linearly with the logarithm of the number of cycles in the initial stages, but eventually saturates.
(4) The technique can be used to provide a record of cyclic deformation received by a component only under certain conditions (e.g. $R = -1$)
(5) The technique has little prospective value in general aeronautical applications.

7. ACKNOWLEDGEMENT

The authors greatefully acknowledge the assistance of M. D. Engellenner with the experimental work.

REFERENCES

1. Miyata, T., Horisawa, H., and Tashiro, T. — Measurement of the Fatigue Life of Motor Parts by AE-Fiol X-ray Study on Strength and Deformation of Metals. Supplement, Society of Materials Science, Japan, pp. 13–18, 1971
2. Dally, J. W., and Panizza, G. A — Conductive Polymers as Fatigue-Damage Indicators. Exp. Mech., vol. 12, pp. 124–29, 1972.
3. Panizza, G. A., and Dally, J. W. — Predicting Failures with Conductive-Polymer Fatigue-Damage Indicators. Exp. Mech., vol. 13, pp. 7–13, 1973.
4. Schulz, L. G. — A Direct Method of Determining Preferred Orientation of a Flat Reflection Sample Using a Geiger Counter X-ray Spectrometer. J. Appl. Phys., vol. 20, pp. 1020–36, 1949.
5. Stüwe, H. P. — Texturbildung bei der Primärrekristallisation (Texture Development During Primary Recrystallisation). Z. Metallkd., vol. 52, pp. 34–44, 1961.
6. Okubo, H. — Electroplating Method of Stress Analysis. Nagoya Univ., Fac. Eng. Mem., vol. 20, pp. 1–143, 1968
7. Segall, R. L., and Partridge, P. G. — Dislocation Arrangements in Aluminium Deformed in Tension or by Fatigue. Philos. Mag., vol. 4, pp. 912–19, 1959.
8. Weissmann, S., Shrier, A., and Greenhut, V. — Dislocation Substructure and Extension of Fatigue Life in Metal Crystals. Trans. ASM, vol. 59, pp. 709–42, 1966.
9. Cooke, R. J., and Beevers, C. J. — The Effect of Load Ratio on the Threshold Stresses for Fatigue Crack Growth in Medium Carbon Steels. Eng. Fract. Mech., vol. 5, pp. 1061–71, 1973.
10. Maddox, S. J. — The Effect of Mean Stress on Fatigue Crack Propagation. Int. J. Fract., vol. 11, pp. 389–408, 1975.

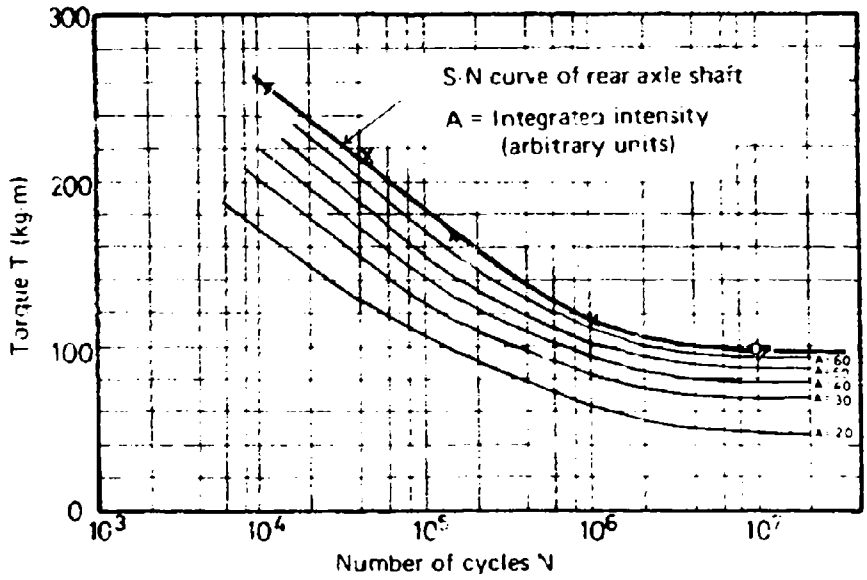

Fig. 1. S/N curve and curves of constant integrated intensity (after Miyata et al. [1]).

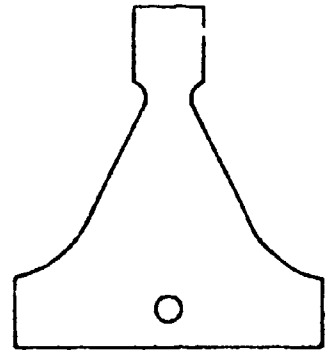

Fig. 2. Constant-stress fatigue specimen used as carrier specimens in most tests.

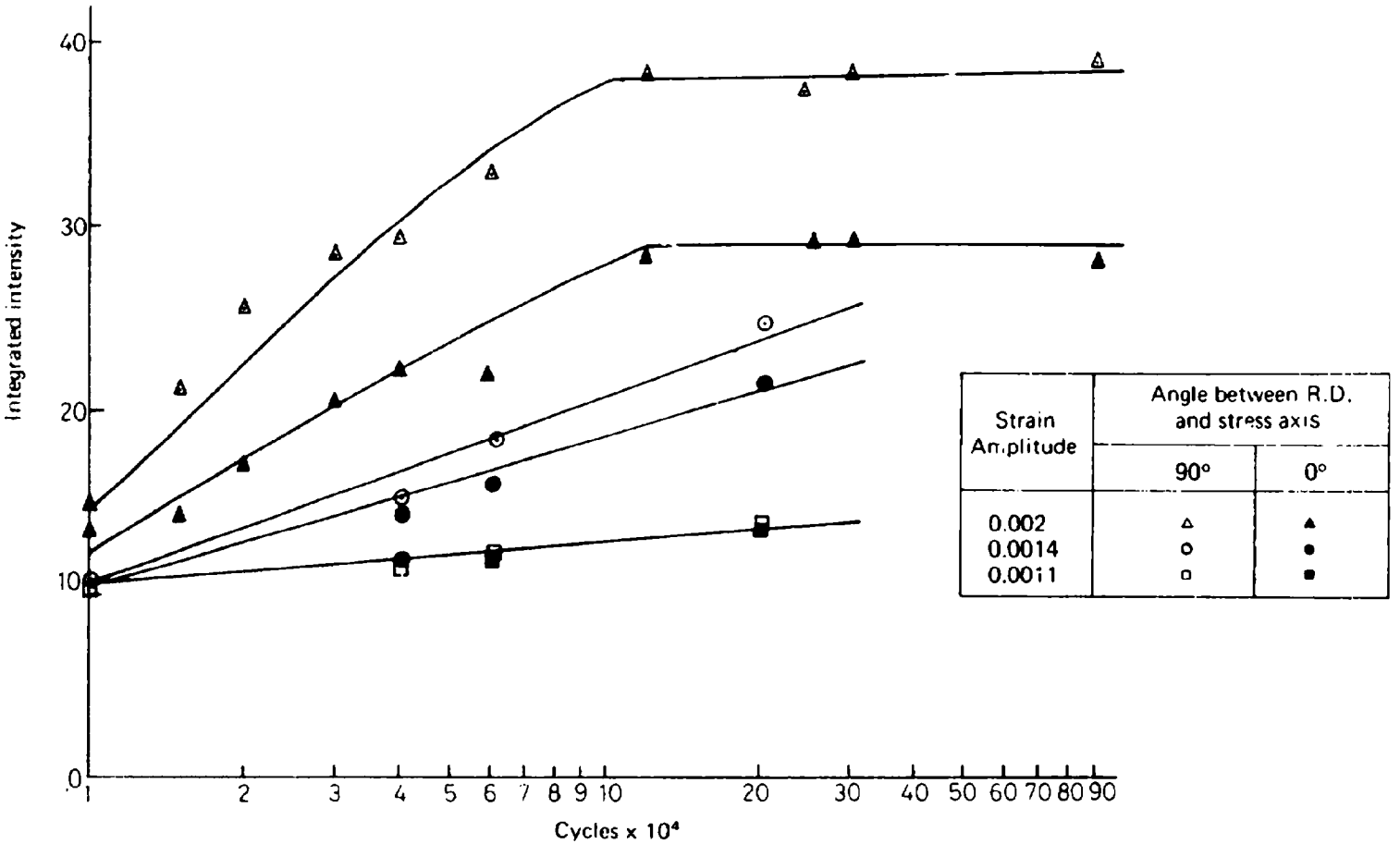

Fig. 3. Variation of integrated intensity with number of cycles for three strain amplitudes and for two orientations of the foil.

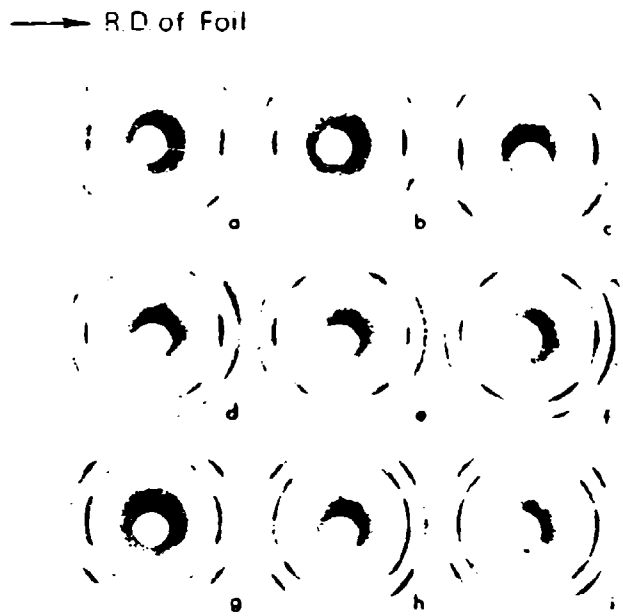

Fig. 4. Transmission X-ray diffraction photographs of aluminium foil (111 and 200 rings); type A foil.
a) as-received condition.
b) 1×10^4 cycles, R.D. perpendicular to stress axis.
c) 1×10^4 cycles, R.D. parallel to stress axis.
d) 4×10^4 cycles, R.D. perpendicular to stress axis.
e) 1.2×10^5 cycles, R.D. perpendicular to stress axis.
f) 9×10^5 cycles, R.D. perpendicular to stress axis.
g) 4×10^4 cycles, R.D. parallel to stress axis.
h) 1.2×10^5 cycles, R.D. parallel to stress axis.
i) 9×10^5 cycles, R.D. parallel to stress axis.

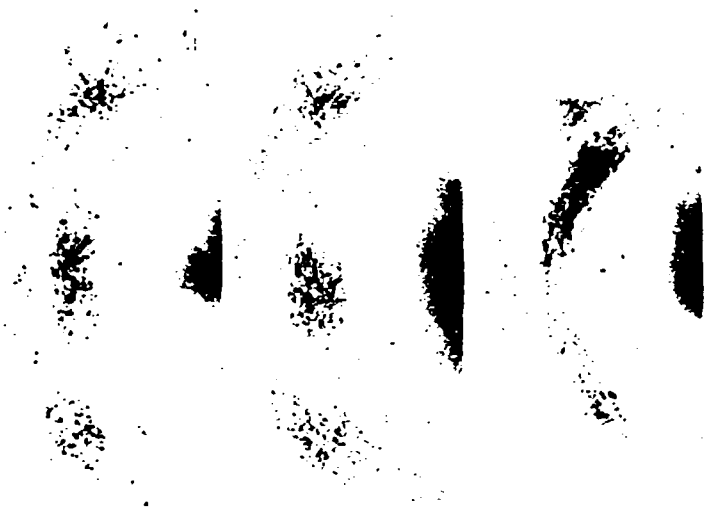

(a) (b) (c)

Fig. 5. Microfocus X-ray photographs showing variation in spot size with fatigue (single-sided film).
a) as-received condition.
b) 1×10^4 cycles, R.D. parallel to stress axis.
c) 9×10^5 cycles, R.D. parallel to stress axis.

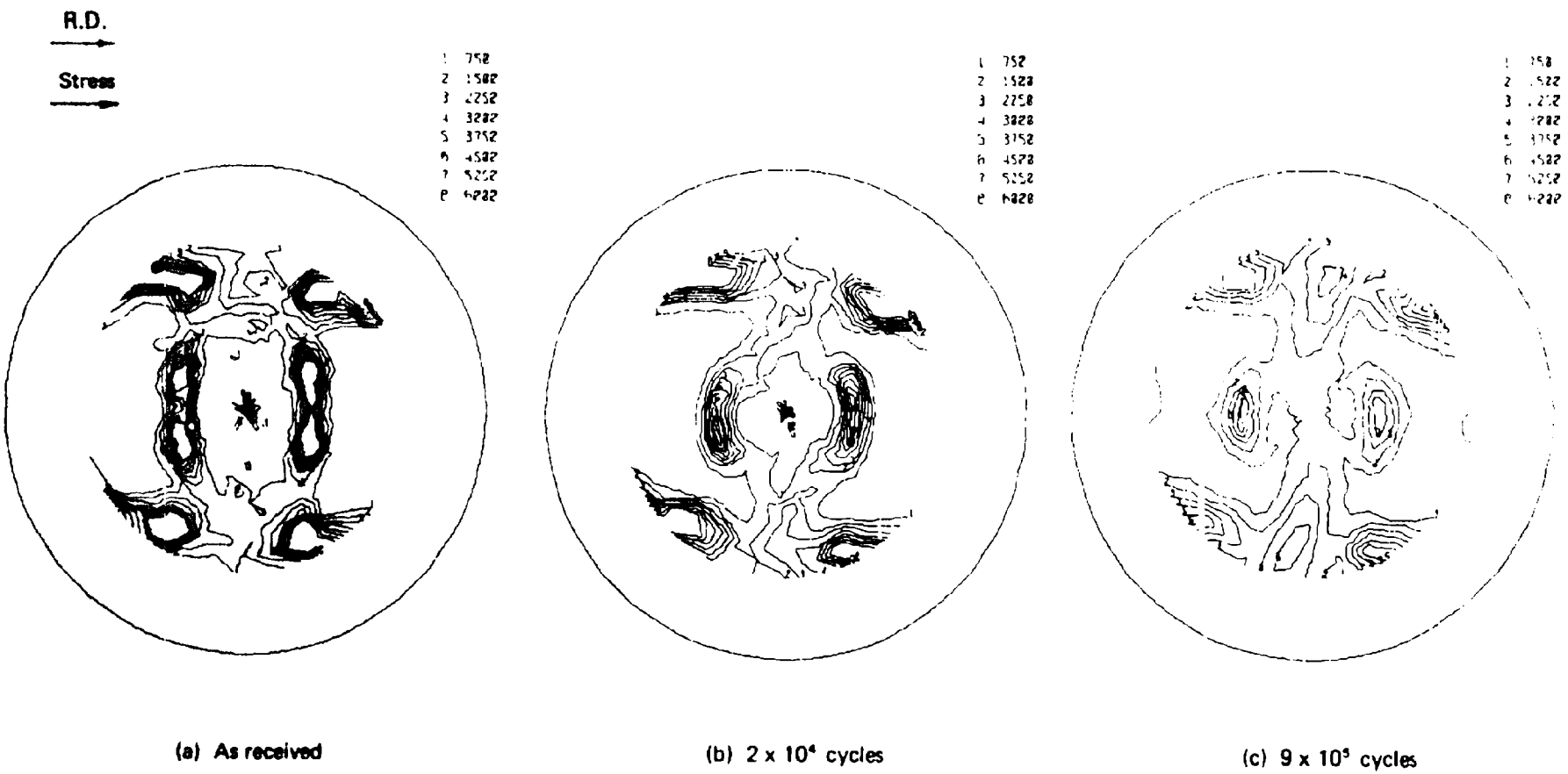

Fig. 6.(a-c) 200 pole figures of aluminium foils, showing the changes in the pole figure for foils oriented with the rolling direction parallel to the stress axis. The contours represent equal counting rates.

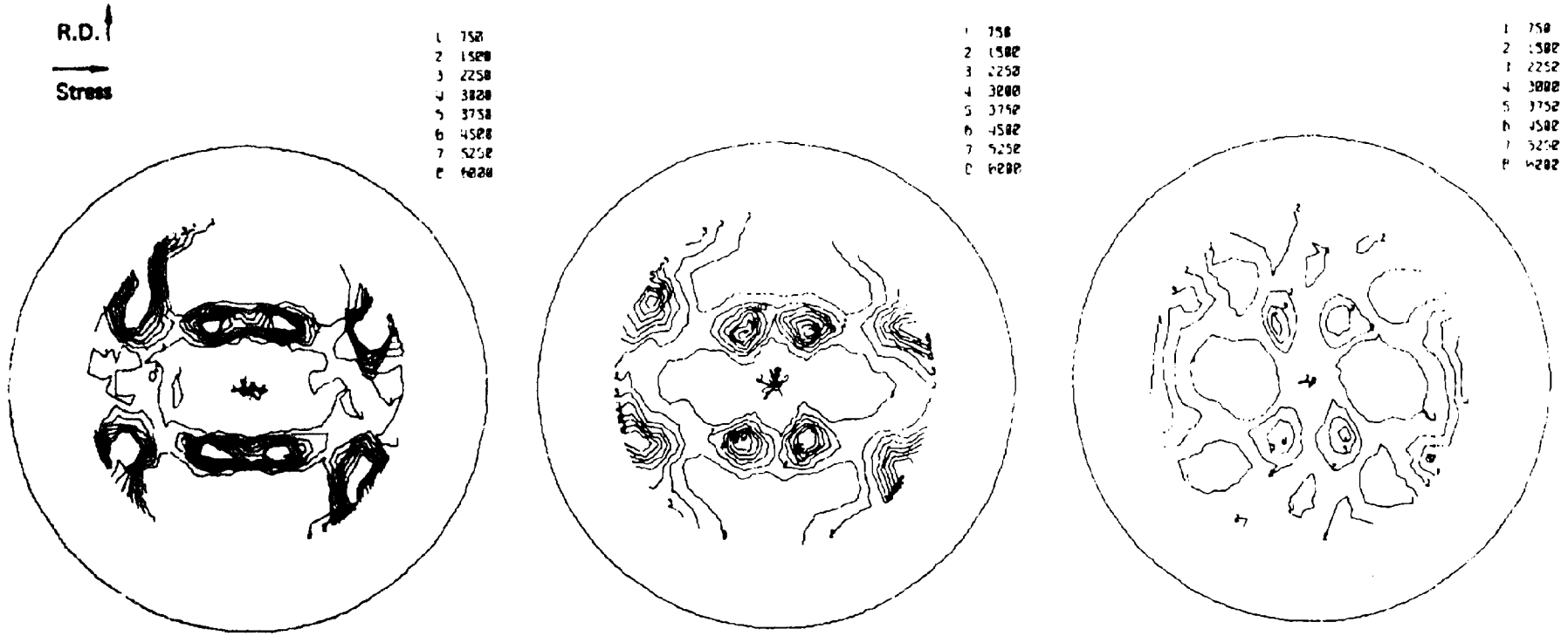

Fig. 6.(d-f) 200 pole figures of aluminium foil, showing the changes for foils with the rolling direction perpendicular to the stress axis. Note that Figs 6(a) and 6(d) are of nominally identical samples in the as-received condition. Allowing for the 90° rotation, they typify the specimen-to-specimen scatter.

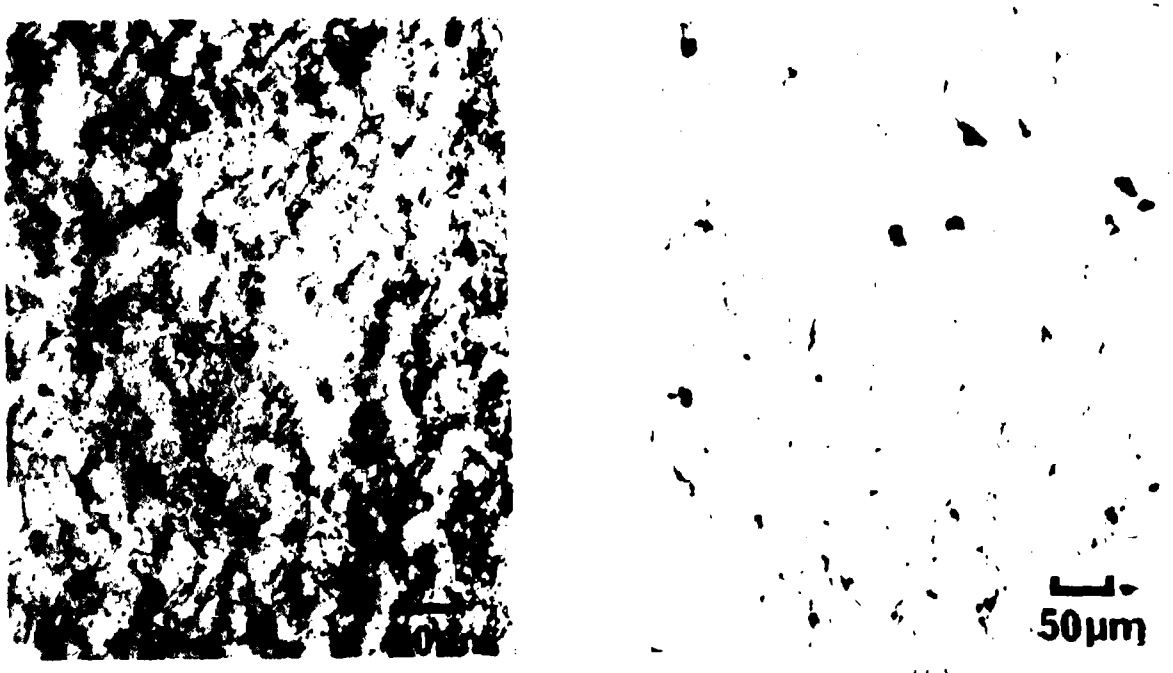

Fig. 7. Slip markings on (a) aluminium foil, (b) steel substrate. The two areas are estimated to correspond to within 20 μm

Fig. 8. Structure of aluminium foil (type A) in reference condition (no fatigue deformation).

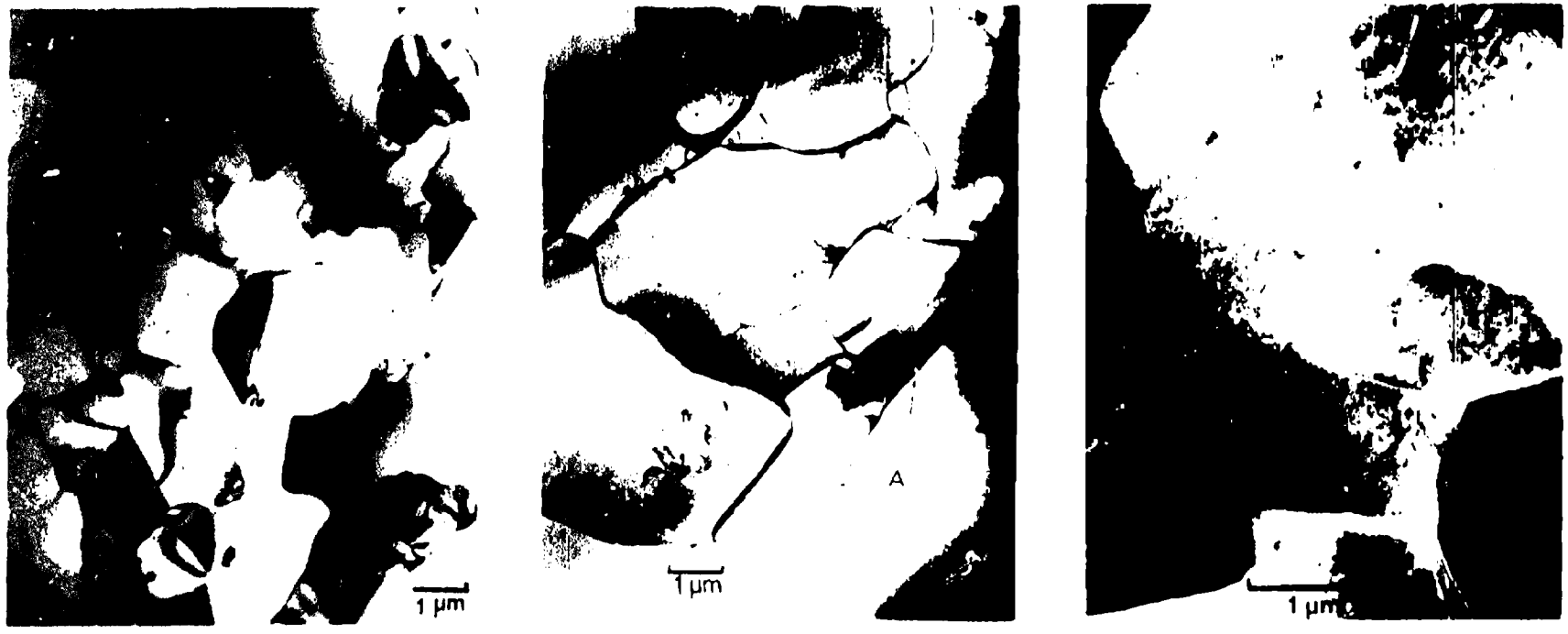

Fig. 9. Structure of aluminium foil tested with rolling direction perpendicular to stress axis, 10^5 cycles. (a) Low magnification, showing cellular structure of subgrain boundaries. (b) Detail of subgrains showing polygonal structure of the subgrain boundaries. A is a high-angle boundary. (c) Same area as (b), imaged with 220 reflection, dark field.

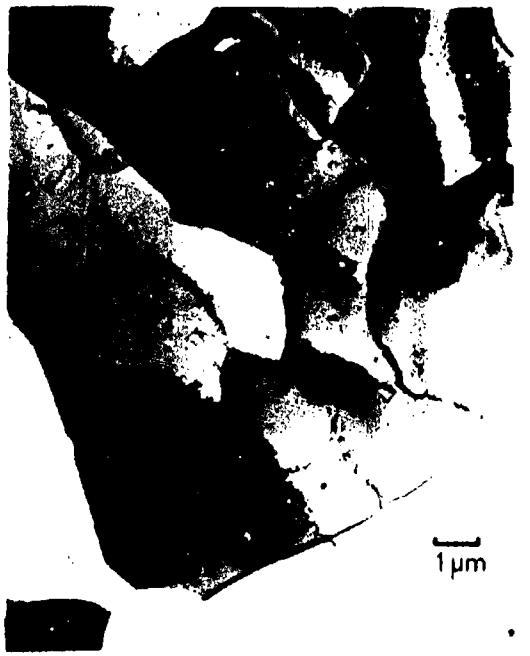

Fig. 10. Structure of aluminium foil (type B) tested with rolling direction parallel to stress axis.

Fig. 11. Structure of aluminium foil (type A) tested in repeated tension.

DISCUSSION

QUESTION —*J. D. Newton*
(SEC, Victoria)

Have you thought of developing the aluminium foils for the assessment of cumulative damage?

Authors' Reply

Our results show that the aluminium foils are sensitive to fatigue cycling at various amplitudes. Miyata *et al.* report that the aluminium-foil technique gives a more accurate assessment of the cumulative damage than does Miner's law. Certainly the aluminium foils can record cumulative damage, but we believe the Japanese claims in this regard to be somewhat premature. Our own experiments were not designed to test this aspect.

QUESTION —*P. Howard*
(ARL)

It seems that the existence of some structural changes due to varying stress has been demonstrated, and that this gives some support to the concept of pre-crack damage.

Authors' Reply

The texture changes we observed in the aluminium foils happen to correlate reasonably well with the progress of fatigue in the substrate, but we do not believe that the texture changes could be related in any direct way with the ultimate development of a fatigue crack.

CLOSING ADDRESS

CLOSING ADDRESS

H. A. WILLS

Retired—Chief Defence Scientist
(formerly Superintendent, Structures and Materials Division, ARL)

The papers in this Symposium combine to give both a synoptic view of the aircraft structural fatigue problem and its solution, as they have developed within the Aeronautical Research Laboratories during a period of 30 years, and also a summary of the current state of knowledge in relevant fields, for example, of fracture mechanics, the micro-mechanisms of fatigue, life monitoring and non-destructive inspection.

In the field of load acquisition and analysis, the nature of atmospheric turbulence and of loads arising from manoeuvres and ground effects are sufficiently well established for preliminary design purposes, as are the methods for translating these effects to stress fluctuations at critical points. For more detailed investigations, fatigue load data acquisition systems such as AFDAS are now available to monitor fluctuating loads and stress on individual aircraft with any desired degree of precision, and also to contribute substantially to the general pool of flight load data.

Several papers have dealt with current developments in the estimation of fatigue life and of safe inspection intervals in safe life or fail safe structures. Although the procedures for achieving a fatigue resistant structure *ab initio* are in theory well known, their achievement in practice is difficult, and the assessment of safety is dependent upon the interpretation of test results on the actual structure in question.

The adoption of risk and reliability theory methods permits the estimates of safe operating limits to be made without adopting some arbitrary specification of the reduced strength level at which the structure becomes unairworthy as a result of fatigue crack growth. (In "conventional" analysis this is usually assumed to be when a crack has grown so that the strength is reduced to around limit strength.) The crux of the problem is the formulation of a realistic model reflecting the properties of crack initiation, crack growth, and strength decay of the family of structures. The crack propagation and strength decay functions vary widely between the different materials and forms of construction. Criteria for flight safety for aircraft of different types may be expressed in terms of either a "limiting permissible average risk rate per hour" or a "limiting permissible probability of failure during the lifetime".

The theory of structural fatigue endeavours to formulate a complete set of equations describing the behaviour of a family of structures having variability of properties and with a variety of critical locations, in which crack growth is preceded by a random damage phase, and in which the macroscopic strains arising only after the commencement of crack growth cause interaction between the stresses at such a crack and at any other critical point. The equations, which may be computer-programmed, are thus potentially useful for prediction purposes and also for analysis of observed behaviour in structural testing, but useful results will depend on the availability of more precise knowledge of the nature of damage and crack initiation and of a realistic mechanism of crack growth from appropriately designed experiments on the actual materials of construction.

Development of the theory of fracture mechanics has thrown new light on estimation of the static (residual) strength of structures containing cracks, and on the propagation of cracks under fatigue loading. In fracture mechanics theory the parameter of significance is the stress intensity factor, and it is seen to be of relevance to the final failure of a cracked structure (unstable crack growth), and to (stable) crack propagation under slow loading or under fatigue conditions. Fracture toughness is a useful basis for comparing high strength materials for a particular application. The sensitivity of fracture toughness to metallurgical structure is both a hazard and a potential advantage to users.

Attention has been drawn in several papers to the great variability in fatigue data - even in those which are obtained from carefully controlled experiments made under carefully controlled laboratory conditions. And further, that the analysis, presentation and interpretation of the data is often a rather subjective process, even when statistically sound and mathematically justifiable techniques are used to present the results in useful form. In a discussion of the subjective quality of S-N curves even when fitted to a single set of S-N data by experienced researchers, it was revealed that, in a cumulative damage situation, these differing S-N curves could lead to estimated lives differing by a factor of 3. There are obviously many more uncertainties involved when data are pooled from different sources.

The paper dealing with load sequence interactions discussed the retardation and acceleration effects on crack growth resulting from the injection of single high loads or single low or negative loads in an otherwise constant amplitude sequence. These effects are qualitatively understood in terms of conditions in the plastic zone at the crack tip, but theoretical formulations have not yet been able to describe the phenomenan adequately. The effects of occasional high loads in inhibiting crack formation and retardation of crack growth have been known for a very long time. It has been proposed before, and it might be worth proposing again, that an initial "proof load" be given as a means of "conditioning" a new structure before it goes into service.

In a detailed discussion of the micro-mechanisms of crack initiation and of crack growth an explanation is offered for the low fracture toughness, and the poor fatigue and stress corrosion properties of the Al-Zn-Mg alloys. It is concluded that the fracture toughness could be improved and the nucleation of fatigue cracks delayed by producing clean alloys, i.e. free from second phase particles rich in Fe and Si—and further improvements in retarding crack growth might result from either increasing the width of precipitation-free zones or preferably by eliminating them altogether.

The paper on D6ac steel investigates the effect for a number of heat treatments which gave approximately the same yield stress but widely different fracture toughnesses. Explanations of these variations were sought in the different micro-structures and failure mechanisms which also affected crack propagation under fluctuating load. The transient effects of step increases and step reductions in alternating load were examined; also the relation between the rate of crack growth and the stress intensity factor. It was concluded that stress intensity factor offers a means of comparing these materials quantitatively as to their crack tolerance and thus provides a basis for estimating crack growth and hence residual strength.

As a means of studying crack propagation involving the behaviour of the plastic zone in the region of the crack tip, a two-component model of elastic and plastic elements in parallel has been proposed, to represent the macro-features of crack behaviour, and to simulate the damaged area of a structure. To substantiate this concept, tests were conducted on test pieces of annealed copper incorporating a key-hole type of stress concentrator, especially designed to permit measurement of crack-opening displacement at the crack tip. Crack growth was found to result from irreversible plastic strain, and the plastic contribution to crack opening controlled the incremental growth of the crack. Just how well this model represents the behaviour of the real materials of construction—and whether it will enable the fatigue behaviour of a structural component to be directly related to a small laboratory test piece—has yet to be demonstrated.

A paper on the endurance testing of aircraft structures at ARL over three decades has supported the contention that full-scale endurance tests are an essential part of airworthiness certification. In addition, associated research investigations have resulted in a number of broad conclusions. Aspects of particular relevance to life prediction were:

(i) the total fatigue behaviour of a new structure cannot be accurately predicted from supposedly representative laboratory specimens, because of the lack of equivalence of the stress redistribution which takes place either from loose fasteners or from crack propagation during the test, nor can it be accurately deduced from the behaviour of vaguely similar structures;

(ii) the effect of a high preload (limit load or above) considerably extends the life for load fluctuations of lower magnitude;

(iii) the introduction of a large negative load, as might occur in a ground-to-air cycle, greatly decreases the fatigue endurance.

It has always been a hope that means would be found to measure directly the deterioration in strength of a structure while in service. ARL tried early on to adapt resistance strain gauges to act as crack detectors, and over the year various attempts have been made to use some sort of strain-sensitive coupon attached to critical areas of the structure to act as fatigue or damage

monitors. The use of aluminium foil has again been investigated by ARL, but the prospects of success of this method appear small.

The physical techniques for detecting cracks and monitoring their growth by non-destructive inspection have made marked progress in recent years, so that no significant manufacturing defect should escape factory inspection. There is also a high degree of confidence that sub-critical cracks will be detected during routine maintenance. The efficiency and limitations of current techniques have been reviewed, and the need stressed for careful selection and training of field operators, and of appropriately designed tests to evaluate their performance. The prospects of newer techniques have been discussed, including acoustic emission, ultra-sound transmission and photo-electron emission which are still in the laboratory stage.

Another paper rightly draws attention to the fact that although environmental agencies, particularly corrosive ones, interact with the fluctuating stress conditions in the initiation and propagation of fatigue cracks, they are generally not given the same detailed attention as other factors affecting the fatigue life. Excuses for this neglect are that corrosion often occurs at hidden places not readily accessible to inspection, that the nature and extent of corrosion is difficult to assess, and that its effect on structural safety is almost impossible to evaluate. The need is expressed for corrosion monitoring using techniques appropriate to the circumstances. Such techniques are now available and should be used on a routine basis. Similarly there is a need for the use by manufacturers of more effective corrosion protection in structurally important areas.

An experimental programme on ultra-high strength steel specimens in unprotected condition showed that the fatigue life was affected both by temperature and humidity (absolute or relative). For relative humidities of less than 100%, it was found that a maximum fatigue life was achieved with a temperature of about 80°C and relative humidity somewhat less than 100%, and this maximum was about double the life obtained at values of temperature and humidity well away from the optimum values. In 100% humidity conditions, with liquid water present on the specimen surface, total lives of about one-tenth of the optimum resulted: both crack initiation and crack propagation were expedited. A possible explanation of the results in terms of a "hydrogen-alloying" phenomenon was proposed. Although some environments are detrimental, the fact that others are beneficial to fatigue life when compared with air should be a stimulant for the search for other beneficial environments, and for strengthening mechanisms in the fatigue process.

The papers of this conference have indicated the great strides that have been made in recent years in applying new theoretical and physical concepts to "life" estimation. But the subject is so diverse and the interacting factors so numerous—each involving a great deal of variability and uncertainty—that continued intensive effort is required to extend the theoretical bases and to provide the essential experimental confirmations. Some of these areas have at least been identified and leads given as to how progress might be made.

It should be remembered that technical innovation sometimes outstrips the scientific base on which it should have been built—on occasions with disastrous results—so it is important to try to anticipate in which direction technology will evolve, and to align research programs to meet the challenge it will provide.

It should also be noted that no other type of terrestrial vehicle, machine or structure needs to be designed, constructed, inspected and proved by test to the same high level of technical efficiency and predictable reliability as an aircraft. As far as human need is concerned the only quality that air transport has to offer is *speed*—and it is the responsibility of aeronautical scientists and technologists to ensure that speed is achieved with the maximum of efficiency, economy and safety.

DISTRIBUTION

AUSTRALIA

Copy No.

DEPARTMENT OF DEFENCE

Central Office

Chief Defence Scientist	1
Executive Controller, ADSS	2
Superintendent, Defence Science Administration	3
Defence Library	4
J.I.O.	5
D.I.S.B.	6-21
Controller, Service Laboratories and Trials	22

Air Force Office

Chief of the Air Staff	23
Chief of Air Force Technical Services	24
Engineering (CAFTS) Library	25
Air Force Scientific Adviser	26
Director General, Aircraft Engineering—Air Force	27
D. Air Eng.	28
Director General, Technical Plans—Air Force	29
H.Q. Support Command (SENGSO)	30
Aircraft Research and Development Unit	31
Library, RAAF Base, Amberley, Qld.	32
Library, RAAF Base, Williamtown, N.S.W.	33
Library, RAAF Base, Richmond, N.S.W.	34
Library, RAAF Base, East Sale, Vic.	35
Library, RAAF Base, Pearce, W.A.	36
Library, RAAF Academy, Point Cook, Vic.	37

Army Office

Army Scientific Adviser	38
Royal Military College	39
US Army Standardisation Group	40

Navy Office

Naval Scientific Adviser	41
Director of Naval Aircraft Engineering	42
Asst. Director Research, Directorate of Naval Aircraft Engineering	43
Superintendent, Aircraft Maintenance and Repair Branch, RAN, Garden Island	44

Aeronautical Research Laboratories

Chief Superintendent	45
Superintendent, Structures Division	46
Divisional File, Structures Division	47
Superintendent, Materials Division	48
Divisional File, Materials Division	49
Library	50

Copy No.

Contributors:

H. A. Wills	51
J. B. Dance	52
B. C. Hoskin	53
A. K. Patterson	54
C. K. Rider	55
D. J. Sherman	56
P. J. Howard	57
J. M. Finney	58
J. Y. Mann	59
R. A. Bruton	60
C. A. Patching	61
A. O. Payne	62
D. G. Ford	63
G. W. Revill	64
Ningaiah	65
S. P. Lynch	66
I. G. Scott	67
J. A. Retchford	68
C. B. Rogers	69
B. J. Wicks	70
N. E. Ryan	71
A. A. Baker	72
M. M. Hutchison	73
D. S. Kemsley	74
R. A. Coyle	75
M. E. Packer	76
L. M. Bland	77

Materials Research Laboratories

Library	78

Weapons Research Establishment

Library	79

Central Studies Establishment

Library	80

Engineering Development Establishment

Library	81

RAN Research Laboratory

Library	82

DEPARTMENT OF PRODUCTIVITY

Government Aircraft Factories

Library	83

Copy No.

DEPARTMENT OF TRANSPORT

Director-General/Library	84
Airworthiness Group (Mr. R. Ferrari)	85

STATUTORY, STATE AUTHORITIES AND INDUSTRY

Australian Atomic Energy Commission (Director) N.S.W.	86
C.S.I.R.O. Central Library	87
C.S.I.R.O. Mechanical Engineering Division (Chief)	88
C.S.I.R.O. Tribophysics Division (Director)	89
Qantas, Library	90
Trans Australia Airlines, Library	91
Gas & Fuel Corporation of Victoria (Research Director)	92
S.E.C. Herman Research Laboratory (Librarian) Victoria	93
Ansett Airlines of Australia, Library	94
BHP Central Research Laboratories	95
BHP Melbourne Research Laboratories	96
Commonwealth Aircraft Corporation (Manager)	97
Commonwealth Aircraft Corporation (Manager of Engineering)	98
Conzinc Riotinto of Australia (Dr. Worner) Victoria	99
Hawker de Havilland Pty. Ltd. (Librarian) Bankstown	100
Hawker de Havilland Pty. Ltd. (Manager) Lidcombe	101
Rolls Royce of Australia Pty. Ltd. (Mr. Mosley)	102
Comalco Research Laboratories (Thomastown, Vic.)	103
Alcoa of Australia	104
Copper and Brass Information Centre, Sydney	105
McPherson's Research Laboratories	106

UNIVERSITIES AND COLLEGES

Adelaide	Barr Smith Library	107
	Professor of Mechanical Engineering	108
Australian National	Library	109
Flinders	Library	110
James Cook	Library	111
La Trobe	Library	112
Melbourne	Engineering Library	113
	Dr. C. J. Osborne, Metallurgy Department	114
	Professor Whitton, Mechanical Engineering	115
Monash	Library	116
	Professor I. J. Polmear, Materials Engineering	117
Newcastle	Library	118
New England	Library	119
New South Wales	Physical Sciences Library	120
	Professor P. T. Fink, Mechanical and Industrial Engineering	121
	Associate Professor R. W. Traill-Nash, Structural Engineering	122
	Professor A. H. Willis, Mechanical and Industrial Engineering	123
Queensland	Library	124

AUSTRALIA (cont.)

		Copy No.
Sydney	Professor G. A. Bird, Aeronautical Engineering	125
	Professor J. W. Roderick, Mechanical Engineering	126
	Professor R. I. Tanner, Mechanical Engineering	127
Tasmania	Engineering Library	128
	Professor A. R. Oliver, Civil and Mechanical Engineering	129
Western Australia	Library	130
R.M.I.T.	Library	131
	Mr. H. Millicer, Aeronautical Engineering	132
	Mr. R. Stokes, Civil Engineering	133

CANADA

Aluminium Laboratories Ltd., Library	134
CAARC Co-ordinator, Structures	135
DeHavilland Aircraft of Canada Ltd.	136
Energy, Mines and Resources Department, Physics and Metallurgy Research Laboratories (Dr. A. Williams)	137
NRC, National Aeronautics Establishment, Library	138

UNIVERSITIES

McGill Library	139
Toronto Institute of Aerophysics	140

FRANCE

AGARD, Library	141
ONERA, Library	142
Service de Documentation, Technique de l'Aeronautique	143

GERMANY

ZLDI	144

INDIA

CAARC Co-ordinator, Materials	145
CAARC Co-ordinator, Structures	146-147
Civil Aviation Department (Director)	148
Defence Ministry, Aero Development Establishment, Library	149
Hindustan Aeronautics Ltd., Library	150
Indian Institute of Science, Library	151
Indian Institute of Technology, Library	152
National Aeronautical Laboratory (Director)	153

INTERNATIONAL COMMITTEE ON AERONAUTICAL FATIGUE

Distributed through Dr. G. S. Jost	154-176

ISRAEL

Technion—Israel Institute of Technology (Professor J. Singer)	177

ITALY

Associazione Italiana di Aeronautica and Astronautica (Professor A. Evla)	178
Aer Macchi (Dr. Bazzochi) Milan	179

	Copy No.
JAPAN	
National Aerospace Laboratory, Library	180
UNIVERSITIES	
Tohuku (Sendai): Library	181
Tokyo: Institute of Space and Aerospace	182
NETHERLANDS	
Delft University of Technology, Professor J. Schijve	183
National Aerospace Laboratory (NLR), Dr. Broek	184
NEW ZEALAND	
Air Department, R.N.Z.A.F. Aero Documents Section	185
Transport Ministry, Civil Aviation Division, Library	186
SWEDEN	
Aeronautical Research Institute	187
SAAB, Library	188
Research Institute of the Swedish National Defence	189
SWITZERLAND	
Armament Technology and Procurement Group	190
Mr. J. Branger, c/-Eidgenössisches Flugzeugwerk, Emmen	191
THAILAND	
Directorate of Aeronautical Engineering, (AVM Jerd Tejasen) RTAF, Bangsue, Bangkok. 3.	192
THE TECHNICAL CO-OPERATION PROGRAMME	
Distributed through Dr. F. P. Bullen	193-202
Distributed through Dr. A. O. Payne	203-208
UNITED KINGDOM	
Australian Defence Science and Technical Representative	209
Mr. A. R. G. Brown, ADR/MAT (MEA)	210
Aeronautical Research Council, N.P.L. (Secretary)	211
C.A.A.R.C., N.P.L. (Secretary)	212
Royal Aircraft Establishment, Farnborough (D. P. Rooke, R. F. W. Anstee, E. Glennie, W. T. Kirkby, P. J. E. Forsyth)	213-217
Royal Aircraft Establishment Library, Bedford	218
Royal Armament Research and Development Establishment, Library	219
Aircraft and Armament Experimental Establishment	220
Military Vehicles Engineering and Experimental Establishment	221
Admiralty Materials Laboratories (Dr. R. G. Watson)	222
National Engineering Laboratories (Superintendent)	223
National Gas Turbine Establishment (Director)	224
National Physical Laboratories Aero Division (Superintendent)	225
British Library, Science Reference Library	226
British Library, Lending Division	227
Naval Construction Research Establishment (Superintendent)	228
C.A.A.R.C. Co-ordinator, Structures	229
Aircraft Research Association, Library	230
British Non-Ferrous Metals Association	231
British Ship Research Association	232

UNITED KINGDOM (cont.)

Copy No.

Central Electricity Generating Board, Materials Research Laboratories, Leatherhead, Surrey (Dr. C. Richards)	233
Fulmer Research Institute Ltd. (Research Director)	234
Motor Industries Research Association (Director)	235
Rolls-Royce (1971) Ltd., Aeronautics Division (Chief Librarian)	236
Science Museum Library	237
Welding Institute, Library	238
Slingsby Sailplanes, Kirkbymoorside	239
Britten-Norman	240
Scottish Aviation, Presswick, Scotland	241
Hawker Siddeley Aviation Ltd., Brough	242
Hawker Siddeley Aviation Ltd., Greengate	243
Hawker Siddeley Aviation Ltd., Kingston-upon-Thames	244
Hawker Siddeley Dynamics Ltd., Hatfield	245
British Aircraft Corporation (Holdings) Ltd., Commercial Aircraft Division	246
British Aircraft Corporation (Holdings) Ltd., Military Aircraft	247
British Aircraft Corporation (Holdings) Ltd., Commercial Aviation Division	248
British Hovercraft Corporation Ltd. (E. Cowes)	249
Fairey Engineering Ltd., Hydraulic Division	250
Short Brothers & Harland	251
Westland Helicopters Ltd.	252

UNIVERSITIES AND COLLEGES

Bristol	Library, Engineering Department	253
Cambridge	Dr. K. J. Miller, Engineering Department	254
	Dr. J. Knott, Metallurgy Department	255
Nottingham	Library	256
Sheffield	Library Department of Fuel Technology	257
Southampton	Library	258
Strathclyde	Library	259
Cranfield Institute of Technology	Library	260
Imperial College	The Head	261

UNITED STATES OF AMERICA

Counsellor Defence Science	262
N.A.S.A. Scientific and Technical Information Facility	263
American Institute of Aeronautics and Astronautics	264
Applied Mechanics Reviews	265
The Chemical Abstracts Service	266
Airforce Flight Dynamics Laboratories, Wright-Patterson A.F.B., Ohio	267
Airforce Materials Laboratory, Wright-Patterson A.F.B., Ohio	268
NASA Langley Research Centre, Hampton, Va. (Dr. W. Elber)	269
NASA Langley Research Centre, Hampton, Va. (Mr. C. M. Hudson)	270
General Dynamics, Fort Worth	271
Bell Helicopter, Fort Worth	272
U.S. Naval Research Laboratories Washington, D.C. (T. W. Crooker)	273
U.S. Naval Research Laboratories, Washington, D.C. (C. D. Beacham)	274
Beechcraft	275
Grumman Aerospace Corporation	276

UNITED STATES OF AMERICA (cont.)

	Copy No.
Rockwell International, Thousand Oaks, Ca. (H. L. Marcus)	277
Materials Science Laboratory, Aerospace Corporation, Ca. (E. G. Kendall)	278
Ford Motor Co., Scientific Laboratory, Dearborn, Michigan (Metallurgy Department)	279
Argonne National Laboratory, Argonne, Illinois (Metallurgy Department)	280
Boeing Co., Head Office	281
Boeing Co., Industrial Production Division	282
Cessna Aircraft Co. (Mr. D. W. Mallonee, Executive Engineer)	283
Lockheed Aircraft Co. (Director)	284
McDonnell Douglas Corporation (Director)	285
Westinghouse Laboratories (Director)	286
United Technologies Corporation, Pratt and Whitney Aircraft Group	287
Battelle Memorial Institute, Library	288
Battelle Memorial Institute, Dr. G. T. Hahn	289

UNIVERSITIES AND COLLEGES

Arizona	Professor B. J. Johnstone, Department of Civil Engineering	290
Brown	Professor J. R. Rice	291
California	Dr. M. Holt, Department of Aerosciences	292
	Library, Guggenheim Aeronautical Laboratories	293
Connecticut	Professor A. J. McEvily	294
Cornell (New York)	Library, Aeronautical Laboratories	295
Florida	Mark H. Clarkson, Department of Aeronautical Engineering	296
Harvard	Professor A. F. Carrier, Division of Engineering and Applied Mathematics	297
Illinois	Professor W. H. Munse, Civil Engineering Department	298
	Professor N. M. Newmark, Talbot Laboratories	299
Johns Hopkins	Professor S. Corrsin, Department of Mechanical Engineering	300
Iowa	Professor R. I. Stephens	301
Lehigh	Professor R. Wei	302
	Professor G. Sih	303
Massachusetts	Professor W. A. Nash, Department of Civil Engineering	304
Pennsylvania	Professor C. Laird, Department of Metallurgy and Materials Science	305
Princeton	Professor G. L. Mellor	306
Stanford	Library, Department of Aeronautics	307
George Washington	Professor Freudenthal	308
Wisconsin	Memorial Library, Serials Department	309
Brooklyn	Library, Polytech Aeronautical Laboratories	310
M.I.T.	Professor R. M. Pelloux	311

Spares 312–400

DOCUMENT CONTROL DATA SHEET

Security classification of this page: Unclassified

1. Document Numbers (a) AR Number: AR-000-724 (b) Document Series and Number: Structures Report 363 Materials Report 104 (c) Report Number: ARL Struc Report 363 ARL Mat – Report – 104	2. Security Classification (a) Complete document: Unclassified (b) Title in isolation: Unclassified (c) Summary in isolation: Unclassified
3. Title: AIRCRAFT STRUCTURAL FATIGUE	
4. Personal Author(s):	5. Document Date: April, 1977 6. Type of Report and Period Covered:
7. Corporate Author(s): Aeronautical Research Laboratories	8. Reference Numbers (a) Task: (b) Sponsoring Agency:
9. Cost Codes: 20-0003, 30-0003	
10. Imprint Melbourne – Aeronautical Research Laboratories 1977	11. Computer Program(s) (Title(s) and Language(s)):
12. Release Limitations (of the document) Approved for public release	

12-0. Overseas:	No.		P.R.	1	A		B		C		D		E	

13. Announcement Limitations (of the information on this page).
No limitation

14. Descriptors:

Aircraft	Life (Durability)	Steels	Aluminium alloys
Fatigue (Materials)	Corrosion	Crack propagation	Reviews
Structures	Non-destructive tests	Aerodynamic loads	Aircraft structures
Aviation safety	Detection	Gusts	Aircraft design
Tests	Reliability	Measurement	Fracture mechanics
Loads (Forces)	Risk	Fibre composites	Histories
Flight	Cracking (Fracturing)		

15. Cosati Codes: 1113 2012

16. *ABSTRACT*

A Symposium on ARL work on Aircraft Structural Fatigue was held in October, 1976 in Melbourne. Nineteen technical papers were presented and these, together with questions and answers, comprise the bulk of the report. The papers cover:

Australian experience and research in Aircraft Structural Fatigue
Fundamentals of fatigue and of fracture mechanics
Data acquisition and interpretation
Structural life prediction
Current research and development in structural and materials fatigue